



Government of **Western Australia**
Department of **Mines and Petroleum**

RECORD 2013/6

YOUANMI AND SOUTHERN CARNARVON SEISMIC AND MAGNETOTELLURIC (MT) WORKSHOP 2013

Compiled by

S Wyche, TJ Ivanic and I Zibra



Geological Survey of Western Australia





Government of **Western Australia**
Department of **Mines and Petroleum**

Record 2013/6

YOUANMI AND SOUTHERN CARNARVON SEISMIC AND MAGNETOTELLURIC (MT) WORKSHOP 2013

Compiled by
S Wyche, TJ Ivanic, and I Zibra

Perth 2014



**Geological Survey of
Western Australia**

MINISTER FOR MINES AND PETROLEUM
Hon. Norman Moore MLC

DIRECTOR GENERAL, DEPARTMENT OF MINES AND PETROLEUM
Richard Sellers

EXECUTIVE DIRECTOR, GEOLOGICAL SURVEY OF WESTERN AUSTRALIA
Rick Rogerson

REFERENCE

Recommended reference to an individual contribution:

Costelloe, RD and Jones, LEA 2013, 2010 Youanmi seismic survey – acquisition and processing, in Youanmi and Southern Carnarvon seismic and magnetotelluric (MT) workshop 2013 compiled by S Wyche, TJ Ivanic and I Zibra: Geological Survey of Western Australia, Record 2013/6, p. 1–6.

Recommended reference to the publication:

Wyche, S, Ivanic, TJ and Zibra, I (compilers) 2013, Youanmi and Southern Carnarvon seismic and magnetotelluric (MT) workshop 2013: Geological Survey of Western Australia, Record 2013/6, 180p.

National Library of Australia Card Number and ISBN 978-1-74168-546-6

Grid references in this publication refer to the Geocentric Datum of Australia 1994 (GDA94). Locations mentioned in the text are referenced using Map Grid Australia (MGA) coordinates, Zones 50 and 51. All locations are quoted to at least the nearest 100 m.

Disclaimer

This product was produced using information from various sources. The Department of Mines and Petroleum (DMP) and the State cannot guarantee the accuracy, currency or completeness of the information. DMP and the State accept no responsibility and disclaim all liability for any loss, damage or costs incurred as a result of any use of or reliance whether wholly or in part upon the information provided in this publication or incorporated into it by reference.

Published 2014 by Geological Survey of Western Australia

This Record is published in digital format (PDF) and is available online at <www.dmp.wa.gov.au/GSWApublications>.

Further details of geological products and maps produced by the Geological Survey of Western Australia are available from:

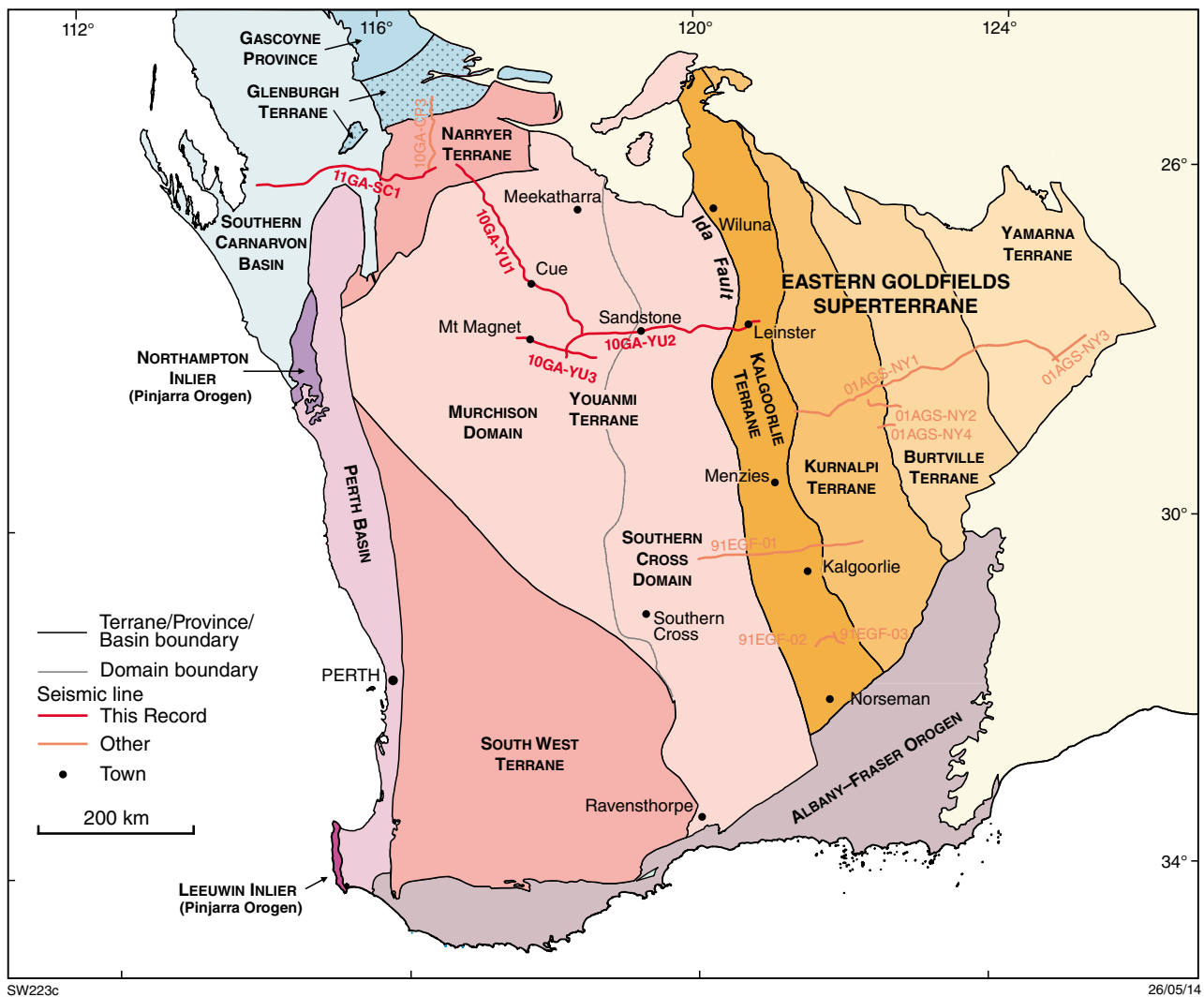
Information Centre
Department of Mines and Petroleum
100 Plain Street
EAST PERTH WESTERN AUSTRALIA 6004
Telephone: +61 8 9222 3459 Facsimile: +61 8 9222 3444
www.dmp.wa.gov.au/GSWApublications

Contents

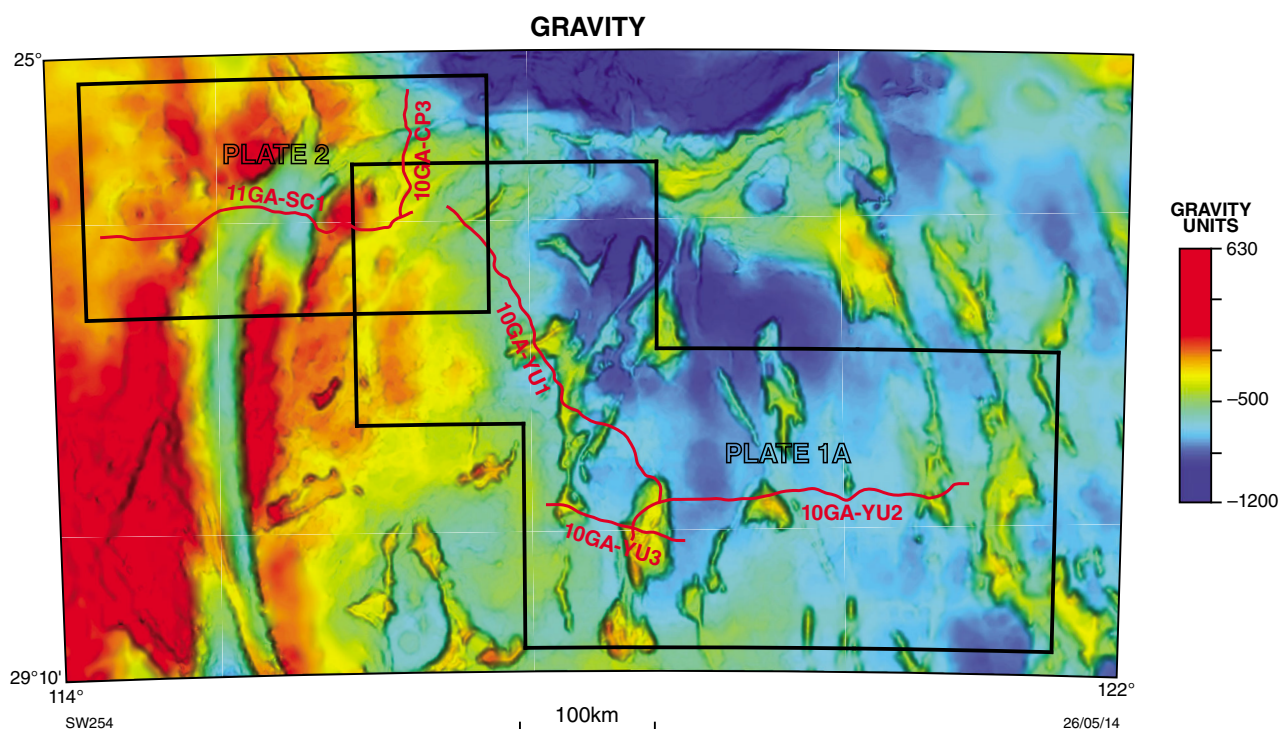
Youanmi seismic survey 2010: acquisition and processing	1
<i>by RD Costelloe and LEA Jones</i>	
Southern Carnarvon seismic survey 2011: acquisition and processing	7
<i>by RD Costelloe</i>	
The Youanmi magnetotelluric (MT) transects.....	13
<i>by PR Milligan, J Duan, T Fomin, A Nakamura, and T Jones</i>	
The nature of the lithosphere in the vicinity of the Youanmi seismic lines	27
<i>by BLN Kennett</i>	
Geology of the northern Yilgarn Craton.....	33
<i>by S Wyche, MJ Pawley, SF Chen, TJ Ivanic, I Zibra, MJ Van Kranendonk, CV Spaggiari, and MTD Wingate</i>	
Interpretation of magnetic and gravity data across the Southern Carnarvon Basin, and the Narryer and Youanmi terranes	65
<i>by K Gessner, T Jones, JA Goodwin, LA Gallardo, PR Milligan, J Brett, and R Murdie</i>	
Main crustal-scale features of the Youanmi seismic transect.....	79
<i>by I Zibra, K Gessner, RJ Korsch, RS Blewett, T Jones, P Milligan, LEA Jones, RD Costelloe, S Wyche, MP Doublier, CE Hall, SF Chen, SS Romano, TJ Ivanic, MJ Pawley, N Patison, BLN Kennett, and MJ Van Kranendonk</i>	
Preliminary interpretation of the Youanmi deep seismic reflection lines for Proterozoic intrusive rocks	81
<i>by TJ Ivanic, MTD Wingate, RJ Korsch, RS Blewett, LEA Jones, S Wyche, I Zibra, MP Doublier, SS Romano, MJ Pawley, MJ Van Kranendonk, K Gessner, CE Hall, SF Chen, N Patison, and RD Costelloe</i>	
Preliminary interpretation of deep seismic line 10GA-YU2: Youanmi Terrane and western Kalgoorlie Terrane.....	87
<i>by I Zibra, K Gessner, MJ Pawley, S Wyche, SF Chen, RJ Korsch, RS Blewett, T Jones, P Milligan, LEA Jones, MP Doublier, CE Hall, SS Romano, TJ Ivanic, N Patison, BLN Kennett, and MJ Van Kranendonk</i>	
Preliminary interpretation of the 2010 Youanmi deep seismic reflection lines and magnetotelluric data for the Windimurra Igneous Complex	97
<i>by TJ Ivanic, RJ Korsch, S Wyche, LEA Jones, I Zibra, RS Blewett, T Jones, P Milligan, RD Costelloe, MJ Van Kranendonk, MP Doublier, CE Hall, SS Romano, MJ Pawley, K Gessner, N Patison, BLN Kennett, and SF Chen</i>	
Preliminary interpretation of deep seismic lines 10GA-YU3 and the southeastern part of 10GA-YU1: Murchison Domain of the Youanmi Terrane	113
<i>by I Zibra, K Gessner, RJ Korsch, RS Blewett, T Jones, P Milligan, LEA Jones, S Wyche, MP Doublier, CE Hall, SF Chen, SS Romano, TJ Ivanic, MJ Pawley, N Patison, BLN Kennett, and MJ Van Kranendonk</i>	
Preliminary interpretation of the northern section of deep seismic line 10GA-YU1: Narryer Terrane to Murchison Domain of the Youanmi Terrane	123
<i>by SS Romano, TJ Ivanic, RJ Korsch, S Wyche, MJ Van Kranendonk, LEA Jones, I Zibra, RS Blewett, T Jones, P Milligan, RD Costelloe, MP Doublier, MJ Pawley, K Gessner, CE Hall, N Patison, BLN Kennett, and SF Chen</i>	
Geological interpretation of deep seismic reflection line 11GA-SC1: Narryer Terrane, Yilgarn Craton and Southern Carnarvon Basin.....	129
<i>by RJ Korsch, MP Doublier, SS Romano, SP Johnson, AJ Mory, LK Carr, Y Zhan, and RS Blewett</i>	
Geodynamic implications of the Youanmi and Southern Carnarvon deep seismic reflection surveys: a ~1300 km traverse from the Pinjarra Orogen to the eastern Yilgarn Craton	147
<i>by RJ Korsch, RS Blewett, S Wyche, I Zibra, TJ Ivanic, MP Doublier, SS Romano, M Pawley, SP Johnson, MJ Van Kranendonk, LEA Jones, N Kositsin, K Gessner, CE Hall, SF Chen, N Patison, BLN Kennett, T Jones, JA Goodwin, P Milligan, and RD Costelloe</i>	
The 2010 Youanmi deep-crustal seismic lines: implications for mineral systems.....	167
<i>by S Wyche, TJ Ivanic, I Zibra, K Gessner, M Doublier, RJ Korsch, and RS Blewett</i>	

Plates

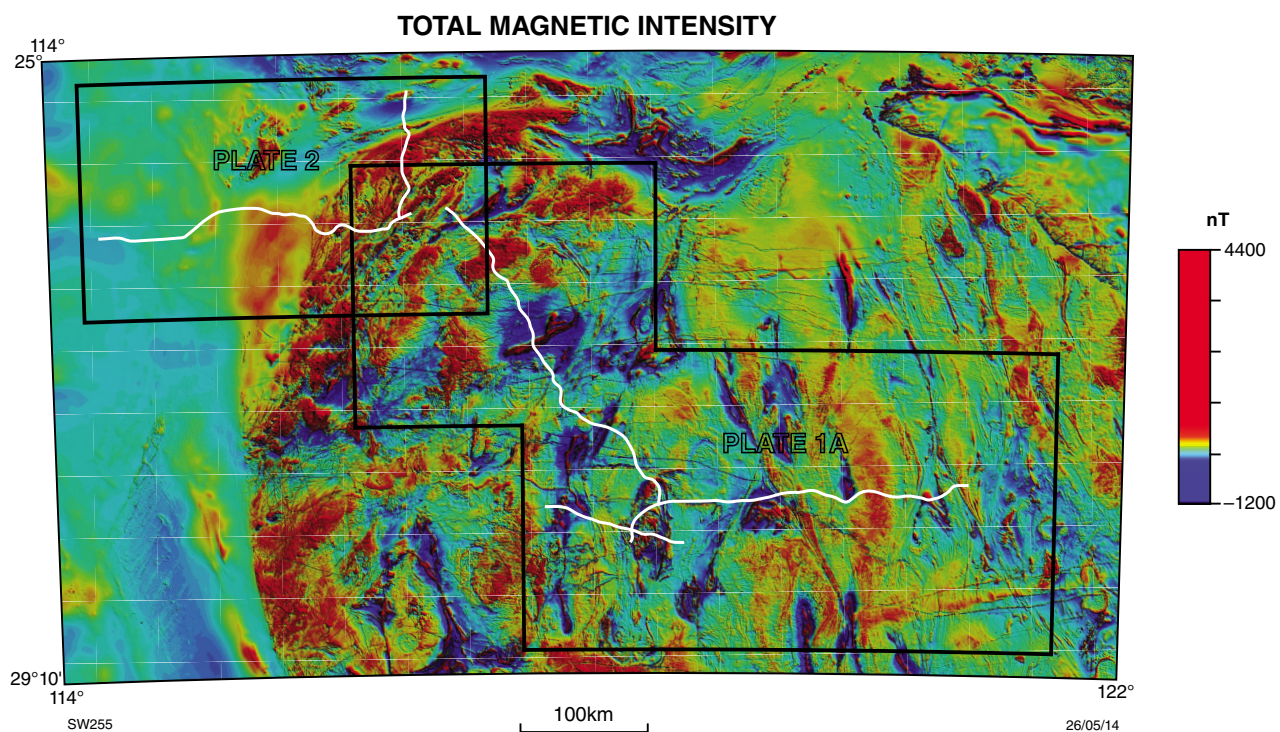
1. Geological interpretation of the northwest Yilgarn Craton
2. Geological interpretation of the northwest Yilgarn Craton margin
3. Geological interpretation of the Youanmi and Southern Carnarvon seismic lines 10GA-YU1, 10GA-YU2, 10GA-YU3, and 11GA-SC1



Frontispiece 1. Major tectonic subdivisions in the Yilgarn region showing locations of deep-crustal seismic traverses



Frontispiece 2. Regional bouguer anomaly gravity image for the northern Yilgarn Craton. Red lines are locations of Youanmi seismic traverses, and areas of Plate 1A and Plate 2 are shown in black outline.



Frontispiece 3. Composite regional TMI aeromagnetic image for the northern Yilgarn Craton. Red lines are locations of Youanmi seismic traverses, and areas of Plate 1A and Plate 2 are shown in black outline.

Youanmi seismic survey 2010: acquisition and processing

by

RD Costelloe¹ and LEA Jones¹

Introduction

Geoscience Australia, in collaboration with the Geological Survey of Western Australia (GSWA), contracted Terrex Seismic to collect the Youanmi Deep Seismic Reflection Survey data in May and June 2010. Deep seismic reflection data and gravity readings were acquired along the three lines comprising the survey (10GA-YU1, 10GA-YU2 and 10GA-YU3) for a total of 694 km (Fig. 1). Magnetotelluric (MT) data, as a part of an ANSIR and AuScope, agreement, were collected at 5 to 20 km spacing along all lines (Milligan et al., this volume). The aim of the survey was to:

- image the northwest Yilgarn Craton to the Ida Fault
- image the transition between the Youanmi Terrane and the Narryer Terrane
- image the Meekatharra structural zone (a focus of gold mineralization).

Seismic acquisition

The reflection seismic survey acquisition began on 21 May 2010, on 10GA-YU1, in the northwest of the Youanmi Terrane near Beringarra Bore at the start of the Beringarra to Cue road. All lines were located on existing roads and tracks. Line 10GA-YU1 continued southeast and finished about 5 km west of Windsor on the Mount Magnet to Sandstone Road. Line 10GA-YU3 was then completed from west to east, starting east of Boogardie Station Homestead and finishing on Windimurra station about 3 km north of Richardson Well. Line 10GA-YU2 was completed from west to east, starting just north of Challa Station Homestead and finishing south of Leinster on 30 June 2010. The location of the survey is shown in Figure 1. Acquisition parameters for the survey are shown in Table 1. The seismic data were collected with 300 live channels spread over 12 km, and with the source array located at the centre of the spread. The maximum offset receiver groups were 6 km from the source. The seismic

data were recorded using a Sercel SN428XL recording system in SEG-D revision 1 8058IEEE demultiplexed format. The energy source was an in-line array of 3 Hemi-60 vibrators with 2 or 3 sweeps per vibration point (VP). The recording system cross-correlated each of the sweeps for each VP with its respective reference sweep and stacked the cross-correlated sweeps, creating a single 20 second record for each VP, which was then written to disk and copied to an LTO2 tape (one tape each day). The LTO2 tapes could easily hold a day's production, for which the greatest daily production was more than 450 VPs. Two sets of acquisition parameters were used, with a VP interval of 80 m (3 sweeps), and of 40 m (2 sweeps). The 40 m VP interval was acquired over greenstone terranes as a way of improving signal penetration through the greenstones.

Seismic reflection processing

The reflection seismic data for the Youanmi survey were processed by the Seismic Acquisition and Processing team of the Onshore Energy and Minerals Division of Geoscience Australia, using the Paradigm Disco/Focus processing software, with Red Hat Enterprise Linux release 4 Operating system on a Sun Fire X4600 M2 server. The basic processing sequence applied to the data is shown in Table 2. A reduced processing stream was used in the field to produce field stacks to QC and monitor data quality while the survey was in progress. As the lines were essentially 2D transects, they were processed using algorithms that are based on assumed 2D geometry. This 2D assumption has implications for processing and for the interpretation of the resulting processed data, which is explained in the description of the key processing steps.

Crooked line geometry definition

The seismic lines followed existing roads and tracks, and hence were not straight. To process crooked line data in 2D using the Common Depth Point (CDP) method, it is necessary to bin the data into common midpoint gathers based on a calculated CDP line. The CDP line is a curve of best fit through the source–receiver midpoints. CDP bin locations are calculated based on a user-supplied CDP

¹ Minerals and Natural Hazards Division, Geoscience Australia, GPO Box 378, Canberra ACT 2601

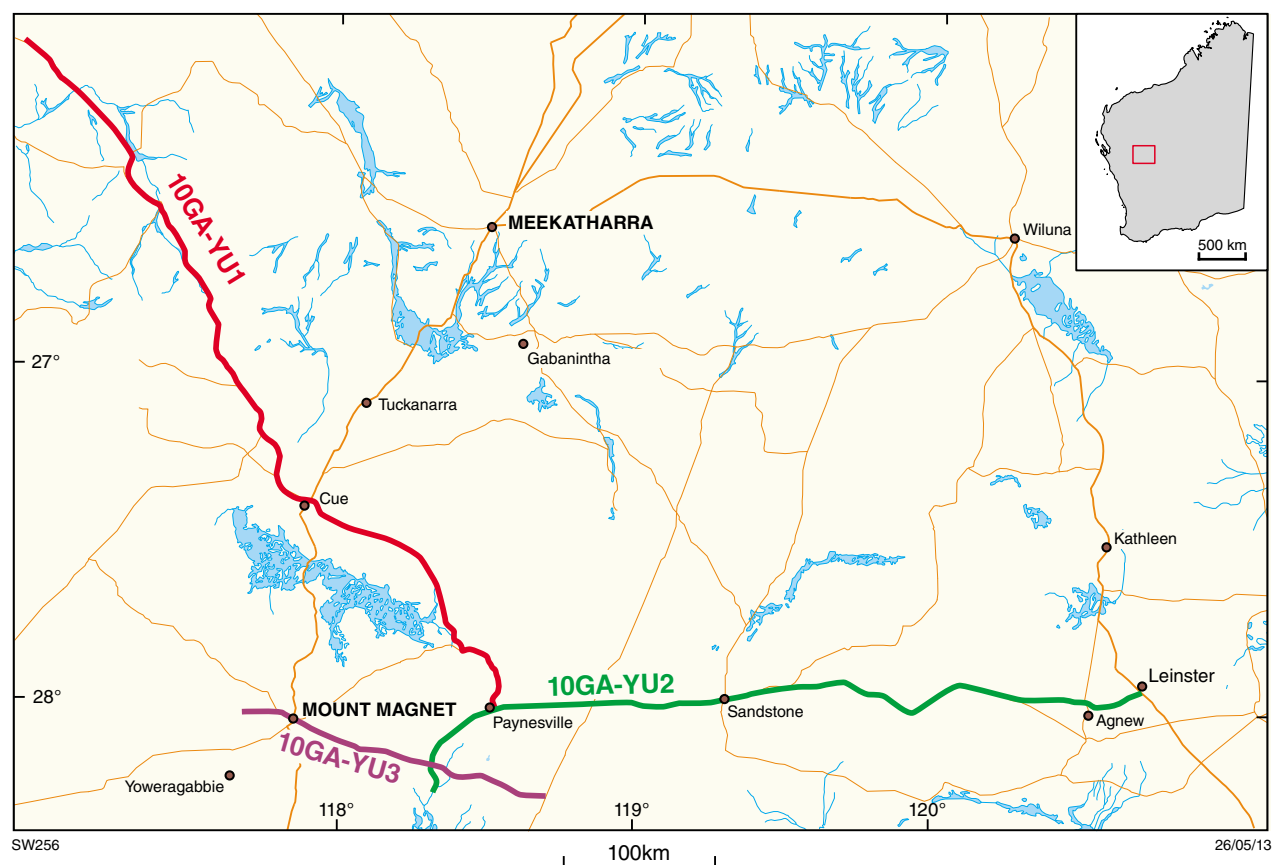


Figure 1. Youanmi Seismic Survey line locations

Table 1. Acquisition Parameters used for the Youanmi Seismic Survey

<i>Lines</i>	10GA-YU1, 10GA-YU2, 10GA-YU3
<i>Source type</i>	3 IVI Hemi-60 vibrators
<i>Source array</i>	15 m pad-to-pad, 15 m moveup
<i>Sweep length</i>	3 x 12 s and 2 x 12 s
<i>Sweep frequency</i>	6-64 Hz, 12-96 Hz, 8-72 Hz and 6-64 Hz, 8-84 Hz
<i>Vibration Point (VP) interval</i>	80 m and 40 m
<i>Receiver group</i>	12 geophones @ 3.3 m spacing
<i>Group interval</i>	40 m
<i>Number of recorded channels</i>	300
<i>Fold (nominal)</i>	75 and 150
<i>Record length</i>	20 s @ 2 ms

Table 2. Seismic reflection processing sequence for the Youanmi lines

Crooked line geometry definition (CDP interval 20 m)
SEG-D to SEG-Y to Disco format conversion, resample to 4 ms
Quality control displays
Inner trace edits
Common midpoint sort
Gain recovery (spherical divergence)
Spectral equalization over 6 to 90 Hz (1000 ms AGC gate)
Application of floating datum residual refraction statics
Velocity analysis
Application of automatic residual statics
Normal moveout correction with stretch mute
Band pass filter
Velocity analysis
Offset regularisation and dip moveout (DMO) correction
Common midpoint stack
Kirchhoff time–space migration
Signal coherency enhancement (digistack 0.6 and fkpwr)
Application of mean datum statics, datum 450 m (AHD), replacement velocity 6000 m/s
Trace amplitude scaling for display

interval and a maximum offset between the CDP location and the calculated source–receiver midpoints. Each trace (source–receiver pair) is allocated to the CDP bin that contains its midpoints. The CDP bins were defined to be 20 metres along the line, and 900, 1800, and 1500 m wide across the line for lines YU1, YU2, and YU3, respectively. The effect of the bin size and midpoint scatter within the bin is most critical at shallow depths. Also, where the line has sharp bends, there is likely to be smearing and poor resolution of shallow data. The effect of bends on deeper data can also be significant, depending on the relative directions of the seismic line and the dip of the structures to be imaged. The CDP lines were processed as if they were straight, ignoring the effects of changing azimuth along the lines. This simplification of the processing to a 2D geometry right at the start of the processing sequence is reasonable for large sections of the lines which are relatively straight; however, it is not possible to correctly migrate, and therefore correctly image, reflectors at significant bends in the lines.

Refraction statics

Variations in surface elevation, weathering layer depth, and weathering layer velocity can produce significant time delays in land seismic data. Variations over a short distance relative to the spread length can degrade the quality of the stack data, as the reflections do not align across the traces to be stacked. Variations over distances longer than a spread length will not significantly affect the stack quality, but can introduce spurious long wavelength structure on the reflections.

Static corrections are applied in the processing stream in order to remove these effects. Static corrections for the Youanmi reflection seismic processing were calculated based on picking first-break refracted arrivals from shot records and creating near surface refractor models of the weathering layer. The refraction statics were applied in two stages using a floating datum. An intermediate step of automatic residual statics produced fine tuning of the corrections. The final statics were calculated relative to a datum of 450 m (Australian Height Datum, AHD) using a replacement velocity of 6000 m/s.

The process of picking first breaks for each shot is time consuming. Although automatic methods of picking the first breaks are used, each set of first breaks needs to be checked and commonly requires editing. Also, the quality of the first break wavelets depends on the nature of the geology at both the source and the receiver arrays. In some parts of the line, a significant proportion of the first-break picks were discarded owing to poor signal-to-noise ratio of the first breaks. The number of picks for each shot contributing to the model may need to vary along the line and the number of layers modelled has to be selected. Once the first breaks for the line have been picked and edited and the number of layers to be modelled is selected, the refractor model can be calculated. The refractor depths and velocities used to calculate the statics are obtained by weighted least squares equations and the conjugate gradient method based on the method of Taner et al. (1988, 1989). Usually, a one-layer or two-layer model can provide a suitable solution to the modelling of the weathering. For the Youanmi lines, single layer models were selected as best representing the weathering over each transect.

Spectral equalization

Spectral equalization is a process used to sharpen the reflection wavelet and suppress low frequency energy, primarily ground roll energy, which is surface wave energy that is generated by the vibrators. The basic processing flow is described in Yilmaz (2001). The frequency spectrum of the data is flattened over a specified frequency range and within a specified time gate. The high-energy, low-frequency surface wave noise is thereby reduced relative to the higher frequency energy of the reflections. The resulting data have better resolution, particularly in the shallow (0–2 s) section. The selection of appropriate frequency range and time gate is based on selective testing and spectral analysis of the data.

Normal moveout correction

Normal moveout (NMO) correction removes time variations across CDP gathers by adjusting for the time delays caused by increasing offset between source and receivers across the gather. The NMO correction is applied as a stacking velocity, which best aligns the reflections in the CDP gather. Velocity analysis requires interactive selection of optimal stack responses and is one of the most time-consuming processes in the processing sequence. Picking velocities at intervals along the lines results in a velocity field varying in time and space (along the line), which maximizes the stack response of the data. Velocity analysis is usually made initially on Spectral Equalized CDP gathers, then after automatic residual statics, and then also after dip moveout. Analyses can also be iterated where required, and areas of complex geology or poor stacking quality may require more closely spaced velocity analyses. The velocity boxes annotated on the seismic sections are the final velocities picked from the dip moveout gathers with all corrections except the mean refraction statics applied. That is, the annotated velocities are the final stacking velocities which were calculated and applied prior to moving the data to its final datum.

Dip moveout correction

Dip moveout (DMO) correction, also known as partial prestack migration, adjusts the NMO correction for the increase in stacking velocity as structural dip increases, and has the effect of correcting the NMO to account for different dips along the line. The process effectively moves reflection energy between traces within and between CDP gathers based on apparent dip of the reflectors, and creates a new set of DMO-corrected CDP gathers. After DMO, intersecting dipping and flat reflections will correctly stack with the same stacking velocity. DMO is a very computer intensive processing step. A time-domain Kirchhoff summation operator method was used based on the work of Deregowski and Rocca (1981).

Common midpoint stack

Common midpoint stack is simply the summing of traces in a CDP gather to produce a single trace at the CDP

location. The traces in the gather are aligned by the NMO and DMO processes to sum optimally. Stacking the data improves the signal to random noise ratio of the data by \sqrt{n} , where n is the number of traces summed (the fold). A nominal fold of 75 and 150 resulted from the different acquisition geometries used for the Youanmi survey.

Post-stack time migration

Migration is the final processing step and moves dipping reflections to their most likely lateral positions. Reflections that appear as dipping on the stacked section will be moved up dip and shortened after migration. Diffraction hyperbolas resulting from discontinuities, such as terminations of reflectors at faults, and which are visible on the stacked section, should collapse to a small region after migration. However, areas of poor signal to noise ratio and sharp bends in the line can produce artefacts in the data, which will not migrate successfully. If there are significant reflections coming from out of plane (i.e. 3D effects), then there will also be areas that cannot be migrated successfully using 2D algorithms. This was certainly the case for parts of the Youanmi survey, which showed apparent 3D structure.

The main parameters to be selected when performing migration are the velocity field and dip ranges to process. The velocity field used is usually a percentage of the stacking velocity. Tests are run on different percentages and the optimum migration velocity selected. The final migrated time section should have dipping reflections in the correct spatial location. A migration velocity field of 90 to 95 percent of the stacking velocities was applied to the Youanmi data. The Kirchhoff time–space migration algorithm used to process the Youanmi data is a numerical approximation of the Kirchhoff integral, as derived in Stolt and Benson (1986), and described in Yilmaz (2001).

The effect of migration on the stacked data is illustrated in Figure 2, which shows stacked and migrated images of part of line 10GA-YU1. The image of the migrated section shows how the migration process collapses diffraction energy and moves dipping reflections to the correct location. It also highlights the 3D nature of the rocks, as the 2D migration process has not removed all crosscutting reflection events. Coherency filters were applied to the data to enhance reflections for the final display images. A full 20 second image of line 10GA-YU1 is shown in Figure 3.

Conclusions

Deep seismic reflection data of 75 and 150 fold, totalling 694 line km, were acquired along existing roads and tracks across the northeast Yilgarn Craton in May and June 2010. The Youanmi seismic data provide images of the full depth of the crust and the upper mantle through this region. The processed data provide valuable information on the nature of the major crustal blocks in this area, and is of a quality that meets the scientific objectives of the project.

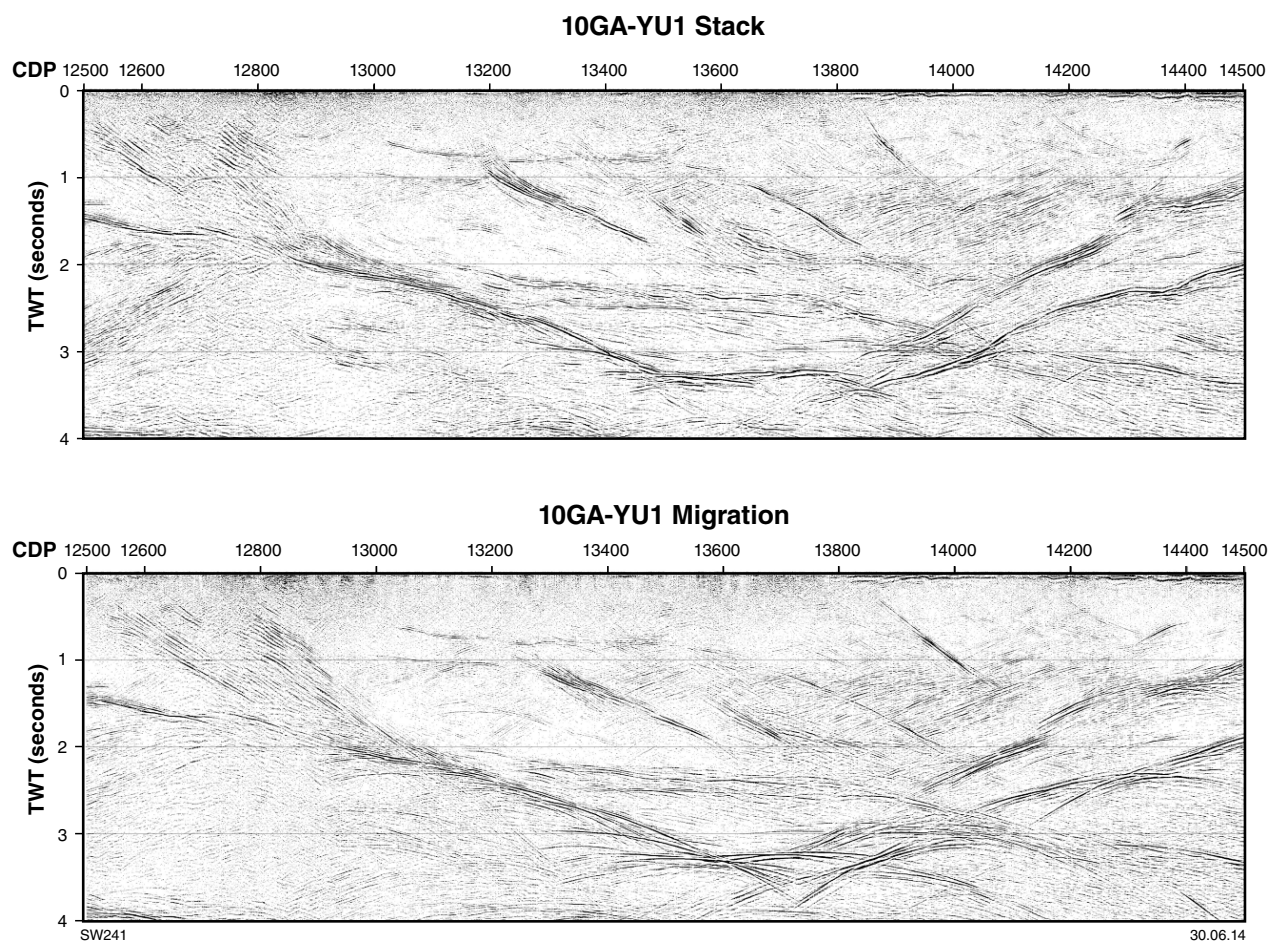


Figure 2. Fragment of the stacked (top) and migrated (bottom) section of line 10GA-YU1

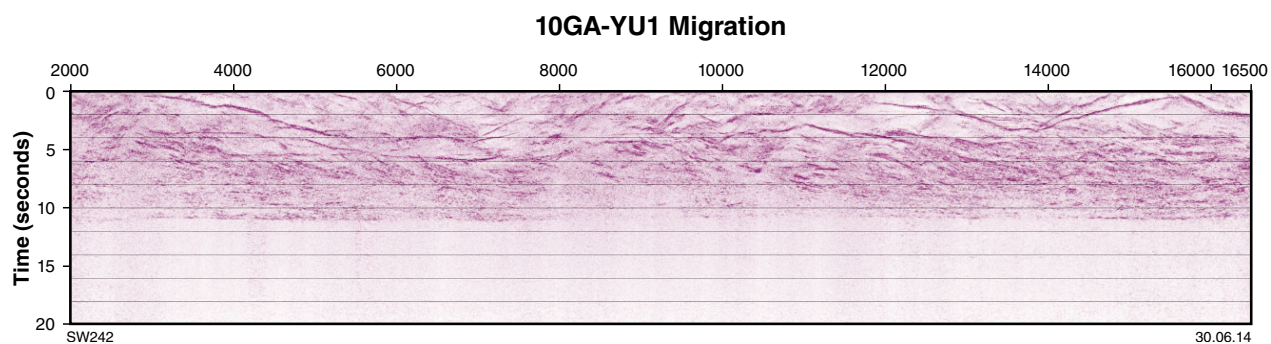


Figure 3. Final migrated section for entire line 10GA-YU1

Acknowledgements

Land access was organized by Geoff Price and Ross Hill, and field data QC was done by Tanya Fomin and Aki Nakamura. Ross Costelloe and Leonie Jones processed the data, and the results were published with the permission of the Chief Executive Officer, Geoscience Australia.

References

- Deregowski, SM and Rocca, F 1981, Geometrical optics and wave theory of constant offset sections in layered media: *Geophysical Prospecting*, v. 29, p. 372–406.
- Milligan, PR, Duan, J, Fomin, T, Nakamura, A and Jones, T 2013, The Youanmi magnetotelluric (MT) transects, *in* Youanmi and Southern Carnarvon seismic and magnetotelluric (MT) workshop 2013 *compiled by* S Wyche, TJ Ivanic and I Zibra: Geological Survey of Western Australia, Record 2013/6, p. 13–25.
- Stolt, RH and Benson, AK 1986, *Seismic migration: theory and practice*: Geophysical Press Ltd, London, UK, 382p.
- Taner, MT, Lu, L and Baysal, E 1988. Unified method for 2-D and 3-D refraction statics with first break picking by supervised learning, *in* Extended abstracts, 58th Annual International Meeting, Society of Exploration Geophysicists, p. 772–774.
- Taner, MT, Wagner, DE, Baysal, E and Lu, L 1989. A unified method for 2-D and 3-D refraction statics: *Geophysics*, v. 63, p. 260–274.
- Yilmaz, O 2001, *Seismic data analysis: processing, inversion, and interpretation of seismic data* (2nd edition): Society of Exploration Geophysicists, Tulsa, Oklahoma, USA, 2027p.

Southern Carnarvon seismic survey 2011: acquisition and processing

by

RD Costelloe¹

Introduction

Geoscience Australia, together with the Geological Survey of Western Australia, under the ongoing National Geoscience Agreement, conducted the Southern Carnarvon Deep Crustal Seismic Reflection Survey in May 2011. Funding for this project was through Geoscience Australia's Onshore Energy Security Program.

The aim of the survey was to image the architecture of the boundary of the Narryer Terrane of the Yilgarn Craton, from its northern juxtaposition against the Gascoyne Province, to the Gascoyne platform of the southern Carnarvon Basin to the west, including the Byro Sub-basin and the Woodleigh impact structure in the Southern Carnarvon Basin.

The survey consisted of one 259.3 km long east–west line, 11GA-SC1, as shown in Figure 1.

Seismic acquisition

Geoscience Australia contracted Terrex Seismic to collect the seismic data. Acquisition commenced on the eastern end of the line near Milly Milly station on the Ballyhunna–Byro Road on 8 May 2011. The acquisition crew progressed westward along the Byro–Woodleigh Road and finished at the North West Coastal Highway on 23 May 2011.

The seismic source was an array of 3 Hemi-50 vibrators, with the geophones in 12 element arrays over 40 m. The spread of 300 active channels was 11 960 m in length, with the vibrators at the centre of the active spread. Acquisition parameters are shown in Table 1. As the survey was conducted along public roads, the seismic crew was supported by a subcontracted traffic control crew who managed road speed signage and third-party traffic around the crew operations.

The western area of the line had experienced significant rain prior to the start of the survey; however, permission was given for the survey to proceed along the roads prior to planned restoration work on the roads. Access along most of the roads was good, and only in one location was the road significantly flooded. At this location, stations 5106 to 5120, an access track on higher ground was available to detour the vehicles. The cables and geophones were laid through a section of scrub which was only accessible by foot, and the vibrators made up for the inaccessible section of the line by shooting an extra four Vibration Points (VPs) on both sides of the detour.

Seismic reflection processing

The data were processed by Velseis Processing Pty Ltd in Brisbane, Queensland (Velseis), and final images and digital data were created at Geoscience Australia. Testing of the data processing sequence was undertaken by Velseis under the supervision of Geoscience Australia.

The data processing parameters were tested on a subset of the data between Common Depth Point (CDP) 6300 and 8000, and from 0 s to 3 s two-way time (TWT), over a section of the Byro Sub-basin of the Southern Carnarvon Basin. The selected parameters were then applied to the whole line. The processing sequence used by Velseis is shown in Table 2, which includes the final data imaging steps performed at Geoscience Australia.

Following is a summary of significant processing steps applied to the data.

Crooked line geometry definition

The first step in processing the seismic data was to define the geometry of the field acquisition, determining source–receiver midpoints and offsets. A CDP line was defined with CDP bins of nominally 20 m width along the line. As the seismic line followed existing roads and tracks, it was not straight, and the CDP line was defined as a line of best fit through the shot–receiver midpoints. Defining the geometry entailed essentially assigning each trace of each shot record to a CDP based on the location of the shot–receiver midpoint for each trace of the record.

¹ Minerals and Natural Hazards Division, Geoscience Australia, GPO Box 378, Canberra ACT 2601

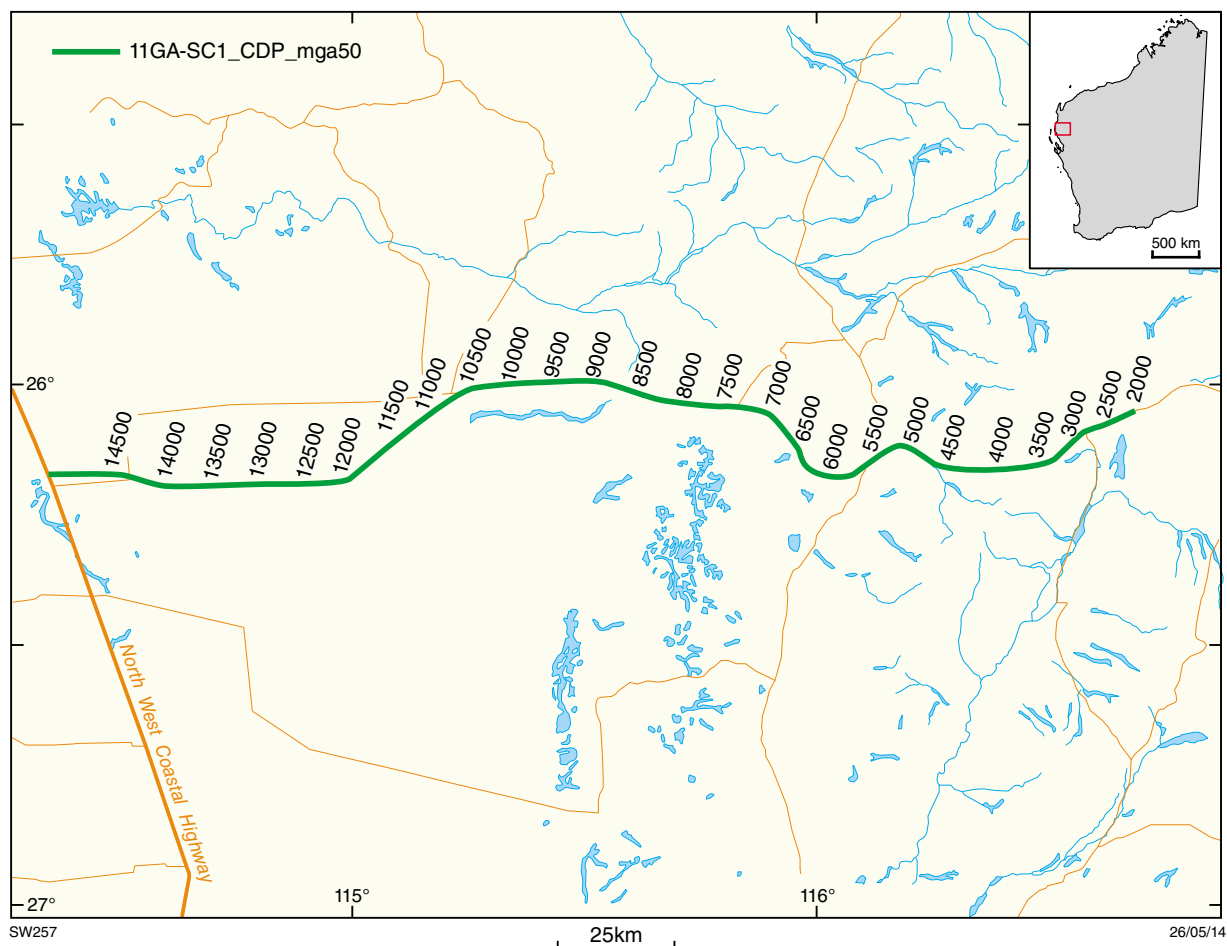


Figure 1. Southern Carnarvon seismic survey line location

Table 1. Acquisition parameters used for the Southern Carnarvon seismic survey

Lines	11GA-SC1
Source type	3 IVI Hemi-50 vibrators
Source array	15 m pad-to-pad, 15 m moveup
Sweep length	3 x 12 s
Sweep frequency	6-64 Hz, 12-96 Hz, 8-72 Hz
Vibration Point (VP) interval	80 m
Receiver group	12 geophones @ 3.3 m spacing
Group interval	40 m
Number of recorded channels	300
Fold (nominal)	75
Record length	20 s @ 2 ms

Velseis binned the data using a method which resulted in unequal CDP bin locations. On tight bends of the line the CDP bins were smaller than the nominal 20 m. Note that, if the stacked or migrated traces are plotted at even trace spacing, the horizontal scale will vary along the line.

Processing the crooked line using a straight line 2D assumption can result in areas where the reflections are poorly imaged, owing to changing azimuth of the line with respect to subsurface structural dip and inherent 3D structures. The processed section does not show significant artefacts of this kind, indicating that the subsurface structures do not exhibit three-dimensionality and that the traverse does not have bends at areas of significant subsurface dip.

Refraction statics

Variations in surface elevation, weathering layer depth and weathering layer velocity can produce significant time delays in land seismic data. Variations over a short distance relative to the spread length can degrade the quality of the stack data, as the reflections do not align across the traces to be stacked. Variations over distances longer than a spread length will not significantly affect the stack quality, but can introduce spurious long wavelength structure on the stacked reflections.

Static corrections were applied in the processing stream in order to remove these effects. For the Southern Carnarvon reflection seismic processing, statics were calculated

Table 2. Seismic reflection processing sequence for the Southern Carnarvon seismic survey

<i>Processing by Velseis</i>
<ul style="list-style-type: none"> • SEG-D to Promax format • Geometry • Resample to 4 ms, zero-phase anti-alias filter • TFD noise attenuation <ul style="list-style-type: none"> (1st pass 0-120 Hz, 7 trace 400 ms window, 100-900 ms application) (2nd pass 0-120 Hz, 7 trace 1000 ms window, 800-20000 ms application) • Gain recovery – TV^2 gain to 4000 ms, 9dB/s gain to 2500 ms • Shot FK - Cut 0-4000 m/s • TFD noise attenuation <ul style="list-style-type: none"> (1st pass 0-15 Hz, 16 trace 400 ms window, 100-2000 ms application) (2nd pass 0-10 Hz, 16 trace 400 ms window, 100-20000 ms application) • Airblast Filter <ul style="list-style-type: none"> TFD noise attenuation (40-120 Hz, 16 trace 400 ms window, 800-2000 ms application) • Trace edits • Gap Deconvolution • Floating Datum refraction and elevation statics (datum 200m, Replacement Velocity 5900 m/s) • Velocity analysis @ 2 km • Automatic Residual statics • Velocity analysis @ 2 km with 1 km infill as required • Automatic residual statics • AGC scaling (500 ms gate) • CRS processing • DMO – Common offset Kirchhoff DMO • Velocity analysis @ 1 km • NMO • NMO Stretch Mute • AGC Scaling (500 ms gate) • Stack • Shift to final datum • Kirchhoff Migration
<i>Processing applied at Geoscience Australia</i>
<ul style="list-style-type: none"> • Signal coherency enhancement • Trace amplitude scaling for display

based on picking first-break refracted arrivals from shot records and creating a near surface refractor model of the weathering layer. The refraction statics were applied in two stages using a floating datum. An intermediate step of automatic residual statics was used to produce fine tuning of the corrections. The final statics were calculated relative to a datum of 200 m (Australian Height Datum, AHD) using a replacement velocity of 5900 ms⁻¹.

Offsets of useful first-break picks were limited to between 200 m and 1000 m to produce picks that were consistent on the same refractor, and this provided a suitable solution to the modelling of the weathering. For seismic line 11GA-SC1, a single layer model was selected as best representing the weathering over the line.

Noise attenuation

One of the main aims of reflection seismic processing is to enhance the reflection signal and attenuate noise in the data. A number of noise attenuation processes were applied to the data, including Time-Frequency Domain (TFD) filtering, shot Frequency-Wavenumber (F-K) filtering, airblast filtering, and bandpass filtering.

The significant noise types apparent on the seismic data include: airblast, which is high-frequency, low-velocity noise originating at the vibrators and travelling across the receiver spread through the air (essentially audible noise); ground roll, which is dispersive low-frequency energy generated by the vibrators and travelling along the surface

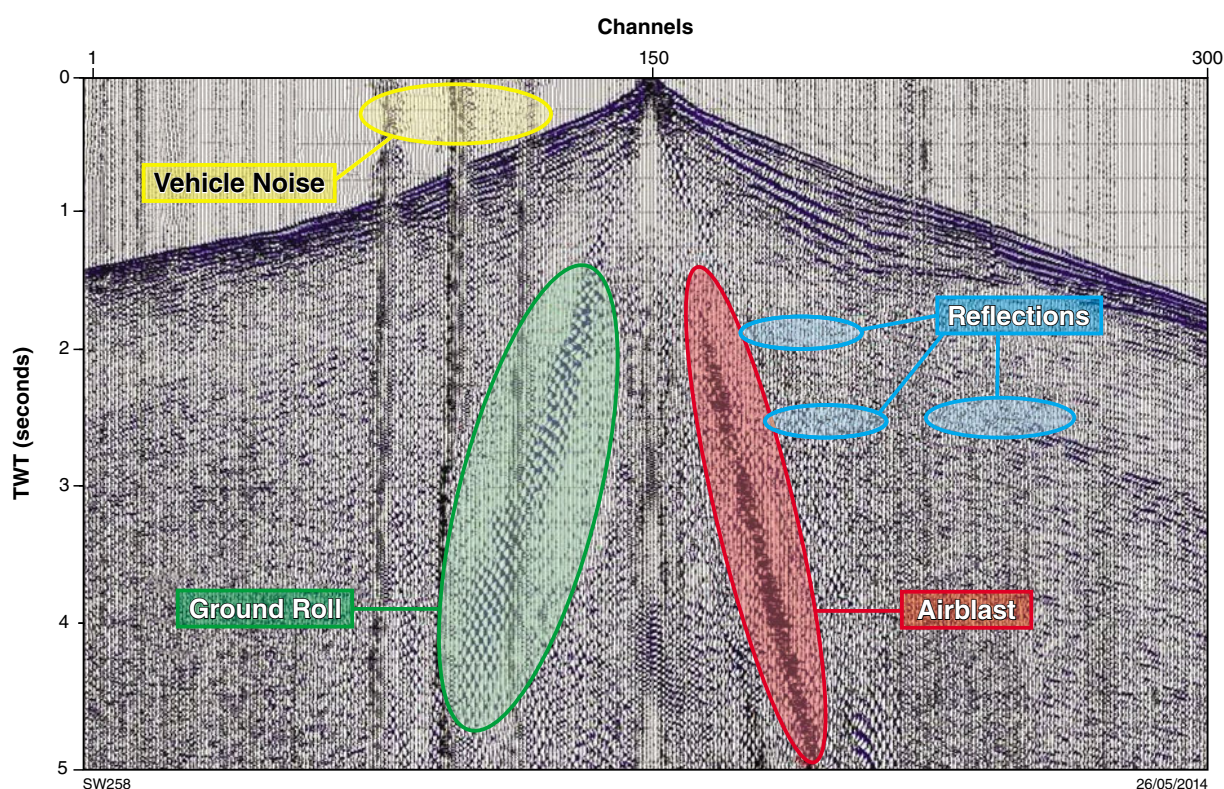


Figure 2. Shot record at VP 3258.5

of the earth and is also known as Rayleigh wave energy; and headwave energy, which travels along the interface between the near-surface low-velocity layers and the high-velocity sub-weathering layer, and shows up on the shot records as the linear first arrival energy (Sheriff and Geldart, 1995). The first-break headwave (or refraction) energy is classed as noise for the purpose of processing the reflection seismic section, although the first-break picks are used in calculating the refraction statics. Wind noise caused by vegetation moving in the wind and generating ground motion can affect the data, and vehicle noise as the line crew drive along the line is often present. Figure 2 shows the first five seconds of a relatively clean record showing some of the noise types that are targeted by the data processing sequence.

TFD filtering was applied at three times in the processing sequence to reduce, respectively, noisy receiver stations, remnant aliased low-frequency ground roll, and high-frequency random noise. The airblast filter targeted the high-frequency airblast noise. The F-K filter was designed to attenuate ground roll and headwave linear noise, both of which could be separated from the reflection signal by their apparent velocity on shot records. Stacking also reduces non-coherent noise including vehicle and wind noise, which is not correlated within or between shots.

Common Reflector Surface (CRS) Processing

CRS processing was applied which rebinned the traces into pre-stack gathers prior to Dip Moveout (DMO) analysis.

Normal moveout correction

Normal moveout (NMO) correction removes time variations across CDP gathers by adjusting for the time delays caused by increasing offset between source and receivers across the gather. The NMO correction is applied as a stacking velocity, which best aligns the reflections in the CDP gather. Velocity analysis requires interactive selection of optimal stack responses and is one of the most time-consuming processes in the processing sequence. The velocity boxes annotated on the seismic sections are the final velocities picked from the dip moveout gathers with all corrections except the mean refraction statics applied; i.e. the annotated velocities are the final stacking velocities which were calculated and applied prior to moving the data to their final datum.

Dip moveout correction

Dip moveout (DMO) correction, also known as partial prestack migration, adjusts the NMO correction for the increase in stacking velocity as structural dip increases, and has the effect of correcting the NMO to account for different dips along the line. The process effectively moves reflection energy between traces within and between CDP gathers based on apparent dip of the reflectors, and creates a new set of DMO-corrected CDP gathers. After DMO, intersecting dipping and flat reflections will correctly stack with the same stacking velocity. DMO is a very computer intensive processing step. A time-domain Kirchhoff summation operator method was used based on the work of Deregowski and Rocca (1981).

Common midpoint stack

Common midpoint stack is simply the summing of traces in a CDP gather to produce a single trace at the CDP location. The traces in the gather are aligned by the NMO and DMO processes to sum optimally. Stacking reduces non-coherent noise, including vehicle and wind noise, which is not correlated within or between shots, and improves the signal to random noise ratio of the data by \sqrt{n} , where n is the number of traces summed (the fold).

A nominal fold of 75 resulted from the acquisition geometry used for the Southern Carnarvon survey.

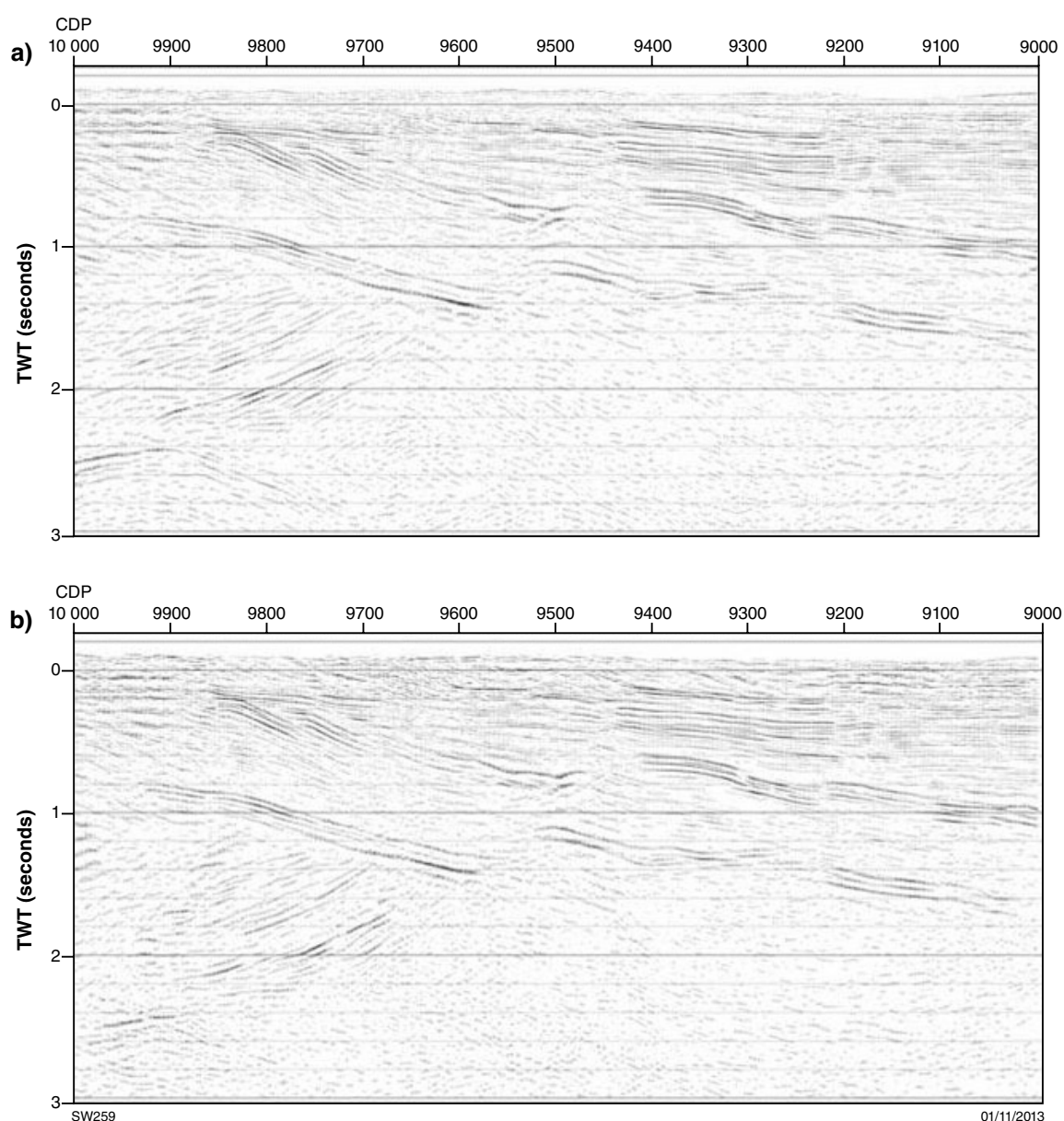


Figure 3. Segment of the stacked (top) and migrated (bottom) section of line 11GA-SC1

Post-stack time migration

Migration is the final processing step and moves dipping reflections to their most likely lateral positions. Reflections that appear as dipping on the stacked section will be moved up dip and shortened after migration. Diffraction hyperbolas resulting from discontinuities, such as terminations of reflectors at faults, and which are visible on the stacked section, should collapse to a small region after migration. The Kirchhoff time–space migration algorithm used to process the Southern Carnarvon data is a numerical approximation of the Kirchhoff integral, as derived in Stolt and Benson (1986), and described in Yilmaz (2001).

The effect of migration on the stacked data is illustrated in Figure 3, which shows stacked and migrated images of part of line 11GA-SC1. The image of the migrated section shows how the migration process collapses diffraction energy and moves dipping reflections to the correct location. Coherency filters were applied to the data to enhance reflections for the final display images.

Conclusions

Deep seismic reflection data of 75 fold, totalling 259 line km, were acquired along existing roads and tracks from the Narryer Terrane of the Yilgarn Craton across to the Gascoyne platform of the Southern Carnarvon Basin in May 2011. The seismic data provide images of the full depth of the crust and the upper mantle through this region. The processed data provide valuable information on the nature of the major crustal blocks and of the structure of the Byro Sub-basin of the Southern Carnarvon Basin.

Acknowledgements

Land access was organized by Emilio Extremera and Jenny Maher, and field data QC was done by Ross Costelloe. Velseis Processing Pty Ltd processed the data, with final imaging produced by Ross Costelloe at Geoscience Australia. Ross Costelloe publishes with the permission of the Chief Executive Officer, Geoscience Australia.

References

- Deregowski, SM and Rocca, F 1981, Geometrical optics and wave theory of constant offset sections in layered media: *Geophysical Prospecting*, v. 29, p. 372–406.
- Sheriff, RE and Geldart, LP 1995, *Exploration seismology*: Cambridge University Press, Cambridge, UK, 628p.
- Stolt, RH and Benson, AK 1986, *Seismic migration: theory and practice*: Geophysical Press Ltd, London, UK, 382p.
- Yilmaz, O 2001, *Seismic data analysis: processing, inversion, and interpretation of seismic data* (2nd edition): Society of Exploration Geophysicists, Tulsa, Oklahoma, USA, 2027p.

The Youanmi magnetotelluric (MT) transects

by

PR Milligan¹, J Duan¹, T Fomin¹, A Nakamura¹, and T Jones¹

Introduction

During the period May to August 2010 magnetotelluric (MT) data were acquired along a total of 690 km of the Youanmi deep seismic reflection traverses 10GA-YU1, 10GA-YU2, and 10GA-YU3 in Western Australia. This was a collaborative project under a National Geoscience Agreement between Geoscience Australia (GA) and the Geological Survey of Western Australia (GSWA). Funding was through the Australian Government's Onshore Energy Security Program (OESP) and the Western Australian Government's Royalties for Regions Exploration Incentive Scheme (EIS).

The aim of the MT survey was to produce information about the electrical conductivity structure of the crust and upper mantle to complement information obtained from deep seismic reflection, gravity, magnetic, and geological data. Together, these data provide new knowledge of the crustal architecture, rock properties, and geodynamics of the region, which is important for helping to determine the potential for both mineral and energy resources.

The MT method uses natural time variations of the geomagnetic field over a range of frequencies to provide electrical conductivity information at varying depths within the Earth by measurement of induced electric currents and magnetic fields. The depth of source signal penetration depends upon the frequency of the signal and also upon the electrical conductivity of Earth itself. Lower frequencies penetrate deeper within the Earth, and more electrically resistive regions also provide deeper penetration of the signal (Chave and Jones, 2012).

Note that both the terms electrical conductivity and resistivity will be used in places; one is the inverse of the other.

MT field measurements and processing

MT measurements were made at field sites by recording two orthogonal horizontal components of the geomagnetic field and the electric field. The horizontal magnetic field variations are the source signal, while the electric components are the induced Earth signal. Vertical magnetic field variations were also measured and are considered to be an induced component.

For the Youanmi survey, two sets of instruments were deployed; broadband measurements were made at sites spaced 5 km apart, whereas long-period measurements were made at sites spaced 15 km apart. Broadband instruments, consisting of induction-coil magnetometers, are used for higher frequency (nearer-surface) measurements, while fluxgate magnetometers, which measure three orthogonal components, are used for lower frequency measurements (deeper penetration). Both deployments used non-polarizing copper/copper sulphate electrodes for measurements of the electric field, and timing of the recorded time series was synchronized by use of GPS clocks. AuScope equipment, based at The University of Adelaide, was used for the survey under ANSIR (National Research Facility in the Earth Sciences) agreement. Figures 1 and 2 show the site locations for long-period and broadband measurements, respectively.

Raw MT data acquired at each field site consist of measurements of time series of the various components of the magnetic and electric fields. Such data are best analysed in the frequency domain, and this processing was undertaken by using the Bounded Influence Remote Reference Processing (BIRRP) robust algorithm of Chave et al. (1987) and Chave and Thomson (2004), and incorporating remote referencing with data from other sites wherever possible. Robust remote reference processing removes outliers and uncorrelated noise from the time series to provide power spectral estimates of the transfer functions between the electric and magnetic fields for each MT site. The spectral estimates were combined into complex frequency-dependent elements of the MT impedance tensor. The impedance values and other fundamental quantities were stored in a standard Electrical Data Interchange (EDI) file. Detailed specifications of the Youanmi MT survey are available in Milligan (2012).

¹ Minerals and Natural Hazards Division, Geoscience Australia, GPO Box 378, Canberra ACT 2601

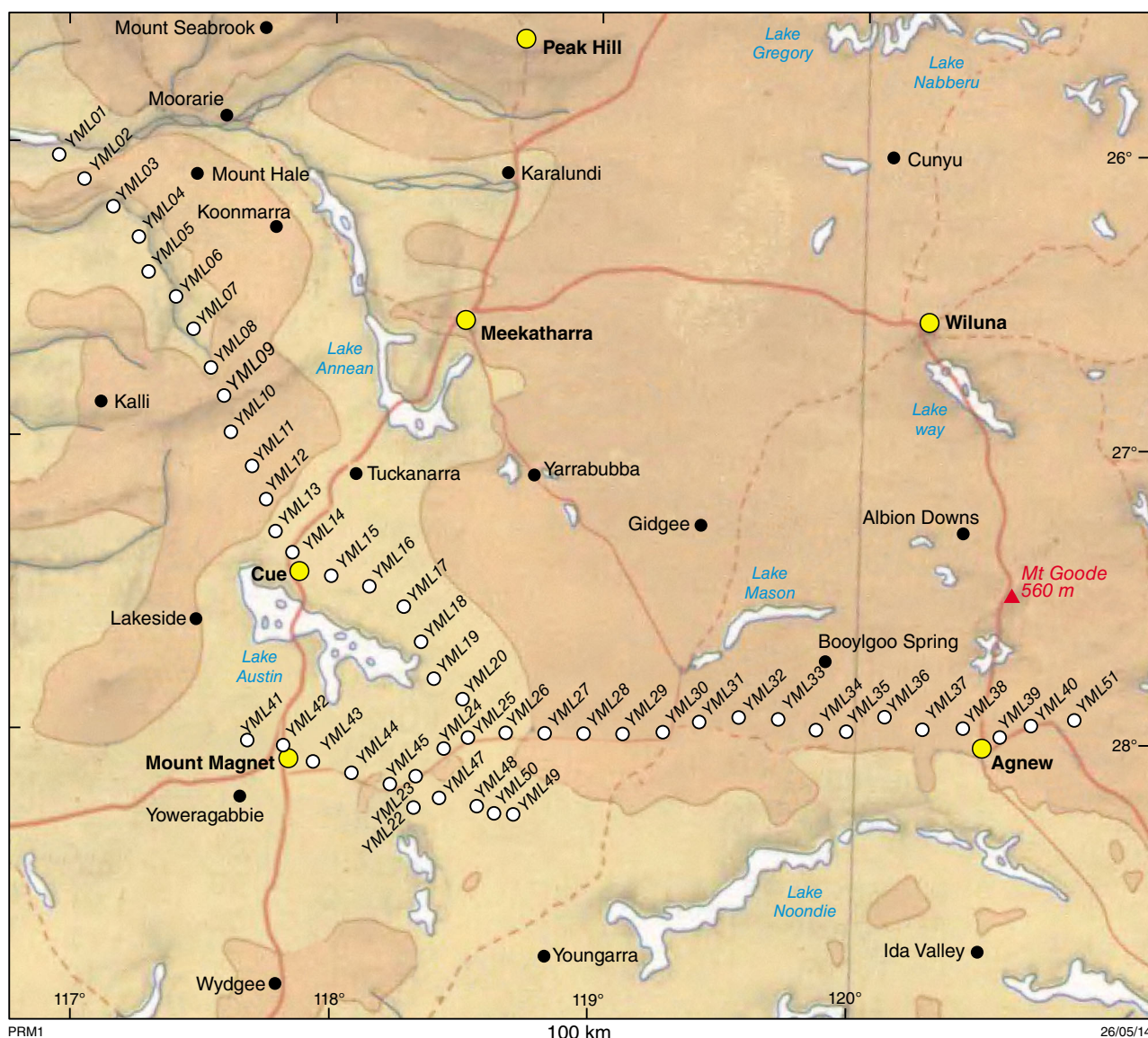


Figure 1. Long-period MT sites, spaced 15 km apart

MT data display and analysis

Magnetotelluric data are commonly displayed in a variety of ways, including graphical and pseudo-section plots and images of apparent resistivity and phase, induction arrow plots of vertical-field transfer-functions, and phase ellipse plots coloured by various parameters of distortion and dimensionality. Only the last two are presented here, for reasons outlined below.

These kinds of displays provide an insight into the variation of the data along profile and with depth, but usually an assumption of one- or two-dimensionality is involved. The data need to be rotated into a common strike direction for a particular profile, determined either from analysis of the data itself, or from assumptions of a geological strike determined from other data.

Induction arrows — often called Parkinson Vectors after Parkinson (1959) — relate changes in the vertical

magnetic field to changes in the horizontal fields as a function of frequency, and point by convention to lateral regions of higher conductivity. The length of the arrow is a function both of the strength of the currents that give rise to the vertical field variations and of the distance of the measuring site from the induced currents. The transfer functions that define the arrows are complex functions of frequency; thus, two arrows are defined, an in-phase arrow and a quadrature-phase arrow. Only the in-phase (real) arrows will be further mentioned here. Responses from shallow sources that are essentially one-dimensional (1D) have arrows that are very small, in which case the direction becomes meaningless. Arrows of significant length and consistency along profile provide an indication of the regional electric strike direction, which will be orthogonal to the direction of the arrow. If the directions vary significantly along profile for each frequency or multiple frequencies, this indicates that the electrical structure is not two-dimensional (2D).

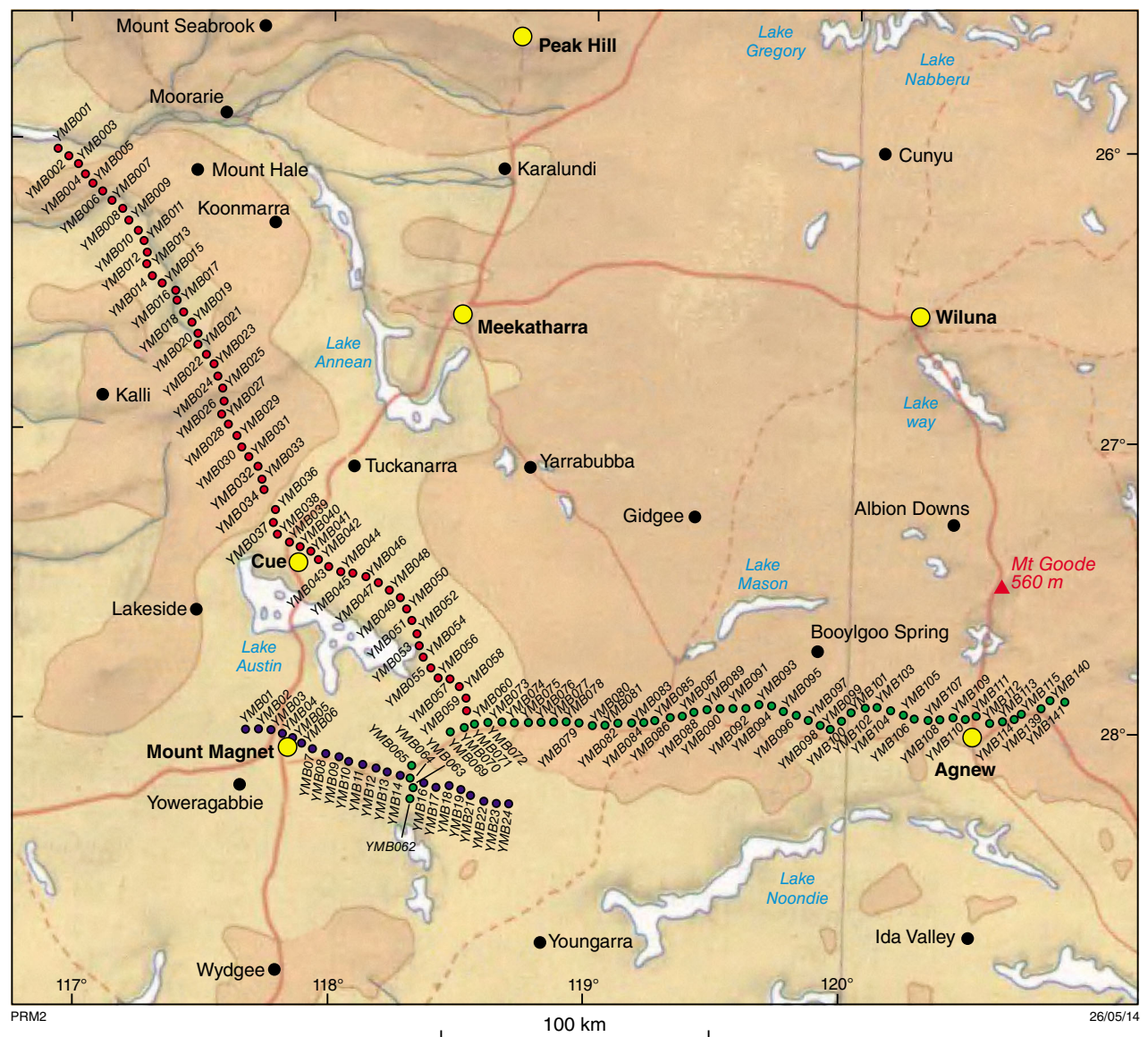


Figure 2. Broadband MT sites, spaced 5 km apart

Figure 3 shows induction arrows for three periods for all the long-period sites. The longest period arrows (black) show a consistency in direction to the west, although the length decreases to the east along the YU2 profile. Shorter period arrows display a consistent clockwise change in direction; the directions of arrows along line YU1 are predominantly to the north-west, while for line YU2 this direction changes to the north-east and then east.

Phase tensor MT analysis (Caldwell et al., 2004) is useful in helping to determine both strike and dimensionality of MT data independently of distortion effects such as static shift. No assumption is made about the underlying conductivity structure in calculation of the phase tensor, which is depicted graphically as an ellipse.

Figure 4a shows long-period phase ellipses and Figure 4b shows broadband phase ellipses for YU1 sites, coloured to indicate those periods in which the data have small skew values and may be considered 1D or 2D in character. If

the data are 1D or 2D, then circles represent 1D data, and ellipses represent 2D data. In the 2D case, the electric strike direction is either parallel to the major axis of the ellipse, or the minor axis. This 90° ambiguity in strike direction cannot be resolved from the phase information alone.

As can be observed by inspection of the ellipses in the figures, the data are not predominantly 1D or 2D in character, but three-dimensional (3D), and a common strike direction for all sites and all periods cannot be successfully determined. This situation also applies to the data from YU2 and YU3 sites.

Inversion modelling and display

Traditional inversion modelling of MT data, such as described here for the Youanmi survey, has used 1D or 2D code. This required the data to be analysed for distortion

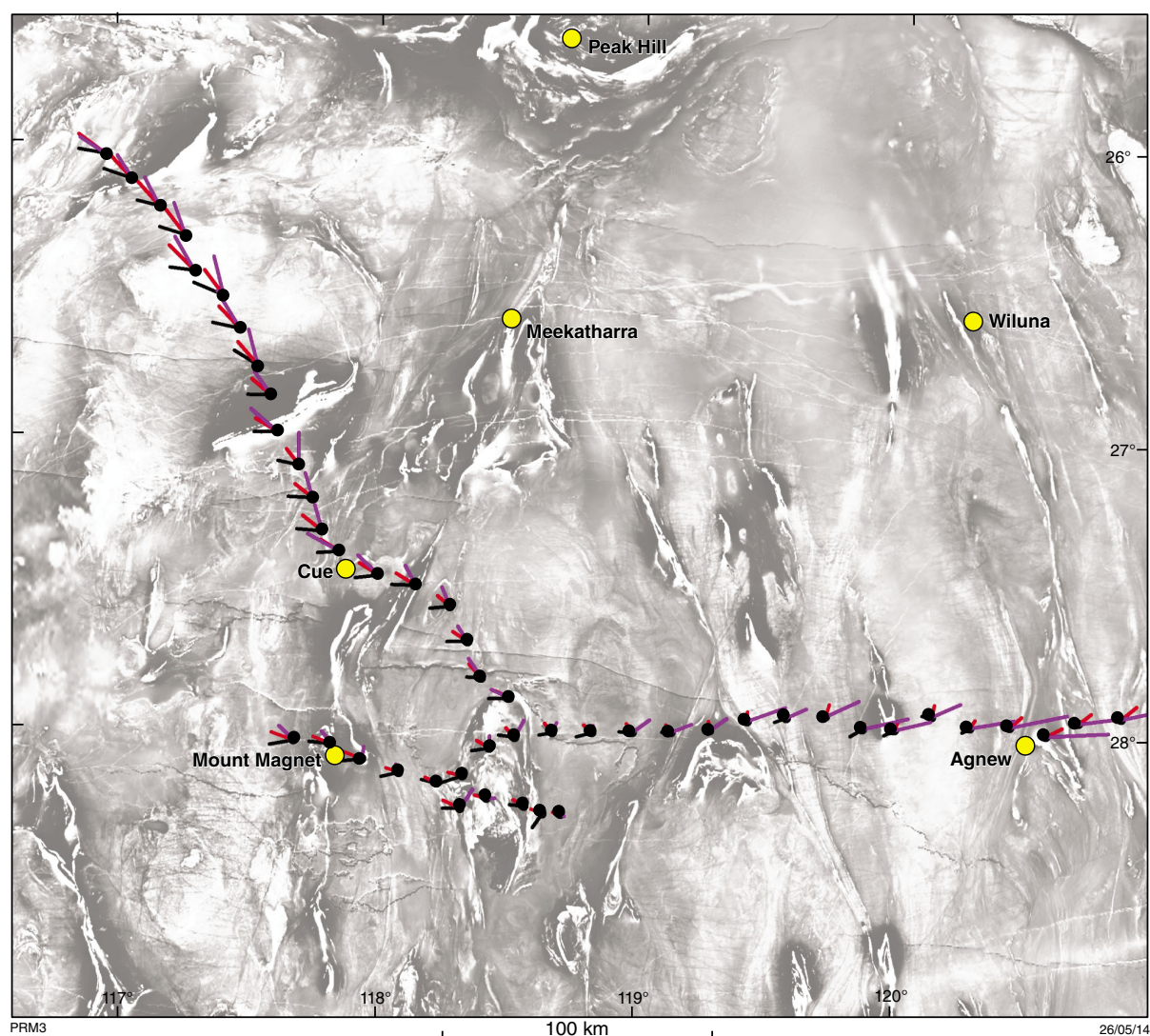


Figure 3. In-phase (real) induction arrows for periods 3276 s (black), 819 s (red) and 68 s (purple). Background image is of total magnetic intensity variably reduced to the pole.

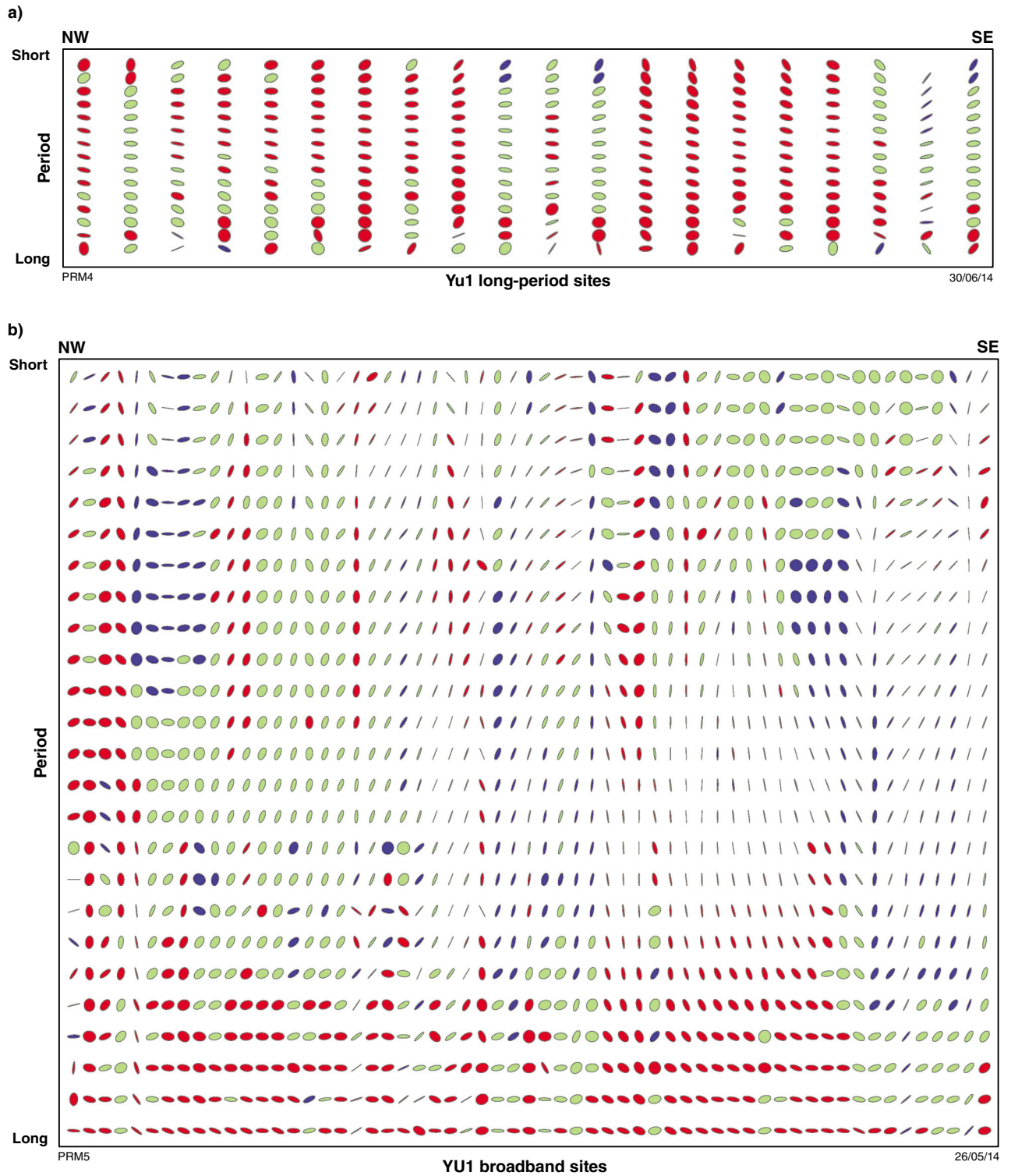
and dimensionality, and either those frequencies that are not 1D or 2D removed prior to modelling, or an attempt made to manipulate the data into 2D form depending upon the type of distortion. Then a constant strike direction must be determined and the data projected onto a linear profile at 90° to the strike direction.

As the information in the previous section shows, the majority of the data acquired for this area cannot be classed as either 1D or 2D, and it is not possible to determine a constant strike direction for any of the three major profiles.

Three-dimensional data require a 3D-modelling approach, even if the data are acquired along profiles (e.g. Patro and Egbert, 2011). This has been undertaken for the Youanmi data using the ModEM code kindly made available to us by Egbert, Kelbert and Meqbel of the College of Atmospheric and Ocean Sciences, Oregon State University (Egbert and Kelbert, 2012).

ModEM has 2D and 3D electromagnetic inversion components written in Fortran 95 and parallelized using MPI controls so that it executes efficiently on large cluster computer systems. GA has compiled the code on the Vayu Sun Constellation Cluster at the National Computational Infrastructure (NCI) Facility <<http://nf.nci.org.au/>>, which has 1492 nodes each containing two quad-core CPUs. To make efficient use of this system, local PC-based software has been written to pre-process the data into the required formats and generate a finite difference model mesh. ModEM is run under the PBS batch system, and output models are manipulated with local software to provide visualizations in either Gocad™ or ArcGIS™ formats.

Three-dimensional meshes used in inversion runs are tailored to the spatial locations of the data so that each MT site is located within its own mesh cell. The input data consist of both broadband and long-period values, with the broadband values culled so that there is no frequency overlap with the long-period values. Conservative error



estimates are applied, and frequencies with significant error outliers are removed. The mesh is well padded with extra cells around the edges to avoid edge effects in the models (Fig. 5).

To conveniently display model data in Gocad or ArcGIS format, values within the model volume are interpolated onto vertical Gocad Sgrid meshes computed at the common depth point (CDP) locations of the seismic profiles. This ensures that the best model information from directly beneath the MT sites is displayed (Fig. 6).

Seismic images and interpretations and magnetic and gravity images (Costelloe and Jones, 2013; Gessner et al., 2013) are also displayed in the Gocad 3D environment, and this enables an exact comparison of the different data types. Figure 7 provides an example of a transparent colour MT image overlying the seismic image along the traverse, and Figure 8 shows the interpretation line work overlaid on the Figure 7 image.

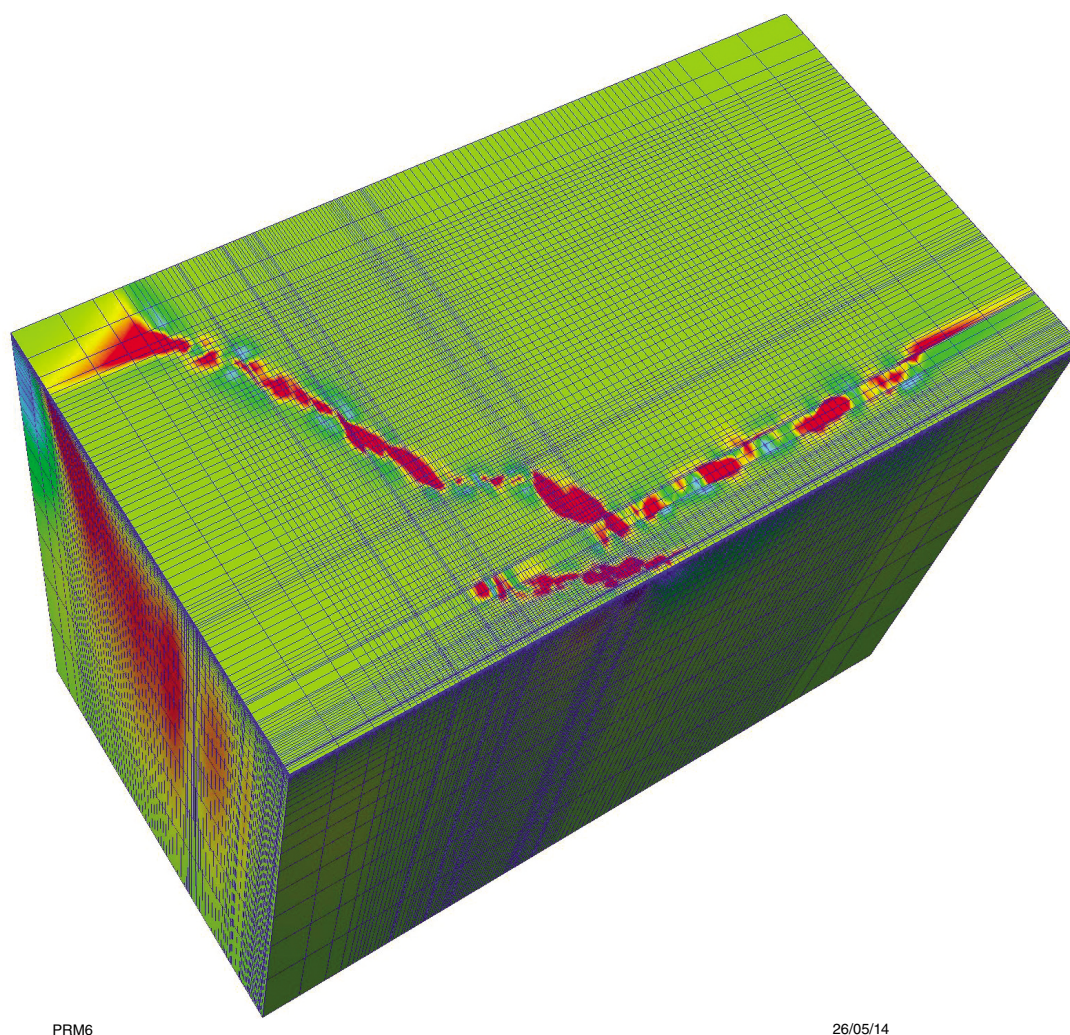
A set of preliminary conductivity images, along with the seismic images and interpretation line work, are displayed in Figures A1 to A6 (see Appendix).

Discussion

The induction arrows previously referred to in Figure 3 show a consistent trend at long periods to the west (from northwest in the far northwest), with diminishing length to the east along the YU2 line. This indicates a regional conductive structure to the west, with lessening influence to the east. This trend is consistent with the arrows determined by Heinson et al. (2011) for the Capricorn MT results to the northwest of the Youanmi survey.

For shorter periods, the arrows are sensitive to shallower conductive structures, and all arrows exhibit a clockwise rotation in direction as the periods become shorter. The shortest period arrows change direction from northwest to northeast and then east at about the location of the Windimurra Complex near the western end of line YU2. There is clearly an influence from conductivity to the east, which becomes more prominent at these short periods than the west or northwesterly influence prominent at the longer periods.

This change in the arrow directions at shorter periods is supported by the conductivity sections shown for line



PRM6

26/05/14

Figure 5. An example 3D finite-difference model mesh

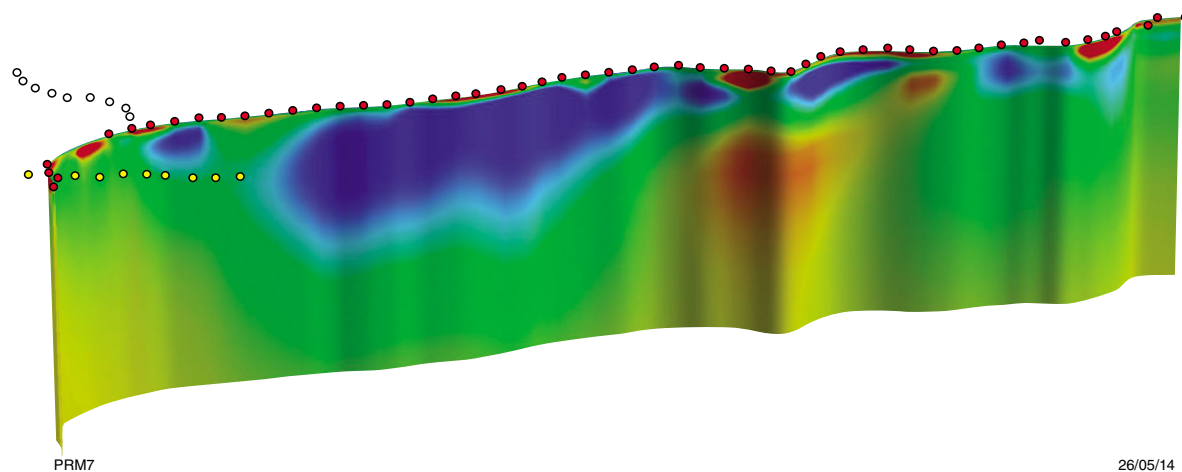


Figure 6. Example conductivity image along line YU2

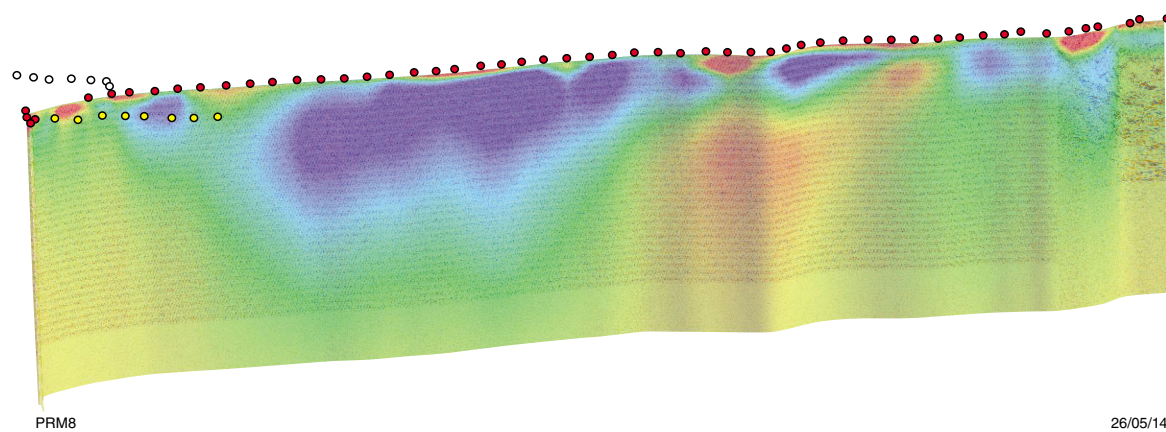


Figure 7. Example conductivity image along line YU2 with transparency to show the underlying seismic image

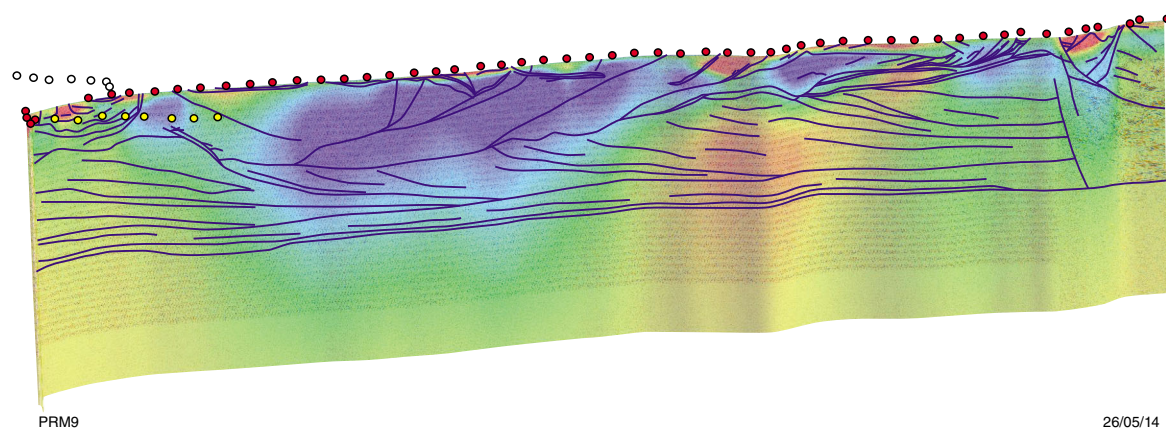


Figure 8. Image of Figure 8 showing seismic interpretation line work

YU2; for example, in Figures A4 and A5. These show that there is a region of low conductivity centred on site YML30 that extends down into the mantle. This may represent the core of the Archean Craton, cold and resistive, and would explain why the arrows point to the more conductive regions to the west and the east.

The reason for the regional direction of long-period arrows to the west or northwest is not clear. They may be influenced to some extent by the coast effect and conductive sediments in basins near the coast (Parkinson, 1979). Alternatively, the crust or upper mantle may generally be more conductive to the west. The deep conductivity structure along line YU1 does indicate a more conductive lower crust and upper mantle at depth, but the measurements along this line may be giving a biased result, as the seismic transect is essentially parallel to the deep geological strike as indicated by the gravity data when upward continued to 20 km (Fig. A7).

The conductivity images of the three lines for regions in the upper to middle crust show features, both conductive and resistive, that correlate well with the interpreted seismic section line work. Each of these lines will be discussed next in detail, and preliminary images are shown in Figures A1 to A6.

Line 10GA-YU1

At the westerly end of line YU1 there is a region of enhanced conductivity from a few kilometres depth down to the middle crust, and this correlates with interpreted banded iron-formations of the Narryer Domain. Other conductive features along this line may be the response of mafic sills, which are abundant. Generally, the upper crustal zone is resistive, but conductive portions of the mafic sills may provide the conductivity anomalies within this generally resistive zone.

There is a particularly resistive zone centred beneath site YMB022 bounded by a triangular arrangement of sills. At the surface beneath site YMB027, a strongly conductive zone dips to the southeast and correlates with a fault-bounded edge of near-surface mafic rocks. A northwesterly dipping mafic sill may also contribute to this zone. Other near-surface occurrences of mafic rocks are closely correlated with high conductivity zones, such as beneath sites YMB033, YMB037, and YMB046. Beneath site YMB055 is a highly conductive zone that extends to about 2 km depth and appears to be associated with granite. Data at this location must be treated with caution as the response is dominated by one site. Southeast beneath sites YMB057 and YMB058 another conductive zone is associated with strongly faulted granite. It is surprising that the mafic and ultramafic rocks at the very southeastern end of the line associated with the Windimurra Igneous Complex do not provide an expression in the MT section.

Line 10GA-YU2

The conductivity features of line YU2 broadly follow the major trends in the seismic interpretation. For the MT data, the upper crustal layers and granite plutons

are generally resistive. The deepening trend of the upper crustal layer to the west corresponds with thickening of the resistive layer until an abrupt change in the depth of the lower crustal layer and thinning of the upper crustal layer in the west, coinciding with the location of the Windimurra Igneous Complex.

As previously mentioned, the resistive layer between YMB077 and YMB094 may represent the heart of the Archean Craton. In the east, the change in conductivity follows well the bottom of the mid-crustal layer (Fig. 8), which contains within, and also its base, mafic sill material. Mafic dykes at site YMB106 are conductive at about 8 km depth. The non-conductive nature of the granites is emphasized at about 10 km depth between sites YMB108 and YMB112. The surface mafic rocks at sites YMB113 and YMB114 have a more conductive expression, and generally east of here the region is more conductive to the Moho.

Line 10GA-YU3

Near-surface zones of the Windimurra Complex towards the eastern end of this line have high conductivity probably associated with the layered mafic upper zone. The resistive nature of the upper crust zone again is shown beneath sites YNB06 to YNB12. To the east and west of this zone the crust generally is more conductive, beneath both the Windimurra Complex and particularly the deeper mafics associated with the Mount Magnet region. MT models indicate there may be a zone of higher conductivity that extends from the mantle to beneath the Windimurra Complex, but this needs to be examined in more detail.

Conclusions

Broadband and long-period MT data have been acquired along the three Youanmi deep seismic reflection transects, and the data have been processed in the frequency domain to produce full complex impedance tensor estimates and magnetic vertical-field transfer functions.

Phase analysis of the impedance tensor estimates shows that the data mostly represent three-dimensional earth conductivity distributions; therefore, one- and two-dimensional modelling is unlikely to be successful. Three-dimensional modelling code, ModEM, has recently been made available to GA, and this has been trialled on the Youanmi data to produce preliminary volumes of conductivity from which the values can be extracted along vertical sections defined from the seismic transect CDP positions.

Conductivity values imaged along the three transects show features that correspond with interpretations of the seismic section images, thus adding confidence to the reliability of the modelling. Induction arrows that change orientation from west to east at shorter periods correspond with a resistive region of the crust along line YU2 which may represent the resistive core of the Archean Craton.

It should be noted that the models presented are preliminary, and that the model space requires further investigation. Inversion modelling with no geological constraints is inherently non-unique, although it is pleasing that first-pass models from the new code provide conductivity sections that relate so well to other independent information.

Data download

The MT impedance tensor data, in EDI format files, can be downloaded from the GA website, which also includes access to the seismic data and images:

<www.ga.gov.au>

Then go to Data/Applications, Free data downloads.

Acknowledgements

This paper forms part of a collaborative project between the Geological Survey of Western Australia and Geoscience Australia. We thank Jenny Maher for project management of the MT acquisition and Geoff Price for help with field acquisition. This paper is published with permission of the Chief Executive Officer, Geoscience Australia.

References

- Caldwell, TG, Bibby, HM and Brown, C 2004, The magnetotelluric phase tensor: *Geophysical Journal International*, v. 158, p. 457–469.
- Chave, AD and Jones, AG (editors) 2012, *The magnetotelluric method: theory and practice*: Cambridge University Press, New York, USA, 552p.
- Chave, AD and Thomson, DJ 2004, Bounded influence magnetotelluric response function estimation: *Geophysical Journal International*, v. 157, no. 3, p. 988–1006.
- Chave, AD, Thomson, DJ and Ander, ME 1987, On the robust estimation of power spectra, coherences, and transfer functions: *Journal of Geophysical Research*, v. 92, no. B1, p. 633–648.
- Costelloe, RD and Jones, LEA 2013, Youanmi seismic survey: 2010 acquisition and processing, *in* Youanmi and Southern Carnarvon seismic and magnetotelluric (MT) workshop 2013 *compiled by* S Wyche, TJ Ivanic and I Zibra: Geological Survey of Western Australia, Record 2013/6, p. 1–6.
- Egbert, GD and Kelbert, A 2012, Computational recipes for electromagnetic inverse problems: *Geophysical Journal International*, v. 189, p. 251–267.
- Heinson, G, Boren, G, Ross, J, Campaña, J, Thiel, S and Selway, K 2011, The Capricorn Orogen magnetotelluric (MT) transect, *in* Capricorn Orogen seismic and magnetotelluric (MT) workshop 2011: extended abstracts *edited by* SP Johnson, AM Thorne and IM Tyler: Geological Survey of Western Australia, Record 2011/25, p. 75–100.
- Gessner, K, Jones, T, Goodwin, JA, Gallardo, LA, Milligan, PR, Brett, J and Murdie, R 2013, Interpretation of magnetic and gravity data across the South Carnarvon Basin, and the Narryer and Youanmi Terranes, *in* Youanmi and Southern Carnarvon seismic and magnetotelluric (MT) workshop 2013 *compiled by* S Wyche, TJ Ivanic and I Zibra: Geological Survey of Western Australia, Record 2013/6, p. 65–77.
- Milligan, PR 2012, Youanmi 2010 magnetotelluric survey: preliminary data release, <www.ga.gov.au>.
- Parkinson, WD 1959, Directions of rapid geomagnetic fluctuations: *Geophysical Journal Royal Astronomical Society*, v. 2, p. 1–14.
- Parkinson, WD 1979, The geomagnetic coast effect: *Reviews of Geophysics and Space Physics*, v. 17, p. 1999–2015.
- Patro, PK and Egbert, GD 2011, Application of 3D inversion to magnetotelluric profile data from the Deccan Volcanic Province of Western India: *Physics of the Earth and Planetary Interiors*, v. 187, p. 33–46.
- Wynne, P and Bacchin, M 2009, *Index of gravity surveys* (2nd edition): Geoscience Australia, Record 2009/7.

Appendix

Preliminary MT section images derived from the 3D inversion modelling compared with seismic images and interpretation line work (Figs A1 to A6) and an image of upward-continued gravity data (Fig. A7). Images in Figures A1, A2, A3, and A6 result from individual image processing of the original log10 conductivity data to enhance the information content.

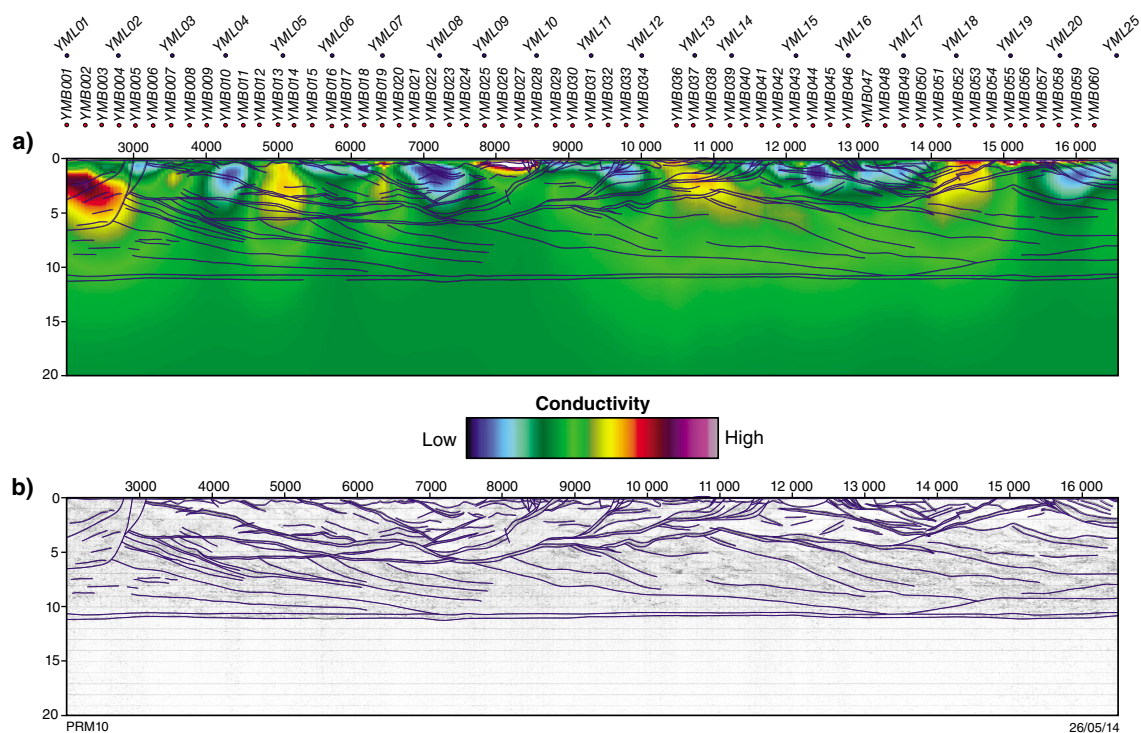


Figure A1. MT inversion model (top) and seismic section (bottom) for line YU1, both overlaid with seismic interpretation line work

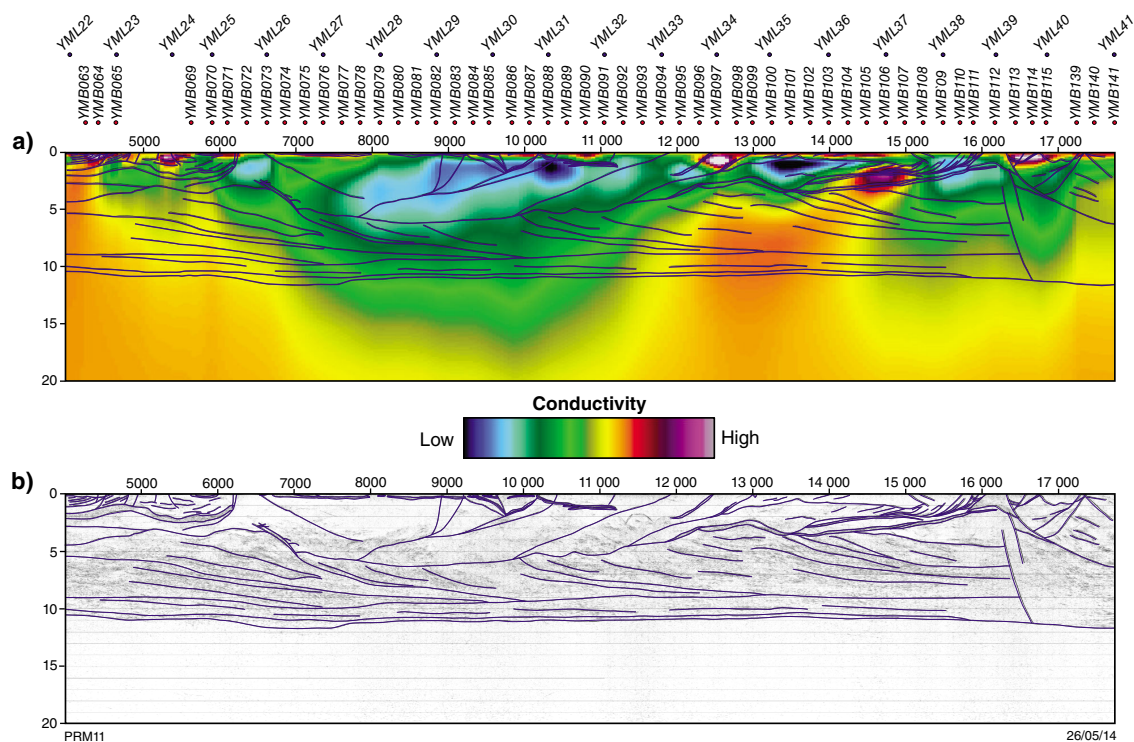


Figure A2. MT inversion model (top) and seismic section (bottom) for line YU2, both overlaid with seismic interpretation line work

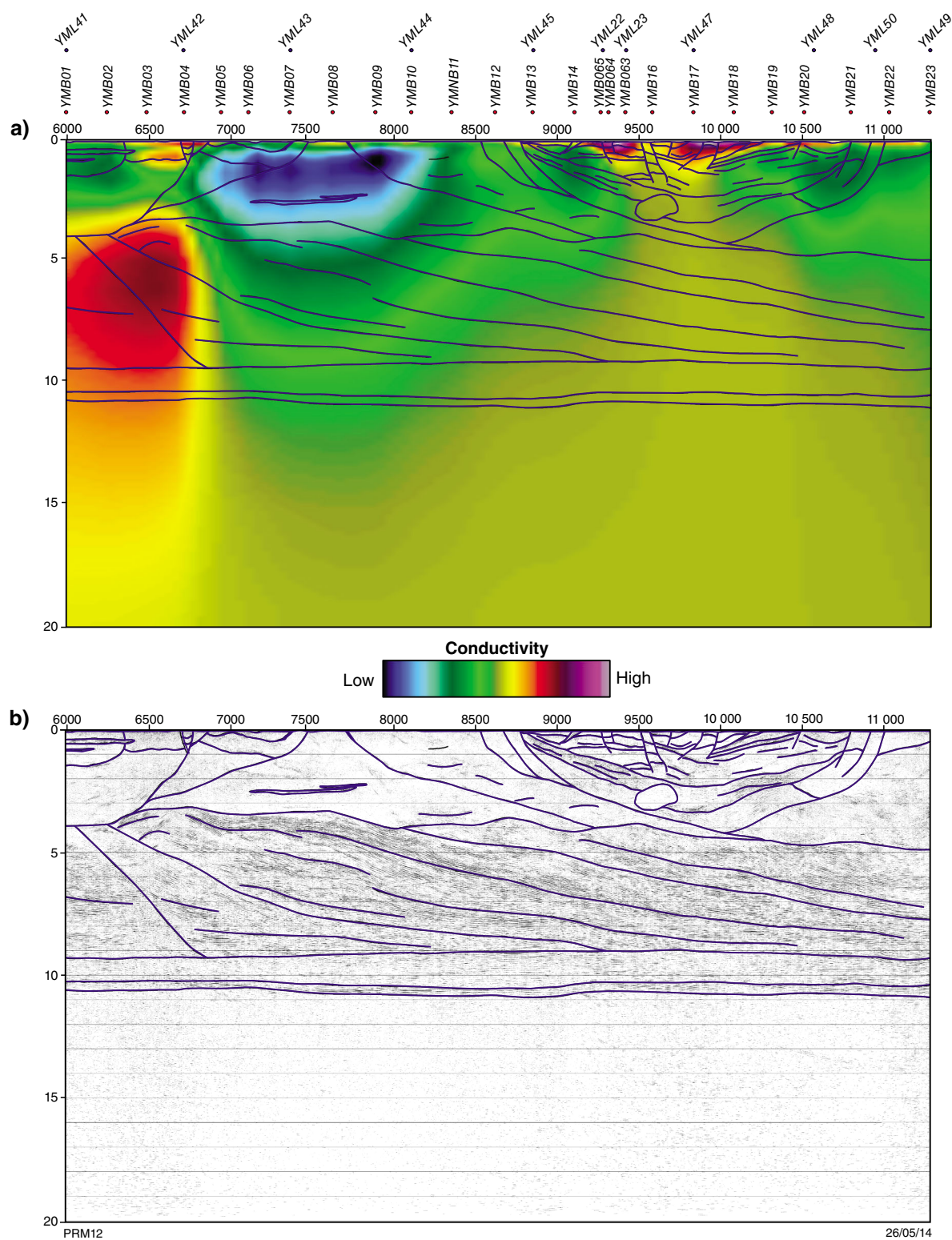


Figure A3. MT inversion model (top) and seismic section (bottom) for line YU3, both overlaid with seismic interpretation line work

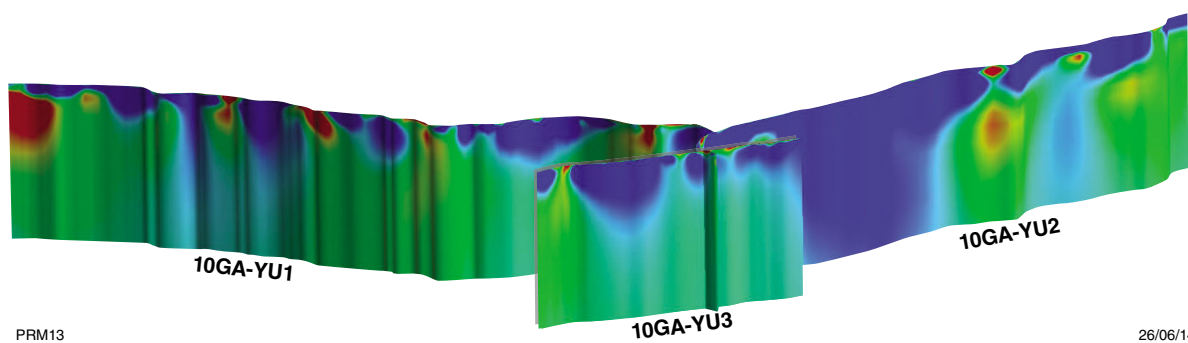


Figure A4. 3D inversion model for all lines interpolated onto vertical sections in Gocad™ using a 'rainbow' colour scale with high conductivity (red) to low conductivity (blue)

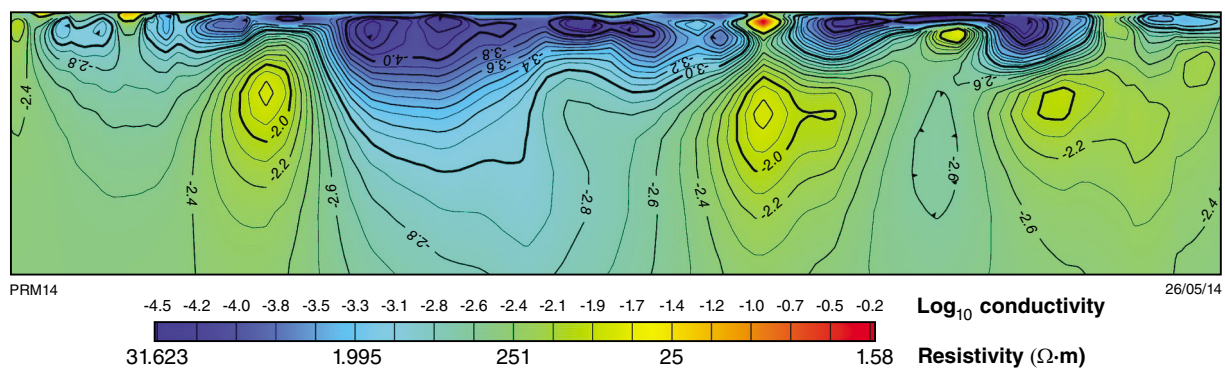


Figure A5. Contoured 3D inversion model for line YU2

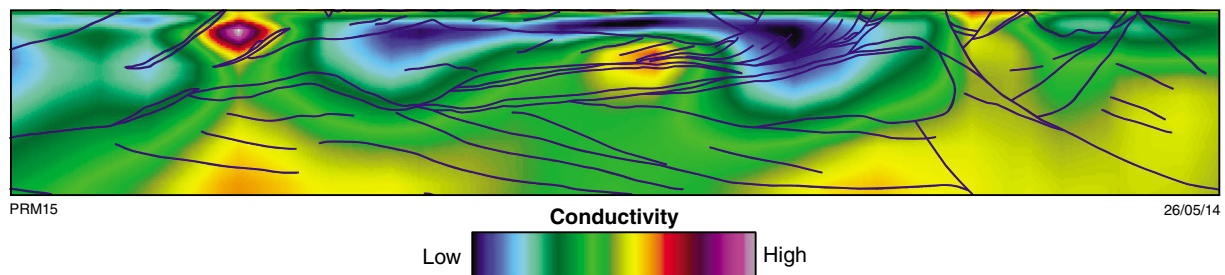


Figure A6. Near-surface section of the eastern end of line YU2, overlaid with seismic interpretation line work

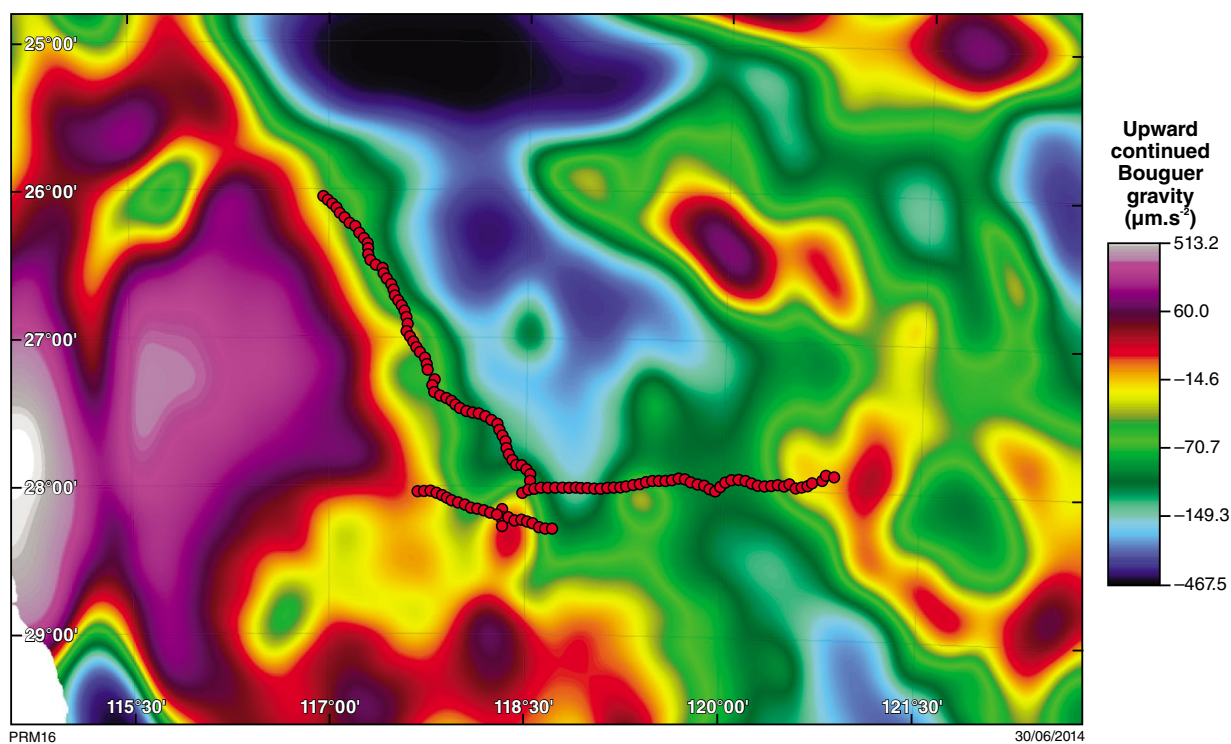


Figure A7. Isostatically corrected Bouguer gravity upward-continued to 20 km (derived from a 400 m grid generated from the Australian National Gravity Database [Wynne and Bacchin, 2009])

The nature of the lithosphere in the vicinity of the Youanmi seismic lines

by

BLN Kennett¹

Introduction

In addition to the recent program of reflection profiling in Western Australia, a range of seismological studies has been made using both artificial and natural sources. Up to the 1980s there was an extensive program of seismic refraction studies, which provided important information on crustal structure. Since 1992, the Australian National University has carried out deployments of portable broadband seismic recorders across Australia. These instruments provide high-fidelity recording of ground motion and record both regional and distant earthquakes. In addition, the national seismic network operated by Geoscience Australia has been augmented in recent years, particularly for tsunami warning. The seismograms from these portable and permanent stations can be analysed to generate information on lithospheric structure beneath the Australian region, both in the crust and uppermost mantle, using a variety of styles of analysis (e.g. Kennett, 2003).

The principal information from regional earthquakes comes from the analysis of the large amplitude surface waves late in the seismograms. These surface waves travel almost horizontally through the lithosphere and, with a sufficient density of crossing paths, can be used in a tomographic inversion to determine 3D structure in the lithospheric mantle. Receiver-based studies at individual stations exploit the conversions and reverberations following the onset of the P-wave energy. From distant earthquakes, information can be extracted about the structure in the crust and uppermost mantle, since the paths arriving at the stations are near vertical.

Additional information has begun to be extracted from the seismic noise field, through the stacked cross-correlation of signals at pairs of stations that provide an approximation to the signal expected for a source at one station recorded at the other location. This ambient noise tomography approach was pioneered in Australia by Saygin (2007) using the continuous data recordings at the portable stations in association with permanent seismic stations to link different experiments. The main signal

comes from high-frequency surface waves, which provide imaging of upper to middle crustal structure, and are particularly sensitive to the presence of sediments (Saygin and Kennett, 2012a,b).

Recently, a major synthesis of the available seismological constraints on lithospheric structure has been carried out to produce the Australian Seismological Reference Model (AuSREM). An overview of the AuSREM model is given in Kennett and Salmon (2012). A detailed description of the crustal component and its construction is presented in Salmon et al. (2012), with a comparable treatment for the mantle component in Kennett et al. (2012). The crustal and mantle components are linked through the Moho model constructed using all available information, including reflection picks (e.g. Kennett et al., 2011; Salmon et al., 2012).

We build on the results from the AuSREM model in this summary of lithospheric properties in the neighbourhood of the Youanmi reflection lines.

Crustal structure

Receiver function studies

A powerful method to extract information on crustal structure is the analysis of the conversions and reverberations immediately following the onset of the P wave for distant earthquakes using the receiver function technique. The two horizontal components of motion are combined to produce records with polarization along (radial) and perpendicular (tangential) to the great circle back to the source. The rotated components are then deconvolved using the vertical component of motion that represents dominantly P waves. In this way, the influence of the source is largely eliminated and attention is focused on wave propagation processes close to the receiver. When there is little energy on the tangential receiver function 3D structural variation is weak, and then an inversion may be made using a radial receiver function for an effective 1D structure in the neighbourhood of the receiver (Shibutani et al., 1996; Sambridge, 1999).

¹ Research School of Earth Sciences, The Australian National University, Canberra ACT 0200, Australia

Alternative approaches use stacking of receiver functions to emphasize features such as the conversion from the crust–mantle boundary, and hence constrain the Moho depth. The moveout pattern of conversions and multiples from different source distances can be used to constrain the depth of seismic boundaries and V_p/V_s ratios (Zhu and Kanamori, 2000). It can also be advantageous to make a partial allowance for the influence of the free surface on the seismograms by a rotation of components in the vertical plane or a transformation (e.g. Reading et al., 2003a).

The first systematic treatments of receiver function results across Australia were made by Clitheroe et al. (2000a,b) with an emphasis on the thickness of the crust and also the base of sediments, and a few of these stations lie in the zone near the Youanmi profile. A particular focus of portable broadband deployments since 2000 has been on Western Australia with a number of deployments that now provide good coverage of the Archean cratons and the Proterozoic Capricorn Orogen. The receiver function studies have provided clear evidence for segmentation of the Yilgarn craton with characteristic crustal structures for the individual terranes (Reading et al., 2003b, 2007, 2012). Stations in the Murchison Domain show a very clear and sharp Moho, which ties well with the reflection results.

AuSREM crustal model

The results from receiver functions provide S wavespeed profiles in the immediate neighbourhood of the seismic stations, together with an estimate of the ratio between P and S wavespeeds. Refraction experiments provide P wavespeed along the line of stations with full crustal penetration only near the midpoints.

From the P/S wavespeed ratio derived from more than 150 receiver functions across the continent we were able to produce a smooth interpolation of the ratio between P and S wavespeeds and used this to convert the S wavespeed distribution of (Saygin and Kennett, 2012b), derived from ambient noise tomography, to an equivalent P wavespeed model. We then combined estimates of the P wavespeed from refraction and receiver function studies with the tomographic results to produce a P wavespeed model for the continent, and offshore where there are refraction experiments.

The resulting model is illustrated in Figure 1 with depth slices at 10 km intervals starting at 5 km depth. The constraints from the ambient noise tomography are rather weak below 25 km, and so there are portions of the model without direct control. We have blanked out those regions that lie further than 200 km from a control point in Figure 1, notably in the Canning Basin at 35 km depth.

At 5 km depth we see the influence of the deep sediments in the Canning Basin, contrasting with the Proterozoic metasediments in the Capricorn Orogen. The transition to the Pinjarra Orogen is evident in slower P wavespeeds along the western coast of Western Australia at 5 km depth, but at greater depth there is very little contrast with the Yilgarn. At 15 and 25 km depth we have only modest velocity variations across the area sampled by the reflection lines, and remain within the crust at 35 km. The thinner crust in the Pilbara is represented by the presence of mantle wavespeeds at 35 km depth, and rather high P wavespeeds are encountered in the southern Yilgarn, which recent reflection work suggests arises within the reflective crust and helps to explain a bimodal distribution of crustal thickness in this area, determined from earlier studies.

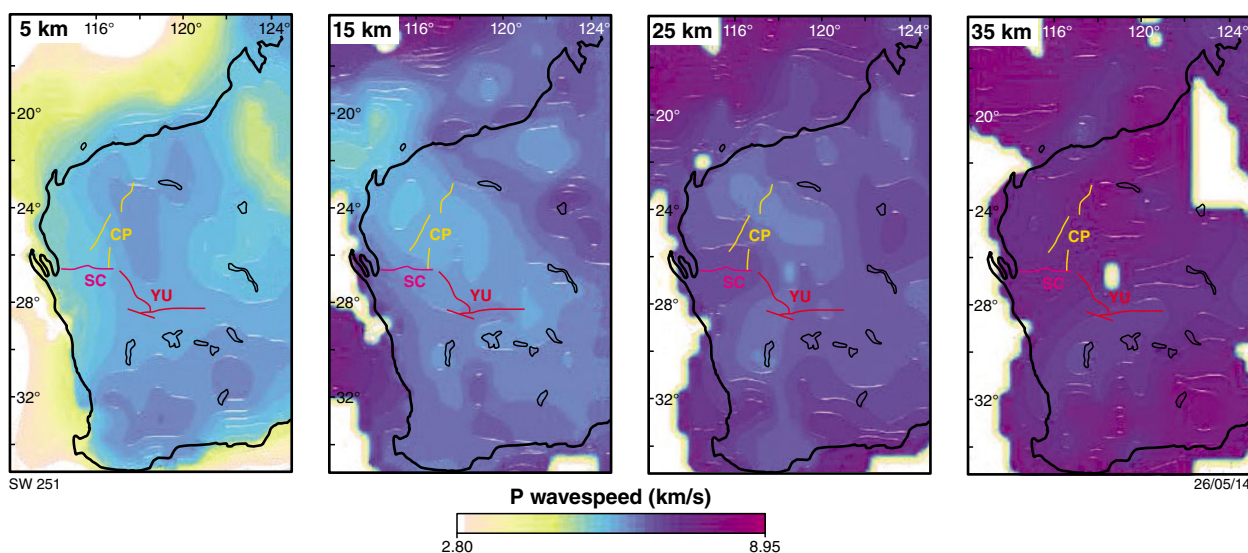


Figure 1. Depth slices through the AuSREM crustal model for P wavespeed for the region around the Youanmi reflection lines. The same wavespeed scale is used for all depths, since mantle speeds are encountered at 15 km offshore. Regions without direct control on wavespeed are blanked out at depth. In each panel the positions of the recent seismic lines are indicated by coloured lines.

Crustal thickness

Kennett et al. (2011) assembled the full suite of available information on the depth to Moho across the continent drawing on results from refraction experiments, receiver functions, and Moho picks from the full suite of crustal reflection profiles across the continent. For refraction or receiver function studies, the crust–mantle boundary is taken at the base of the transition to mantle seismic velocities (P wavespeeds above 7.9 km/s or shear wavespeeds above 4.4 km/s). On the reflection records, the Moho is taken at the base of the set of crustal reflectors and converted to depth using an average crustal velocity of 6 km/s.

The estimates of crustal thickness in the northern Yilgarn, Capricorn Orogen and the Pilbara are summarized in Figure 2. There is a close correspondence in the estimates from the different techniques and station deployments even though the methods of analysis differ significantly. Fortunately most of the portable seismic stations appear to lie in zones without any dramatic steps in the Moho. The profile of crust thickness in the northern Yilgarn from the receiver function studies is very similar to that seen on the reflection profile, and in consequence the receiver function results provide a check on the calibration of the time–depth conversion for the reflection results.

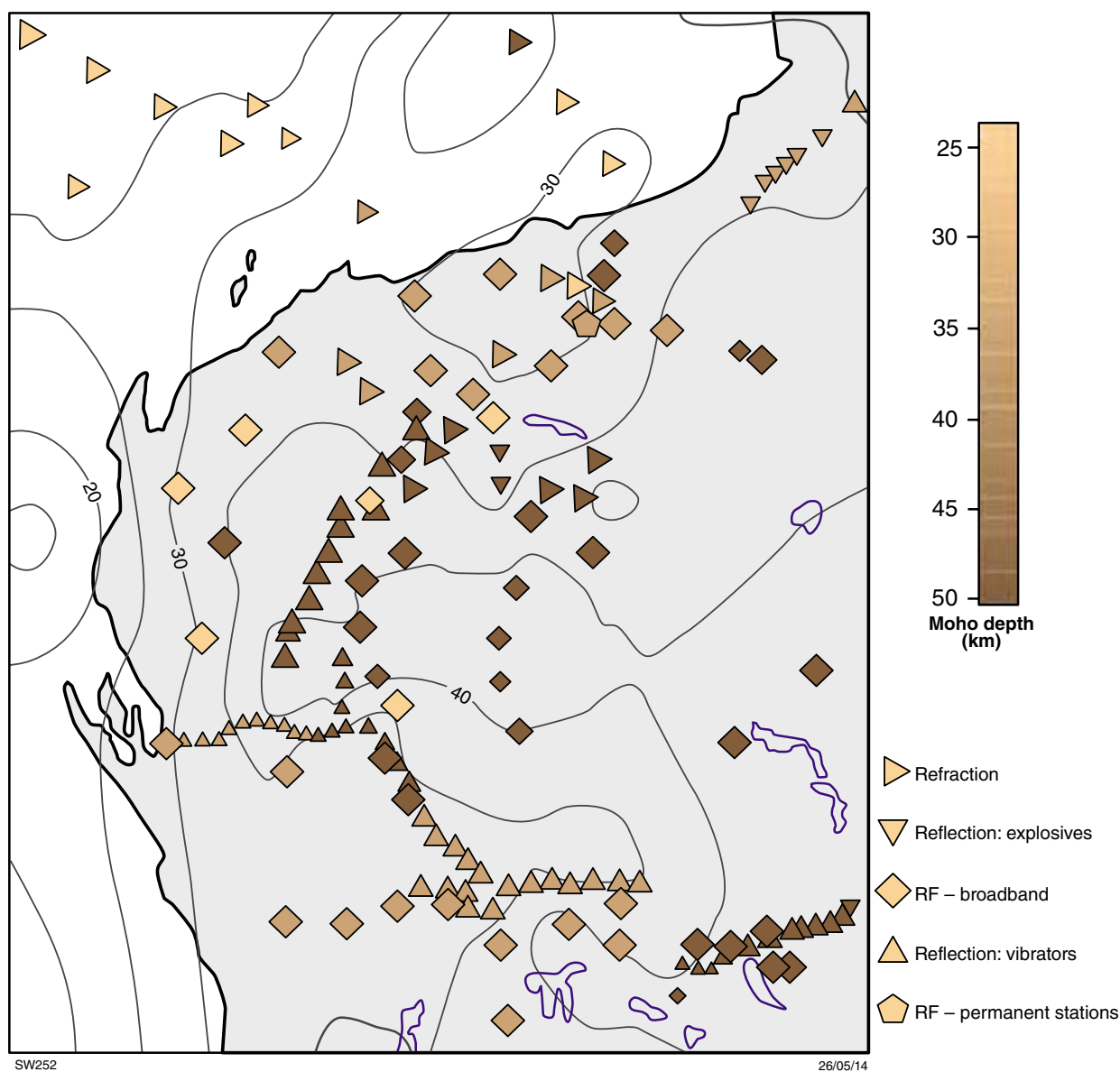


Figure 2. Estimates of crustal thickness derived from refraction experiments (triangles) and receiver function studies (diamonds – broad-band stations, pentagons – short-period stations, less reliable results indicated by smaller symbols). Moho estimates from reflection work are indicated by the dense lines of triangles. The contours of Moho depth are derived from a continent-wide synthesis (Kennett et al., 2011).

The background contour plot of the Moho in Figure 2 is taken from the continent-wide synthesis of results, using all receiver functions and the refraction data from the compilation of Collins et al. (2003), with additional control from reflection experiments (Kennett et al., 2011; Salmon et al., 2012).

Surface wave tomography

The earthquake belts to the north of Australia along the Indonesian arc into New Guinea and to the east in the Tonga–Fiji zone provide frequent seismic events of suitable magnitude to be recorded well in Australia. There are less common events to the south along the mid-oceanic ridge between Australia and Antarctica, but these are important in providing additional directional control. A number of different techniques has been used to analyse the large-amplitude surface waves that arrive late in the seismogram, and 3D models of the seismic shear wavespeed distribution have been extracted from the combinations of results from many paths (Debayle and Kennett, 2000, 2003; Yoshizawa and Kennett, 2004; Kennett et al., 2004a,b; Fishwick et al., 2005, 2008; Fichtner et al., 2009, 2010). Most of the methods rely on some approximations to wave propagation in three dimensions, but the work of Fichtner et al. (2009, 2010) used full seismogram calculations in a 3D model. In consequence, the frequency range used is restricted to prevent excessive computational requirements. Fortunately the results with this sophisticated analysis indicate that the longer wavelength features obtained with the approximate methods are confirmed.

We can now have considerable confidence in the main structures in the lithosphere at a horizontal scale of about 200 km and a vertical resolution around 30 km. Figure 3 illustrates the shear wave structure in western Australia using the AuSREM mantle model developed in a collaboration between the authors of a number of different studies (Yoshizawa and Kennett, 2004; Fichtner

et al., 2010; Fishwick and Rawlinson, 2012). This new model benefits from the incorporation of more paths than in any individual study and includes the use of techniques that provide improved resolution at depth. The variations in seismic S-wave velocity are displayed in terms of the absolute shear wavespeed at each depth, with the neutral colour chosen to represent typical continental values.

Regions with faster S wavespeed than the continental reference are indicated by bluish tones, and zones with slower S wavespeed are shown in tones of brown in Figure 3. Reductions in seismic wavespeed are expected from the influence of temperature or the presence of volatiles. Faster wavespeeds are produced by cooler temperatures, but the very fast wavespeeds seen in Figure 3 are very difficult to produce by temperature alone and suggest the presence of chemical heterogeneity.

The mantle lithosphere deeper than 100 km is marked by distinct fast seismic wavespeeds, but at about 75 km there is an indication of somewhat reduced wavespeeds (Fig. 3a) in the east of Western Australia, that may be linked in part to the presence of thickened crust. This feature is not associated with enhanced seismic attenuation as might be expected if the cause was a concentration of radioactivity in the uppermost mantle.

At 75 km, the Paterson Orogen is marked by very high seismic wavespeeds, and there is also a distinct rather fast patch in the northern Yilgarn. There is no distinctive mantle feature associated with the Capricorn Orogen, though we note that at 225 km the Capicorn and Pilbara regions show somewhat lower shear wavespeeds than in the Yilgarn. The surface wave tomography results are consistent with a situation in which the Capricorn is more strongly coupled to the Pilbara Craton than to the Yilgarn to the south. The Youanmi reflection lines traverse a zone that shows high seismic wavespeeds to at least 225 km depth, placing it among the thickest seismic lithosphere on the Australian continent.

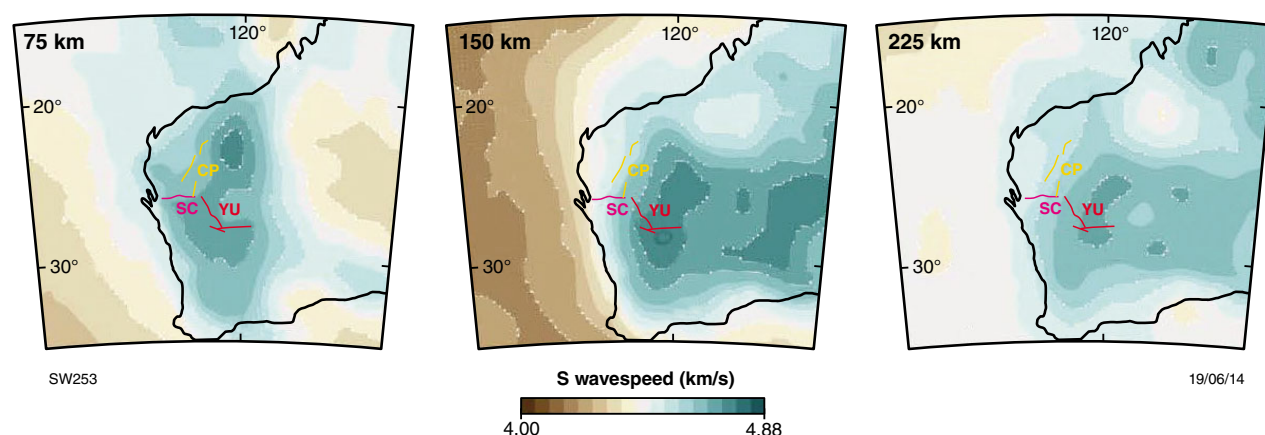


Figure 3. Seismic shear-wavespeed structure in Western Australia from the AuSREM mantle model, largely controlled by surface wave tomography. (a)–(c) Continental-scale measurements of seismic wavespeed variation 75, 150, and 225 km depth, respectively, inferred from the analysis of surface waves. In each panel the position of the recent reflection seismic lines are indicated by coloured lines.

Discussion and conclusions

The AuSREM model for lithospheric structure in the Australian region provides valuable controls on 3D variability that can be helpful in the interpretation of other classes of information, such as reflection seismic profiles. The crustal component of AuSREM builds on information from artificial and natural sources, using refraction experiments, near receiver studies using distant earthquakes, and continent-wide tomography exploiting ambient seismic noise. In the uppermost mantle, surface-wave tomography is the main source of information on 3D S wavespeed variation, with the most reliable results available below 75 km depth. At shallower depths, there is a strong influence from the crustal structure along the various paths and crustal structure can be mapped into the uppermost mantle, especially where the crust is thick.

The crust in the northern Yilgarn shows only moderate variability in seismic wavespeed superimposed on a mild gradient in depth in a crust of rather similar thickness (around 40 km). This means that the time sections from the seismic reflection processing can be interpreted almost directly as depth sections along the profiles. However, there will be influences from off-line structures in the complex 3D configuration of reflectors that cannot be fully taken into account in line-oriented processing.

The results for the area around the Youanmi reflection lines show a strong distinction in the crust between the Yilgarn Craton with crust thinner than 40 km, and the Capricorn Orogen where the crust thickens significantly. The mantle beneath the Capricorn Orogen appears to have greater affinities with the Pilbara, and does not share the rather high shear wavespeeds seen beneath the Yilgarn extending to 200 km depth and more.

Acknowledgements

The deployments of portable broadband stations across Australia have depended on the efforts of many people often working in trying circumstances. Particular thanks are due to John Grant, Steve Sirotjuk, and Qi Li for their major role in maintaining equipment and logistics, and to Armando Arciadiaco for field support and a critical role in data handling and organization. Receiver function results draw on the work of Drs Geoff Clitheroe, Anya Reading, Steve Revets, Erdinc Saygin, Michelle Salmon, and Elizabeth Vanacore. Particular thanks go to Anya Reading for her systematic studies of seismic structure in Western Australia, which have been very significant in the construction of the crustal wavespeed distribution.

References

- Clitheroe, G, Gudmundsson, O and Kennett, BLN 2000a, Sedimentary and upper-crustal structure of Australia from receiver functions: *Australian Journal of Earth Sciences*, v. 47, p. 209–216.
- Clitheroe, G, Gudmundsson, O and Kennett, BLN 2000b, The crustal thickness of Australia: *Journal of Geophysical Research*, v. 105, p. 13697–13713.
- Collins, CDN, Drummond, BJ and Nicoll, MG 2003, Crustal thickness patterns in the Australian continent: *Geological Society of America Special Papers*, v. 372, p. 121–128.
- Debayle, E and Kennett, BLN 2000, The Australian continental upper mantle: structure and deformation inferred from surface waves: *Journal of Geophysical Research*, v. 105, p. 25443–25540.
- Debayle, E and Kennett, BLN 2003, Surface-wave studies of the Australian region, in *Evolution and dynamics of the Australian plate edited by RR Hillis and RD Müller*: Geological Society of America, Special Publications 372, p. 25–40.
- Fichtner, A, Kennett, BLN, Igel, H and Bunge, HP 2009, Full seismic waveform tomography for upper-mantle structure in the Australasian region using adjoint methods: *Geophysical Journal International*, v. 179, p. 1703–1725.
- Fichtner, A, Kennett, BLN, Igel, H and Bunge, HP 2010, Full seismic waveform tomography for radially anisotropic structure: New insights into the past and present states of the Australasian upper mantle: *Earth and Planetary Science Letters*, v. 290, p. 270–280.
- Fishwick, S, Heintz, M, Kennett, BLN, Reading, AM and Yoshizawa, K 2008, Steps in lithospheric thickness within eastern Australia, evidence from surface wave tomography: *Tectonics*, v. 27 (TC4009), doi:10.129/2007TC002116.
- Fishwick, S, Kennett, BLN and Reading, AM 2005, Contrasts in lithospheric structure within the Australian craton—insights from surface wave tomography: *Earth and Planetary Science Letters*, v. 231, p. 163–176.
- Fishwick, S and Rawlinson, N 2012, 3-D structure of the Australian lithosphere from evolving seismic datasets: *Australian Journal of Earth Sciences*, v. 59, p. 809–826.
- Kennett, BLN 2003, Seismic structure in the mantle beneath Australia, in *Evolution and dynamics of the Australian Plate edited by RR Hillis and RD Müller*: Geological Society of America, Special paper no. 372, p. 7–23.
- Kennett, BLN, Fichtner, A, Fishwick, S and Yoshizawa, K 2012, Australian Seismological Reference Model (AuSREM): mantle component: *Geophysical Journal International*, v. 192, doi:10.1093/gji/ggs065.
- Kennett, BLN, Fishwick, S and Heintz, M 2004a, Lithospheric structure in the Australian region: a synthesis of surface wave and body wave studies: *Exploration Geophysics*, v. 35, p. 258–266.
- Kennett, BLN, Fishwick, S and Reading, AM 2004b, Contrasts in mantle structure beneath Australia – relation to the Tasman Lines?: *Australian Journal of Earth Sciences*, v. 51, p. 563–569.
- Kennett, BLN and Salmon, M 2012, AusREM: Australian seismological reference model: *Australian Journal of Earth Sciences*, v. 59, p. 1091–1103.
- Kennett, BLN, Salmon, M, Saygin, E and AusMoho Working Group 2011, AusMoho: the variation of Moho depth in Australia: *Geophysical Journal International*, v. 187, no. 2, p. 946–958.
- Reading, AM, Kennett, BLN and Dentith, MC 2003b, Seismic structure of the Yilgarn Craton, Western Australia: *Australian Journal of Earth Sciences*, v. 50, p. 427–438.
- Reading, AM, Kennett, BLN and Goleby, B 2007, New constraints on the seismic structure of West Australia: evidence for terrane stabilization prior to assembly of an ancient continent: *Geology*, v. 35, p. 379–382.
- Reading, AM, Kennett, BLN and Sambridge, M 2003a, Improved inversion for seismic structure using transformed S-wavevector receiver functions: removing the effect of the free surface: *Geophysical Research Letters*, v. 30, p. 1981.
- Reading, AM, Tkalcic, H, Kennett, BLN, Johnson, SP and Sheppard, S 2012, Seismic structure of the crust and uppermost mantle of the Capricorn and Paterson Orogens and adjacent cratons, Western Australia, from passive seismic transects: *Precambrian Research*, v. 196–197, p. 295–308.

- Salmon, M, Kennett, BLN and Saygin, E 2012, Australian Seismological Reference Model (AuSREM): crustal component: *Geophysical Journal International*, v. 192, p. 190–206.
- Sambridge, MS 1999, Geophysical inversion with a neighbourhood algorithm: I. Searching a parameter space: *Geophysical Journal International*, v. 138, p. 479–494.
- Saygin, E 2007, Seismic receiver and noise correlation based on studies in Australia: Australian National University, Canberra, PhD thesis (unpublished).
- Saygin, E and Kennett, BLN 2012a, Ambient noise tomography for the Australian Continent: *Tectonophysics*, v. 481, p. 116–125, doi:10.106/j.tecto.2008.11.013.
- Saygin, E and Kennett, BLN 2012b, Crustal structure of Australia from ambient seismic noise tomography: *Journal of Geophysical Research: Solid Earth*, v. 117, no. B1, doi:10.1029/2011JB008403.
- Shibutani, T, Sambridge, M and Kennett, BLN 1996, Genetic algorithm inversion for receiver functions with application to crust and uppermost mantle structure beneath Eastern Australia: *Geophysical Research Letters*, v. 23, p. 1829–1832.
- Yoshizawa, K and Kennett, BLN 2004, Multimode surface wave tomography for the Australian region using a three-stage approach incorporating finite frequency effects: *Journal of Geophysical Research: Solid Earth*, v. 109, no. B2, doi:10.129/2002JB002254.
- Zhu, L and Kanamori, H 2000, Moho depth variation in southern California from teleseismic receiver functions: *Journal of Geophysical Research*, v. 105, p. 2969–2980.

Geology of the northern Yilgarn Craton

by

**S Wyche, MJ Pawley¹, SF Chen, TJ Ivanic, I Zibra,
MJ Van Kranendonk², CV Spaggiari, and MTD Wingate**

Introduction

The Paleoproterozoic to Neoproterozoic Yilgarn Craton in Western Australia (Fig. 1) is a highly mineralized granite–greenstone terrain. Granites comprise more than 70% of the craton with the remainder consisting of greenstone or supracrustal successions with distinct temporal and spatial associations. The Yilgarn Craton hosts world-class deposits of gold and nickel, and significant iron and volcanic-hosted massive sulfide (VHMS) base-metal deposits. Economic iron deposits are confined to the western part of the craton.

The Yilgarn Craton has been divided into terranes defined on the basis of distinct sedimentary and magmatic associations, geochemistry, and ages of volcanism (Fig. 1; Cassidy et al., 2006; Pawley et al., 2012). The Narryer and South West Terranes in the west are dominated by granite and granitic gneiss with minor supracrustal greenstone inliers, whereas the Youanmi Terrane and the Eastern Goldfields Superterrane contain substantial greenstone belts separated by granite and granitic gneiss. The Eastern Goldfields Superterrane comprises the Kalgoorlie, Kurnalpi, Burtville and Yamarna Terranes.

The Ida Fault (Fig. 1), which marks the boundary between the western Yilgarn Craton and the Eastern Goldfields Superterrane, is a major structure that extends to the base of the crust (Drummond et al., 2000). Various geophysical techniques, including deep-crustal seismic (Drummond et al., 2000; Goleby et al., 2003), seismic receiver-function analysis (Reading et al., 2007), and magnetotelluric surveys (Dentith et al., 2013), show the Yilgarn crust to be between 32 and 46 km thick, with the shallowest Moho beneath the Youanmi Terrane. The crust is thicker in the southwest, and thickest in the eastern part of the Eastern Goldfields Superterrane (Kennett et al., 2011). Seismic and gravity data suggest that the greenstones are 2–7 km thick (Swager et al., 1997).

Isotopic data, including Sm–Nd data (Fig. 2; Champion and Cassidy, 2007) and Lu–Hf data (Griffin et al., 2004; Mole et al., 2010; Ivanic et al., 2012; Wyche et al., 2012), show that the terrane subdivisions of the Yilgarn Craton reflect regions with distinctive crustal histories. The Narryer Terrane, which contains both the oldest detrital zircons yet found on Earth (back to c. 4400 Ma; Wilde et al., 2001) and the oldest rocks in Australia (back to c. 3730 Ma; Kinny et al., 1988), shows abundant evidence of very old model ages. The Youanmi Terrane has a more mixed history, whereas the Eastern Goldfields Superterrane is distinctly more juvenile than the terranes to the west.

Deformation histories have been described for the Eastern Goldfields Superterrane (e.g. Blewett et al., 2010); the Southern Cross Domain (e.g. Chen et al., 2001, 2004); the Murchison Domain (e.g. Van Kranendonk et al., 2013); and the South West Terrane (Wilde et al., 1996). However, although there are many common elements to the deformation history across the craton, particular regions are characterized by deformation that reflects their overall magmatic and tectonic history.

The supracrustal rock record in the Yilgarn Craton dates back to at least c. 3080 Ma in the Youanmi and Narryer Terranes in the west (Wang et al., 1998; Yeats et al., 1996; Rasmussen et al., 2010; Van Kranendonk et al., 2013) and c. 2960 Ma in the Burtville Terrane in the northeast (Pawley et al., 2012). However, greenstone successions across most of the craton are dominated by rocks that formed after c. 2820 Ma.

In the central Youanmi Terrane, a cycle of mafic–ultramafic to felsic volcanism between c. 2820 and 2735 Ma is likely due to a major plume that produced large mafic–ultramafic layered intrusions between c. 2820 and 2800 Ma (Ivanic et al., 2010), coincident with similar, but less voluminous, magmatism in the eastern part of the craton (Wyche et al., 2012). This event may have resulted in partial break-up of the early Yilgarn Craton with rifting in the east (Czarnota et al., 2010) and incipient rifting marked by younger Nd model ages and the layered intrusions in the Youanmi Terrane (Ivanic et al., 2010). A protracted period of mafic to felsic volcanism and associated sedimentation continued from c. 2800 Ma until

1 Geological Survey of South Australia, Department of Manufacturing Innovation Trade Resources and Energy, Level 4, 101 Grenfell Street, Adelaide SA 5000

2 School of Biological, Earth and Environmental Sciences, University of New South Wales, Sydney NSW 2052

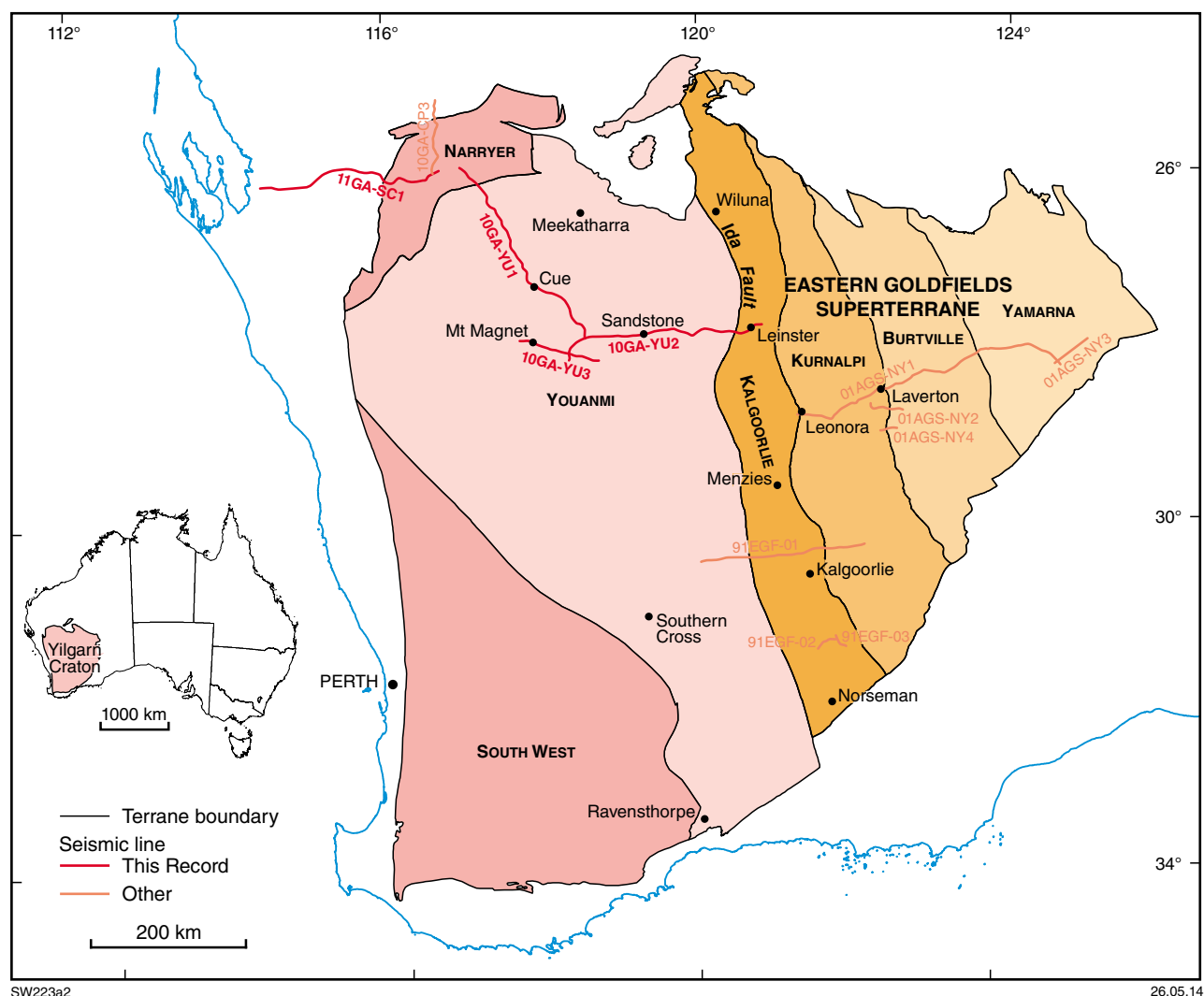


Figure 1. Subdivision of the Yilgarn Craton (modified from Pawley et al., 2012) showing locations of seismic lines

c. 2735 Ma. Wyman and Kerrich (2012) proposed that the presence of boninite-like rocks in the Murchison Domain at this time is due to subduction-related magmatism associated with the closing of a rift formed during the plume event. Calc-alkaline volcanism was dominant after c. 2760 Ma, and broadly coincided with a period of mafic tonalite–trondhjemite–granodiorite (TTG) and enriched high-field-strength element (HFSE) granite magmatism (Cassidy et al., 2002; Van Kranendonk et al., 2013).

The last recognized regional greenstone-forming event in the Youanmi Terrane was a mafic to felsic volcanic cycle between c. 2740 and 2720 Ma (Chen et al., 2003; Van Kranendonk et al., 2013), which was contemporaneous with high-Ca TTG granite magmatism (Cassidy et al., 2002).

Except for rare greenstones in the South West Terrane (Allibone et al., 1998), after c. 2715 Ma volcanic activity and greenstone development in the Yilgarn Craton was restricted to the Eastern Goldfields Superterrane. Andesite-

dominated calc-alkaline volcanism in the eastern Kurnalpi Terrane (Fig. 1; Barley et al., 2008) and dacitic volcanism in the northern Kalgoorlie Terrane (Rosengren et al., 2005) were prevalent between c. 2715 and 2705 Ma (Fiorentini et al., 2005; Kositsin et al., 2008). Barley et al. (2008) interpreted the andesite-dominated successions as oceanic intra-arc volcanic centres.

In the Eastern Goldfields Superterrane, a major plume event at c. 2700 Ma (Campbell and Hill, 1988; Barnes et al., 2012) produced voluminous komatiites, which occur as both high-level intrusions and flows (Trofimovs et al., 2004; Fiorentini et al., 2005, 2010). They are preserved in a distinct north-northwesterly trending belt, about 600 km long and up to 100 km wide, between Norseman and Wiluna (Fig. 1). The mafic–ultramafic succession also contains tholeiitic and komatiitic basalts (Leshner, 1983; Squire et al., 1998; Said and Kerrich, 2009). It is well constrained in age to between c. 2710 Ma and 2692 Ma (Kositsin et al., 2008) and partly overlaps in age with the andesite-dominated calc-alkaline volcanism. The

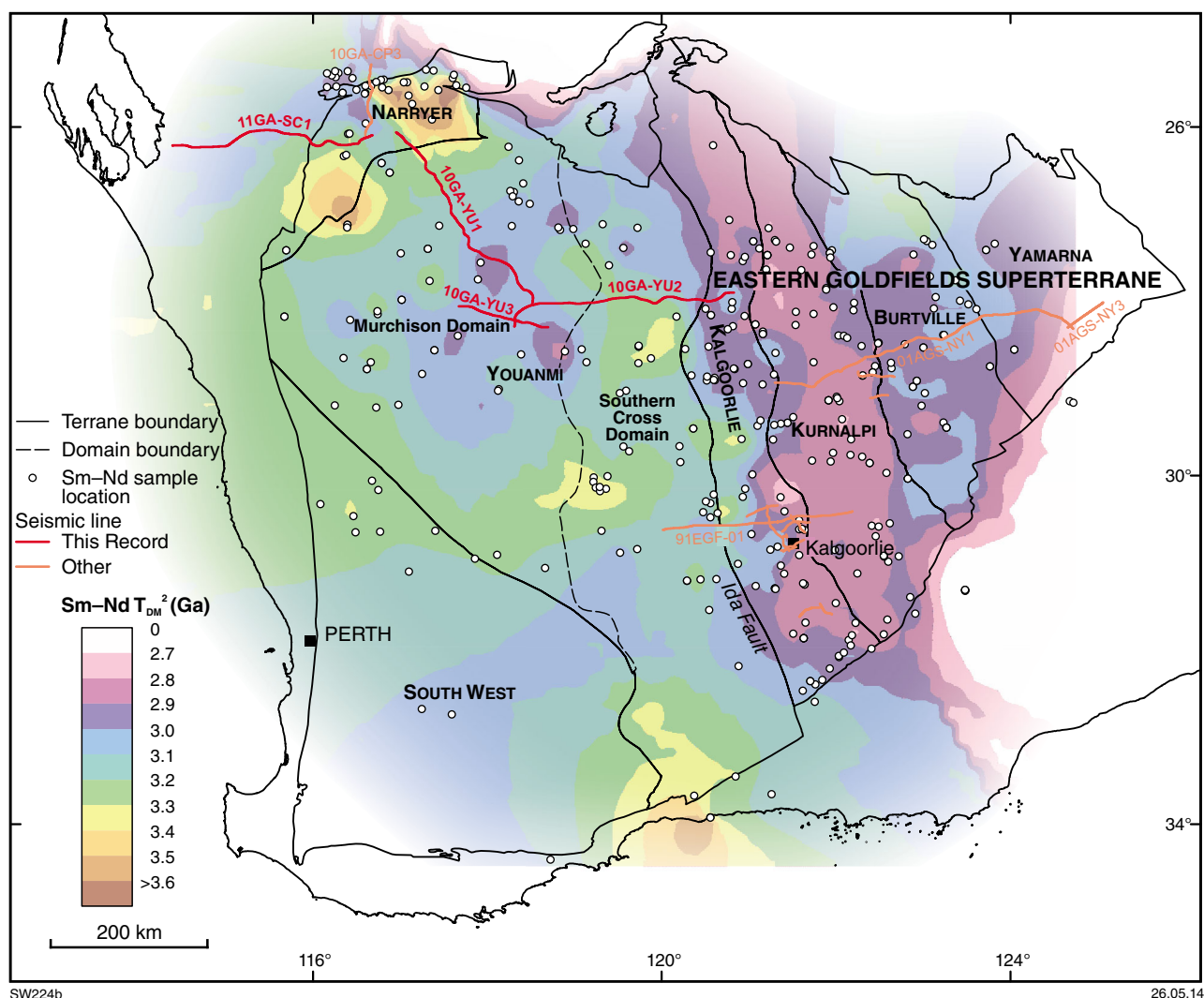


Figure 2. Nd depleted-mantle model age map for the Yilgarn Craton (modified from Champion and Cassidy, 2007)

Norseman–Wiluna komatiites, which host major nickel deposits, are not only younger than ultramafic rocks in the Youanmi Terrane, but also differ in chemical character. Komatiites of the Youanmi Terrane include Al-depleted, and Al-undepleted and Ti-enriched varieties, whereas those in the Norseman–Wiluna belt are Al-undepleted (Barnes et al., 2007).

Abundant SHRIMP geochronological data on greenstones from throughout the Eastern Goldfields Superterrane (GSWA, 2013) suggest that thinner and more sparsely distributed komatiite units in the Kurnalpi Terrane are mainly the same age as the more voluminous material in the Kalgoorlie Terrane and may represent thin flows or channel deposits which have travelled farther as result of paleotopography. Barnes et al. (2012) have shown that similar geochemical patterns in basalts in the same relative stratigraphic positions are associated with the c. 2700 Ma komatiite event across the Eastern Goldfields Superterrane.

Between c. 2692 and 2680 Ma, volcanic centres in the western part of the Kurnalpi Terrane produced bimodal (basalt–rhyolite) volcanic and associated intrusive and

sedimentary rocks, coinciding with the main period of high-HFSE granite magmatism (Cassidy et al., 2002). Barley et al. (2008) interpreted these ‘Gindalbie’ successions as representing an arc-rift environment. Gindalbie-style volcanism, which locally hosts VHMS mineralization, overlapped in age with, and was succeeded by, TTG magmatism and associated sedimentary rocks and mafic intrusions represented by the Black Flag Group in the Kalgoorlie Terrane. The deposition of the Black Flag Group between c. 2690 and 2660 Ma coincided with voluminous high-Ca TTG granite magmatism in the Eastern Goldfields Superterrane (Champion and Cassidy, 2007). Krapež and Hand (2008) interpreted the Black Flag Group (their ‘Kalgoorlie Sequence’) as representing a strike-slip intra-arc basin, whereas Squire et al. (2010) argued that they are the result of volcanism and sedimentation associated with extensional deformation due to the emplacement of large granite batholiths. Felsic volcanic and associated plutonic rocks of this age have also been recorded in a poorly exposed bimodal greenstone succession in the Yamarna Terrane in the far east of the Eastern Goldfields Superterrane (Fig. 1; Pawley et al., 2012).

The youngest supracrustal successions in the Yilgarn Craton are the so-called 'late basins', which rest unconformably on all earlier greenstones in the Eastern Goldfields Superterrane. Likely deposited in a very short time (c. 10 m.y.) after c. 2665 Ma (Squire et al., 2010), they preserve fluvial and deep-marine facies, which Krapež and Barley (2008) interpreted as having formed in a tectonic-escape corridor after arc closure. The late-basin sedimentary rocks, which include turbidites through to coarse, braided-stream sediments (Krapež et al., 2008), and contain a range of detrital zircon ages, post-date the cessation of TTG granite magmatism. They contain material derived from both proximal and distal sources during ongoing extension and uplift (Squire et al., 2010).

Finally, the cessation of greenstone deposition was accompanied by craton-wide low-Ca granite magmatism (Cassidy et al., 2002). There are several distinct periods of granite emplacement. Most coincide with periods of crustal development and greenstone deposition in various parts of the craton. The latest period of granite emplacement, after c. 2655 Ma, consisted of widespread low-Ca granite without contemporaneous greenstone deposition (Cassidy et al., 2002; Mole et al., 2012). A distinctive belt of alkaline granites, emplaced at this time, appears to coincide with deeply penetrating crustal structures and is mainly restricted to the Kurnalpi Terrane (Smithies and Champion, 1999).

Geodynamic models proposed for the Yilgarn Craton embrace ensialic rifts (e.g. Groves and Batt, 1984; Hallberg, 1986), plumes (e.g. Campbell and Hill 1988; Barnes et al., 2012; Van Kranendonk et al., 2013), accretionary settings (e.g. Barley et al., 1989; Myers, 1990a), and combinations of plume and accretionary tectonics (e.g. Czarnota et al., 2010). There is still no consensus as to an overarching geodynamic model for the craton.

Recently, Begg et al. (2010) have suggested that the komatiite distribution in the Eastern Goldfields is controlled by the presence of older blocks within the craton which are underlain by a thick component of subcontinental lithospheric mantle (SCLM). Mantle plumes that encountered the thick lithosphere were deflected towards the thinner lithosphere adjacent to protocraton margins. In the case of the Eastern Goldfields, Barnes et al. (2012) and Barnes and Fiorentini (2012) suggested that a plume that impacted SCLM below the Youanmi Terrane was deflected to the boundary between the Youanmi Terrane and the older components of the Eastern Goldfields Superterrane where it generated voluminous komatiites. It is possible that there are other old SCLM margins within the Yilgarn Craton; for example, marked by the zone of relatively juvenile crust in the middle of the Youanmi Terrane. Mole et al. (2010) suggested that the distribution of nickel deposits in the southern part of the Youanmi Terrane might be controlled by variations in lithospheric thickness in that region.

The seismic transects 10GA-YU1, 10GA-YU2, 10GA-YU3 and 11GA-SC1 traverse the northern Yilgarn Craton

from its western margin crossing the Narryer Terrane, the Youanmi Terrane, and the western margin of the Eastern Goldfields Superterrane.

Yilgarn granites

Champion and Sheraton (1997) divided Archean granites and granitic gneisses of the Eastern Goldfields Superterrane into:

...two major groups (high-Ca and low-Ca), and three minor groups (high-HFSE (high field strength elements), mafic, and syenitic). The high-Ca group (68–77% SiO₂) with high Al₂O₃, Na₂O and Sr, and low Y, shares many features with typical Archean tonalite-trondhjemite suites, but has higher K₂O, Rb, and Th contents. The low-Ca group (70–76% SiO₂) differs from the high-Ca group in having lower Al₂O₃, CaO, and Na₂O, but higher K₂O, Rb, Th, Zr, Y, La and Ce contents. Granites of the high-HFSE, mafic and syenitic groups form a minor component (10–20%) of the Eastern Goldfields granites. The siliceous (74–77% SiO₂) high-HFSE granites . . . are characterized by high TiO₂, total FeO, MgO, Y, Zr and Ce, but only moderate Rb, Th and Pb contents. The A-type syenites (50–68% SiO₂) are distinguished by their high total alkalies and mainly occur along tectonic lineaments. The mafic group (55–70% SiO₂) is lithologically diverse and exhibits a wide range of K₂O, Rb, Th, La and Ce contents. (Champion and Sheraton, 1997, p. 109)

Cassidy et al. (2002) extended the granite subdivisions of Champion and Sheraton (1997) to the west across the northern part of the Youanmi Terrane and collected a large body of geochronological data that indicate that peak granite magmatism took place at different times in the Yilgarn Craton. In the Murchison and Southern Cross Domains of the Youanmi Terrane, several peaks of magmatism are evident between c. 3010 and 2630 Ma. However, the c. 2800 Ma peaks appear to be less well represented in the Southern Cross Domain than in the Murchison Domain. These peaks are broadly coincident with periods of felsic volcanism. The majority of Eastern Goldfields Superterrane granites are younger than c. 2720 Ma. Both the Youanmi Terrane and the Eastern Goldfields Superterrane show a marked change from dominantly high-Ca to dominantly low-Ca magmatism at 2655–2650 Ma, although the peak age of low-Ca magmatism decreases from east to west across the craton. Inherited zircon ages in the Youanmi Terrane and Eastern Goldfields Superterrane mainly follow known ages for older granites and greenstones.

Van Kranendonk et al. (2013) and Ivanic et al. (2012) have built on the work of Champion and Sheraton (1997) and Cassidy et al. (2002) in the Murchison Domain, where they have integrated the geochemical and geochronological character of mapped granites with the newly developed stratigraphic system for the region (see Murchison Domain below).

Eastern Goldfields Superterrane

Stratigraphy

Poor exposure, deep weathering, lack of detailed geochronology, and structural and metamorphic overprints preclude description of detailed stratigraphy in many of the Yilgarn greenstones. East of the Ida Fault (Fig. 1), local stratigraphy has been established in some greenstone belts (e.g. Kositsin et al., 2008) but detailed regional stratigraphy has been described only for the southern part of the Kalgoorlie Terrane.

The southern Kalgoorlie Terrane (Woodall, 1965; Gresham and Loftus-Hills, 1981; Swager et al., 1995) comprises a lower mafic–ultramafic succession consisting of the Lunnon Basalt, Kambalda Komatiite (including the Silver Lake and Tripod Hill members), Devon Consols Basalt, Kapai Slate, and Paringa Basalt (Fig. 3). The mafic–ultramafic succession is unconformably overlain by the Black Flag Group, which comprises extensive volcanoclastic rocks, rhyolitic to dacitic volcanic rocks, intrusive mafic complexes, and minor mafic volcanic rocks (Squire et al., 2010). The late-basin sediments are represented in this area by polymictic conglomerate of the Kurrawang Formation, which contains a variety of clasts, including banded iron-formation and granite, that

indicate a distal provenance, probably in the Youanmi Terrane (Krapež et al., 2008). In less-deformed areas, many primary igneous features and textures are still visible despite locally complete replacement by alteration assemblages.

The abundant pillow lavas and hyaloclastites in basalts, the presence of marine sediments, and quench textures in komatiites and basalts indicate a submarine eruption of the mafic–ultramafic succession (Hill et al., 1995; Squire et al., 1998; Said and Kerrich, 2009). Squire et al. (1998) proposed that the Lunnon Basalt is either distal to a shield volcano, or represents a ponded lava field in an extensional basin distant from the eruptive centre. Similarly, Hill et al. (1995) suggested that the komatiite flows at Kambalda are distal deposits in contrast with the thick, cumulate dunite bodies to the north and northwest of Kalgoorlie, which are proximal to the eruptive centre.

The nature of basement to the mafic–ultramafic succession in the Kalgoorlie region is unknown. Xenocrystic zircon age data (Compston et al., 1986) and trace-element and isotopic data suggest the mafic–ultramafic succession may have been generated through varying degrees of crustal contamination (Arndt and Jenner, 1986) and mixing of a depleted mantle source with an enriched subcontinental lithospheric mantle (Said and Kerrich, 2009). Model age data based on Lu–Hf analyses on zircons have peaks after 3.5 Ga, and mainly after 3.1 Ga. This is significantly younger than the earliest model age recognized in the Youanmi Terrane (Wyche et al., 2012).

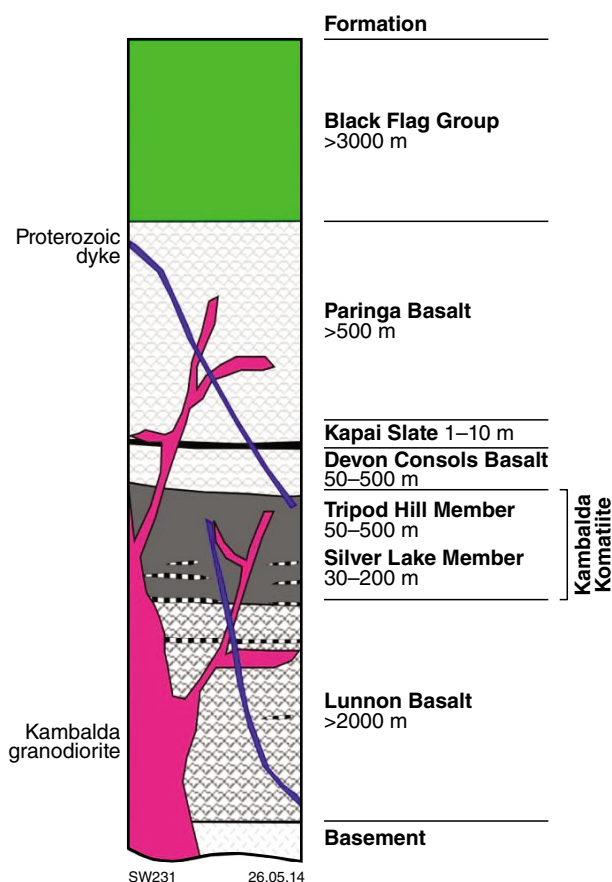


Figure 3. Kambalda stratigraphy (modified from Beresford et al., 2005)

Structure and metamorphism

Building on the regional framework established by Swager (1997), Blewett et al. (2010) produced a six-stage, integrated structural-event framework (Fig. 4) for the Eastern Goldfields Superterrane to account for the documented magmatic, depositional, structural, and metamorphic history (Czarnota et al., 2010). In this scheme, the period of greenstone deposition between c. 2715 and 2705 Ma, characterized by calc-alkaline and komatiite magmatism, was a time of dominantly extensional tectonics that marked the initiation of regional-scale granite doming (Blewett et al., 2010).

Deposition of the Black Flag Group, between c. 2690 and 2660 Ma, was accompanied by the widespread emplacement of a high-Ca TTG granite suite. Granite doming was probably coeval with local contraction indicated by upright folding and dextral shearing at this time. The peak period of granite doming began during the last depositional phase of the Black Flag Group (Squire et al., 2010). Ongoing doming and extension produced the clastic late-basin sediments. After the cessation of high-Ca magmatism, low-Ca granite magmatism, which appears to be the result of melting of a middle to lower crustal source of TTG/high-Ca composition (Champion and Cassidy, 2007), was accompanied by a major contractional deformation, which produced both upright folds and regional-scale sinistral shearing, which may have reactivated earlier structures. Subsequent, relatively minor, brittle contractional and extensional events affected the now rigid Yilgarn Craton (Czarnota et al., 2010).

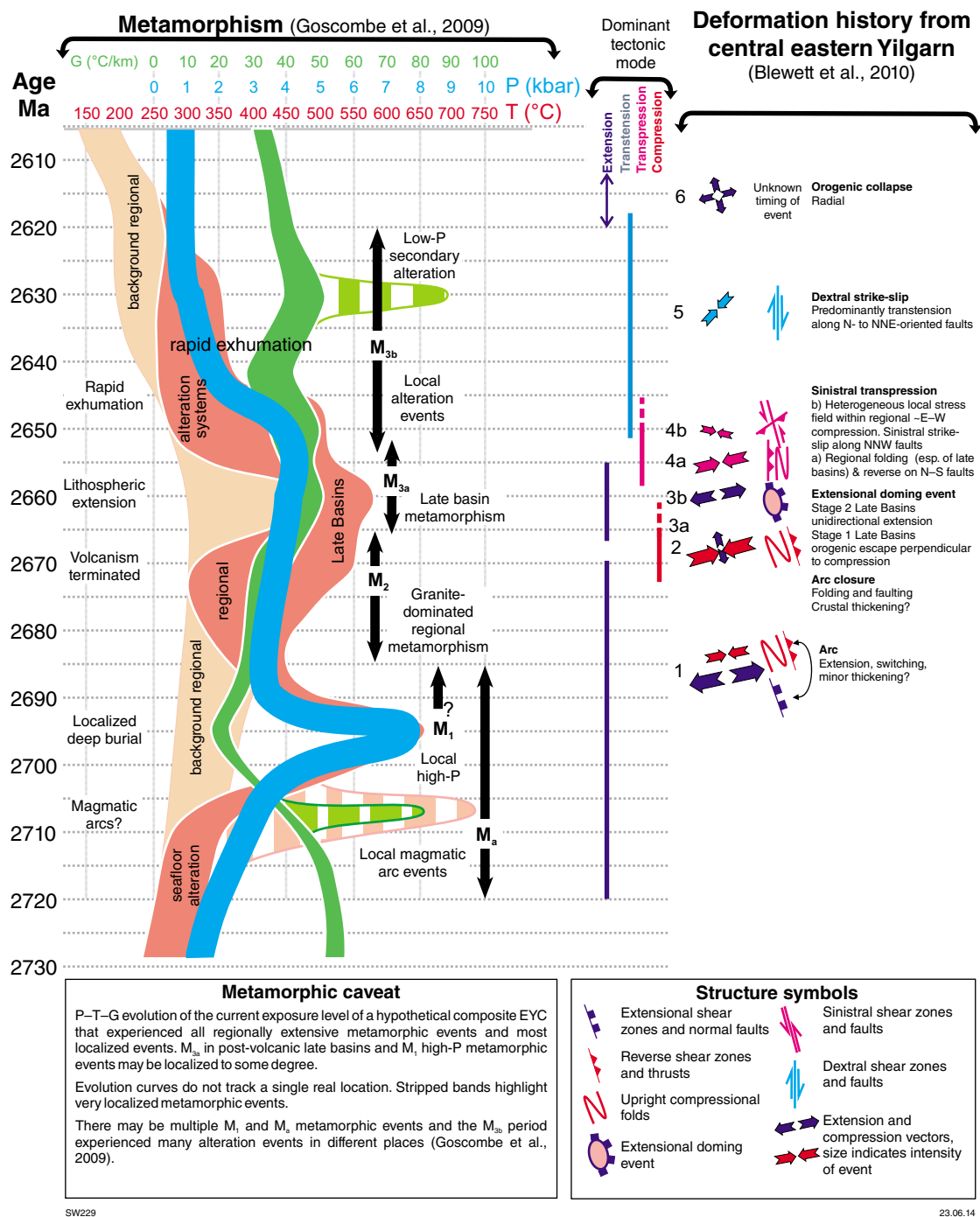


Figure 4. Metamorphic and structural history of the Eastern Goldfields Superterrane (modified from Czarnota et al., 2010)

Local evidence of early, low-pressure granulite-facies metamorphism, consistent with a high geothermal gradient (Fig. 4; Goscombe et al., 2009), was contemporaneous with the eruption of the Norseman–Wiluna komatiites. Later medium-pressure metamorphism was most likely due to exhumation of deep-seated early structures around granite domes (Goscombe et al., 2009). Subsequent periods of low-pressure metamorphism, accompanied by moderate to high geothermal gradients, reflect exhumation during granite doming prior to and during late-basin development. Very low pressures and geothermal gradients mark the end of the period of granite doming and the initiation of widespread exhumation (Goscombe et al., 2009).

Kalgoorlie Terrane in the Agnew–Leinster region

Stratigraphy

The Agnew–Wiluna greenstone belt lies within the Kalgoorlie Terrane of Cassidy et al. (2006). The southern end of the belt is divided into two lobes separated by the Leinster Anticline (Fig. 5; Plate 1), which is occupied by the Leinster granodiorite (Duuring et al., 2012). The eastern lobe consists of the ‘Leinster district’ of Duuring et al. (2012) and the western lobe is the ‘Agnew – Mount White district’ of Duuring et al. (2012). The Leinster district hosts the nickel deposits of the Leinster nickel camp and the Agnew – Mount White district hosts the numerous gold deposits of the Agnew gold camp.

Stratigraphy in the Leinster district has been described by Duuring et al. (2007, 2010, 2012). The succession is bounded to the east by the Perseverance Fault and to the west by granodiorite. Greenstone units trend broadly south-southeasterly, parallel to the belt margins. Dips in greenstones are to the west and younging is to the east, indicating that the stratigraphy is overturned. The stratigraphic succession is similar to that described to the north at Mount Keith (Fiorentini et al., 2005), with basalt at the base overlain by a complex succession of sedimentary and felsic volcanic and volcanoclastic rocks. The succession contains multiple intervals of ultramafic rocks including komatiite. The ultramafic rocks, which host the Perseverance, Rockys Reward and Harmony nickel deposits, are strongly deformed with the deformation obscuring relationships with the adjacent country rocks and there may be some structural repetition (Trofimovs et al., 2003). However, Barnes et al. (2011) argued that the original stratigraphy at Perseverance is preserved. The age of felsic volcanic rocks from the mine succession at Rockys Reward is c. 2720 Ma (Nelson, 1997; Duuring et al., 2012).

Platt et al. (1978), Liu et al. (1998), and Beardsmore (2002) have described the stratigraphy in the southern part of the Agnew – Mount White district. Here, the three main packages consist of a lower mafic–ultramafic succession, a middle siliciclastic succession (dominated by feldspathic detritus), and an upper siliciclastic succession (dominated by quartz-rich detritus).

The basal mafic–ultramafic package comprises a series of komatiite and basalt units, distinguishable on textural grounds, which are intruded by mafic sills and layered complexes. The lowermost basalt crops out as highly strained rocks on the western limb of the Lawlers Anticline and in the core of the Leinster Anticline, and is overlain by komatiite and pyroxene spinifex-textured komatiitic basalt. This lower ultramafic unit appears to be distinct unit that is not recognized in the Kalgoorlie region.

Basalt, which overlies the ultramafic rocks, appears to grade from magnesian near the base to tholeiitic near the top. The upper part may correspond to the Lunnon Basalt of the Kalgoorlie Group of Swager et al. (1995). It contains several thin, clastic sedimentary units. The overlying, thick unit of komatiite includes minor komatiitic basalt layers. This komatiite unit, informally called the Agnew komatiite, is a prominent marker unit which defines the major folds in the area and is considered to be contemporaneous with the Kambalda Komatiite in the Kalgoorlie region (Swager et al., 1995). Mafic rocks that overlie the Agnew komatiite include pyroxene spinifex-textured basalt, massive, undifferentiated basalt, feldspar-phyric basalt, and dolerite. A thin unit of volcanogenic sandstone, probably from the lower part of the Vivien Formation sedimentary unit immediately above the mafic–ultramafic succession, has a maximum depositional age of 2692 ± 3 Ma (Kositicic et al. 2008), identical to the age of the Kapai Slate at Kambalda.

The mafic–ultramafic succession has been intruded by numerous mafic sills and layered complexes. These are most common below the Agnew komatiite where there are two thick, composite intrusions of dolerite and gabbro with minor, continuous, thin layers of pyroxenite and peridotite. Despite having similar internal zonation, the lower complex is hosted by magnesian basalt, whereas the upper complex is hosted by tholeiitic basalt, arguing against the structural duplication of a single unit.

The mafic–ultramafic succession in the Agnew area is overlain by two sedimentary rock packages. To the east, in the Mount White Syncline, a package of variably metamorphosed feldspar- and quartz-bearing sandstones and mudstones with minor conglomerate has a polymodal detrital age population with a maximum depositional age of 2692 ± 3 Ma (Kositicic et al. 2008), and has been assigned to the late stage of the Black Flag Group of Squire et al. (2010). On the western limb of the Lawlers Anticline, the mafic–ultramafic rocks have a faulted contact with a sedimentary sequence that includes a thin basal package of conglomerate and sandstone and thick quartz-rich clastic sedimentary rocks, the ‘late-basin’ sediments of the Scotty Creek Formation, which has a maximum depositional age of c. 2662 Ma (Kositicic et al., 2008). This age is similar to that of the Jones Creek Conglomerate to the north (Krapež et al., 2000). Squire et al. (2010) has correlated these rocks with their late Merougil Group in the Kalgoorlie area on the basis of the limited zircon age range and the dominance of volcanic-derived quartz grains.

The stratigraphic position of mafic rocks in the core of the Mount White Syncline is uncertain. The succession contains gabbro, pillow basalt, and clastic sedimentary

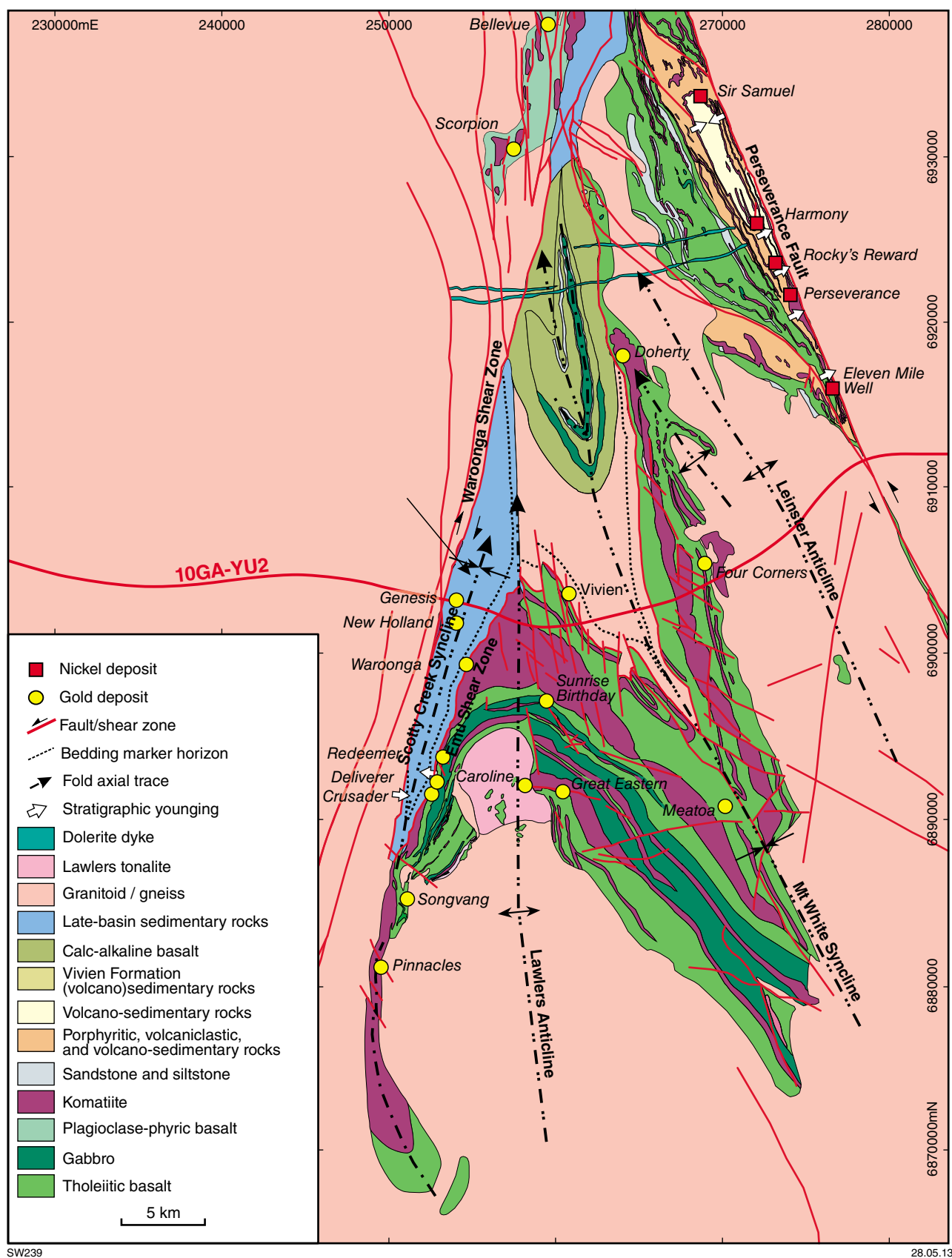


Figure 5. Interpreted geology map of the Agnew – Mount White district showing the distribution of rock types, gold and nickel deposits, and major structural relationships (modified from Duuring et al., 2012)

rocks (Platt et al., 1978; Liu et al., 1998) that are not obvious repetitions of lower parts of the succession and may be equivalent to mafic components of the Black Flag Group in the Kalgoorlie area, as described by Krapež and Hand (2008).

Deformation

Duuring et al. (2012) described a multi-stage deformation history for the southern end of the Agnew–Wiluna greenstone belt. Following Platt et al. (1978), the earliest recognizable fabric is a layer-parallel foliation due to recumbent folding and thrust imbrication. The prominent regional fold structures such as the Lawlers Anticline formed during east-northeast – west-southwest compression at c. 2665 Ma, which coincided with the cessation of felsic volcanism and the emplacement of high-Ca granites into the Lawlers structure (Blewett et al., 2010; Duuring et al., 2012). This was the time of peak (amphibolite facies) metamorphism (Goscombe et al., 2009). Doming associated with the emplacement of the granites produced a radiating pattern of mineral stretching lineations (Blewett et al., 2010). The clastic ‘late-basin’ sedimentary successions at Jones Creek and Scotty Creek, which were deposited at this time, are interpreted by Blewett et al. (2010) as the products of exhumation associated with doming, and by Squire et al. (2010) as being, at least in part, reworked pyroclastic deposits related to the waning phase of felsic volcanism. Subsequent west-northwest – east-southeast compression (Fig. 4; D_{4b} of Blewett et al., 2010) folded the clastic successions, tightened existing folds and produced the north-northwesterly trending, sinistral transpressional Perseverance Fault. The main movement on the Emu and Waroonga shear zones, which bound the Scotty Creek Syncline (Fig. 5), overprints earlier structures and may correspond to D_5 of Blewett et al. (2010).

The Ida Fault, which separates the Youanmi Terrane from the Eastern Goldfields Superterrane, is evident as a geophysical and satellite-image lineament in the Kalgoorlie region where it shows in seismic-reflection data as a shallowly east-dipping feature that displaces the Moho in a normal sense. However, it is not clear which surface feature in the Agnew district corresponds to the Ida Fault and it may be overprinted by subsequent reverse movement on the Waroonga Shear Zone (Liu and Chen, 1998; Zibra et al., 2013b).

Youanmi Terrane

Second-generation regional mapping, SHRIMP geochronology, and regional granite geochemistry and isotope data (Cassidy et al., 2002) suggest that the Southern Cross and Murchison Domains of the Youanmi Terrane (Fig. 1; Cassidy et al., 2006) do not represent allochthonous terranes that have come together during an accretionary event, as previously thought (Myers, 1995). However, within these domains, some parts clearly have ages and tectonic histories different from others. For example, the Ravensthorpe greenstone belt in the south of the Southern Cross Domain (Witt, 1999)

contains c. 2950 Ma calc-alkaline volcanic rocks that host Cu–Zn–Au mineralization in an association that may have more in common with parts of the Murchison Domain than with other greenstone belts in the Southern Cross Domain. This may reflect the presence of cryptic terranes within the Youanmi Terrane as suggested by Lu–Hf isotopic studies (Griffin et al., 2004; Mole et al., 2010; Wyche et al., 2012).

The Youanmi Terrane is bounded to the west by the Darling Fault system, to the north by the Capricorn Orogen, to the southeast by the Albany–Fraser Orogen, and to the southwest by the South West Terrane. The boundary with the Narryer Terrane has been taken to be the Balbalinga and Yalgar faults of Myers (1993). However, recent structural studies in the Jack Hills area (Spaggiari, 2006, 2007a,b; Spaggiari et al., 2008) have demonstrated a complex structural history involving a significant component of Proterozoic deformation. The boundary with the South West Terrane is poorly defined (Myers, 1993). The boundary with the Eastern Goldfields Superterrane is marked by the Ida Fault and Waroonga shear zone.

The Youanmi Terrane is isotopically distinct from other terranes with Sm–Nd and Lu–Hf data showing several discrete episodes of crustal formation and reworking (Champion and Cassidy, 2007; Griffin et al., 2004; Wyche et al., 2012; Ivanic et al., 2012). Detrital zircon ages from quartzites in the Southern Cross Domain and inherited zircon ages from intrusive and volcanic rocks across the Youanmi Terrane date back to >4000 Ma (Nelson, 1997; Wyche, 2007), suggesting the presence of ancient basement, although no such rocks have yet been discovered.

Large-scale structural architecture

Widespread and voluminous granitic magmatism in the Youanmi Terrane between c. 2720 and 2600 Ma ended with the intrusion of several suites of post-tectonic granites (c. 2640 to 2600 Ma, see Murchison Domain section). All granites are crustal melts and represent an extremely long period of crustal reworking (Rey et al., 2003). The peculiar tectonic style in such ‘hot orogens’ includes the development of rhomb-shaped networks of anastomosing, steep shear zones in the upper crust rooted in a weak, partially molten and horizontally layered mid- to lower crust (see Riller et al., 2012, for a review). This kind of crustal architecture is expected to prevent significant crustal thickening. Large-scale thrust systems generated during compression are generally associated with significant components of horizontal displacement that eventually leads to lateral escape associated with orogen-parallel extension (Cagnard et al., 2006).

Because the Neoarchean lithosphere is regarded as hot and weak as a result of extensive mantle melting and high internal heat from radioactivity, Neoarchean tectonics is thought to have been largely accommodated by shearing of partially molten gneisses and by syntectonic granitic magmatism. However, direct field examples of such strain localization are relatively scarce, and little is known as yet about emplacement style and about the relationship between granite emplacement and regional

deformation. The Archean Yilgarn Craton, which is made up of volumetrically dominant granites and granitic gneiss (about 80%: Myers and Swager, 1997), is a natural laboratory for studying the effect of melting on continental deformation. However, structural investigations have traditionally focussed on solid-state structures (e.g. Blewett et al., 2010, for a review).

From Figure 6, it is evident that the Youanmi Terrane is dissected by a network of terrane-scale shear zones (length >100 km). Since these shear zones are interconnected, their rheology likely controlled the rheology of the whole crustal section. The understanding of the structural and rheological evolution of these shear zones is therefore an essential prerequisite for the formulation of any tectonic model. Where exposed, these shear zones are typically steep, centred on elongate granitic plutons and flanked by strongly deformed and dismembered greenstone packages. Metagranitic rocks are typically L–S tectonites, displaying a prominent and shallowly plunging mineral or stretching lineation. In contrast, adjacent greenstone-derived mafic schists and gneisses are commonly S tectonites, showing a weakly to moderately developed, steep mineral lineation, suggesting that these shear zone segments are in fact transpressional zones where strain has been strongly partitioned between felsic and mafic tectonites (Fossen et al., 1994, fig. 11).

Strain partitioning seems more pronounced along northeasterly and northwesterly trending segments, where conjugate systems developed locally, at least during the latest stages of shearing. Northerly trending, linked, high-strain zones appear dominated by coaxial shearing (e.g. Chen et al., 2001, 2004). As a whole, this shear zone network reflects east–west shortening and north–south extension. However, recent studies (in progress) indicate that the structural features described in Chen et al. (2001) represent just the very late solid-state shear increments. Several lines of evidence indicate that these shear zones were active for at least 20 Ma, during several episodes of incremental pluton emplacement. In this respect, the northeasterly trending corridor between Mount Magnet and Meekatharra is a key study area (Figs 6 and 7). Here, the main structure belonging to the shear zone network described above is represented by the Cundimurra Shear Zone (CMSZ, Fig. 7), which preserves evidence of shearing during incremental pluton emplacement (c. 2680–2650 Ma), and then under retrograde conditions down to greenschist facies temperatures (Fig. 8). Its activity can be constrained to the time span c. 2680–2620 Ma (based on age of the Garden Rock Monzogranite, Fig. 6, which post-dates the Cundimurra Shear Zone). The Cundimurra Shear Zone post-dates the emplacement of the adjacent Lakeside and Yarraquin granites (Fig. 7), which are large composite plutons associated with migmatites (c. 100 km long × 50 km wide in map view). These plutons show widespread evidence of deformation during and immediately after pluton crystallization (Zibra, 2012). Therefore, they can be regarded as large, partially molten shear zones, not readily detectable in geophysical images (compare Figs 6 and 7), which accommodate the

emplacement of granite–migmatite domes. The northerly trending, steeply dipping, magmatic to high-temperature solid-state structures preserved in these plutons were likely controlled by active large-scale structures, and therefore by the regional stress field that was prevalent in the Youanmi Terrane at c. 2700 Ma. As discussed in Zibra et al. (2013a, this volume), two seismic lines intersect these granitic bodies (YU1 and YU3, Figs 6 and 7), offering a unique opportunity to constrain their three-dimensional architecture.

Southern Cross Domain

The Southern Cross Domain (Fig. 2) contains at least three greenstone successions. The oldest rocks yet identified lie in the southern part of the domain where the Ravensthorpe greenstone belt contains c. 2950 Ma calc-alkaline volcanic rocks (Witt, 1998, 1999). This is similar to the age of the felsic volcanic succession which hosts the base metal mineralization at Golden Grove in the Murchison Domain (Wang et al., 1998). Felsic volcanic rocks older than 2900 Ma have also been found in the Lake Johnston greenstone belt (Wang et al., 1998).

In the centre and north of the Southern Cross Domain, greenstone belts along the eastern and western sides of the domain commonly preserve quartz-rich sedimentary units at the base of the volcano-sedimentary succession, with maximum depositional ages greater than 3100 Ma (Wyche, 2007). They are similar in character to clastic sedimentary rocks at Mount Narryer (Williams and Myers, 1987) and the Jack Hills (Eriksson and Wilde, 2010) in the Narryer Terrane, and the Jimperding greenstone belt in the South West Terrane (Wilde, 2001), which also contain very old detrital zircons with maximum depositional ages older than 3100 Ma.

The most widespread and abundant greenstone successions in the Southern Cross Domain typically contain abundant banded iron-formation and chert, interbedded with mafic and subordinate ultramafic rocks, overlain by a mafic-dominated succession (Chen et al., 2003). SHRIMP U–Pb zircon ages older than 2800 Ma on intrusive mafic rocks (Riganti et al., 2010) and detrital zircons in sedimentary rocks (Romano et al., 2010) within this dominant greenstone succession suggest a correlation of at least part of the succession with the Norie Group in the Murchison Domain (Van Kranendonk et al., 2012).

The youngest greenstone succession in the Southern Cross Domain is best known in the Marda–Diemals greenstone belt where it consists of the c. 2730 Ma calc-alkaline Marda Complex and clastic sedimentary Diemals Formation (Hallberg et al., 1976; Chen et al., 2003; Morris et al., 2007). However, other greenstone belts also contain felsic volcanic rocks (Wang et al., 1998). For example, c. 2720 Ma dacite in the Gum Creek greenstone belt (Bodorkos et al., 2006) appears to be part of a widespread but very poorly exposed younger greenstone succession that also contains clastic sedimentary rocks, including abundant graphitic shale.

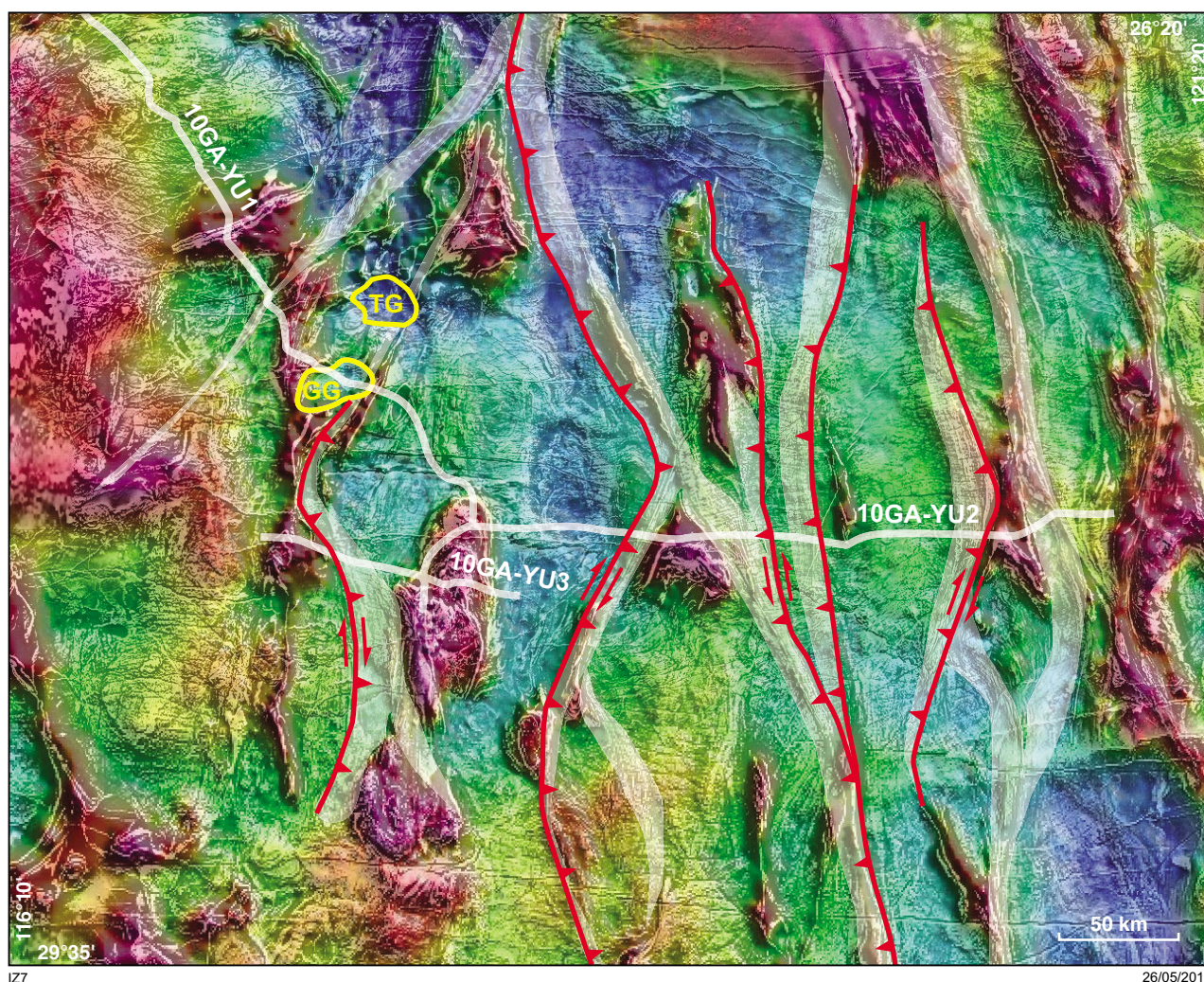


Figure 6. Geophysical image (gravity on aeromagnetic) showing the trace of the terrane-scale network of late-orogenic shear zones (red), that likely controlled the rheology of the whole crustal section. The post-kinematic plutons Garden Rock Monzogranite (GG) and Taincrow Granite (TG), post-dating the development of the shear zone network, are outlined in yellow.

Booylgoo Range greenstone belt

The Booylgoo Range greenstone belt (Fig. 9) is a north-northwesterly trending, faulted syncline that is exposed over a distance of about 40 km, and is up to 6 km wide. Images of aeromagnetic data suggest that the belt may be more than 50 km long. The greenstone belt is surrounded, and locally intruded, by biotite monzogranite. The granite is typically undeformed to weakly deformed, except at the granite–greenstone contact along some parts of the western side of the greenstone belt where deeply weathered granite is strongly deformed, indicating at least a locally sheared contact. The succession in the Booylgoo greenstone belt is very similar in character to that described for the Marda–Diemals greenstone belt to the south (Chen et al., 2003).

The Booylgoo Range greenstone belt contains two intervals of banded iron-formation, which are responsible

for significant topographic relief. Younging is indicated by pillow structures in basalt. Part of the succession on the western side of the belt has been excised by layer-parallel faulting that may have coincided with the upright folding event that produced the Mount Anderson Syncline (Fig. 9) or with the east-verging reverse faults associated with the Waroonga Shear Zone (Liu and Chen, 1998; Zibra et al., 2013b, this volume). All rocks have been metamorphosed at greenschist or amphibolite facies.

The lowest exposed unit in the Booylgoo Range greenstone belt is a banded iron-formation which may be tightly refolded at the southern end of the belt. It is overlain by mainly basaltic mafic rocks with thin interbeds of banded iron-formation and shale. The major ridge-forming component of the greenstone belt is a series of prominent units of banded iron-formation that include interbeds of weathered rock. Deeply weathered ultramafic rock outcrops between banded iron-formation units on the

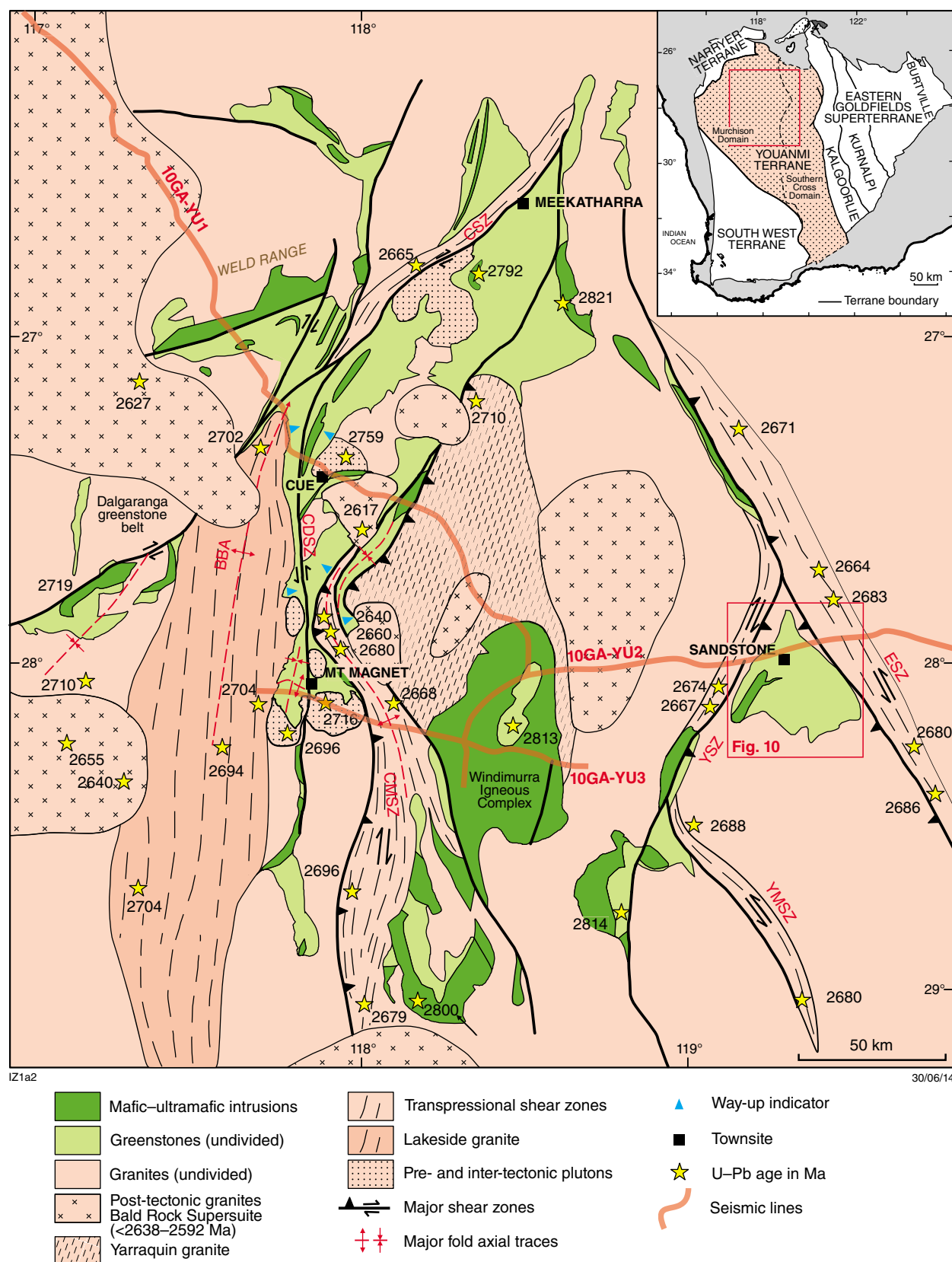


Figure 7. Simplified geological map of northern Youanmi Terrane. BBA – Big Bell anticline; CMSZ – Cundimurra Shear Zone; CDSZ – Cuddingwarra Shear Zone; CSZ – Chunderloo Shear Zone; ESZ – Edale Shear Zone; YSZ – Youanmi Shear Zone; YMSZ – Yuinmery Shear Zone. Modified from Zibra (2012)

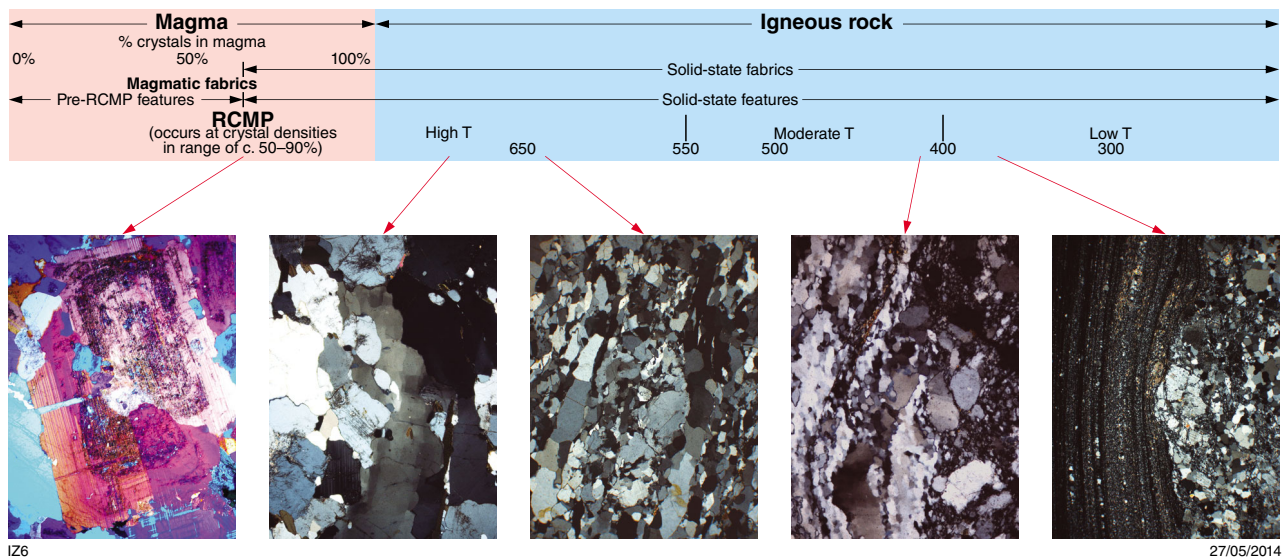


Figure 8. Summary of the wide range of microstructures preserved in the Cundimurra Granite, testifying that deformation started during pluton crystallization and continued during cooling to greenschist facies temperatures

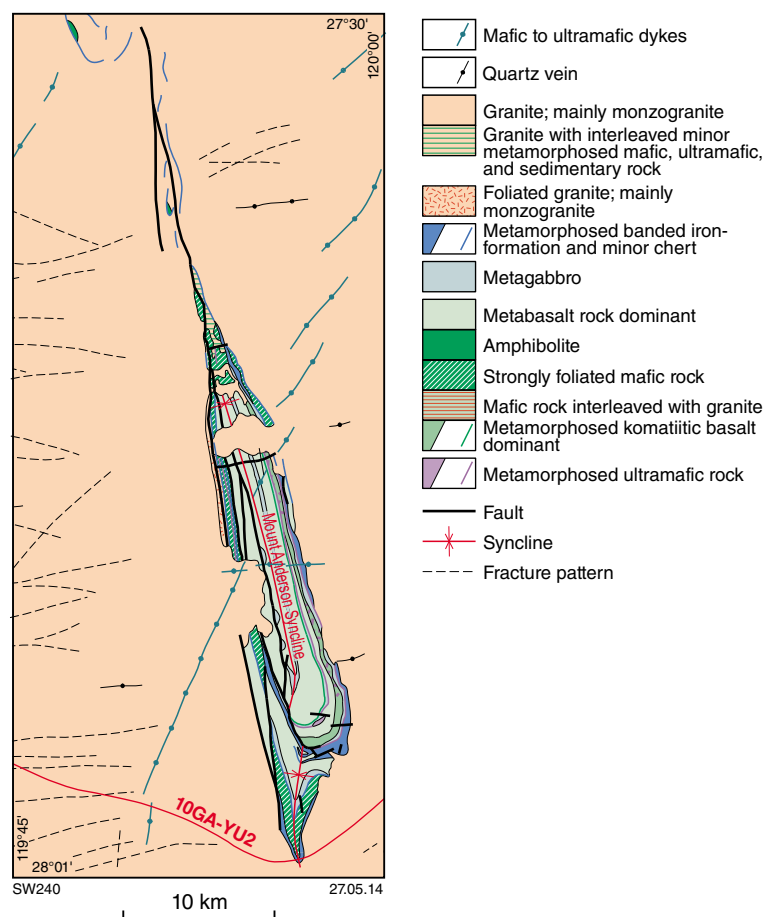


Figure 9. Simplified geological map of the Booylgoo Range greenstone belt showing main structures and lithotypes

eastern side of the belt. The major banded iron-formation interval is overlain in the south by a strongly differentiated mafic-ultramafic body. This unit is less evident in the north where it is most commonly exposed as a medium-grained gabbro. The top of the differentiated body is commonly marked by a thin unit of grey shale. Above the grey shale, pyroxene spinifex-textured basalt is overlain by massive basalt, which is in turn overlain by a second differentiated mafic-ultramafic sill. The upper part of the exposed succession includes a differentiated gabbroic body in a dominantly basaltic succession.

Sandstone greenstone belt

The Sandstone greenstone belt (Chen, 2005) occupies a triangular area between the northeasterly trending Youanmi Shear Zone and the northwesterly trending Edale Shear Zone, with the northern apex of the triangle at the junction of the shear zones, and the southern margin disrupted by granite intrusions (Fig. 10). The triangle is approximately 40 km along its southern margin, and 35 km from south to north. Greenstones are locally well exposed in the western, eastern, and southeastern parts. Stewart et al. (1983) interpreted greenstones in the Sandstone area as a regional-scale, north-plunging anticline that largely defined the stratigraphy of the Sandstone greenstone belt. In that interpretation, the lower part of their stratigraphic column was composed of ultramafic rocks and komatiitic basalt; the middle part consisted mainly of tholeiitic basalt, banded iron-formation, and chert, with minor gabbro and ultramafic rocks; and the upper part was dominated by shale, with minor gabbro and limestone.

However, Chen (2005) has reinterpreted the northerly plunging anticline of Stewart et al. (1983) as the doubly plunging Sandstone Syncline (Fig. 10). In this interpretation, an early, tight syncline has been refolded to form a complex, greenstone-belt-scale synclinorium which has been extensively intruded by granite along its southern margin. Structural complexity, poor exposure, and lack of geochronological data make it difficult to establish an overall stratigraphy for the Sandstone greenstone belt (Chen, 2005). A structurally lower, mafic-dominated succession is preserved mainly on the limbs of the regional-scale Sandstone Syncline. This part of the succession contains at least two intervals of abundant banded iron-formation with local subordinate clastic metasedimentary and Mg-rich meta-igneous rocks, including komatiitic basalt and tremolite-chlorite(-talc) schist (Fig. 10).

Rare outcrop, extensive coverage by mineral exploration drillholes, areas of silica caprock, and local outcrop of serpentinized peridotite in the central-southern part of the Sandstone greenstone belt indicate the presence of widespread ultramafic rocks (dominantly komatiite) that appear to occupy a structurally high position in the stratigraphy (Chen, 2005). The stratigraphic relationship of this ultramafic-dominated succession with the structurally

lower, mafic-dominated succession described above is uncertain due to the poor exposure. They may be unconformable, separated by a fault, or the ultramafic-dominated succession may be the intensely folded and detached top part of the mafic-dominated succession in this area (Chen, 2005). The apparent abundance of ultramafic rocks in the Sandstone greenstone belt is unusual in the northern part of the Southern Cross Domain (Chen, 2005) but there are major komatiite-hosted nickel deposits at Forrestania (Collins et al., 2012) and Lake Johnston (Heggie et al., 2012a,b) to the south.

The only geochronological constraint from within the Sandstone greenstone belt is from porphyritic microgranite that intrudes ultramafic rocks in the Bulchina gold mine south of Sandstone (Fig. 10). This rock has a U–Pb zircon age of 2731 ± 14 Ma (Nelson, 2004), and a SHRIMP U–Pb monazite age of 2731 ± 3 Ma (Nelson, 2005).

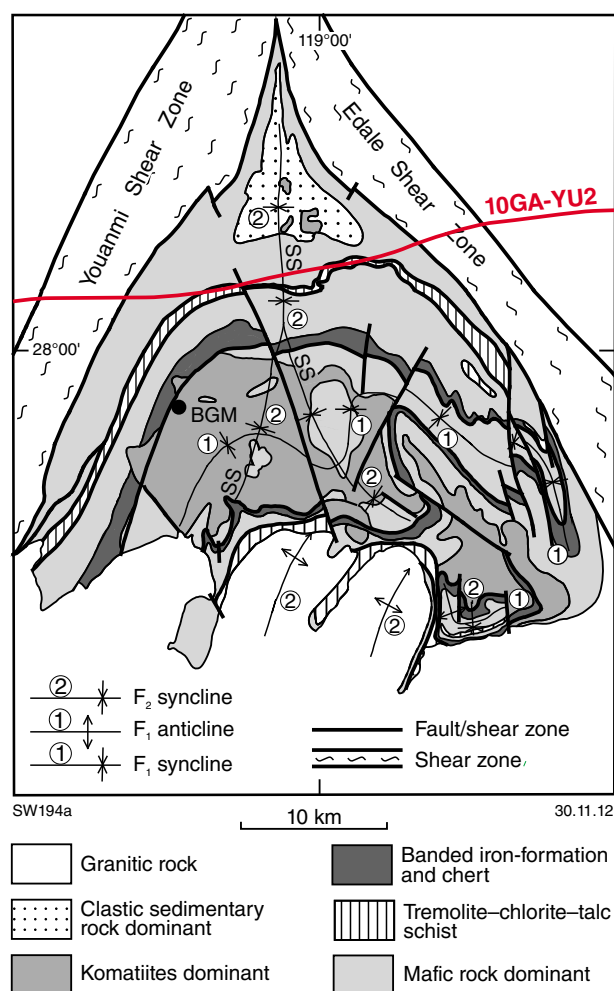


Figure 10. Interpreted geological map of the Sandstone greenstone belt showing path of seismic line 10GA-YU2. BGM – Bulchina gold mine; SS – Sandstone Syncline

Murchison Domain

The Murchison Domain occupies the western half of the Youanmi Terrane (Fig. 11). To the east it is bounded by the Southern Cross Domain along the Youanmi Shear Zone. To the northwest, the poorly defined boundary with the Narryer Terrane is overprinted by voluminous granite plutons. The southern boundary with the South West Terrane is also poorly defined.

The exposed Murchison Domain comprises approximately 60% granitic plutons and 40% greenstone belts, which have a large component of layered mafic–ultramafic intrusions.

Stratigraphy

Four autochthonous volcano-sedimentary groups have been defined for the Murchison Supergroup in the Murchison Domain, based on contact relationships, geochronology, geochemistry, and lithology (Fig. 12; Van Kranendonk et al., 2012). The oldest known components of the Murchison Supergroup lie in the southern part of Murchison Domain, where greenstones in the Mount Gibson and Golden Grove areas have been dated at c. 2935 Ma and c. 2960–2945 Ma, respectively (Yeats et al., 1996; Wang et al., 1998).

At Golden Grove, the c. 2960–2945 Ma felsic volcanic succession (>1 km thickness) is unconformably overlain by a unit of banded iron-formation and volcanoclastic mass-flow sedimentary rocks that contain zircon populations dated at 2945 ± 4 Ma and 2809 ± 5 Ma (Wang, 1998), the latter of which is interpreted as the maximum age of deposition of this unit. The c. 2809 Ma population lies within the upper range of the widespread Norie Group (c. 2820–2800 Ma), which forms the lowermost stratigraphic unit across the better exposed and more thoroughly studied northern part of the domain. The Norie Group consists of several kilometres thickness of stratigraphy with a lowermost unit of interbedded Ti-rich, Al-depleted komatiites and komatiitic volcanoclastic rocks (Barley et al., 2000) and a thick succession of pillowed and massive tholeiitic basalt (Murrouli Basalt; Watkins and Hickman, 1990). Conformably overlying the Murrouli Basalt is the Yaloginda Formation, which consists of rhyolite, fine- to medium-grained felsic volcanoclastic sedimentary rocks, and interbedded units of ferruginous shale and banded iron-formation dated at 2814 ± 3 to 2806 ± 4 Ma (Van Kranendonk and Ivanic, 2009). Norie Group volcanism was accompanied by the emplacement of very large (up to 7 km thick and 80 km diameter) layered mafic–ultramafic igneous complexes of the Meeline Suite (c. 2810 Ma) and Narndee Igneous Complex (c. 2800 Ma; Ivanic et al., 2010).

The c. 2800–2740 Ma Polelle Group conformably overlies the Norie Group. It consists of four conformable formations: the thin, basal quartzitic Coodardy Formation; the lower Meekatharra Formation of dominantly tholeiitic basalt, komatiitic basalt, komatiite, and thin interflow felsic volcanoclastic sedimentary rocks (c. 2800–2760 Ma); the intermediate Greensleeves Formation of andesitic to rhyolitic volcanic and volcanoclastic rocks

(c. 2760–2740 Ma); and interbedded banded iron-formation, shale, and felsic volcanoclastic rocks of the Wilgie Mia Formation (c. 2760–2740 Ma). The younger stage of volcanism was accompanied by emplacement of the Gnanagooragoo Igneous Complex (Fig. 13), a thick, differentiated mafic–ultramafic intrusion that was emplaced below and within the banded iron-formation of the Wilgie Mia Formation in the Weld Range at some time between c. 2752 Ma, the age of a plagioclase feldspar crystal tuff unit, and c. 2740 Ma, the age of a cross-cutting granitic intrusion (Wang, 1998; Van Kranendonk et al., 2010). The absolute thicknesses of the formations of the Polelle Group are difficult to determine due to deformation. However, they appear to be at least 5 km thick.

The c. 2735–2710 Ma Glen Group, which unconformably overlies the Polelle Group (Van Kranendonk et al., 2010), consists of the lower Ryansville Formation of clastic sedimentary rocks and the conformably overlying Wattagee Formation of komatiitic basalt and subordinate rhyolite. Deposition of the Glen Group was coeval with emplacement of widespread, thick, differentiated gabbro sills of the Yalgowra Suite. As the top contact of the group is not exposed, the thickness of 2 km is a minimum estimate. The cumulative thickness of the Yalgowra Suite sills is approximately 1 km.

Mafic Suites

Four components of mafic–ultramafic intrusive rocks have been identified in the northern part of the Murchison Domain (Figs 12 and 13; Ivanic et al., 2010). They include three suites of mafic–ultramafic intrusive rocks: the c. 2810 Ma Meeline Suite, the c. 2800 Ma Boodanoo Suite, and the c. 2720 Ma Yalgowra Suite (Ivanic et al., 2010); and the Gnanagooragoo Igneous Complex, which has not been assigned to one of the mafic–ultramafic suites.

- The Meeline Suite consists of five large, layered mafic–ultramafic complexes. All are >3 km thick and contain similar elements, including igneous layering that ranges in composition from dunite through to anorthosite with thick layers of magnetitite. For further details, see Windimurra Igneous Complex.
- The Boodanoo Suite consists of the Narndee Igneous Complex, which is located south of the Windimurra Igneous Complex (Fig. 13). The Narndee Igneous Complex is compositionally distinctive in that it contains a large volume of hornblende gabbro, a larger proportion of ultramafic rocks, and lacks the characteristic magnetitite layers of Meeline Suite intrusive complexes. It is thus considered to have been derived from different parent magma to that of the Windimurra Igneous Complex (Scowen, 1991). As with the Meeline Suite, the Narndee Igneous Complex was emplaced into the Norie Group at shallow crustal levels of between 3 and 9 km, estimated from pyroxene geobarometry (Scowen, 1991). A SHRIMP U–Pb age on zircon and baddeleyite of 2800 ± 6 Ma from a gabbro-norite (GSWA 191056, Ivanic et al., 2010) is consistent with a Sm–Nd whole-rock isochron for the Narndee Igneous Complex of 2824 ± 80 Ma (Scowen, 1991).

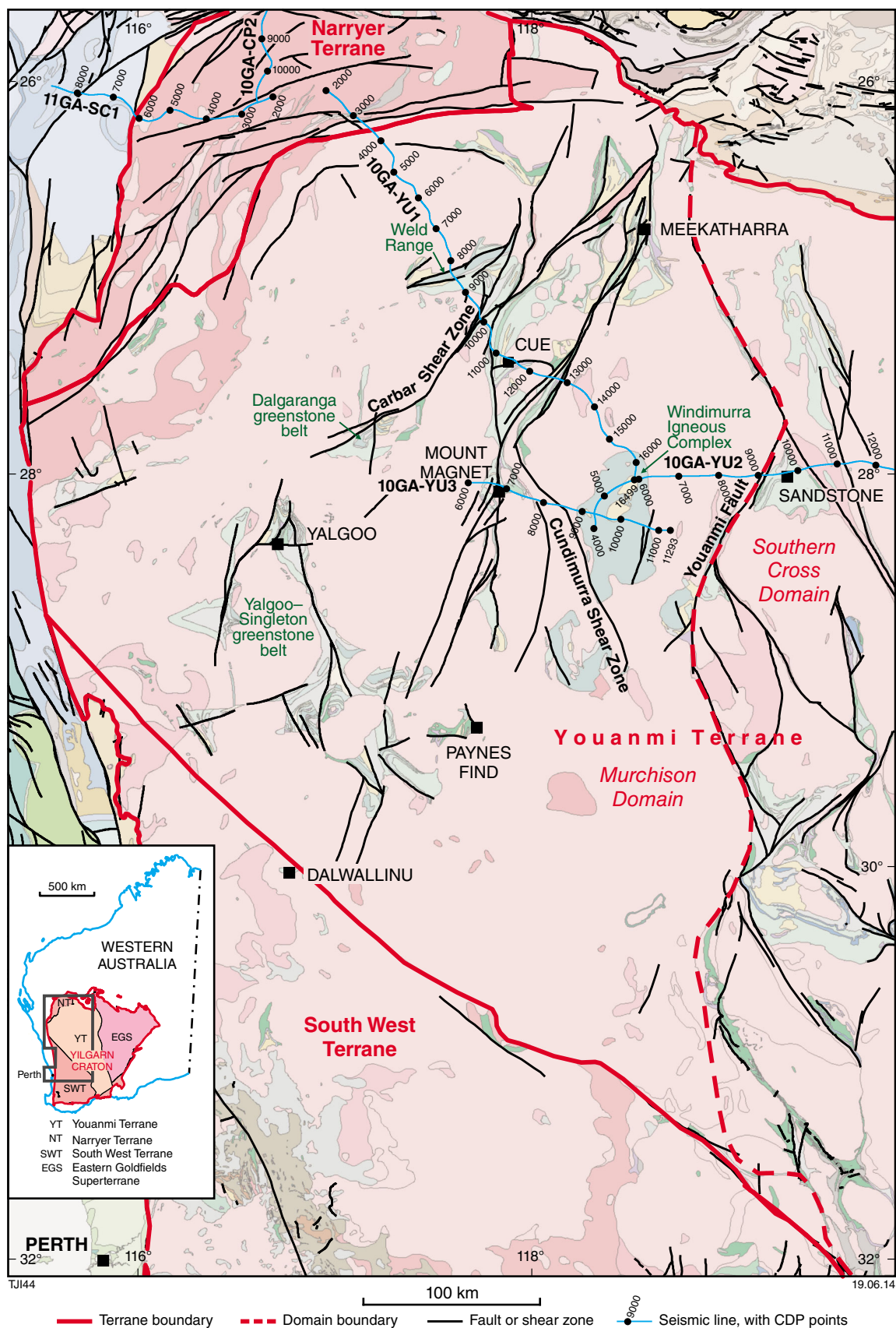


Figure 11. Map showing the extent of the Murchison Domain and its major greenstone belts relative to adjacent terranes and the Southern Cross Domain. The Meekatharra – Mount Magnet greenstone belt (not labelled) accounts for the majority of supracrustal rocks in the Murchison Domain. The location of five seismic lines 09GA-CP3, 10GA-SC1, 10GA-YU1, 10GA-YU2, and 10GA-YU3 are shown, and 1:500 000-scale geology is displayed in the background.

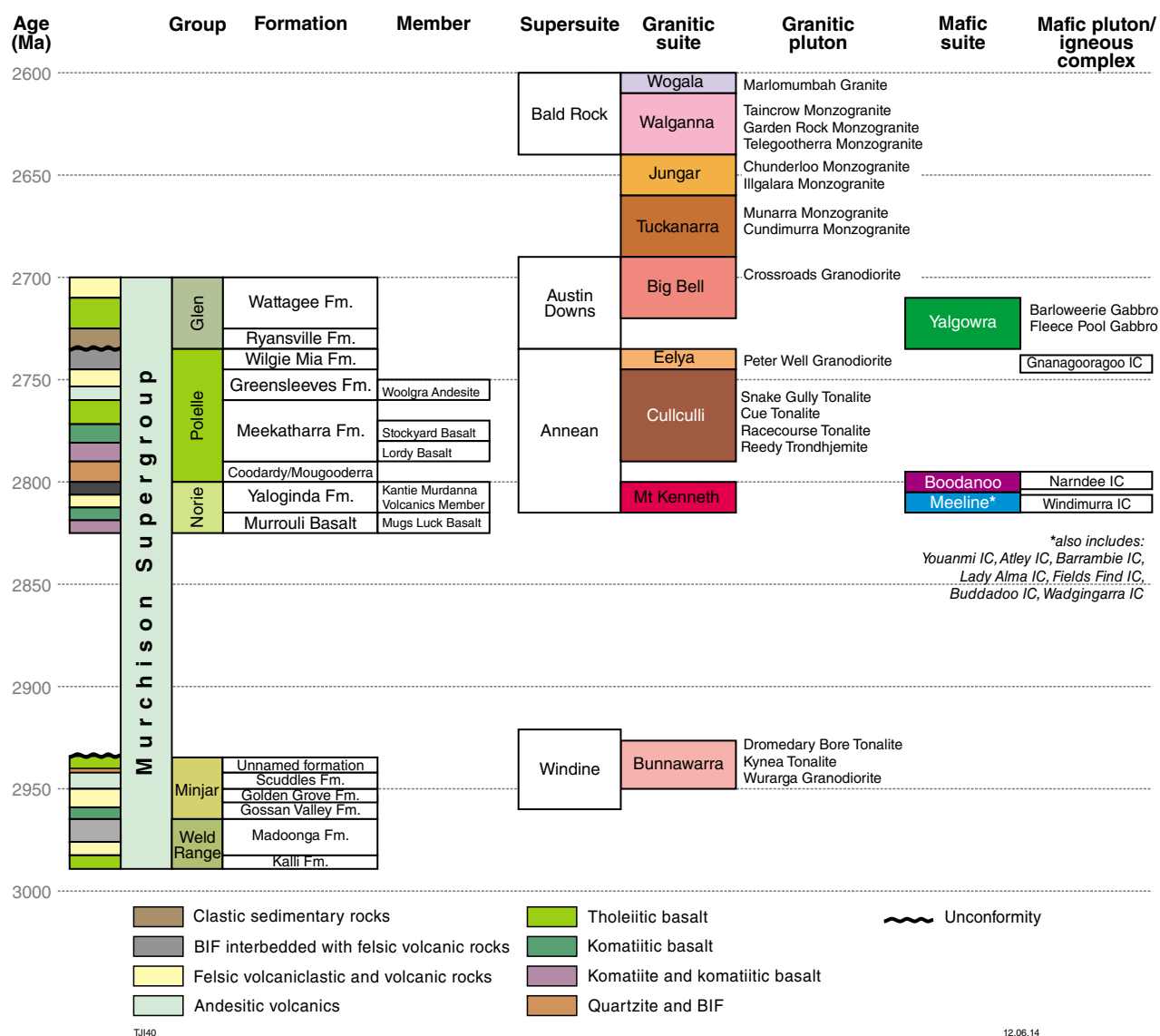
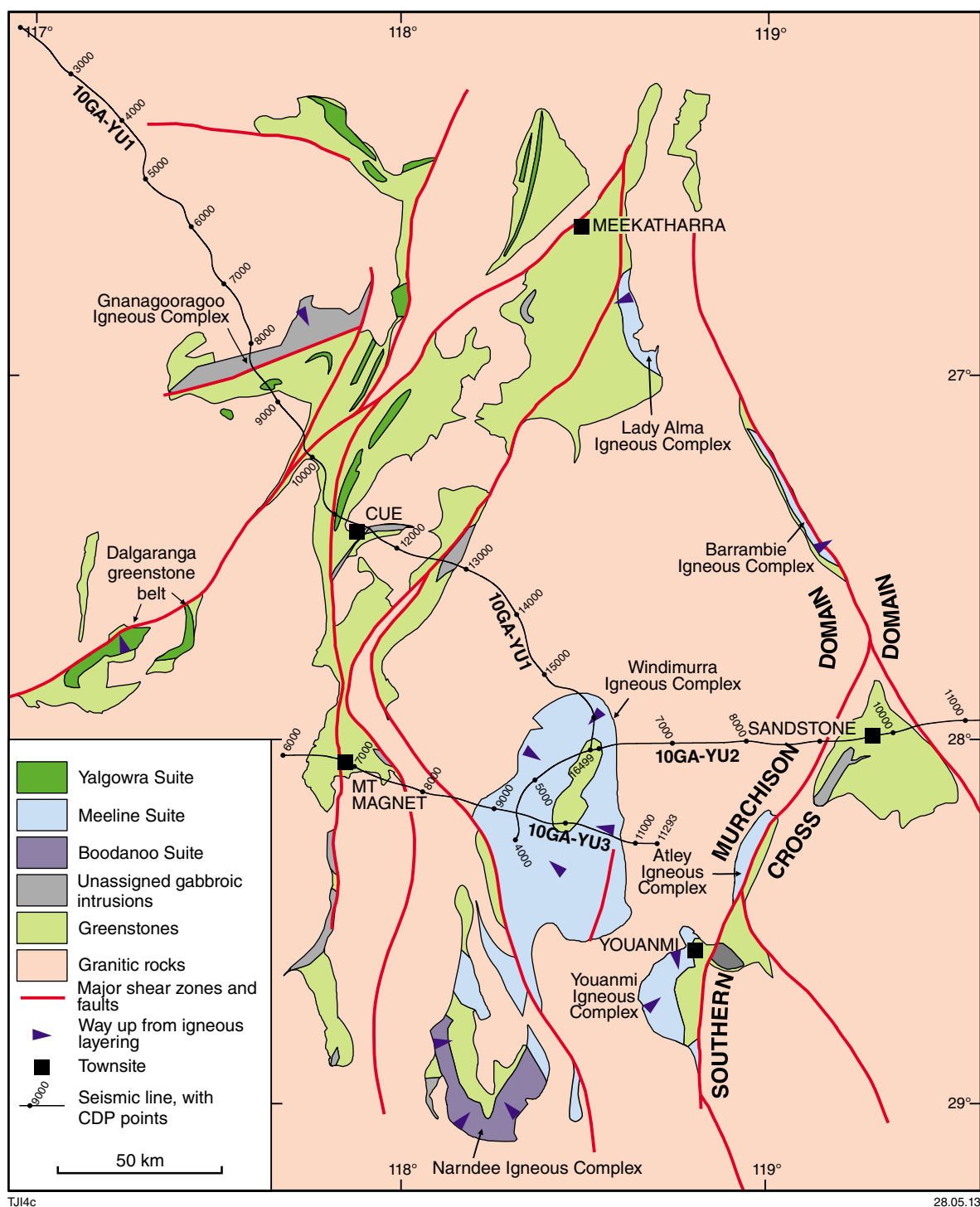


Figure 12. Stratigraphic scheme for the Murchison Domain, divided into three main columns for supracrustal rocks, granitic rocks and mafic-ultramafic intrusive rocks

- The Gnanagooragoo Igneous Complex is a thick, differentiated mafic-ultramafic intrusion that was emplaced below and within the banded iron-formations of the Weld Range (Wilgie Mia Formation). At lower stratigraphic levels, the complex consists of a funnel-shaped intrusion of ultramafic cumulate rocks that have been explored for PGE–Cr–Au and Ni–Co mineralization (Parks, 1998). At stratigraphically higher levels, thick, sheeted sills of homogeneous gabbro and dolerite split apart c. 2785 Ma felsic volcanoclastic rocks and interbedded banded iron-formations (M Wingate, 2013, written comm., 15 January 2013). Geological constraints indicate it was emplaced after c. 2785 Ma but before c. 2735 Ma.
- Thick differentiated mafic-ultramafic sills of the Yalgowra Suite are associated with the komatiitic basalts of the Glen Group (Wattagee Formation). These sills are predominantly hosted in felsic volcanoclastic rocks of the Greensleeves Formation (Pollelle Group) but are absent from the Glen Group (Fig. 3; Van Kranendonk et al., 2012).

In summary, suites of mafic-ultramafic rocks were emplaced as layered intrusions during periods of mafic volcanism. The most voluminous intrusions belong to the c. 2820 Ma Meeline Suite and include the Windimurra Igneous Complex (2500 km²), which hosts significant vanadium mineralization in magnetite layers.



TJ14c

28.05.13

Figure 13. Simplified geological map of the northern Murchison Domain, highlighting the location of mafic–ultramafic intrusive suites relative to greenstone belts and shear zones. Also shown is the igneous differentiation way-up direction for the major igneous complexes. The locations of three seismic lines are also shown (10GA-YU1, 10GA-YU2, 10GA-YU3). Modified from Ivanic et al. (2010)

Granitic suites

Eight suites of granitic rocks have been described for the northern Murchison Domain, based on composition, cross-cutting relationships, and age (Figs 12 and 14). A ninth, older occurrence of granites has been recorded in the Mount Gibson area in the far southern part of the domain, where c. 2935 Ma monzogranite intrudes the base of greenstones and is contemporaneous with subvolcanic felsic porphyritic intrusions emplaced higher up within the greenstones (Yeats et al., 1996).

In the northern part of the domain, widespread synvolcanic granitic rocks (Annean Supersuite) were emplaced at the same time as the deposition of the Norie and Polelle Groups (c. 2815–2740 Ma). Three geochemically distinct suites have been identified within the supersuite, the oldest being the Mount Kenneth Suite (Ivanic et al., 2012). Plutons from this suite intruded into the upper and marginal regions of large layered mafic–ultramafic igneous complexes of the Meeline and Boodanoo Suites between c. 2815 and 2800 Ma, and are considered to represent local melts generated by the thermal effects of the emplacement of these complexes. Contemporaneous with the Polelle Group, the Cullculli Suite (c. 2785–2735 Ma) is composed dominantly of tonalite–trondhjemite–granodiorite (TTG), which commonly exhibit a distinctive, mafic, clotty texture consisting of elliptical hornblende ± biotite clots ranging in size from 1 to 8 cm (Van Kranendonk et al., 2010). Some plutons of the Cullculli Suite also contain syn-plutonic mafic dykes, while others are mafic tonalite with 15–20% hornblende phenocrysts. The Eelya Suite includes granitic rocks which are particularly enriched in high-field-strength elements (HFSE; Cassidy et al., 2002).

The felsic intrusive rocks of the Austin Downs Supersuite are assigned to the Big Bell Suite, which includes tonalitic to monzogranitic rocks ranging in age from c. 2724 to 2690 Ma.

The c. 2690–2670 Ma Tuckanarra Suite consists of tonalitic to monzogranitic rocks which intrude greenstone belts, and the c. 2665–2640 Ma Jungar Suite includes mainly K-feldspar porphyritic monzogranites.

The post-tectonic Bald Rock Supersuite of undeformed granites is subdivided into two suites: the c. 2630–2610 Ma Walganna Suite of biotite ± muscovite monzogranite to syenogranite that ranges from coarsely K-feldspar porphyritic to coarse-grained and equigranular, and the c. 2605 Ma Wogala Suite of fluorite-bearing alkali granite.

Granitic suites in relation to Lu–Hf and geochemical data

The Murchison Domain contains a remarkable record of continuous, but geochemically evolving, granite magmatism over c. 210 m.y., from the oldest syn-volcanic granites at c. 2810 Ma to the youngest post-tectonic granites at c. 2600 Ma. The earliest granites in this sequence (c. 2810–2800 Ma) are shallow crustal melts associated with adjacent, contemporaneous, large, layered mafic–ultramafic igneous complexes. This event, the major phase of juvenile input into the crust, has been interpreted

to be the result of impingement of a mantle plume into the base of the lithosphere. Isotopic data indicate the plume tapped a 3.04 Ga mantle source (Ivanic et al., 2010, 2012). The involvement of 3.04 Ga source material (i.e. basement material of Golden Grove Group age) was important from c. 2810–2650 Ma (Fig. 15b) and the involvement of older basement in the source was significant at least at c. 2750 Ma and c. 2620 Ma. The postulated plume activity at c. 2810 Ma was the precursor of a protracted series of events that would eventually lead to cratonization of the domain (Fig. 15c).

A diverse but systematically evolving range of granitic compositions continued from c. 2760 to 2600 Ma. During this time, the intrusion of primitive, isotopically juvenile hornblende tonalites evolved to more fractionated compositions through time. Ivanic et al. (2012) proposed that granites were also sourced at progressively shallower levels, which is likely the result of conductive heat transferring upwards after the final greenstone sequences had been deposited (Fig. 15c). This evolution signifies not only nearly continuous crustal melting over this period, but a change in the source of melts from early melting of deep-crustal amphibolites (generating TTG) to later melting of mid-crustal rocks (the older TTG) generating monzogranites of the Tuckanarra and Jungar Suites, and possible remelting of these and older basement material to generate the Bald Rock Supersuite.

This continuous and progressive evolution of melts ended with cratonization of the domain, probably resulting in almost complete depletion of the lower middle crust. During the most voluminous granitic activity from c. 2700 to 2650 Ma, this depletion likely resulted in the composition of the lower middle crust changing from amphibolite to depleted, garnet-bearing granulite. Weakness in the middle to lower crust due to the extent of melting at this time may be responsible for greenstone sinking and soft-crust deformation (Fig. 15c; Van Kranendonk et al., 2012). The change in granite compositions at c. 2645 Ma is interpreted to reflect renewed heat input at the base of the crust, possibly as a result of delamination of garnet-rich, lower crustal residuum such as an eclogitic layer (Fig. 15c; cf. Smithies and Champion, 1999). This process would have allowed melts to source more evolved material as shown in more negative εHf compositions at this time (Fig. 15a). Delamination could also allow the development of widespread melts (Bald Rock Supersuite) to continue for an extended period. However, a major delamination event would not be required if there had been significant upper crustal insulation. The greenstone blanketing effect, as suggested by Rey et al. (2003) for the period c. 2750–2650 Ma, is compatible with the model proposed above where it would have been most important from c. 2720–2680 Ma (see ‘blanketing?’ in Fig. 15c).

The process of intra-crustal differentiation, as proposed for Eastern Goldfields Superterrane (Campbell and Hill, 1988; Hill et al., 1989) may be applicable in the Murchison Domain and is also consistent with a plume heat source (Ivanic et al., 2010). The shallowing of depth of melting in the Murchison Domain granitic rocks from c. 2765–2600 Ma, as documented by the progressive

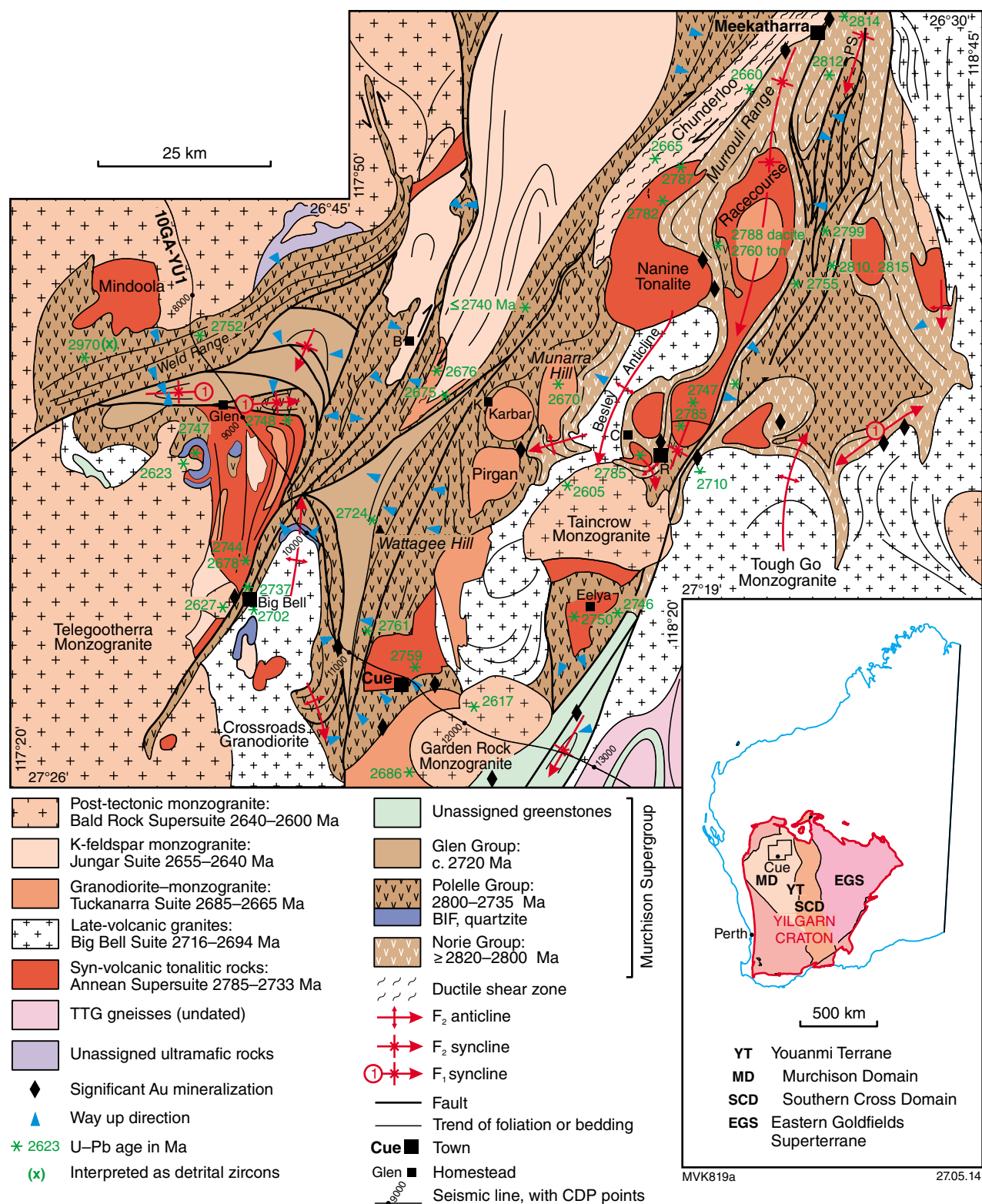


Figure 14. Interpreted bedrock geology map of the Cue to Meekatharra area of the Murchison Domain showing the distribution of supracrustal groups, granitic suites and supersuites, available age data, and major structural features. Interpretation is based on 1:100 000-scale mapping, geochronology and interpretation of aeromagnetic data. G – Gabanintha, PS – Polelle Syncline. The location of seismic line 10GA-YU1 is also shown.

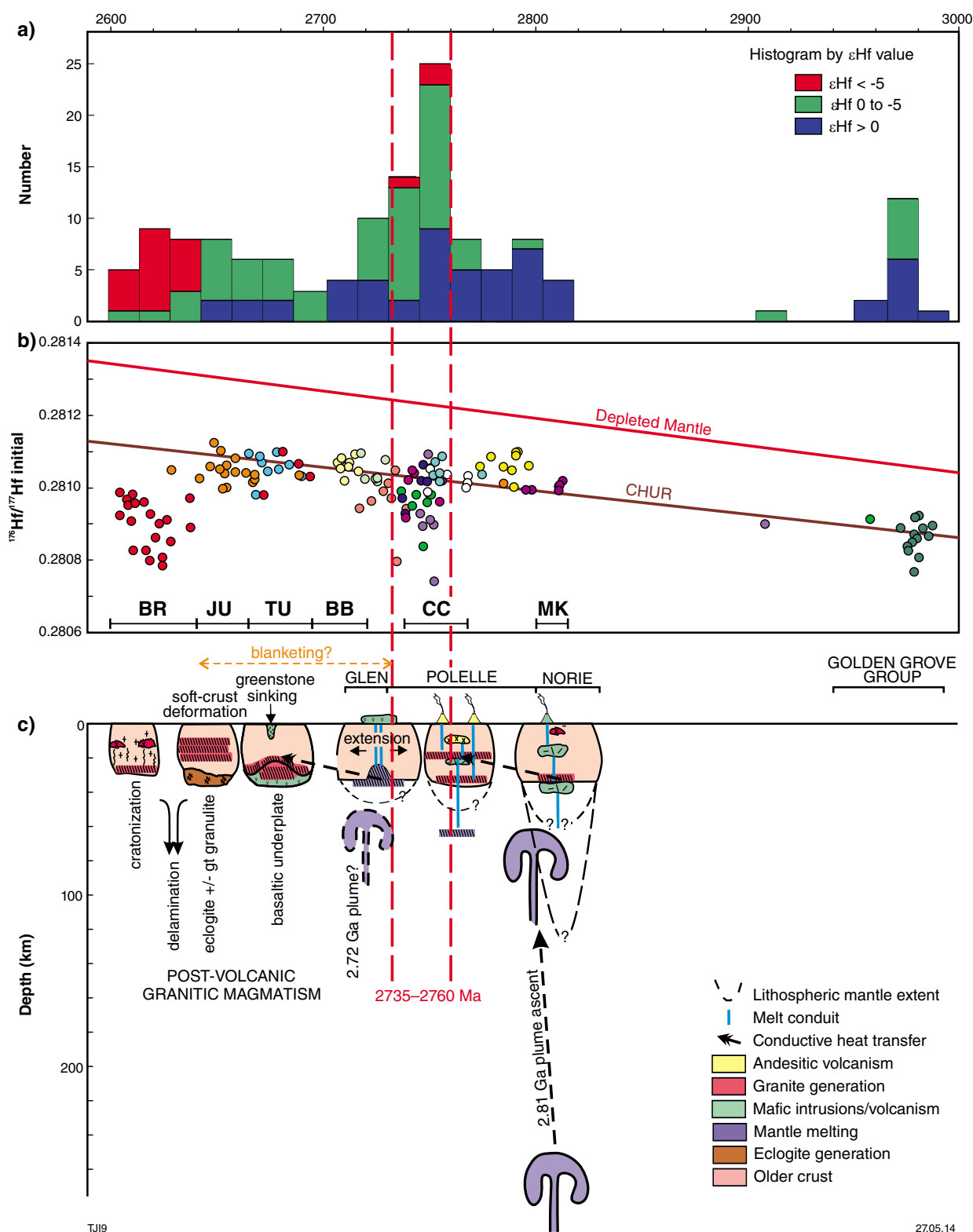


Figure 15. Summary tectonic evolution diagram: a) Histogram of ϵ_{Hf} vs age (Ma). Red bars indicate periods of coeval radiogenic and nonradiogenic sources; b) $^{176}\text{Hf}/^{177}\text{Hf}_i$ vs age in Ma (axis at top of part (a)) for data from this study (samples are shown with single unique colours); depleted mantle and chondritic uniform reservoir (CHUR) evolution model lines shown for reference. Selected suites and supersuites shown at bottom of diagram for reference (BR – Bald Rock Supersuite, JU – Jungar Suite, TU – Tuckanarra Suite, BB – Big Bell Suite, CC – Cullculli Suite, MK – Mount Kenneth Suite); c) Tectonic evolution illustrated with six diagrammatic cross-sections through the lithosphere (and asthenosphere) (age axis at top of part (a)). Deep melting (>200 km, Barley et al., 2000) is indicated in the deep-sourced 2.81 Ga plume and the possibility of a second plume is shown at c. 2.72 Ga. The significant departure of ϵ_{Hf} to extremely negative values (less than -5) is highlighted by vertical dashed red lines across the whole diagram (between 2760 and 2735 Ma) and shown to overlap with the onset of diverse melt sources found during deposition of the Polelle Group.

evolution of the Sm–Nd (Cassidy et al., 2002) and Lu–Hf (Ivanic et al., 2012) isotope systems, indicates that differentiation through time and space is the key process that determined the composition of this part of the Yilgarn Craton before cratonization and stabilization.

Geology of the Windimurra Igneous Complex

Introduction

The Windimurra Igneous Complex (Fig. 16), which is located in the eastern part of the Murchison Domain (Fig. 11), is the largest, relatively intact and exposed, mafic–ultramafic intrusion in Australia (Ivanic et al., 2010). The complex is the type example of the c. 2810 Ma Meeline Suite and has been directly dated at 2813 ± 3 Ma (Wingate et al., 2012). Primary igneous layering features are well preserved and the layering is typically concentric and inward dipping. There are several economic vanadium deposits hosted within the magnetitites of the upper zone. The central-northern part of the complex is overlain by the rhyolitic Kantie Murdana Volcanics Member, also dated at 2813 ± 3 Ma (Nelson, 2001).

The coherent main body of the complex extends for 85 km north–south and 37 km east–west, and covers an area of c. 2500 km². Additional regions of intrusive rock associated with the complex are metamorphosed and occur as sheared lenses to the south and east of the main body, east of the Challa Shear Zone. Based on aeromagnetic images, these features are up to 25 km long north–south and 5 km wide east–west. The Windimurra Igneous Complex is the westernmost of the identified igneous complexes in the Meeline Suite. However, it is possible that intrusions belonging to the Meeline Suite form part of the Yalgoo–Singleton greenstone belt which lies some 150 km to the southwest.

There is an overall progression from more mafic rocks in the lower zone to large volumes of leucocratic rocks in the middle and upper zones. Within these zones, megacycllicity on an approximately 200 m scale can be related to at least 13 documented reversals in the chemostratigraphy (Ahmat, 1986). The exposed complex has an extremely felsic overall composition compared to other layered gabbros worldwide. However, it is possible that this may be accounted for by a large volume of ultramafic zone material at depth.

Igneous stratigraphy

The stratigraphy of the Windimurra Igneous Complex (Fig. 17) is comparable in composition and thickness to many other large layered mafic–ultramafic intrusions worldwide, and others in the Murchison Domain. The cumulative thickness of the exposed layers of gabbroic and ultramafic rocks is 13 km where they exhibit lateral aggradation or offlap geometry (Ahmat, 1986). This may represent a true thickness of about 6 km as suggested by the observation that shallower dips (as low as 10°) are

present in the upper parts of the complex and examples of onlap have also been noted in several localities around the complex. The Shephards Discordant Zone, which is at least 20 km long, represents a significant break in the igneous stratigraphy (several kilometres). However, the precise origin of this feature is still not fully understood (Ahmat, 1986; Bunting, 2004). It is possible that the Shephards Discordant Zone separates the complex into two main parts: an older eastern lobe and a younger, transgressive western lobe, both of which contain a lower, middle and upper zone of similar nature. Figure 18 shows a possible multi-stage evolution for the various components of the complex.

The complex is divided into eight parts: a border zone, ultramafic zone, lower zone, middle zone, upper zone, roof zone and Corner Well Gabbro and other unassigned units. See Ivanic et al. (2013, this volume) for further details.

Narryer Terrane

The Narryer Terrane is one of Earth's oldest crustal fragments and contains the oldest known rocks in Western Australia. The terrane is situated in the northwestern part of the Yilgarn Craton and comprises granitic rocks and granitic gneisses ranging in age from early through to late Archean (Kinny et al., 1988; Nutman et al., 1991; Pidgeon and Wilde, 1998). These are interlayered with: 1) deformed and metamorphosed supracrustal rocks (including the extensive metasedimentary rocks at Mount Narryer and Mount Murchison; Williams and Myers, 1987), and 2) local areas of banded iron-formation, mafic and ultramafic intrusive rocks, and metasedimentary rocks (Williams and Myers, 1987; Myers, 1988a; Kinny et al., 1990).

The oldest components of the Narryer Terrane are a dismembered layered igneous complex (anorthosite–gabbro–ultramafic intrusion) known as the Manfred Complex, and felsic intrusive rocks of the Meeberrie Gneiss (Myers and Williams, 1985; Myers, 1988b). Leucogabbro and meta-anorthosite inclusions, belonging to the Manfred Complex and included within syenogranitic Dugel Gneiss, have a magmatic SHRIMP U–Pb zircon age of 3730 ± 6 Ma (Kinny et al., 1988). Rocks of the Meeberrie Gneiss are generally migmatitic and the oldest component has a similar, maximum, SHRIMP U–Pb zircon age of 3730 ± 10 Ma (Kinny and Nutman, 1996).

Both the Meeberrie Gneiss and the Manfred Complex were intruded by various felsic magmas (Dugel and Eurada Gneisses) before a major magmatic event at c. 3300 Ma, accompanied by deformation and amphibolite to granulite facies metamorphism (Kinny et al., 1988; Myers, 1988a; Nutman et al., 1991, 1993; Pidgeon and Wilde, 1998). Further felsic magmatism is believed to have occurred at c. 3100 Ma (Nutman et al., 1991). These events took place prior to deposition of the supracrustal sequences predominantly exposed in the Jack Hills greenstone belt and the Mount Narryer region (Compston and Pidgeon, 1986; Maas and McCulloch, 1991).

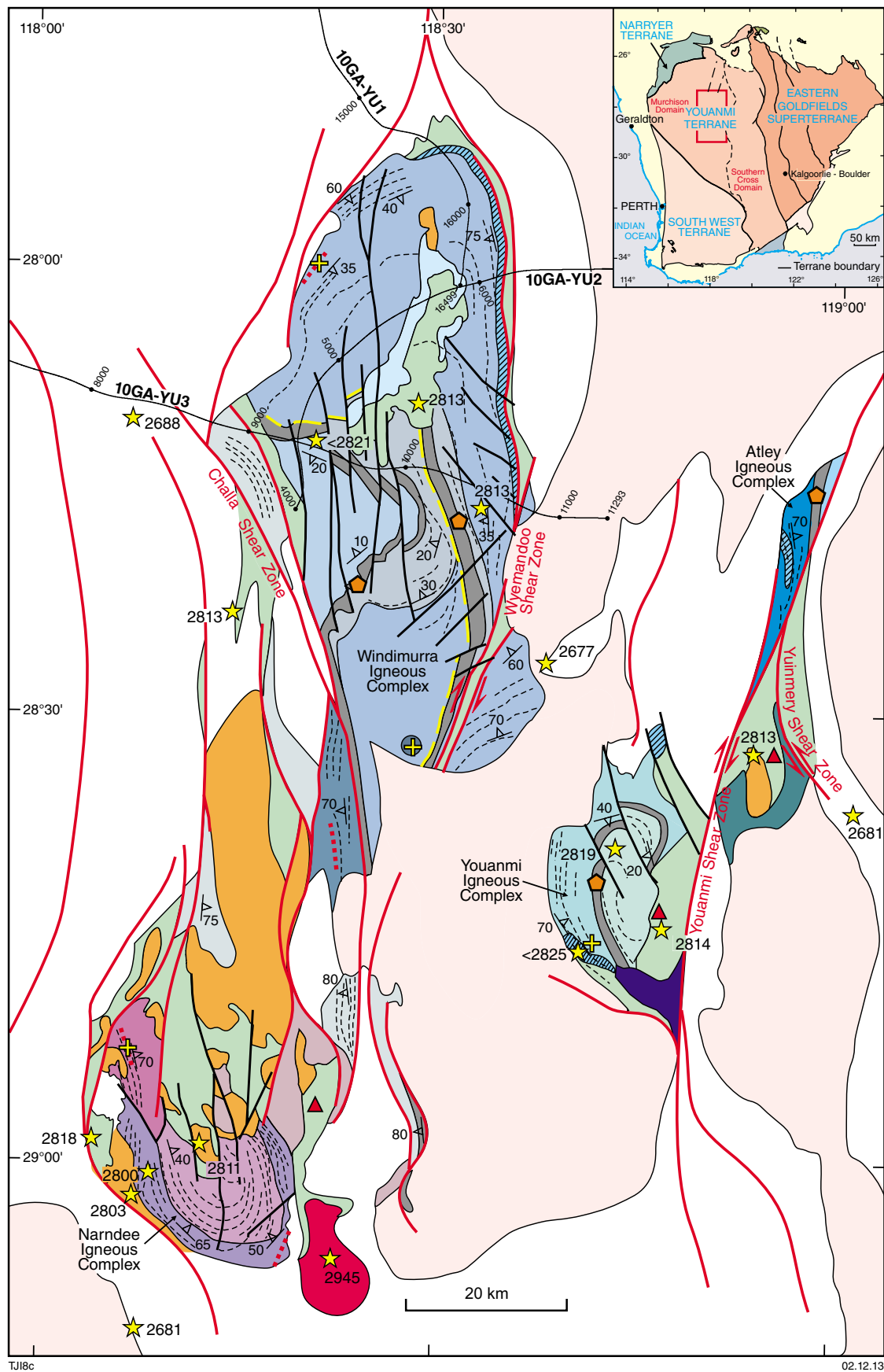
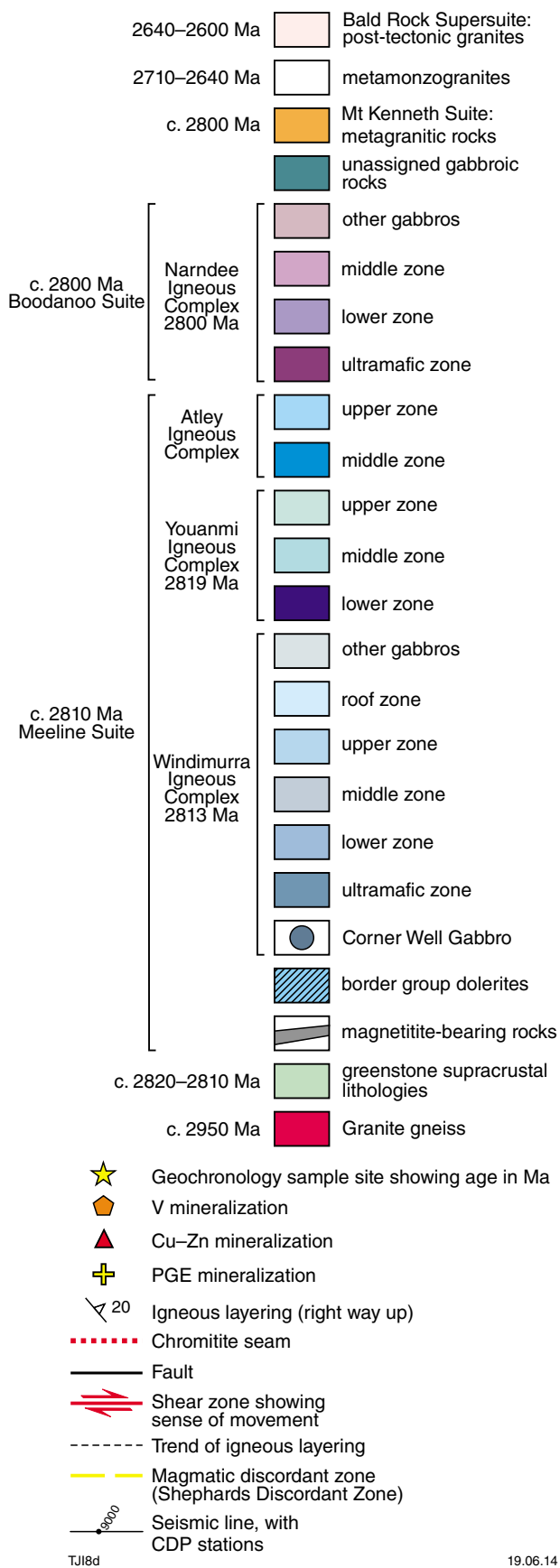


Figure 16. Interpreted geological map of the Windimurra, Narndee, Youanmi and Atley Igneous Complexes, highlighting available geochronological data and mineralization styles. Note the location of the Shephards Discordant Zone in the Windimurra Igneous Complex and the location of three seismic lines (10GA-YU1, 10GA-YU2, 10GA-YU3). See also Legend overleaf.



TJ18d

19.06.14

Figure 16. Legend

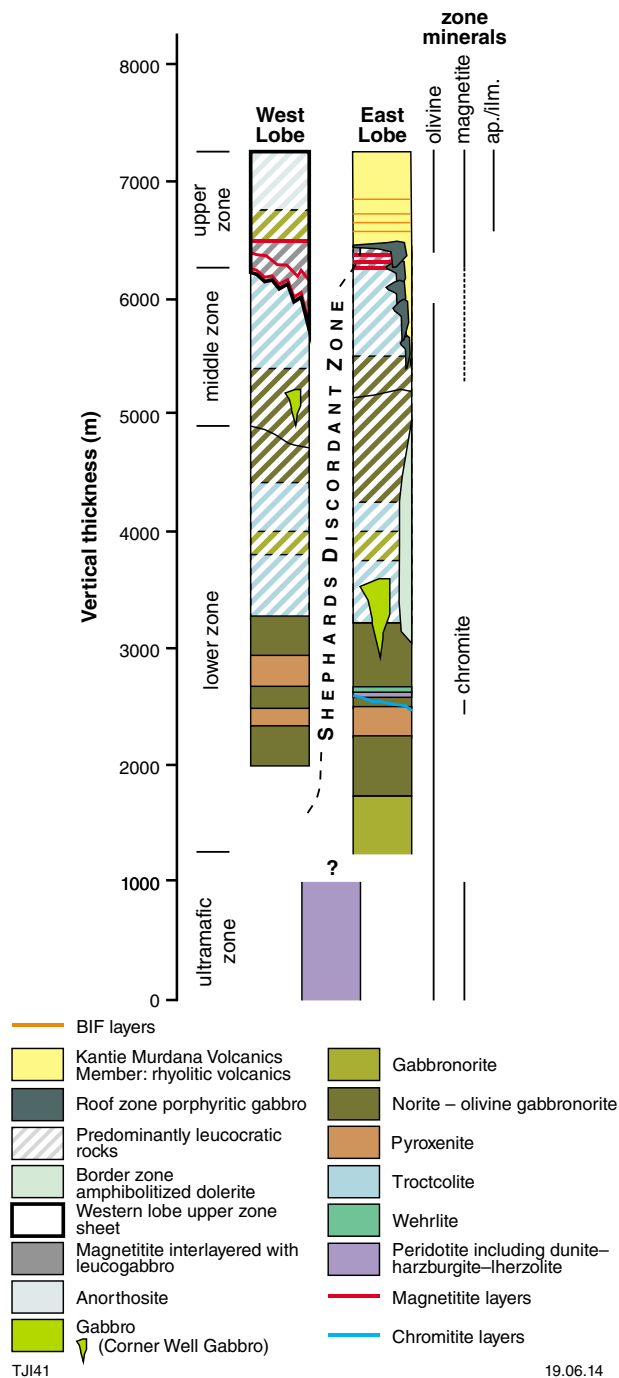


Figure 17. Igneous stratigraphic column for the Windimurra Igneous Complex showing true thickness for all major components of the complex as derived from observations made at the surface. The complex is divided into an eastern and western lobe along the Shephards Discordant Zone. Note major oxide horizons of chromite-rich and magnetite-rich lithologies

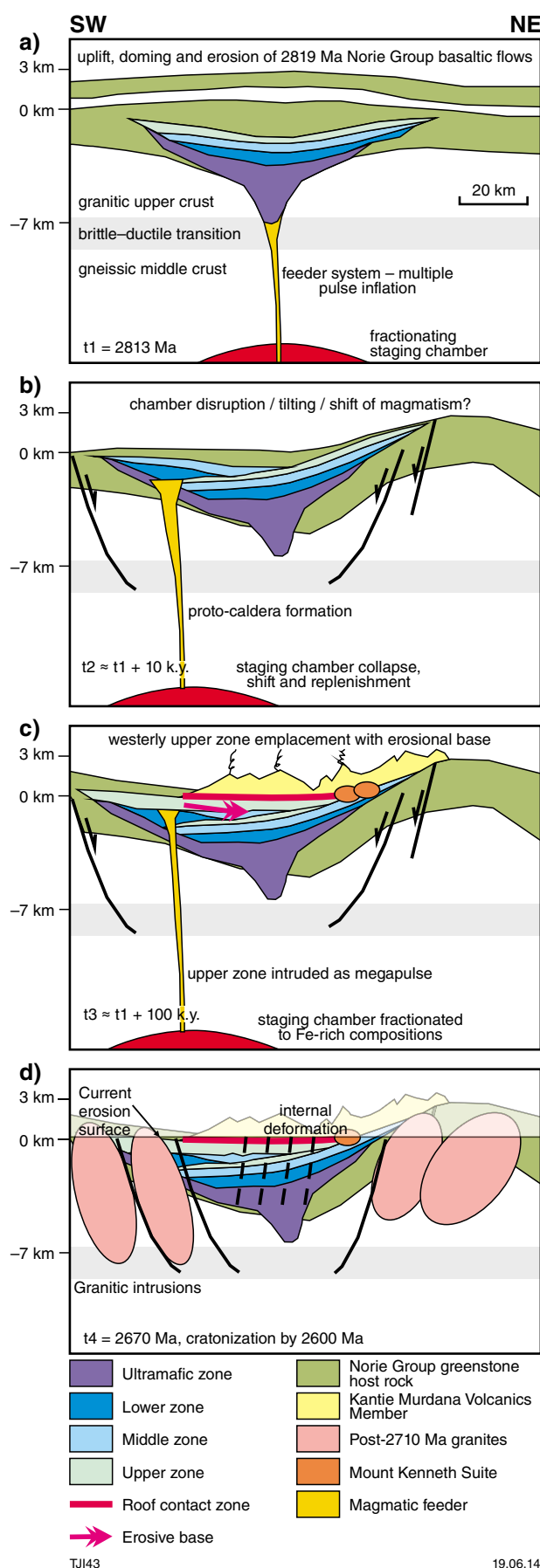


Figure 18. A possible multi-stage evolution for the various components of the Windimurra Igneous Complex

The southern margin of the Narryer Terrane and its boundary to the Youanmi Terrane is defined by the Balbalinga and Yalgar Faults. The latter is interpreted as a major dextral strike-slip fault (Myers, 1990b, 1993) but the structural history of this fault is poorly understood, and the boundary is likely to be reworked and cryptic (Nutman et al., 1993). The early Archean gneisses of the Narryer Terrane have been interpreted as an allochthon that was thrust over approximately 3000–2920 Ma granitic crust of the Youanmi Terrane, prior to or during late Archean granitic magmatism that stitches the terranes (Nutman et al., 1993). Although there is evidence of deformation prior to the intrusion of these granites, the deformation that produced the main tectonic grain across both terranes is believed to have occurred under amphibolite facies conditions between c. 2750 and 2620 Ma (Myers, 1990b).

The Jack Hills greenstone belt, which is the only coherent greenstone belt within the Narryer Terrane, lies along the interpreted southern margin. It comprises greenschist- to amphibolite-facies banded iron-formation, mafic and ultramafic rocks, and both Archean and Paleoproterozoic metasedimentary rocks (Spaggiari, 2007a). Amphibolite- to granulite-facies metasedimentary rocks at Mount Narryer, as in the Jack Hills greenstone belt, contain detrital zircons that are older than 4000 Ma (Williams and Myers, 1987; Compston and Pidgeon, 1986; Wilde et al., 2001). Rasmussen et al. (2010) obtained an age of c. 3080 Ma from monazite and authigenic xenotime in banded iron-formation from the Jack Hills. This is a minimum depositional age for at least part of the succession. Various studies have shown the age of the youngest detrital zircon population in the typical quartzite and conglomerate succession to be >3000 Ma (e.g. Crowley et al., 2005). However, detrital zircon grains as young as c. 1220 have been reported from clastic sedimentary units within the belt (Cavosie et al., 2004; Dunn et al., 2005; Grange et al., 2010). Wilde (2010) has found zircons as young as c. 1598 Ma in rocks, interpreted as volcanic rocks, on the southern side of the belt.

The Paleoproterozoic Capricorn Orogeny produced intracratonic, predominantly greenschist facies, dextral transpressional reworking of both the northern and southern margins of the Narryer Terrane. These effects are evident in the Errabiddy Shear Zone (e.g. Occhipinti and Reddy, 2004), the Jack Hills greenstone belt (Spaggiari, 2007a,b), and the Yarlalweelor Gneiss Complex in the northeastern part of the Narryer Terrane (e.g. Occhipinti et al., 2004).

Proterozoic Intrusive Rocks

The region of the Youanmi seismic traverses is transected by numerous Proterozoic mafic dykes and sills (Fig. 19), many of which can be attributed to large igneous provinces (LIPs) within the Yilgarn Craton (Table 1). The majority are dolerite dykes, typically 5–30 m wide, 50–300 km long, and trending mainly east to east-northeast. Many sills have also been recognized at the surface, which are also up to 50 m thick with outcrop over distances of up to 300 km.

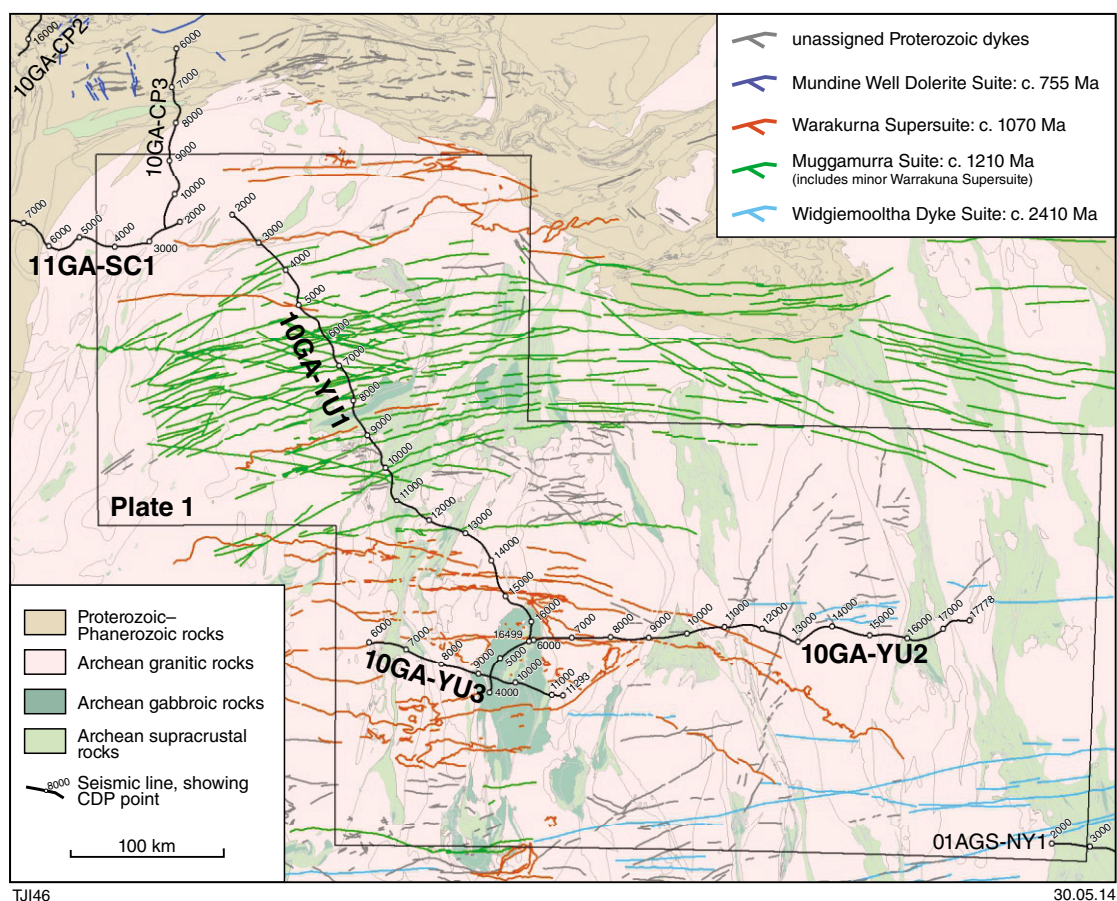


Figure 19. Distribution of Proterozoic dykes and sills in the northern Yilgarn Craton

Table 1. Proterozoic LIPs and dyke swarms in the northwest Yilgarn Craton

LIP	Age (Ma)	Region	Components
Warakurna	1070	Northwestern and central Yilgarn Craton	ENE-trending dolerite dykes and plugs in northwest; Shallow-dipping dolerite sills in northern and central areas
Marnda Moorn	1210	Nothwestern, western, and southern Yilgarn Craton margins	Dolerite, gabbro, and diorite dykes subparallel to craton margins; ENE-trending in northwest (Muggamurra dyke swarm); mainly NNW-trending in west (Boyagin dyke swarm)
Widgiemooltha	2410	Craton-wide	E- and ENE-trending dykes, mainly dolerite and gabbro

Easterly and east-northeasterly trending gabbro or norite dykes in the southern and southeastern parts of the traverse region (Fig. 19) belong to the Widgiemooltha Dyke Suite, which is intruded across the entire Yilgarn Craton. Several Widgiemooltha dykes can be traced, either in outcrop or in aeromagnetic images, for up to 600 km, and most dykes are several metres to hundreds of metres thick. U–Pb, Rb–Sr, and Sm–Nd geochronology of dykes in the southern Yilgarn Craton indicates an age of c. 2410 Ma, and paleomagnetic data can be used to correlate several dykes in the northern parts of the craton with those in the south.

Dyke density is highest in the northwestern Murchison Domain in a 100 km-wide zone from CDP 5700 to

CDP 10300 on line 10GA-YU1 (Fig. 19). These dykes mostly belong to the Muggamurra dyke swarm (Marnda Moorn LIP, c. 1210 Ma) but some may be related to the Warakurna LIP (Wingate et al., 2004). The Muggamurra Dyke Suite includes swarms of dolerite, gabbro, and diorite dykes, which are concentrated mainly around the margins of the Yilgarn Craton, but also extend into the centre of the craton. East-southeasterly trending, poorly exposed dykes in the northeastern part of Figure 19 are correlated tentatively with the Muggamurra swarm, but are not dated. In aeromagnetic images, they appear to cut across the Yerrida Basin and so must be younger than 1800 Ma.

The c. 1070 Ma Warakurna LIP (Wingate et al., 2004) consists of mafic igneous rocks emplaced over about 1.5 million km² in western and central Australia. In the northwestern Yilgarn Craton (Fig. 19), several east-northeasterly trending dykes and small intrusions of medium-grained dolerite overlap in part with the c. 1210 Ma Muggamurra swarm. In the northern and southern parts of the traverse area, and extending for several hundred kilometres into the central and eastern Yilgarn Craton, subhorizontal or shallowly dipping gabbro sills, typically several metres thick, produce prominent west-northwesterly trending, sinuous aeromagnetic anomalies.

Sills up to 30 m thick, assigned to the Warakurna LIP, have been identified in outcrop west and north of the Windimurra Igneous Complex. They include sills south and north of line 10GA-YU3 and also at CDP 6300 on that line. They also include the Mount Holmes Gabbro sill, which crosses line 10GA-YU2 at CDP 6500. The Mount Holmes Gabbro sill, which crops out near Sandstone and is probably the sill interpreted at about CDP 10300 on line 10GA-YU2 (Plate 2), has a crystallization age of c. 1070 Ma (U–Pb SHRIMP date on baddeleyite, Wingate et al., 2008). This sill extends >200 km east from the Windimurra Igneous Complex to the Eastern Goldfields Superterrane (Fig. 19).

References

- Ahmat, AL 1986, Petrology, structure, regional geology and age of the gabbroic Windimurra complex, Western Australia: University of Western Australia, Perth, Western Australia, PhD thesis (unpublished), 279p.
- Allibone, AH, Windh, J, Etheride, MA, Burton, D, Anderson, G, Edwards, PW, Miller, A, Graves, C, Fanning, CM and Wysoczanski, R 1998, Timing relationships and structural controls on the location of Au–Cu mineralisation at the Boddington gold mine: *Economic Geology*, v. 93, p. 245–270.
- Arndt, NT and Jenner, GA 1986, Crustally contaminated komatiites and basalts from Kambalda, Western Australia: *Chemical Geology*, v. 56, p. 229–255.
- Barley, ME, Brown, SJA, Krapež, B and Kositcin, N 2008, Physical volcanology and geochemistry of a Late Archaean volcanic arc: Kurnalpi and Gindalbie Terranes, Eastern Goldfields Superterrane, Western Australia: *Precambrian Research*, v. 161, p. 53–76.
- Barley, ME, Eisenlohr, BN, Groves, DI, Perring, CS and Vearncombe, JR 1989, Late Archean convergent margin tectonics and gold mineralization: A new look at the Norseman–Wiluna Belt, Western Australia: *Geology*, v. 17, no. 9, p. 826.
- Barley, ME, Kerrich, R, Reudavy, I and Xie, Q 2000, Late Archaean Ti-rich, Al-depleted komatiites and komatiitic volcanoclastic rocks from the Murchison Terrane in Western Australia: *Australian Journal of Earth Sciences*, v. 47, no. 5, p. 873–883.
- Barnes, S-J, Leshner, CM and Sproule, RA 2007, Geochemistry of komatiites in the Eastern Goldfields Superterrane, Western Australia, and the Abitibi Greenstone Belt, Canada, and implications for the distribution of associated Ni–Cu–PGE deposits: *Applied Earth Science*, v. 116, p. 167–187.
- Barnes, S-J and Fiorentini, ML, 2012, Komatiite magmas and sulfide nickel deposits: a comparison of variably endowed Archean terranes: *Economic Geology*, v. 107, p. 755–780.
- Barnes, S-J, Fiorentini, ML, Duuring, P, Grguric, BA and Perring, CS, 2011, The Perseverance and Mount Keith Ni deposits of the Agnew–Wiluna Belt, Yilgarn Craton, Western Australia: *Reviews in Economic Geology*, v. 17, p. 51–88.
- Barnes, S-J, Van Kranendonk, MJ and Sonntag, I 2012, Geochemistry and tectonic setting of basalts from the Eastern Goldfields Superterrane, Yilgarn Craton: *Australian Journal of Earth Sciences*, v. 59, no. 5, p. 707–735.
- Beardsmore, TJ 2002, The geology, tectonic evolution and gold mineralization of the Lawlers region: a synopsis of present knowledge: Barrick Gold of Australia Ltd, Confidential Technical Report 1026, 279p.
- Begg, GC, Hronsky, JMA, Arndt, NT, Griffin, WL, O'Reilly, S and Hayward, N 2010, Lithospheric, cratonic, and geodynamic setting of Ni–Cu–PGE sulfide deposits: *Economic Geology*, v. 105, p. 1057–1070.
- Beresford, S, Stone, WE, Cas, R, Lahaye, Y and Jane, M 2005, Volcanological controls on the localization of the komatiite-hosted Ni–Cu–(PGE) Coronet Deposit, Kambalda, Western Australia: *Economic Geology*, v. 100, p. 1457–1467.
- Blewett, RS, Czarnota, K and Henson, PA 2010, Structural-event framework for the eastern Yilgarn Craton, Western Australia, and its implications for orogenic gold: *Precambrian Research*, v. 183, p. 203–209.
- Bodorkos, S, Love, GJ, Nelson, DR and Wingate, MTD 2006, 179239: porphyritic metadacite, Montague Well; *Geochronology Record* 647: Geological Survey of Western Australia, 4p.
- Bunting, JA 2004, The nickel–PGE potential of the Nardee and Windimurra intrusions; Apex Minerals NL: Geological Survey of Western Australia, Statutory mineral exploration report, A69643 (unpublished).
- Cagnard, F, Durrieu, N, Gapais, D, Brun, J-P and Ehlers, C 2006, Crustal thickening and lateral flow during compression of hot lithospheres, with particular reference to Precambrian times: *Terra Nova*, v. 18, p. 72–78.
- Campbell, IH and Hill, RI 1988, A two-stage model for the formation of the granite–greenstone terrains of the Kalgoorlie–Norseman area, Western Australia: *Earth and Planetary Science Letters*, v. 90, p. 11–25.
- Cassidy, KF, Champion, DC, McNaughton, N, Fletcher, IR, Whitaker, AJ, Bastrakova, IV and Budd, A 2002, The characterisation and metallogenic significance of Archaean granitoids of the Yilgarn Craton, Western Australia: Minerals and Energy Research Institute of Western Australia (MERIWA), Project no. M281/AMIRA Project no. 482, Report no. 222 (unpublished).
- Cassidy, KF, Champion, DC, Krapež, B, Barley, ME, Brown, SJA, Blewett, RS, Groenewald, PB and Tyler, IM 2006, A revised geological framework for the Yilgarn Craton, Western Australia: Geological Survey of Western Australia, Record 2006/8, 8p.
- Cavosie, AJ, Wilde, SA, Liu, D, Weiblen, PW, and Valley, JW, 2004, Internal zoning and U–Th–Pb chemistry of Jack Hills detrital zircons: a mineral record of early Archean to Mesoproterozoic (4348–1576 Ma) magmatism: *Precambrian Research*, v. 135, p. 251–279.
- Champion, DC and Cassidy, KF 2007, An overview of the Yilgarn and its crustal evolution, in *Proceedings edited by FP Bierlein and CM Knox-Robinson: Geoscience Australia; Geoconferences (WA) Inc. Kalgoorlie '07, Kalgoorlie, Western Australia, 25–27 September 2007*, Kalgoorlie, Western Australia: Geoscience Australia, Record 2007/14, p. 8–13.
- Champion, DC and Sheraton, JW 1997, Geochemistry and Nd isotope systematics of Archaean granites of the Eastern Goldfields, Yilgarn Craton, Australia: implications for crustal growth processes: *Precambrian Research*, v. 83, p. 109–132.

- Chen, SF 2005, Geology of the Atley, Rays Rocks, and southern Sandstone 1:100 000 sheets: Geological Survey of Western Australia, 1:100 000 Geological Series Explanatory Notes, 42p.
- Chen, SF, Libby, JW, Greenfield, JE, Wyche, S and Riganti, A 2001, Geometry and kinematics of large arcuate structures formed by impingement of rigid granitoids into greenstone belts during progressive shortening: *Geology*, v. 29, no. 3, p. 283–286.
- Chen, SF, Libby, JW, Wyche, S and Riganti, A 2004, Kinematic nature and origin of regional-scale ductile shear zones in the central Yilgarn Craton, Western Australia: *Tectonophysics*, v. 394, p. 139–153.
- Chen, SF, Riganti, A, Wyche, S, Greenfield, JE and Nelson, DR 2003, Lithostratigraphy and tectonic evolution of contrasting greenstone successions in the central Yilgarn Craton, Western Australia: *Precambrian Research*, v. 127, p. 249–266.
- Collins, JE, Hagemann, SG, McCuaig, TC and Frost, KM 2012, Structural controls on sulfide remobilization at the Flying Fox Ni–Cu–PGE deposit, Forrestania Greenstone Belt, Western Australia: *Economic Geology*, v. 107, p. 1433–1455.
- Compston, W and Pidgeon, RT 1986, Jack Hills, evidence of more very old detrital zircons in Western Australia: *Nature*, v. 321, p. 766–769.
- Compston, W, Williams, IS, Campbell, IH and Gresham, JJ, 1986, Zircon xenocrysts from the Kambalda volcanics: age constraints and direct evidence for older continental crust below the Kambalda–Norseman greenstones: *Earth and Planetary Science Letters*, v. 76, p. 299–301.
- Crowley, JL, Myers, JS, Sylvester, PJ and Cox, RA 2005, Detrital zircons from the Jack Hills and Mount Narryer, Western Australia: evidence for diverse >4.0 Ga source rocks: *Journal of Geology*, v. 11, p. 239–263.
- Czarnota, K, Champion, DC, Goscombe, B, Blewett, RS, Cassidy, KF, Henson, PA and Groenewald, PB 2010, Geodynamics of the eastern Yilgarn Craton: *Precambrian Research*, v. 183, p. 175–202.
- Dentith, MC, Evans, S, Thiel, S, Gallardo, L, Joly, A and Romano, SS 2013, A magnetotelluric traverse across the southern Yilgarn Craton: Geological Survey of Western Australia, Report 121, 43p.
- Drummond, BJ, Goleby, BR and Swager, CP 2000, Crustal signature of Late Archean tectonic episodes in the Yilgarn craton, Western Australia: evidence from deep seismic sounding: *Tectonophysics*, v. 329, p. 193–221.
- Dunn, SJ, Nemchin, AA, Cawood, PA, and Pidgeon, RT, 2005, Provenance record of the Jack Hills metasedimentary belt: Source of the Earth's oldest zircons: *Precambrian Research*, v. 138, p. 235–254.
- Duuring, P, Bleeker, W and Beresford, SW 2007, Structural modification of the komatiite-associated Harmony nickel sulphide deposit, Leinster, Western Australia: *Economic Geology*, v. 102, p. 277–297.
- Duuring, P, Bleeker, W, Beresford, SW, Fiorentini, ML and Rosengren, NM 2012, Structural evolution of the Agnew–Wiluna greenstone belt, Eastern Yilgarn Craton and implications for komatiite-hosted Ni sulfide exploration: *Australian Journal of Earth Sciences*, v. 59, no. 5, p. 765–791.
- Duuring, P, Bleeker, W, Beresford, SW and Hayward, N, 2010, Towards a volcanic-structural balance: relative importance of volcanism, folding and remobilisation of nickel sulphides at the Perseverance Ni–Cu–(PGE) deposit, Western Australia: *Mineralium Deposita*, v. 45, p. 281–311.
- Eriksson, KA and Wilde, SA 2010, Palaeoenvironmental analysis of Archean siliciclastic sedimentary rocks in the west central Jack Hills belt, Western Australia with new constraints on ages and correlations: *Journal of the Geological Society of London*, v. 167, p. 827–840.
- Fiorentini, ML, Barley, ME, Pickard, A, Beresford, SW, Rosengren, NM, Cas, RAF and Duuring, P 2005, Age constraints of the structural and stratigraphic architecture of the Agnew–Wiluna greenstone belt: implications for the age of komatiite-felsic association and interaction in the Eastern Goldfields Province, Western Australia: *Minerals and Energy Research Institute of Western Australia (MERIWA), Project no. M356, Report no. 255 (unpublished)*.
- Fiorentini, M, Beresford, SW, Rosengren, NM, Barley, ME and McCuaig, TC 2010, Contrasting komatiite belts, associated Ni–Cu–(PGE) deposit styles and assimilation histories: *Australian Journal of Earth Sciences*, v. 57, p. 543–566.
- Fossen, H, Tikoff, B and Teyssier, C, 1994, Strain modeling of transpressional and transtensional deformation: *Norsk Geologisk Tidsskrift*, v. 74, p. 134–145.
- Geological Survey of Western Australia 2013, Geochronology (GeoVIEW.WA): Department of Mines and Petroleum, <www.dmp.wa.gov.au/geochron/>, viewed January 2013.
- Goleby, BR, Blewett, RS, Groenewald, PB, Cassidy, KF, Champion, DC, Jones, LEA, Korsch, RJ, Shevchenko, S and Apak, SN 2003, The 2001 Northeastern Yilgarn Deep Seismic Reflection Survey: *Geoscience Australia, Record 2003/28*, 143p.
- Goscombe, B, Blewett, RS, Czarnota, K, Groenewald, PB and Maas, R 2009, Metamorphic evolution and integrated terrane analysis of the Eastern Yilgarn Craton: rationale, methods, outcomes and interpretation: *Geoscience Australia, Record 2009/23*, 270p.
- Grange, ML, Wilde, SA, Nemchin, AA and Pidgeon, RT 2010, Implications of Mesoproterozoic sedimentation at Jack Hills, Western Australia: evidence from zircons hosted within quartzite cobbles in the metaconglomerates: *Earth and Planetary Science Letters*, v. 292, p. 158–169.
- Gresham, JJ and Loftus-Hills, GD 1981, The geology of the Kambalda nickel field, Western Australia: *Economic Geology*, v. 76, p. 1372–1416.
- Griffin, WL, Belousova, EA, Shee, SR, Pearson, NJ and O'Reilly, SY 2004, Archean crustal evolution in the northern Yilgarn Craton: U–Pb and Hf–isotope evidence from detrital zircons: *Precambrian Research*, v. 127, p. 19–41.
- Groves, DI and Batt, WD 1984, Spatial and temporal variations of Archean metallogenic associations in terms of evolution of granitoid–greenstone terrains with particular emphasis on the Western Australian shield, in *Archean geochemistry — the origin and evolution of the Archean continental crust*, edited by A Kroner, GN Manson and AM Goodwin: Berlin, Springer-Verlag, p. 73–98.
- Hallberg, JA 1986, Archean basin development and crustal extension in northeastern Yilgarn Block, Western Australia: *Precambrian Research*, v. 31, p. 133–156.
- Hallberg, JA, Johnston, C and Bye, SM 1976, The Archean Marda igneous complex, Western Australia: *Precambrian Research*, v. 3, p. 111–136.
- Heggie, GJ, Fiorentini, ML, Barnes, S-J and Barley, ME 2012, Maggie Hays Ni deposit: Part 1. Stratigraphic control on the style of komatiite emplacement in the 2.9 Ga Lake Johnston greenstone belt, Yilgarn Craton, Western Australia: *Economic Geology*, v. 107, no. 5, p. 797–816.
- Hill, RET, Barnes, S-J, Gole, MJ and Dowling, SJ 1995, The volcanology of komatiites as deduced from field relationships in the Norseman–Wiluna greenstone belt, Western Australia: *Lithos*, v. 34, p. 159–188.
- Hill, RI, Campbell, IH and Compston, W 1989, Age and origin of granitic rocks in the Kalgoorlie–Norseman region of Western Australia: implications for the origin of Archean crust: *Geochimica et Cosmochimica Acta*, v. 53, p. 1259–1275.
- Ivanic, TJ, Korsch, RJ, Wyche, S, Jones, LEA, Zibra, I, Blewett, RS, Jones, T, Milligan, PR, Costelloe, RD, Van Kranendonk, MJ, Doublier, MP, Hall, CE, Romano, SS, Pawley, MJ, Gessner, K, Patisson, N, Kennett, BLN and Chen, SF 2013, Preliminary interpretation of the 2010 Youanmi deep seismic reflection lines and magnetotelluric data for the Windimurra Igneous Complex, in *Youanmi and Southern Carnarvon seismic and magnetotelluric (MT) workshop 2013 compiled by S Wyche, TJ Ivanic and I Zibra: Geological Survey of Western Australia, Record 2013/6*, p. 97–111.

- Ivanic, TJ, Van Kranendonk, MJ, Kirkland, CL, Wyche, S, Wingate, MTD and Belousova, E 2012, Zircon Lu–Hf isotopes and granite geochemistry of the Murchison Domain of the Yilgarn Craton: evidence for reworking of Eocarchean crust during Meso–Neoproterozoic plume-driven magmatism: *Lithos*, v. 148, p. 112–127.
- Ivanic, TJ, Wingate, MTD, Kirkland, CL, Van Kranendonk, MJ and Wyche, S 2010, Age and significance of voluminous mafic–ultramafic magmatic events in the Murchison Domain, Yilgarn Craton: *Australian Journal of Earth Sciences*, v. 57, p. 597–614.
- Kennett, BLN, Salmon, M, Saygin, E and AusMoho Working Group 2011, AusMoho: the variation of Moho depth in Australia: *Geophysical Journal International*, v. 187, no. 2, p. 946–958.
- Kinny, PD and Nutman, AP 1996, Zirconology of the Meeberrie gneiss, Yilgarn Craton, Western Australia: an early Archaean migmatite: *Precambrian Research*, v. 78, p. 165–178.
- Kinny, PD, Williams, IS, Froude, DO, Ireland, TR and Compston, W 1988, Early Archaean zircon ages from orthogneisses and anorthositic at Mount Narryer, Western Australia: *Precambrian Research*, v. 38, p. 325–341.
- Kinny, PD, Wijbrans, JR, Froude, DO, Williams, IS and Compston, W 1990, Age constraints on the geological evolution of the Narryer Gneiss Complex, Western Australia: *Australian Journal of Earth Sciences*, v. 37, no. 1, p. 51–69.
- Kositcin, N, Brown, SJA, Barley, ME, Krapež, B, Cassidy, KF and Champion, DC 2008, SHRIMP U–Pb zircon age constraints on the Late Archaean tectonostratigraphic architecture of the Eastern Goldfields Superterrane, Yilgarn Craton, Western Australia: *Precambrian Research*, v. 161, p. 5–33.
- Krapež, B and Barley, ME 2008, Late Archaean synorogenic basins of the Eastern Goldfields Superterrane, Yilgarn Craton, Western Australia: Part III. Signatures of tectonic escape in an arc–continent collision zone: *Precambrian Research*, v. 161, no. 1–2, p. 183–199.
- Krapež, B, Barley, ME and Brown, SJA 2008, Late Archaean synorogenic basins of the Eastern Goldfields Superterrane, Yilgarn Craton, Western Australia. Part I. Kalgoorlie and Gindalbie Terranes: *Precambrian Research*, v. 161, p. 135–153.
- Krapež, B, Brown, SJA, Hand, J, Barley, ME and Cas, RAF 2000, Age constraints of recycled crustal and supracrustal sources of Archaean metasedimentary sequences, Eastern Goldfields Province, Western Australia: evidence from SHRIMP zircon dating: *Tectonophysics*, v. 332, no. 1–2, p. 89–133.
- Krapež, B and Hand, JL 2008, Late Archaean deep-marine volcanoclastic sedimentation in an arc-related basin: the Kalgoorlie Sequence of the Eastern Goldfields Superterrane, Yilgarn Craton, Western Australia: *Precambrian Research*, v. 161, p. 89–113.
- Leshner, CM 1983, Localization and genesis of komatiite-associated Fe–Ni–Cu sulphide mineralization at Kambalda, Western Australia: The University of Western Australia, Perth, Western Australia, PhD thesis (unpublished), 199p.
- Liu, SF and Chen, SF 1998, Structural framework of the northeastern Yilgarn Craton and implications for hydrothermal gold mineralisation: AGSO Research Newsletter, no. 29.
- Liu, SF, Griffin, TJ, Wyche, S, Westaway, JM and Ferguson, KM 1998, Geology of the Sir Samuel 1:100 000 sheet: Geological Survey of Western Australia, 1:100 000 Geological Series Explanatory Notes, 25p.
- Maas, R and McCulloch, MT 1991, The provenance of Archaean clastic metasediments in the Narryer Gneiss Complex, Western Australia: trace element geochemistry, Nd isotopes, and U–Pb ages for detrital zircons: *Geochimica et Cosmochimica Acta*, v. 55, p. 1914–1932.
- Mole, DR, Fiorentini, ML, Thébaud, N, McCuaig, TC, Cassidy, KC, Kirkland, CL, Wingate, MTD, Romano, SS, Doublier, MP and Belousova, EA 2012, Spatio-temporal constraints on lithospheric development in the southwest-central Yilgarn Craton, Western Australia: *Australian Journal of Earth Sciences*, v. 59, no. 5 (Archaean evolution — Yilgarn Craton), p. 625–656.
- Mole, DR, Fiorentini, ML, Thébaud, N, McCuaig, TC, Cassidy, KF, Barnes, S-J, Belousova, EA, Mudrovska, I and Doublier, MP 2010, Lithospheric controls on the localization of komatiite-hosted nickel-sulfide deposits: evolving early Earth, in *Fifth International Archaean Symposium Abstracts edited by IM Tyler and CM Knox-Robinson*: Geological Survey of Western Australia, Record 2010/8, p. 101.
- Morris, PA, Riganti, A and Chen, SF 2007, Evaluating the provenance of Archaean sedimentary rocks of the Diemals Formation (central Yilgarn Craton) using whole-rock chemistry and precise U–Pb zircon chronology: *Australian Journal of Earth Sciences*, v. 54, p. 1123–1136.
- Myers, JS 1988a, Early Archaean Narryer Gneiss Complex, Yilgarn Craton, Western Australia: *Precambrian Research*, v. 38, p. 279–307.
- Myers, JS, 1988b, Oldest known terrestrial anorthosite at Mount Narryer, Western Australia: *Precambrian Research*, v. 38, p. 309–323.
- Myers, JS 1990a, Precambrian tectonic evolution of part of Gondwana, southwestern Australia: *Geology*, v. 18, p. 537–540.
- Myers, JS, 1990b, Western Gneiss Terrane, in *Geology and mineral resources of Western Australia: Geological Survey of Western Australia, Memoir 3*, p. 13–31.
- Myers, JS 1993, Precambrian history of the West Australian Craton and adjacent orogens: *Annual Review of Earth and Planetary Sciences*, v. 21, p. 453–485.
- Myers, JS 1995, The generation and assembly of an Archaean supercontinent: evidence from the Yilgarn Craton, Western Australia, in *Early Precambrian Processes edited by MP Coward and AC Reis*: Geological Society, London, Special Publication 95, p. 143–154.
- Myers, JS and Swager, C 1997, The Yilgarn Craton, in *Greenstone belts edited by M de Wit and LD Ashwal*: Clarendon Press, Oxford, UK, p. 640–656.
- Myers, JS and Williams, IR 1985, Early Precambrian crustal evolution at Mount Narryer, Western Australia: *Precambrian Research*, v. 27, no. 1–3, p. 153–163.
- Nelson, DR 1997, Evolution of the Archaean granite–greenstone terranes of the Eastern Goldfields, Western Australia: SHRIMP U–Pb zircon constraints: *Precambrian Research*, v. 83, no. 1–3, p. 57–81.
- Nelson, DR 2001, 169003: vesicular rhyolite, Carron Hill: *Geochronology Record 170*: Geological Survey of Western Australia, 4p.
- Nelson, DR 2004, 165364: quartz-feldspar porphyry, Bulchina: *Geochronology dataset 57*; in *Compilation of geochronology data, June 2006 update*: Geological Survey of Western Australia.
- Nelson, DR 2005, 165364: quartz-feldspar porphyry, Bulchina: *Geochronology dataset 532*; in *Compilation of geochronology data, June 2006 update*: Geological Survey of Western Australia.
- Nutman, AP, Bennett, VC, Kinny, PD and Price, R 1993, Large-scale crustal structure of the northwestern Yilgarn Craton, Western Australia: evidence from Nd isotopic data and zircon geochronology: *Tectonics*, v. 12, p. 971–981.
- Nutman, AP, Kinny, PD, Compston, W and Williams, IS 1991, SHRIMP U–Pb zircon geochronology of the Narryer Gneiss Complex, Western Australia: *Precambrian Research*, v. 52, p. 275–300.
- Ochipinti, SA and Reddy, SM 2004, Deformation in a complex crustal-scale shear zone: Errabiddy Shear Zone, Western Australia, in *Flow Processes in Faults and Shear Zones edited by GI Alsop, RE Holdsworth, KJW McCaffrey and M Hand*: Geological Society of London, Special Publication 224, p. 229–248.
- Parks, J 1998, The Weld Range platinum group element deposit, in *geology of Australian and Papua New Guinean mineral deposits edited by DA Berkman and DH Mackenzie*: Australasian Institute of Mining and Metallurgy, Monograph 22, p. 279–286.
- Pawley, MJ, Wingate, MTD, Kirkland, CL, Wyche, S, Hall, CE, Romano, SS and Doublier, MP 2012, Adding pieces to the puzzle: episodic crustal growth and a new terrane in the northeast Yilgarn Craton, Western Australia: *Australian Journal of Earth Sciences*, v. 59, p. 603–623.

- Pidgeon, RT, and Wilde, SA, 1998, The interpretation of complex zircon U–Pb systems in Archaean granitoids and gneisses from the Jack Hills, Narryer Gneiss Terrane, Western Australia: *Precambrian Research*, v. 91, p. 309–332.
- Platt, JP, Allchurch, PD and Rutland, RWR 1978, Archaean tectonics in the Agnew supracrustal belt, Western Australia: *Precambrian Research*, v. 7, p. 3–30.
- Rasmussen, B, Fletcher, IR, Muhling, JR and Wilde, SA 2010, In situ U–Th–Pb geochronology of monazite and xenotime from the Jack Hills belt: implications for the age of deposition and metamorphism of Hadean zircons: *Precambrian Research*, v. 180, p. 26–46.
- Reading, AM, Kennett, BLN and Goleby, B 2007, New constraints on the seismic structure of West Australia: evidence for terrane stabilization prior to assembly of an ancient continent: *Geology*, v. 35, p. 379–382.
- Rey, PF, Philippot, P and Thebaud, N 2003, Contribution of mantle plumes, crustal thickening and greenstone blanketing to the 2.75–2.65 Ga global crisis: *Precambrian Research*, v. 127, p. 43–60.
- Riganti, A, Wyche, S, Wingate, MTD, Kirkland, CL and Chen, SF 2010, Constraints on ages of greenstone magmatism in the northern part of the Southern Cross Domain, Yilgarn Craton, in *Fifth International Archaean Symposium Abstracts edited by IM Tyler and CM Knox-Robinson*: Geological Survey of Western Australia, Record 2010/18, p. 119–122.
- Riller, U, Cruden, AR, Boutelier, D and Schrank, C 2012, The causes of sinuous crustal-scale deformation patterns in hot orogens: Evidence from scaled analogue experiments and the southern Central Andes: *Journal of Structural Geology*, v. 37, p. 65–74.
- Romano, SS, Doublier, MP, Mole, DR, Thébaud, N, Wingate, MTD and Kirkland, CL 2010, Age constraints in the southern part of the southern cross domain of the Yilgarn Craton, in *Fifth International Archaean Symposium Abstracts edited by IM Tyler and CM Knox-Robinson*: Geological Survey of Western Australia, Record 2010/8, p. 206.
- Rosengren, NM, Cas, RAF, Beresford, SW and Palich, BM 2005, Reconstruction of an extensive Archaean dacitic submarine volcanic complex associated with the komatiite-hosted Mt Keith nickel deposit, Agnew–Wiluna Greenstone Belt, Yilgarn Craton, Western Australia: *Precambrian Research*, v. 161, p. 34–52.
- Said, N and Kerrich, R 2009, Geochemistry of coexisting depleted and enriched Paringa Basalts, in the 2.7 Ga Kalgoorlie Terrane, Yilgarn Craton, Western Australia: evidence for a heterogeneous mantle plume event: *Precambrian Research*, v. 174, p. 287–309.
- Scowen, PAH 1991, The geology and geochemistry of the Narndee intrusion: Australian National University, Canberra, Australian Capital Territory, PhD thesis (unpublished), 214p.
- Smithies, RH and Champion, DC 1999, Late Archaean felsic alkaline igneous rocks in the Eastern Goldfields, Yilgarn Craton, Western Australia: a result of lower crustal delamination?: *Journal of the Geological Society, London*, v. 156, p. 561–576.
- Spaggiari, CV 2006, Interpreted bedrock geology of the northern Murchison Domain, Youanmi Terrane, Yilgarn Craton: Geological Survey of Western Australia, Record 2006/10, 19p.
- Spaggiari, CV 2007a, The Jack Hills greenstone belt, Western Australia — Part 1: Structural and tectonic evolution over >1.5 Ga: *Precambrian Research*, v. 155, p. 204–228.
- Spaggiari, CV 2007b, Structural and lithological evolution of the Jack Hills greenstone belt, Narryer Terrane, Yilgarn Craton, Western Australia: Geological Survey of Western Australia, Record 2007/3, 49p.
- Spaggiari, CV, Wartho, J-A and Wilde, SA 2008, Proterozoic deformation in the northwest of the Archaean Yilgarn Craton, Western Australia: *Precambrian Research*, v. 162, p. 354–384.
- Squire, RJ, Allen, CM, Cas, RAF, Campbell, IH, Blewett, RS and Nemchin, AA 2010, Two cycles of voluminous pyroclastic volcanism and sedimentation related to episodic granite emplacement during the late Archaean: Eastern Yilgarn Craton, Western Australia: *Precambrian Research*, v. 183, no. 2, p. 251–274.
- Squire, RJ, Cas, RAF, Clout, JMF and Behets, R 1998, Volcanology of the Lunnon Basalt and its relevance to nickel sulfide-bearing trough structures at Kambalda, Western Australia: *Australian Journal of Earth Sciences*, v. 46, p. 695–715.
- Stewart, AJ, Williams, IR and Elias, M (compilers) 1983, Youanmi, Western Australia: Geological Survey of Western Australia, 1:250 000 Geological Series Explanatory Notes, 58p.
- Swager, CP 1997, Tectono-stratigraphy of late Archaean greenstone terranes in the southern Eastern Goldfields, Western Australia: *Precambrian Research*, v. 83, p. 11–42.
- Swager, CP, Goleby, BR, Drummond, BJ, Rattenbury, MS and Williams, PR 1997, Crustal structure of granite–greenstone terranes in the Eastern Goldfields, Yilgarn Craton, as revealed by seismic profiling: *Precambrian Research*, v. 83, p. 43–56.
- Swager, CP, Griffin, TJ, Witt, WK, Wyche, S, Ahmat, AL, Hunter, WM and McGoldrick, PJ 1995, Geology of the Archaean Kalgoorlie Terrane — an explanatory note (reprint of Record 1990/12): Geological Survey of Western Australia, Report 48, 26p.
- Trofimovs, J, Davis, BK and Cas, RAF 2004, Contemporaneous ultramafic and felsic intrusive and extrusive magmatism in the Archaean Boorara Domain, Eastern Goldfields Superterrane, Western Australia, and its implications: *Precambrian Research*, v. 131, p. 283–304.
- Trofimovs, J, Tait, MA, Cas, RAF, McArthur, A and Beresford, SW 2003, Can the role of thermal erosion in strongly deformed komatiite–Ni–Cu–(PGE) deposits be determined? Perseverance, Agnew–Wiluna Belt, Western Australia: *Australian Journal of Earth Sciences*, v. 50, p. 199–214.
- Van Kranendonk, MJ and Ivanic, TJ 2009, A new lithostratigraphic scheme for the northeastern Murchison Domain, Yilgarn Craton, in *Geological Survey of Western Australia Annual Review 2007–08*: Geological Survey of Western Australia, p. 34–53.
- Van Kranendonk, MJ, Ivanic, TJ, Wingate, MTD, Kirkland, CL and Wyche, S 2013, Long-lived, autochthonous development of the Archaean Murchison Domain, and implications for Yilgarn Craton tectonics: *Precambrian Research*, v. 229, p. 49–92.
- Van Kranendonk, MJ, Ivanic, TJ, Wyche, S, Wilde, SA and Zibra, I (compilers) 2010, A time transect through the Hadean to Neoproterozoic geology of the western Yilgarn Craton — a field guide: Geological Survey of Western Australia, Record 2010/19, 69p.
- Wang, Q 1998, Geochronology of the granite–greenstone terranes in the Murchison and Southern Cross Provinces of the Yilgarn Craton, Western Australia: Australian National University, Canberra, PhD thesis (unpublished), 186p.
- Wang, Q, Schiøtte, L and Campbell, IH 1998, Geochronology of supracrustal rocks from the Golden Grove area, Murchison Province, Yilgarn Craton, Western Australia: *Australian Journal of Earth Sciences*, v. 45, p. 571–577.
- Watkins, KP and Hickman, AH 1990, Geological evolution and mineralization of the Murchison Province, Western Australia: Geological Survey of Western Australia, Bulletin 137, 267p.
- Wilde, SA 2001, Jamperding and Chittering metamorphic belts, southwestern Yilgarn Craton, Western Australia — a field guide: Geological Survey of Western Australia, Record 2001/12, 24p.
- Wilde, SA 2010, Proterozoic volcanism in the Jack Hills Belt, Western Australia: some implications and consequences for the World’s oldest zircon population: *Precambrian Research*, v. 183, p. 9–24.

- Wilde, SA, Middleton, MF and Evans, BJ 1996, Terrane accretion in the southwestern Yilgarn Craton: evidence from a deep seismic crustal profile: *Precambrian Research*, v. 78, p. 179–196.
- Wilde, SA, Valley, JW, Peck, WH and Graham, CM 2001, Evidence from detrital zircons for the existence of continental crust and oceans on the Earth 4.4 Gyr ago: *Nature*, v. 409, p. 175–178.
- Williams, IR and Myers, JS 1987, Archaean geology of the Mount Narryer region, Western Australia: Geological Survey of Western Australia, Report 22, 32p.
- Wingate, MTD, Bodorkos, S and Kirkland, CL 2008, 178113: gabbro sill, Kurrajong Bore; Geochronology Record 732: Geological Survey of Western Australia, 7p.
- Wingate, MTD, Kirkland, CL and Ivanic, TJ 2012, 194747: metagabbro, Malamiter Well; Geochronology Record 1013: Geological Survey of Western Australia, 4p.
- Wingate, MTD, Pirajno, F and Morris, PA 2004, Warakurna large igneous province: a new Mesoproterozoic large igneous province in west-central Australia: *Geology*, v. 32, no. 2, p. 105–108.
- Witt, WK 1998, Geology and mineral resources of the Ravensthorpe and Cocanarup 1:100 000 sheets: Geological Survey of Western Australia, Report 54, 152p.
- Witt, WK 1999, The Archaean Ravensthorpe Terrane, Western Australia: synvolcanic Cu–Au mineralization in a deformed island arc complex: *Precambrian Research*, v. 96, no. 3–4, p. 143–181.
- Woodall, R 1965, Structure of the Kalgoorlie goldfield, in *Geology of Australian Ore Deposits* (2nd edition) edited by J McAndrew: 8th Commonwealth Mining and Metallurgical Congress, Australia and New Zealand, 1965; Publications 1, p. 71–79.
- Wyche, S 2007, Evidence of pre-3100 Ma crust in the Youanmi and Southwest Terranes and Eastern Goldfields Superterrane, of the Yilgarn Craton, in *Earth's Oldest Rocks* edited by MJ Van Kranendonk, RH Smithies and VC Bennett: Elsevier BV, *Developments in Precambrian Geology* 15, p. 113–123.
- Wyche, S, Kirkland, CL, Riganti, A, Pawley, MJ, Belousova, E and Wingate, MTD 2012, Isotopic constraints on stratigraphy in the central and eastern Yilgarn Craton, Western Australia: *Australian Journal of Earth Sciences*, v. 59, no. 5 (Archean evolution — Yilgarn Craton), p. 657–670.
- Wyman, DA and Kerrich, R 2012, Geochemical and isotopic characteristics of Youanmi terrane volcanism: the role of mantle plumes and subduction tectonics in the western Yilgarn Craton: *Australian Journal of Earth Sciences*, v. 59, no. 5 (Archean evolution — Yilgarn Craton), p. 671–694.
- Yeats, CJ, McNaughton, NJ and Groves, DI 1996, SHRIMP U–Pb geochronological constraints on Archean volcanic-hosted massive sulfide and lode gold mineralization at Mount Gibson, Yilgarn Craton, Western Australia: *Economic Geology*, v. 91, p. 1354–1371.
- Zibra, I 2012, Syndeformational granite crystallisation along the Mount Magnet Greenstone Belt, Yilgarn Craton: evidence of large-scale magma-driven strain localisation during Neoproterozoic time: *Australian Journal of Earth Sciences*, v. 59, no. 5, p. 793–806.
- Zibra, I, Gessner, K, Korsch, RJ, Blewett, RS, Jones, T, Milligan, PR, Jones, LEA, Wyche, S, Doublier, MP, Hall, CE, Chen, SF, Romano, SS, Ivanic, TJ, Pawley, MJ, Patison, N, Kennett, BLN and Van Kranendonk, MJ 2013a, Preliminary interpretation of deep seismic lines 10GA-YU3 and the southeastern part of 10GA-YU1: Murchison Domain of the Youanmi Terrane, in *Youanmi and Southern Carnarvon seismic and magnetotelluric (MT) workshop 2013 compiled by S Wyche, TJ Ivanic and I Zibra*: Geological Survey of Western Australia, Record 2013/6, p. 113–122.
- Zibra, I, Gessner, K, Pawley, MJ, Wyche, S, Chen, SF, Korsch, RJ, Blewett, RS, Jones, T, Milligan, PR, Jones, LEA, Doublier, MP, Hall, CE, Romano, SS, Ivanic, TJ, Patison, N, Kennett, BLN and Van Kranendonk, MJ 2013b, Preliminary interpretation of deep seismic line 10GA-YU2: Youanmi Terrane and western Kalgoorlie Terrane, in *Youanmi and Southern Carnarvon seismic and magnetotelluric (MT) workshop 2013 compiled by S Wyche, TJ Ivanic and I Zibra*: Geological Survey of Western Australia, Record 2013/6, p. 87–95.

Interpretation of magnetic and gravity data across the Southern Carnarvon Basin, and the Narryer and Youanmi Terranes

by

K Gessner, T Jones¹, JA Goodwin¹, LA Gallardo², PR Milligan¹, J Brett, and R Murdie

Introduction

Magnetic and gravity data provide important information on the physical properties of rocks within the Earth's crust and, in turn, reveal information on the crust's geological structure. To complement existing high-resolution total magnetic intensity (TMI) data, new gravity data were collected along the traverses of the Youanmi survey (10GA-YU1, 10GA-YU2, and 10GA-YU3), and the Southern Carnarvon survey (11GA-SC1) (Frontispiece 1), together with the acquisition of deep seismic reflection data for both surveys and magnetotelluric data for the Youanmi survey. This Report provides an interpretation of the gravity and magnetic data covering the Southern Carnarvon Basin, the Narryer Terrane, and the Youanmi Terrane. The interpretation is based on a regional analysis of gravity and magnetic grids, forward modelling of gravity data, interpretation of seismic reflection data, and cross-gradient joint inversion of gravity and magnetic data along the traverses of the Youanmi survey.

Magnetics

The source dataset used to generate images, multiscale edges, and cross-gradient joint inversions is 'WA_80m_Mag_Merge_landsea_v1_2010' (GSWA, 2010). This grid combines merged magnetic field data from onshore and offshore Western Australia and is generated from Federal and State government data sets acquired with a line spacing of 500 metres or less, with the addition of selected open-file proprietary data sets. The Magnetic anomaly map of Australia Edition 5 (Milligan et al., 2010) has been used as a base reference grid and is also used to complete the background areas where closer spaced data are not available. The horizontal datum and projection are Geocentric Datum of Australia 1994 (GDA94), geodetic. The grid cell size is 0.0008333 degrees of arc (~80 m). The data are in units of nanotesla (nT).

Modelling techniques

Potential field data

Gravity

The forward modelling and joint inversion studies used a gravity grid that incorporated data from the Australian National Gravity Database (ANGD) (Wynn, 2009), plus new data collected along the Youanmi seismic transects at regular intervals of 400 m. The data were gridded at 0.005 degrees of arc grid cell spacing. For the purpose of forward modelling and joint inversion, gravity data were extracted from the new grid along the seismic transects as defined by the Common Depth Points (CDP) to ensure the accurate co-location of the gravity profiles with the seismic lines.

Multiscale edge detection

Multiscale edge detection involves computation of the maximum horizontal gradients of potential-field data for multiple levels of upward continuation (Archibald et al., 1999). These gradients are initially computed at point locations and form strings of points, referred to as 'worms', for each upward continuation level. Worms of different upward continuation levels represent discontinuities in physical rock properties, which relate to stratigraphic, intrusive, or faulted contacts in the Earth's crust. Archibald et al. (1999) and Holden et al. (2000) proposed that worms derived from higher upward continuation levels can be interpreted as originating from physical property contrasts of greater depth. This feature, however, must be treated with caution due to the inherently ambiguous depth information of potential-field data. At lower continuation levels, the attitude of the surfaces is more likely to reflect the dip direction of the property contrasts (but not the angle).

¹ Minerals and Natural Hazards Division, Geoscience Australia, GPO Box 378, Canberra ACT 2601

² Earth Science Division, Centro de Investigación Científica y de Educación Superior de Ensenada (CICESE), Ensenada, B.C., Mexico

Forward modelling

Forward calculations of gravity anomalies were produced for models derived from the seismic interpretations of Korsch et al. (2013, this volume). The geometries of bodies described in those interpretations were maintained and the density values for these bodies manipulated within reasonable ranges. The calculated gravity anomalies were compared to the observed gravity data to infer density values for the rock bodies interpreted in the seismic data. The primary objective of this process was to determine where the seismically inferred models correlate with the observed gravity field and where inconsistencies exist. Postulating why these inconsistencies exist can provide a new perspective on the crustal architecture.

Models were created using ModelVision v11.0 software, extending from 0 to 60 km depth. Two-dimensional polygons, representing cross-sections of geology along the seismic line, were drawn and extended to 200 km in strike length (100 km either side of the profile) and 100 km beyond the ends of the seismic line to avoid edge effects. Rock property data from Emerson (1990), Telford et al. (1990), Christensen and Mooney (1995), Poudjom Djomani, et al. (2001) and Rudnick et al. (1995) were used as a starting point to assign average lithospheric density values to each model.

In this study, only the observed gravity data were used for forward modelling purposes. Magnetic data across the region are dominated by short-wavelength anomalies and relate to near-surface features that bear little relation to the crustal-scale interpretations made in this study. Forward modelling of potential-field data is inherently non-unique; therefore, consistency between seismic interpretations and the observed potential-field data represents only the validity of a single interpretation. Further investigation of the model space (including the addition of geological constraints) should be undertaken in order to improve the confidence of these interpretations.

Cross-gradient joint inversion

Cross-gradient joint inversion is an integrative method for different geophysical datasets, with the aim to search for multiple geophysical models that match structurally, and fit multiple datasets (Gallardo and Meju, 2003, 2004). This approach has been applied intensively to data combinations including: electrical resistivity and seismic travel time data (Gallardo and Meju, 2004; Linde et al., 2006), electromagnetic and seismic refraction data (Moorkamp et al., 2011; Hu et al., 2009; Gallardo and Meju, 2007), and gravity and magnetic data (Gallardo et al., 2012; Moorkamp et al., 2011).

The application of cross-gradient joint inversion to gravity and magnetic data is very practical since these data types are widely available in many regions where access is difficult and which generally cover large areas. Despite this, the sole application of these datasets, due to the known limitation on depth resolution, requires careful handling and processing in order to achieve models that

become geologically meaningful (see Hornby et al., 2001; Fregoso and Gallardo, 2009).

A cross-gradient strategy that has proven particularly appropriate for crustal structure studies in the Eastern Goldfields Superterrane of the Yilgarn Craton (Gallardo and Thebaud, 2012) is used here to constrain the crustal structure along the Youanmi traverses. We aimed to use the cross-gradient algorithm of Gallardo (2007) to find two models that describe the subsurface: one for the distribution of density contrast, driven by the gravity data, and one for the distribution of magnetization determined by the magnetic data. These sections should structurally resemble each other as measured by the cross product of their property gradients. To deal with the ambiguity inherent in unconstrained gravity and magnetic data modelling, we simplified our models by assuming that only negligible density and magnetization contrast exists below 20 km depth. While this approach may disregard some features of the deep structure still visible in a deep seismic section, it allows the variations of density and magnetic susceptibility to better relate to the architecture of the more heterogeneous upper crust. For the sake of numerical stability we favour smooth over highly heterogeneous models, as measured by the Laplacian operator of the physical properties (Twomey, 1977; Tikhonov and Arsenin, 1977).

Input data preparation

The data were processed using methods described in Gallardo and Thebaud (2012) and Gallardo et al. (2012). A constant value of 80 mGal was subtracted from the high-resolution gravity grid previously mentioned. This value corresponds to the lowest gravity anomaly associated with the lowest density crust (exposed at the surface as a major granitic crustal domain) that can be used as a reference for the density of other crustal regions with inferred similar geology. For the inversion processing, an overall standard deviation for data errors of 0.1 mGal was assumed and set as the optimal misfit value.

The TMI data show a flat regional trend and an average of zero, indicating that deep geomagnetic effects were corrected and that most magnetic anomalies should occur within the upper crust in the studied region. In order to cope with the crooked trace of the seismic sections and the influence of this on the declination in relation to the local profile azimuth, we reduced the magnetic anomaly to the magnetic pole, using the following parameters which represent an average of the geomagnetic field for the studied area for January 1998: inclination -61.43 degrees, declination $+0.3$ degrees, average intensity of the geomagnetic field 56184.5 nT. We noted that magnetic anomalies of deviated polarity, such as those associated with magnetic remanence, may not have been fully rectified by this process. This leaves spurious polarities in the resulting anomalies that may propagate into the resulting models. For the inversion we assumed that the errors have a standard deviation of 30 nT, and set this value as the target misfit for the three profiles.

Geophysical model parameterization and initial guess

The model was divided into regular cells of 1 km width along the distance of the seismic sections. The cell width was increased logarithmically until the potential-field section extended 100 km beyond the seismic section limits. Following the same procedure, the transverse section of the profiles was extended for more than 100 km on each side. These dimensions are set to account for any regional data trend that may still exist in each individual section, and to focus on the study area. Cell thicknesses are set to vary with depth, ranging from 100 m at the surface, to 2 km at 20 km depth. We note that, as beyond this depth no heterogeneities are assumed to exist, further discretization is not necessary. The initial model was set to zero-density and zero-magnetization contrast and, as described in Gallardo et al. (2012), the inversion goes through four iterative steps to gradually add heterogeneities and fit the local data.

Selection of optimal models

To achieve optimal models, the level of smoothness of the models was adjusted progressively. All the models presented fitted the dataset, were structurally cross-related, concentrated the heterogeneities in the first 18 km of the crust, and were therefore deemed as representative of the major local heterogeneities within the upper crust.

Geophysical interpretation results

Potential-field grids and worms

Southern Carnarvon survey

Along seismic reflection survey 11GA-SC1, the magnetic (Fig. 1) and gravity (Figs 2, 3) fields change character along northeasterly to north-trending gradients, which separate distinct domains and highlight internal geological structures (Frontispiece 1; Korsch et al., 2013, this volume). A marked gravity low (Figs 2, 3) coincides with the Errabiddy corridor (Plate 2) that separates the Narryer and Glenburgh Terranes (Frontispiece 3), where gravity values are generally higher. However, interpretation of the TMI image is less conclusive; the magnetic patterns of the Narryer and Glenburgh Terranes, when compared to the Pinjarra Orogen and the Errabiddy Shear Zone, are distinct in both the grid (Fig. 1) and the magnetic worms (Fig. 4).

Youanmi surveys

The observed regional gravity trend across the northwest Yilgarn Craton (Figs 2, 3) shows a pronounced east–west gradient with a gravity high in the west, ranging from about -45 to -50 mGal, and a regional low of about -120 mGal in the east. The 20 km upward continuation

of the Bouguer gravity grid (Fig. 3) shows an east–northeasterly gradient that is consistent from southeast to northwest across the area of study, and separates a regional gravity high in the west of the central Yilgarn from a gravity low centred near 119°E and 27°S . The long-wavelength north–northwest gravity gradient is oriented at a small angle to the seismic reflection line 10GA-YU1, whereas line 10GA-YU2 crosses the lower part of the negative anomaly just west of longitude 119°E .

Multiscale edge detection of the gravity data shows a north–south trending structure that intersects 10GA-YU1 near CDP 1200 and 10GA-YU3 CDP 7000 near Mount Magnet (Fig. 5). Other north–south worms intersect 10GA-YU2 at CDP 9000 near the Sandstone region, and between CDPs 1500 and 1600, at the eastern end of the line; the latter presumably relates to the boundary between the Youanmi Terrane and the Eastern Goldfields Superterrane. Worms of shorter lengths and with east–northeasterly trends relate to the Narryer–Murchison domain boundary near CDP 3000 of 10GA-YU1, and the Weld Range near CDP 9000. The Windimurra Igneous Complex is defined well by gravity worms intersecting 10GA-YU3 between CDP 9000 and 11000.

The magnetic field along 10GA-YU1 is mainly characterized by short-wavelength (kilometre to tens of kilometres) anomalies related to greenstone belts including banded iron-formation, dykes and sills, and also to lithological variation within the Windimurra Igneous Complex (Plate 1; Figs 1, 4). The Jack Hills greenstone belt intersects 10GA-YU1 near CDP 3000, the Weld Range banded iron-formations between 8000 and 9000, and the Windimurra Igneous Complex near the southern end of the line. A north–northeasterly trending anomaly just west of CDP 13000 likely relates to the Tuckabianna Synform, a thin, folded greenstone sequence in the hanging wall of the Cundimurra Shear Zone (Zibra et al., 2013, this volume). Seismic reflection traverse 10GA-YU1 is also intersected by a number of east–west oriented dykes (Fig. 1). Magnetic anomalies along 10GA-YU2 include the Windimurra Igneous Complex at its western end, a sill between CDP 6000 and 7000, structures related to the sheared western and eastern margins of the Sandstone greenstone belt (Chen et al., 2004) between CDP 9000 and 10000, the Booylgoo Range greenstone belt near CDP 13000, and the Agnew greenstone belt at the eastern end of the line. Seismic reflection traverse 10GA-YU3 is intersected by the Mount Magnet greenstone belt near its western end, and the Windimurra Igneous Complex in the west.

Forward modelling of the Southern Carnarvon seismic line (11GA-SC1)

A crucial part of the seismic interpretation process is testing the seismic interpretation against other data. In this case, forward models were generated to test the seismic interpretation against gravity data. The crust along the 11GA-SC1 line is modelled with a density of 2.83 g/cm^3 to reflect the mean density of continental crust

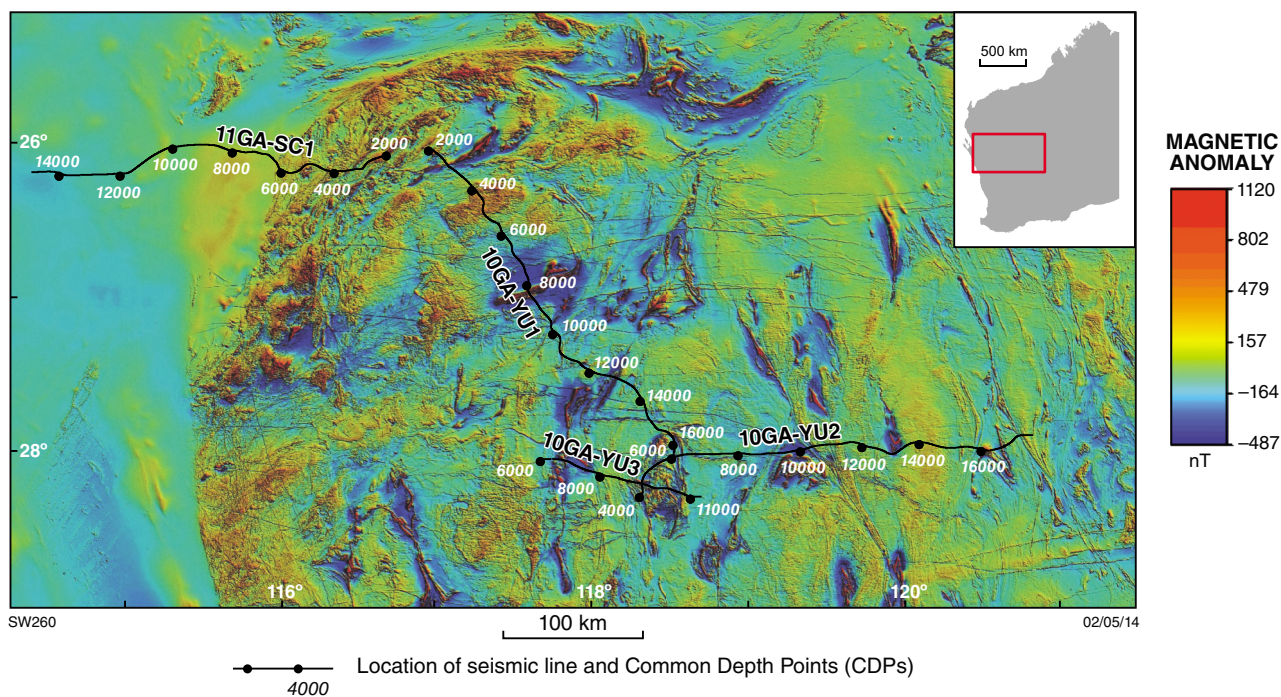


Figure 1. Magnetic anomaly map of the study area

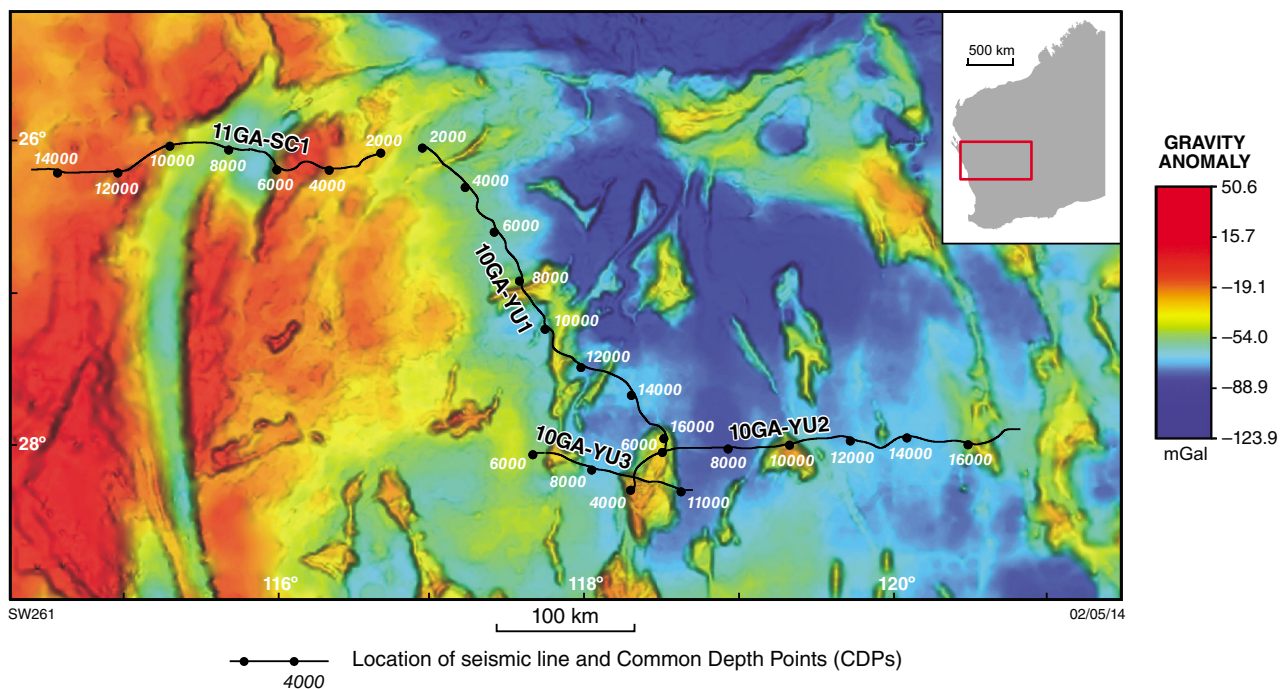


Figure 2. Gravity anomaly map of the study area

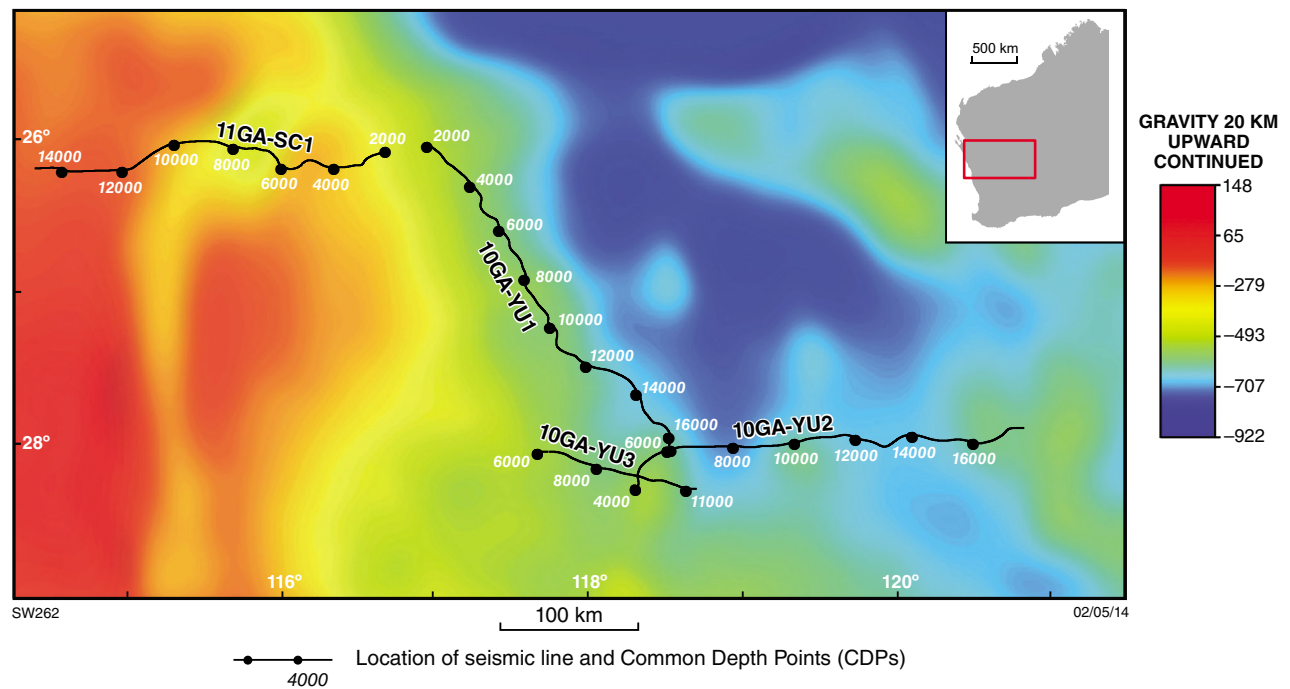


Figure 3. Gravity anomaly map of the study area upward continued to 20 km

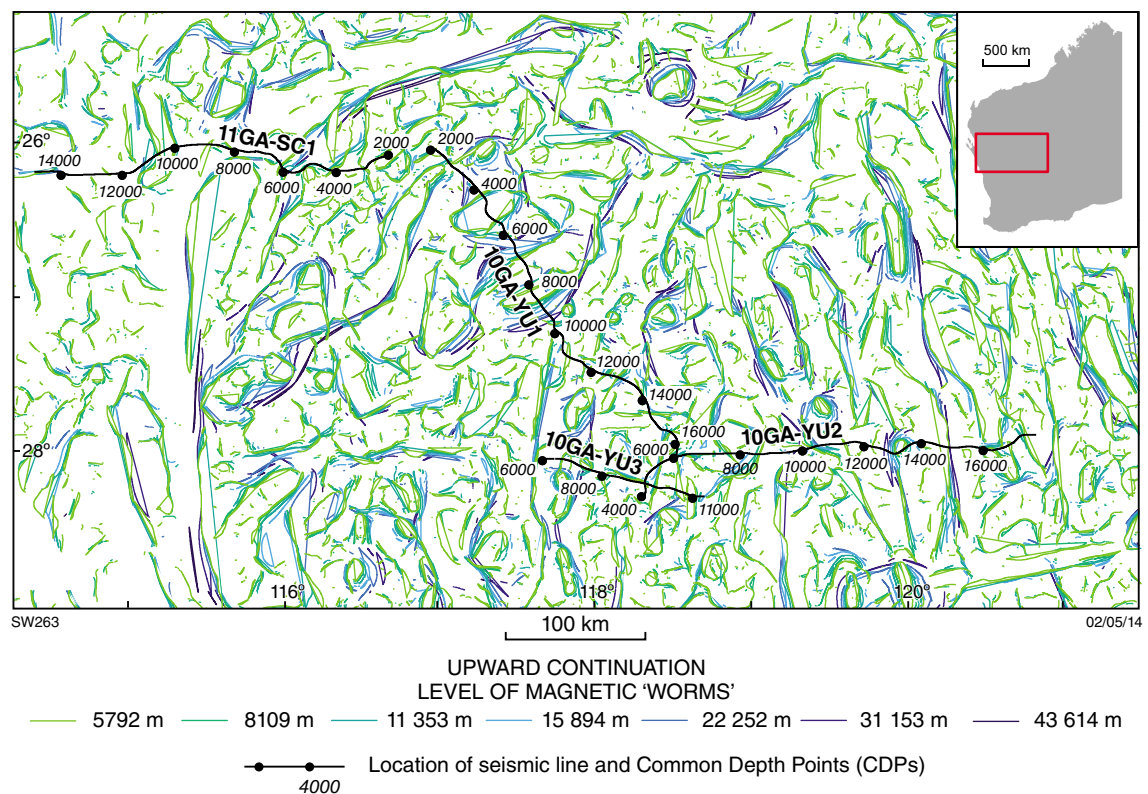


Figure 4. Multiscale edges ('worms') of magnetic field

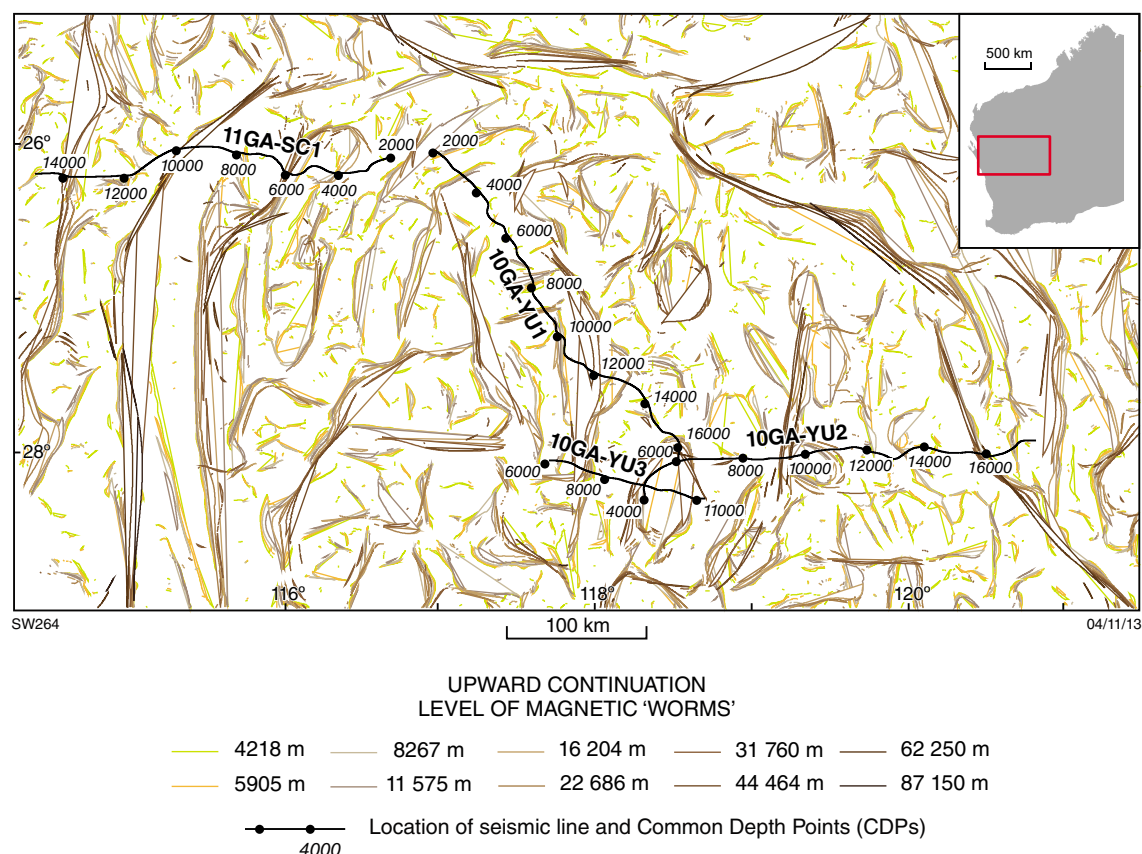


Figure 5. Multiscale edges ('worms') of gravity field

(Christensen and Mooney, 1995) and the upper mantle is modelled with a density of 3.30 g/cm^3 (Poudjom Djomani et al., 2001). This Moho topography creates a broad wavelength regional low at CDP 8000. This regional trend increases to the east and west, varying with the depth of the crust–mantle boundary.

The Southern Carnarvon Basin is modelled with a density of 2.40 g/cm^3 to reflect the density of sedimentary rock (Emerson, 1990). This model component generates the contrast caused by the east end of the Southern Carnarvon Basin at CDP 6400, where it is faulted against the Narryer Terrane (Plate 2 and Frontispiece 1).

Following the seismic interpretation (Korsch et al., 2013, this volume), the remaining crustal layers were included (Fig. 6). Middle (10–20 km) to lower (20–40 km) crustal layers of the Narryer Terrane, Errabiddy Shear Zone, Paradise Zone, and Pinjarra Orogen were included to match the gravity profile, with densities ranging between 2.70 and 2.85 g/cm^3 . These densities are consistent with amphibolite to granulite facies felsic to intermediate rocks (Rudnick et al., 1995). The upper crustal portion of the Narryer Terrane, from CDP 3400–6200, consists of amphibolite to granulite facies felsic rocks and was modelled with densities in the range of 2.60 – 2.82 g/cm^3 (Rudnick et al., 1995).

The gravity profile suggests that the geology is more complex than represented in the interpretation, hence further divisions were made based on form lines in the western portion of the Narryer Terrane, which was divided into upper and lower crustal blocks to reflect an increase of density with depth (Fig. 6). Similarly, the amphibolite to granulite facies felsic rocks of the Narryer Terrane from CDP 3400–6200 were separated so that the central block could be represented as a denser layer to those on the east and west (Fig. 6). These changes allowed the gravity high of -1 mGal at the eastern end of the line to be modelled with an improved fit to the observed data.

A final modification was to change the density of the upper crustal block (2–11 km depth) from CDP 10000–10500. This block was originally modelled with a density of 2.76 g/cm^3 as part of the Pinjarra Orogen. However, the gravity profile suggests there is a low density feature in this region and so the density was changed to 2.50 g/cm^3 to reflect this (Fig. 6). This suggests that this upper crustal block has a density significantly different to that of the average for the Pinjarra Orogen. Overall, the results of the forward modelling suggest that the interpretation of seismic line 11GA-SC1 is plausible as the geometries can reproduce the observed gravity data with acceptable densities.

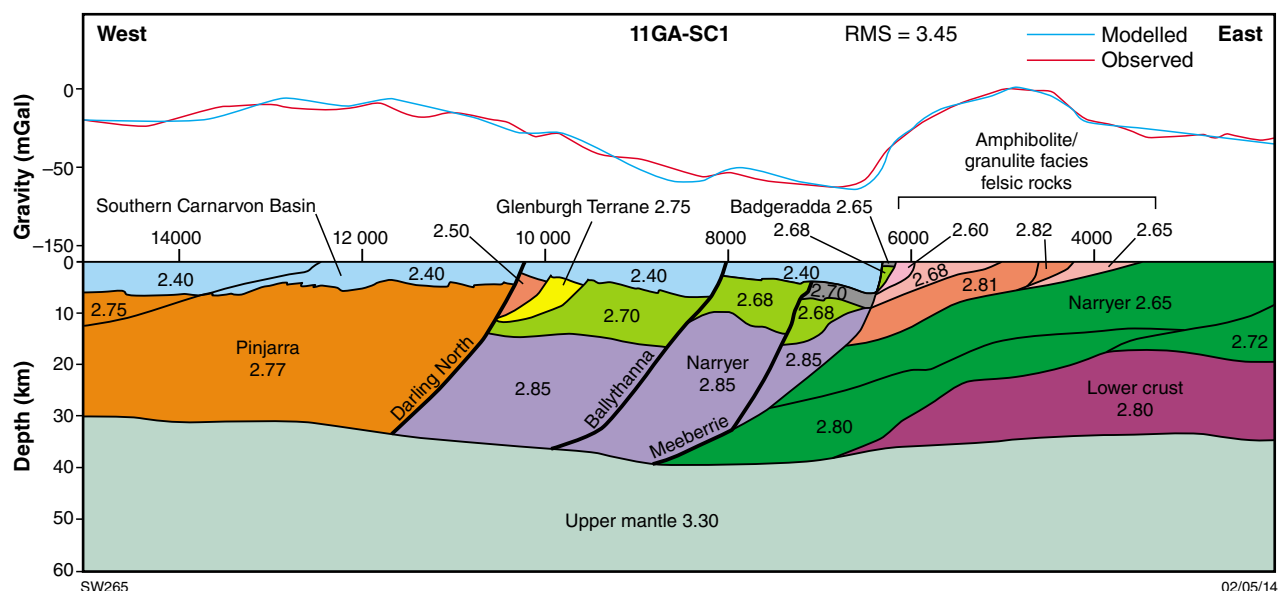


Figure 6. Forward model along Southern Carnarvon survey (11GA-SC1)

Forward modelling of 10GA-YU1

The gravity profile along 10GA-YU1 is characterized by a southeasterly decrease, with intermittent high-amplitude, short-wavelength anomalies resulting from dense greenstone belts that trend north–south (Fig. 7). Between these peaks, the observed data suggest a number of near-surface geological bodies, characterized by a series of closely spaced peaks and troughs. These high-frequency anomalies are interpreted to be the result of irregularly shaped granites and sills located near the surface. Using reasonable density values for the interpreted rock units, the gravity data are generally in agreement with the crustal architecture interpreted in the seismic data. To account for the regional variation, the middle to lower crust has been modelled with laterally varying densities (modelled at 2.89 – 2.83 g/cm³), and this variation may represent metamorphic and/or compositional variation within the Yarraquin Seismic Province.

The northwestern end of the line contains a sharp high-amplitude anomaly situated near the Cargarah Shear Zone, most likely associated with banded iron-formations within the Jack Hills, as identified in the surface geology. The steep negative gradient to the northwest of this anomaly is poorly matched by the calculated response and can be accounted for by modelling low-density sediments at the surface, not interpreted in the seismic data.

There are three peaks between CDPs 7000 and 14000 that correlate with felsic volcanic and mafic intrusive rocks in the vicinity of the Weld Range and Wattagee Hill volcanics of the Murchison Supergroup. A number of banded iron-formations have been identified within these units and may also contribute to the high amplitude (35 mGal) anomalies.

At the southern end of the line, there is a broad high-amplitude anomaly related to the Windimurra Igneous Complex, also seen along profiles 10GA-YU2 and 10GA-YU3 (Ivanic et al., 2013, this volume). The Windimurra Igneous Complex was modelled using a constant density of 2.95 g/cm³ for the ultramafic zone and 2.815 g/cm³ for the overlying zone. The same values were used across all three lines and provide a good overall fit between the observed and calculated responses.

Due to the nature of forward modelling, we have assumed that all bodies extend either side of the line by 5–10 times their depth extent (see description in Forward modelling section). This assumption is generally accepted for profiles that run orthogonal to geological strike. Figure 3 shows the upward continued (20 km) gravity response, illustrating that 10GA-YU1 was collected along strike of a significant boundary in the gravity data. This may introduce non-trivial errors into model-determined densities and could be investigated further through forward modelling either side of the line.

Forward modelling of 10GA-YU2

Seismic line 10GA-YU2 crosses the Ida Fault, a major tectonic boundary in the Yilgarn Craton, which separates the Youanmi and Kalgoorlie Terranes and delineates the western extent of the Eastern Goldfields Superterrane. The seismic interpretation indicates a distinct change in the lower crustal character west of the Ida Fault (Zibra et al., 2013, this volume) and has been modelled by a notable increase in density for both the upper and lower crust (Fig. 8).

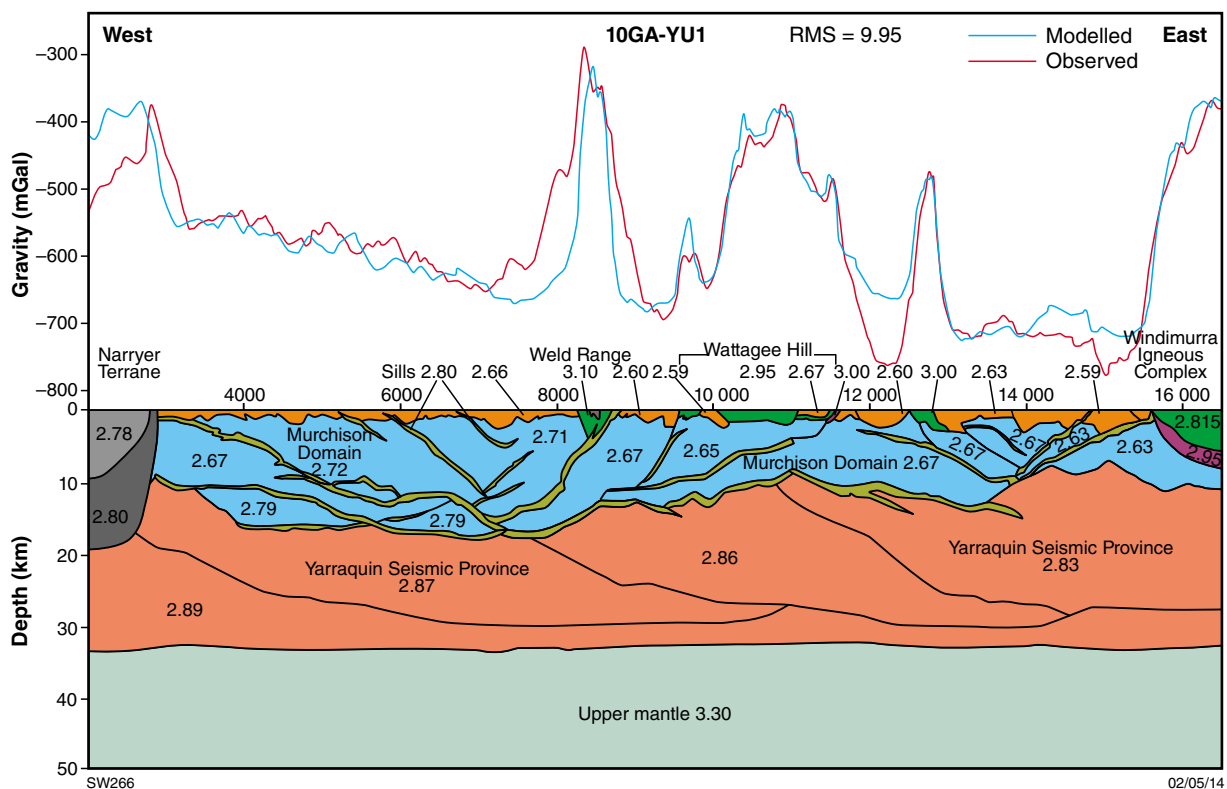


Figure 7. Forward model along 10GA-YU1

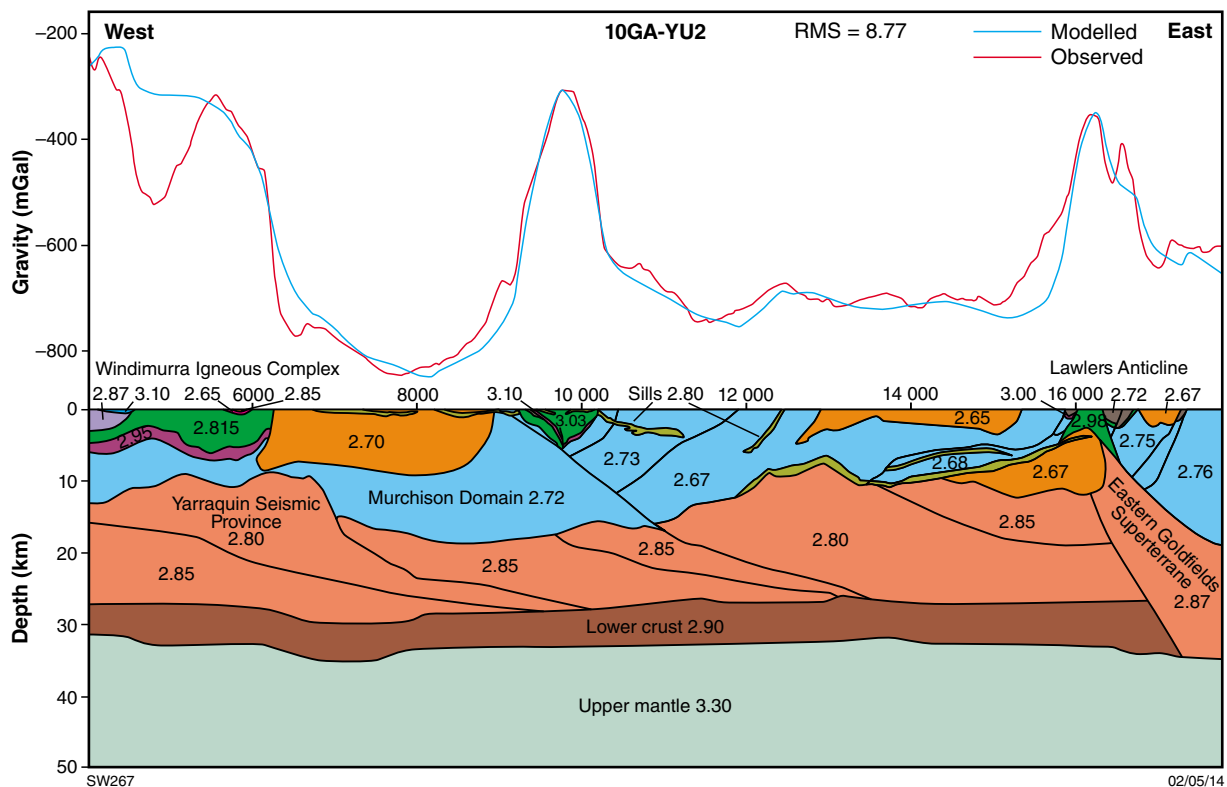


Figure 8. Forward model along 10GA-YU2

The largest mismatch over the model space is around the Windimurra Igneous Complex. Due to a significant bend in the seismic line between CDP 4000 and 6000, the gravity profile runs close to the western edge of the complex. As a result, the observed response will be significantly affected by low density sedimentary rocks to the west, which are not taken into account in this forward model as they occur out of section.

There are two other broad, high-amplitude anomalies that reach -30 and -35 mGal in the observed gravity data at approximately CDP 10000 and 16000, respectively. These have been attributed to the Sandstone and Booylgoo greenstone belts and the Lawlers Anticline. A large, dome-shaped granitic unit — the Lawlers Tonalite — has been modelled beneath the Lawlers Anticline. This is consistent with interpretations by Blewett et al. (2010), who proposed syn-extensional plutonism in the region. However, this low density body to the west of the Lawlers Anticline causes a steep negative gradient in the modelled response that does not match very well with the observed gravity data.

Forward Modelling of 10GA-YU3

There are two broad, high-amplitude anomalies that dominate the overall gravity response along seismic line 10GA-YU3 (Fig. 9). These correspond to the Mount Magnet area to the west and the Windimurra Igneous Complex to the east. The regional trend is east dipping and correlates with a shallowing lower crust from east to west. The largest mismatch across the model space exists over the Windimurra Igneous Complex, where short-wavelength features in the observed gravity are not accounted for in the seismic interpretation. The internal structure of the Windimurra Igneous Complex requires a higher model resolution if short-wavelength features are to be resolved. However, the gravity data tend to agree with the general 'bowl shape' interpreted for the Windimurra Igneous Complex at depth (Ivanic et al., 2013, this volume). The Mount Magnet anomaly dips to the east and was modelled using bodies of 2.95 g/cm³ for mafic units and 3.10 g/cm³ for ultramafic units.

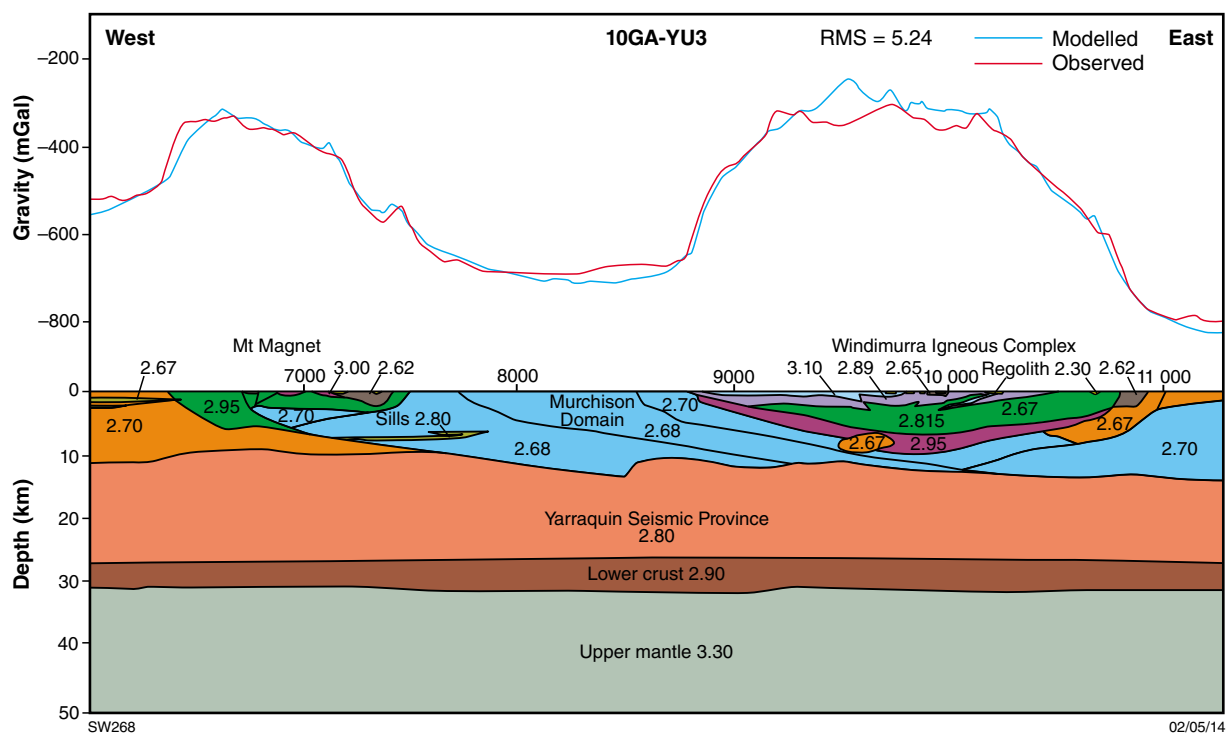


Figure 9. Forward model along 10GA-YU3

Cross-gradient joint inversion

Reading of the combined geophysical parameters

The results of the cross-gradient joint inversion are presented as curves and ‘geospectral’ images using a colour scale that combines information on gravity and magnetic data (Fig. 10). The values for density and magnetic susceptibility are set between reasonable bounds for average rock properties. The average rock property values identify major crustal rock types such as gneiss and metasedimentary (green), magnetic igneous intrusive (red), non-magnetic igneous intrusive (yellow), and ultramafic (brown) rocks (Fig. 10). It should be noted that property contrasts along the profile are deemed accurate in general, whereas the estimated depths of features are less reliable, as they generally depend on the general dip of structures near the surface.

Inversion of 10GA-YU1

The gravity and magnetic field profiles and the inversion model along 10GA-YU1 (Fig. 11) show a long-wavelength south-southeasterly trend of decreasing gravity relative to a flatter magnetic response with a broad, elevated anomaly near CDP 5000. Both the gravity and magnetic fields display many short-wavelength variations with coinciding peaks near the Jack Hills greenstone belt, the Weld Range, the Tuckabianna Synform, and the Windimurra Igneous Complex. There are areas that display a negative correlation between low gravity and a flat magnetic response between the Tuckabianna Synform and the Windimurra Igneous Complex. There are also two narrow features where high gravity values coincide with low magnetization, one just north of Weld Range near CDP 8000, and a second one — likely a dyke — near CDP

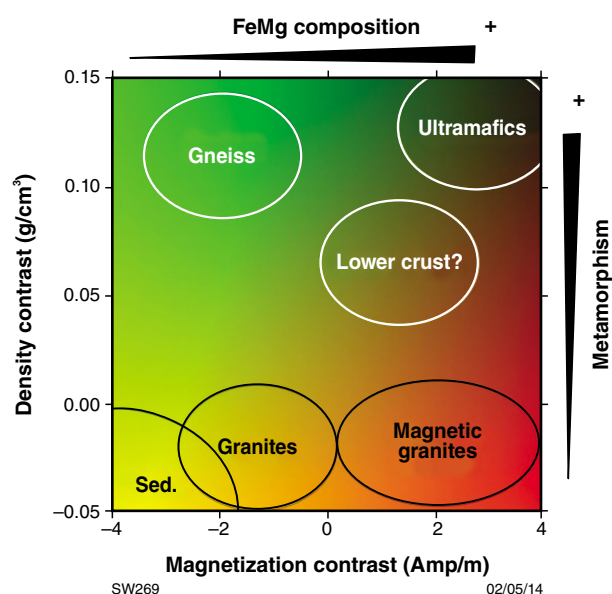


Figure 10. Colour scale for geospectral images

15000. The decrease in gravity corresponds with an overall increase of less reflective upper crust towards the south.

In general, features with common physical properties alternate at a 10–20 km wavelength in most of the central and southern portion of 10GA-YU1, which suggests a variation between low and moderate levels of magnetization, and a large range of densities. This pattern is similar to the magnetotelluric data along the same profile (Milligan et al., 2013, this volume). The northern part shows a stronger magnetic response, and the inversion predicts a relatively magnetic and moderately dense lower crustal affinity for Narryer Terrane rocks north of the Jack Hills greenstone belt. Rocks with properties similar to these are predicted to form the middle crust along most of the section, with the exception of the area near the Windimurra Igneous Complex, where mafic and ultramafic rocks are predicted to be much denser. The overall pattern suggests that the region of relatively magnetic and moderately dense lower crustal rocks in 10GA-YU1 correlates well with the reflective lower crust named the Yarraquin Seismic Province (Korsch et al., 2013, this volume).

Inversion of 10GA-YU2

The gravity and magnetic field profiles and the inversion model along 10GA-YU2 (Fig. 12) show a relatively low level of magnetization with short-amplitude variations within the Windimurra Igneous Complex and at the eastern end of the line, and a pronounced trough between CDP 9000 and 10000. Gravity is highly variable, with high levels within the Windimurra Igneous Complex, the Sandstone greenstone belt, and the eastern end of the line. Gravity values are very low between the Windimurra Igneous Complex and the Sandstone greenstone belt, and low between there and the boundary to the Eastern Goldfields. Within the Windimurra Igneous Complex, broad peaks of high gravity coincide with a pattern of shorter wavelength magnetic anomalies. The magnetic response is relatively flat in the areas of low gravity and shows a negative correlation with the gravity high near the Sandstone greenstone belt. Both fields have common peaks near the eastern end of the profile.

In general, features with common physical property gradients alternate at a longer wavelength in 10GA-YU2 compared to 10GA-YU1, probably because fewer greenstone belts are intersected. Similarly to 10GA-YU1, the topography of relatively magnetic and moderately dense lower crust imaged in section 10GA-YU2 correlates well with the reflective lower crustal Yarraquin Seismic Province (Korsch et al., 2013, this volume). The Yarraquin sequence in section 10GA-YU2 has a similar response in the magnetotelluric profile (Milligan et al., 2013, this volume).

Inversion of 10GA-YU3

In the gravity and magnetic field profiles and the inversion model along 10GA-YU3 (Fig. 13), broad peaks of high gravity coincide with a pattern of shorter wavelength magnetic anomalies within the Windimurra Igneous Complex, which appears to be surrounded by low density

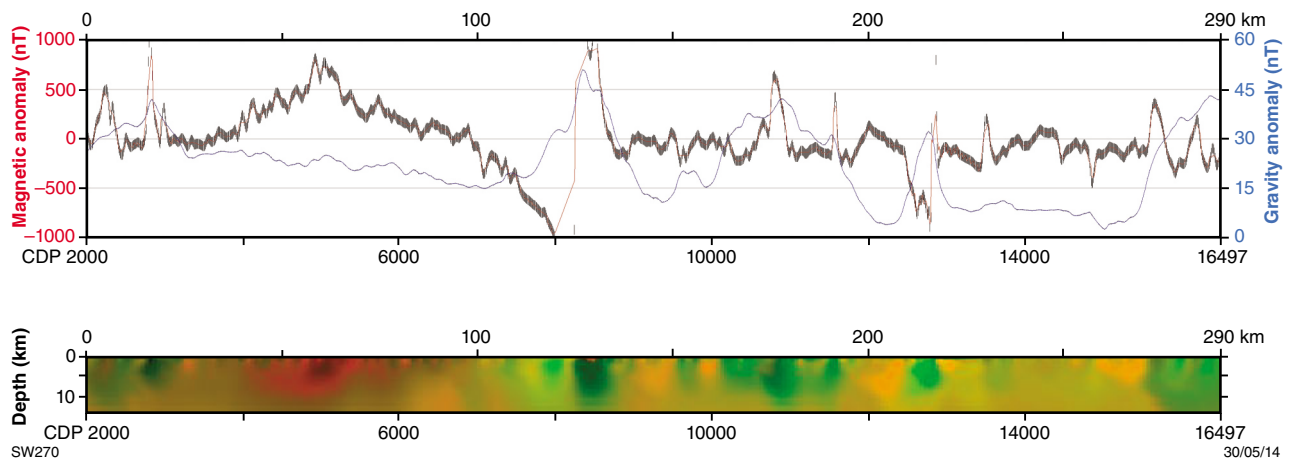


Figure 11. Profiles of magnetic and gravity anomalies, and geospectral image along 10GA-YU1: potential field curves (top) and cross-gradient joint inversion (bottom)

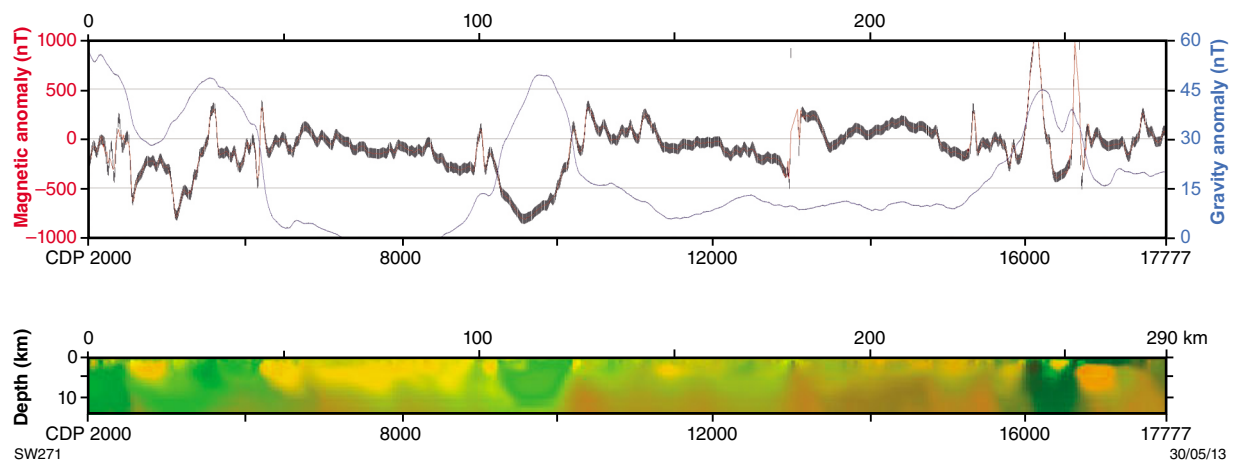


Figure 12. Profiles of magnetic and gravity anomalies, and geospectral image along 10GA-YU2: potential field curves (top) and cross-gradient joint inversion (bottom)

material with moderate to high magnetization levels. The Mount Magnet greenstone belt stands out as a prominent feature of high density and relatively low magnetization in the upper crust, except for a spike related to banded iron-formations at Mount Magnet. Even though the lower crust is very reflective in the seismic data, the upper crustal signature of the Mount Magnet greenstone belt dominates the entire section. This may be an example of where a broad wavelength anomaly in the upper crust is propagated to greater depths — one of the potential pitfalls of the cross-gradient joint inversion method that need to be considered during interpretation, when assessing what is geologically plausible. The area between the Mount Magnet greenstone belt and the Windimurra Igneous Complex consists of the low-density and weakly to moderately magnetic Cundimurra granite. The Cundimurra granite is underlain by the Yarraquin seismic province, which also extends below and east of the Windimurra Igneous Complex (Ivanic et al., 2013, fig. 7f, this volume).

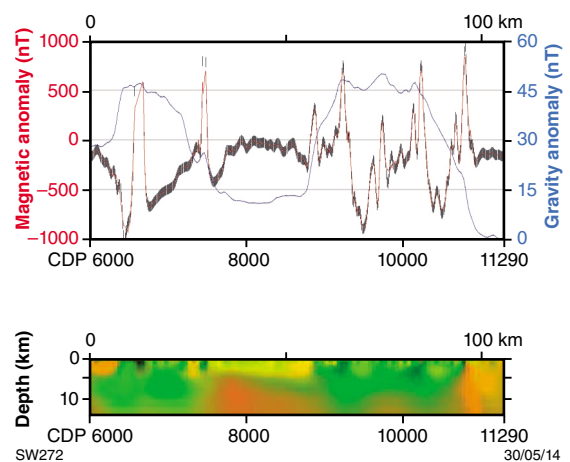


Figure 13. Profiles of magnetic and gravity anomalies, and geospectral image along 10GA-YU3: potential field curves (top) and cross-gradient joint inversion (bottom)

Conclusions

The grids, worms, inversions, and models presented here share many characteristics with surface observations and, in case of the Youanmi survey, also with the magnetotelluric data (Milligan et al., 2013, this volume). Therefore, they help to constrain the deep structure of the Paleozoic Southern Carnarvon Basin, the Neoproterozoic Pinjarra Orogen, the Archean to Proterozoic Glenburgh Terrane, and of the Archean Narryer, Youanmi and Kalgoorlie terranes of the Yilgarn Craton.

A striking feature of the potential-field data, and the forward models and inversions from which they were derived, is the occurrence of pronounced gradients in gravity related to the terrane boundaries in the northwest Yilgarn Craton, and also the long-wavelength gravity pattern within the Murchison Domain. The southern margin of the pronounced gravity low in the Murchison Domain is intersected by seismic reflection line 10GA-YU2, where the overall flat Moho suggests that the gravity low is related to the relatively small thickness of the Yarraquin seismic province and the presence of extensive granite in the upper crust. Whether it is this combination of physical property distribution or some other structural situation that causes the large gravity low in the Murchison Domain must remain speculation at this stage.

The potential-field data along the Southern Carnarvon survey appear to vary as a function of the spatial extent of the Southern Carnarvon Basin, and where its basement changes from Pinjarra to Glenburgh and Narryer affinity. Along the Youanmi survey, the variations in the potential-field data appear to be controlled by the thickness of the lower crust, and the spatial extent of granitic bodies and greenstone belts.

A striking feature of the potential-field data, and the forward models and inversions from which they were derived, is the occurrence of pronounced gradients in gravity in the northwest Yilgarn Craton, and also the long-wavelength gravity pattern within the Murchison Domain. The southern margin of the pronounced gravity low in the Murchison Domain is intersected by seismic reflection line 10GA-YU2, where the overall flat Moho suggests that the gravity low is related to the relatively small thickness of the Yarraquin seismic province and the presence of extensive granite in the upper crust. Whether it is this particular combination of physical property distribution or some other structural situation that causes the large gravity low in the Murchison Domain must remain speculation at this stage. This uncertainty highlights the challenge of understanding the reason for long wavelength gravity patterns across the Yilgarn Craton, and also along its Proterozoic margins. It is likely that variations in physical properties of Earth's crust alone are not sufficient to explain these gravity gradients. For a coherent understanding of gravity patterns across the Yilgarn Craton and models that take into account regional changes in mantle properties such as age-based density variations (Aitken et al., 2013) may need to be considered.

References

- Aitken, ARA, Salmon, ML and Kennett, BLN 2013, Australia's Moho: a test of the usefulness of gravity modelling for the determination of Moho depth: *Tectonophysics*, v. 609, p. 468–479.
- Archibald, N, Gow, P and Boschetti, F 1999, Multiscale edge analysis of potential-field data: *Exploration Geophysics*, v. 30, p. 38–44.
- Bouguer gravity anomaly map of Australia 2010: Geoscience Australia, Canberra, ACT, <www.geoscience.gov.au/gadds>, viewed December 2010.
- Blewett, RS, Czarnota, K and Henson, PA 2010, Structural-event framework for the eastern Yilgarn Craton, Western Australia, and its implications for orogenic gold: *Precambrian Research*, v. 183, p. 203–209.
- Chen, SF, Libby, JW, Wyche, S and Riganti, A 2004, Kinematic nature and origin of regional-scale ductile shear zones in the central Yilgarn Craton, Western Australia: *Tectonophysics*, v. 394, p. 139–153.
- Christensen, NI and Mooney, WD 1995, Seismic velocity structure and composition of the continental crust: A global view: *Journal of Geophysical Research: Solid Earth*, v. 100, no. B6, p. 9761–9788.
- Fregoso, E and Gallardo, LA 2009, Cross-gradients joint 3D inversion with applications to gravity and magnetic data: *Geophysics*, v. 74, p. L31–L42.
- Emerson, DW 1990, Notes on mass properties of rocks — density, porosity, permeability: *Exploration Geophysics*, v. 21, p. 209–216.
- Gallardo, LA 2007, Multiple cross-gradient joint inversion for geospectral imaging: *Geophysical Research Letters*, v. 34, L19301.
- Gallardo, LA, Fontes, SL, Meju, MA, Buonora, MP and Lugao, PP 2012, Robust geophysical integration through structure-coupled joint inversion and multispectral fusion of seismic reflection, magnetotelluric, magnetic, and gravity images: Example from Santos Basin, offshore Brazil: *Geophysics*, v. 77, p. B237–B251.
- Gallardo, LA and Meju, MA 2003, Characterization of heterogeneous near-surface materials by joint 2D inversion of dc resistivity and seismic data: *Geophysical Research Letters*, v. 30, p. 1658.
- Gallardo, LA and Meju, MA 2004, Joint two-dimensional DC resistivity and seismic travel time inversion with cross-gradients constraints: *Journal of Geophysical Research Solid Earth*, v. 109, p. B03311.
- Gallardo, LA and Meju, MA 2007, Joint two-dimensional cross-gradient imaging of magnetotelluric and seismic travel time data for structural and lithological classification: *Geophysical Journal International*, v. 169, p. 1261–1272.
- Gallardo, LA and Thebaud, N 2012, New insights into Archean granite-greenstone architecture through joint gravity and magnetic inversion: *Geology*, v. 40, p. 215–218.
- Geological Survey of Western Australia 2010, Magnetic merged grid of Western Australia (version 1 – superseded): Geological Survey of Western Australia, <www.dmp.wa.gov.au/16942.aspx#17072>, viewed December 2010.
- Holden, DJ, Archibald, NJ, Boschetti, F and Jessell, MW 2000, Inferring geological structures using wavelet-based multiscale edge analysis and forward models: *Exploration Geophysics*, v. 31, p. 617–621.
- Hornby, P, Boschetti, F and Horowitz, FG 2001, Ambiguity analysis and joint inversion of potential-field and other data: CSIRO Exploration & Mining, Nedlands, Western Australia, 29p.
- Hu, WY, Abubakar, A and Habashy, TM 2009, Joint electromagnetic and seismic inversion using structural constraints: *Geophysics*, v. 74, p. R99–R109.

- Ivanic, TJ, Korsch, RJ, Wyche, S, Jones, LEA, Zibra, I, Blewett, RS, Jones, T, Milligan, PR, Costelloe, RD, Van Kranendonk, MJ, Doublier, MP, Hall, CE, Romano, SS, Pawley, MJ, Gessner, K, Patison, N, Kennett, BLN and Chen, SF 2013, Preliminary interpretation of the 2010 Youanmi deep seismic reflection lines and magnetotelluric data for the Windimurra Igneous Complex, *in* Youanmi and Southern Carnarvon seismic and magnetotelluric (MT) workshop 2013 *compiled by* S Wyche, TJ Ivanic and I Zibra: Geological Survey of Western Australia, Record 2013/6, p. 97–111.
- Korsch, RJ, Blewett, RS, Wyche, S, Zibra, I, Ivanic, TJ, Doublier, MP, Romano, SS, Pawley, MJ, Johnson, SP, Van Kranendonk, MJ, Jones, LEA, Kositsin, N, Gessner, K, Hall, CE, Chen, SF, Patison, N, Kennett, BLN, Jones, T, Goodwin, JA, Milligan, PR and Costelloe, RD 2013, Geodynamic implications of the Youanmi and Southern Carnarvon deep seismic reflection surveys: a ~1300 km traverse from the Pinjarra Orogen to the eastern Yilgarn Craton, *in* Youanmi and Southern Carnarvon seismic and magnetotelluric (MT) workshop 2013 *compiled by* S Wyche, TJ Ivanic and I Zibra: Geological Survey of Western Australia, Record 2013/6, p. 147–166.
- Linde, N, Binley, A, Tryggvason, A, Pedersen, LB and Reil, A 2006, Improved hydrogeophysical characterization using joint inversion of cross-hole electrical resistance and ground-penetrating radar traveltimes data, *Water Resources Research*, v. 42, no. 12, p. W12404.
- Milligan, PR 2010, The Magnetic anomaly map of Australia Edition 5: Geoscience Australia, Canberra, ACT, <<http://data.gov.au/dataset/magnetic-anomaly-map-of-australia-5th-edition-1-5-million-scale-2010>>, viewed December 2010.
- Milligan, PR, Duan, J, Fomin, T, Nakamura, A and Jones, T 2013, The Youanmi magnetotelluric (MT) transects, *in* Youanmi and Southern Carnarvon seismic and magnetotelluric (MT) workshop 2013 *compiled by* S Wyche, TJ Ivanic and I Zibra: Geological Survey of Western Australia, Record 2013/6, p. 13–25.
- Moorkamp, M, Heincke, B, Jegen, M, Roberts, AW and Hobbs, RW 2011, A framework for 3-D joint inversion of MT, gravity and seismic refraction data: *Geophysical Journal International*: v. 184, p. 477–493.
- Poudjom Djomani, YH, O'Reilly, SY, Griffin, WL and Morgan, P 2001, The density structure of subcontinental lithosphere through time: *Earth and Planetary Science Letters*, v. 184, no. 3, p. 605–621.
- Rudnick, RL and Fountain, DM 1995, Nature and composition of the continental crust: a lower crustal perspective: *Reviews of Geophysics*, v. 33, p. 267–309.
- Telford, WM and Sheriff, RE 1990, *Applied geophysics*: Cambridge University Press, Cambridge, UK, 770p.
- Tikhonov, AN and Arsenin, VY 1977, *Solutions of ill-posed problems*, in *Scripta Series in Mathematics*: Winston & Sons, New York, USA, 258p.
- Twomey, S 1977, *Introduction to the mathematics of inversion in remote sensing and indirect measurement*: Elsevier, Amsterdam, The Netherlands, 253p.
- Wynn, P 2009, *Index of gravity surveys*, 2nd edition: Geoscience Australia Record, 2009/007
- Zibra, I, Gessner, K, Pawley, MJ, Wyche, S, Chen, SF, Korsch, RJ, Blewett, RS, Jones, T, Milligan, PR, Jones, LEA, Doublier, MP, Hall, CE, Romano, SS, Ivanic, TJ, Patison, N, Kennett, BLN and Van Kranendonk, MJ 2013, Preliminary interpretation of deep seismic line 10GA-YU2: Youanmi Terrane and western Kalgoorlie Terrane, *in* Youanmi and Southern Carnarvon seismic and magnetotelluric (MT) workshop 2013 *compiled by* S Wyche, TJ Ivanic and I Zibra: Geological Survey of Western Australia, Record 2013/6, p. 87–95.

Main crustal-scale features of the Youanmi seismic transect

by

**I Zibra, K Gessner, RJ Korsch¹, RS Blewett¹, T Jones¹, P Milligan¹, LEA Jones²,
RD Costelloe¹, S Wyche, MP Doublier, CE Hall, SF Chen, SS Romano, TJ Ivanic,
MJ Pawley³, N Patison, BLN Kennett⁴, and MJ Van Kranendonk⁵**

Introduction

This chapter gives an overview of prominent, large-scale features evident on the seismic traverses. Observations relating to discrete features will be discussed in following chapters dedicated to segments of particular lines.

and Kalgoorlie Terranes. The Moho becomes progressively deeper eastward in the Yilgarn Craton, down to about 15.5 s TWT (46 km) at the eastern end of the northeastern Yilgarn seismic transect (AGS01-NY1; Goleby et al., 2004).

These features will be discussed in the relevant chapters of this volume.

The Moho

In all three Youanmi seismic lines, the Mohorovičić discontinuity (Moho) is interpreted to be the obvious sharp transition between the highly reflective lower crust and the poorly reflective uppermost mantle (see also Korsch et al., 2013, this volume). In these seismic profiles, the Moho appears as a well-defined, flat and laterally continuous surface mostly between 10.5 and 11 s two-way time (TWT), corresponding to about 31–33 km depth. The Moho appears remarkably flat, even under the major Youanmi–Narryer terrane boundary. However, there are two intervals along line 10GA-YU2 that show different depth character:

- To the east of the Windimurra Igneous Complex (CDP 6200–7700), the Moho deepens down to 12.5 s (or possibly even to 13.5 s) TWT over a distance of about 50 km. This variation in Moho depth is symmetrical at each end of the interval.
- Near the eastern end of line (CDP >16500), the Moho gradually deepens down to 11.5 s TWT. This is in the vicinity of the boundary between the Youanmi

Divisions within the crust

On the basis of geometry and seismic character, the continental crust imaged by the seismic lines can be subdivided into three main structural domains (see also Korsch et al., 2013, this volume). Above the Moho, between about 11 and 9 s TWT, the seismic transect includes strong horizontal reflections, which are laterally continuous at the scale of the whole seismic transect; that is, at the scale of hundreds of kilometres. Such morphology, together with the absence of any important vertical offset of the Moho, suggests that there are possibly no mantle-penetrating shear zones in the Youanmi lithosphere. The Neoarchean deposition of continuous, 5–15 km thick, subaqueous continental flood basalt successions typical of Archean terranes requires Moho temperatures much greater than 650°C at the time of eruption (Flament et al., 2011); that is, temperatures were about 250°C hotter in Archean cratons than present-day Moho temperatures (Artemieva, 2009). The description of high-temperature shear fabrics in Archean lower crust (e.g. Sandiford, 1989) suggests that Archean continental geotherms were significantly hotter than their present-day counterparts, allowing the flow of hot, ductile and partially molten lower crust. This is consistent with metamorphic studies in both the Superior Province (Canada) and the Yilgarn Craton, showing that temperatures of up to 750°C were reached at a depth of 15–20 km (e.g. Easton, 2000). Therefore, we suggest that the weak lower continental crust in the Youanmi Terrane provided a first-order decoupling horizon between the stronger lithospheric mantle and the middle to upper crust.

Studies of exposed lower crustal sections indicate that layering resulting from deformation and metamorphism of lithological units with different acoustic impedances

1 Minerals and Natural Hazards Division, Geoscience Australia, GPO Box 378, Canberra ACT 2601

2 Energy Division, Geoscience Australia, GPO Box 378, Canberra ACT 2601

3 Geological Survey of South Australia, Department of Manufacturing Innovation Trade Resources and Energy, Level 4, 101 Grenfell Street, Adelaide SA 5000

4 Research School of Earth Sciences, The Australian National University, Canberra ACT 0200

5 School of Biological, Earth and Environmental Sciences, The University of New South Wales, Sydney NSW 2052

(e.g. clusters of fine layers of mafic granulite within granitic or charnockitic mylonite), combined with mantle-derived magma underplating, is able to produce the high reflectivity commonly observed at lower crustal levels (Ji et al., 1997; Meissner et al., 2006).

In the Youanmi seismic lines, the lower crust grades upward into the middle crust (between about 3 and 9 s TWT) characterized by strong, east-dipping reflections, which display overall listric geometry, with a gradual upward steepening of the major reflections. This region forms the upper part of the Yarraquin Seismic Province of Korsch et al. (2013, this volume). In all three seismic lines, the transition between the middle and lower crust is gradual, and confined between 8 and 9 s TWT. The uppermost part of the mid-crustal, highly reflective domain is characterized by a complex topography, where individual packages of reflections show an upward convex profile giving rise to a crustal-scale, consistently east-dipping, imbricate fan geometry (Plate 3).

In contrast with the middle to lower crust, the uppermost portion of the present-day Youanmi continental crust contains thin (i.e. <500 m minimum thickness) sets of reflections, which are both east- or west-dipping, and isolated within generally transparent to poorly reflective domains. Particularly along lines 10GA-YU1 and 10GA-YU2, some of these prominent and isolated reflections can be confidently interpreted as Proterozoic mafic sills. This interpretation is mainly based on: 1) the modelled seismic response of high acoustic-impedance layers; 2) the absence of either any deflection or offset of markers overprinted by these reflections; and 3) good surface geology control — the uppermost portions of these reflections can be matched confidently with regional-scale mafic sills exposed at the surface and identifiable by geophysical means (Plate 1; Ivanic et al., 2013, this volume).

References

Artemieva, IM 2009, The continental lithosphere: Reconciling thermal, seismic, and petrologic data: *Lithos*, v. 109, p. 23–46.

Easton, RM 2000, Metamorphism of the Canadian Shield, Ontario, Canada. I. The Superior Province: *Canadian Mineralogist*, v. 38, p. 287–317.

Flament, N, Rey, PF, Coltice, N, Dromart, G and Olivier, N 2011, Lower crustal flow kept Archean continental flood basalts at sea level: *Geology*, v. 39, p. 1159–1162.

Goleby, BR, Blewett, RS, Korsch, RJ, Champion, DC, Cassidy, KF, Jones, LEA, Groenewald, PB and Henson, PA 2004, Deep seismic reflection profiling in the Archaean northeastern Yilgarn Craton, Western Australia: implications for crustal architecture and mineral potential: *Tectonophysics*, v. 388, p. 119–133.

Ivanic, TJ, Wingate, MTD, Korsch, RJ, Blewett, RS, Jones, LEA, Wyche, S, Zibra, I, Doublier, MP, Romano, SS, Pawley, MJ, Van Kranendonk, MJ, Gessner, K, Hall, CE, Chen, SF, Patison, NL and Costelloe, RD 2013, Preliminary interpretation of the Youanmi deep seismic reflection lines for Proterozoic intrusive rocks, in *Youanmi and Southern Carnarvon seismic and magnetotelluric (MT) workshop 2013 compiled by S Wyche, TJ Ivanic and I Zibra*: Geological Survey of Western Australia, Record 2013/6, p. 81–85.

Ji, S, Long, C, Martignole, J and Salisbury, M 1997, Seismic reflectivity of a finely layered, granulite-facies ductile shear zone in the southern Grenville Province (Quebec): *Tectonophysics*, v. 279, p. 113–133.

Korsch, RJ, Blewett, RS, Wyche, S, Zibra, I, Ivanic, TJ, Doublier, MP, Romano, SS, Pawley, MJ, Johnson, SP, Van Kranendonk, MJ, Jones, LEA, Kositsin, N, Gessner, K, Hall, CE, Chen, SF, Patison, N, Kennett, BLN, Jones, T, Goodwin, JA, Milligan, PR and Costelloe, RD 2013, Geodynamic implications of the Youanmi and Southern Carnarvon deep seismic reflection surveys: a ~1300 km traverse from the Pinjarra Orogen to the eastern Yilgarn Craton, in *Youanmi and Southern Carnarvon seismic and magnetotelluric (MT) workshop 2013 compiled by S Wyche, TJ Ivanic and I Zibra*: Geological Survey of Western Australia, Record 2013/6, p. 147–166.

Meissner, R, Rabbal, W and Kern, H 2006, Seismic lamination and anisotropy of the Lower Continental Crust: *Tectonophysics*, v. 416, no. 1–4p. 81–99.

Sandiford, M 1989, Horizontal structures in granulite terrains: A record of mountain building or mountain collapse?: *Geology*, v. 17, p. 449–452.

Preliminary interpretation of the Youanmi deep seismic reflection lines for Proterozoic intrusive rocks

by

TJ Ivanic, MTD Wingate, RJ Korsch¹, RS Blewett¹, LEA Jones², S Wyche, I Zibra, MP Doublier, SS Romano, MJ Pawley³, MJ Van Kranendonk⁴, K Gessner, CE Hall, SF Chen, N Patison, and RD Costelloe¹

Introduction

The region of the Youanmi seismic traverses is transected by numerous Proterozoic mafic dykes and sills (Fig. 1), many of which can be attributed to large igneous provinces (LIPs) within the Yilgarn Craton (Table 1 in Wyche et al., 2013, this volume). The majority occur as dolerite dykes, typically 5–30 m wide, 50–300 km long, and trending mainly east to east-northeast. Many sills have also been recognized at the surface, some of which are up to 50 m thick with a surface expression of up to 300 km length.

Easterly and east-northeasterly trending gabbro or norite dykes in the southern and southeastern parts of the traverse region (Fig. 1) are part of the c. 2410 Ma Widgiemooltha Dyke Suite. This suite occurs across the entire Yilgarn Craton, but is not well represented in the region of the Youanmi seismic lines. The c. 1210 Ma Muggamurra dyke swarm (Fig. 1) is part of the Marnda Moom LIP comprising dolerite, gabbro and diorite dykes, which are concentrated mainly around the margins of the Yilgarn Craton, but also extend into the centre of the craton. The c. 1070 Ma Warakurna LIP consists of mafic igneous rocks emplaced over about 1.5 million km² in western and central Australia. In the northwestern Yilgarn Craton and the southern parts of the traverse area, subhorizontal or shallowly dipping gabbro sills, typically several metres thick, produce prominent west-northwesterly trending, sinuous aeromagnetic anomalies.

Seismic expression of mafic sills

To generate a seismic reflection from an interface, there must first be a change in acoustic impedance, which is the product of density and seismic P-wave velocity.

Representative values of density are 2.65 g/cm³ for granite and 2.95 g/cm³ for dolerite. Seismic P-wave velocities are more variable within each rock type, but typically range from 6000 to 6500 ms⁻¹ for granite and 6500 to 7000 ms⁻¹ for dolerite (Christensen, 1982). The reflection coefficient (ratio of reflected to incident amplitude) calculated from the middle range of these values is approximately 0.09, a relatively large value. In contrast, the reflection coefficient between sand and shale in a sedimentary basin is typically <0.05. Thus strong reflections should be characteristic of a felsic–mafic interface.

The seismic response to changing thickness of a horizontal mafic sill embedded in felsic material is shown in Figure 2. The consequence of this simple model is that thick sills should be marked by a pair of reflected wavelets, with the lower reflection having opposite polarity to the upper one. This can be seen clearly over a distance of 10 km for a shallow sill imaged on line 10GA-YU2 (Fig. 3). Assuming a P-wave velocity of 6500 ms⁻¹, this sill varies in thickness from approximately 170 to 180 m. Deeper, less continuous sills on line 10GA-YU2 have with the same pattern of pairs of reflections, with reversed polarity for the lower one (Fig. 4). At CDP 10650, the upper sill is approximately 180 m thick, whereas the lower is approximately 190 m thick. Thinning towards the east is obvious for another sill at about 1.1 s below CDP 10950. The model in Figure 2 shows that, with thinning of the sill, the reflections from the top and bottom will become closer, and by 25 m thickness they will have merged to produce a single stronger asymmetrical reflected event. Thus, thin sills will have a different seismic response from thick sills.

The above discussion uses the polarity convention that an increase in impedance should correspond to a trough (red). Polarity is one of the most difficult issues with seismic surveys. The refracted first arrival from base of weathering, however, corresponds to an impedance contrast, and this appears as a trough on the shot records. Additional stacking velocity analysis indicates an increase in interval velocity near the top of a sill and a decrease at the base. Over such a short two-way travel time interval, it is not possible to obtain a very accurate estimate of interval velocity, but it is typically about 6500 ms⁻¹ with an error of possibly ± 250 ms⁻¹. Note that the original stacking velocity function, while not picking top and bottom of every sill, was close enough to provide a good stacked image of the tops and bottoms of the sills.

- 1 Minerals and Natural Hazards Division, Geoscience Australia, GPO Box 378, Canberra ACT 2601
- 2 Energy Division, Geoscience Australia, GPO Box 378, Canberra ACT 2601
- 3 Geological Survey of South Australia, Department of Manufacturing Innovation Trade Resources and Energy, Level 4, 101 Grenfell Street, Adelaide SA 5000
- 4 School of Biological, Earth and Environmental Sciences, The University of New South Wales, Sydney NSW 2052

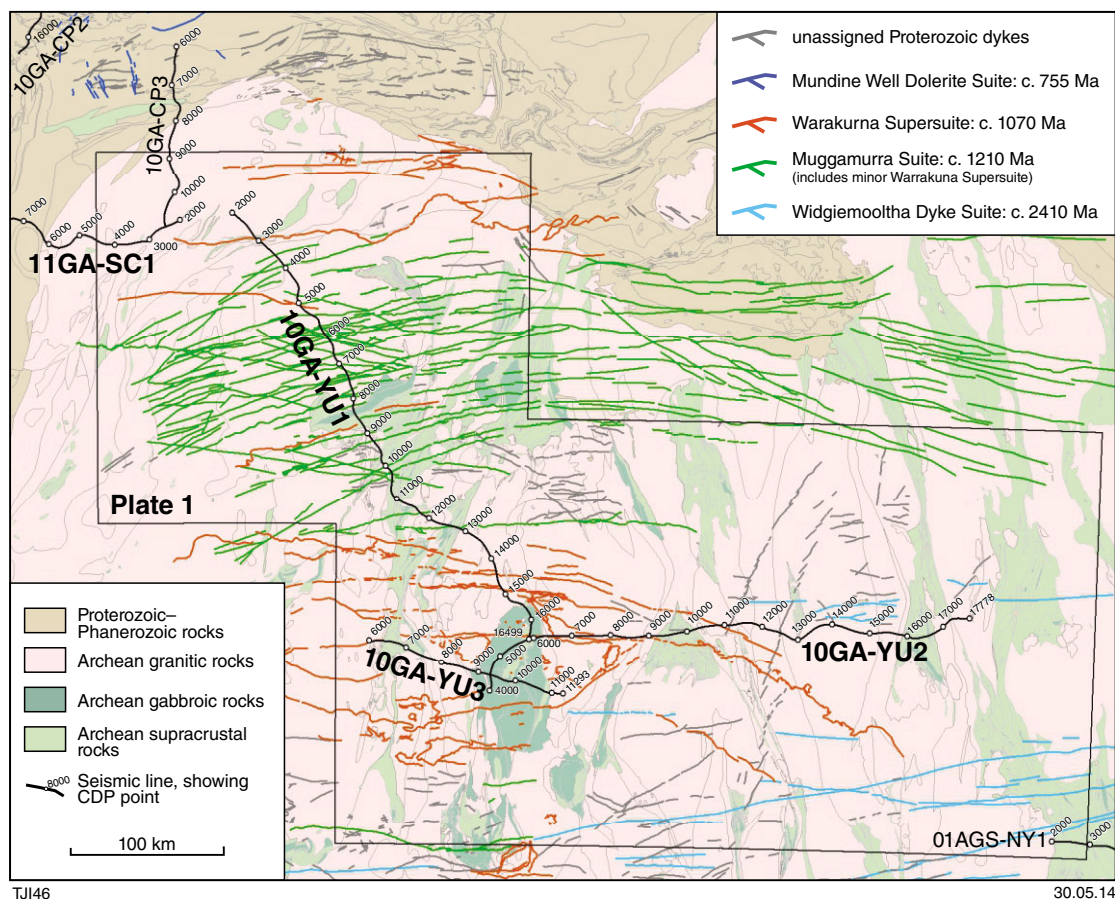


Figure 1. Interpreted geological map of the northern Yilgarn Craton showing suites of Proterozoic dykes and sills in the region of the Youanmi seismic lines

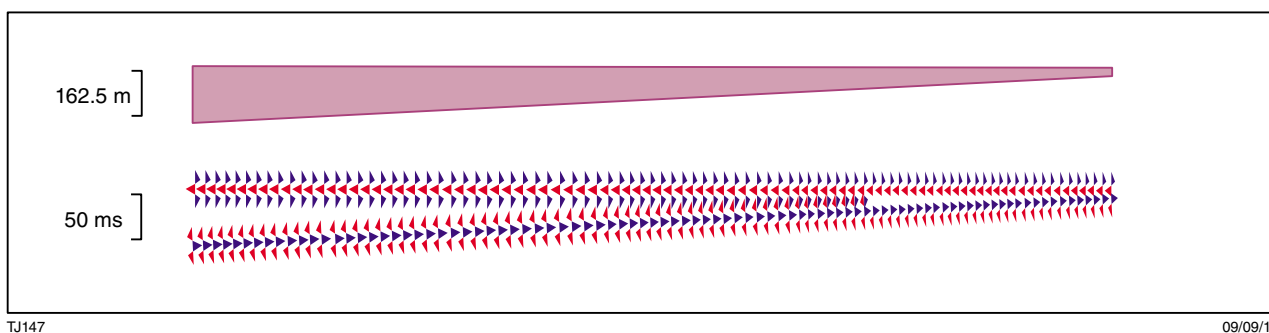


Figure 2. Modelled seismic response of a mafic sill, using a 40 Hz peak frequency zero phase Ricker wavelet. The polarity convention is that the acoustic impedance increase at the top of the sill corresponds to a trough (red). It is assumed that the impedance decreases by the same amount at the bottom of the sill, so the two reflected wavelets are equal in amplitude but opposite in polarity. The time–depth relationship uses an interval of 6500 ms-1 for the sill. The thickness of the sill decreases from 180 m to 25 m. Note the increase in amplitude (tuned response) as the sill thins (right hand edge).

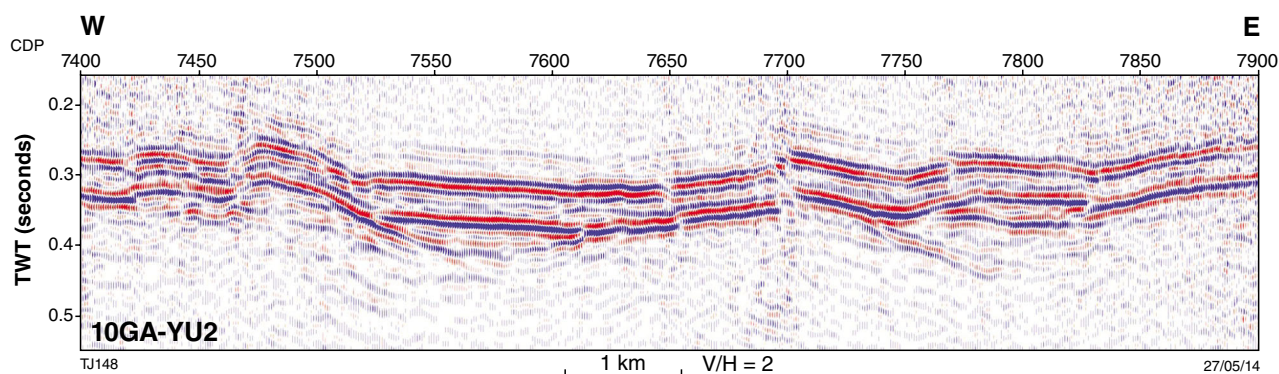


Figure 3. Detailed image of a shallow sill on line 10GA-YU2. The vertical exaggeration is x2, assuming an average crustal velocity of 6000 ms^{-1} . Note the reversal in polarity of the bottom reflection compared with top, as in the model in Figure 2. The two-way travel time thickness varies from about 56 ms in the west to about 52 ms in the east. Additional stacking velocity analyses picking the top and bottom of the sill lead to an estimate of approximately 6500 ms^{-1} for the interval velocity.

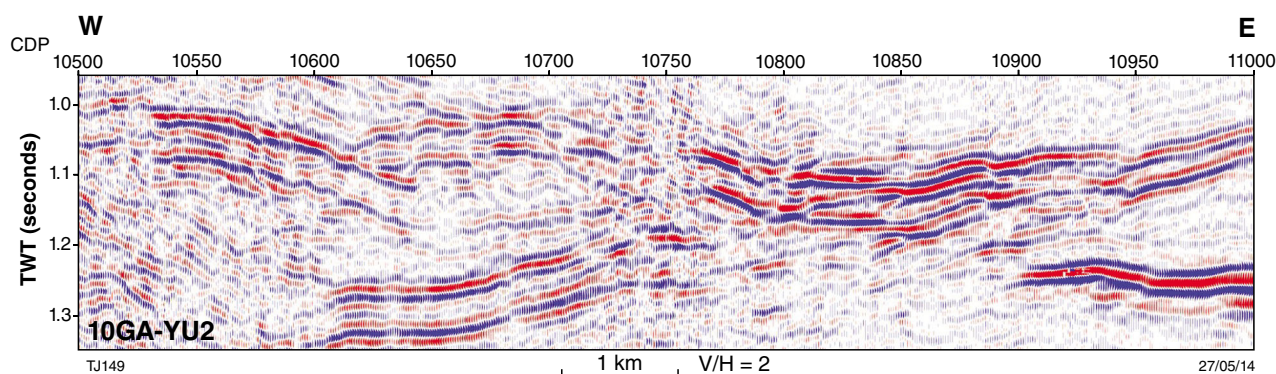


Figure 4. Detailed image of deeper sills on line 10GA-YU2. The vertical exaggeration is x2, assuming an average crustal velocity of 6000 ms^{-1} . Note the occurrence of pairs of reflections with reversal in polarity of the bottom reflection compared with top, as in the model in Figure 2. At CDP 10650, the upper sill at about 1 s TWT is 56 ms thick, whereas the lower sill at about 1.3 s TWT is 60 ms thick, both with an interval velocity of approximately 6500 ms^{-1} .

General observations for Youanmi seismic

Mafic sills are some of the most striking features in the Youanmi seismic lines and, as described above, are seismically highly reflective, with a characteristic seismic reflection signature. They are similar in geometry and seismic character to dolerite sills in Sweden imaged in seismic sections and intersected in a deep bore hole (Juhlin, 1990), and to sills imaged in Canada (Welford and Clowes, 2004). Map patterns show intense Proterozoic sill and dyke intrusions in the vicinity of the Youanmi seismic traverses (Fig. 1). These correspond at depth with regions of abundant, planar, shallow-dipping, strong reflections typically down to 3 s two-way travel time (TWT), but locally down to 5.5 s TWT (Plate 3). In many places, but especially at the Waroonga Shear Zone on line 10GA-YU2 (Plate 1), these strong reflections clearly truncate, and are unaffected by, reflections associated with the ductile

shear zone. Strong reflections in the middle crust beneath the Weld Range area on 10GA-YU1 are also transected by these planar and locally stepped sets of reflections. To the north and east of the Windimurra Igneous Complex, surface expressions of these reflections correspond to Proterozoic sills. Sills intruded into the Youanmi Terrane have been dated at c. 1070 Ma (Wingate et al., 2008) and assigned to the Warakurna Large Igneous Province (LIP), which extends over at least 1.5 million km^2 in western and central Australia (Wingate et al., 2004). Particularly good sill expressions in the seismic data are observed at the northwestern end of line 10GA-YU1, where they have been interpreted to extend for up to 90 km (Plate 2). Sill-related reflections are less common in seismic line 10GA-YU3 (Plate 2).

Some sills are clearly intruded along shear zones, which commonly link into higher-level splay faults (e.g. at about CDP 15800 on line 10GA-YU2, Plate 2). A subhorizontal shear zone, intruded by a sill at about 5.5 s TWT depth

between about CDP 3900 and 5600 on line 10GA-YU1 (Plate 1), has a sinistral (top to the northwest) sense of tectonic transport. A major sill has been emplaced at the contact between the Youanmi Terrane and the Yarraquin Seismic Province (Romano et al., 2013, this volume), and this sill (or sills) extends for a distance of over 180 km on line 10GA-YU1 (Plate 2). The Youanmi Terrane has also been intruded by extensive suites of mafic dykes (see Plate 1), but because they are typically subvertical, they have not been imaged in the seismic sections.

Specific interpretations for 10GA-YU1

In line 10GA-YU1, mafic sills are common for 130 km between the Narryer Terrane and Cue (CDP 2900–11500), then again for 65 km north of the Windimurra Igneous Complex (CDP 12000–15500). In the Narryer–Cue area, a dense swarm of dykes of the c. 1210 Ma Muggamurra Dyke Suite (e.g. Wingate, 2007), each up to 50 m wide, is recognized from aeromagnetic survey images and exposed intermittently at the surface. Interspersed with the Muggamurra intrusions, however, are dykes related to the c. 1070 Ma Warakurna LIP. Therefore, it is possible that some dykes, none of which is visible in the seismic data, were feeders to large sills at 3–5 s TWT that have an apparent dip of 10–20° to the southeast (Plate 1). Since limited number of sills have been dated in the northern Yilgarn, it is also possible that some may belong to the c. 1210 Ma Marnda Moorn Supersuite.

In the region to the north of the Windimurra Igneous Complex, dyke density is high near a strong reflection that intersects the surface (approximate CDP 15500). This could represent a Proterozoic sill which forms part of a composite lopolith. The lower part of this sill complex, which is not exposed at the surface, appears to terminate against the Windimurra Igneous Complex. This seismic truncation may represent either a loss of signal beneath the strongly layered lower zone of the Windimurra Igneous Complex, or indicate that the sill may have been deflected around the resistant mass of the northern part of the complex.

The V-shaped pattern of many of the sills in 10GA-YU1 indicate intersection of sills with a lopolithic (saucer-shaped) geometry. Approximately circular map patterns of sills in the vicinity of the Windimurra Igneous Complex also attest to this geometry. These lopolithic sills have the appearance that they are somewhat interconnected to adjacent sill intrusions, thus forming a network of stacked sills which intrude the upper 10 km of crust (see Summary and implications section).

Specific interpretations for 10GA-YU2

Line 10GA-YU2 crosses a region of dykes and a sill to the east of the Windimurra Igneous Complex (CDP 6500–11000). The sill is exposed north of the line where it is composed of dolerite, is approximately 30 m thick,

has margins containing abundant granitic xenoliths, and dips approximately 5° to the northeast. The location of the sill coincides with the surface intersection of a thin band of apparently east-dipping reflections on the seismic line. The sill is continuous at a very shallow depth (about 0.3 s TWT) until it reaches the Sandstone greenstone belt. There are several outcrops of the sill, again with a xenolith-rich marginal facies, to the south of the line in the Sandstone greenstone belt and extending about 200 km to the east-southeast, including the locality dated at c. 1070 Ma (Wingate et al., 2008). Perturbations of sills and dykes are seen beneath the Sandstone region in the seismic line, probably owing to the structural complexity and competency contrasts in the rocks in this area. Another large sill apparently affects a region from 1.5–3.5 s TWT between the Booylgoo Range greenstone belt and the Waroonga Shear Zone (c. 65 km strike length; CDP 13000–16000) where these strong reflections clearly cross-cut the ductile listric faults of the west-dipping parts of the Waroonga Shear Zone (circled area, Fig. 5). As for line 10GA-YU1, these sills are interpreted to belong to the Warakurna Large Igneous Province.

Specific interpretations for 10GA-YU3

In the region of line 10GA-YU3, there are many aeromagnetic anomalies interpreted to represent a subhorizontal sill, or sills, although there are few surface exposures. There are sill-like reflections at the western end of the line at 0.5 s TWT (CDP 6000–6400) and also beneath Mount Magnet at 2.5 s TWT (approximate CDP 7500). The location and orientation of this seismic line has resulted in very few intersections with sill-related reflections, although there are outcrops of sills and abundant sill-related aeromagnetic anomalies within a few kilometres north and south of this line. As for line 10GA-YU1, these sills are interpreted to belong to the c. 1070 Ma Warakurna Large Igneous Province.

Summary and Implications

Modelling shows that the minimum thickness of sills detected in the Youanmi seismic lines is approximately 25 m. Some of the sills may be up to 180 m thick. The geometry of the sills imaged in 10GA-YU1 (Plate 3) is typically lopolithic (saucer-shaped) and apparently part of an interconnected network that steps upwards into overlying lopolithic sills. In detail, the upturned edges of the saucer form are not so clearly evident, so they are more like stepped shallow cones. Their interconnected nature is in close agreement with recent models for vertical magma transport (e.g. Cartwright and Hansen, 2006), and indicative of a single and efficient magmatic plumbing system. In addition, the lopolith geometry is in agreement with modelling of shallowly intruded sills within sedimentary basins (e.g. Galerne et al., 2011; Galland et al., 2009). Thus, data presented here indicate that neither shallow intrusive levels nor a strongly layered substrate is necessary for sills to assume this type of geometry.

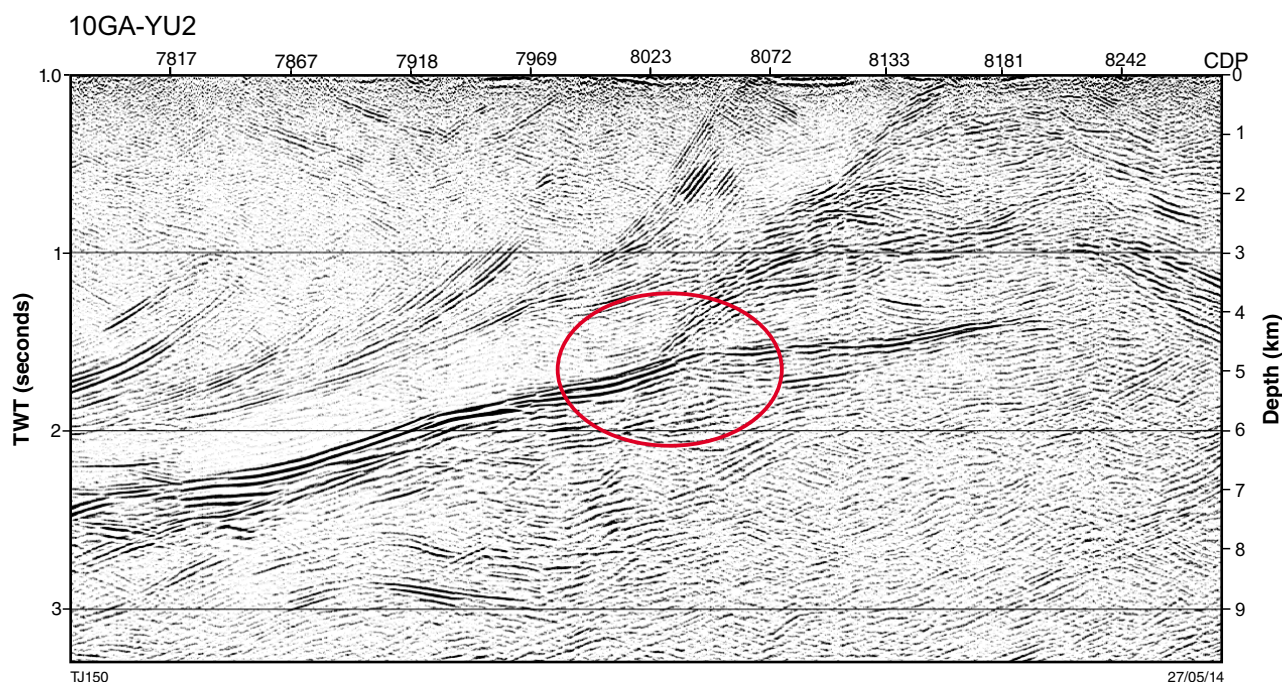


Figure 5. Detail from seismic line 10GA-YU2 showing the truncation of Archean features adjacent to the listric Waroonga Shear Zone by a Proterozoic sill

Although easterly and east-northeasterly trending dykes of the Muggamurra Dyke Suite are particularly dense in a 100 km wide zone between CDP 5700–10300 on line 10GA-YU1 (Fig. 1), they are not evident in the seismic data owing to their steeply dipping orientations. Similarly, dykes belonging to the Widgiemooltha Dyke Suite (Fig. 1) are not evident in the seismic data.

The highly reflective, shallow-dipping sills evident in the three Youanmi seismic lines are attributed to the Warakurna Supersuite, extend for several hundreds of kilometres, and may be up to 200 m thick. It has only recently been recognized that the Warakurna LIP had such far-reaching distribution and volume within the western Yilgarn Craton. Cumulate settling behaviour may have occurred in at least some of these sills, and some of the thicker sills identified in the seismic lines are prospective for orthomagmatic Cu–Ni–PGE deposits.

References

- Cartwright, J and Hansen, T 2006, Magma transport through the crust via interconnected sill complexes: *Geology*, v. 34, p. 929–932.
- Christensen, NI 1982, Seismic velocities, in *Handbook of Physical Properties of Rocks, Volume II* edited by RS Carmichael: CRC Press, Florida, USA, p 1–228.
- Galerne, CY, Galland, O, Neumann, E-R and Planke, S 2011, 3D relationships between sills and their feeders: evidence from the Golden Valley Sill Complex (Karoo Basin) and experimental modelling: *Journal of Volcanology and Geothermal Research*, v. 202, p. 189–199.
- Galland, O, Planke, S, Neumann, E-R and Malthe-Sorensen, A 2009, Experimental modelling of shallow magma emplacement: Application to saucer-shaped intrusions: *Earth and Planetary Science Letters*, v. 277, p. 373–383.
- Juhlin, C 1990, Interpretation of the reflections in the Siljan Ring area based on results from the Gravberg-1 borehole: *Tectonophysics*, v. 173, p. 345–360.
- Romano, SS, Ivanic, TJ, Korsch, RJ, Wyche, S, Van Kranendonk, MJ, Jones, LEA, Zibra, I, Blewett, RS, Jones, T, Milligan, PR, Costelloe, RD, Doublier, MP, Pawley, MJ, Gessner, K, Hall, CE, Patison, N, Kennett, BLN and Chen, SF 2013, Preliminary interpretation of the northern section of deep seismic line 10GA-YU1: Narryer Terrane to Murchison Domain of the Youanmi Terrane, in *Youanmi and Southern Carnarvon seismic and magnetotelluric (MT) workshop 2013 compiled by S Wyche, TJ Ivanic and I Zibra*: Geological Survey of Western Australia, Record 2013/6, p. 123–128.
- Welford, JK and Clowes, RM 2004, Deep 3-D seismic reflection imaging of Precambrian sills in southwestern Alberta, Canada: *Tectonophysics*, v. 388, p. 161–172.
- Wingate, MTD 2007, Proterozoic mafic dykes in the Yilgarn Craton, in *Proceedings of Geoconferences (WA) Inc. Kalgoorlie '07 Conference* edited by FP Bierlein and CM Knox-Robinson: Geoscience Australia, Record 2007/14, p. 80–84.
- Wingate, MTD, Bodorkos, S, and Kirkland, CL 2008, 178113: gabbro sill, Kurrajong Bore; Geochronology Record 732: Geological Survey of Western Australia, 7p.
- Wingate, MTD, Pirajno, F and Morris, PA 2004, Warakurna large igneous province: a new Mesoproterozoic large igneous province in west-central Australia: *Geology*, v. 32, no. 2, p. 105–108.
- Wyche, S, Pawley, MJ, Chen, SF, Ivanic, TJ, Zibra, I, Van Kranendonk, MJ, Spaggiari, CV and Wingate MTD 2013, Geology of the northern Yilgarn Craton, in *Youanmi and Southern Carnarvon seismic and magnetotelluric (MT) workshop 2013 compiled by S Wyche, TJ Ivanic and I Zibra*: Geological Survey of Western Australia, Record 2013/6, p. 33–63.

Preliminary interpretation of deep seismic line 10GA-YU2: Youanmi Terrane and western Kalgoorlie Terrane

by

I Zibra, K Gessner, MJ Pawley¹, S Wyche, SF Chen, RJ Korsch², RS Blewett¹,
T Jones¹, P Milligan¹, LEA Jones³, MP Doublier, CE Hall, SS Romano, TJ Ivanic,
N Patison, BLN Kennett⁴, and MJ Van Kranendonk⁵

Introduction and aims of the seismic survey

Deep seismic reflection line 10GA-YU2 runs from near Challa homestead within the Windimurra Igneous Complex in the central part of the Murchison Domain to the western side of the northern part of the Eastern Goldfields Superterrane in the east (Frontispiece 1, Plate 1A). The interpretation presented here covers that part of the line from its eastern end to the eastern edge of the Windimurra Igneous Complex. The western end of the line, where it crosses the Windimurra Igneous Complex, is described by Ivanic et al (2013a, this volume). The overall east–west orientation of the line is nearly orthogonal to the strike of the major geological structures in this part of the Neoarchean Youanmi Terrane.

The principal objectives of seismic line 10GA-YU2 were to determine: 1) the nature of the contact and the geometric relationship between the Eastern Goldfields Superterrane and the Youanmi Terrane; 2) the three-dimensional architecture of the structures associated with the Sandstone greenstone belt near the central part of the line; 3) the nature of the Moho and the architecture of the unexposed middle to lower continental crust in the depth dimension.

The preliminary interpretation of seismic line 10GA-YU2 is constrained by outcrop geology along the section line, as well as by the interpretation of gravity, magnetic and

geochronology data for the region. The seismic line crosses two greenstone belts separated by broad areas dominated by poorly exposed, post-tectonic granite suites (Plate 1A). In the magnetic anomaly map (Frontispiece 2), these areas are characterized by featureless or weakly developed magnetic patterns that are discordant to the main north-striking, map-scale structures. We have used the locations of these post-tectonic intrusive bodies as boundaries to subdivide the seismic line into three segments: 1) from the eastern end of the line to west of the Waroonga Shear Zone, including the Lawlers Anticline; 2) the Sandstone area; 3) the Windimurra area (see Ivanic et al., 2013a, this volume).

The Lawlers area and the Waroonga Shear Zone

Local geological setting

The eastern end of seismic line 10GA-YU2 traverses the southern part of the economically important Agnew–Wiluna greenstone belt and the Waroonga Shear Zone (Fig. 1), which, in this area, forms the boundary between the Eastern Goldfields Superterrane and the Youanmi Terrane (Cassidy et al., 2006). The rock assemblages and major structures in this area are described below from east to west. The eastern end of the seismic line starts in granite to the east of the Perseverance Fault, in the northern part of the Kalgoorlie Terrane of the Eastern Goldfields Superterrane.

The Perseverance Fault (Eisenlohr et al., 1993; Blewett and Hitchman, 2006) marks the eastern boundary of the c. 2720–2660 Ma Agnew–Wiluna greenstone belt, which can be divided into two areas, based on differing rock associations. The eastern association forms a linear belt that extends from Perseverance northwards to Wiluna, and comprises mafic to ultramafic volcanic and intrusive rocks, with c. 2710 Ma felsic volcanic rocks that are about the same age as the komatiites (Duuring et al., 2012; Fiorentini et al., 2005; Fig. 1 and Plate 1A). Blewett and

1 Geological Survey of South Australia, Department of Manufacturing Innovation Trade Resources and Energy, Level 4, 101 Grenfell Street, Adelaide SA 5000

2 Minerals and Natural Hazards Division, Geoscience Australia, GPO Box 378, Canberra ACT 2601

3 Energy Division, Geoscience Australia, GPO Box 378, Canberra ACT 2601

4 Research School of Earth Sciences, The Australian National University, Canberra ACT 0200

5 School of Biological, Earth and Environmental Sciences, The University of New South Wales, Sydney NSW 2052

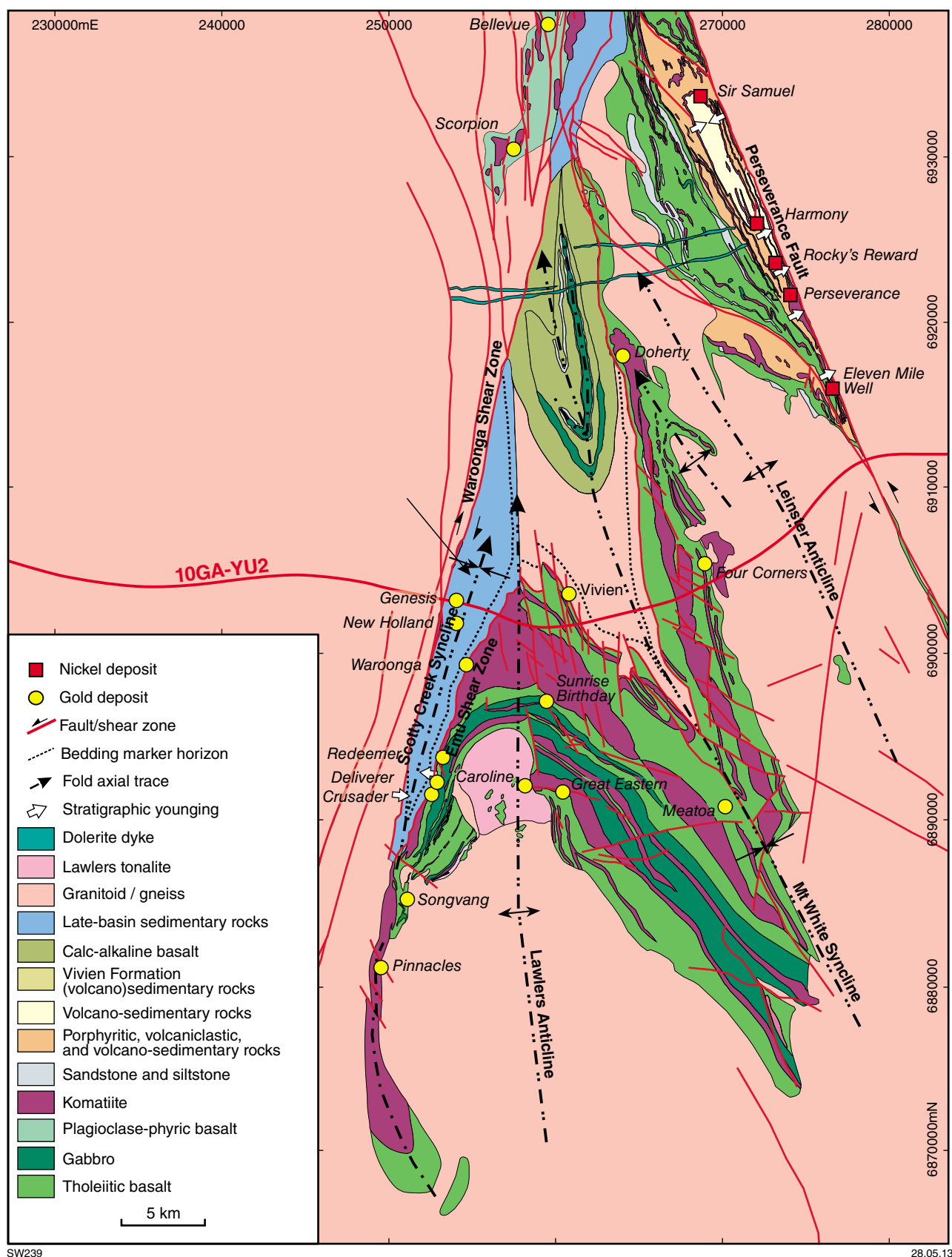


Figure 1. Interpreted geology map of the Lawlers – Mount White district showing the distribution of rock types, gold and nickel deposits, and major structural relationships (modified from Duuring et al., 2012).

Hitchman (2006) assigned shear zones in the western part of this greenstone package to their Bardoc fault system. The seismic line crosses the southern, unexposed end of these greenstones.

The second association traversed by the seismic line (Fig. 1) can be divided into two parts (see Wyche et al., 2013, this volume): 1) a lower succession of mafic and ultramafic volcanic and intrusive rocks with minor siliciclastic sedimentary rocks in the Lawlers Anticline and Mount White Syncline; and 2) two overlying texturally, spatially, and temporally distinct successions of volcanoclastic to siliciclastic sedimentary rocks, which have a more uneven distribution. The latter include: the Vivien Formation, a succession of feldspathic, volcanoclastic sedimentary rocks, with a maximum depositional age of c. 2692 Ma (Kositcin et al., 2008), which crops out in the Mount White Syncline; and the Scotty Creek Formation of quartz-rich volcanoclastic sandstones, which have a maximum depositional age c. 2662 Ma (Dunphy et al., 2003), in the Scotty Creek Syncline. Both of the younger sedimentary successions have faulted contacts with the underlying mafic–ultramafic greenstones, although the presence of basal conglomerates with clasts that are similar to the underlying rocks suggests these contacts are modified unconformities (Squire et al., 2010).

The supracrustal rocks have been multiply deformed, with the major structures including a set of kilometre-scale, north-trending tight folds with steep axial planes. From east to west, these include the Leinster Anticline, the Mount White Syncline, the Lawlers Anticline, and the Scotty Creek Syncline. Shear zones are commonly developed along the axial planes and limbs of these folds. The age of deformation is constrained by the intrusion of the Lawlers Tonalite into the Lawlers Anticline (Beardmore, 2002; Blewett et al., 2010) at c. 2665 Ma (DC Champion, written communication, 23 January, 2013), which is coincident with the c. 2662 Ma maximum depositional age of the Scotty Creek Formation (Dunphy et al., 2003). The Scotty Creek Formation is a typical ‘late-basin’ sediment, which was likely deposited during doming associated with the emplacement of the Lawlers Tonalite (Blewett et al., 2010).

The Scotty Creek Syncline (Fig. 1) is bounded to the east by the Emu Fault and to the west by the Waroonga Shear Zone. The Emu Fault is a reactivated unconformity that separates the Scotty Creek Formation from the <2686 Ma feldspathic sedimentary rocks to the north and the greenstones to the south. The locally derived clasts in the basal conglomerates (Squire et al., 2010) imply there was only minor movement along this structure, despite it being an important control on mineralization.

Although the Waroonga Shear Zone forms the terrane boundary between the Eastern Goldfields Superterrane and the Youanmi Terrane in the vicinity of the seismic line, it overprints the Ida Fault to the north and south of the Lawlers area, which is considered to be the major terrane boundary (Cassidy et al., 2006). Because of this overprinting, the relationship of the Ida Fault to the Waroonga Shear Zone is not evident in surface exposures. The Ida Fault is a long-lived, craton-scale

feature, which may have started as an extensional fault that played a major role in controlling the distribution of the c. 2720–2660 Ma greenstone successions of the Eastern Goldfields Superterrane. The fault was reactivated during the subsequent deformation events that affected the Eastern Goldfields Superterrane (Blewett et al., 2010), with the last stage of movement interpreted to have been at c. 2640 Ma (Nelson, 1996). Greenstones in the Burtville Terrane, to the east of the Kalgoorlie Terrane, are similar to those of the Youanmi Terrane with respect to age and lithostratigraphic associations. This suggests that, although the Ida Fault may have accommodated extension and deposition in the Eastern Goldfields Superterrane at c. 2720 Ma, it may not represent a suture that formed at this time between two distinct blocks of crust (Pawley et al., 2012). Nevertheless, Wyche et al. (2012) found that the Ida Fault is a boundary between blocks of crust that have different crustal growth histories. Hafnium isotope model-age data from the Youanmi Terrane indicate a crustal history dating back to c. 4200 Ma, whereas the hafnium isotope data from the Eastern Goldfields Superterrane do not show evidence of significant crustal development before c. 3100 Ma (Wyche et al., 2012).

The Waroonga Shear Zone (Liu and Chen, 1998) is a steep, north-striking structure, largely obscured by regolith. However, it is readily seen in geophysical images (Plate 2) and appears to be about 100 km long by about 20 km wide. A nearly continuous, east–west cross-section through the Waroonga Shear Zone is exposed in its central part, in an area immediately south of the seismic line (Zibra et al., 2014; Fig. 1). Here, it consists of strongly deformed gneissic granodiorite and granite, together with xenoliths of banded iron-formation, and mafic and ultramafic gneisses, which probably represent greenstone remnants, along with both concordant and discordant granitic dykes and pegmatites. The Waroonga Shear Zone was described originally as a dextral strike-slip shear zone displaying subvertical foliation, associated with a shallow-plunging mineral lineation (e.g. Platt et al., 1978). Liu and Chen (1998) recognized that the Waroonga Shear Zone was west-dipping and, based on the curvilinear, concave-to-the-west geometry, proposed that the shear zone was the result of an indenting, rigid granite body.

Recent detailed structural investigations, however, offer a slightly different picture of the Waroonga Shear Zone. Whereas the main gneissic foliation strikes consistently north and dips steeply to the west across the whole study area, the pattern of mineral and stretching lineations in granitic gneisses indicate there are two major structural domains. The western domain shows a steeply west-plunging lineation associated with top-to-east shear sense indicators, whereas the eastern domain preserves a prominent subhorizontal lineation in metagranites. Microstructural observations and P–T estimates indicate that both domains recorded shearing within the magmatic state during emplacement of the granitic protoliths. In contrast, solid-state structures associated with cooling are restricted to the easternmost portion of the Waroonga Shear Zone, along the contact with the Scotty Creek Formation. Consequently, rather than being a discrete structure, the Waroonga Shear Zone is proposed to be a broad zone of deformation that extends from the

Scotty Creek Syncline westwards for about 20 km. This zone records a history of early thrusting, followed by transpression, during emplacement of the granitic protolith of the Waroonga gneiss, and continuing during subsequent cooling to lower amphibolite facies metamorphic conditions (Zibra et al., in prep.). The age of granite emplacement and shearing along the Waroonga Shear Zone is bracketed by the c. 2662 Ma maximum depositional age of the Scotty Creek Formation, and the 2655 ± 4 Ma post-kinematic intrusion of granite along the western side of the Waroonga Shear Zone (Fletcher et al., 2001).

Preliminary seismic interpretation

The eastern section of seismic line 10GA-YU2 is characterized by the progressive deepening of the Moho discontinuity from about 11 s two-way travel time (TWT), which represents the common Moho depth along the three Youanmi seismic lines, to about 12 s TWT towards the Eastern Goldfields Superterrane. This trend is a craton-scale feature, as suggested by previously acquired seismic traverses, which indicates that the continental crust thickens eastward down to about 15.5 s TWT at the easternmost margin of the Yilgarn Craton (Goleby et al., 2000). This deepening of the Moho appears to be related to a series of ramp-and-flat segments, which are likely related to the major crustal-penetrating structures (Goleby et al., 2003). In the Lawlers Anticline area, the incipient Moho deepening could be related to the some large-scale structures, described below.

Above the Moho, crustal reflectivity in the Lawlers Anticline area includes the first-order features described in Korsch et al. (2013, this volume). The lower crust is characterized by moderately developed, horizontal to shallowly east-dipping reflections, and the middle crust by prominent east-dipping reflections with overall listric geometry. Together, the lower and middle crust constitute the Yarraquin Seismic Province. The upper crust is characterized by well-developed, relatively discrete reflections which have various orientations (Fig. 2).

Features in the upper crust

Along seismic line 10GA-YU2, seismic reflections in the upper crust can commonly be correlated with structures and rocks exposed at the surface. From east to west, these surface features include:

- The Perseverance Fault, recognizable as a moderately east-dipping feature at about CDP 17330, and traceable by short, discontinuous reflections.
- The Bardoc fault system, apparently represented by a pair of subparallel reflections, also at about CDP 17330, which dip moderately to the west. These reflections are truncated at about 4 s TWT by an east-dipping set of reflections, here called the Table Hill Shear Zone.
- The unexposed greenstone belt south of Perseverance, forming a west-dipping wedge between the Perseverance Fault and Bardoc fault system.
- The west-dipping limb of the Leinster Anticline, interpreted as a wedge of greenstone, between CDP 16500 and 16750, dipping to the west. The east limb of the anticline appears to have been intruded by later granite.
- The Mount White Syncline seen at about CDP 16400. The faults along the limbs that separate the syncline from the neighbouring Leinster and Lawlers anticlines can be seen at about CDP 16600 and CDP 16300, respectively. The eastern fault appears to be truncated by the western fault at about 2 s TWT, with the listric, western fault continuing down to apparently merge with the Table Hill Shear Zone.
- The Lawlers Anticline, which forms a prominent area of relatively reflective crust that projects to the surface between CDP 16350 and 16050. The western limb of the Lawlers Anticline appears to continue to a greater depth than the Scotty Creek Syncline, where it is intersected by a shallowly dipping reflector, interpreted to be a sill (see below), at about 2 s TWT.
- Greenstones within the Lawlers Anticline have a convex upwards contact with a relatively low-reflectance zone, interpreted to be the Lawlers Tonalite. The tonalite appears to form a subhorizontal wedge-shaped body that tapers westwards from about 2 s TWT thickness beneath the Lawlers Anticline, to pinch out at about CDP 14300.
- To the west, the upper margin of the pluton may form the footwall of the Emu Fault and be part of the broader Waroonga Shear System. The contact is locally obscured, however, by a highly reflective sill (see below), which may have exploited this surface.
- To the east, the contact between the greenstones and the tonalite appears to continue at a moderate dip, forming a feature called here the Table Hill Shear Zone, which continues to the east end of the line at about 6.5 s TWT. This structure appears to truncate the Bardoc fault system.
- The Emu Fault, which is clearly imaged in the uppermost part of the crust, where it forms the west-dipping boundary between the highly reflective mafic rocks of the Lawlers Anticline to the east, and the weakly reflective Scotty Creek Formation to the west. At deeper levels (i.e. below about 1 s TWT), it is unclear whether the Emu Fault: 1) continues at a steep dip at the contact with the Lawlers Anticline before flattening along the upper margin of the Lawlers Tonalite; 2) shallows to form the base of the Scotty Creek Formation; or 3) splits to form both structures.
- The Scotty Creek Syncline, which can be seen in the seismic line at about CDP 16000, where it forms a thin, tapering wedge, which flattens out to the west where it terminates at a depth of about 4 s TWT, at CDP 15300. The structure that underlies the syncline merges with the basal surface of the Waroonga Shear, suggesting that the syncline and the bounding Emu Fault may be geodynamically linked with the Waroonga Shear Zone.

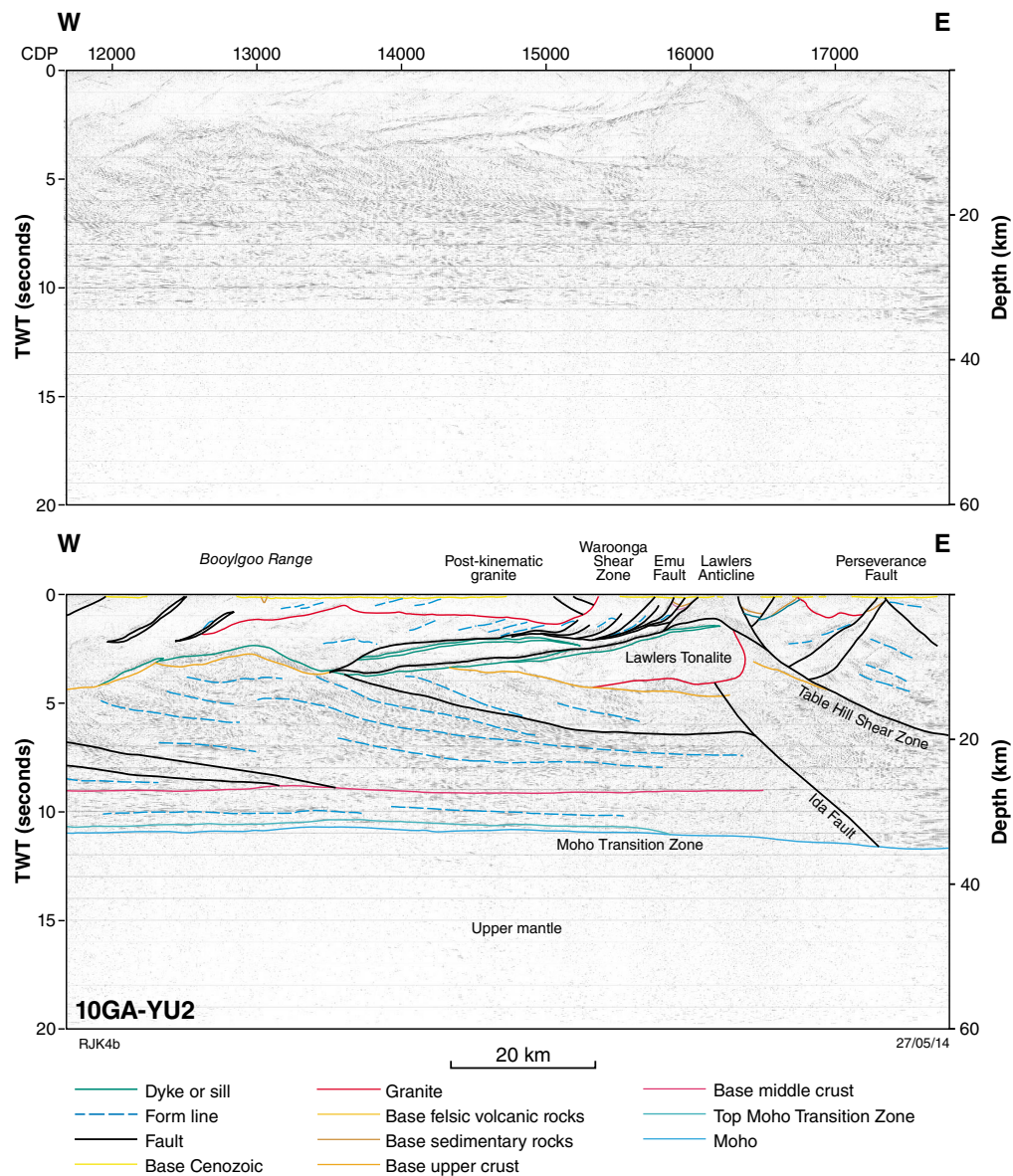


Figure 2. Migrated seismic section for the eastern end of the seismic line 10GA-YU2, showing both uninterpreted and interpreted versions

- The Waroonga Shear Zone, as traditionally mapped, seen at about CDP 15850, where it forms a listric, west-dipping structure, which flattens out at about 4 s TWT. This set of reflections then forms a clear, subhorizontal, broadly undulating set of reflections that can traced westwards to at least CDP 14700. Between the Waroonga Shear Zone and CDP 15300, there is a series of prominent, west-dipping, listric reflections, which form imbricates that floor into the basal surface. This set of structures, along with the Scotty Creek Syncline, form the Waroonga Shear Zone described by Zibra et al. (2014).
- Two sets of reflections that represent the basal structures of the Waroonga Shear Zone appear to intersect at about CDP 13000 at a depth of about 4 s TWT. The crust between the two structures has very low seismic reflectivity and it is unclear if this is younger granite, or if it is part of the older crust of the Youanmi Terrane.
- A post-kinematic monzogranite, which intruded the western side of the Waroonga Shear Zone, imaged as a thin, poorly reflecting body, with a subhorizontal floor at about 1 s TWT that extends westward for several tens of kilometres, to about CDP 13000. The monzogranite truncates a series of underlying, strong, west-dipping reflections, which are likely associated with the Waroonga Shear Zone (Fig. 2), indicating it has a greater extent than seen at the surface. The western boundary of the monzogranite corresponds to another important west-dipping structure, which is a poorly-exposed, craton-scale, north-striking shear zone, evident in aeromagnetic images (Frontispiece 3), running along the western side of the Booylgoo Range greenstone belt.

Sills

Seismic line 10GA-YU2 includes two strong sets of narrow, shallowly west-dipping reflections, which are interpreted as Proterozoic mafic sills, as the lower reflection projects into the Lawlers Tonalite (Fig. 2; see Ivanic et al., 2013b, this volume). These reflections extend from about 2 s TWT at CDP 15800 to about 3–4 s TWT at CDP 13600, and broadly correspond to the base of the Waroonga Shear Zone, suggesting that they may have been emplaced along pre-existing structures. This interpretation is based on two observations: 1) the reflections do not offset or displace the nearby reflections which they truncate; and 2) there are similar reflections in the Sandstone area (see below), where they can be matched with exposed mafic sills.

The Ida Fault

The Ida Fault is interpreted to be located below the Lawlers Tonalite, where a diffuse, moderately east-dipping zone separates subhorizontal reflections to the west from east-dipping reflections to the east. This zone can be traced from the lower contact of the Lawlers Tonalite at about 4 s TWT at CDP 16200 to the base of the crust at about CDP 17300, where it broadly coincides with the steepening of the Moho at the Youanmi Terrane – Eastern Goldfields Superterrane transition. This structure is not recognizable in the upper crust, where it has likely been obliterated by the intrusion of the c. 2665 Ma Lawlers Tonalite.

The diffuse nature of this structure is possibly the result of fluid flow from deep sources, which could be associated with the gold mineralization in the Lawlers area. A similar relationship is seen to the east in the Eastern Goldfields Superterrane, where crustal-scale structures, which were imaged in the 01AGS-NY1 seismic line, were correlated with mineralized fault systems that formed domain and terrane boundaries (Goleby et al., 2004).

An alternative interpretation is that the Ida Fault may have coincided with the lower contact of the greenstones in the Lawlers Anticline (forming a detachment), before being folded during the formation of the Lawlers Anticline and intruded by the c. 2665 Ma Lawlers Tonalite. In this interpretation, the Ida Fault corresponds to the Table Hill Shear Zone.

Despite interpreting the location of the Ida Fault, the boundary between the Youanmi Terrane and the Eastern Goldfields Superterrane does not appear to be clear-cut. For example, the seismic image suggests that: 1) the Lawlers Tonalite continues as a tapering body to the west before terminating at CDP 14300; 2) possible Youanmi crust continues under the Scotty Creek Syncline to abut the Lawlers Dome at about CDP 15900; and 3) the Scotty Creek Syncline continues westward as a thin wedge-shaped belt to CDP 15300. The interfingering of the two terranes supports the suggestion that the boundary is long-lived and dynamic (Blewett et al., 2010).

The Waroonga Shear Zone

The seismic line supports the interpretation, based on outcrop studies, that the Waroonga Shear System is a broad, complex zone of deformation (Zibra et al., 2014). In the upper crust, a series of west-dipping, listric reflections merge into a basal structure that can be traced to the surface exposure of the sheared granite–greenstone contact, suggesting that they are part of the same deformation system. The presence of these listric reflections under the c. 2655 Ma post-kinematic monzogranites (Fig. 2, Plate 3) indicates that this was a very wide deformation zone. The Scotty Creek Syncline forms a west-dipping wedge, which also links into the same basal structure, suggesting it has been affected by the same deformation. Brittle deformation associated with mineralization in the Scotty Creek Formation is probably due to a later overprinting event. In summary, the Waroonga Shear Zone is interpreted as a broad zone with a complex, domainal history of thrusting, transpression and folding (Zibra et al., 2014), which can be traced across strike for at least 20 km.

The Sandstone area

Local geological setting

West of the Waroonga Shear Zone, seismic line 10GA-YU2 traverses a region of granite dominated by low-Ca or late granites of Cassidy et al. (2002). Greenstone stratigraphy in the Booylgoo Range and Sandstone greenstone belts is described by Wyche et al. (2013, this volume). The most significant mapped structures in this part of the line are the northwest-striking Edale and northeast-striking Youanmi Shear Zones, which bound the Sandstone greenstone belt to the east and west, respectively. The age of movement on these shear zones has not been constrained but it postdates c. 2667 Ma, the age of the youngest deformed granite within the Youanmi Shear Zone (Nelson, 2002).

Another significant feature along this part of the line is a series of outcrops of a mafic sill which is evident on aeromagnetic images as a shallow-dipping feature (Fig. 3). The sill has a U–Pb baddeleyite age of c. 1070 Ma, has been attributed to the Warakurna Supersuite (Wingate et al., 2008), and is described in more detail in Ivanic et al. (2013b, this volume).

Preliminary seismic interpretation

In our interpretation, the Sandstone greenstone belt has a synformal shape and closes downward at about 2 s TWT (Fig. 3). Field observations suggest that the three-dimensional architecture of the belt is probably more complex and includes large-scale, refolded folds (see Wyche et al., 2013, this volume). In agreement

with field observations, seismic data indicate that the greenstone belt is bounded by the Youanmi and Edale shear zones. To the west, the exposed Youanmi Shear Zone intersects line 10GA-YU2 at about CDP 9100. The seismic profile shows that this structure is a listric shear zone that roots within the highly reflective lower crust. To the east of the Sandstone greenstone belt, the Edale Shear Zone, which intersects the seismic line at about CDP 10450, can be viewed as a west-dipping, listric structure that ends against the Youanmi Shear Zone (at about 2.5 s TWT, Fig. 3). There are two other strong sets of reflections parallel to the Edale Shear Zone farther to the east. The easternmost reflection reaches the surface at about CDP 13000 and corresponds to the north-trending Booylgoo Range greenstone belt, exposed in the area immediately north of seismic line (Plate 1A). Another strong, west-dipping set of reflections reaches the surface at about CDP 12500 (Fig. 3), corresponding to a broad north-striking shear zone within granite along the west of the Booylgoo greenstone belt, which can also be seen in aeromagnetic images (Plate 1A). Strongly deformed granodiorite, apparently within the structure about 25 km south of the seismic line, has an emplacement age

of c. 2686 Ma (Wingate et al., 2012a) and is intruded by undeformed monzogranite with a magmatic age of c. 2671 Ma (Wingate et al., 2012b). The west-dipping reflections, including the Edale Shear Zone, may represent back thrusts produced during a late stage of craton-scale contraction (Chen et al., 2001). The geometrical relationship between the Youanmi and Edale shear zones is similar to that between the Ida Fault and the Bardoc Shear Zone in seismic line 91-EGF01 (Drummond et al., 2000), the so-called ‘Y-front’ geometry of Drummond and Goleby (1998).

West of the Sandstone greenstone belt, the lower to middle crust displays listric east-dipping reflections — an architecture that is characteristic of all the Youanmi seismic profiles. We recognize two major crustal-scale shear zones, both rooted in the lower crust below the Sandstone greenstone belt:

- The lowermost shear zone is very shallow dipping (c. 10°) and passes beneath the Windimurra Igneous Complex. It can be followed along line 10GA-YU3, where it correlates with the exposed Wattle Creek

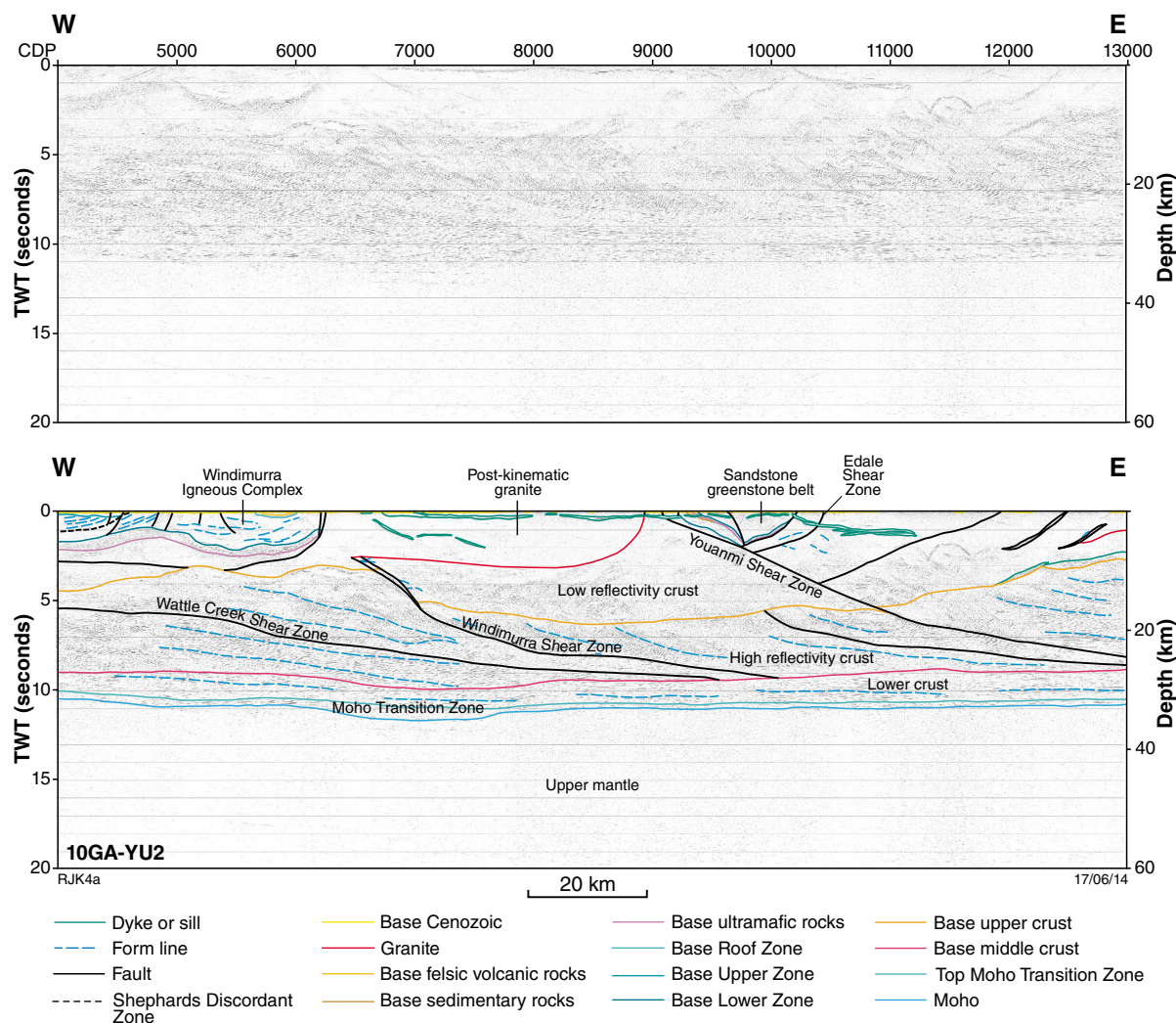


Figure 3. Migrated seismic section for the central part of the seismic line 10GA-YU2, centred on the Sandstone area, showing both uninterpreted and interpreted versions

Shear Zone, developed along the boundary between the Mount Magnet greenstone belt and the Lakeside Granite (Zibra, 2012). This feature is discussed in more detail in the interpretation of line 10GA-YU3 (Zibra et al., 2013, this volume).

- Above the Wattle Creek Shear Zone, a steeper shear zone displays a ramp-and-flat geometry and is associated with thrusting and duplication of the highly reflective middle crust, which reaches about 2.5 s TWT at CDP 6500 (Fig. 3). This crustal thickening is mirrored by a deepening of the Moho (centred at about CDP 7000). The uppermost segment of this shear zone is truncated by a large, sheetlike, post-tectonic granite intrusion, which extends from the Sandstone greenstone belt to the Windimurra Igneous Complex. Before the emplacement of the post-tectonic granite, this shear zone would have reached the present-day surface level near the eastern boundary of the Windimurra Igneous Complex. Therefore, we have called this feature the Windimurra Shear Zone.

The structures identified near the western end of seismic line 10GA-YU2 are likely to be intersected by seismic lines 10GA-YU1 and 10GA-YU3. Therefore, the structural architecture of this area could potentially be well constrained by building a 3D geological map. The sector characterized by the deepening of the Moho, centred at about CDP 7000, does not show any obvious link with the large-scale shear zones, suggesting that its high reflectivity could be due to an underplated mafic sill, which is interlayered with the more felsic lower crust.

Conclusions

- Near the eastern end of seismic line 10GA-YU2, the Moho discontinuity progressively deepens from about 11–12 s TWT towards the Eastern Goldfields Superterrane.
- Above the Moho, we recognize a horizontally layered lower crust overlain by a middle crust characterized by prominent east-dipping reflections with overall listric geometry.
- The Lawlers Anticline is cored by the Lawlers Tonalite. To the east, this structure is flanked by the east-dipping Table Hill Shear Zone, which appears to be a major structure that truncates shears in the upper crust.
- The Ida Fault, considered to be the terrane boundary between the Youanmi Terrane and Eastern Goldfields Superterrane, is interpreted to be a moderately east-dipping structure, which has been truncated by the Lawlers Tonalite.
- To the west, the west-dipping Waroonga Shear System is a broad zone of deformation that can be traced for over 20 km.

- The Sandstone greenstone belt is bounded to the west by the east-dipping Youanmi Shear Zone. This crustal-scale structure is linked to the west-dipping Edale Shear Zone and associated upper crustal structures, which were active during the very late stages of deformation.
- The lower crustal segment of Wattle Creek Shear Zone, exposed west of Mount Magnet and identified on seismic line 10GA-YU3, could be rooted under the Sandstone greenstone belt. This hypothesis should be tested by three-dimensional modelling.

References

- Beardsmore, TJ 2002, The geology, tectonic evolution and gold mineralization of the Lawlers region: a synopsis of present knowledge: Barrick Gold of Australia Ltd, Confidential Technical Report 1026, 279p.
- Blewett, RS, Czarnota, K and Henson, PA 2010b, Structural-event framework for the eastern Yilgarn Craton, Western Australia, and its implications for orogenic gold: *Precambrian Research*, v. 183, p. 203–209.
- Blewett, RS and Hitchman, AP (editors) 2006, Final report – 3D Geological models of the eastern Yilgarn Craton, Project Y2: Geoscience Australia, Record 2006/05, 276p.
- Chen, SF, Libby, JW, Greenfield, JE, Wyche, S and Riganti, A 2001, Geometry and kinematics of large arcuate structures formed by impingement of rigid granitoids into greenstone belts during progressive shortening: *Geology*, v. 29, no. 3, p. 283–286.
- Cassidy, KF, Champion, DC, Krapež, B, Barley, ME, Brown, SJA, Blewett, RS, Groenewald, PB and Tyler, IM 2006, A revised geological framework for the Yilgarn Craton, Western Australia: Geological Survey of Western Australia, Record 2006/8, 8p.
- Cassidy, KF, Champion, DC, McNaughton, N, Fletcher, IR, Whitaker, AJ, Bastrakova, IV and Budd, A 2002, The characterisation and metallogenic significance of Archaean granitoids of the Yilgarn Craton, Western Australia: Minerals and Energy Research Institute of Western Australia (MERIWA), Project no. M281/AMIRA Project no. 482, Report no. 222 (unpublished).
- Drummond, BJ and Goleby, BR 1998, Yilgarn crustal structure revealed in five seismic profiles, in *Geodynamics and gold exploration in the Yilgarn*, workshop abstracts, edited by SE Wood: Australian Geodynamics Cooperative Research Centre, p. 23–31.
- Drummond, BJ, Goleby, BR and Swager, CP 2000, Crustal signature of Late Archean tectonic episodes in the Yilgarn craton, Western Australia: evidence from deep seismic sounding: *Tectonophysics*, v. 329, p. 193–221.
- Dunphy, JM, Fletcher, IR, Cassidy, KF and Champion, DC 2012, Compilation of SHRIMP U–Pb geochronological data, Yilgarn Craton, Western Australia, 2001–2002: Geoscience Australia, Record 2003/15, 139p.
- Duuring, P, Bleeker, W, Beresford, SW, Fiorentini, ML and Rosengren, NM 2012, Structural evolution of the Agnew–Wiluna greenstone belt, Eastern Yilgarn Craton and implications for komatiite-hosted Ni sulfide exploration: *Australian Journal of Earth Sciences*, v. 59, no. 5, p. 765–791.
- Eisenlohr, BN, Groves, DI, Libby, J and Vearncombe, JR 1993, The nature of large scale shear zones and their relevance to gold mineralization, Yilgarn block: Mineral and Energy Research Institute of Western Australia, Report 122, 161p.

- Fiorentini, ML, Barley, ME, Pickard, A, Beresford, SW, Rosengren, NM, Cas, RAF and Duuring, P 2005, Age constraints of the structural and stratigraphic architecture of the Agnew–Wiluna greenstone belt: implications for the age of komatiite-felsic association and interaction in the Eastern Goldfields Province, Western Australia: Minerals and Energy Research Institute of Western Australia (MERIWA), Project no. M356 (unpublished report no. 255).
- Fletcher, IR, Dunphy, JM, Cassidy, KF and Champion, DC 2001, Compilation of SHRIMP U–Pb geochronological data, Yilgarn Craton, Western Australia, 2000–2001: Geoscience Australia, Record 2001/47, 111p.
- Goleby, BR, Bell, B, Korsch, RJ, Sorjonen-Ward, P, Groenewald, PB, Wyche, S, Bateman, R, Fomin, T, Witt, W, Walshe, J, Drummond, BJ and Owen, AJ 2000, Crustal structure and fluid flow in the Eastern Goldfields, Western Australia: Australian Geological Survey Organisation, Record 2000/34, 109p.
- Goleby, BR, Blewett, RS, Groenewald, PB, Cassidy, KF, Champion, DC, Jones, LEA, Korsch, RJ, Schevshenko, S and Apak, SN 2003, The 2001 northeastern Yilgarn deep seismic reflection survey: Geoscience Australia, Record 2003/28, 143p.
- Goleby, BR, Blewett, RS, Korsch, RJ, Champion, DC, Cassidy, KF, Jones, LEA, Groenewald, PB and Henson, P 2004, Deep seismic reflection profiling in the Archaean northeastern Yilgarn Craton, Western Australia: implications for crustal architecture and mineral potential: *Tectonophysics*, v. 388, p. 119–133.
- Ivanic, TJ, Korsch, RJ, Wyche, S, Jones, LEA, Zibra, I, Blewett, RS, Jones, T, Milligan, PR, Costelloe, RD, Van Kranendonk, MJ, Doublier, MP, Hall, CE, Romano, SS, Pawley, MJ, Gessner, K, Patison, N, Kennett, BLN and Chen, SF 2013a, Preliminary interpretation of the 2010 Youanmi deep seismic reflection lines and magnetotelluric data for the Windimurra Igneous Complex, *in* Youanmi and Southern Carnarvon seismic and magnetotelluric (MT) workshop 2013 *compiled by* S Wyche, TJ Ivanic and I Zibra: Geological Survey of Western Australia, Record 2013/6, p. 97–111.
- Ivanic, TJ, Wingate, MTD, Korsch, RJ, Blewett, RS, Jones, LEA, Wyche, S, Zibra, I, Doublier, MP, Romano, SS, Pawley, MJ, Van Kranendonk, MJ, Gessner, K, Hall, CE, Chen, SF, Patison, NL and Costelloe, RD 2013b, Preliminary interpretation of the Youanmi deep seismic reflection lines for Proterozoic intrusive rocks, *in* Youanmi and Southern Carnarvon seismic and magnetotelluric (MT) workshop 2013 *compiled by* S Wyche, TJ Ivanic and I Zibra: Geological Survey of Western Australia, Record 2013/6, p. 81–85.
- Korsch, RJ, Blewett, RS, Wyche, S, Zibra, I, Ivanic, TJ, Doublier, MP, Romano, SS, Pawley, MJ, Johnson, SP, Van Kranendonk, MJ, Jones, LEA, Kositsin, N, Gessner, K, Hall, CE, Chen, SF, Patison, N, Kennett, BLN, Jones, T, Goodwin, JA, Milligan, PR and Costelloe, RD 2013, Geodynamic implications of the Youanmi and Southern Carnarvon deep seismic reflection surveys: a ~1300 km traverse from the Pinjarra Orogen to the eastern Yilgarn Craton, *in* Youanmi and Southern Carnarvon seismic and magnetotelluric (MT) workshop 2013 *compiled by* S Wyche, TJ Ivanic and I Zibra: Geological Survey of Western Australia, Record 2013/6, p. 147–166.
- Kositsin, N, Brown, SJA, Barley, ME, Krapež, B, Cassidy, KF and Champion, DC 2008, SHRIMP U–Pb zircon age constraints on the Late Archaean tectonostratigraphic architecture of the Eastern Goldfields Superterrane, Yilgarn Craton, Western Australia: *Precambrian Research*, v. 161, p. 5–33.
- Liu, SF and Chen, SF 1998, Structural framework of the northeastern Yilgarn Craton and implications for hydrothermal gold mineralisation: AGSO Research Newsletter, no. 29.
- Nelson, DR 1996, 112117: bitoite monzogranite, Clark Well; *Geochronology Record* 498, Geological Survey of Western Australia, 4p.
- Nelson, DR 2002, 169069: foliated biotite syenogranite, Bell Chambers Well; *Geochronology Record* 107: Geological Survey of Western Australia, 4 p.
- Pawley, MJ, Wingate, MTD, Kirkland, CL, Wyche, S, Hall, CE, Romano, SS and Doublier, MP 2012, Adding pieces to the puzzle: episodic crustal growth and a new terrane in the northeast Yilgarn Craton, Western Australia: *Australian Journal of Earth Sciences*, v. 59, no. 5, p. 603–623.
- Platt, JP, Allchurch, PD and Rutland, RWR 1978, Archaean tectonics in the Agnew supracrustal belt, Western Australia: *Precambrian Research*, v. 7, p. 3–30.
- Squire, RJ, Allen, CM, Cas, RAF, Campbell, IH, Blewett, RS and Nemchin, AA 2010, Two cycles of voluminous pyroclastic volcanism and sedimentation related to episodic granite emplacement during the late Archean: Eastern Yilgarn Craton, Western Australia: *Precambrian Research*, v. 183, no. 2, p. 251–274.
- Wingate, MTD, Bodorkos, S, and Kirkland, CL, 2008, 178113: gabbro sill, Kurrajong Bore; *Geochronology dataset* 732: Geological Survey of Western Australia, 7p.
- Wingate, MTD, Kirkland, CL, Riganti, AR and Wyche, S 2012a, 185986: granodiorite gneiss, Flat Topped Hill; *Geochronology Record* 1081: Geological Survey of Western Australia, 4p.
- Wingate, MTD, Kirkland, CL, Riganti, AR and Wyche, S 2012b, 185985: biotite metamonzogranite, Flat Topped Hill; *Geochronology Record* 1080: Geological Survey of Western Australia, 4p.
- Wyche, S, Kirkland, CL, Riganti, A, Pawley, MJ, Belousova, E and Wingate, MTD 2012, Isotopic constraints on stratigraphy in the central and eastern Yilgarn Craton, Western Australia: *Australian Journal of Earth Sciences*, v. 59, p. 657–670.
- Wyche, S, Pawley, MJ, Chen, SF, Ivanic, TJ, Zibra, I, Van Kranendonk, MJ, Spaggiari, CV and Wingate MTD 2013, Geology of the northern Yilgarn Craton, *in* Youanmi and Southern Carnarvon seismic and magnetotelluric (MT) workshop 2013 *compiled by* S Wyche, TJ Ivanic and I Zibra: Geological Survey of Western Australia, Record 2013/6, p. 33–63.
- Zibra, I 2012, Syndeformational granite crystallisation along the Mount Magnet Greenstone Belt, Yilgarn Craton: evidence of large-scale magma-driven strain localisation during Neoproterozoic time: *Australian Journal of Earth Sciences*, v. 59, no. 5, p. 793–806.
- Zibra, I, Gessner, K, Korsch, RJ, Blewett, RS, Jones, T, Milligan, PR, Jones, LEA, Wyche, S, Doublier, MP, Hall, CE, Chen, SF, Romano, SS, Ivanic, TJ, Pawley, MJ, Patison, N, Kennett, BLN and Van Kranendonk, MJ 2013, Preliminary interpretation of deep seismic lines 10GA-YU3 and the southeastern part of 10GA-YU1: Murchison Domain of the Youanmi Terrane, *in* Youanmi and Southern Carnarvon seismic and magnetotelluric (MT) workshop 2013 *compiled by* S Wyche, TJ Ivanic and I Zibra: Geological Survey of Western Australia, Record 2013/6, p. 113–122.
- Zibra, I, Pawley, MJ and Wyche, S 2014, Linking grain-scale to crustal scale structures along the Youanmi seismic line: Geological Survey of Western Australia, Record 2014/8, 34p.

Preliminary interpretation of the 2010 Youanmi deep seismic reflection lines and magnetotelluric data for the Windimurra Igneous Complex

by

TJ Ivanic, RJ Korsch¹, S Wyche, LEA Jones², I Zibra, RS Blewett¹, T Jones¹, P Milligan¹, RD Costelloe¹, MJ Van Kranendonk³, MP Doublier, CE Hall, SS Romano, MJ Pawley⁴, K Gessner, N Patison, BLN Kennett⁵, and SF Chen

Introduction

The Windimurra Igneous Complex, located in the eastern part of the Murchison Domain (Fig. 1), is the largest, relatively intact and exposed, mafic–ultramafic intrusion in Australia (Ivanic et al., 2010). The complex is the type example of the c. 2810 Ma Meeline Suite of the Murchison Supergroup (Van Kranendonk et al., 2013) and has been directly dated at 2813 ± 3 Ma (Wingate et al., 2012). Primary igneous layering features are well preserved and the layering is typically concentric and inward dipping. There are several economic vanadium deposits hosted within the magnetitites of the upper zone. The central-northern part of the complex is overlain by the rhyolitic Kantie Murdana Volcanics Member of the Yaloginda Formation (Fig. 2), also dated at 2813 ± 3 Ma (Nelson, 2001).

The coherent main body of the complex has a surface expression that extends for 85 km north–south and 37 km east–west, and covers an area of c. 2500 km². Additional regions of intrusive rock associated with the complex are metamorphosed and occur as sheared lenses to the south and east of the main body, east of the Challa Shear Zone. Based on aeromagnetic images, these features extend for up to 25 km north–south by 5 km east–west. The Windimurra Igneous Complex is the westernmost of the identified igneous complexes in the Meeline

Suite. However, it is possible that intrusions belonging to the Meeline Suite form part of the Yalgoo–Singleton greenstone belt, which lies about 150 km to the southwest.

There is an overall progression from more mafic rocks in the lower zone to large volumes of leucocratic rocks in the middle and upper zones. Within these zones, megacyclicity on an approximately 200 m scale can be related to at least 13 documented reversals in the chemostratigraphy (Ahmat, 1986). The exposed complex has an extremely felsic overall composition compared to other layered gabbros worldwide. It is possible, however, that this may be accounted for by a large volume of ultramafic material at depth.

Igneous stratigraphy

The stratigraphy of the Windimurra Igneous Complex is broadly comparable in composition and thickness to many other large layered mafic–ultramafic intrusions worldwide, such as the Bushveld Complex, and others in the Murchison Domain (Fig. 3). Where they exhibit lateral aggradation or offlap geometry (Ahmat, 1986), the cumulative thickness of the exposed layers of gabbroic and ultramafic rocks is 13 km. Prior to this seismic survey, this was thought to represent a true thickness of about 6 km, as suggested by the observation that shallower dips (as low as 10°) are present in the upper parts of the complex; examples of onlap have also been noted in several localities around the complex (e.g. Ivanic et al. 2010). The Shephards Discordant Zone (SDZ), which is known to have a strike length at the surface for at least 20 km, represents a significant discordant break of several kilometres in the igneous stratigraphy (Fig. 4). The precise origin of this feature, however, is still not fully understood (Ahmat, 1986; Bunting, 2004). It is possible that the SDZ separates the complex into two main parts: an older eastern lobe and a younger, transgressive western lobe, both of which contain a lower, middle and upper zone of similar nature. Figure 5 shows a possible multi-stage evolution for the various components of the complex.

-
- 1 Minerals and Natural Hazards Division, Geoscience Australia, GPO Box 378, Canberra ACT 2601
 - 2 Energy Division, Geoscience Australia, GPO Box 378, Canberra ACT 2601
 - 3 School of Biological, Earth and Environmental Science, The University of New South Wales, Sydney NSW 2052
 - 4 Geological Survey of South Australia, Department of Manufacturing Innovation Trade Resources and Energy, Level 4, 101 Grenfell Street, Adelaide SA 5000
 - 5 Research School of Earth Sciences, The Australian National University, Canberra ACT 0200

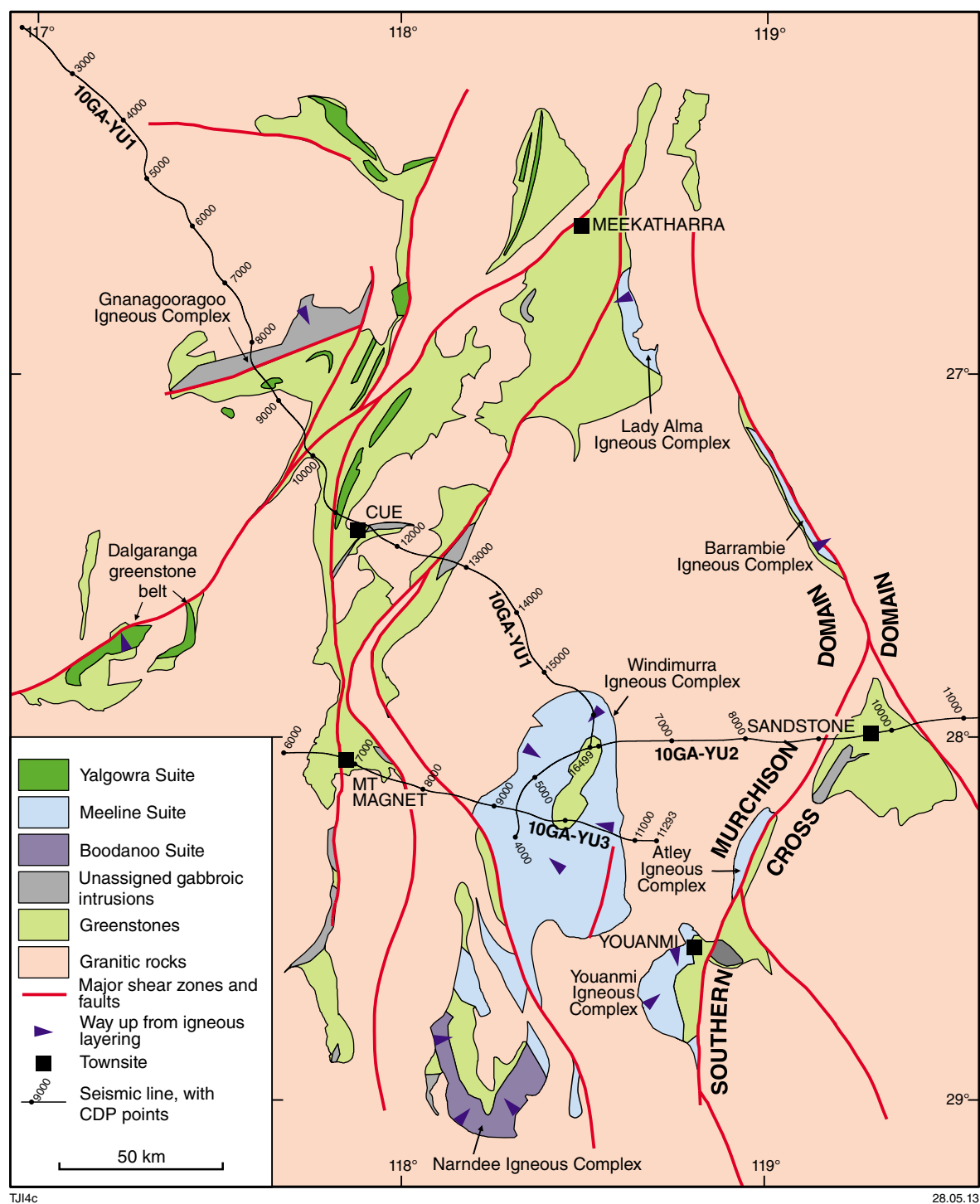


Figure 1. Simplified geological map of the northern Murchison Domain, highlighting the location of mafic-ultramafic intrusive suites relative to greenstone belts and shear zones. Also shown is the igneous differentiation way-up direction for the major igneous complexes and the locations of three seismic lines (10GA-YU1, 10GA-YU2, 10GA-YU3). Modified from Ivanic et al. (2010).

The complex is divided into eight parts (Figs 2 and 4; see Fig. 7 for rock codes).

1. A doleritic **border zone** (A-ANwb; equivalent to the border group of Ahmat, 1986) along the boundary between sheared supracrustal rocks and the lower-zone gabbros. This is thought to represent the chilled original magma, although it is typically metamorphosed and altered. Examples of granulite facies contact metamorphism of pelitic xenoliths and wall rocks that belong to the Norie Group are preserved at the margins of the complex. Pyroxene mineral barometry from gabbros shows that the Windimurra Igneous Complex was emplaced at pressures around 400 MPa (Ahmat, 1986), at middle crustal depths.
2. The **ultramafic zone** (A-ANwu), which is only exposed in the small outcrops close to Muleryon Hill, is characterized by abundant peridotite with common accessory disseminated chromite.
3. The **lower zone** (A-ANwl) hosts olivine-rich gabbros and gabbro-norites, which grade upwards into more leucocratic gabbroic rocks, typically without oxides. These rocks are modally layered on a centimetre to metre scale and the rock types are repeated on a 200 m vertical scale. Several kilometres of lower zone are apparently repeated in the western lobe, west of the SDZ.
4. The **middle zone** (A-ANwm) is composed of troctolitic rocks with intercumulus magnetite, which are layered in a way similar to the lower zone. This zone appears to be completely repeated in the western lobe, west of the SDZ.
5. The **upper zone** (A-ANwz) is marked by the incoming of vast thicknesses of cumulus magnetite and the disappearance of Mg-olivine. Within a few hundred metres of the base of the upper zone, Fe-olivine appears as a cumulus phase with magnetite. The majority of rocks in this zone are composed of magnetite-bearing leuconorite and anorthosite, with magnetite locally abundant. The upper zone of the eastern lobe is truncated by the SDZ, whereas the upper zone of the western lobe appears to have intruded as a single pulse that scoured down into the cumulates of the middle zone.
6. The **Corner Well Gabbro** is a late phase of gabbroic pipes, <1 km in diameter, which intruded into the middle and lower zones.
7. The **roof zone** (A-ANwr) of the Windimurra Igneous Complex represents the chilled contact zone with roof pendants: rhyolites of the c. 2813 Ma Kantie Murdana Volcanics Member (Nelson, 2001) and tonalitic rocks of the c. 2813 Ma Mount Kenneth Suite (Ivanic et al., 2012). This zone overlies the central part of the lower zone towards the north of the complex, and also truncates surface exposure of the SDZ area.
8. In several locations along the Challa Shear Zone are **unassigned units** of the complex; these are detached

from any known stratigraphy and do not have a distinctive composition. Knowledge of these units is also poor because the outcrop is very minor (Ivanic, 2011) due to the proximity of the Challa salt lake system. They include: Boodanoo Hill area, Watsons Well area, West Challa area, Moolyawarda Hill area, North Bore area (east).

In addition to the eight parts described above, there may be several other components to the complex:

- a significant ultramafic zone directly underlying the lower zone, and not exposed at the surface
- amphibolitic xenoliths within metagranitic rocks in a 50 km radius around the complex
- the entire Atley Igneous Complex (Fig. 2) was possibly once part of the Windimurra Igneous Complex
- significant thicknesses of portions of the complex may have been lost through erosion
- an area of high gravity response to the south of the Narndee Igneous Complex, approximately 30 x 30 km, may be a sinistrally displaced part of the western lobe of the Windimurra Igneous Complex (i.e. with about 80 km displacement).

Contact relations and structural overprint

In several places around its northwestern, northern and eastern sides, the Windimurra Igneous Complex is in sheared contact with host rocks of the Norie Group. In these areas, some xenoliths of supracrustal country rocks are preserved, which suggests that the complex intruded into host rocks of the Norie Group. The border zone was formed by chilling of magma along these contacts at that time.

The roof zone is thought to represent a complex zone of late-stage intrusive gabbroic rocks that were chilled locally at their upper contact with the Kantie Murdana Volcanics Member. Contact metamorphism is thought to have caused recrystallization of rhyolitic rocks of this member. The metatonalitic rocks of the Mount Kenneth Suite are locally intrusive into the lower zone and roof zone of the complex and are possibly contemporaneous with the Kantie Murdana Volcanics Member.

Metamonzogranites of the Big Bell, Tuckanarra and Jungar Suites are in sheared contact with the lower, middle, upper and border zones of the complex, where it is evident that they truncate many of the Windimurra igneous layers on aeromagnetic maps. These layers are locally deformed into parallelism with shear zones and metamonzogranites. Granites of the Walganna Suite intrude across the southern part of the complex, where they are interpreted to have cut across sheared layering of the complex (Ivanic, 2011, 2012a,b). In addition, lithium-rich pegmatites of the Wogala Suite crosscut layers of the lower zone of the complex.

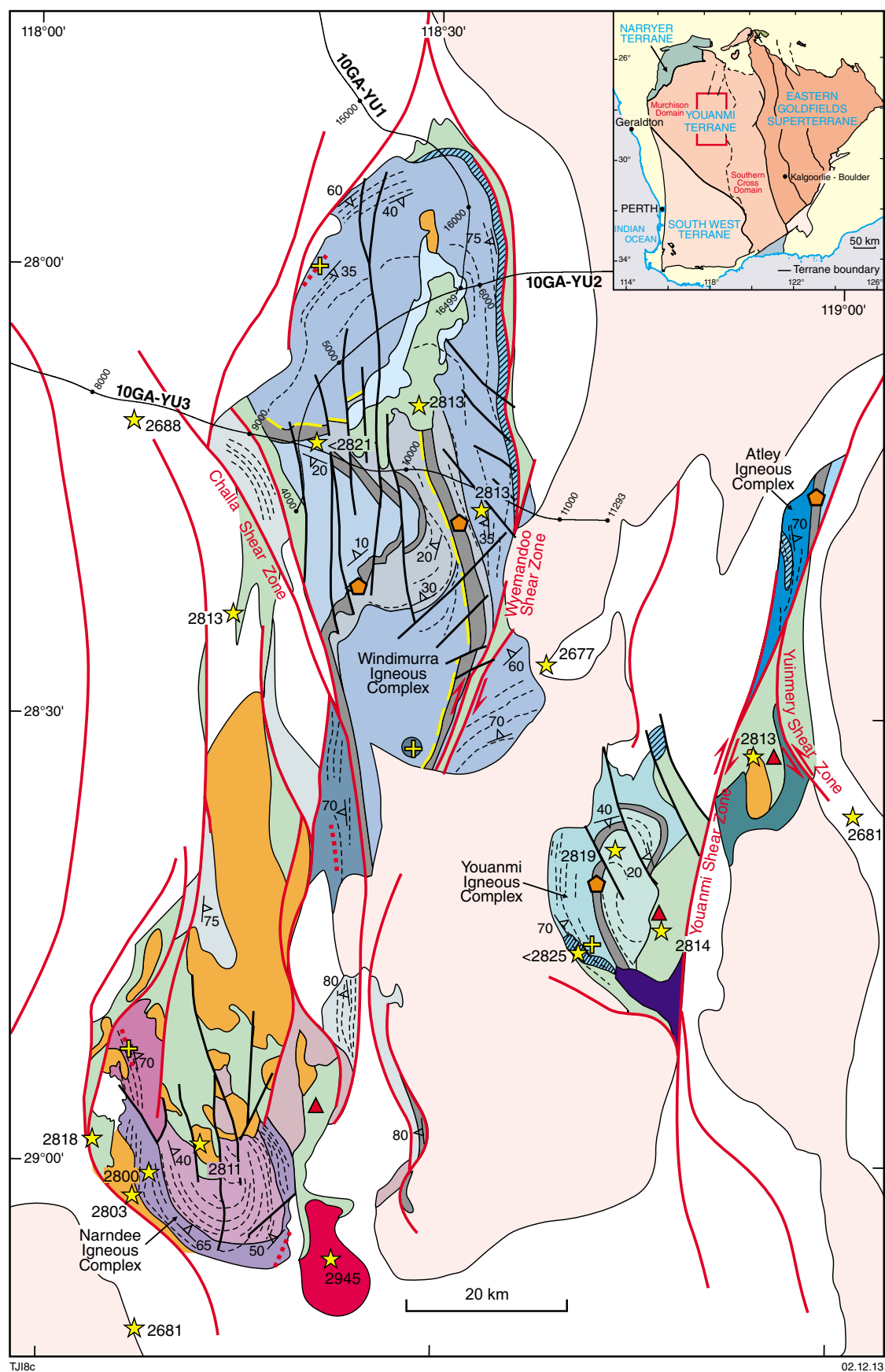


Figure 2. Interpreted geological map of the Windimurra, Narndee, Youanmi and Atley Igneous Complexes, highlighting available geochronological data and mineralization styles. Note the location of the Shephards Discordant Zone in the Windimurra Igneous Complex and the location of three seismic lines (10GA-YU1, 10GA-YU2, 10GA-YU3).

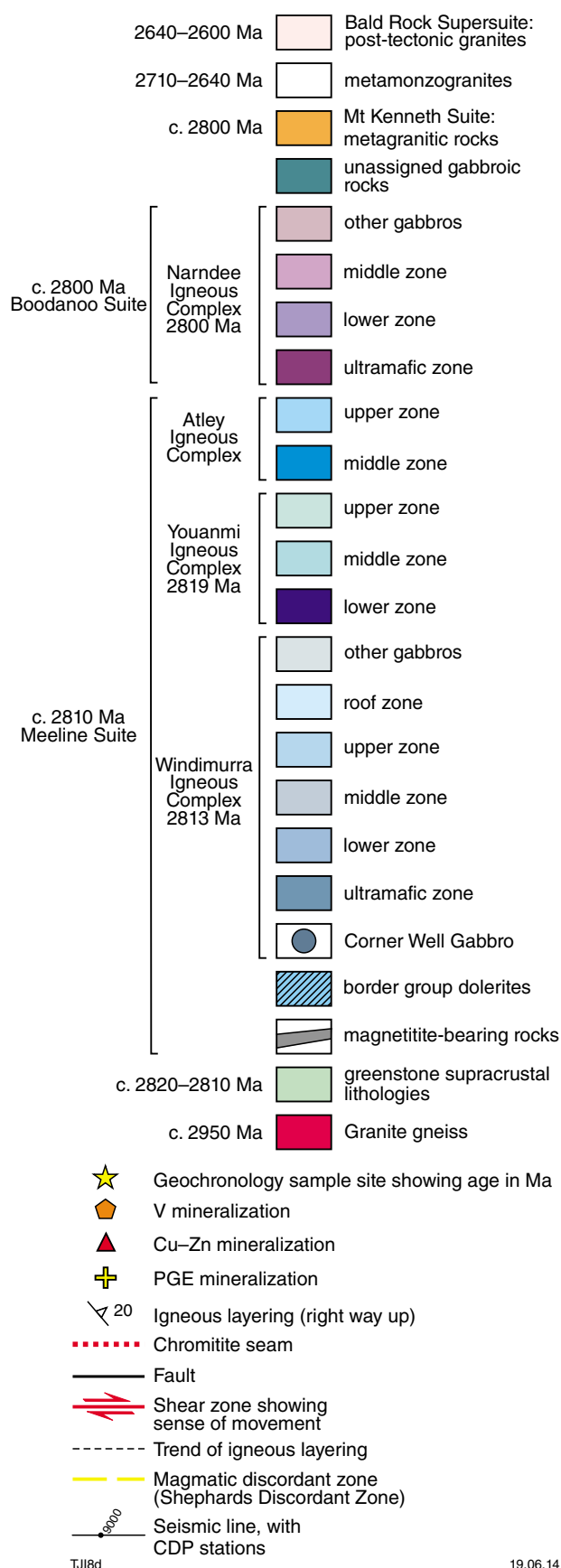


Figure 2. Legend

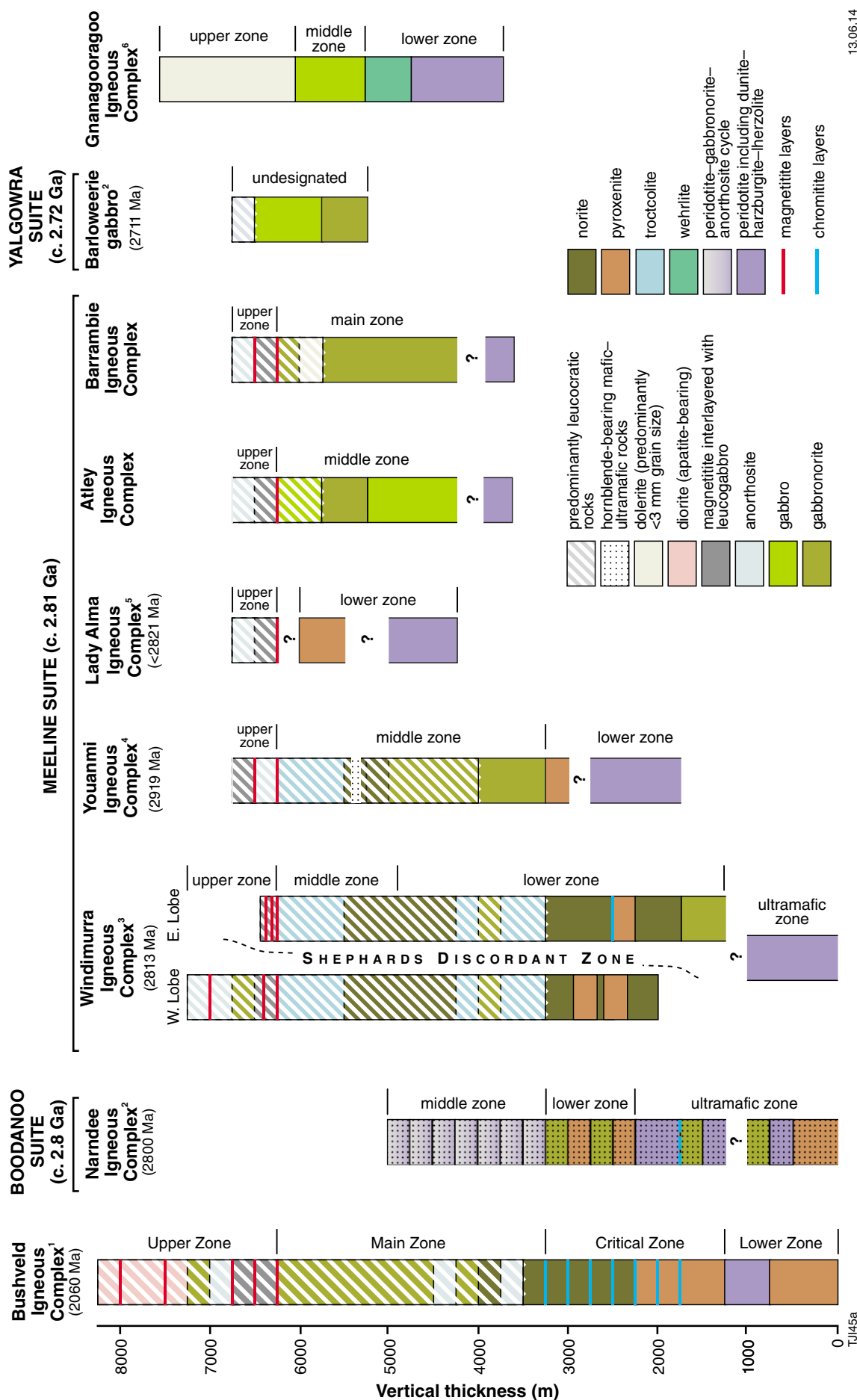
There are other shear zones around the northern and eastern parts of the complex, where metagranitic rocks are typically in contact with sheared supracrustal rocks (Fig. 2). The Yarloo Shear Zone deforms metagranitic rocks at the northwest of the complex and appears to be crosscut in the south by the Challa Shear Zone. The Wyemadoo Shear Zone in the southeast of the complex dextrally displaces igneous layering and the SDZ. It contains lenses of metamorphosed supracrustal rocks and amphibolitized lenses of the complex. There is also another minor shear zone which brings supracrustal rocks into contact with the complex in the Mingyngura area, which is in the northeast of the complex.

Folding on a 500 m scale is evident in the Kantie Murdana Volcanics Member, and also in supracrustal rocks immediately to the north of the complex. The axial planes are typically steep and northerly striking with an associated, moderately north-plunging lineation. This is consistent with an overall east–west shortening and moderate northward downwarping of the entire complex as also indicated by its overall ovoid map pattern. A synformal fold axis is indicated on the WINDIMURRA and CHALLA 1:100 000 map sheets (Ivanic, 2012a,b).

Abundant northerly striking, steeply-dipping brittle faults in the central part of the main body of the complex offset the igneous layers and the SDZ. These are consistent with extensional faulting (including antithetic faults) and 50–500 m of offset, based on map patterns. A set of northeasterly striking brittle faults in the south part of the main body of the complex dextrally offset the Wyemadoo Shear Zone, with strike-slip displacement of up to 1000 m, based on map patterns. Another set of brittle faults in the northeastern part of the complex strikes northwest and dextrally offsets igneous layering, the border zone, and lateral shear zones around the complex by between 50 and 3000 m.

Introduction to the seismic lines in the vicinity of the Windimurra Igneous Complex

In April 2010, the position of each of the three seismic lines 10GA-YU1, 10GA-YU2 and 10GA-YU3 was planned to traverse particular parts of the Windimurra Igneous Complex, utilizing existing roads and tracks, to provide sufficient data for a 3D seismic interpretation of the complex. This goal was greatly enhanced by the inclusion of line 10GA-YU3, which had five particular foci: 1) to image across what was thought to be the some of the deepest parts of the complex, as seen in gravity data (Fig. 6); 2) to image across the SDZ and provide evidence for the mechanism of emplacement of rocks to the west of this zone; 3) to image and trace the extent of economically significant magnetitite horizons of the upper zone of the complex; 4) to image across the Challa Shear Zone and the associated Cundimurra Monzogranite pluton; and 5) to image across the Mount Magnet greenstone belt.



13.06.14

Figure 3. Comparative igneous stratigraphic columns (simplified) for layered igneous complexes of the Murchison Domain, compared with the Bushveld Igneous Complex. Stratigraphy is aligned with occurrence of the lowermost upper zone, typically associated with thick magnetite horizons in the Meeline Suite. Note identified chromitite horizons in comparison to the critical zone of the Bushveld Igneous Complex. Notes: (1) adapted from Cawthorn and Wairaven (1998); (2) age from Ivanic et al. (2010); (3) age from Wingate et al. 2012; (4) Gill (2011); (5) Wang (2009); (6) zones adapted from Parks (1998).

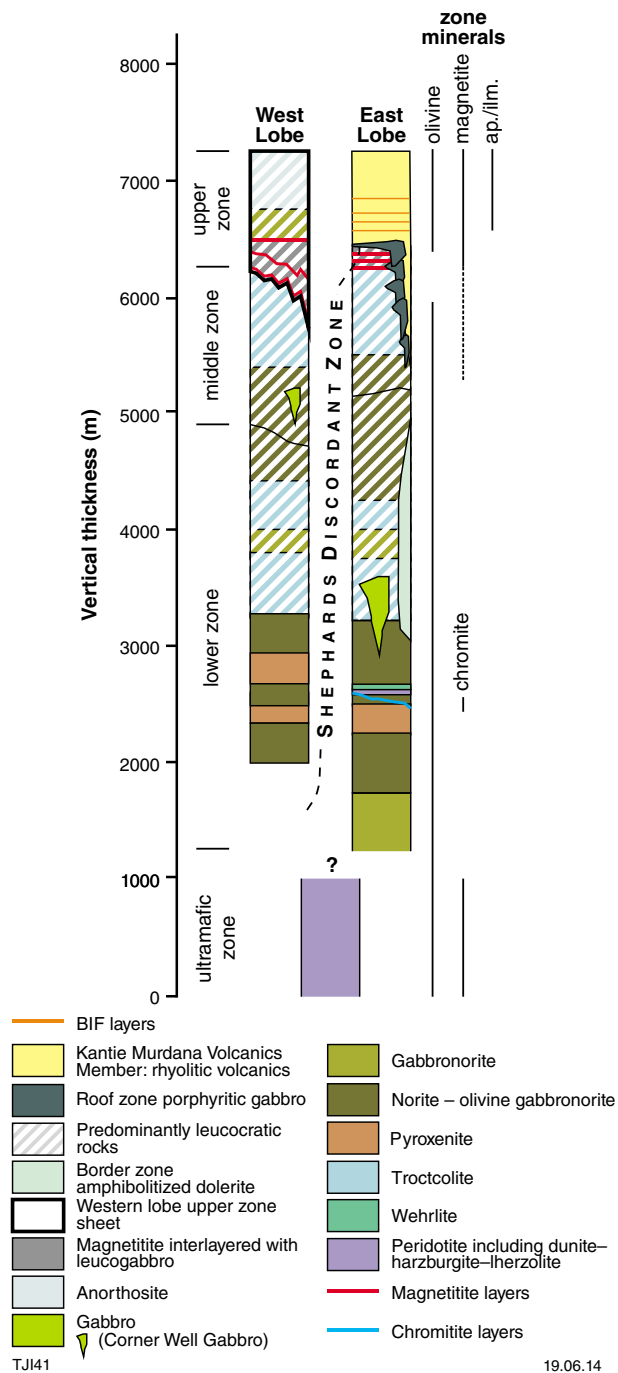
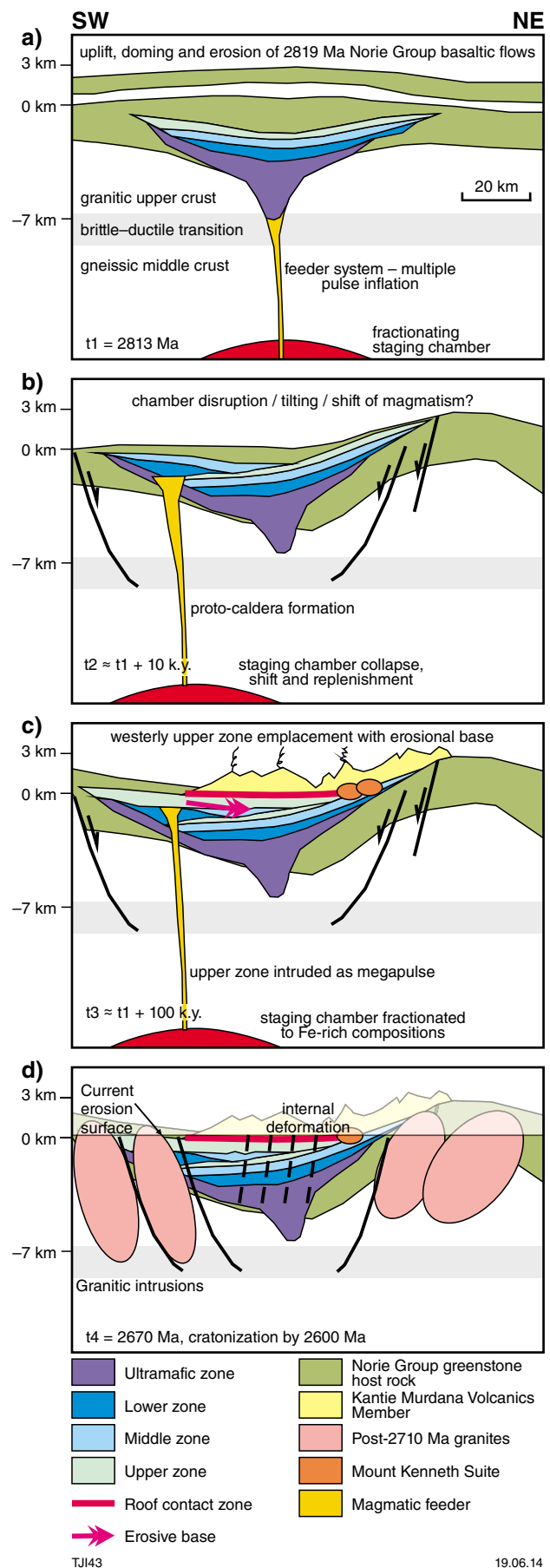


Figure 4. (above) Igneous stratigraphic column for the Windimurra Igneous Complex showing true thickness for all major components of the complex as derived from observations made at the surface. The complex is divided into an eastern and western lobe along the Shephards Discordant Zone. Note major oxide horizons of chromite-rich and magnetite-rich rock types.

Figure 5. (right) Simplified model for the formation of the Windimurra Igneous Complex. a) initial stage of intrusion into the Norie Group, formation of the Western lobe; b) Formation of the Eastern lobe; c) Formation of the upper zone of the eastern lobe, Mount Kenneth Suite and Kantie Murdana Volcanics Member; d) Formation of Tuckanarra and Jungar Suite granitic rocks, deformation and erosional features



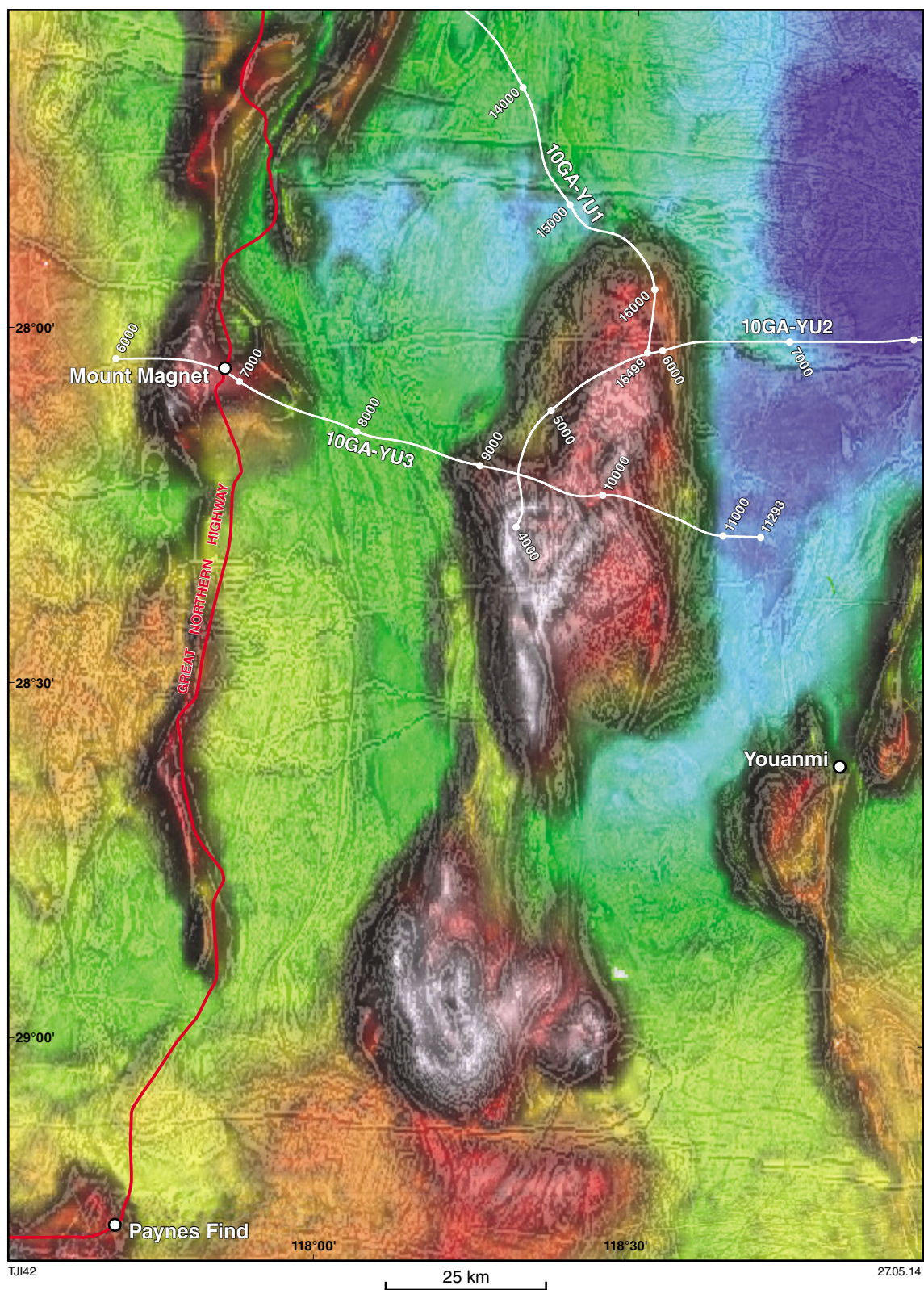


Figure 6. Location of the Youanmi seismic lines in the vicinity of the Windimurra Igneous Complex (cf. Fig. 2) in relation to gravity data (colour) and magnetic data (shading)

Details of seismic acquisition and processing for the Windimurra Igneous Complex, along with observations on the seismic characteristics were given by Jones et al. (2012). Seismic processing obtains seismic velocity in two ways: bedrock velocity as a by-product of refraction statics analysis, and interval velocity, as a derivative of stacking velocity analysis. High bedrock and interval velocities (approximately 6500 ms⁻¹) correspond with the location of the Windimurra Igneous Complex. Seismic attenuation is low, resulting in high frequency and good resolution down to the base of the complex, thus facilitating detailed interpretation.

The interpretations of the seismic data are presented in Plate 3 and discussed below. An initial 3D interpretation was carried out in Geomodeller™ which, in addition to the seismic data, utilized field observations across the complex, as well as gravity and magnetic surveys. That interpretation is presented at the end of this chapter, and a more detailed 3D interpretation is in progress.

Interpretation of for the seismic lines across the Windimurra Igneous Complex

General interpretations

In the vicinity of the Windimurra Igneous Complex, the Moho is slightly elevated by 0.3 s two-way travel time (TWT, about 1 km), compared to the northern Murchison Domain. The higher seismic velocities within the complex are not sufficient to explain this difference. Apart from this, there are flat and relatively uniform reflections below 9 s TWT (about 27 km depth) within the Moho transition zone. Between 3 and 9 s TWT (4 and 9 s TWT on 10GA-YU3, about 12 and 27 km depth, respectively), there is a series of strong reflections dipping distinctly at about 15° to the east. This is interpreted to be the layered, intermediate middle crust with a strongly listric geometry (see previous chapters of this volume). There is a distinctive region of this middle crust as shallow as 2.4 s TWT (about 7.2 km) just to the north of the complex (seen in line 10GA-YU1). This region deepens to a more typical level for the Murchison Domain of 4 s TWT (about 12 km) towards the central and southern parts of the complex (see Plate 3).

In one seismic zone with no distinctive features (e.g. 10GA-YU1, CDP15500–16000 at 2–3 s TWT) upper crustal granitic rocks are interpreted to overlie the strongly anisotropic middle crust and underlie the Windimurra Igneous Complex. Some of these granitic rocks are in sheared contact with the ultramafic zone at the base of the complex, and are attributed to the Tuckanarra and Big Bell suites, as these units can be traced to surface outcrops. However, some of these granitic rocks at depth may include older suites (<2813 Ma), which acted as a basement to the complex. Some of these basement granites may belong to the Mount Kenneth Suite which, when exposed at the surface, are typically deformed and interlayered with felsic supracrustal rocks of the Norie

Group. In addition, there are several instances where the seismic data show crosscutting granitic plutons of the Bald Rock Supersuite, some of which can be related to surface exposures of this unit.

Using information from all the Youanmi seismic lines, the general form of the Windimurra Igneous Complex is a shallow, funnel-shaped cone, with inward-dipping reflections. The seismic character is twofold with a lower region of very strongly layered and reflective features, and an upper region of less strongly reflective, but still layered, features. In each of the seismic lines, these layered features in both seismic regions typically follow the outer (funnel-shaped) form of the complex as a whole, in two dimensions at least. The upper region, however, has some layering complexity visible in its central part on 10GA-YU3 (Fig. 7c).

The maximum true thickness of the lower region is 1 s TWT (about 3 km) and the maximum thickness of the upper region is 2.3 s TWT (about 6.9 km), both evident on 10GA-YU3. Therefore, a minimum estimate for the maximum true thickness of the complex is 10.5 km. Table 1 summarizes vertical thicknesses of zones within the Windimurra Igneous Complex, and of the complex as a whole.

In terms of stratigraphic thickness — that is, in a perpendicular transect of continuous igneous stratigraphic layering in 2D, where layering is not truncated — the maximum thickness observed is 3.1 s TWT (9.3 km), again on 10GA-YU3. This stratigraphic estimate is thicker than that estimated for the 8.1 km thick Rustenberg Layered Series of the Bushveld Igneous Complex (e.g. Cawthorn and Walraven, 1998).

Thermomechanical modelling of the dynamics of magma emplacement suggests a transition from vertical to horizontal flow for large intrusions at the brittle–ductile transition (Brown, 2007, and references therein). Therefore, the depth of the base of the funnel-form of the complex potentially provides an estimate for the brittle–ductile transition at c. 2810 Ma of about 10 km. This is probably reasonable, since the contact with the overlying and contemporaneous Kantie Murdana Volcanics Member is observed above the central parts of the complex. This vast thickness suggests that mafic–ultramafic intrusions in the Archean may have greater thicknesses than any known Proterozoic–Phanerozoic example.

The ultramafic zone is characterized by strongly layered, high-frequency reflections, whereas the lower zone is seismically less reflective, with more discrete reflective horizons. Reflections in the ultramafic zone likely correspond to cyclical cumulates of peridotite, chromitite, pyroxenite and gabbro, which are interlayered on an approximate 100 m scale. For the lower zone, the lithologic contrast between pyroxenitic and anorthositic layers on an approximate 300 m vertical scale (as observed at the surface) is consistent with the abundance and magnitude of these more discrete reflections.

The regions of middle and upper zones on the seismic lines appear similar, due to the presence of high-density contrasts in the lithologies of these zones (i.e. anorthosite, gabbro, magnetitite and dunite, with the last two more

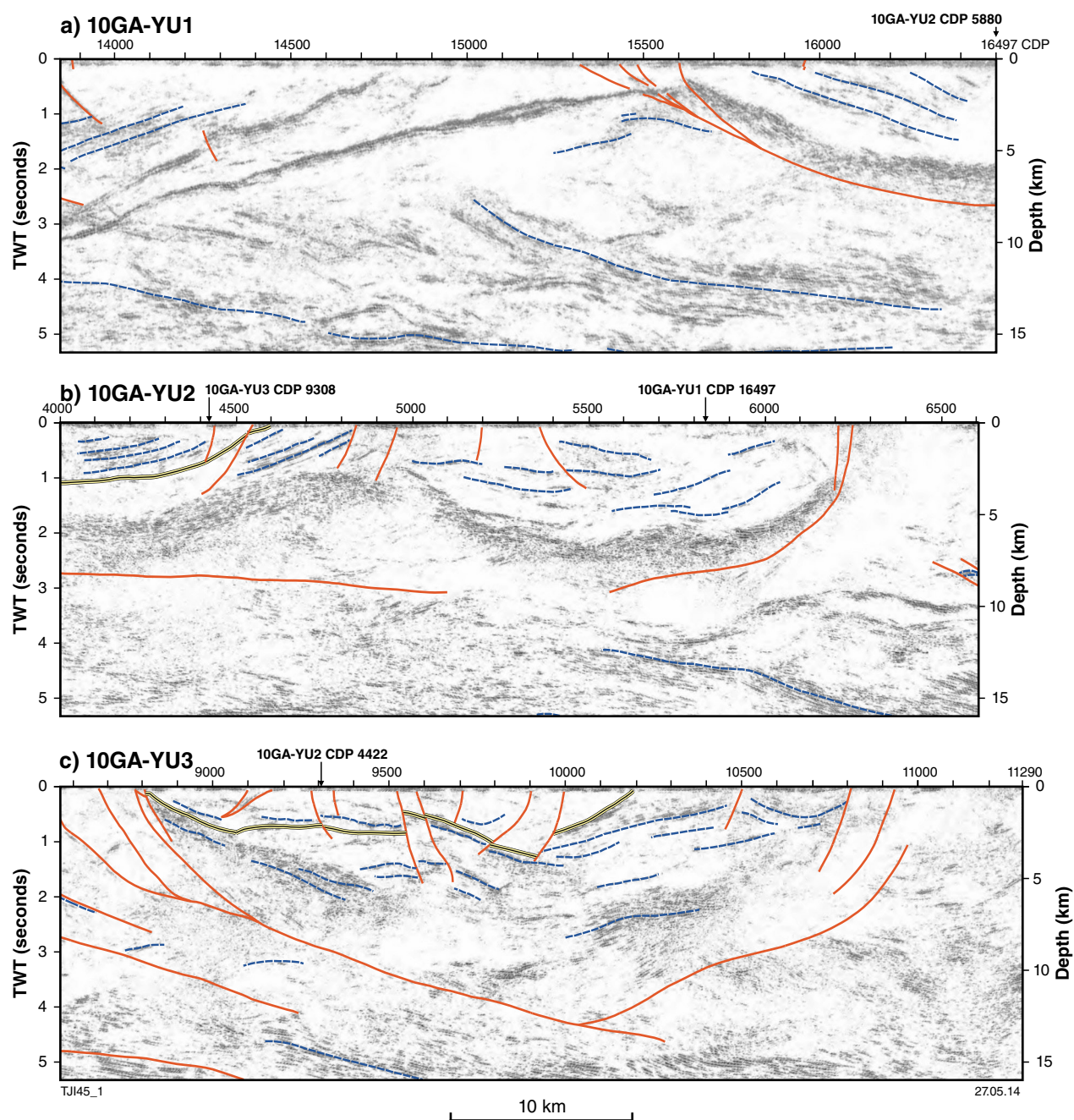


Figure 7: a) Seismic data from 10GA-YU1 showing interpreted structural features; b) seismic data from 10GA-YU2 showing interpreted structural features; c) seismic data from 10GA-YU3 showing interpreted structural features; d) seismic interpretation of 10GA-YU1; e) seismic interpretation of 10GA-YU2; f) seismic interpretation of 10GA-YU3. Zones of the Windimurra Igneous Complex are identified in rock unit codes as: wr – roof zone, wz – upper zone, wm – middle zone, wl – lower zone, wu – ultramafic zone, wb – border zone.

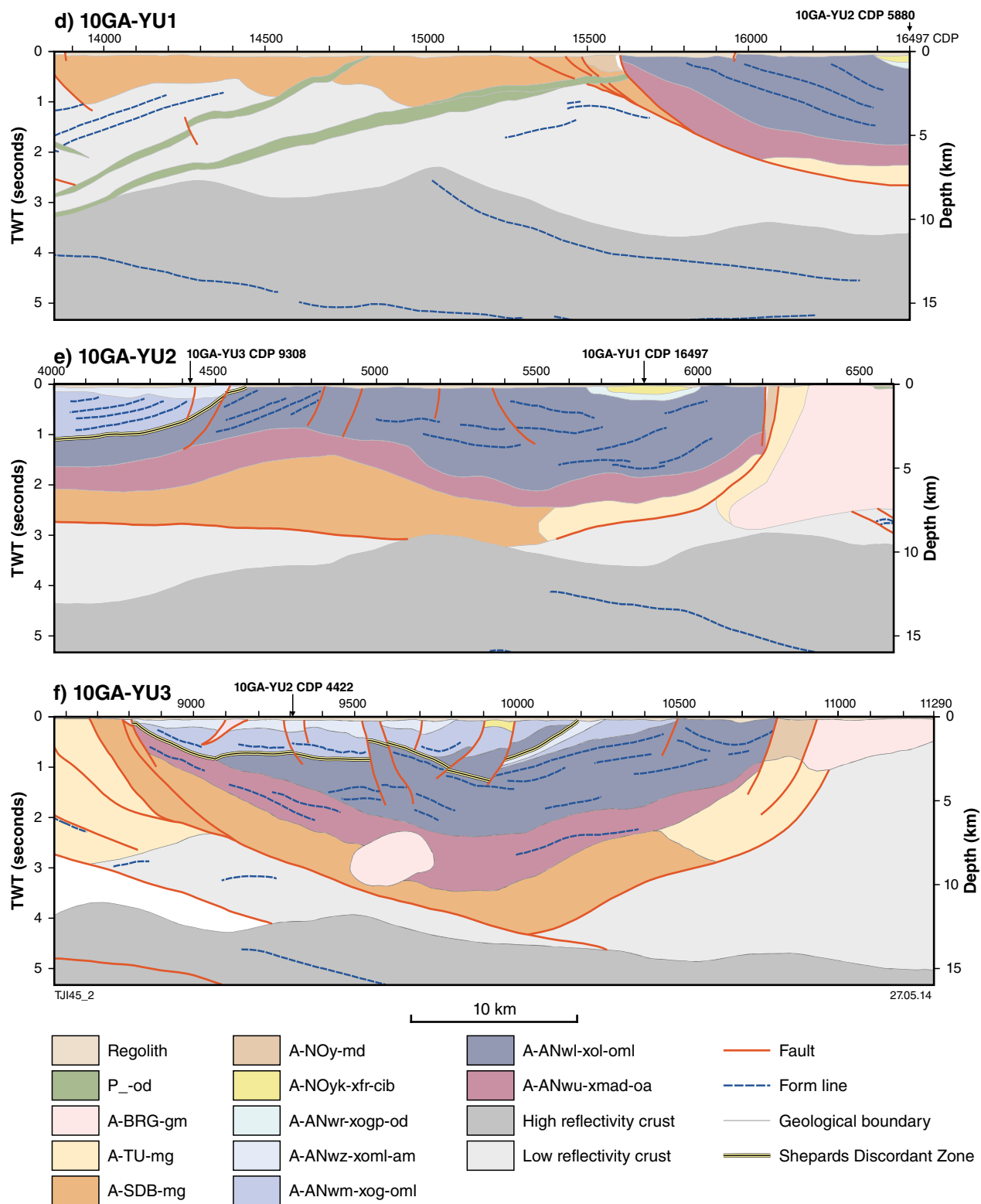


Figure 7. Continued

common in the upper zone). The upper zone appears to be well constrained in the upper seismic region where very flat-lying reflections in 10GA-YU2 and 10GA-YU3 are evident. This is consistent with the dip of layering as observed at the surface. It is also consistent with the interpretation that this layer intruded as a crosscutting sheet into at least the middle zone of the western lobe of the complex, and possibly into its lower zone and various zones of the eastern lobe. This truncation is evident in the 10GA-YU2 and 10GA-YU3 (Fig. 7 b,c,e,f).

Each seismic line shows that layering within the roof zone of the complex and the overlying Kantie Murdana Volcanics Member crosscuts all other zones of the complex, which is again consistent with surface observations. These contacts appear to dip at a shallow angle ($<10^\circ$).

A preliminary 3D model for the complex was generated using Geomodeller and incorporated map data and geophysical surveys as well as preliminary interpretation of the three seismic lines (Ivanic et al., in prep). The model yielded a 3D form for the zones of the intrusion that is consistent with surface and seismic data. The model confirmed the broad funnel-shaped form and the inward-dipping nature of the main subdivisions of the complex.

Preliminary MT conductivity models in the vicinity of the Windimurra Igneous Complex

The preliminary magnetotelluric (MT) conductivity model for seismic line 10GA-YU1 shows moderate to low conductivity for the ultramafic and lower zones of the complex (Plate 3). This feature appears to be a single, long-wavelength region. Higher conductivity is evident in the surrounding foliated granitic rocks, possibly indicating interconnected conductive minerals in these rocks; for example, within the biotite foliation planes.

The preliminary MT conductivity model for seismic line 10GA-YU2 shows three short-wavelength anomalies in the upper parts of the Windimurra Igneous Complex, corresponding to the magnetite-rich upper zone and roof zone. The lower and ultramafic zones are represented by relatively long-wavelength conductivity features of moderate strength. A 10 km low conductivity feature to the east of the complex on this line is thought to represent late granitic plutons (see Plate 3).

The preliminary MT conductivity model for seismic line 10GA-YU3 shows relatively uniform, moderate upper crustal conductivity beneath the Windimurra Igneous Complex. This moderate conductivity is modelled to include the majority of the ultramafic and lower zones of the complex. There is an extremely conductive inward-dipping region, however, which corresponds with the western lobe of the complex above the SDZ, and hence a region of the complex which is thought to be occupied by the magnetite-rich middle and upper zones. This region dips approximately 25° inwards.

Specific interpretations of seismic data for 10GA-YU1 (CDP 15300–16497)

As the line traverses the complex from the north, it progresses up-stratigraphy through the lower zone and, at the southernmost part of the line, it crosses into surface exposures of the Kantie Murdana Volcanics Member (see Fig. 7a,d). This line terminates at CDP 5880 of 10GA-YU2.

- At CDP 15300, the west-dipping Yarloo Shear Zone has been inferred using aeromagnetic interpretation. Exposure is poor in the area, however, and so this feature is not well described. Granitic rocks in the vicinity have a steeply dipping, northerly striking foliation, oriented at a low angle to the seismic line. Thus, they are expressed only as shallow-dipping reflections on this section. The shear zone is interpreted to be within metagranitic rocks of the c. 2700 Ma Big Bell Suite.
- Felsic schists assigned to the Norie Group, Yaloginda Formation, including metasedimentary rocks (A-NOy-md on Fig 7c,f), which mantle the Windimurra Igneous Complex, are not reflective but are interpreted to occur in a small wedge immediately to the north of the complex between shear zones. Rocks of this unit are only exposed in a small outcrop (200 x 200 m) north of the complex (Zibra et al., 2013).
- Relatively shallow-dipping reflections characterize the lower zone of the complex. Corresponding surface exposures of modally layered gabbroic cumulates are known to have similar dips of $15\text{--}30^\circ$ across this region, compatible with these reflections.
- Towards the southern end of the line (closer to the centre of the complex), dips are shallow to almost horizontal, as shown by the reflections in the lower zone towards the southern limit of the line.
- Estimates from this line indicate that the maximum thickness and depth-to-the-base of the lower zone are approximately 5 and 5.5 km, respectively.
- Estimates from this line indicate that the maximum thickness and depth-to-the-base of the ultramafic zone are approximately 1.5 and 6.5 km, respectively.
- The roof zone is interpreted as lying above horizontal reflections of the macro-rhythmically layered lower zone.
- The Kantie Murdana Volcanics Member is interpreted as lying above the roof zone with a shallowly southward-dipping contact.
- Strong reflections to the north of the Windimurra Igneous Complex, with an apparent dip of 10° north, at approximately 1 s TWT, are interpreted to be part of an extensive Proterozoic sill complex. This unit may crosscut the zones of the Windimurra Igneous

Complex but, as they are likely to have a similar density and seismic velocity, they may not be visible in seismic data within the gabbroic layers. This sill is likely part of the typically shallowly dipping Mount Holmes Gabbro sill, which outcrops to the east of the Windimurra Igneous Complex and is readily visible in seismic line 10GA-YU2.

- There is an extensional fault at CDP 15900 (10GA-YU1), which appears to cut the regolith horizon and offset this down to the north. The apparent displacement on the seismic line is approximately 50 m.

Specific interpretations of seismic data for 10GA-YU2 (CDP 4000–6900)

In map view, seismic line 10GA-YU2 starts in the centre of the upper zone of the complex, proceeds towards the northwestern edge and, as the line bends around to the east, traverses the middle of the lower zone, and continues out to the eastern edge of the complex (Fig. 2). At CDP 4422 the line intersects 10GA-YU3 and at CDP 5880 it intersects the end of 10GA-YU1 (Fig. 7b,e).

- A minimum thickness of approximately 4 km is estimated for the complex at CDP 4850, where the line extends to its northwesternmost location.
- Estimates from this line indicate that the maximum thickness and depth-to-the-base of the upper zone are approximately 0.9 and 1.0 km, respectively.
- Estimates from this line indicate that the maximum thickness and depth-to-the-base of the middle zone are approximately 2.8 and 3.1 km, respectively.
- Estimates from this line indicate that the maximum thickness and depth-to-the-base of the lower zone are approximately 6.1 and 6.3 km, respectively.
- Estimates from this line indicate that the maximum thickness and depth-to-the-base of the ultramafic zone are approximately 2.0 and 7.1 km, respectively.
- Dips in the ultramafic zone and lower zone support an interpretation of an overall bowl-shaped form for the Windimurra Igneous Complex, with steeper dips at the margins (about 20°) and subhorizontal reflections in the interior. As the seismic line approaches the margin of the complex in two places, this bowl shape is duplicated in this section.
- The SDZ is interpreted as a south-dipping horizon towards the southern end of the line, which cuts into lower-zone stratigraphy and is overlain by middle- and upper-zone material.
- Very shallow dipping (apparent dip of 0–5°) reflections from CDP 4000 to CDP 4500 are interpreted to represent the magnetitite-rich base of the upper zone, which can be seen to truncate moderately dipping middle zone material (with an apparent dip of 5–15°).
- A shallow, bowl-shaped region above reflective, layered gabbroic rocks (centred at CDP 5800) has an estimated maximum thickness of 1 km in the line of section. This is interpreted to be composed of 500 m thickness of the roof zone of the Windimurra Igneous Complex, and 500 m thickness of the overlying Kantie Murdana Volcanics Member.
- The Proterozoic Mount Holmes Gabbro sill is interpreted at shallow levels to the east of the complex, and dips 5° to the northeast, as noted in surface outcrops adjacent to the seismic line.

Specific interpretations of seismic data for 10GA-YU3 (CDP 8600–11290)

Seismic line 10GA-YU3 provides an east–west cross section across the complex from CDP 8800 to CDP 10800 (Fig. 7c,f). In the west, the line intersects the sheared western contact of the complex and continues through to CDP 9308, where it intersects 10GA-YU2. The line then crosses the SDZ, 2 km north of the Windimurra vanadium openpit, and continues out past the eastern extent of the complex, across an unexposed contact with metasedimentary rocks within the Wyemandoo Shear Zone. The line finishes in post-tectonic granitic rocks of the Bald Rock Supersuite.

- Estimates from this line indicate that the maximum thickness and depth-to-the-base of the upper zone are approximately 0.9 km and 2.5 km, respectively.
- Estimates from this line indicate that the maximum thickness and depth-to-the-base of the middle zone are approximately 2.5 km and 3 km, respectively.
- Estimates from this line indicate that the maximum thickness and depth-to-the-base of the lower zone are approximately 6.0 km and 6.3 km, respectively.
- Estimates from this line indicate that the maximum thickness and depth-to-the-base of the ultramafic zone are approximately 3.2 km and 10.5 km, respectively.
- The seismically non-reflective zone beneath the western part of the complex is interpreted to be an intersection with a homogeneous granitic pluton, possibly of the Bald Rock Supersuite.
- The SDZ has an apparent dip which varies from close to horizontal to east-dipping in the western part of the complex. At CDP 10000, this zone is cut by a brittle fault, to the east of which the zone dips to the west at approximately 30° apparent dip.
- Form lines within the complex have a shallow dip and form a broadly inward-dipping structure related to primary igneous layering.

- A 3 km thickness of metasedimentary rocks of the Norie Group is interpreted east of the Wyemando Shear Zone in a seismically non-reflective region (CDP 10800 to 10930). This is based primarily on the extrapolation of surface observations and aeromagnetic data.
- A seismically non-reflective region at the base of the complex is interpreted to represent a crosscutting granitic body (CDP 9500 to 10000 at 2 to 3 s TWT). This is attributed to the Bald Rock Supersuite (post-tectonic granite) as it appears to postdate any deformational structures. However, its precise form is not clear.
- An approximately 2–3 km thick, flat-lying sheet of Bald Rock Supersuite granitic rock is interpreted in the seismically non-reflective region in the east of the line (CDP 10930 to 11290 at 0.1 to 1.2 s TWT).
- The Yarloo and Challa shear zones are interpreted to dip to the east. Both merge into the larger Cundimurra Shear Zone at a depth of approximately 7 km beneath the middle of the Windimurra Igneous Complex.
- A significant ultramafic zone, approximately 3 km thick at its maximum, likely underlies the entire complex. The presence of a basal component of the Windimurra Igneous Complex effectively accounts for the missing ultramafic zone (Ivanic et al., 2010; Ahmat, 1986), and therefore militates against the possibility (Bunting, 2004) that the Narndee Igneous Complex represents the ultramafic portion of the Windimurra Igneous Complex. The bulk composition is, therefore, much less Ca and Al rich than previously anticipated (Ahmat, 1986) and closer to a tholeiitic/komatiitic basalt composition.
- The ultramafic zone cannot be traced to the surface using the seismic data. However, regions along the northern margin of the complex (e.g. on line 10GA-YU1) are identified as having the shallowest parts of this zone at about 600 m depth. The western margin also has a region of shallow ultramafic zone material, identified at CDP 8800 on 10GA-YU3.
- Approximately half of the western lobe of the complex has been displaced along the Challa Shear Zone and detached from the main body of the complex. Some of this material may lie unexposed beneath granites to the south of the Narndee Igneous Complex, coincident with a gravity high.
- The Challa Shear Zone dips approximately 70° to the east-northeast. This dip decreases below 3 km depth to approximately 45°.
- The deepest part of the complex identified is in the central part where it is intersected by the 10GA-YU3 seismic line, approximately 10.5 km below the present erosion level. This is likely close to the maximum thickness of the complex, although slightly deeper regions may be present immediately south of this point.
- The interpretation of the SDZ as marking the base of the western lobe of the complex remains plausible, consistent with seismic data.
- An intrusion of a flat slab of 1 km thick upper zone material in the western lobe (in the vicinity of the Canegrass Ti–V–Fe prospect) is consistent with seismic data in 10GA-YU2 and 10GA-YU3.

Table 1 provides summary vertical thicknesses of the zones within the Windimurra Igneous Complex.

Conclusions and implications

- An overall funnel-shaped form for the Windimurra Igneous Complex is supported by the seismic data. The complex appears relatively intact and coherent in its main part, with local modification by strike-slip shear zones, brittle faulting, and crosscutting granitic plutons.
- A two-stage stratigraphy consisting of an eastern and western lobe is consistent with seismic data. The eastern lobe is considered to represent the initial intrusive form, evolving from an ultramafic zone through to the lower, middle and upper zones. Subsequently, a second lobe (western lobe) intruded in the southwest and cuts across the lower, middle and upper zones of the eastern lobe.

Table 1. Dimensions of components of the Windimurra Igneous Complex as obtained from seismic data, assuming an average crustal seismic velocity of 6000 ms⁻¹.

Zone	Max. vertical thickness (km)	Max. cumulative perpendicular thickness (km)	Maximum depth-to-base (km)	Primary source
Complex as a whole	10.1	13.7	10.5	10GA-YU3
Ultramafic	3.2	3.2	10.5	10GA-YU3
Lower	6.1	6.3	6.2	10GA-YU2
Middle	2.3	2.8	3.1	10GA-YU2
Upper	0.9	1.0	2.5	10GA-YU3
Shephard's Discordant Zone	–	–	3.8	10GA-YU3
Roof Zone	0.3	0.4	0.8	10GA-YU2
Kantie Murdana Volcanics Member	0.5	0.5	0.7	10GA-YU2

- A strongly reflective, west-dipping slab (about 30°) of upper zone material (including the unit at the Windimurra vanadium openpit) in the eastern lobe is apparent from seismic data in 10GA-YU3, down to at least 3 km depth.
- The Kantie Murdana Volcanics Member appears to overlie up to 1 km thickness of gabbroic rocks in the roof zone of the complex. Seismic data suggest that both of these units crosscut zones of the eastern and western lobes of the complex.
- A preliminary 3D model for the Windimurra Igneous Complex has been constructed and is consistent with seismic interpretations and surface observations.

References

- Ahmat, AL 1986, Petrology, structure, regional geology and age of the gabbroic Windimurra complex, Western Australia: The University of Western Australia, Perth, Western Australia, PhD thesis (unpublished), 279p.
- Brown, M 2007, Crustal melting and melt extraction, ascent and emplacement in orogens: mechanisms and consequences: *Journal of the Geological Society*, v. 164, p. 1–22.
- Bunting, JA 2004, The nickel–PGE potential of the Narndee and Windimurra intrusions; Apex Minerals NL: Geological Survey of Western Australia, Statutory mineral exploration report, A69643 (unpublished).
- Cawthorn, RG and Walraven, F 1998, Emplacement and crystallization time for the Bushveld complex: *Journal of Petrology*, v. 39, no. 9, p. 1669–1687.
- Gill, M 2011, The petrogenesis and FeTiO accumulation of the Youanmi Igneous Complex (Yilgarn Craton), Western Australia: University of Tasmania, Honours thesis (unpublished).
- Ivanic, TJ 2009, Madoonga, WA Sheet 2444: Geological Survey of Western Australia, 1:100 000 Geological Series.
- Ivanic, TJ 2011, Coolamaninu, WA Sheet 2540: Geological Survey of Western Australia, 1:100 000 Geological Series.
- Ivanic, TJ 2012a, Challa, WA Sheet 2541: Geological Survey of Western Australia, 1:100 000 Geological Series.
- Ivanic, TJ 2012b, Windimurra, WA Sheet 2641: Geological Survey of Western Australia, 1:100 000 Geological Series.
- Ivanic, TJ, Van Kranendonk, MJ, Kirkland, CL, Wyche, S, Wingate, MTD and Belousova, E 2012, Zircon Lu–Hf isotopes and granite geochemistry of the Murchison Domain of the Yilgarn Craton: evidence for reworking of Eocarchean crust during Meso–Neoproterozoic plume-driven magmatism: *Lithos*, v. 148, p. 112–127.
- Ivanic, TJ, Wingate, MTD, Kirkland, CL, Van Kranendonk, MJ and Wyche, S 2010, Age and significance of voluminous mafic–ultramafic magmatic events in the Murchison Domain, Yilgarn Craton: *Australian Journal of Earth Sciences*, v. 57, p. 597–614.
- Jones, LEA, Ivanic, TJ and Costelloe, RD 2012, Seismic reflection imaging of the mafic–ultramafic Windimurra Igneous Complex, Yilgarn Craton, Western Australia, in *Extended abstracts volume: 22nd Australian Society of Exploration Geophysicists international conference and exhibition*, Brisbane, Australia, 26 February 2012, p. 1–4, 4p.
- Nelson, DR 2001, 169003: vesicular rhyolite, Carron Hill; *Geochronology Record 170*: Geological Survey of Western Australia, 4p.
- Parks, J 1998, Weld Range platinum group element deposit, in *Geology of Australian and Papua New Guinean mineral deposits edited by DA Berkman and DH Mackenzie*: The Australian Institute of Mining and Metallurgy, Monograph 22, p. 279–286.
- Scowen, PAH 1991, The geology and geochemistry of the Narndee intrusion: Australian National University, Canberra, Australian Capital Territory, PhD thesis (unpublished), 214p.
- Van Kranendonk, MJ, Ivanic, TJ, Wingate, MTD, Kirkland, CL and Wyche, S 2013, Long-lived, autochthonous development of the Archean Murchison Domain, and implications for Yilgarn Craton tectonics: *Precambrian Research*, v. 229, p. 49–92.
- Wang, Q 1998, Geochronology of the granite–greenstone terranes in the Murchison and Southern Cross Provinces of the Yilgarn Craton, Western Australia: Australian National University, Canberra, PhD thesis (unpublished), 186p.
- Wingate, MTD, Kirkland, CL and Ivanic, TJ 2012, 194747: metagabbro, Malamiter Well; *Geochronology Record 1013*: Geological Survey of Western Australia, 4p.
- Zibra, I, Ivanic, TJ and Chen, SF 2013, Wynyangoo, WA Sheet 2542: Geological Survey of Western Australia, 1:100 000 Geological Series.

Preliminary interpretation of deep seismic lines 10GA-YU3 and the southeastern part of 10GA-YU1: Murchison Domain of the Youanmi Terrane

by

I Zibra, K Gessner, RJ Korsch, RS Blewett¹, T Jones¹, P Milligan¹,
LEA Jones², S Wyche, MP Doublier, CE Hall, SF Chen, SS Romano,
TJ Ivanic, MJ Pawley³, N Patison, BLN Kennett⁴, and MJ Van Kranendonk⁵

Introduction and aims of the seismic survey

Deep seismic reflection line 10GA-YU3 is oriented approximately east–west, broadly normal to the strike of the major geological structures in this portion of the Neoproterozoic Youanmi Terrane (Fig. 1). In the west, the line starts within the Lakeside Granite, near the western margin of the Mount Magnet greenstone belt, and then continues east for about 105 km to the eastern margin of the Windimurra Igneous Complex. The southeastern half of line 10GA-YU1 is subparallel to line 10GA-YU3, so that the two lines cross the same structures and plutons along strike. This allows an opportunity to investigate the three-dimensional architecture of this part of the belt. These two segments are therefore treated together in this section.

The principal objectives of seismic reflection lines 10GA-YU3 and 10GA-YU1, where they cross the Murchison Domain of the Youanmi Terrane, were to determine: 1) the three-dimensional architecture of the structures associated with the four main granitic plutons exposed in the area (see below); 2) the three-dimensional architecture of structures associated with the highly mineralized Mount Magnet, Cue, Big Bell and Tuckabianna greenstones; and 3) the nature of the Moho discontinuity and the three-dimensional architecture of the unexposed middle to lower continental crust.

The preliminary interpretation of these seismic transects is based on the seismic reflection data, and constrained by outcrop geology along the section line, as well as by gravity, magnetic and geochronological data for the

region. The interpretation of the easternmost parts of the 10GA-YU3 and 10GA-YU1 lines is incorporated elsewhere in this volume (Ivanic et al., 2013, this volume).

Local geological setting

Introduction

In the Murchison Domain, the northeast-trending corridor between Mount Magnet and Meekatharra represents a key area for understanding the deformational style of the Neoproterozoic crust, in particular the interplay between progressive magmatism and deformation of metamorphic granite–greenstone terranes. The area includes c. 2810–2720 Ma greenstone successions intruded by c. 2720–2590 Ma granitic rocks, although some older, typically small granitic plutons with emplacement ages of c. 2800–2750 Ma are preserved within greenstone packages. In the Murchison area, granitic plutons range from pre- to post-kinematic, systematically showing differences in size, shape and aspect ratio, depending on the role these plutons played during the development of the Neoproterozoic crustal structure preserved in the northwestern part of the Yilgarn Craton. A comprehensive summary of the greenstone stratigraphy and granitic suites for the Murchison Domain was given by Van Kranendonk et al. (2013).

The most main structure in the area is the Cundimurra Shear Zone (Fig. 1). This is a transpressional shear zone centred on the Cundimurra Monzogranite, which preserves evidence of shearing during incremental pluton emplacement (c. 2680–2660 Ma; Schiøtte and Campbell, 1996), and during retrograde conditions down to low- to greenschist facies temperatures (Zibra et al., 2014a,b). The Cundimurra Shear Zone postdates the emplacement of the adjacent Lakeside and Yarraquin granite plutons (Fig. 1), which are approximately 100 × 50 km composite plutons associated with migmatites. Conversely, the shear zone is cut by the c. 2620 Ma Garden Rock Monzogranite (Fig. 1; Wang, 1998). The Lakeside and Yarraquin granite plutons show widespread evidence of melt-present deformation, and also high-temperature, solid-state deformation to

1 Minerals and Natural Hazards Division, Geoscience Australia, GPO Box 378, Canberra ACT 2601

2 Energy Division, Geoscience Australia, GPO Box 378, Canberra ACT 2601

3 Geological Survey of South Australia, Department of Manufacturing Innovation Trade Resources and Energy, Level 4, 101 Grenfell Street, Adelaide SA 5000

4 Research School of Earth Sciences, The Australian National University, Canberra ACT 0200

5 School of Biological, Earth and Environmental Sciences, The University of New South Wales, Sydney NSW 2052

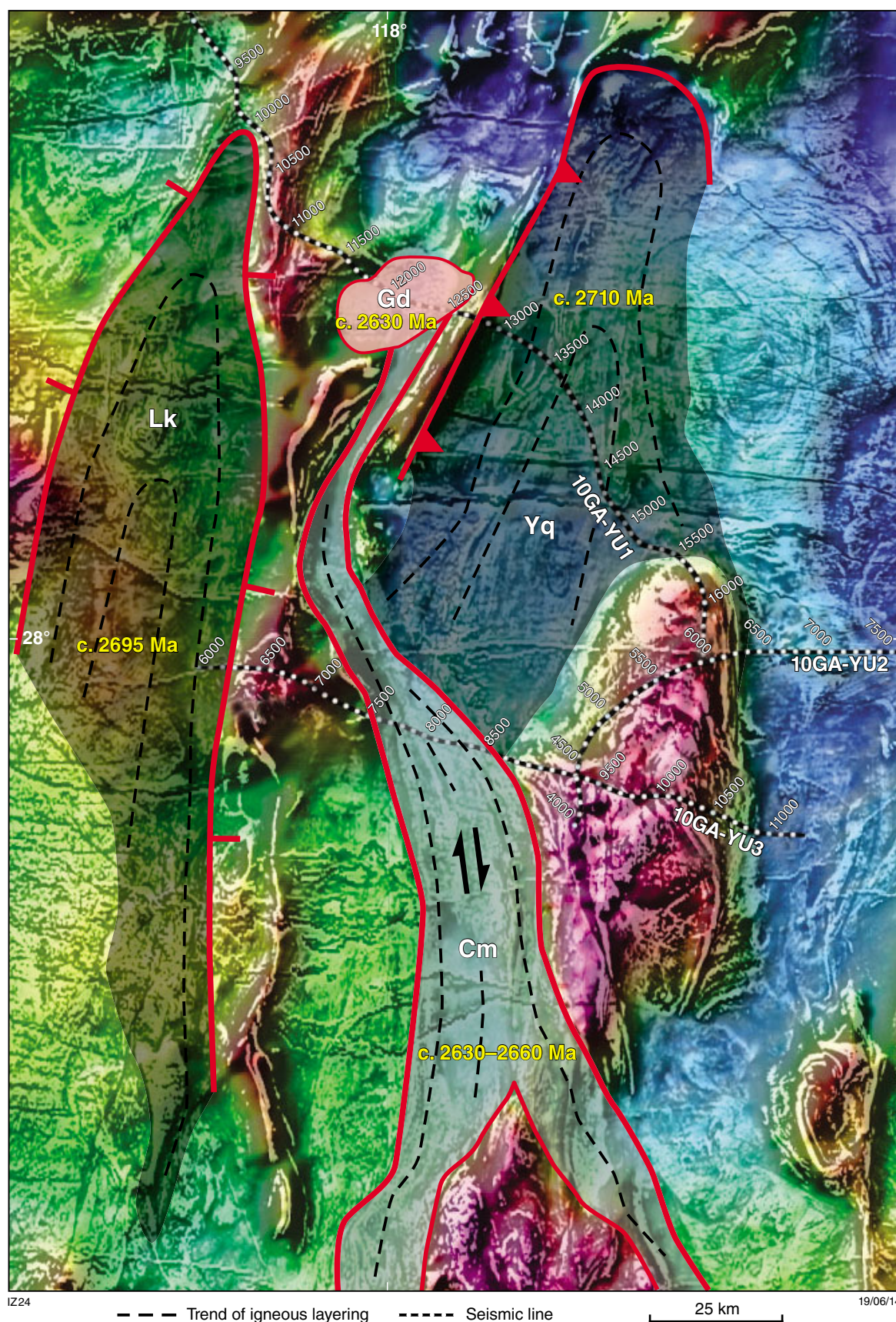


Figure 1. Geophysical image (gravity on aeromagnetic) centred on the Cundimurra pluton (Cm), which coincides with the dextral transpressional Cundimurra Shear Zone. Map view field relations and geochronology indicate that the Cundimurra Shear Zone postdates both the Yarraquin and the Lakeside plutons (Yq and Lk, respectively). All the regional-scale structures are truncated by the post-tectonic Garden Rock Monzogranite (Gd).

accommodate the emplacement of granite–migmatite domes (Zibra, 2012). Based on detailed structural analysis, these plutons can be regarded as large-scale, partially molten shear zones, even though the fabrics which relate to this shearing are not readily detectable in geophysical images (e.g. compare Figs 1, 2). Field and microstructural observations suggest that the north-striking, steeply dipping magmatic to high-temperature solid-state structures preserved in these plutons were likely controlled by active large-scale structures, and therefore by the regional stress field which was prevalent in the Youanmi Terrane at about 2700 Ma.

Yarraquin pluton

The Yarraquin pluton is a north-striking gneissic complex (approximately 100 × 40 km; Fig. 1) exposed on line

10GA-YU1 between the Tuckabianna Syncline (at about CDP 12800) and the Windimurra Igneous Complex (at about CDP 15600). It is mainly composed of high-temperature granitic gneiss (Fig. 3), including numerous xenoliths of mafic gneiss and paragneiss, which likely represent fragments of greenstone packages that were dismembered during granite emplacement and subsequent high-temperature shearing. Here, the main rock types include ultramafic schist, (locally garnet-bearing), amphibolite, gabbro, banded iron-formation, sillimanite-bearing mica schist and quartzite (Fig. 4). These rock types are locally exposed, and they are readily detectable in aeromagnetic images (Fig. 2). Composite xenoliths are typically narrow and elongate, ranging in size from a few metres to a few kilometres along strike. They define two major structures, named here as the Mingimbia and Fred folds, which are well defined by geophysical

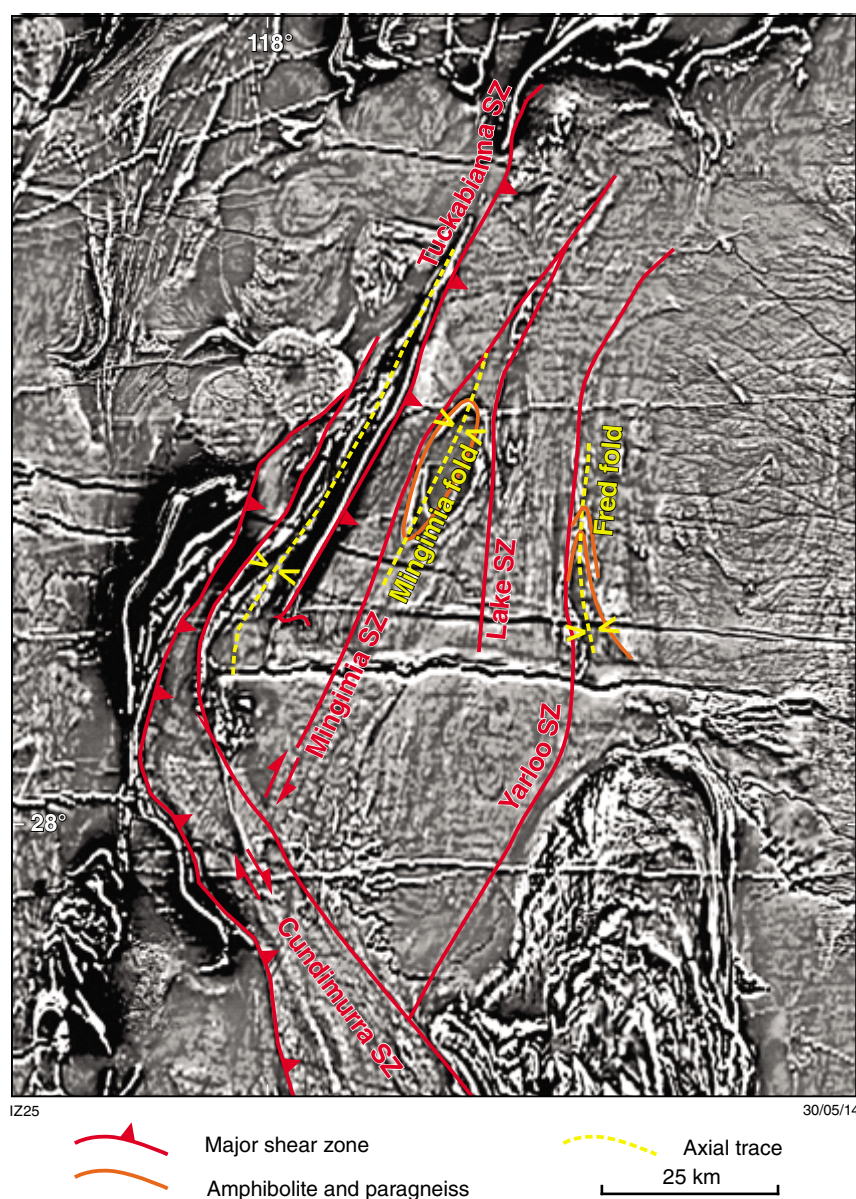


Figure 2. Aeromagnetic image centred on the Yarraquin pluton, showing its main internal structures and relationships with adjacent plutons



IZ28

01/11/13

Figure 3. Layered granitic gneiss displaying north-striking high-temperature fabric in the Fred area greenstones



IZ29

01/11/13

Figure 4. Transposed bedding in strongly foliated, ferruginous quartzite

images (Fig. 2) and partly exposed at the surface. In the exposed portion of the Fred fold, field relations indicate that early, east-trending folds were refolded by north-trending, upright folds. Therefore, it is likely that the pattern visible in the aeromagnetic map derives from large-scale superposed folds. Both structures are flanked by large-scale shear zones (Fig. 2), described in detail in the following section. Granitic rocks are typically poorly exposed, so lithological and structural features are not well constrained. Nevertheless, the exposed Yarraquin pluton is granodioritic to monzogranitic in composition, with tonalites common along the exposed western pluton margins. The main steep, north-northeasterly striking fabric ranges from a magmatic to a high-temperature, solid-state fabric, whereas shear zones along the margins of the pluton typically developed under mid-amphibolite

facies conditions. No evidence of a pervasive overprint lower than amphibolite facies has been observed. A sample collected along the northwestern margin of the pluton provided an emplacement age of 2710 ± 10 Ma (Wang et al., 1995), which could be representative of the tonalitic marginal facies but not necessarily of the whole pluton.

Lakeside pluton

The north-trending Lakeside pluton (about 150×50 km) is exposed between the north-striking, sinistral Cuddingwarra Shear Zone (CDSZ; Fig. 7 in Wyche et al., 2013, this volume) and the northeast-striking, dextral Chunderloo Shear Zone. The eastern pluton boundary against the Mount Magnet greenstones (Fig. 7 in Wyche et al., 2013, this volume) is represented by the kilometre-scale Wattle Creek Shear Zone, which was active during and after pluton crystallization at c. 2700 Ma (Fig. 6; see also Zibra, 2012). Here, granitic rocks occupy a lozenge-shaped area centred along the core of the north-northeasterly trending Big Bell antiform (BBA, fig. 7 in Wyche et al., 2013, this volume; CDP 10000 on 10GA-YU1; Fig. 5). These granites are mostly unaffected by the greenschist-facies shearing event which gave rise to the regional shear zones, allowing the study of syn-emplacement and syn-crystallization structures. In this area, the dominant granite type is mesocratic, porphyritic to equigranular, biotite tonalite to monzogranite, displaying north-trending magmatic to high-temperature, solid-state fabrics (Fig. 7). These rocks are intruded by medium-grained leucogranite and meso- to leucocratic microgranite dykes. Monzogranites include metre- to kilometre-scale xenoliths represented by microtonalitic to microgranitic gneiss and subordinate, coarse-grained granodioritic gneiss. In the Cue area, these high-grade tonalite–trondhjemite–granodiorite (TTG) gneisses provided an emplacement age of c. 2720 Ma (Van Kranendonk et al., 2013).

Cundimurra Monzogranite

The Cundimurra Monzogranite is a narrow (between 5 and 10 km wide and 100 km long), north-trending, elongate pluton, which extends south from just southeast of Cue to the Narndee Igneous Complex (Fig. 1). It consists mainly of medium-grained, biotite-bearing monzogranite associated with tonalite and porphyritic monzogranite characterized by 2–5 cm K-feldspar phenocrysts. These rocks are intruded by muscovite-bearing leucogranite and pegmatitic to aplitic veins. Leucocratic veins contain muscovite and, less commonly, garnet. The Cundimurra Monzogranite records several generations of deformation fabrics which developed during emplacement and subsequent cooling from emplacement temperatures down to greenschist conditions. Magmatic features are better preserved in the central portion of the pluton, and in the core of the body, away from the sheared intrusive contacts with the greenstone belts. Magmatic features mainly include a north-striking, steep foliation, which is typically associated with a shallow-plunging lineation. Schlieren fabric is commonly seen in the monzogranites. Solid-state fabrics are best developed near the boundaries

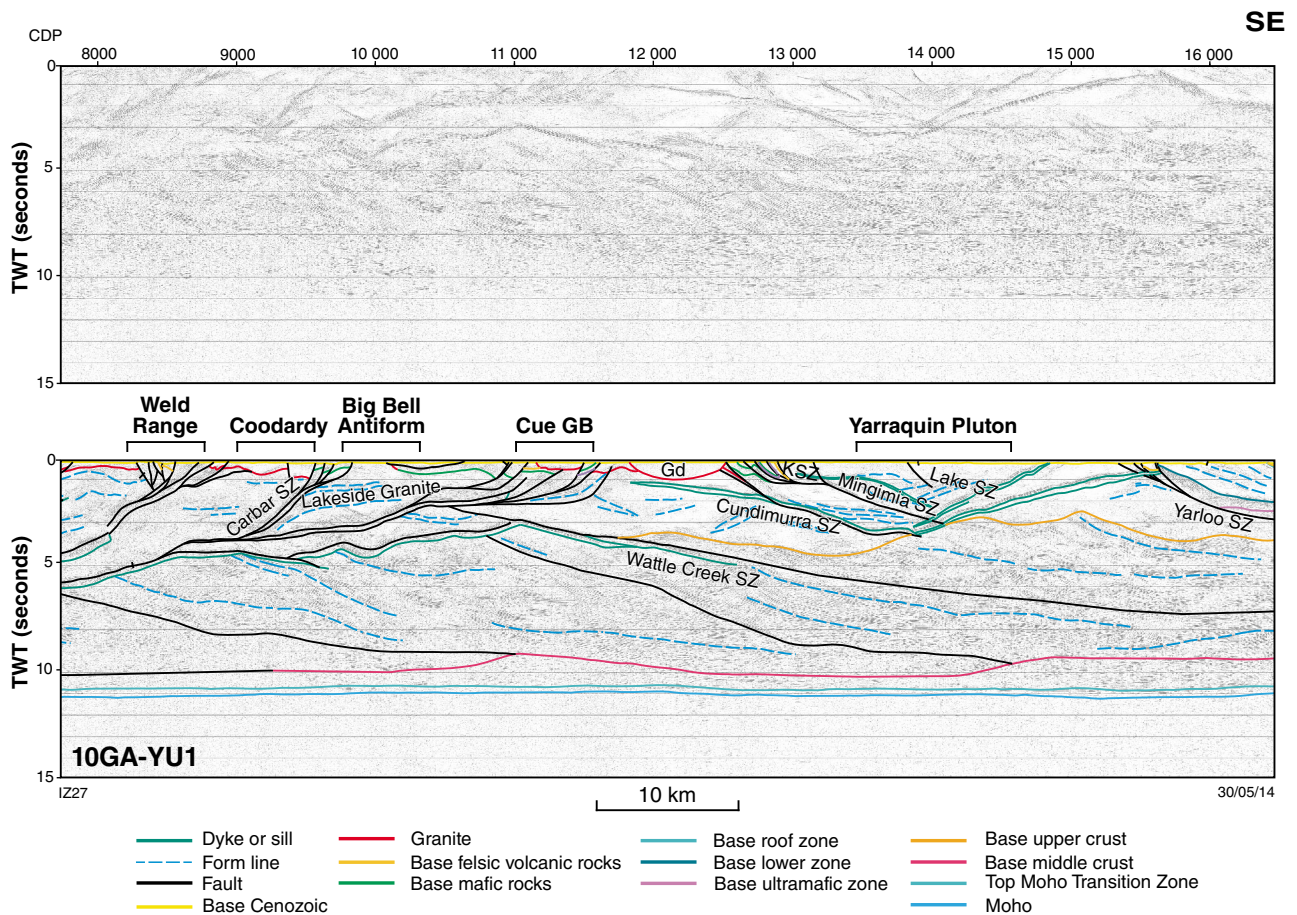


Figure 5. Migrated seismic section for the seismic line 10GA-YU1, between the Weld Range and the northern edge of the Windimurra Igneous Complex, showing both uninterpreted and interpreted versions. Gd – Garden Rock Monzogranite

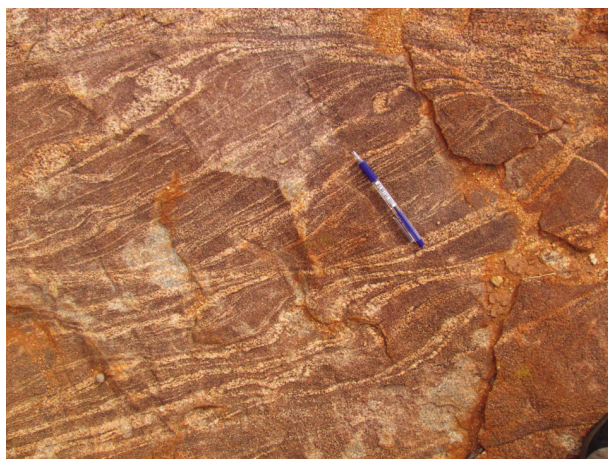


Figure 6. Migmatitic TTG gneiss from the Wattle Creek Shear Zone. Leucosome-injected dextral shear bands indicate syndeformational partial melting

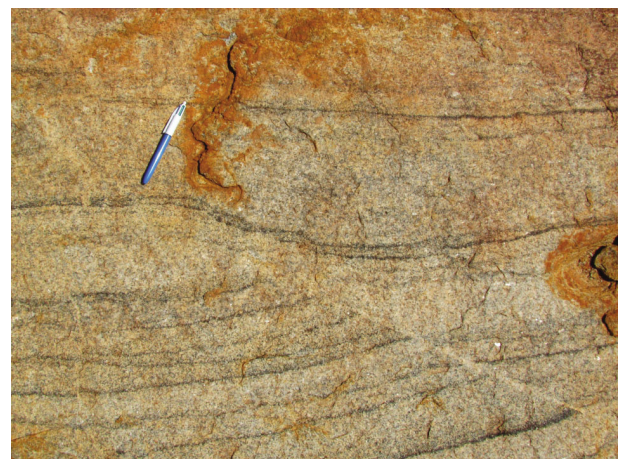


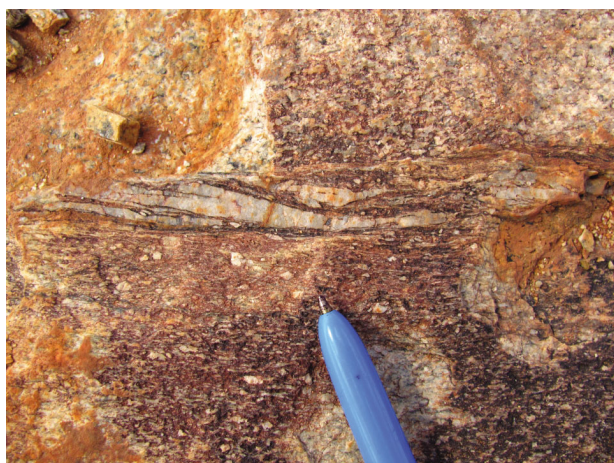
Figure 7. Metre-scale dextral, synmagmatic fault offsetting schlieren layering in equigranular monzogranite

with greenstone belts. At these boundaries, a steep, north-striking, dextral mylonitic foliation is associated with a subhorizontal stretching lineation. Local, small-scale, melt-filled shear zones suggest that magma crystallization likely took place during dextral strike-slip shearing (Fig. 8). In contrast, the north-striking foliation in the adjacent greenstone belts bears a steeply plunging mineral lineation, and amphibolites are commonly $S > L$ tectonites. These observations suggest that transpressional deformation along the Cundimurra Shear Zone was strongly partitioned between the felsic and the mafic components (e.g. Fossen and Tikoff, 1998). Within the metagranites, the gneissic foliation is locally overprinted by thin, retrograde sinistral shear zones (Fig. 9), which typically have a few metres of horizontal displacement. This minor sinistral reactivation is restricted to the northwest-striking segment of the shear zone (i.e. where



IZ32 30/05/14

Figure 8. High-temperature gneissic fabric in metatonalite near the western Cundimurra pluton boundary. The north-striking, steep foliation bears subhorizontal mineral lineation and is postdated by decimetre-scale melt-segregation pockets, indicating that the transpressional shear zone was active during pluton crystallization



IZ33 30/05/14

Figure 9. Horizontal pavement showing sinistral ultramylonite associated with a quartz vein, overprinting at a low angle higher temperature gneissic fabric in porphyritic granite near CDP 7800 on 10GA-YU3

it is intersected by seismic line 10GA-YU3, Fig. 1) and probably represents a very late shearing stage, during which deformation was accommodated by a set of the conjugate structures (Chen et al., 2001). Over the whole pluton, metamorphic conditions, estimated by microstructural means, range from upper amphibolite to mid-greenschist facies (Fig. 8 in Wyche et al., 2013, this volume). Higher temperature fabrics are locally preserved in the Wynyangoo Hill area, whereas the lower temperature fabrics dominate in the central and northern portions of the body. Overall, the observed geometries indicate that shearing was associated with a major component of horizontal displacement, which, in some places, started before complete pluton crystallization. The two greenstone belts flanking the granitic suite are unrelated, suggesting that the displacement along the transpressional shear zones may be on the order of tens of kilometres.

Garden Rock Monzogranite

All regional-scale structures are post-dated by discordant post-tectonic plutons belonging to the c. 2630–2590 Ma Bald Rock Supersuite (Van Kranendonk et al., 2013). In the central Murchison Domain, the Garden Rock Monzogranite (centred around CDP 12000 on 10GA-YU1) truncates the Cundimurra Shear Zone. This post-tectonic pluton is a key element in constraining the tectonic evolution of the area. The Garden Rock Monzogranite is a medium-sized, slightly east–west elongated, undeformed pluton (about 20 × 10 km, Fig. 1) with a steep, concentric, magmatic foliation that is parallel to pluton boundaries and is clearly discordant to the regional structures. Primary magmatic features include aligned euhedral feldspar (and locally hornblende) phenocrysts, aligned mafic microgranular enclaves (Fig. 10), and schlieren layering. Microstructures are characterized by Type I magmatic microfabric (Zibra et al., 2012), where no sign of crystal plastic deformation is detectable. An emplacement age of 2617 ± 24 Ma has been obtained by Wang (1998). A new geochronology sample collected by GSWA is currently being processed.



IZ34 30/05/14

Figure 10. Horizontal pavement in the Garden Rock Monzogranite showing steeply dipping primary magmatic fabric highlighted by euhedral feldspar, and a microgranular, hornblende-bearing diorite enclave

Preliminary seismic interpretation

The Moho is imaged as a sharp and flat discontinuity located at about 11 s two-way travel time (TWT) in both lines 10GA-YU3 and 10GA-YU1. The two lines also share a common deep-crustal architecture, including a highly reflective and horizontally layered lower crust overlain by a middle crust characterized by prominent, east-dipping reflections with overall listric geometry (Figs 5, 11). In their uppermost portions, mid-crustal reflection packages show an arcuate geometry, which is most commonly interpreted as a ramp anticline associated with a hangingwall cutoff in a thrust system (Van der Velden et al., 2006). This is consistent with the duplication of some reflections which is observable in several domains. The most convincing examples occur at about 5 s TWT at about CDP 12000 and CDP 8500 on line 10GA-YU1 and 10GA-YU3, respectively (Figs 5, 11). In both cases, the duplication of mid-crustal arcuate reflection packages beneath the Cundimurra Granite suggests that they could be different expressions of the same structure. This hypothesis needs to be tested by three-dimensional modelling. In the upper crust, the three major syntectonic plutons described above share some important first-order geometric features. The seismic images show that these bodies are wedge-shaped and east-dipping. Moreover, pluton floors are rooted within the highly reflective mid-crust at about 5 s TWT. Each pluton has some specific features, which are described in the following.

Deep structure of the Yarraquin pluton

In the western part of the Yarraquin pluton, line 10GA-YU1 runs nearly perpendicular to the main structural grain while, farther east, it progressively rotates and runs at low angle (about 30°) to the main fabric, introducing some distortion in the imaged structures. In addition, some exposed, east-trending Proterozoic mafic sills generate strong, west-dipping reflections that overprint Archean structures (Fig. 5). Despite these complications, the Yarraquin pluton can be identified as a wedge-shaped body, rooted towards the east under the base of the Windimurra Igneous Complex. The geological map shows that this pluton pinches out immediately north of line 10GA-YU3. This suggests that, on line 10GA-YU3, the pluton has been imaged underneath the gabbroic complex (Fig. 11), which is consistent with what can be seen on line 10GA-YU1. The exposed Mingimnia and Fred folds are connected at depth with highly reflective packages so that these structures are imaged as synforms that close downward between 1 and 2 s TWT. In plan view, the Mingimnia Fold shows a double fold closure north and south of line 10GA-YU1. Consistent with field observations, this pattern suggests that this structure likely derives from a north-northeasterly trending fold superposed on an earlier east-trending fold.

The Yarraquin pluton is associated with four major, partially exposed shear zones, which are evident in

the aeromagnetic map and imaged in the seismic profile (Figs 2, 5). From west to east, they include the Tuckabianna, Mingimnia, Lake and Yarloo Shear Zones. The Tuckabianna Shear Zone corresponds to the western boundary of the pluton against the Tuckabianna Syncline. This contact is well exposed along the eastern side of the greenstone belt and has been interpreted as a sheared intrusive contact reflecting amphibolite-facies thrusting of the Yarraquin pluton over the Tuckabianna Syncline (Zibra et al., 2012). In this area, the Tuckabianna Syncline has an east-dipping axial plane, which closes downward at about 2 s TWT (Fig. 5). The Mingimnia Shear Zone flanks the western limb of the Mingimnia Fold. The seismic image shows that this is a deep structure with listric geometry, which merges into the Tuckabianna Shear Zone at about 2 s TWT (Fig. 5). The Lake Shear Zone flanks the eastern limb of the Mingimnia Fold (at about CDP 13800) and merges into the Mingimnia Shear Zone about 25 km north of the seismic line (Fig. 2). It is well imaged in the upper crust, but is hard to see below about 2 s TWT, mainly because of the strong reflections associated with the Proterozoic sills (Fig. 5). It is likely, however, that the Lake Shear Zone merges into the Mingimnia Shear Zone near CDP 14500, at about 4 s TWT, within the highly reflective middle crust. Map (Fig. 2) and field observations suggest that these three shear zones are truncated by discordant post-tectonic plutons, which, although still undated, are tentatively assigned to the c. 2640–260 Ma Bald Rock Supersuite. The easternmost Yarloo Shear Zone flanks the western side of the Fred area greenstones and the western side of the Windimurra Igneous Complex, where it is truncated by the Cundimurra Shear Zone (Figs 1, 2). The seismic profile indicates that the Yarloo Shear Zone developed along the roof of the Yarraquin pluton and likely represents the sheared intrusive contact against the base of the Windimurra Igneous Complex, as can be seen in both lines 10GA-YU1 and 10GA-YU3.

Deep structure of the Lakeside pluton and associated structures between Cue and the Weld Range

Like the Yarraquin pluton, the Lakeside Granite is intersected by both lines 10GA-YU1 and 10GA-YU3. However, line 10GA-YU3 only clips the eastern margin of the pluton (Figs 1, 11). The exposed Wattle Creek Shear Zone developed along the boundary between the wedge-shaped and east-rooted Mount Magnet greenstone belt and the Lakeside Granite (Zibra, 2012). This large-scale structure is imaged well in line 10GA-YU3 (Fig. 11), and may also be seen in the deep-crustal portion of line 10GA-YU2. It can be interpreted as a dextral transpressional, synmagmatic shear zone which accommodated the emplacement of the Lakeside Granite (Zibra, 2012). The solid-state component of the Wattle Creek Shear Zone (Zibra, 2012) can be seen as a local transtensional shear zone, which developed in its hangingwall during the final stage of pluton emplacement. The emplacement age of the Lakeside Granite (c. 2700 Ma) provides the minimum age for this pluton-related structure. The Wattle Creek Shear Zone is

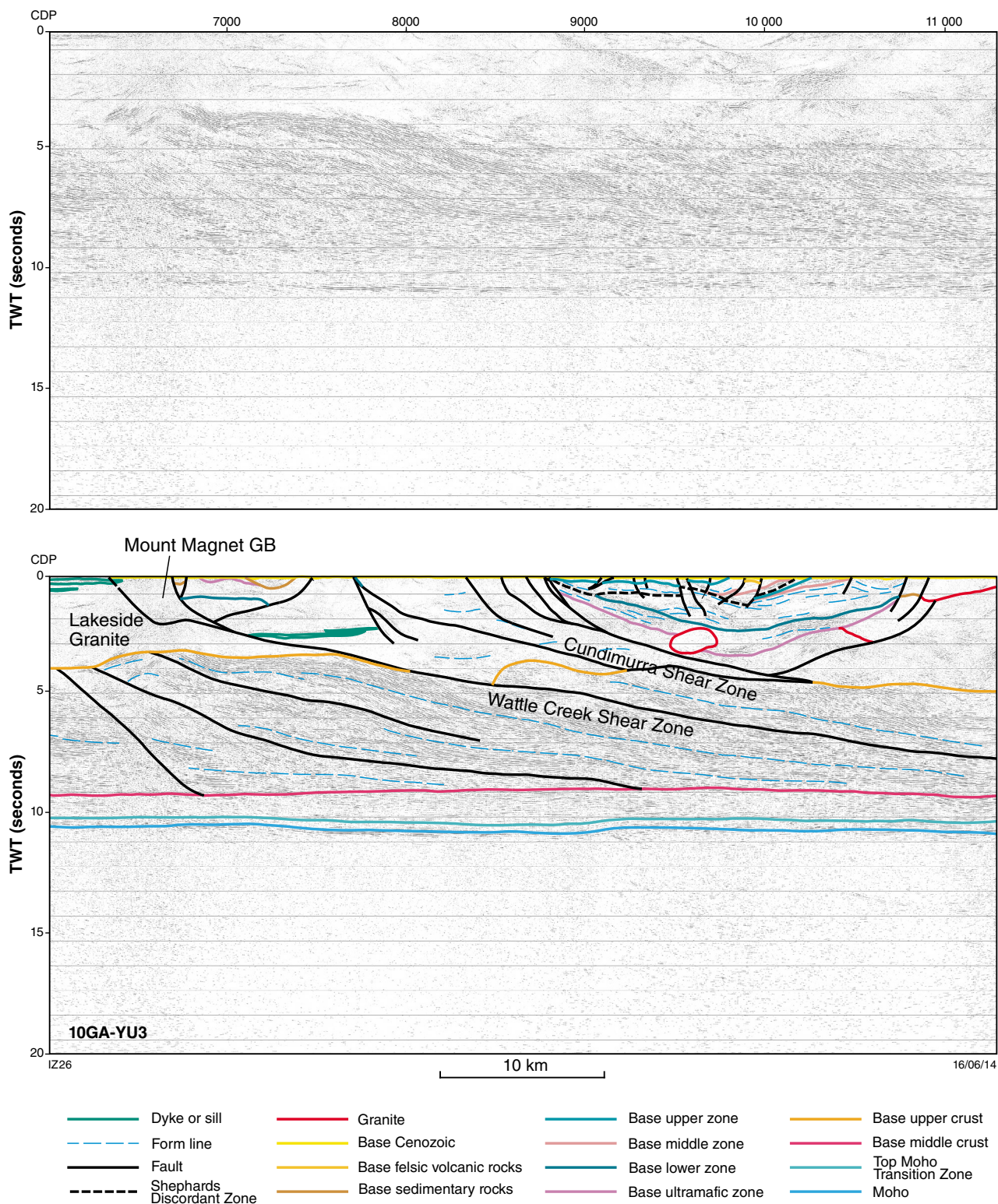


Figure 11. Migrated seismic section for the seismic line 10GA-YU3 between the Lakeside Granite and the eastern edge of the Windimurra Igneous Complex, showing both uninterpreted and interpreted versions

also visible on line 10GA-YU1 (Plate 3), where it appears truncated by a network of west-dipping, anastomosing structures. These younger, upper crustal shear zones reach the surface between Big Bell and Cue (Fig. 5, between CDPs 11000 and 11700 on line 10GA-YU1) and therefore likely control the geometry of the highly mineralized Cue region.

Between about CDP 10000 and 11000, line 10GA-YU1 runs parallel to the eastern limb of the Big Bell antiform, thus presenting a distorted image of this structure (Fig. 5). The network of west-dipping reflections flanking the western limb of the Big Bell antiform could correspond to the Carbar Shear Zone, interpreted as a west-dipping thrust, and the Chunderloo Shear Zone (Fig. 2 in Spaggiari, 2006). The c. 2660 Ma emplacement age of the Chunderloo pluton (Van Kranendonk et al., 2013) provides the maximum age of this west-dipping shear zone. Farther west, the seismic image indicates that the Weld Range lies in the hangingwall of another west-dipping structure, which reaches the surface near CDP 8750, corresponding to the western limb of the Coodardy antiform (Fig. 5). The seismic profile also shows that the Carbar/Chunderloo Shear Zone juxtaposes two antiforms, suggesting that this structure originated within the synform that linked the Big Bell and the Coodardy antiforms.

Deep structure of the Cundimurra Monzogranite

The Cundimurra pluton and the associated shear zone are well imaged in seismic lines 10GA-YU1 and 10GA-YU3 (Figs 5, 11). Line 10GA-YU1 intersects the pluton along its northernmost and narrowest portion (at about CDP 12500), where it is truncated by the Garden Rock Monzogranite (Figs 1, 5). In this area, primary magmatic structures are nearly completely transposed by the greenschist-facies, solid-state overprint associated with the latest activity on the dextral transpressional Cundimurra Shear Zone (Zibra et al., 2014a,b). The pervasive gneissic foliation transposing primary internal lithology contacts likely enhanced pluton reflectivity. Therefore, the Cundimurra pluton is readily imaged along line 10GA-YU1 as a narrow, wedge-shaped body emplaced at the base of the Tuckabianna Syncline (Fig. 5), truncated at depth by the east-dipping Cundimurra Shear Zone. This structure has listric geometry and can be followed down to about 5 s TWT, where it is rooted within the highly reflective middle crust. This portion of 10GA-YU1 also shows that the Garden Rock Monzogranite can be interpreted as a relatively thin sill, floored at about 1 s TWT depth and clearly transecting the local structures (Fig. 5).

Line 10GA-YU3 intersects the Cundimurra pluton 20 km east of Mount Magnet (at about CDP 7750–8750), immediately west of the Windimurra Igneous Complex. In this area, the pluton is about 15 km wide and primary magmatic structures are preserved within anastomosing, high- to medium-temperature, solid-state shear zones (Zibra et al., 2014a,b). This set of superposed structures is well imaged in line 10GA-YU3, where high-strain zones can be seen as east-dipping listric structures rooted

beneath the Windimurra Igneous Complex between the Yarraquin pluton and the highly reflective middle crust. These shear zones truncate, fold and displace older reflections that likely represent (emplacement-related) internal pluton contacts and compositional layering.

Conclusions

1. The three main large-scale syntectonic plutons intersected by seismic lines 10GA-YU1 and 10GA-YU3 are linked to important, crustal-scale, east-dipping shear zones.
2. The minimum age of the east-dipping structures is c. 2700 Ma, corresponding to the age of the Yarraquin pluton and Lakeside Granite.
3. Local west-dipping structures observed along line 10GA-YU1 are restricted to the uppermost 3–5 s TWT, where they postdate the east-dipping shear zones.
4. A maximum age of c. 2660 Ma (emplacement age of the Chunderloo Monzogranite) is proposed for the development of the west-dipping structures in the Cue – Weld Range area.
5. The different seismic patterns shown by the Cundimurra Monzogranite along the two seismic lines perfectly matches field and microstructural observations, and reflect a multistage structural evolution developed during pluton emplacement and subsequent syndeformational cooling.

References

- Chen, SF, Libby, JW, Greenfield, JE, Wyche, S and Riganti, A 2001, Geometry and kinematics of large arcuate structures formed by impingement of rigid granitoids into greenstone belts during progressive shortening: *Geology*, v. 29, p. 283–286.
- Fossen, H and Tikoff, B 1998, Extended models of transpression and transtension, and application to tectonic settings, *in* Continental Transpressional and Transtensional Tectonics *edited by* RE Holdsworth, RA Strachan and JE Dewey: Geological Society, London, Special Publication 135, p. 15–33.
- Ivanic, TJ, Korsch, RJ, Wyche, S, Jones, LEA, Zibra, I, Blewett, RS, Jones, T, Milligan, PR, Costelloe, RD, Van Kranendonk, MJ, Doublier, MP, Hall, CE, Romano, SS, Pawley, MJ, Gessner, K, Patison, N, Kennett, BLN and Chen, SF 2013, Preliminary interpretation of the 2010 Youanmi deep seismic reflection lines and magnetotelluric data for the Windimurra Igneous Complex, *in* Youanmi and Southern Carnarvon seismic and magnetotelluric (MT) workshop 2013 *compiled by* S Wyche, TJ Ivanic and I Zibra: Geological Survey of Western Australia, Record 2013/6, p. 97–111.
- Schiøtte, L and Campbell, IH 1996, Chronology of Mount Magnet granite–greenstone terrain, Yilgarn Craton, Western Australia: implications for field based predictions of the relative timing of granitoid emplacement: *Precambrian Research*, v. 78, p. 237–260.
- Spaggiari, CV 2006, Interpreted bedrock geology of the northern Murchison Domain, Youanmi Terrane, Yilgarn Craton: Geological Survey of Western Australia, Record 2006/10, 19p.
- Van der Velden, AJ, Cook, FA, Drummond, BJ and Goleby, BR 2006, Reflections of the Neoproterozoic: A global perspective: *AGU Geophysical Monograph* 164, p. 255–265.

- Van Kranendonk, MJ, Ivanic, TJ, Wingate, MTD, Kirkland, CL and Wyche, S, 2013, Long-lived, autochthonous development of the Archean Murchison Domain, and implications for Yilgarn Craton tectonics: *Precambrian Research*, v. 229, p 49–92.
- Wang, Q 1998, Geochronology of the granite–greenstone terranes in the Murchison and Southern Cross Provinces of the Yilgarn Craton, Western Australia: Australian National University, Canberra, PhD thesis (unpublished), 186p.
- Wang, LG, McNaughton, NJ and Groves, DI 1995, New geochronological data for granitoid intrusions in the Reedy's area, Murchison Province, Western Australia: constraints on genesis of gold mineralization, *in* Australian Conference on Geochronology and Isotope Geoscience, Perth, Western Australia, Workshop Programme and Abstract, p. 37.
- Wyche, S, Pawley, MJ, Chen, SF, Ivanic, TJ, Zibra, I, Van Kranendonk, MJ, Spaggiari, CV and Wingate MTD 2013, Geology of the northern Yilgarn Craton, *in* Youanmi and Southern Carnarvon seismic and magnetotelluric (MT) workshop 2013 *compiled by* S Wyche, TJ Ivanic and I Zibra: Geological Survey of Western Australia, Record 2013/6, p. 33–63.
- Zibra, I 2012, Syndeformational granite crystallisation along the Mount Magnet greenstone belt, Yilgarn Craton: evidence of large-scale magma-driven strain localisation during Neoproterozoic time: *Australian Journal of Earth Sciences*, v. 59, p. 793–806.
- Zibra, I, Kruhl, JH, Montanini, A, Tribuzio, R 2012, Shearing of magma along a high-grade shear zone: evolution of microstructures during the transition from magmatic to solid-state flow: *Journal of Structural Geology*, v. 37, p. 150–160.
- Zibra, I, Pawley, MJ and Wyche, S 2014a, Linking grain-scale to crustal-scale structures along the Youanmi seismic line: Geological Survey of Western Australia, Record 2014/8, 34p.
- Zibra, I, Smithies, RH, Wingate, MTD and Kirkland, CL 2014b, Incremental pluton emplacement during inclined transpression: *Tectonophysics*, v. 623, p. 100–122.

Preliminary interpretation of the northern section of deep seismic line 10GA-YU1: Narryer Terrane to Murchison Domain of the Youanmi Terrane

by

SS Romano, TJ Ivanic, RJ Korsch¹, S Wyche, MJ Van Kranendonk³, LEA Jones², I Zibra, RS Blewett¹, T Jones¹, P Milligan¹, RD Costelloe¹, MP Doublier, MJ Pawley⁴, K Gessner, CE Hall, N Patison, BLN Kennett⁵, and SF Chen

Introduction

In this chapter, we describe the seismic character of the northern part of deep seismic line 10GA-YU1 (Fig. 1), which starts in the northwest in the Narryer Terrane and crosses into the Murchison Domain of the Youanmi Terrane. We present an initial interpretation of the results, taking into account existing knowledge of the geology, geochronology and geochemistry, as determined from previous surface observations and analysis. The southern section of this line (CDP >10000) is described by Zibra et al. (2013a, this volume), in parallel with parts of seismic line 10GA-YU3, which intersects units along strike from those in the southern section of 10GA-YU1. Ivanic et al. (2013a, this volume) covers the interpretation of the Windimurra Igneous Complex and surrounding rocks on seismic line 10GA-YU1 from CDP 15000 to 16497, and lines 10GA-YU2 and 10GA-YU3.

The Moho

The Moho is interpreted to occur at the base of a moderately reflective package, below which the nonreflective material is considered to represent the upper mantle (Fig. 2). The interpreted Moho is relatively continuous at a depth of about 10 s two-way travel time (TWT) (about 30 km) (Plates 1, 3). In the seismic section, the Moho varies in seismic reflectivity from a moderately reflective crust–mantle transition zone about 0.3–0.6 s TWT thick (about 1–2 km), to generally poor reflectivity, particularly in the central

part of the seismic section. A strongly reflective crust–mantle transition zone is a persistent feature across most of the Youanmi seismic lines

Crustal terranes and seismic provinces

On the basis of seismic character and the presence of discrete, crustal-scale structures, the basement in section 10GA-YU1 has been divided into two terranes and one seismic province — the Narryer Terrane, the Murchison Domain of the Youanmi Terrane, and the Yarraquin Seismic Province.

Narryer Terrane

The Narryer Terrane is exposed to the north of the Yalgarr Fault (CDP 3100), and is interpreted to extend westwards, in the subsurface beneath the Southern Carnarvon Basin, to the Darling Fault System (Plate 2), which is imaged in deep seismic line 11GA-SC1 (Korsch et al., 2013a, this volume). In the west, the Narryer Terrane lies above the Yarraquin Seismic Province, down to a crustal level of about 6 s TWT (18 km). The Narryer Terrane is moderately to weakly reflective, and is dominated by reflections with an apparent dip to the west in the 11GA-SC1 line. Forward modelling of the gravity data indicates that the crust of the Narryer Terrane is denser than the crust below the Murchison Domain (Gessner et al., 2013, this volume). Surface mapping by Myers (1997) indicates that structures in the Narryer Terrane in the vicinity of the seismic line strike either to the northeast or east-northeast. The Narryer Terrane is interpreted to have been thrust southeastwards over the Yarraquin Seismic Province and the Murchison Domain along the Yalgarr Fault.

Between CDPs 2000 and 2819, the seismic section crosses a mix of migmatite and granitic gneiss (Plate 1). These include slivers of metamorphosed greenstones, such as amphibolite, banded iron-formation, and ultramafic rocks (Elias, 1982), between CDPs 2430–2640.

-
- 1 Minerals and Natural Hazards Division, Geoscience Australia, GPO Box 378, Canberra ACT 2601
 - 2 School of Biological, Earth and Environmental Sciences, University of New South Wales, Sydney NSW 2052
 - 3 Energy Division, Geoscience Australia, GPO Box 378, Canberra ACT 2601
 - 4 Geological Survey of South Australia, Department of Manufacturing Innovation Trade Resources and Energy, Level 4, 101 Grenfell Street, Adelaide, SA 5000 Australia
 - 5 Research School of Earth Sciences, The Australian National University, Canberra ACT 0200

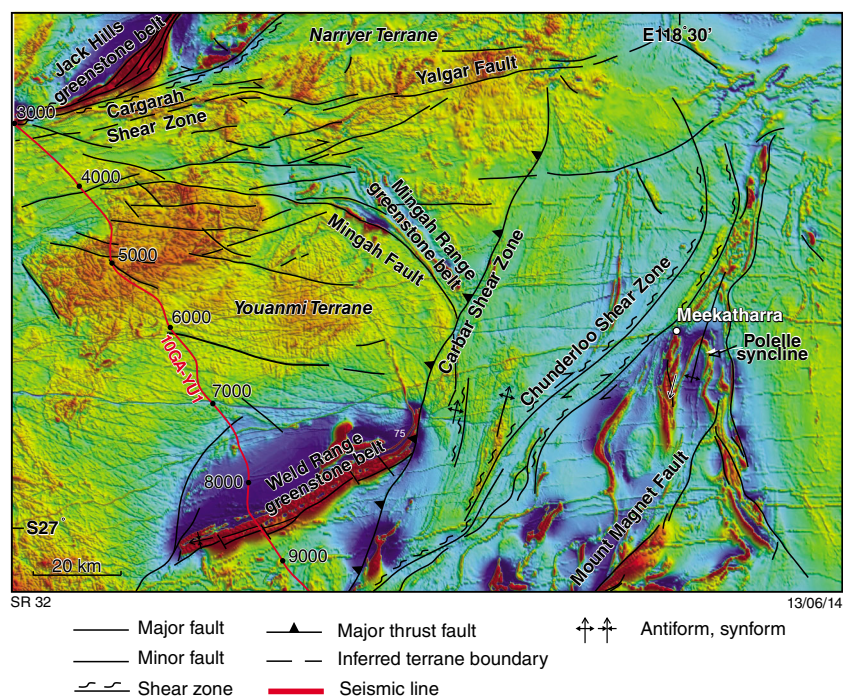


Figure 1. Aeromagnetic image (total magnetic intensity, reduced to pole) showing main structures in the vicinity of the northern end of 10GA-YU1 (modified from Spaggiari, 2006)

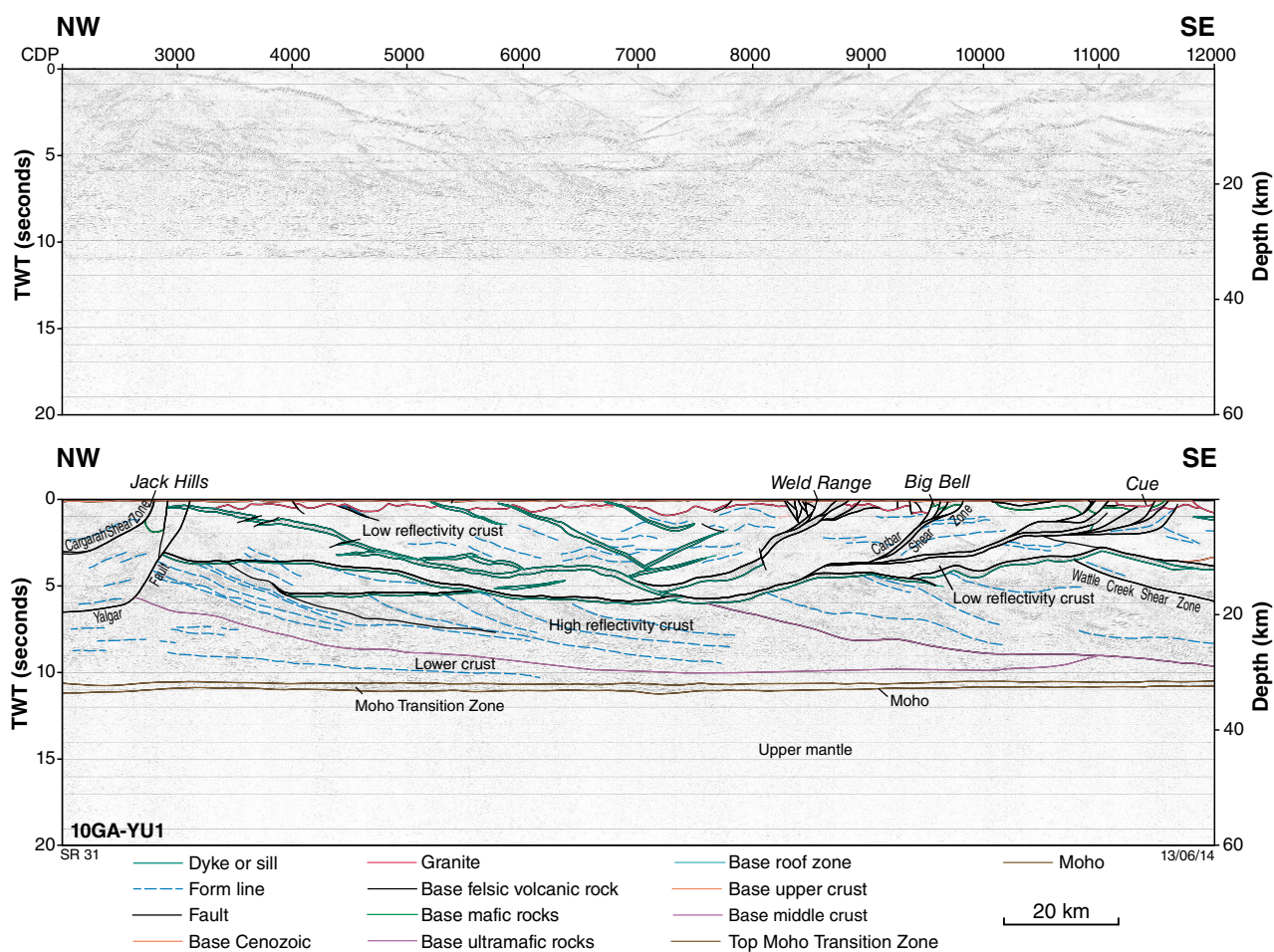


Figure 2. Migrated seismic section for the northern end of seismic line 10GA-YU1, from the beginning of the line to just south of Cue, showing both uninterpreted and interpreted versions

Southeast of the Jack Hills greenstone belt (CDPs 2980–3100), the granitic gneiss and migmatite contain evidence of Archean magmatism and metamorphism

Yarraquin Seismic Province

The lower crustal reflective package is named the Yarraquin Seismic Province (Korsch et al., 2013b, this volume) and forms the lower crust to the entire Youanmi Terrane, from the Yalgar Fault in the west to the Ida Fault in the east (Zibra et al., 2013a,b, this volume), and the Narryer Terrane. As rocks of the Yarraquin Seismic Province have not been identified at the surface, there are no direct constraints on their lithology or age.

At the eastern end of the Southern Carnarvon seismic line, 11GA-SC1, the Yarraquin Seismic Province is highly reflective and its upper, subhorizontal surface is interpreted to be the Yalgar Fault (Myers, 1990), based on a tie from this seismic section (Korsch et al., 2013a, this volume).

East of the Yalgar Fault on line 10GA-YU1, the Yarraquin Seismic Province can be subdivided into a deeper, more reflective zone, roughly at a lower crustal level (below 6 s TWT, about 18 km), and a shallower, less reflective zone, roughly at a lower to mid crustal level (3–6 s TWT, about 9–18 km).

Combining lines 11GA-SC1 and 10GA-YU1 indicates that the Narryer Terrane was thrust over the Murchison Domain, thereby exhuming a deeper crustal level, potentially along structures which later were active during the Proterozoic. However, rocks beneath the Narryer Terrane are comparable in seismic character to those which underlie the Murchison Domain. The interpreted continuity of a seismic province below the southeastern Narryer Terrane and Murchison Domain is supported by recently acquired Lu–Hf data from the Murchison Domain, which indicate widespread sampling of ancient, Narryer Terrane-aged crust by Neoproterozoic granites (Ivanic et al., 2012).

Jack Hills greenstone belt

The Jack Hills greenstone belt is a narrow, 70 km long, northeasterly trending, curvilinear belt, imaged in seismic line 10GA-YU1 between CDPs 2820 and 2980. The greenstone belt is defined by an area with low seismic reflectivity. It has a concave contact with the underlying crust in the Narryer Terrane, at a depth of about 2 s TWT (about 6 km).

The greenstone belt contains chert and banded iron-formation, as well as rare mafic–ultramafic rocks, interleaved with, and overlain by, metasedimentary rocks, some of which are Proterozoic in age (Spaggiari et al., 2007). Both the sedimentary rocks on the northwestern side of the greenstone belt and the mafic–ultramafic rocks on the southeastern side, have a weak reflectivity response in the seismic profile. In the gravity forward model (Gessner et al., 2013, this volume), the greenstone belt is marked by

change of gravity properties on the northwestern side that are related to a thick sedimentary package. The greenstone belt has undergone a long history of deformation and metamorphism, from c. 3300 to 1075 Ma, including late dextral transpressional shearing along the Proterozoic Cargarah Shear Zone (Spaggiari et al., 2008).

Cargarah Shear Zone

The Cargarah Shear Zone (Spaggiari et al., 2007, 2008) has a dextral sigmoidal geometry, and significant dextral transpressional shearing is interpreted to have taken place during the Capricorn Orogeny (c. 1830–1780 Ma; Spaggiari, 2007, Spaggiari et al., 2008).

On seismic line 10GA-YU1, the Cargarah Shear Zone is interpreted as a major structure within the Narryer Terrane, just to the northwest of the Yalgar Fault. It is an approximately 2 km-wide, northerly dipping, listric shear zone, which is evident at the surface where it coincides with the Jack Hills greenstone belt between CDPs 2820 and 2980. In line 10GA-YU1, it can be traced down to 3.6 s TWT (about 11 km), and can also be seen in the Southern Carnarvon seismic section (11GA-SC1). There it has been interpreted to sole onto the Yalgar Fault at about CDP 3800 (Korsch et al., 2013a, this volume).

A minor, steeply dipping fault at CDP 2900, south of the Cargarah Shear Zone, is imaged as a splay structure of the Yalgar Fault, rooting into it at about 4 s TWT (about 12 km).

Terrane-bounding structures

Yalgar Fault

The easterly trending, steeply north-dipping listric Yalgar Fault (CDP 3100; Myers, 1990) marks the boundary between the Murchison Domain of the Youanmi Terrane and the Narryer Terrane (Plate 3). Moreover, it offsets the underlying lower crust of the Yarraquin Seismic Province beneath the Narryer Terrane and the middle crust of the Yarraquin Seismic Province underneath the Murchison Domain. In this seismic section, the middle crust of the Yarraquin Seismic Province appears to be missing beneath the Narryer Terrane.

At a depth of about 21 km, the Yalgar Fault flattens significantly. The overall crustal-scale structure can be described as a west-northwesterly dipping ramp structure, which reaches the Moho in the Southern Carnarvon line (11GA-SC1), and cuts the 10GA-YU1 seismic line at about 7 s TWT (about 21 km). At about CDP 2800, the ramp steepens. The steep angle at the currently exposed segment of the ramp is most likely due to a late, secondary reactivation of the structure. The surface expression of the Yalgar Fault is interpreted as a series of younger (Proterozoic), reworked, post-amalgamation structures, possibly controlled by the ancestral Yalgar Fault (Spaggiari et al., 2008).

Murchison Domain of the Youanmi Terrane

Large-scale crustal features

The crust east of the Yalgar Fault can be subdivided vertically. The lower and middle crust in this seismic line are different in seismic character from the upper crust of the Murchison Domain and the Narryer Terrane, and are therefore assigned to the Yarraquin Seismic Province (Korsch et al., 2013b, this volume). Beneath the upper crust of the Murchison Domain, the Yarraquin Seismic Province can be subdivided into moderately reflective lower crust containing horizontal to southeast-dipping reflections, and highly reflective middle crust marked by strong southeast-dipping reflections (Fig. 2). These reflections are decoupled from structures and reflections in the upper crust, and are subparallel to the listric, east-dipping, crustal-scale shear zones that sole into the lower crust.

The upper crust in the Murchison Domain is only moderately reflective. Reflections interpreted as shear zones and sills are subparallel to the major structural grain north of Big Bell (about CDP 11000). The deepest extent of the Murchison Domain is at CDP 7180, where it is interpreted to reach a depth of about 7 s TWT (about 21 km).

Yalgar Fault to Weld Range (CDPs 3100–8264)

Granite and gneiss immediately south of the Yalgar Fault are assigned to the Murchison Domain of the Youanmi Terrane. From CDP 3100 to CDP 4000, however, granite and minor granitic gneiss have not been subdivided further. North of Weld Range, an extensive area of monzogranite belongs to the Bald Rock Supersuite (Ivanic, 2009). Most of these granitic rocks are deeply weathered. They are interpreted in the seismic section from CDP 4000 to CDP 8264 as nonreflective monzogranite of the Walganna Suite, part of the Bald Rock Supersuite (c. 2640–2600 Ma; Van Kranendonk et al., 2013). These granitic rocks have a flat-lying fabric, and are interpreted to form a sheet-like intrusion underlain by undifferentiated felsic crust.

Greenstone succession from Weld Range to Big Bell (CDPs 8246–11000)

The granitic rocks cropping out to the north of the Weld Range are interpreted to intrude into the base of the Weld Range greenstone stratigraphy, the westernmost supracrustal rocks of the Murchison Supergroup to be intersected along this line. Off the section in this area, approximately 10 km to the east-northeast, is the large, layered mafic–ultramafic intrusive base to the

Gnanagooragoo Igneous Complex. However, this feature is not interpreted along the line of section and only the upper zone of the complex (see Fig. 3 in Ivanic et al., 2013a, this volume) is extensive enough to be intersected by 10GA-YU1. Approximately 6 km to the west, the Kalli volcanic succession is interpreted to be the base of the southward-younging succession in the Weld Range. Some of this material may have an age of c. 2960 Ma, based on detrital zircon ages (e.g. GSWA 193972, Wingate et al., 2012).

At the surface, along the seismic line from CDP 8264 to CDP 8430, the Weld Range succession begins in steeply dipping (approximately 70° S) felsic volcanic rocks and banded iron-formation of the Wilgie Mia Formation of the Polelle Group (with an across-strike extent of 3.5 km). This supracrustal succession is extensively intruded by dolerite of the Gnanagooragoo Igneous Complex (Plate 1). This region forms a wedge-shaped area of strong reflections down to approximately 2 s TWT (about 6 km depth), at which point they intersect what is interpreted to be a north-dipping Proterozoic dolerite sill and low-reflectivity crustal material of the Murchison Domain (Fig. 2).

At CDP 8430, the Wilgie Mia Formation is unconformably overlain by more shallowly dipping siliciclastic rocks of the Ryansville Formation of the Glen Group. Overall, the Glen Group is more shallowly dipping than the Polelle Group, and units of the basaltic Wattagee Formation are interpreted to underlie the Ryansville Formation with a contact dipping approximately 40° to the north.

Although not exposed along this part of the seismic section, the Meekatharra Formation of the Polelle Group is interpreted to underlie rocks of the Glen Group. The Glen Group rocks form a north-dipping wedge of strong reflections from about CDP 8700 to CDP 9000 at 1–2 s TWT (about 3–6 km depth). The overlying and cross-cutting metagranitic rocks of the Annean Supersuite are interpreted to form the apex of a large antiformal region.

Minor faults and other structures

Mingah Fault

The Mingah Fault bounds the southern part of the Mingah Range greenstone belt (Plate 1). It is an extensional fault and is likely to be part of a bigger scoop-like structural feature, which may include a dextral strike-slip component. In the vicinity of the Mingah Range, the fault dips moderately to the south and is itself truncated by the Carbar Shear Zone corridor on its southern extension.

The Mingah Fault is interpreted to intersect the 10GA-YU1 seismic line in two places (Fig. 3). In the north, it crosses the line at about CDP 4000 where it is interpreted to a depth of 0.8 s TWT (about 2.4 km), but might extend to a depth of 4 s TWT (about 12 km). It may develop a listric character which extends to the transition

of the upper crust to the Yarraquin Seismic Province. In the south, the Mingah Fault is interpreted to cross the seismic line near the northwestern boundary of the Carbar Shear Zone, at CDP 9300, near Big Bell, where it has been intruded by granite (Fig. 2).

In keeping with the the interpretation of the Mingah Fault as a large-scale, scoop-like structure, the general trend of greenstone belts changes along the fault. In the vicinity of the Mingah Range (Plate 1), greenstone belts trend to the west-northwest north of the fault, whereas in the south, they are north-northeasterly striking. To compensate for east–west compression, there was inferred dextral strike-slip movement along Carbar Shear Zone, which is part of a broader shear corridor west of Big Bell (CDP 9570–11 000).

Carbar Shear Zone

The Carbar Shear Zone is part of a broader corridor (CDP 9570–11000) with numerous splay faults east of the Weld Range and Mingah Range greenstone belts. Spaggiari (2006) interpreted the Carbar Shear Zone as a major, northwest-dipping thrust separating the Weld Range and Mingah Range greenstone belts from the Meekatharra structural zone. In the seismic profile, the Carbar Shear Zone appears as a northwest-dipping listric structure, with splay faults flooring at about 1.5 s TWT (about 4.5 km) near CDP 9500. The Carbar Shear Zone soles into the Chunderloo Shear Zone at CDP 9040 at a depth of 3.5 s TWT (about 10.5 km). This implies that the Carbar Shear Zone is a thrust slice related to a wider thrust corridor. In addition, it may have been locally reactivated with a dextral strike-slip component like the Chunderloo Shear Zone (Spaggiari, 2006).

Mafic sills

There is a very distinctive pattern of discrete, shallow-dipping, strong reflections between the surface and 5 s TWT (and possibly as deep as 6 s TWT) along most of line 10GA-YU1. The packages of reflections occupy up to 0.25 s TWT, but are typically 0.1s TWT, and are most abundant in the Youanmi Terrane from CDP 3100 to CDP 15650. They are interpreted to be a widespread, interconnected mafic sill network related to the c. 1075 Ma Warakurna Supersuite (Warakurna Large Igneous Province, Wingate et al., 2004; Ivanic et al., 2013b, this volume).

Some of the sills appear to have locally exploited existing shear zones. They follow existing west-dipping shear zones within the Coodardy Antiform and the Cue greenstone belt (Fig. 2). The root zone of this particular shear-intrusion pattern is at about CDP 7180 at a depth of about 6 s TWT (about 18 km). It appears that a northern branch of the sill network was slightly offset by the Yalgar Fault at a depth of about 0.4 s TWT (about 1.2 km), implying relatively young movement on the fault. A similar, flat-lying feature is imaged north of the Cargarah Shear Zone. If this is interpreted as a continuation of the sill, it implies an offset along these structures, and an older intrusion age for the sills. If this sill does indeed belong to the Warakurna Large Igneous Province, then the Yalgar Fault and the Cargarah Shear Zone may have been active after 1070 Ma. Alternatively, the continuation of the sill crossing the Jack Hills greenstone belt (CPDs 2820–2900) has not been imaged in the seismic section, due to alteration or lithology contrast, and the sill is continuous and post-tectonic, or intruding along already existing structures.

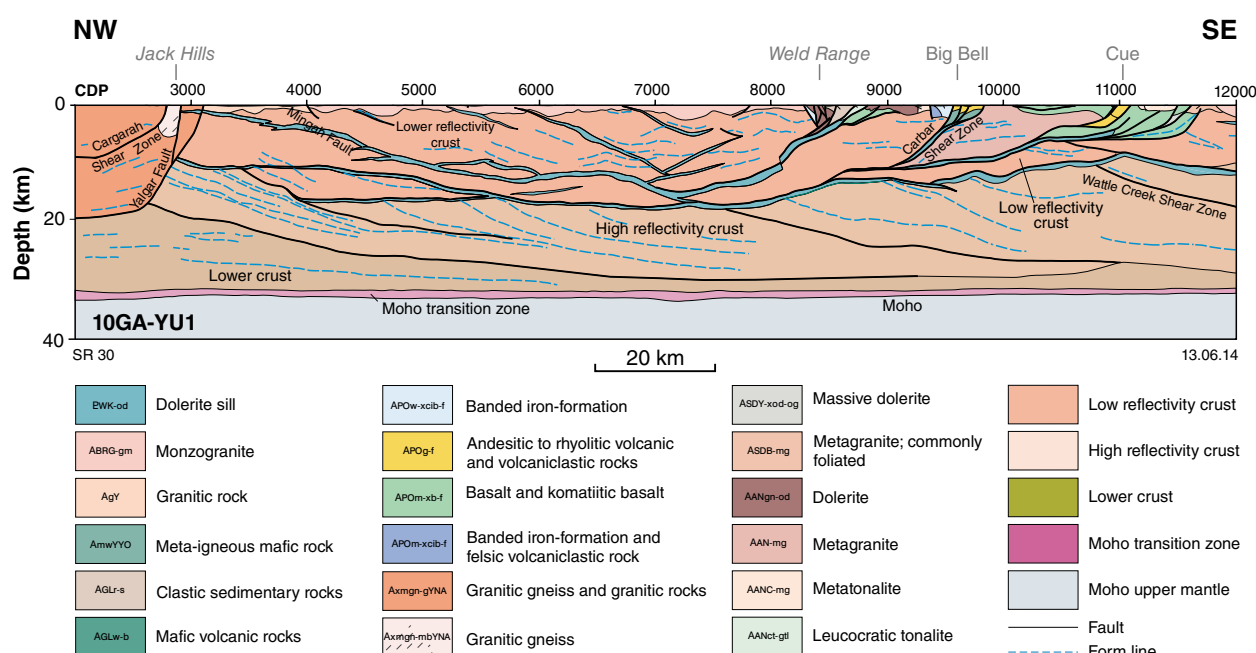


Figure 3. Interpreted geology for the northern end of seismic line 10GA-YU1, from the beginning of the line to just south of Cue

Minor flat-lying thrust faults within the sill network appear to offset several sills. These structures could be older than the sills, which may have exploited older zones of weakness or they could have formed during intrusion to create space.

Crustal architecture along 10GA-YU1

Seismic line 10GA-YU1 transects a geologically complex area with a long structural history of over two billion years, and images the contact between the Narryer Terrane and the Youanmi Terrane.

Terrane boundaries and suture zones

The Yalgir Fault is interpreted to mark the boundary between the Narryer Terrane and the Youanmi Terrane. Seismic cross sections 10GA-YU1 and 11GA-SC1 show its depth extent and trace, and that it offsets the Narryer Terrane and the underlying Yarraquin Seismic Province. The deep-crustal 3D geometry displays crustal-scale ramp architecture for this structure and southeasterly movement along it, in which the Narryer Terrane was thrust over the Youanmi Terrane. The steep section of the ramp is the current exposed boundary between the Narryer and Youanmi Terrane.

References

- Elias, M (compiler) 1982, Beale, Western Australia: Geological Survey of Western Australia, 1:250 000 Geological Series Explanatory Notes, 22p.
- Gessner, K, Jones, T, Goodwin, JA, Gallardo, LA, Milligan, PR, Brett, J and Murdie, R 2013, Interpretation of magnetic and gravity data across the South Carnarvon Basin, and the Narryer and Youanmi Terranes, *in* Youanmi and Southern Carnarvon seismic and magnetotelluric (MT) workshop 2013 *compiled by* S Wyche, TJ Ivanic and I Zibra: Geological Survey of Western Australia, Record 2013/6, p. 65–77.
- Ivanic, TJ 2009, Madoonga, WA Sheet 2444: Geological Survey of Western Australia, 1:100 000 Geological Series.
- Ivanic, TJ, Van Kranendonk, MJ, Kirkland, CL, Wyche, S, Wingate, MTD and Belousova, E 2012, Zircon Lu–Hf isotopes and granite geochemistry of the Murchison Domain of the Yilgarn Craton: evidence for reworking of Eocarchean crust during Meso–Neocarchean plume-driven magmatism: *Lithos*, v. 148, p. 112–127.
- Ivanic, TJ, Korsch, RJ, Wyche, S, Jones, LEA, Zibra, I, Blewett, RS, Jones, T, Milligan, PR, Costelloe, RD, Van Kranendonk, MJ, Doublier, MP, Hall, CE, Romano, SS, Pawley, MJ, Gessner, K, Patison, N, Kennett, BLN and Chen, SF 2013a, Preliminary interpretation of the 2010 Youanmi deep seismic reflection lines and magnetotelluric data for the Windimurra Igneous Complex, *in* Youanmi and Southern Carnarvon seismic and magnetotelluric (MT) workshop 2013 *compiled by* S Wyche, TJ Ivanic and I Zibra: Geological Survey of Western Australia, Record 2013/6, p. 97–111.
- Ivanic, TJ, Wingate, MTD, Korsch, RJ, Blewett, RS, Jones, LEA, Wyche, S, Zibra, I, Doublier, MP, Romano, SS, Pawley, MJ, Van Kranendonk, MJ, Gessner, K, Hall, CE, Chen, SF, Patison, NL and Costelloe, RD 2013b, Preliminary interpretation of the Youanmi deep seismic reflection lines for Proterozoic intrusive rocks, *in* Youanmi and Southern Carnarvon seismic and magnetotelluric (MT) workshop 2013 *compiled by* S Wyche, TJ Ivanic and I Zibra: Geological Survey of Western Australia, Record 2013/6, p. 81–85.
- Korsch, RJ, Doublier, MP, Romano, SS, Johnson, SP, Mory, AJ, Carr, LK, Zhan, Y and Blewett, RS 2013a, Geological interpretation of deep seismic reflection line 11GA-SC1: Narryer Terrane, Yilgarn Craton and Southern Carnarvon Basin, *in* Youanmi and Southern Carnarvon seismic and magnetotelluric (MT) workshop 2013 *compiled by* S Wyche, TJ Ivanic and I Zibra: Geological Survey of Western Australia, Record 2013/6, p. 129–145.
- Korsch, RJ, Blewett, RS, Wyche, S, Zibra, I, Ivanic, TJ, Doublier, MP, Romano, SS, Pawley, MJ, Johnson, SP, Van Kranendonk, MJ, Jones, LEA, Kositsin, N, Gessner, K, Hall, CE, Chen, SF, Patison, N, Kennett, BLN, Jones, T, Goodwin, JA, Milligan, PR and Costelloe, RD 2013b, Geodynamic implications of the Youanmi and Southern Carnarvon deep seismic reflection surveys: a ~1300 km traverse from the Pinjarra Orogen to the eastern Yilgarn Craton, *in* Youanmi and Southern Carnarvon seismic and magnetotelluric (MT) workshop 2013 *compiled by* S Wyche, TJ Ivanic and I Zibra: Geological Survey of Western Australia, Record 2013/6, p. 147–166.
- Myers, JS 1990, Yilgarn Craton — Western Gneiss Terrane, *in* *Geology and mineral resources of Western Australia*: Geological Survey of Western Australia, Memoir 3, p. 13–32.
- Myers, JS (compiler) 1997, Byro, WA Sheet SG50-10 (2nd edition): Geological Survey of Western Australia, 1:250 000 Geological Series.
- Spaggiari, CV 2006, Interpreted bedrock geology of the northern Murchison Domain, Youanmi Terrane, Yilgarn Craton: Geological Survey of Western Australia, Record 2006/10, 19p.
- Spaggiari, CV, Pidgeon, RT and Wilde, SA 2007, The Jack Hills greenstone belt, Western Australia — Part 2: Lithological relationships and implications for the deposition of >4.0 Ga detrital zircons: *Precambrian Research*, v. 155, p. 261–286.
- Spaggiari, CV, Wartho, J-A and Wilde, SA 2008, Proterozoic deformation in the northwest of the Archean Yilgarn Craton, Western Australia: *Precambrian Research*, v. 162, p. 354–384.
- Van Kranendonk, MJ, Ivanic, TJ, Wingate, MTD, Kirkland, CL and Wyche, S 2013, Long-lived, autochthonous development of the Archean Murchison Domain, and implications for Yilgarn Craton tectonics: *Precambrian Research*, v. 229, p. 49–92.
- Wingate, MTD, Kirkland, CL and Ivanic, TJ 2012, 193972: metarhyolite clast in volcanoclastic breccia, Weld Range; *Geochronology Record* 1011: Geological Survey of Western Australia, 4p.
- Wingate, MTD, Pirajno, F and Morris, PA 2004, Warakurna Large Igneous Province: a new Mesoproterozoic large igneous province in west-central Australia: *Geology*, v. 32, no. 2, p. 105–108.
- Zibra, I, Gessner, K, Korsch, RJ, Blewett, RS, Jones, T, Milligan, PR, Jones, LEA, Wyche, S, Doublier, MP, Hall, CE, Chen, SF, Romano, SS, Ivanic, TJ, Pawley, MJ, Patison, N, Kennett, BLN and Van Kranendonk, MJ 2013a, Preliminary interpretation of deep seismic lines 10GA-YU3 and the southeastern part of 10GA-YU1: Murchison Domain of the Youanmi Terrane, *in* Youanmi and Southern Carnarvon seismic and magnetotelluric (MT) workshop 2013 *compiled by* S Wyche, TJ Ivanic and I Zibra: Geological Survey of Western Australia, Record 2013/6, p. 113–122.
- Zibra, I, Gessner, K, Pawley, MJ, Wyche, S, Chen, SF, Korsch, RJ, Blewett, RS, Jones, T, Milligan, PR, Jones, LEA, Doublier, MP, Hall, CE, Romano, SS, Ivanic, TJ, Patison, N, Kennett, BLN and Van Kranendonk, MJ 2013b, Preliminary interpretation of deep seismic line 10GA-YU2: Youanmi Terrane and western Kalgoorlie Terrane, *in* Youanmi and Southern Carnarvon seismic and magnetotelluric (MT) workshop 2013 *compiled by* S Wyche, TJ Ivanic and I Zibra: Geological Survey of Western Australia, Record 2013/6, p. 87–95.

Geological interpretation of deep seismic reflection line 11GA-SC1: Narryer Terrane, Yilgarn Craton and Southern Carnarvon Basin

by

RJ Korsch¹, MP Doublier, SS Romano, SP Johnson, AJ Mory, LK Carr², Y Zhan, and RS Blewett¹

Introduction and aims of the seismic survey

As part of its Onshore Energy Security Program, Geoscience Australia in conjunction with the Geological Survey of Western Australia under its Exploration Incentive Scheme, acquired 259 line km of vibroseis-source, deep-seismic reflection data along a single east–west traverse through the Southern Carnarvon Basin. The transect, 11GA-SC1, referred to as the Southern Carnarvon seismic line, was acquired during May–June 2011 and extended from the Gascoyne Platform of the southern Carnarvon Basin at the North West Coastal Highway, through the Byro Sub-basin, to the Narryer Terrane of the northwest Yilgarn Craton (Frontispiece 1, Fig. 1) close to Milly Milly homestead in the east. Here, we report the results of an initial geological interpretation of the seismic data.

Near its eastern end, the Southern Carnarvon seismic line ties to the southern end of seismic line 10GA-CP3, part of the Capricorn seismic survey described by Johnson et al. (2011a). Initially, the aim of the survey was also to tie the Southern Carnarvon line to the northwestern end of line 10GA-YU1, part of the Youanmi seismic survey (Romano et al., 2013, this volume; Zibra et al., 2013, this volume), but wet conditions at the start of acquisition made the proposed easternmost point inaccessible, resulting in a gap of about 28 km between the eastern end of line 11GA-SC1 and the northwestern end of line 10GA-YU1 (Frontispiece 1, Fig. 1).

The Southern Carnarvon seismic line was designed, in part, to evaluate:

- the architecture of the Southern Carnarvon Basin and, in particular, the Byro Sub-basin
- the potential of the Byro Sub-basin for structural and stratigraphic hydrocarbon traps, including the effects of the Late Ordovician to Carboniferous

(450–300 Ma) Alice Springs Orogeny, and younger extensional events

- the architecture and deep structure of the Archean Narryer Terrane, in the northwest Yilgarn Craton, which is the oldest terrane in the craton, and the region which contains the oldest known crust in Australia
- the relationship, in the subsurface beneath the Southern Carnarvon Basin, between the Archean Narryer Terrane, the Archean to Proterozoic Glenburgh Terrane of the Gascoyne Province, and the Mesoproterozoic to Neoproterozoic Pinjarra Orogen.

Seismic acquisition and processing

The seismic reflection data along line 11GA-SC1 were acquired in 2011, with project management undertaken by the Seismic Acquisition and Processing Section from Geoscience Australia. For the seismic line, 75-fold seismic reflection data were acquired to 20 s two-way travel time (TWT), providing an image of the crust and upper mantle to a depth of about 60 km (Fig. 2). Details of the acquisition and processing techniques are provided in Costelloe et al. (2013, this volume). Depth estimates provided here were calculated assuming an average crustal velocity of 6000 ms⁻¹, so that 1 s TWT is approximately equal to 3 km depth, with the exception of sedimentary rocks in the Southern Carnarvon basin, where we assume velocities of 4000–5000 ms⁻¹.

Geological setting

Seismic line 11GA-SC1 transects a geologically complex area which represents a triple junction between three major basement blocks, the Glenburgh Terrane, the Narryer Terrane and the Pinjarra Orogen (Frontispiece 1). Although these tectonic units are poorly exposed along the transect or only occur in the subsurface, elsewhere they have been shown to have a long and complex tectonometamorphic and magmatic history spanning more than two billion years.

¹ Minerals and Natural Hazards Division, Geoscience Australia, GPO Box 378, Canberra, ACT 2601

² Energy Division, Geoscience Australia, GPO Box 378, Canberra, ACT 2601

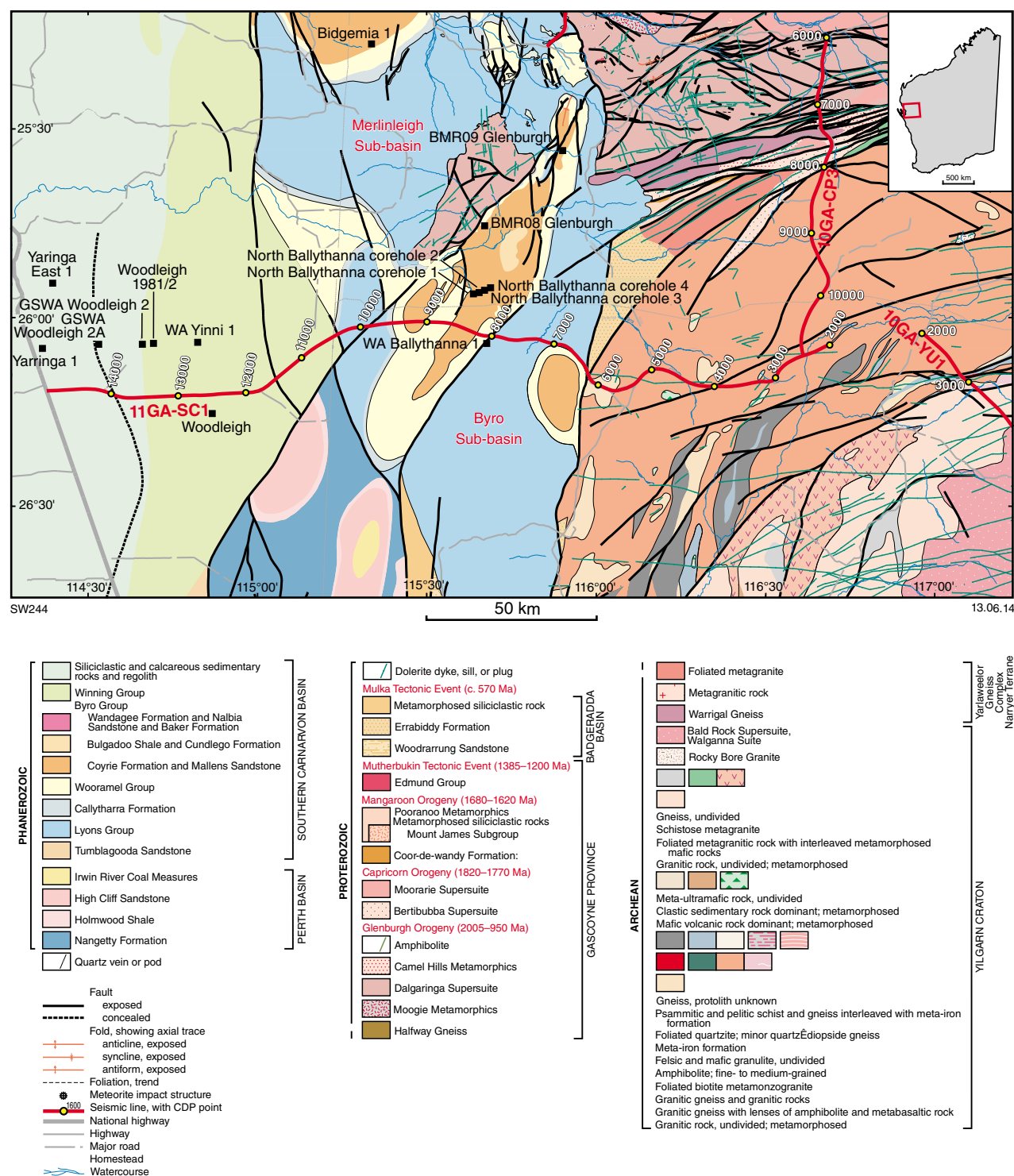


Figure 1. Solid geology map of the Southern Carnarvon basin and surrounding regions, showing the location of the Southern Carnarvon line 11GA-SC1, along with Capricorn seismic line 10GA-CP3 and the southern part of Capricorn seismic line 10GA-CP2, and the northwestern part of Youanmi seismic line 10GA-YU1.

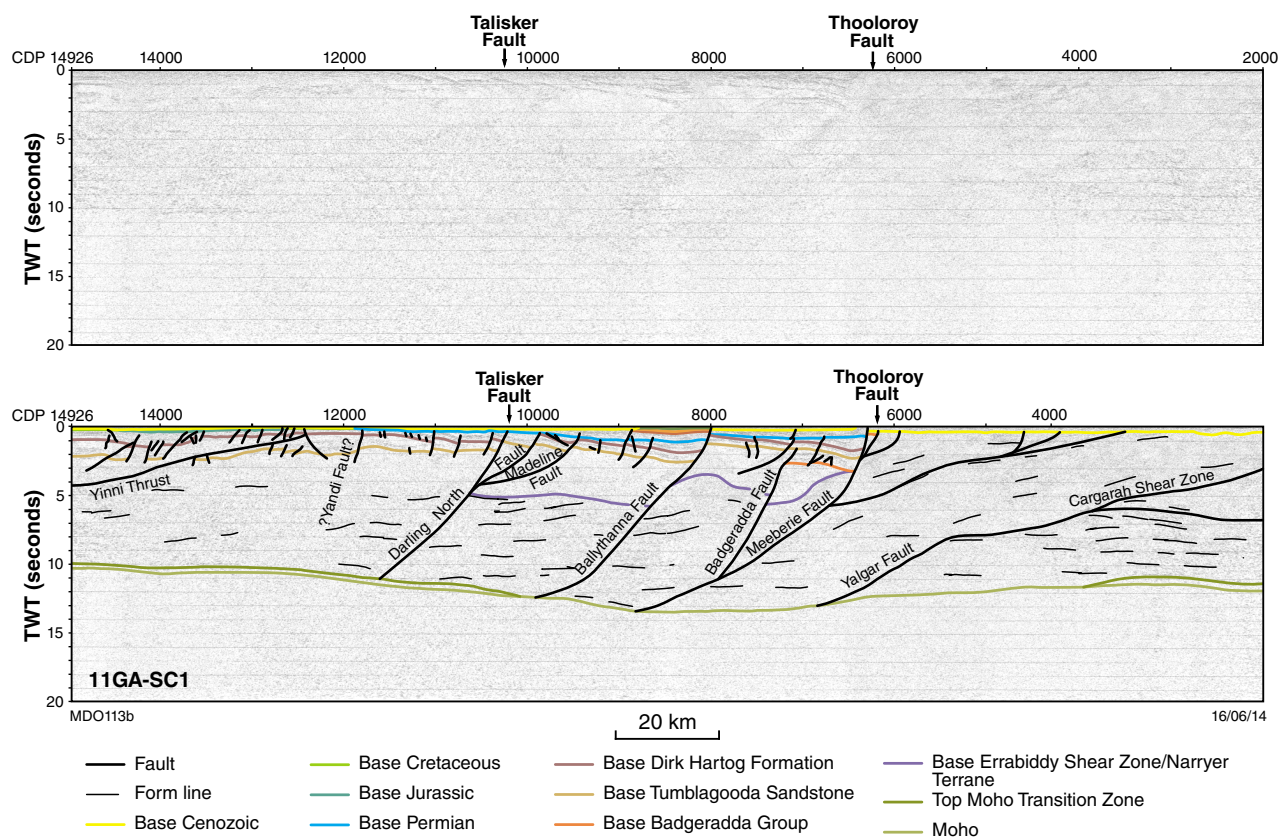


Figure 2. Migrated section for seismic line 11GA-SC1, showing both uninterpreted and interpreted versions. Display is to 60 km depth, and shows vertical scale equal to the horizontal scale, assuming a crustal velocity of 6000 ms⁻¹.

Narryer Terrane, Yilgarn Craton

The geology of the Archean Narryer Terrane is described in the contribution by Wyche et al. (2013, this volume).

Glenburgh Terrane

The Glenburgh Terrane consists of: 1) a basement of heterogeneous granitic gneisses (the Halfway Gneiss) with ages between c. 2555 and 2430 Ma; 2) an overlying package of continent-derived siliciclastic metasedimentary rocks (the c. 2240–2125 Ma Moogie Metamorphics); 3) a c. 2000 Ma belt of metagranitic rocks (the Dalgaringa Supersuite), which are interpreted to have formed in a continental-margin volcanic arc; and 4) arc-related metasedimentary rocks (the c. 2000–1955 Ma Camel Hills Metamorphics), which are in tectonic contact with both the arc rocks and the deformed northern margin of the Yilgarn Craton.

The oldest tectonic unit, the Halfway Gneiss, consists of heterogeneous, variably pegmatite-banded, granitic gneisses. The protoliths have crystallization ages between c. 2555 and 2430 Ma, but also contain abundant older inherited zircons, some of which are as old as c. 3447 Ma (Johnson et al., 2011c). Although no older crust (>2555 Ma) is exposed, the Lu–Hf compositions and crustal model ages of both magmatic and inherited

zircons indicate a long crustal history ranging back to c. 3700 Ma (Johnson et al., 2011b). These isotopic data also demonstrate that large parts of the terrane, presumably representing the middle and lower crust (none of these rocks are currently exposed), formed via juvenile crustal growth processes between c. 2730 and 2600 Ma. Formation of the c. 2555–2430 Ma gneisses occurred mainly by the in situ reworking of these older crustal components. A comparison of the U–Pb zircon ages and zircon–Hf isotopic compositions of the Halfway Gneiss with those of the bounding Pilbara and Yilgarn Cratons indicates that the Halfway Gneiss (and thus the Glenburgh Terrane) is exotic to, and evolved independently from, these cratons (Johnson et al., 2011b). The Glenburgh Terrane is interpreted to have collided and accreted with the Pilbara Craton during the c. 2215–2145 Ma Ophthalmian Orogeny (Occhipinti et al., 2004; Johnson et al., 2010; Johnson et al., 2011b,d).

The Moogie Metamorphics are dominated by psammitic schists, the protoliths to which were deposited across the Glenburgh Terrane sometime between c. 2240 and 2125 Ma. The timing of deposition is essentially coincident with the c. 2215–2145 Ma Ophthalmian Orogeny, and these protoliths are interpreted to represent a proforeland basin deposited in response to uplift of the southern margin of the Pilbara Craton during the collision and accretion of the Glenburgh Terrane with the Pilbara Craton (Occhipinti et al., 2004; Johnson et al.,

2010, 2011b). The Moogie Metamorphics are probably approximately time-equivalent to the Beasley River Quartzite of the lower Wyloo Group, which was deposited in a retroforeland basin during the Ophthalmian Orogeny (Martin and Morris, 2010).

Following this collision on the northern margin of the Glenburgh Terrane, continental-margin arc-magmatic activity was initiated along the southern margin at c. 2080 Ma (Johnson et al., 2010, 2011b). Although magmatic rocks with ages between c. 2080 and 2005 Ma are not exposed within the province, detrital and inherited zircons of this age, with slightly evolved Lu–Hf compositions, are abundant within the volcanoclastic metasedimentary rocks of the 2000–1955 Ma Camel Hills Metamorphics (Johnson et al., 2010, 2011b), and within the granitic gneisses of the 2005–1985 Ma Dalgaringa Supersuite.

The Dalgaringa Supersuite is exposed in the southern part of the province, within the Paradise Zone, and consists of massive, foliated, and gneissic granitic rocks which have major, trace, and rare earth element concentrations consistent with formation in a suprasubduction zone setting (Sheppard et al., 2004). Their whole-rock Sm–Nd, and magmatic zircon Lu–Hf, isotopic signatures indicate the incorporation of Neoarchean granitic gneisses with isotopic compositions similar to those of the Halfway Gneiss (Sheppard et al., 2004; Johnson et al., 2011b), suggesting that magmatism occurred in a continental margin arc, termed the Dalgaringa Arc, which formed along the southern margin of the Glenburgh Terrane. This magmatic event records the progressive closure and northward subduction of an oceanic tract under the previously amalgamated Pilbara Craton – Glenburgh Terrane. The older parts of the Dalgaringa Supersuite (c. 2005–1985 Ma), including lenses of pelitic diatexite and mafic granulite, were deformed and metamorphosed at high temperatures and pressures during the D_{1g} event (c. 2005–1985 Ma) of the c. 2005–1950 Ma Glenburgh Orogeny. This event is interpreted to reflect the construction of the arc in the middle crust (Johnson et al., 2010, 2011b).

Terminal ocean closure, the collision between the Pilbara Craton – Glenburgh Terrane and the Yilgarn Craton, and the formation of the West Australian Craton, all took place during the c. 1965–1950 Ma D_{2g} event of the Glenburgh Orogeny (Johnson et al., 2010, 2011b). The collision resulted in the underthrusting of the Glenburgh Terrane beneath the Narryer Terrane of the Yilgarn Craton along the moderately south-dipping Cardilya Fault (Johnson et al., 2011d). Late backthrusting was responsible for the imbrication of the northern Yilgarn Craton margin with Glenburgh Terrane lithologies along the Errabiddy Shear Zone. High-grade tectonometamorphism during the D_{2g} collision event was accompanied by the intrusion of granitic stocks and dykes of the 1965–1945 Ma Bertibubba Supersuite. These granitic rocks are the first common magmatic element of the northern margin of the Yilgarn Craton, the Yarlalweelor Gneiss Complex, the Errabiddy Shear Zone, and the Paradise Zone of the Glenburgh Terrane. Therefore, suturing of the combined Pilbara Craton – Glenburgh Terrane with the Yilgarn Craton, and thus the assembly of the West Australian Craton, was complete by this time.

Pinjarra Orogen

The Mesoproterozoic to Neoproterozoic Pinjarra Orogen lies along the western margin of Western Australia, and consists of medium- to high-grade metasedimentary and meta-igneous rocks within three basement inliers (Myers, 1990a): the Northampton, Mullingarra, and Leeuwin Inliers, including the Naturaliste Plateau. It also includes several, disparate sedimentary basins — the Badgeradda, Yandanooka and Moora Groups — which unconformably overly the high-grade basement rocks of the Mullingarra Inlier and granite–greenstone terranes of the Yilgarn Craton. The high-grade rocks of the orogen are separated from the Yilgarn Craton by the Darling Fault, which also truncates the Badgeradda and Moora Basins.

The geological evolution of the orogen is poorly constrained, but reconnaissance U–Pb dating of monazite and zircon indicate that deformation, metamorphism and granite magmatism took place between c. 1080 and 990 Ma in the Northampton and Mullingarra Inliers, and at c. 750–520 Ma in the Leeuwin Inlier in the south (Bruguier et al., 1999; Kriegsman et al., 1999; Ksienzyk et al., 2012). Limited detrital zircon U–Pb age data from the Badgeradda Basin indicate deposition sometime after c. 1090 Ma (GSWA, unpublished data). However, since these rocks are essentially undeformed, they must have been deposited after the main c. 1080–990 Ma tectonic event that affected the northern part of the orogen; that is, they are possibly younger than c. 990 Ma.

In the region of seismic line 11GA-SC1, the Pinjarra Orogen is exposed about 140 km to the south, in the Northampton Inlier, but aeromagnetic and gravity images (e.g. Frontispieces 2, 3) imply that these rocks extend northward beyond the seismic traverse under sedimentary cover of the Southern Carnarvon Basin. The inlier is dominated by granulite facies paragneisses that have been multiply deformed and intruded by granite and pegmatite (Bruguier et al., 1999). The metasedimentary rocks are dominated by detrital zircons with ages <2000 Ma, and include major Mesoproterozoic components as young as c. 1150 Ma, indicating deposition of the sedimentary rocks after this time (Ksienzyk et al., 2012). Deformation and metamorphism took place at 800–900°C and 5–6 kbar sometime between c. 1083 and c. 1079 Ma (Bruguier et al., 1999; Ksienzyk et al., 2012), and post-tectonic granite and pegmatite were emplaced at c. 1065 Ma and c. 990 Ma (Bruguier et al., 1999), respectively. The driver for this tectonic activity is currently unknown. About 18 km to the north of the seismic line, drillhole GSWA Woodleigh 1 intersected gneissic granite basement beneath Cretaceous sediments within the Woodleigh Impact Structure (Mory et al., 2001). Preliminary U–Pb SHRIMP dating of complex zircons from the gneissic granite has yielded a preliminary crystallization age for the granite of c. 1300 Ma and a preliminary metamorphic age for high-grade metamorphism of c. 1195 Ma (GSWA, unpublished data). These data confirm the presence of Pinjarra Orogen-type crust in the seismic line beneath sedimentary rocks of the Gascoyne Platform of the Southern Carnarvon Basin.

Current models for the tectonic evolution of the Pinjarra Orogen imply an allochthonous setting for the high-grade metamorphic rocks (Myers, 1990a; Bruguier et al., 1999;

Cobb et al., 2001; Fitzsimons 2001, 2003; Ksienzyk et al., 2012). Fitzsimons (2001, 2003) highlighted the synchronicity in deformation and metamorphism between the Pinjarra Orogen and the Albany–Fraser Orogen, and suggested that the high-grade rocks in the Northampton and Mullingar Inliers originally formed about 800 km to the south, in the Albany–Fraser Orogen, and were transported to their present position by dextral strike-slip movement on the Darling Fault prior to c. 755 Ma, sealed by the emplacement of voluminous mafic sills of the Mundine Well Dolerite Suite across the Northampton Inlier, Gascoyne Province and western margin of the Yilgarn Craton. In contrast, Ksienzyk et al. (2012) suggested that the high-grade rocks formed part of a para-autochthonous oceanic island-arc system which received sedimentary detritus from the Albany–Fraser Orogen to the south. The collision of the magmatic arc with the western margin of the West Australian Craton, along the Darling Fault, was the driver for Late Mesoproterozoic high-grade metamorphism and deformation. Both models imply that Narryer Terrane crust does not occur beneath the orogen, and that the contact between the Pinjarra Orogen high-grade rocks and the Yilgarn Craton is a discrete major crustal-scale structure, possibly the Darling Fault.

Badgeradda Basin

Approximately 70 km south of seismic line 11GA-SC1, between the Darling and Meeberrie Faults (Frontispiece 1), unfossiliferous sedimentary rocks of the Badgeradda Group (Perry and Dickins, 1960; see also Condon, 1965) unconformably overlie Archean rocks of the Narryer Terrane. The group contains folded sandstone, shale and conglomerate with an estimated maximum thickness of about 3000 m, and has been intruded by undated east–west trending dolerite dykes. The presence of cross-bedded, coarse-grained feldspathic quartz sandstone indicates local derivation.

Age constraints on these rocks are limited but U–Pb SHRIMP dating of detrital zircons from the Woodrarrung Sandstone yielded a late Mesoproterozoic preliminary maximum depositional age of c. 1080 Ma (GSWA, unpublished data). The oldest detrital zircon grains have ages of about 1800 Ma (GSWA, unpublished data), indicating no input from the Narryer Terrane, which is the basement on which the Group was deposited. The Badgeradda Group is inferred to continue to the north, in the subsurface beneath the Byro Sub-basin of the Southern Carnarvon Basin, and an outcrop is crossed by the seismic line at about CDP 6200.

Southern Carnarvon Basin

The Southern Carnarvon Basin covers an area of 188 000 km², of which about 90 000 km² is onshore. Offshore, and 500 km to the north of seismic line 11GA-SC1, the Northern Carnarvon Basin contains a thick succession of mainly Mesozoic clastic sediments and is the premier petroleum-producing province in Australia; whereas, onshore, the basin contains mostly Paleozoic

sedimentary rocks overlain by a thin and mostly flat-lying Mesozoic succession. The Southern Carnarvon seismic line 11GA-SC1 (Frontispiece 1, Fig. 1) extends east–west across lower Paleozoic strata in the west (Gascoyne Platform), which are covered by Mesozoic and Cenozoic sediments, and Permian depocentres of the Byro Sub-basin in the east. The Gascoyne Platform and Byro Sub-basin are separated by the Talisker Fault, which is a splay fault of the Darling North Fault System (Hocking et al., 1987; Carr et al., 2012). Major tectonic events that have affected the basin include mid-Carboniferous folding, faulting and erosion, Permian extension, and Jurassic–Cretaceous continental breakup (Mory et al., 2003).

In terms of resources, the Southern Carnarvon Basin has potential for hydrocarbons, whereas its potential for geothermal energy and coal is low. Ghori (1999) found excellent to fair, albeit thin, source-rock intervals in the Silurian Dirk Hartog Group and the Upper Devonian Gneudna Formation on the Gascoyne Platform to the north of the seismic line, as well as thicker source rock intervals within the Permian succession of the adjacent Merlinleigh Sub-basin. The Permian, and possibly also the older stratigraphic units, extend into the Byro Sub-basin, implying that it has at least fair hydrocarbon-generating potential. The thick sedimentary succession in the Byro Sub-basin and along the Darling Fault indicates that low heat flows are likely and the thick basal sandstone of the Gascoyne Platform succession is likely to allow dissipation of heat that is too rapid to be prospective for geothermal energy. Coal deposits other than the small Talisker deposit (le Blanc Smith, 1990), preserved in a small syncline 70 km south of the seismic line, are unlikely because the stratigraphic level of that deposit (Keogh Formation) has a limited distribution in the region due to erosion.

Constraints on the stratigraphy of the Southern Carnarvon Basin are provided by several wells, including Hamelin Pool 1 and 2, Yaringa 1, Woodleigh 1982-1 and GSWA Ballythanna 1. Hamelin Pool 2 and Yaringa 1, 6 km and 14 km to the northwest of the seismic line, respectively, were drilled into the upper part of the Ordovician Tumblagooda Sandstone, and were used to constrain the interpretation of the stratigraphic succession at the western end of the seismic line. Woodleigh 1982-1, located 4 km south of the line, intersected 90 m of Cretaceous strata and a 101 m-thick section of probable Lower Jurassic age overlying carbonates of the Silurian Dirk Hartog Group (Iasky et al., 2001). GSWA Ballythanna 1 lies on seismic line 11GA-SC1 (CDP 8120, Fig. 3), about 2 km west of the Ballythanna Fault. It intersected the Permian Keogh and Callytharra formations, and the uppermost Lyons Group, before drilling was terminated. Permian outcrops, and several water and coal-exploration boreholes, also help to constrain the interpretation.

Preliminary interpretation of seismic line 11GA-SC1

The east–west orientation of the seismic line is essentially perpendicular to the long axis of the Byro Sub-basin,

and to the major faults that bound the basin and which separate the Pinjarra Orogen from the Narryer Terrane (Frontispieces 1–3). In the western half of the seismic line, the Southern Carnarvon Basin is concealed by younger Cenozoic sedimentary deposits, and information from available drillholes was used to constrain the geological interpretation (Fig. 3). Outcrop geology and drillholes were used to constrain the interpretation of the Byro Sub-basin. For the Narryer Terrane, limited outcrop was projected along strike onto the seismic line to assist the interpretation. Apart from within the Southern Carnarvon Basin, the crust in the vicinity of the seismic section has variable reflectivity, with local parts of the section containing strong reflections but most having only moderate to low reflectivity (Fig. 2).

The Moho is interpreted to occur principally at the base of a weakly to moderately reflective package, below which the nonreflective material is interpreted to represent the upper mantle. The depth of the interpreted Moho varies from about 10 s two-way travel time (TWT) (about 30 km) at the western end of the line and about 11.6 s TWT (about 35 km) at the eastern end of the line, to >13 s TWT (nearly 40 km) beneath the Byro Sub-basin (Figs 2, 4). In the seismic section, the Moho varies in seismic reflectivity

from a moderately reflective crust–mantle transition zone about 0.3–0.6 s TWT thick (about 1–2 km) to areas, particularly in the central part of the seismic section, where it is generally poorly imaged. A strongly reflective crust–mantle transition zone is a persistent feature across most of the Youanmi seismic lines (e.g. Zibra et al., 2013, this volume), as well as in other seismic surveys in younger Proterozoic and Paleozoic terranes elsewhere (e.g. North Queensland, Korsch et al, 2012; Canada, Hammer and Clowes, 1997; Clowes and Oueity, 2010).

Crustal terranes, seismic provinces and basins

On the basis of seismic character and presence of discrete, crustal-scale structures, the basement beneath the Southern Carnarvon Basin in section 11GA-SC1 has been divided into five major components: the Narryer Terrane, the Yarraquin Seismic Province, the Errabiddy Shear Zone, the Glenburgh Terrane, and the Pinjarra Orogen (Fig. 4). These tectonic units, as well as the overlying sedimentary basins are discussed in more detail below.

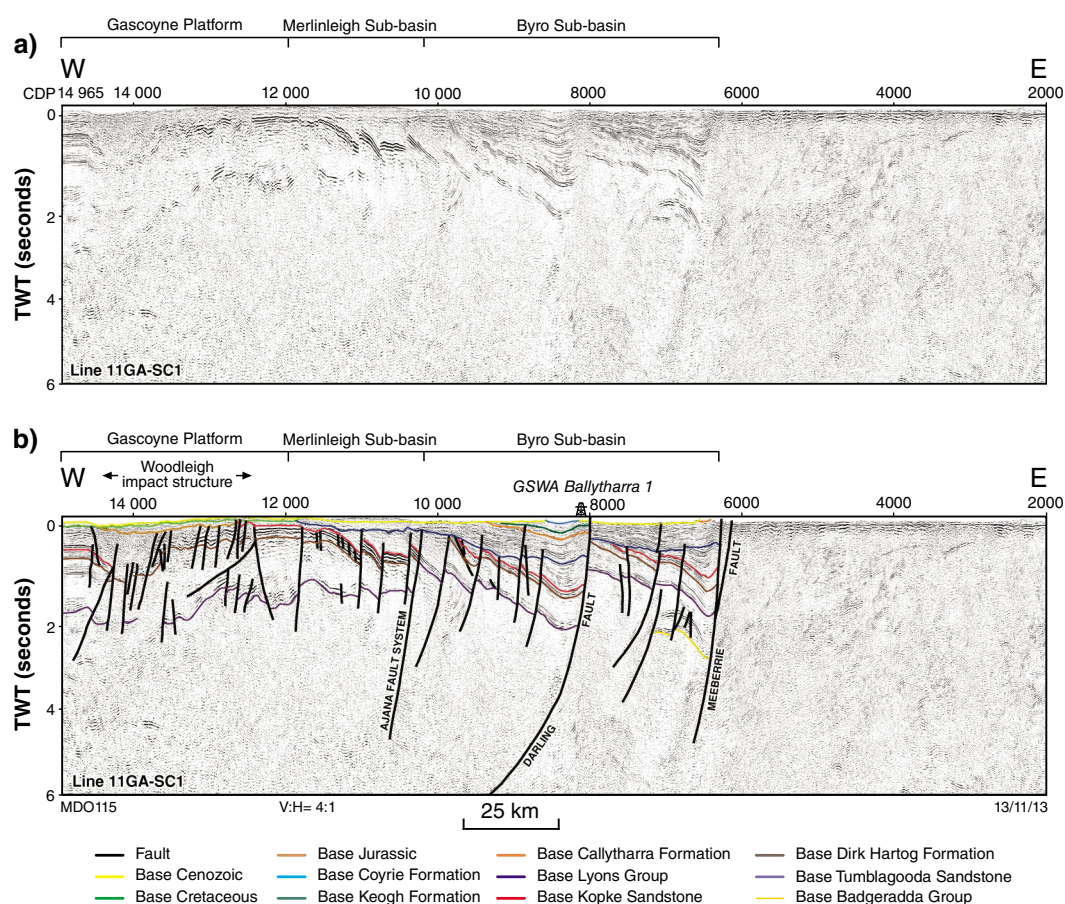


Figure 3. Geological interpretation of part of migrated seismic section 11GA-SC1 across the southern Carnarvon Basin, displayed with a vertical exaggeration of x4, assuming an average crustal velocity of 6000 ms⁻¹

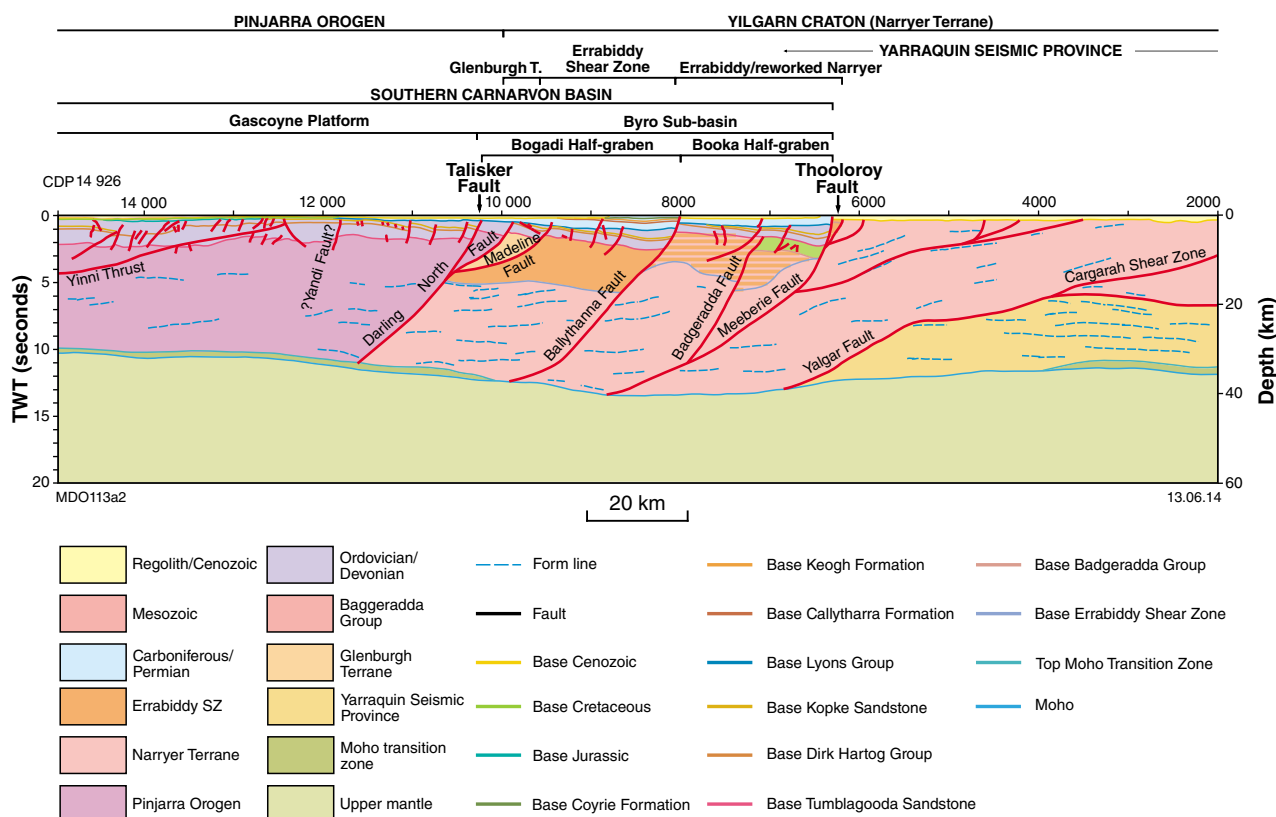


Figure 4. Geological interpretation of seismic line 11GA-SC1, showing the distribution of the basins and provinces

Narryer Terrane

The Narryer Terrane is exposed to the east of the Meeberrie Fault, and is interpreted to extend to the west in the subsurface, beneath the Byro Sub-basin, to the Darling North Fault (Figs 2, 4). It lies above the Yarraquin Seismic Province in the east, and then extends down to the Moho at about CDP 6800 (Fig. 2). The terrane is moderately to weakly reflective, and is dominated mainly by reflections with an apparent westerly dip. Surface mapping by Myers (1997) indicates that the structures in the Narryer Terrane in the vicinity of the seismic line strike either to the northeast or east-northeast, and are steeply dipping to subvertical. The west-dipping fault interpreted in the seismic section at CDP 3500 separates granulite facies rocks to the west from amphibolite facies rocks to the east, with a sliver of amphibolite facies rocks occurring between the faults at CDPs 4200 and 4600. This interpretation agrees well with the potential field modelling (Gessner et al. 2013, this volume).

On seismic line 10GA-YU1, the Cargarah Shear Zone (Spaggiari, 2007) is interpreted to lie within the Narryer Terrane, just to the northwest of the Yalgar Fault (Plates 1, 3; Romano et al., 2013, this volume). We have projected the Cargarah Shear Zone into the Southern Carnarvon seismic section, and interpreted it as the base

of a package of west-dipping reflections at a depth of about 2.8 s TWT (about 8.5 km) at the eastern margin of the section, and have interpreted it to sole onto the Yalgar Fault at about CDP 3800 (Fig. 2).

The Thooloroy Fault (named after Thooloroy Well) is a minor fault that separates domains of different aeromagnetic signature within the northwestern Narryer Terrane (Fig. 5). It is truncated by the Meeberrie Fault at about 2 s TWT (about 6 km) depth at about CDP 6310.

Yarraquin Seismic Province

At the eastern end of the Southern Carnarvon seismic line, the lower crust is highly reflective and, based on a jump tie from seismic line 10GA-YU1 to the east (Romano et al., 2013, this volume), its upper subhorizontal surface is interpreted to be the Yalgar Fault (Myers, 1990b). This lower crustal reflective package is termed the Yarraquin Seismic Province (Korsch et al., 2013, this volume) and forms the lower crust to the entire Youanmi Terrane, from the Yalgar Fault in the west to the Ida Fault in the east (Romano et al. 2013, this volume; Zibra et al., 2013, this volume; Korsch et al., 2013, this volume). As we have not been able to track these rocks to the surface, we have no direct constraints on their lithology or age.

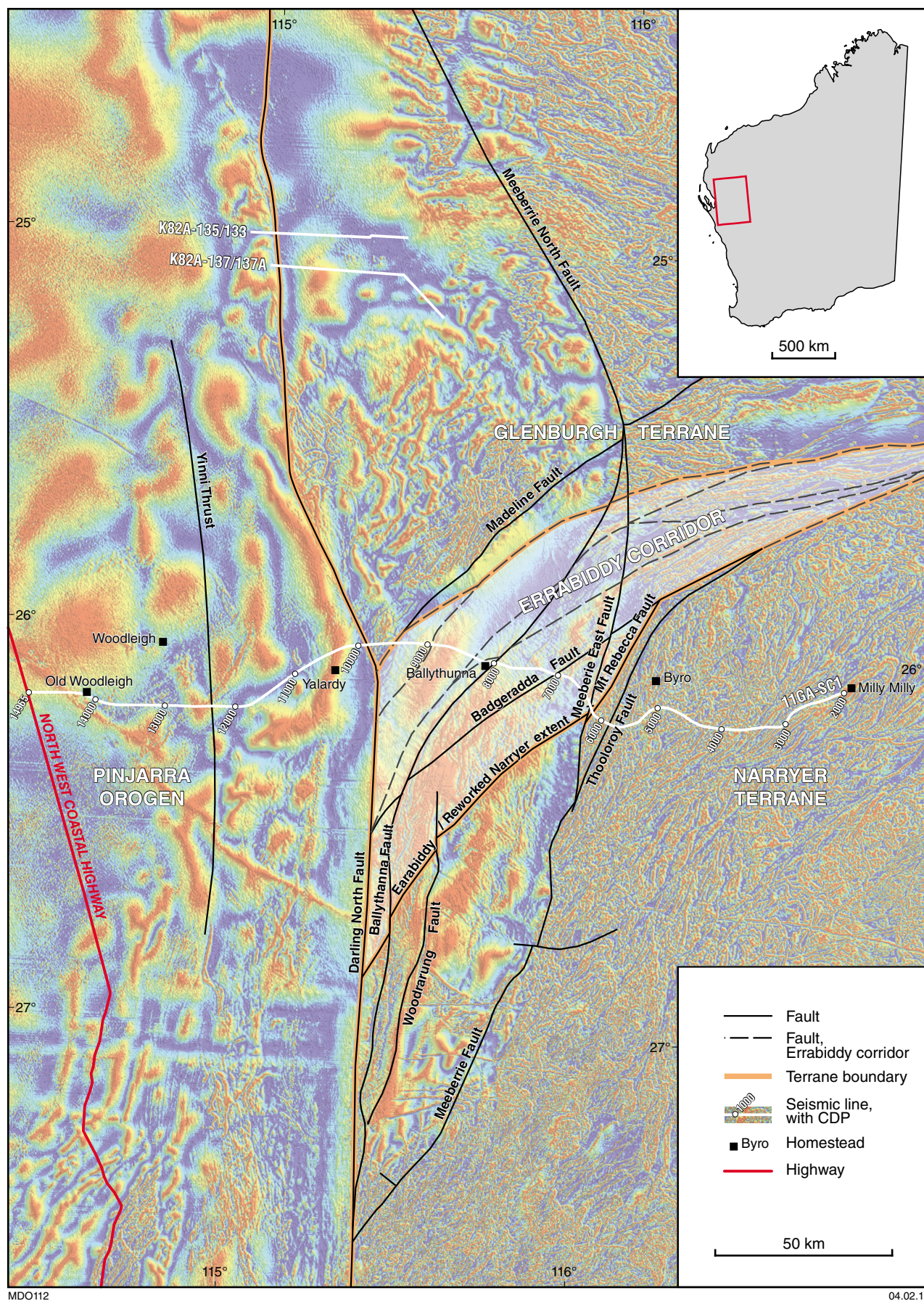


Figure 5. Aeromagnetic image showing interpretation of the key faults and shear zones in the vicinity of seismic line 11GA-SC1 in the regional context

Glenburgh Terrane

The Glenburgh Terrane is interpreted to form a small wedge-shaped sliver between the Darling North and Madeline Faults between CDP 9430 and 9860 (Fig. 4). The package is moderately reflective, showing moderate to steep westerly dipping reflections, and is up to 2 s TWT (about 6 km) thick. The terrane is overlain by Ordovician and younger sedimentary rocks of the Southern Carnarvon Basin, which here are up to 1.5 s TWT (about 3–4 km) thick. About 10 km north of the transect, the Glenburgh Terrane is exposed in the Carrandibby Inlier, where its southern margin and contact with sedimentary rocks of the Southern Carnarvon Basin is marked by the Madeline Fault (Figs 5 and 6). The inlier is composed of tectonically imbricated granitic gneisses of the c. 2555–2430 Ma Halfway Gneiss and c. 2005–1970 Ma Dalgaringa Supersuite, with kilometre-scale rafts of metasedimentary rocks belonging to the c. 2240–2125 Ma Moogie Metamorphics. The detail observed in the seismic data is insufficient to subdivide this terrane into more discrete components. To the east of the Madeline Fault (CDP 9430) a weakly reflective package extending over an interval of

up to 3 s TWT (about 9 km thick) lies above the Narryer Terrane (Fig. 4), and contains several arcuate imbricate faults. This section is interpreted as part of the Errabiddy Shear Zone, and most likely contains strongly deformed rocks from both the Narryer and Glenburgh Terranes (also see Johnson et al., 2011d). To the east of the Ballythanna Fault (CDP 8010), the Errabiddy Shear Zone grades into the strongly reworked margin of the Narryer Terrane, and the generally nonreflective character of this package makes it difficult to further subdivide this unit.

Pinjarra Orogen

The Pinjarra Orogen is interpreted to extend westwards from the Darling North Fault (CDP 9860) to beyond the western end of the seismic section (Fig. 2). The orogen is uniformly weakly reflective and, at this stage, it has not been subdivided. The uniformity of seismic character implies that Pinjarra Orogen crust extends in the subsurface from the base of the Southern Carnarvon Basin to the Moho, and is unlikely to be underlain by rocks of the Narryer or Glenburgh terranes

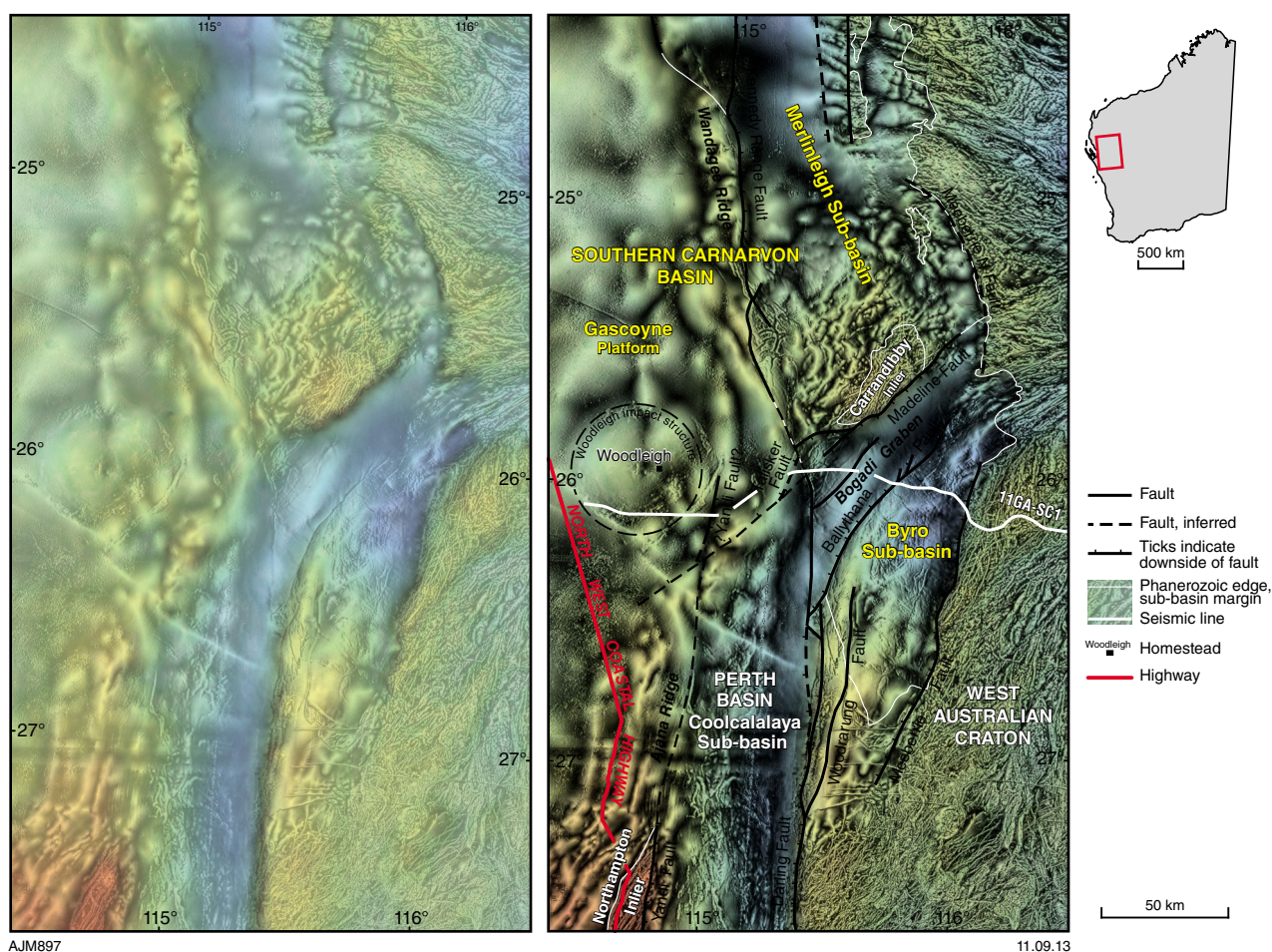


Figure 6. Phanerozoic structures and basins on top of a grey-scale aeromagnetic image draped on gravity

Badgeradda Basin

Within the seismic section, between CDPs 6400 and 7200, there is a package of reflections below the interpreted position of the Tumblagooda Sandstone (Figs 2, 4), and subparallel to it, which we interpret as the late Mesoproterozoic Badgeradda Group. The reflections making up this set extend up to 1 s TWT (about 3 km thick) and rest unconformably on the underlying basement. We have not been able to map the reflections farther to the west than about CDP 7200, and hence terminate the Badgeradda Group at the Badgeradda Fault (Fig. 2).

Immediately to the east of the Meeberrie Fault, in the vicinity of the seismic line, a thin wedge of sedimentary rocks is exposed, which is also mapped as the Badgeradda Group. This is interpreted within the seismic section as a thin sliver between the Mount Rebecca Fault at CDP 6180 and the Meeberrie Fault at CDP 6300. The Mount Rebecca Fault represents an early stage of extensional faulting along the Meeberrie Fault system. It is truncated by the Meeberrie Fault at about 2.3 s TWT (about 7 km) depth, at about CDP 6380.

Southern Carnarvon and Perth Basins

Seismic line 11GA-SC1 crosses the Gascoyne Platform in the west and the Byro Sub-basin east of this, both within the Southern Carnarvon Basin. There are some faults, identified on the seismic line, that extend from the adjoining Gascoyne Platform to the north and from the Coolcalalaya Sub-basin (Perth Basin) to the south (Fig. 6). Historically, the latter sub-basin has been placed within the Perth Basin (e.g. Playford et al., 1975) but neither its northern nor southern limits can be delineated precisely due to data limitations, and it is likely that the sub-basin represents a transitional zone (Mory et al., 1998). A major difference between the Perth and Southern Carnarvon Basins is the change in controlling faults from the down-to-the-west Darling Fault and southern segment of the Darling North Fault in the Perth Basin, to the down-to-the-east Kennedy Range Fault System (at least in the Merlinleigh Sub-basin) in the Southern Carnarvon Basin. From this perspective, it could be argued that the Byro Sub-basin is better placed in the Perth Basin.

An as yet unresolved interpretation problem is the lateral continuation of the westerly-dipping Talisker Fault at CDP 10400 in the Phanerozoic, which cannot be resolved on either the gravity or aeromagnetic images. This structure is the eastern boundary of the Gascoyne Platform, and appears to be a splay fault of the Darling North Fault (Figs 2, 4). It is possible that the splay was propagated from a decollement zone in the basement, which may explain the high obliquity of this boundary to the seismic line between the Gascoyne Platform and Coolcalalaya Sub-basin (Fig. 6).

Byro Sub-basin

Seismic line 11GA-SC1 (Fig. 4) shows that the Byro Sub-basin consists of two, relatively thick half graben, bounded by the west-dipping faults. The eastern one, controlled by the Meeberrie Fault, is called the Booka Half-graben. The

western one, controlled by the west-dipping Ballythanna Fault, represents the southwest-trending Bogadi Half-graben, which extends into the Coolcalalaya Sub-basin, or abuts against it. The seismic line cuts across the Bogadi Half-graben obliquely, and does not intersect its northern margin. This margin is formed by a southeast-dipping fault, which largely follows and reactivates a Proterozoic basement structure (the Madeline Fault, see below), but deviates from it west of the Carrandibby Inlier and swings into an easterly trend (Fig. 6). Calculations from stacking velocities on the seismic line suggest that the sedimentary successions in the two half-graben next to the major faults are about 5600 m and 5000 m thick, respectively. Two distinct sedimentary packages are interpreted: a lower unit ranging from the Ordovician Tumblagooda Sandstone to the Lower Devonian Kopke Sandstone, and an upper Permian unit, separated from the lower unit by an angular unconformity. Faulting and tilting between the two units is attributed to tectonism related to the Alice Springs Orogeny. The Permian rocks show some thickening into both the Ballythanna and Meeberrie Faults, implying they are syn-extensional deposits. Although these crustal-scale faults must merge within the basement, the convergence of these two faults towards the northeastern part of the Byro Sub-basin, based on the aeromagnetic data and outcrop, cannot be resolved, due to Cenozoic cover and the dominance of shallow cross-cutting Precambrian features in the aeromagnetic data in that area. It is possible that at least some of the vertical displacement is taken up by the Meeberrie North Fault, which runs from the southeastern margin of the Merlinleigh Sub-basin into the Byro Sub-basin. Both synthetic and antithetic faults mapped in both the upper and lower successions are interpreted to relate to these extensional events.

Merlinleigh Sub-basin

The Merlinleigh Sub-basin is an elongate, north-northwesterly trending depocentre in the Southern Carnarvon Basin (Figs 1, 6, 7) containing a sedimentary succession of up to 8000 m thickness, of which the greater part is the Upper Carboniferous to Lower Permian succession, which thickens westwards towards the Kennedy Range Fault System (Iasky et al., 1998). The sub-basin is separated from the Byro Sub-basin to the south by the Carrandibby Inlier, and abuts against the Gascoyne Platform to the west along the Kennedy Range Fault System. In places, this boundary somewhat arbitrarily crosses relay ramps within this down-to-the-east fault zone. To the east and south, the Paleozoic rocks onlap onto basement of the West Australian Craton, although aeromagnetic data indicate a fault boundary south of 25°S akin to the Meeberrie Fault on the eastern edge of the Byro Sub-basin, here designated as the Meeberrie North Fault.

Gascoyne Platform

The Gascoyne Platform is an area of shallow Lower Paleozoic strata, mostly covered by a thin Cretaceous sedimentary succession, which lies west of the main Permian depocentres of the Merlinleigh, Byro and Coolcalalaya Sub-basins (Fig. 6). The wells Hamelin Pool 2 (about 6 km to the north of the seismic line at its western end) and Yaringa 1 (about 14 km to the north)

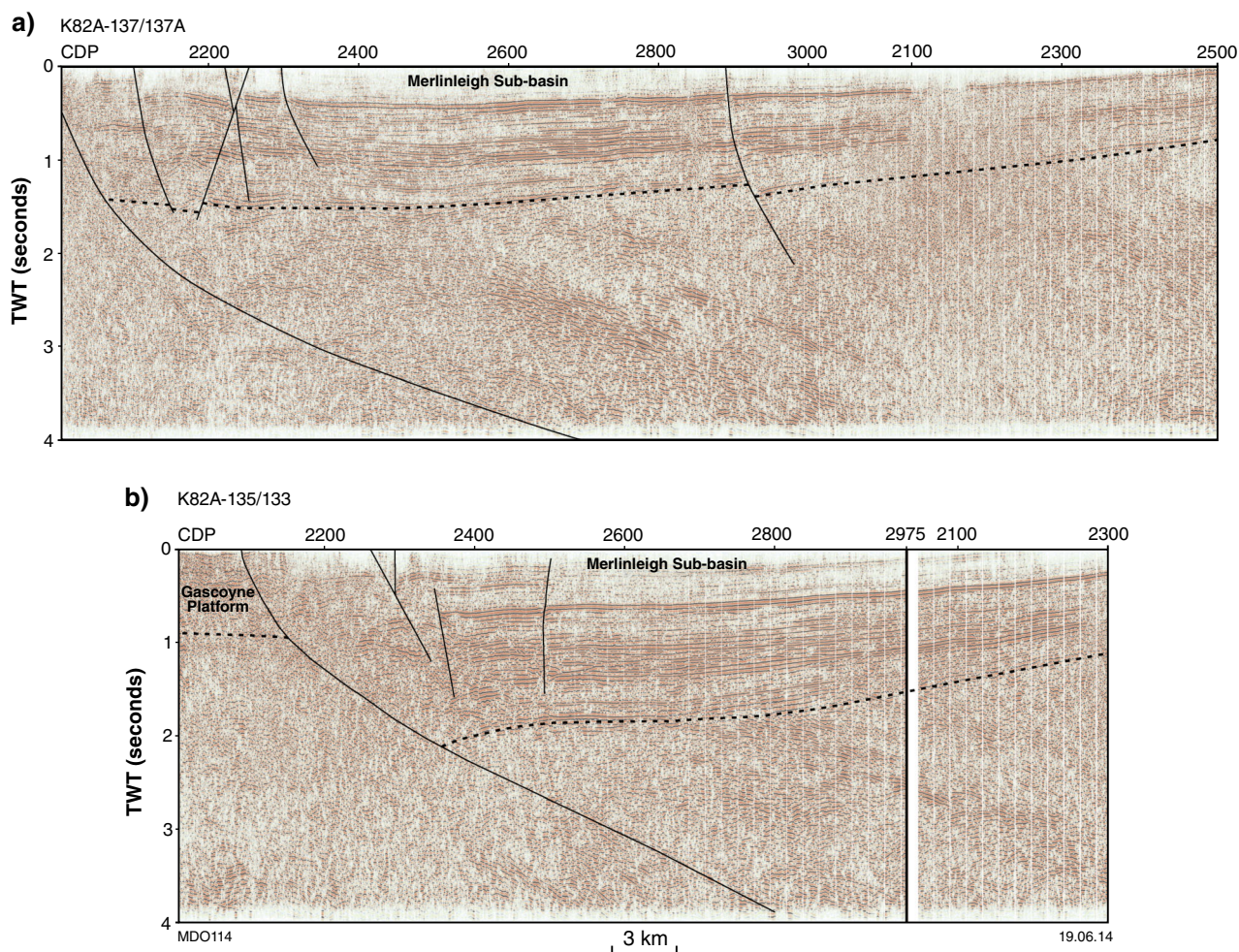


Figure 7. Interpreted versions of the migrated sections for seismic lines K82A-137/137A (a) and K82A-135/133 (b). Note the opposite polarity of the half-graben compared with the Byro Sub-basin in Figure 3. See Figure 5 for location.

intersected a thin Cretaceous succession above a Lower Devonian siliciclastic section, Silurian carbonates of the Dirk Hartog Group, and the Tumblagooda Sandstone of likely Ordovician age (Iasky and Mory, 1999). Our interpretation suggests that the Southern Carnarvon Basin succession is about 4 km thick at the western end of the seismic section. Permian strata extend as far west as about CDP 11900 in the seismic section (Fig. 3), but thin dramatically and unconformably overlie tilted and faulted older Paleozoic rocks west of the Byro Sub-basin. Modelling of maturity data from the Silurian succession shows that it has never been deeply buried across most of the Gascoyne Platform, thereby implying limited, if any, Permian deposition within that sub-basin (Ghori, 1999; Ghori et al., 2005).

Coolcalalaya Sub-basin

The Coolcalalaya Sub-basin lies south of seismic line 11GA-SC1 between the Ajana Ridge of the Gascoyne Platform and the Northampton Inlier to the west, and Byro Sub-basin or West Australian Craton to the east (Fig. 6). It is estimated to contain up to 8500 m of Paleozoic

strata (Mory et al., 1998). The southwest-oriented aeromagnetic feature, which appears to represent a deep southern extension of the Madeline Fault System, was somewhat arbitrarily chosen by Hocking (1994) as the northwestern limit of the Coolcalalaya Sub-basin. This feature is here taken as the entire northern boundary, as the new aeromagnetic data do not reveal any northwesterly oriented features that Hocking (1994) assumed for the northeastern limit of the sub-basin. This is still not an entirely satisfactory definition, as the boundary with the Byro Sub-basin is along a subsidiary fault (here designated as Darling North Fault), whereas the major Phanerozoic down-to-the-west throw along the Darling Fault farther south appears to transfer into the Byro Sub-basin along the northeast-trending Ballythanna Fault. The western boundary of the sub-basin is assumed to be an east-dipping fault extending north from the Yandi Fault along the east margin of the Northampton Inlier (Fig. 6). Whereas this appears to align with the west-dipping fault evident on the seismic line at approximately CDP 11800, the correlation is somewhat ambiguous as there is not a clear differentiation of such a fault from bedding on the aeromagnetic data north of the Northampton Inlier.

Terrane-bounding structures

Darling Fault and Darling North Fault

The approximately 1000 km-long, predominantly north–south oriented, Darling Fault and its northern extension, the Darling North Fault, is one of the most distinctive topographic, gravity and aeromagnetic features on the Australian continent (Fig. 5). The fault intersects the seismic line at CDP 9870, represents the eastern boundary of the Pinjarra Orogen, and truncates and terminates all structures and crustal blocks to the east (i.e. Narryer Terrane, Errabiddy Shear Zone, Glenburgh Terrane; Fig. 5). The structure transects the entire crustal profile, cutting Permian strata at the surface, and can be traced down to the Moho.

Errabiddy Shear Zone and reworked Narryer Terrane

The Errabiddy Shear Zone is best defined farther east where, in seismic line 10GA-CP3, it is imaged as an easterly striking zone of imbricate faults, which lie within the upper 10–15 km of the crust, and have an overall south-verging sense of movement (Johnson et al., 2011d). The internal structure and lithological make-up of the zone is poorly resolved due to low seismic reflectivity (Johnson et al., 2011d) and the Errabiddy Shear Zone is not exposed in the vicinity of seismic line 11GA-SC1 where it is buried beneath rocks of the Southern Carnarvon Basin. Nevertheless, aeromagnetic and gravity images (Fig. 5) suggest that the shear zone swings gently to the southwest into the plane of the seismic section, and is truncated by the Darling North Fault at CDP 10600, between about 4–5 s TWT (about 12 to 15 km) depth in the west (Figs 2, 4, 5). The extent of the Errabiddy Shear Zone to the east is difficult to estimate as it grades into the strongly reworked margin of the Narryer Terrane, which is very similar in seismic character. Hence, east of the Ballythanna Fault, at CDP 8010, both units are combined where they overlie the Narryer Terrane. The contact with the Narryer Terrane is not exposed, but is interpreted to rise in the crust east of CDP 7000, which causes the eastward pinching out of the Errabiddy Shear Zone – reworked Narryer Terrane at CDP 6480 and 3.2 s TWT (about 12.5 km). The contact is offset by the Ballythanna and Badgeradda faults, respectively.

Within line 11GA-SC1, the Errabiddy Shear Zone is imaged as a series of arcuate, imbricate faults, the base of which lies at 5.5 s TWT (about 16 km). The general asymmetry of the faults implies thrust movements towards the southeast. The internal structure and lithological make-up of the zone is poorly resolved, due to the weakly reflective nature of the crust (Figs 2, 4). In general, the Errabiddy Shear Zone is of similar character in this line to that in seismic line 10GA-CP3 (Johnson et al., 2011d). The moderately south-dipping Cardilya Fault, which marks the suture between the Glenburgh and Narryer Terranes farther east in 10GA-CP3 (Johnson et al., 2011d), is not imaged in the Southern Carnarvon section, probably because the fault dips out of the plane of section. The crust is thickest beneath the Errabiddy Shear Zone, however,

where the Moho reaches a maximum depth of 13.5 s TWT (about 40 km), and this may be due to crustal thickening during the collision of the Glenburgh and Narryer Terranes during the c. 2005–1950 Ma Glenburgh Orogeny (Johnson et al., 2010, 2011b,d).

Due to the masking effect by the overlying sediments of the Byro Sub-basin and, farther south, by the Badgeradda Group, the southern extent of the Errabiddy Shear Zone – reworked Narryer Terrane is difficult to estimate. The boundary as shown in Figure 5 is interpreted from aeromagnetic data.

Basin-bounding structures

With the possible exception of the Kennedy Fault System, all major faults within the Southern Carnarvon Basin are reactivated and are related to basement faults and shear zones, which presumably have a pre-Phanerozoic history, and are mostly of crustal scale. This implies that they are laterally continuous features within the basement, as shown in Figure 5. Their (extensional) reactivation, however, can be restricted to fault segments only, which are commonly bounded by cross-cutting basement features. One example is the intersection between the Meeberrie Fault and the Errabiddy Shear Zone (Figs 5, 6). Furthermore, the reactivated faults can have an antithetic orientation with respect to the basement fault, or also deviate from the trace of the basement fault in response to the stress field (e.g. Meeberrie Fault; Figs 5, 6).

Meeberrie and Meeberrie North Faults

Within the seismic section, below the Southern Carnarvon Basin, the Meeberrie Fault (van de Graaff et al., 1977) is interpreted as an internal fault within the Narryer Terrane, and both it and its northern extension, the Meeberrie North Fault, pass through the entire crust to the Moho (Figs 2, 4, 5). Nevertheless, this fault marks the eastern edge of the Booka Half-graben of the Byro Sub-basin, and was an active extensional fault controlling the deposition of the basin fill during the formation of the half-graben during the Permian. Later, there was minor inversion on the fault to produce the small hangingwall anticline on the western side of the fault, as seen in the seismic section between CDPs 6300 and 6500 (Figs 2, 3). Timing of this contraction is only constrained to after deposition of the Permian sediments. Within the basement, the Meeberrie North Fault is interpreted to merge with the Ballythanna Fault to the north of the seismic line (Fig. 5).

Ballythanna Fault

In the vicinity of the seismic line, the Ballythanna Fault trends northeast–southwest (Frontispiece 2, Fig. 5), crossing the seismic line at CDP 8010. Within the basement, it is interpreted to merge farther to the north with the Meeberrie North Fault (Fig. 5), and is also interpreted to cut through the Yarlalweelor Gneiss Complex – Errabiddy Shear Zone and the Narryer Terrane to the Moho (Figs 2, 4). The major Phanerozoic period of movement on the fault, as seen in the seismic section

(Figs 2, 3), was during the Permian, when the fault was the active bounding fault to the Bogadi Half-graben. This extensional movement also displaced the base of the Errabiddy Shear Zone, with a down-to-the-west extensional sense of displacement (Fig. 2). Later, there was a period of minor inversion on the fault to form the Ballythanna Hill Anticline in the hangingwall between CDPs 8010 and 8220 (Fig. 3). The only age constraint on this inversion is that it was after deposition of the Permian sediments. The Ballythanna Fault is an interesting feature, as it apparently acted as a transfer fault transferring extensional movement from the Darling to the Meeberrie fault systems. Hence, on a regional scale, the Bogadi Half-graben can be interpreted as a Permian pull-apart basin, bounded by the Madeline and Ballythanna faults, and formed during dextral transtension.

Talisker Fault

The Talisker Fault, which is crossed by the seismic line at CPD 10 200, is a significant fault in the architecture of the Southern Carnarvon Basin as it separates the Byro Sub-basin from the Gascoyne Platform. At CDP 10550, at a depth of 4.3 s TWT (about 13 km), it merges with the Darling North Fault, which is the primary basement fault (Fig. 5). Its possible lateral continuation south of the boundary with the Coolcalalaya Sub-basin is not known (Fig. 6).

Other structures

Yalgar Fault

The Yalgar Fault is a major fault, mapped at the surface, which separates the Narryer Terrane from the Murchison Domain of the Youanmi Terrane to the southeast (Myers, 1990b; Spaggiari, 2007; Wilde and Spaggiari, 2007). Its projected surface trace was crossed by seismic line 10GA-YU1, where it is interpreted to be a listric fault dipping to the northwest and cutting deep into the crust (Romano et al., 2013, this volume). In seismic line 11GA-YU1, it separates the Narryer Terrane from the Murchison Domain, but below about 3 s TWT (about 9 km) it separates the Narryer Terrane from the Yarraquin Seismic Province (Korsch et al., 2013, this volume). In the Southern Carnarvon seismic section, the Yalgar Fault is confined to the lower crust, and forms the boundary between the Narryer Terrane and the underlying Yarraquin Seismic Province (Fig. 2).

Cargarah Shear Zone

On seismic line 10GA-YU1, the Cargarah Shear Zone (Spaggiari, 2007) is interpreted to be within the Narryer Terrane, just to the northwest of the Yalgar Fault (Romano et al., 2013, this volume). We have jump tied the two seismic sections and correlated the Cargarah Shear Zone into the Southern Carnarvon seismic section, with the shear zone interpreted to be the base of a package of west-

dipping reflections at a depth of about 2.8 s TWT (about 8.5 km) at its eastern margin (Fig. 2). We have interpreted the Cargarah Shear Zone to sole onto the Yalgar Fault at about CDP 3800. This supports the contention, above, that the Cargarah Shear Zone lies entirely within the Narryer Terrane.

Badgeradda Fault

Within the vicinity of the seismic section, the Badgeradda Fault is interpreted to be a steep thrust fault and to mark the western limit of the sedimentary rocks of the Badgeradda Group (Fig. 2). It is also interpreted to displace the base of the Yarlalweelor Gneiss Complex – Errabiddy Shear Zone. Because the fault does not appear to cut the Tumblagooda Sandstone at the base of the Southern Carnarvon Basin, its time of movement is constrained to be after deposition of the Badgeradda Group and before deposition of the Ordovician Tumblagooda Sandstone.

Yinni Thrust

The Yinni Thrust (new name, after Yinni Tank) is interpreted as a shallowly west-dipping shear zone within the Pinjarra Orogen. It began as a top-to-the-east thrust, which exhumed a deeper structural level of Pinjarra Orogen prior to the deposition of the Ordovician Tumblagooda Sandstone. The basement of granitic gneiss has been drilled in GSWA Woodleigh 1 (Mory et al., 2001; see above under Pinjarra Orogen). The Yinni Thrust was later reactivated as an extensional fault, and can be traced to the base of the Silurian Dirk Hartog Group. It does not reach the surface within the seismic section because it is masked at 0.4 s TWT (about 1.3 km) by an east-dipping extensional fault which cuts the line at CDP 12435. Nevertheless, it is included in the diagrammatic sketch on Figure 5.

Woodleigh impact structure

The western part of the Southern Carnarvon seismic line crosses the southern part of the Woodleigh impact structure, which is buried beneath thin Jurassic to Cretaceous strata (Iasky et al., 2001). Subhorizontal dips in the Ordovician – Early Devonian rocks, to the west of a zone of down-to-the-west extensional faults (west of CDP 11800, Fig. 3), indicate that the diameter of the impact structure is about 51 km, which is significantly smaller than the 120 km diameter for the structure proposed by Glikson et al. (2005). This size is also consistent with the eastward deterioration of reflections in seismic line W65G-003, located about 15 km to the north. The diameter of the structure appears to closely match the distribution of the lower Jurassic Woodleigh Formation, a siliciclastic lacustrine deposit which is up to 300 m thick (intersected in GSWA Woodleigh 2A; Mory et al., 2001), thereby suggesting a possible earliest Jurassic age for the structure (compared to a latest Devonian age proposed by Glikson et al., 2005).

Crustal architecture along 11GA-SC1

Seismic line 11GA-SC1 transects a geologically complex area with a long structural history of over two billion years, and images a triple junction between three major basement blocks: the Glenburgh Terrane, the Narryer Terrane and the Pinjarra Orogen. Figures 3 and 4 synthesize the preliminary interpretation of seismic line 11GA-SC1, with Figure 5 showing the structural interpretation of aeromagnetic and gravity data, combined with surface geological constraints, with a focus on the basement architecture. It is complemented by Figure 6, which shows the main Phanerozoic structures.

Terrane boundaries and suture zones

In seismic line 11GA-SC1, the Yalgar Fault separates the Yarraquin Seismic Province from the Narryer Terrane, but on seismic line 10GA-YU1 the fault separates the Narryer Terrane from the Youanmi Terrane. The two terranes have differing crustal reflectivities, suggesting that they are discrete blocks of continental crust (Fig. 5). Thus, the Yalgar Fault is interpreted to mark the site of a suture zone, with collision occurring at, or just before, c. 2750 Ma (see discussion in Korsch et al., 2013, this volume).

The Errabiddy Shear Zone represents the upper crustal portion of the suture zone between the Glenburgh and Narryer terranes, although the Cardilya Fault is not imaged in seismic line 11GA-SC1. Collision and suturing took place during the c. 2005–1950 Ma Glenburgh Orogeny (Johnson et al., 2010, 2011b), which is also recorded by the uplift and retrogression of granulite facies rocks in the Narryer Terrane (Muhling, 1988). The shear zone represents a zone of imbrication and contains lithologies from both the Glenburgh and Narryer Terranes.

The Darling Fault and its northern extension, the Darling North Fault, represent the suture zone that separates the Pinjarra Orogen from the West Australian Craton. There is no evidence in the seismic data to indicate the presence of the Narryer Terrane, Glenburgh Terrane or Yarraquin Seismic Province crust beneath the Pinjarra Orogen, supporting the models of Myers (1990a), Bruguier et al. (1999), Cobb et al. (2001), Fitzsimons (2001, 2003) and Ksienzyk et al. (2012), that rocks of the Pinjarra Orogen formed in an allochthonous setting with regard to their current position against the West Australian Craton. The late Mesoproterozoic ages for high-grade metamorphism and deformation obtained from paragneisses within the Northampton Inlier (Ksienzyk et al., 2012), and of meta-igneous rocks from the Woodleigh 1 drill core (GSWA, unpublished data), suggest that collision and suturing of the Pinjarra Orogen to the West Australian Craton along the Darling – Darling North Faults took place sometime between c. 1300 and 1080 Ma.

The Badgeradda Basin

The Badgeradda Basin unconformably overlies rocks of the Narryer Terrane and, in the seismic section, is restricted to a small imbricate fault system bounded by the Badgeradda Fault in the west and the Meeberrie Fault in the east, and a small sliver immediately east of the Meeberrie Fault (Fig. 1). The package is about 1 s TWT (about 3 km) in thickness, but it is not evident which faults controlled deposition of the basin. The group is only gently deformed and was probably deposited after high-grade metamorphism of paragneisses in the Northampton Inlier, but before deposition of the Ordovician Tumblagooda Sandstone, which unconformably overlies it. Deposition of the Tumblagooda Sandstone also postdates the last movement on the Badgeradda Fault, indicating thrust movement on this fault sometime between c. 990 and 485 Ma.

Fault reactivation and deposition of the Southern Carnarvon Basin

The Madeline Fault postdates the Errabiddy structures, and separates the Glenburgh Terrane *sensu stricto* from imbricated Glenburgh Terrane – Narryer Terrane lithologies in the Errabiddy Shear Zone. It is well defined in aeromagnetic data, and appears to represent the southwestern extension of the Deadman Fault (Fig. 5), which has acted as a sinistral shear zone during the Mulka Tectonic Event at c. 570 Ma (Bodorkos and Wingate, 2007). During the Early Permian, the fault was reactivated as a south- to southeast-dipping extensional fault, forming the northern boundary of the Bogadi Half-graben, complementing and running subparallel to the Ballythanna Fault where it traverses the Byro Sub-Basin. The extensional offset seems to diminish towards the northeast, where the fault is masked by Permian sediments. To the west, the Permian fault deviates from the basement structure and swings into an easterly trend (Fig. 6).

The Darling Fault and its northern extension, the Darling North Fault, represent the suture zone that separates the Pinjarra Orogen from the West Australian Craton, and records a long tectonic history of movement. Based on our structural interpretations of aeromagnetic and gravity data, and surface geology, at some stage it acted as a significant sinistral strike-slip fault. This is indicated by the change of trend of the Errabiddy Shear Zone into a southwest to south-southwest direction, which is interpreted to reflect drag along the Darling North Fault. The drag is most pronounced for the Errabiddy structures, suggesting an older period of sinistral shearing, prior to the formation of the Madeline and Badgeradda faults. The major Phanerozoic movement along the Ballythanna and Meeberrie Faults was during the Permian, when these structures controlled the sedimentation of the Bogadi Half-graben and the Booka Half-graben of the Byro Sub-basin. Accordingly, they crosscut and offset all previous structures (Fig. 5). In the seismic data, both structures are interpreted to transect the crust, which may indicate an earlier history of movement.

Petroleum potential of the Southern Carnarvon Basin

Ghori (1999) found excellent to fair source-rock intervals within the Permian succession of the Merlinleigh Sub-basin, and also in thin intervals within the Silurian Dirk Hartog Group and the Upper Devonian Gneudna Formation on the Gascoyne Platform to the north of the seismic line. Total organic carbon (TOC) content within the Gneudna Formation is up to about 13%, and up to 16% within the Permian in those sub-basins (Ghori, 1999; Mory et al, 2003). The Permian, and possibly also the older, units extend into the Byro Sub-basin, implying that it has at least fair hydrocarbon-generating potential. Low maturities across much of the Gascoyne Platform indicate it could not have generated significant quantities of hydrocarbons. Nevertheless, it is feasible that there has been migration of hydrocarbons from the Permian depocentres into fault traps along the eastern margin of the Gascoyne Platform. In the Byro Sub-basin, small fault-related traps, especially along the Ballythanna Fault, may also be prospective. Post-Permian structures, however, are likely to have compromised the integrity of such conventional plays, implying the more favourable exploration targets are shale-gas prospects within the Permian succession.

Summary

In our interpretation of seismic line 11GA-SC1, we have investigated the crustal architecture of an area which transects the western margin of the West Australian Craton. It allows tracking the evolution of major structures that control the architecture of the basement and the economically significant overlying Southern Carnarvon Basin through time, and greatly improves the confidence in the placement and lateral extent of these structures. The Byro Sub-basin of the Southern Carnarvon Basin is shown to consist of two half-graben, both of which contain two major sedimentary packages: a Permian package unconformably overlying an Ordovician to Devonian one. The angular unconformity resulted from deformation and erosion in the Carboniferous during the Alice Springs Orogeny. The preliminary interpretation unmasks the Darling Fault – Darling North Fault system as the suture between the West Australian Craton and the Pinjarra Orogen. It also suggests that the Ballythanna and Meeberrie faults are crustal-scale faults with a pre-Phanerozoic history. They are rooted in the Darling North Fault (Fig. 5), and converge and merge to the north of the seismic line. In the Permian, they were reactivated as extensional structures. The change of trend of the structural corridor of the Errabiddy Shear Zone from east–west into a southwest to south-southwest direction is interpreted to be caused by bending during sinistral strike-slip faulting along the Darling North Fault.

Acknowledgements

This paper forms part of a collaborative project between Geoscience Australia and the Geological Survey of Western Australia. We thank the following for their contributions to the project: Jenny Maher, for project management during the planning, acquisition and processing phase of the seismic data; Narelle Neumann and Tristan Kemp for project management during the interpretation phase of the project; Lindsay Hight and Weiping Zhang for producing the maps and digital versions of the interpretations of the seismic sections, respectively; and Narelle Neumann for reviewing this extended abstract. RJK, LKC and RSB publish with permission of the Chief Executive Officer, Geoscience Australia.

References

- Bodorkos, S and Wingate, MTD 2007, The contribution of geochronology to GSWA's mapping programs: current perspectives and future directions, in GSWA 2007 extended abstracts: promoting the prospectivity of Western Australia: Geological Survey of Western Australia, Record 2007/2, p. 10–11.
- Bruguier, O, Bosch, D, Pidgeon, RT, Byrne, DI and Harris, LB 1999, U–Pb chronology of the Northampton Complex, Western Australia – evidence for Grenvillean sedimentation, metamorphism and deformation and geodynamic implications: Contributions to Mineralogy and Petrology v. 136, p. 258–272.
- Carr, LK, Korsch, RJ, Mory, AJ, Hocking, RM, Marshall, SK, Costelloe, RD, Holzschuh, J and Maher, JL 2012, Structural and stratigraphic architecture of Australia's frontier onshore sedimentary basins: the Western Officer and Southern Carnarvon basins, Western Australia: APPEA Journal and Conference Proceedings, v. 52, 4p (CD-ROM).
- Cobb, MM, Cawood, PA, Kinny, PD and Fitzsimons, ICW 2001, SHRIMP U–Pb zircon ages from the Mullingarra Complex, Western Australia: isotopic evidence for allochthonous blocks in the Pinjarra Orogen and implications for East Gondwana assembly, in 2001: A structural odyssey: Geological Society of Australia, Abstracts 64, p. 21–22.
- Condon, MA 1965, The geology of the Carnarvon Basin, Western Australia, Part 1: Pre-Permian stratigraphy: Bureau of Mineral Resources, Australia, Bulletin 77, 82p.
- Clowes, RM and Oueity, J 2010, The nature of the Moho transition in NW Canada from combined near-vertical and wide-angle seismic reflection studies, in 14th International Symposium on Deep Seismic Profiling of the Continents and their Margins compiled by DM Finlayson: Geoscience Australia, Record 2010/24, p. 40.
- Costelloe, RD 2013, 2011 Southern Carnarvon seismic survey: acquisition and processing, in Youanmi and Southern Carnarvon seismic and magnetotelluric (MT) workshop 2013 compiled by S Wyche, TJ Ivanic and I Zibra: Geological Survey of Western Australia, Record 2013/6, p. 7–12.
- Fitzsimons, ICW 2001, The Neoproterozoic evolution of Australia's western margin. Geological Society of Australia Abstracts 65, 39–42.
- Fitzsimons, ICW 2003, Proterozoic basement provinces of southern and south-western Australia, and their correlation with Antarctica, in Proterozoic East Gondwana: Supercontinent Assembly and Breakup edited by M Yoshida, BF Windley and S Dasgupta: Geological Society, London, Special Publications 206, p. 93–130.

- Gessner, K, Jones, T, Goodwin, JA, Gallardo, LA, Milligan, PR, Brett, J and Murdie, R 2013, Interpretation of magnetic and gravity data across the South Carnarvon Basin, and the Narryer and Youanmi Terranes, *in* Youanmi and Southern Carnarvon seismic and magnetotelluric (MT) workshop 2013 *compiled by* S Wyche, TJ Ivanic and I Zibra: Geological Survey of Western Australia, Record 2013/6, p. 65–77.
- Ghori, KAR 1999, Silurian–Devonian petroleum source-rock potential and thermal history, Carnarvon Basin, Western Australia: Geological Survey of Western Australia, Report 72, 88p.
- Ghori, KAR, Mory, AJ and Iasky, RP 2005, Modeling petroleum generation in the Paleozoic of the Carnarvon Basin, Western Australia: Implications for prospectivity: American Association of Petroleum Geologists, Bulletin, v. 89, p. 27–40
- Glikson, AY, Mory, AJ, Iasky, RP, Pirajno, F, Golding, SD and Uysal, IT 2005, Woodleigh, Southern Carnarvon Basin, Western Australia: history of discovery, Late Devonian age, and geophysical and morphometric evidence for a 120 km-diameter impact structure: Australian Journal of Earth Sciences, v. 52, p. 545–553.
- Hammer, PTC and Clowes, RM 1997, Moho reflectivity patterns – a comparison of Canadian Lithoprobe transects: Tectonophysics, v. 269, p. 179–198.
- Hocking, RM, 1994, Subdivisions of Western Australian Neoproterozoic and Phanerozoic sedimentary basins: Geological Survey of Western Australia, Record 1994/4, 84p.
- Hocking, RM, Moors, HT and van de Graaff, WJE 1987, Geology of the Carnarvon Basin, Western Australia: Geological Survey of Western Australia, Bulletin 133, 289p.
- Iasky, RP, Mory, AJ, Ghori, KAR and Shevchenko, SI, 1998, Structure and petroleum potential of the southern Merlinleigh Sub-basin, Carnarvon Basin, Western Australia: Geological Survey of Western Australia, Report 61, 63p.
- Iasky, RP and Mory, AJ 1999, Geology and petroleum potential of the Gascoyne Platform, structure, Southern Carnarvon Basin, Western Australia: Geological Survey of Western Australia, Report 69, 46p.
- Iasky, RP, Mory, AJ and Blundell, KA 2001, The geophysical interpretation of the Woodleigh impact structure, Southern Carnarvon Basin, Western Australia: Geological Survey of Western Australia, Report 79, 41p.
- Johnson, SP, Sheppard, S, Rasmussen, B, Wingate, MTD, Kirkland, CL, Muhling, JR, Fletcher, IR and Belousova, E 2010, The Glenburgh Orogeny as a record of Paleoproterozoic continent–continent collision: Geological Survey of Western Australia, Record 2010/5, 54p.
- Johnson, SP, Cutten, HN, Tyler, IM, Korsch, RJ, Thorne, AM, Blay, OA, Kennett, BLN, Blewett, RS, Joly, A, Dentith, MC, Aitken, ARA, Goodwin, JA, Salmon, M, Reading, A, Boren, G, Ross, J, Costelloe, RD and Fomin, T 2011d, Preliminary interpretation of deep seismic reflection lines 10GA-CP2 and 10GA-CP3: crustal architecture of the Gascoyne Province, and Edmund and Collier Basins, *in* Capricorn Orogen seismic and magnetotelluric (MT) workshop 2011: extended abstracts *edited by* SP Johnson, AM Thorne and IM Tyler: Geological Survey of Western Australia, Record 2011/25, p. 49–60.
- Johnson, SP, Sheppard, S, Rasmussen, B, Wingate, MTD, Kirkland, CL, Muhling, JR, Fletcher, IR and Belousova, EA 2011b, Two collisions, two sutures: punctuated pre-1950 Ma assembly of the West Australian Craton during the Ophthalmian and Glenburgh Orogenies: Precambrian Research, v. 189, no. 3–4, p. 239–262.
- Johnson, SP, Sheppard, S, Wingate, MTD, Kirkland, CL and Belousova, EA 2011c, Temporal and hafnium isotopic evolution of the Glenburgh Terrane basement: an exotic crustal fragment in the Capricorn Orogen: Geological Survey of Western Australia, Report 110, 27p.
- Johnson, SP, Thorne, AM and Tyler, IM (editors) 2011a, Capricorn Orogen seismic and magnetotelluric (MT) workshop 2011: extended abstracts: Geological Survey of Western Australia, Record 2011/25, 120p.
- Korsch, RJ, Huston, DL, Henderson, RA, Blewett, RS, Withnall, IW, Fergusson, CL, Collins, WJ, Saygin, E, Kositsin, N, Meixner, AJ, Chopping, R, Henson, PA, Champion, DC, Hutton, LJ, Wormald, R, Holzschuh, J and Costelloe, RD 2012, Crustal architecture and of North Queensland, Australia: insights from deep seismic reflection profiling: Tectonophysics, v. 572–573, p. 76–99.
- Korsch, RJ, Blewett, RS, Wyche, S, Zibra, I, Ivanic, TJ, Doublier, MP, Romano, SS, Pawley, MJ, Johnson, SP, Van Kranendonk, MJ, Jones, LEA, Kositsin, N, Gessner, K, Hall, CE, Chen, SF, Patisson, N, Kennett, BLN, Jones, T, Goodwin, JA, Milligan, PR and Costelloe, RD 2013, Geodynamic implications of the Youanmi and Southern Carnarvon deep seismic reflection surveys: a ~1300 km traverse from the Pinjarra Orogen to the eastern Yilgarn Craton, *in* Youanmi and Southern Carnarvon seismic and magnetotelluric (MT) workshop 2013 *compiled by* S Wyche, TJ Ivanic and I Zibra: Geological Survey of Western Australia, Record 2013/6, p. 147–166.
- Kriegsman, LM, Moller, A and Nelson, DR 1999, P–T–t–D path and detrital zircon geochronology of the Northampton Block, Western Australia: a Mesoproterozoic, collision-induced foreland rift. European Union of Geosciences Conference EUG 10, Journal of Conference Abstracts, v. 4(1), p. 433.
- Ksienzyk, AK, Jacobs, J, Boger, SD, Kosler, J, Sircombe, KN and Whitehouse, MJ 2012, U–Pb ages of metamorphic monazite and detrital zircon from the Northampton Complex: evidence of two orogenic cycles in Western Australia: Precambrian Research, v. 198–199, p. 37–50.
- le Blanc Smith, G 1990, A review of the coal resources in Western Australia: Geological Survey of Western Australia, Basins and Fossil Fuels Report 1990/3 (unpublished).
- Martin, DM and Morris, PA 2010, Tectonic setting and regional implications of ca 2.2 Ga mafic magmatism in the southern Hamersley Province, Western Australia: Australian Journal of Earth Sciences, v. 57, no. 7, p. 911–931.
- Mory, AJ, Iasky, RP and Shevchenko, SI 1998, The Coolcalalaya Sub-basin — a forgotten frontier ‘between’ the Perth and Carnarvon Basins, W.A., *in* The sedimentary basins of Western Australia 2 *edited by* PG Purcell and RR Purcell: Petroleum Exploration Society of Australia Symposium, Perth, WA, 1998, Proceedings, p. 614–622.
- Mory, AJ, Pirajno, F, Glikson, AY and Coker, J (compilers) 2001, GSWA Woodleigh 1, 2, and 2a well completion report, Woodleigh impact structure, Southern Carnarvon Basin, Western Australia: Geological Survey of Western Australia, Record 2001/6, 147p.
- Mory, AJ, Iasky, RP and Ghori, KAR 2003, A summary of the geological evolution and petroleum potential of the Southern Carnarvon Basin, Western Australia: Geological Survey of Western Australia, Report 86, 26p.
- Muhling, JR 1998, The nature of Proterozoic reworking of early Archaean gneisses, Mukalo Creek Area, Southern Gascoyne Province, Western Australia: Precambrian Research, v. 40–41, p. 341–362.
- Myers, JS 1990a, Precambrian tectonic evolution of part of Gondwana, southwestern Australia: Geology, v. 18, p. 537–540.
- Myers, JS 1990b, Western Gneiss Terrane, *in* Geology and mineral resources of Western Australia: Geological Survey of Western Australia, Memoir 3, p. 13–32.
- Myers, JS 1997, Byro, WA, Sheet SG 50-10 (2nd edition): Geological Survey of Western Australia, 1:250 000 Geological Series.

- Occhipinti, SA, Sheppard, S, Passchier, C, Tyler, IM and Nelson, DR 2004, Palaeoproterozoic crustal accretion and collision in the southern Capricorn Orogen: the Glenburgh Orogeny: *Precambrian Research*, v. 128, p. 237–255.
- Perry, WJ and Dickins, JM 1960, The geology of the Badgeradda area, Western Australia. Bureau of Mineral Resources, Report 46, 38p.
- Playford, PE, Cope, RN, Cockbain, AE, Low, GH and Lowry, DC 1975, Phanerozoic, in *The geology of Western Australia: Geological Survey of Western Australia, Memoir 2*, p. 223–433.
- Romano, SS, Ivanic, TJ, Korsch, RJ, Wyche, S, Van Kranendonk, MJ, Jones, LEA, Zibra, I, Blewett, RS, Jones, T, Milligan, PR, Costelloe, RD, Doublier, MP, Pawley, MJ, Gessner, K, Hall, CE, Patisson, N, Kennett, BLN and Chen, SF 2013, Preliminary interpretation of the northern section of deep seismic line 10GA-YU1: Narryer Terrane to Murchison Domain of the Youanmi Terrane, in *Youanmi and Southern Carnarvon seismic and magnetotelluric (MT) workshop 2013 compiled by S Wyche, TJ Ivanic and I Zibra: Geological Survey of Western Australia, Record 2013/6*, p. 123–128.
- Sheppard, S, Occhipinti, SA and Tyler, IM 2004, A 2005–1970 Ma Andean-type batholith in the southern Gascoyne Complex, Western Australia: *Precambrian Research*, v. 128 (Assembling the Palaeoproterozoic Capricorn Orogen), p. 257–277.
- Spaggiari, CV 2007, Structural and lithological evolution of the Jack Hills greenstone belt, Narryer Terrane, Yilgarn Craton: *Geological Survey of Western Australia, Record 2007/3*, 49p.
- van de Graaff, WJE, Hocking, RM, and Denman, PD 1977, Revised stratigraphic nomenclature and interpretation in the East-Central Carnarvon Basin, W.A.: Geological Survey of Western Australia, Annual Report 1976, 37–39.
- Wilde, SA and Spaggiari C, 2007, The Narryer Terrane, Western Australia: a review, in *Earth's oldest rocks edited by MJ Van Kranendonk, RH Smithies and VC Bennett: Developments in Precambrian Geology*, v. 15, p. 275–304.
- Wyche, S, Pawley, MJ, Chen, SF, Ivanic, TJ, Zibra, I, Van Kranendonk, MJ, Spaggiari, CV and Wingate MTD 2013, Geology of the northern Yilgarn Craton, in *Youanmi and Southern Carnarvon seismic and magnetotelluric (MT) workshop 2013 compiled by S Wyche, TJ Ivanic and I Zibra: Geological Survey of Western Australia, Record 2013/6*, p. 33–63.
- Zibra, I, Gessner, K, Korsch, RJ, Blewett, RS, Jones, T, Milligan, PR, Jones, LEA, Wyche, S, Doublier, MP, Hall, CE, Chen, SF, Romano, SS, Ivanic, TJ, Pawley, MJ, Patisson, N, Kennett, BLN and Van Kranendonk, MJ 2013, Preliminary interpretation of deep seismic lines 10GA-YU3 and the southeastern part of 10GA-YU1: Murchison Domain of the Youanmi Terrane, in *Youanmi and Southern Carnarvon seismic and magnetotelluric (MT) workshop 2013 compiled by S Wyche, TJ Ivanic and I Zibra: Geological Survey of Western Australia, Record 2013/6*, p. 113–22.

Geodynamic implications of the Youanmi and Southern Carnarvon deep seismic reflection surveys: a ~1300 km traverse from the Pinjarra Orogen to the eastern Yilgarn Craton

by

RJ Korsch¹, RS Blewett¹, S Wyche, I Zibra, TJ Ivanic, MP Doublier, SS Romano, M Pawley², SP Johnson, MJ Van Kranendonk³, LEA Jones, N Kositsin¹, K Gessner, CE Hall, SF Chen, N Patison, BLN Kennett⁵, T Jones¹, JA Goodwin¹, P Milligan¹, and RD Costelloe¹

Introduction

In May and June 2010, 695 line kilometres of vibroseis-source, deep seismic reflection, gravity and magnetotelluric (MT) data were acquired along three traverses (10GA-YU1, 10GA-YU2, and 10GA-YU3), collectively referred to as the Youanmi seismic survey. The lines started in the northwestern part of the Archean Yilgarn Craton, in the Narryer Terrane, and crossed the Murchison and Southern Cross Domains of the Youanmi Terrane, before ending to the east of the Waroonga Fault in the westernmost part of the Kalgoorlie Terrane, a component of the Eastern Goldfields Superterrane (Frontispiece 1; Plate 1). The survey was funded through the Western Australian Government's Royalties for Regions Exploration Incentive Scheme (EIS), with acquisition, processing and interpretation being managed by Geoscience Australia (GA) as part of its Onshore Energy Security Program.

A key aim of the Youanmi seismic survey was to image the crustal architecture in the region. Specific aims to understand the regional geodynamics were to:

- image deep structure in the Narryer Terrane, the oldest component of the Yilgarn Craton, and the region which contains the oldest known crust in Australia
- image the contact between the Narryer Terrane and the adjacent, highly mineralized Murchison Domain of the Youanmi Terrane

- compare the nature, orientation, and crustal penetration of mineralized and unmineralized structures
- image the Ida Fault, the boundary between the Youanmi Terrane and the Kalgoorlie Terrane in the Eastern Goldfields Superterrane, and compare the deep structure in the adjacent terranes
- link with previously acquired deep-crustal seismic traverses in the Eastern Goldfields Superterrane.

In May 2011, 259 line kilometres of vibroseis-source, deep seismic reflection data were acquired along a single east-west traverse (11GA-SC1) across the Paleozoic Southern Carnarvon Basin and the Archean Narryer Terrane of the northwest Yilgarn Craton, and is referred to as the Southern Carnarvon seismic survey. The traverse went from near the Milly Milly homestead in the east (on the Narryer Terrane) to the North West Coastal Highway in the west (on the Gascoyne Platform of the Southern Carnarvon Basin) (Frontispiece 1; Plate 1). In the subsurface beneath the Southern Carnarvon Basin, the traverse crossed basement of the Paleoproterozoic Yarlalweelor Gneiss Complex – Errabiddy Shear Zone, the Glenburgh Terrane of the Gascoyne Province, and the Mesoproterozoic–Neoproterozoic Pinjarra Orogen. The seismic line was acquired by Geoscience Australia, as part of its Onshore Energy Security Program, in conjunction with the Geological Survey of Western Australia, as part of its Exploration Incentive Scheme.

The Southern Carnarvon seismic line was designed, in part, to evaluate:

- the architecture of the Southern Carnarvon Basin, and, in particular the Byro Sub-basin
- the architecture and deep structure of the Archean Narryer Terrane, in the northwest Yilgarn Craton, which is the oldest terrane in the craton, and the region which contains the oldest known crust in Australia
- the relationship, in the subsurface beneath the Southern Carnarvon Basin, between the Archean

1 Minerals and Natural Hazards Division, Geoscience Australia, GPO Box 378, Canberra ACT 2601

2 Geological Survey of South Australia, Department of Manufacturing Innovation Trade Resources and Energy, Level 4, 101 Grenfell Street, Adelaide SA 5000

3 School of Biological, Earth and Environmental Sciences, University of New South Wales, Kensington NSW 2052

4 Energy Division, Geoscience Australia, GPO Box 378, Canberra ACT 2601

5 Research School of Earth Sciences, Australian National University, Canberra ACT 0200

Narryer Terrane, the Yarlalweelor Gneiss Complex-Errabiddy Shear Zone, the Glenburgh Terrane, and the Pinjarra Orogen.

Companion papers in this volume present summaries of the geological evolution of the region (Wyche et al., 2013, this volume), interpretations of the four seismic lines (Zibra et al., 2013a,b, this volume; Ivanic et al., 2013a, this volume; Romano et al., 2013, this volume; Korsch et al., 2013, this volume), and discussions of the potential field geophysics (Gessner et al., 2013, this volume) and magnetotellurics (Milligan, 2013, this volume). The approximate northwest-southeast to east-west orientation of the seismic lines is essentially perpendicular to the major domains and structures in the region (Frontispiece 1–3; Plate 1), and provides crustal-scale geometries which can be compared with existing geological interpretations. Overall, the crust in the vicinity of the seismic sections has variable reflectivity, with some parts of the section containing strong reflections, and other areas having very low reflectivity (Figs 1–4).

Here, we discuss some of the geodynamic implications which arise from interpretation of the new deep seismic reflection data obtained during the Youanmi and Southern Carnarvon seismic surveys. Of particular interest are the relationships at a crustal scale between the terranes within the Yilgarn Craton, and the relationship of the Yilgarn Craton to younger provinces to its north and west. For example, are the crustal elements allochthonous? Is there evidence for sutures between the terranes within the Yilgarn Craton? Is there evidence for a suture between the Pinjarra Terrane and the Narryer Terrane? The current surveys build on the existing network of deep-crustal seismic surveys, and will improve the understanding of the crustal structure and geodynamics of Western Australia.

Moho

In the region of the Youanmi and Southern Carnarvon seismic surveys, the Moho is mostly imaged as a sharp discontinuity, and is interpreted to occur at the base of strongly reflective packages, the nonreflective material below which is considered to represent the upper mantle (Figs 1–4). In places, however, particularly on line 11GA-SC1, the Moho is poorly imaged, and the transition from crust to mantle appears gradational.

In the Youanmi seismic sections, the Moho has a highly reflective crust–mantle transition zone about 0.3–1.0 s TWT (approximately 1–3 km) thick, which is a persistent feature across most parts of the seismic lines (e.g. Zibra et al., 2013a,b, this volume; Romano et al., 2013, this volume) (Figs 1–3). A highly reflective crust–mantle transition zone is not confined to Archean rocks, as it is a relatively common feature seen in other seismic surveys

in younger Proterozoic and Paleozoic terranes elsewhere (e.g. North Queensland, Korsch et al., 2012; Canada, Hammer and Clowes, 1997; Clowes and Oueity, 2010). In line 11GA-SC1, however, the transition zone is only developed near each end of the line and is absent in the central part (Fig. 4). The character of the Moho, as imaged on the Youanmi seismic lines, is in strong contrast to what is observed on the lines from the Capricorn survey to the north where, in general, the Moho was not well imaged (Korsch et al., 2011a) and was difficult to interpret in many places. Beneath the Archean Pilbara Craton, for example, the Moho is very poorly defined.

Over the entire length of the Youanmi seismic survey, the Moho is extraordinarily flat and sharp, at approximately 11 s two-way travel time (TWT; about 33 km depth). There are two areas where the apparent reflectivity of the Moho is only weak. One area is on line 10GA-YU1, between CDPs 8100 and 9400 (Fig. 1), approximately below the Weld Range greenstone belt, and the other is at the eastern end of Line 10GA-YU2, between CDPs 14900 and 16000 (Fig. 2), immediately west of the Ida Fault, approximately below the Waroonga Shear Zone.

In the Southern Carnarvon seismic line, the Moho is interpreted to occur at the base of a weakly to moderately reflective package, below which the nonreflective material is considered to represent the upper mantle (Fig. 4). Compared to the Moho interpreted on the Youanmi seismic lines (Figs 1–3), the interpreted Moho is not flat, varying from a depth of about 10 s TWT (approximately 30 km) at the western end of the line and about 11.6 s TWT (approximately 35 km) at the eastern end of the line, to >13 s TWT (nearly 40 km) beneath the Byro Sub-basin, at about CDP 8000 (Fig. 4).

Crustal architecture

In the region of the Youanmi and Southern Carnarvon seismic sections, the upper crust can be subdivided into several discrete provinces, domains and basins, based principally on surface geological mapping and the interpretation of potential-field data (Fig. 5). By comparison, the middle to lower crust, in the vicinity of the Youanmi seismic survey, appears to have a very consistent seismic character, over a distance of nearly 600 km, which is very different in seismic character to that imaged in the upper crust. Thus, we term the middle to lower crust, beneath the Youanmi Terrane, the Yarraquin Seismic Province (new name, after Yarraquin well), and we describe it below. Following Korsch et al. (2010), we use the term ‘seismic province’ to refer to a discrete volume of middle to lower crust, which cannot be traced to the surface, and whose crustal reflectivity is different to that of laterally or vertically adjoining provinces.

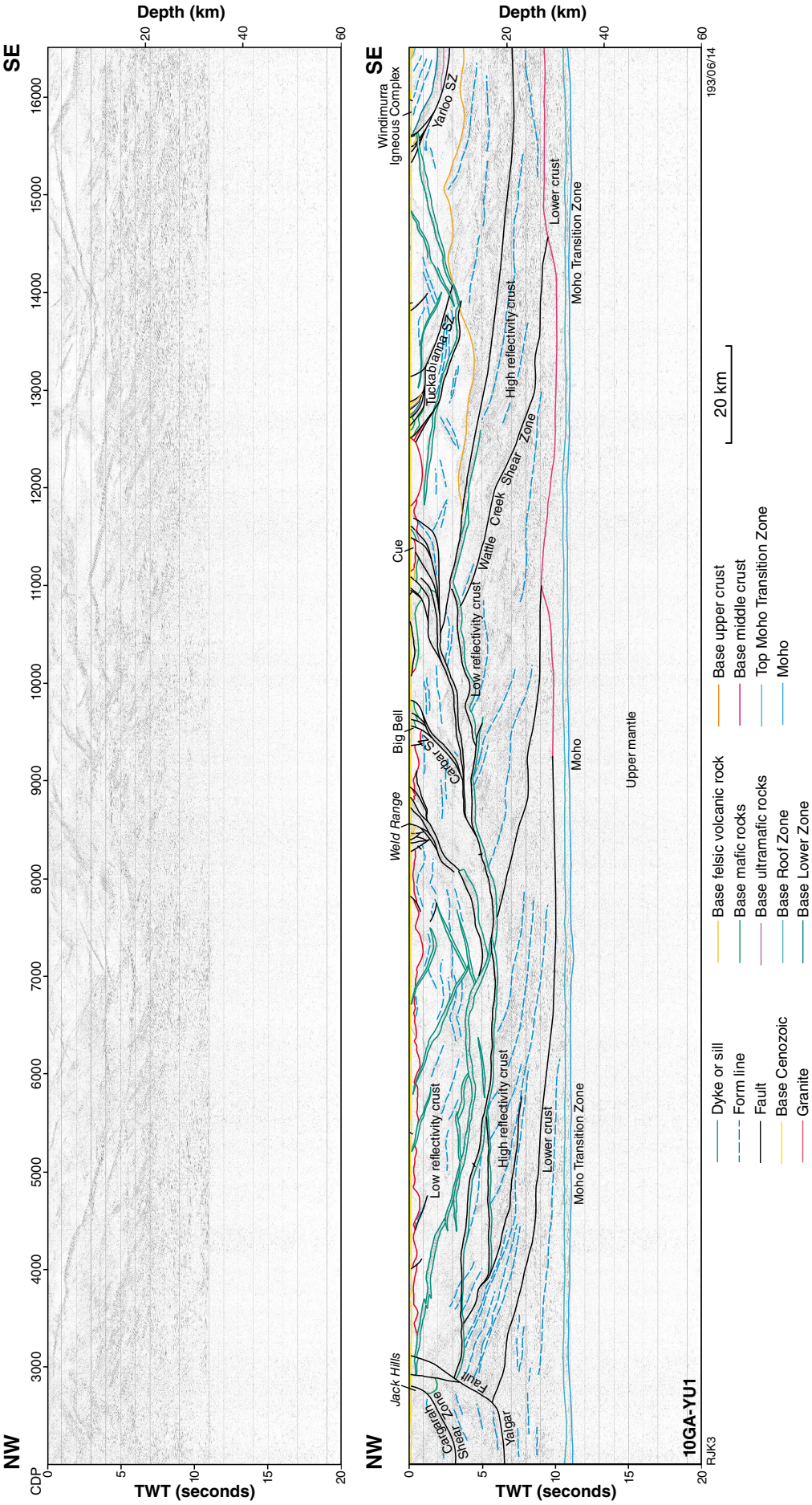


Figure 1. Migrated section for seismic line 10GA-YU1, showing both uninterpreted and interpreted versions. Display is to 60 km depth, and shows vertical scale equal to the horizontal scale, assuming a crustal velocity of 6000 ms⁻¹ for the entire section.

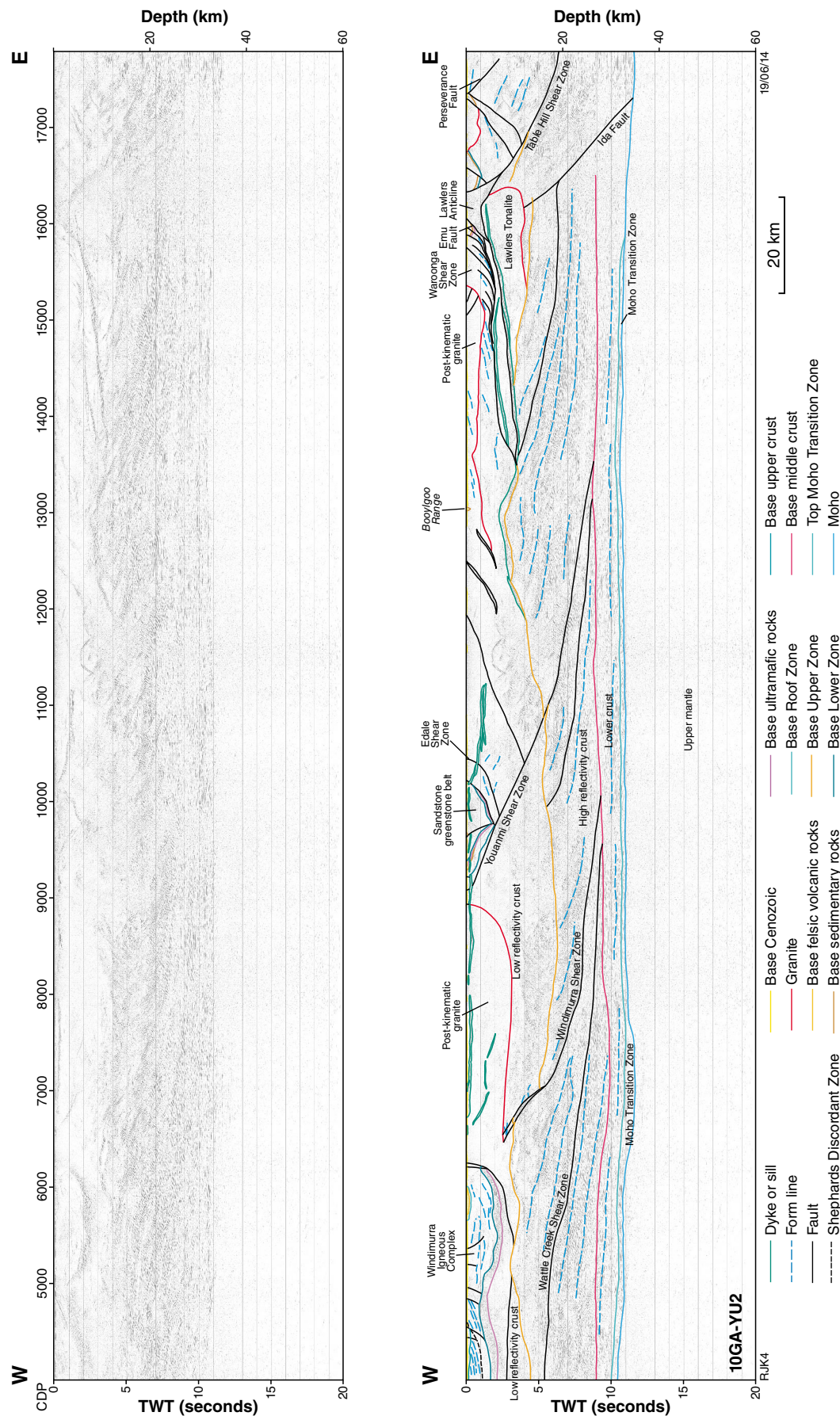


Figure 2. Migrated section for seismic line 10GA-YU2, showing both uninterpreted and interpreted versions. Display is to 60 km depth, and shows vertical scale equal to the horizontal scale, assuming a crustal velocity of 6000 ms⁻¹.

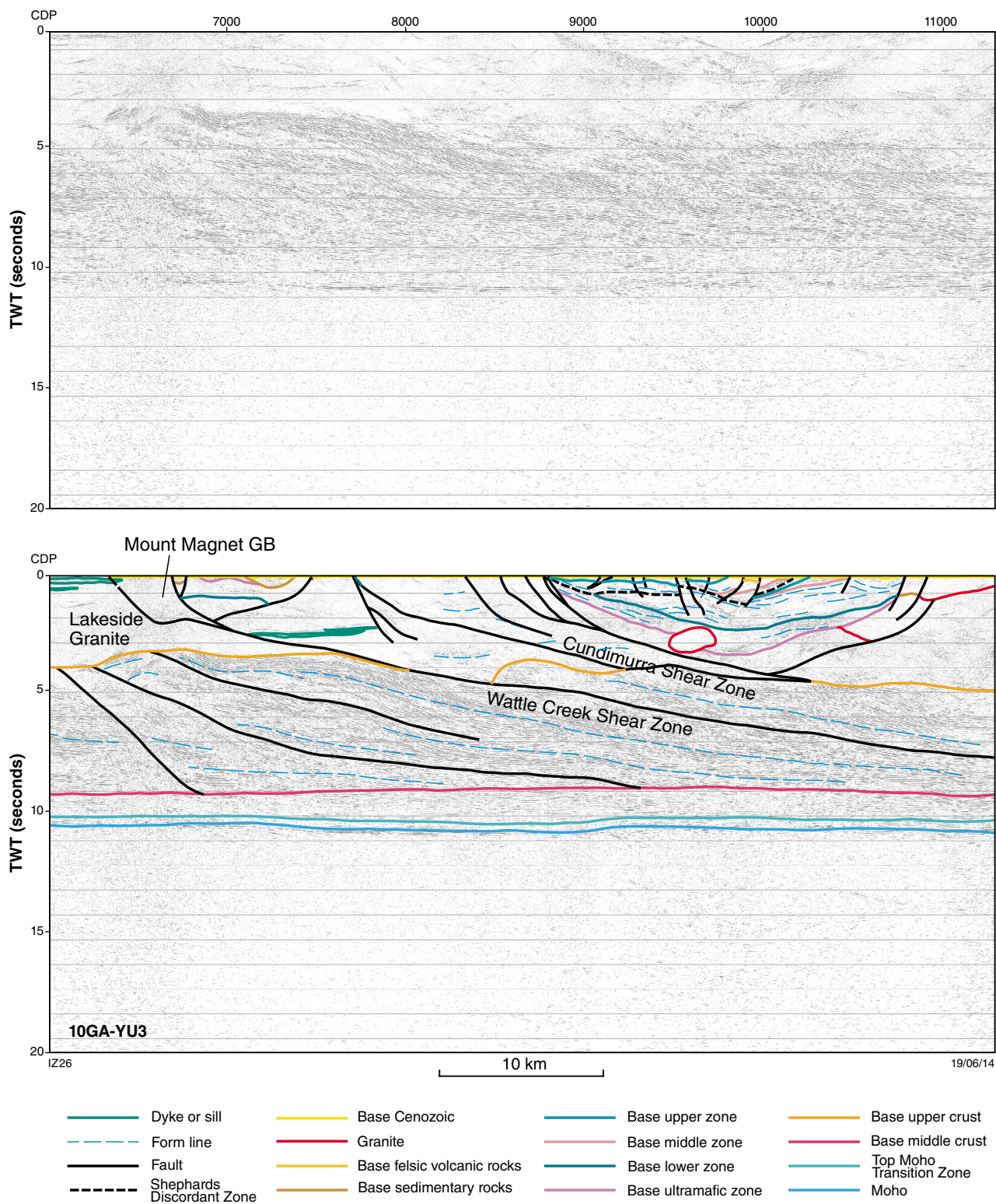


Figure 3. Migrated section for seismic line 10GA-YU3, showing both uninterpreted and interpreted versions. Display is to 60 km depth, and shows vertical scale equal to the horizontal scale, assuming a crustal velocity of 6000 ms⁻¹.

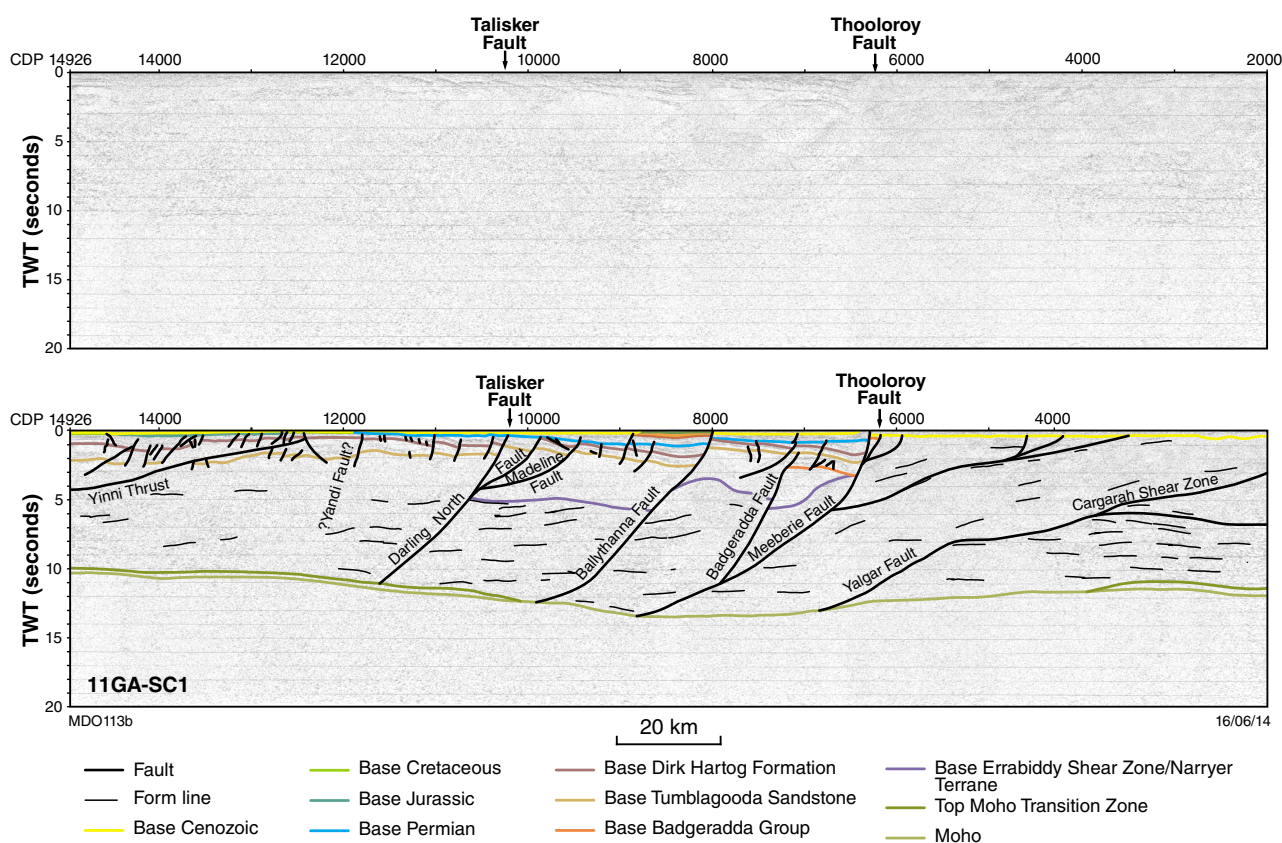


Figure 4. Migrated section for seismic line 11GA-SC1, showing both uninterpreted and interpreted versions. Display is to 60 km depth, and shows vertical scale equal to the horizontal scale, assuming a crustal velocity of 6000 ms⁻¹.

Yilgarn Craton

The Yilgarn Craton in Western Australia is a large (1000 × 1000 km) Archean granite–greenstone terrain which forms a major part of the West Australian Craton and represents well over one billion years of craton formation. The craton has been subdivided into several terranes (Frontispiece 1; Cassidy et al., 2006; Pawley et al., 2012), and consists of metamorphosed mafic and felsic volcanic and intrusive rocks, and metasedimentary units, intruded by granite and gneissic granite, all of which formed mainly between c. 3050 and 2620 Ma (Cassidy et al., 2006). In the northwest, however, in the Narryer Terrane, there are rocks which are c. 3730 Ma (Kinny et al., 1988), and are the oldest known rocks in Australia. Detrital zircons up to c. 4404 Ma also occur in the Narryer Terrane (Wilde et al., 2001). These are the oldest known terrestrial material on Earth (Froude et al., 1983) and have been the subject of intense study (see summary in Cavosie et al., 2007). Detrital zircons up to 4350 Ma have been described from the Southern Cross Domain of the Youanmi Terrane (Wyche et al., 2004).

Narryer Terrane

The Narryer Terrane has been imaged on seismic lines 11GA-SC1 (Korsch et al., 2013, this volume) and

10GA-YU1 (Romano et al., 2013, this volume), providing a cross section across the terrane between the Pinjarra Orogen in the west and the Youanmi Terrane in the east. The northern margin of the terrane against the Gascoyne Province was imaged on the previously acquired seismic line 10GA-CP3 (Johnson et al., 2011a).

At the surface, the Yalgar Fault is the interpreted boundary between the Narryer Terrane and the Youanmi Terrane. This fault is known to have been active in the Proterozoic (e.g. Spaggiari, 2007) and is interpreted on line 10GA-YU1 as a fault which is listric to the northwest, flattening at a depth of about 6.5 s TWT (approximately 20 km) (Fig. 1). We have jump-tied the fault across the 28 km gap to line 11GA-SC1, where it is interpreted to be subhorizontal, before ramping down to meet the Moho at about CDP 6800 (Fig. 4). We interpret the western boundary of the Narryer Terrane to be the Darling North Fault which, in seismic line 11GA-SC1, is a west-dipping, crustal-scale fault at CDP 9860, cutting through almost the entire crust to the Moho (Fig. 4).

In the seismic sections, the Narryer Terrane is only moderately to weakly reflective, with the reflections having a predominant apparent dip to the northwest in line 10GA-YU1 (Fig. 1) and an apparent dip to the west in line 11GA-SC1 (Fig. 4). Overall, however, the upper 3 s TWT of the Narryer Terrane are typically more reflective than the upper 3 s TWT of the Youanmi Terrane to the southeast.

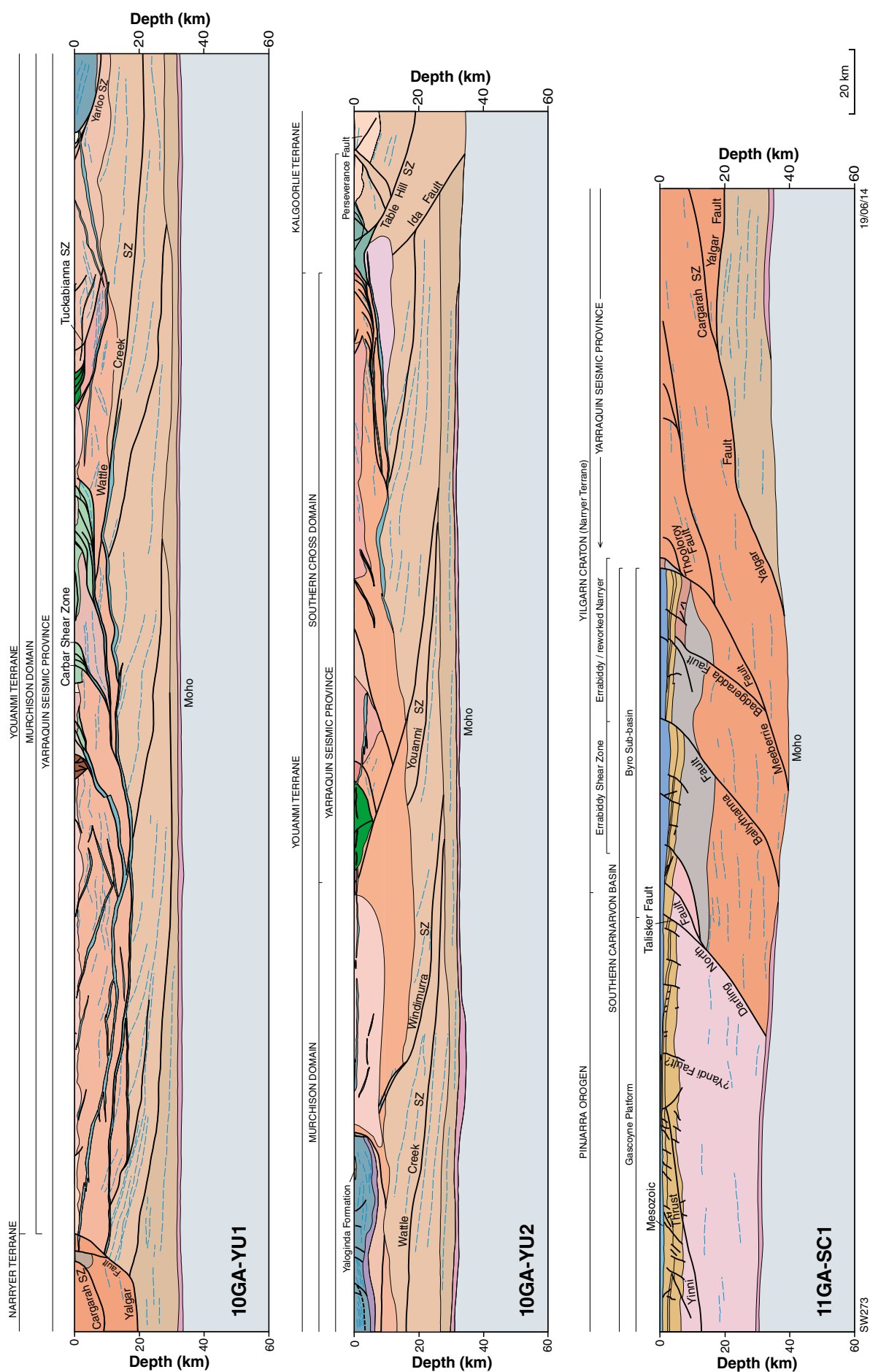


Figure 5. Geological interpretation of seismic lines 11GA-SC1, 10GA-YU1 and 10GA-YU2, showing the distribution of terranes within the Yilgarn Craton and other key provinces and basins. For full Legend, see Plates 1B and 3.

Youanmi Terrane

All of seismic line 10GA-YU3 and most of lines 10GA-YU1 and 10GA-YU2 were located on the Youanmi Terrane (Frontispiece 1; Plate 1). In all three seismic sections, the crust is seen to consist of three layers:

- An upper crust which, in general, is only weakly to moderately reflective and quite variable in thickness, ranging from about 2.4 s TWT (approximately 7 km) at about CDP 15050 on line 10GA-YU1 (Fig. 1) to about 6.3 s TWT (approximately 19 km) at about CDP 8500 on line 10GA-YU2 (Fig. 2),
- A strongly reflective middle crust, within which the reflections are listric to the southeast and east, and soling onto the top of the lower crust (Figs 1–3). The middle crust is of variable thickness, ranging from about 3.5 s TWT (approximately 11 km) at about CDP 8800 on line 10GA-YU2 (Fig. 2) to about 7.3 s TWT (approximately 22 km) at about CDP 14300 on line 10GA-YU1 (Fig. 1),
- A relatively thin, moderately to strongly reflective lower crust (Figs 1–3), ranging from about 1.0 s TWT (approximately 3 km) thickness at about CDP 13800 on line 10GA-YU1 to about 5.5 s TWT (approximately 17 km) thickness at about CDP 2700 on line 10GA-YU1 (Fig. 1). At the base of the lower crust, there is a thin (approximately 1–3 km) crust–mantle transition zone which is highly reflective (see above).

Because of the very distinct change in the seismic character at the boundary between the upper and middle crust, we here confine the Youanmi Terrane (*sensu stricto*) to only the upper crust, which consists of the granite–greenstone units, and define its base as the contact between the relatively non-reflective upper crust and the package of strong reflections in the middle crust with listric apparent dips to the southeast or east. We combine the middle and lower crust into the Yarraquin Seismic Province (see below).

The Youanmi Terrane has been subdivided into the western Murchison Domain and the eastern Southern Cross Domain (Cassidy et al., 2006), the boundary being the Youanmi Shear Zone (CDP 9080 on seismic line 10GA-YU2, Fig. 2), which Cassidy et al. (2006) considered to be a relatively late structure. Seismically, the two domains appear indistinguishable, supporting the proposal by Wyche (2007) that the two domains are not allochthonous terranes, but are contiguous. Cassidy et al. (2006) considered that the Youanmi Terrane possibly represents the nucleus, or protocraton, onto which the Narryer Terrane and Eastern Goldfields Superterrane were accreted.

Key seismic features of the Youanmi Terrane, which are described in detail in Zibra et al. (2013a,b, this volume), Romano et al. (2013, this volume) and Ivanic et al. (2013a, this volume), are:

- several phases of granite and gneissic granite intrusions, which volumetrically form much of the

Youanmi Terrane. Although there are some granites with ages up to c. 3010 Ma, the majority are younger than c. 2720 Ma (Cassidy et al., 2006; Ivanic et al., 2012; Van Kranendonk et al., 2012). Seismically, the granites are typically weakly to non-reflective, with weak parallel reflections probably due to gneissic fabric in deformed granites. The post-tectonic, low-Ca granites are typically non-reflective and appear as thin sheets in the seismic profiles. Good examples are the Skinny Bore Granite, centred on about CDP 8000 on line 10GA-YU2 (Fig. 2) and The Bore Granite, centred on about CDP 14600 on line 10GA-YU2 (Fig. 2).

- greenstone belts, consisting of mafic and felsic volcanic successions and associated sedimentary rocks, are as old as c. 3000 Ma in the Youanmi Terrane (Pidgeon and Wilde, 1990; Van Kranendonk et al., 2012). The greenstone belts have variable seismic reflectivity and most seem to be related to faults that cut deep into the crust, such as the Weld Range greenstone belt, centred on about CDP 8400 on line 10GA-YU1 (Fig. 1), the Sandstone greenstone belt, centred on about CDP 9700 on line 10GA-YU2 (Fig. 2), and the Mount Magnet greenstone belt, centred on about CDP 7000 on line 10GA-YU3 (Fig. 3).
- Archean mafic–ultramafic intrusions, for example, the Windimurra Igneous Complex, dated at c. 2810 Ma (see Ivanic et al., 2010), and whose seismic architecture is described in detail by Ivanic et al. (2013a, this volume).

One of the most striking features in the Youanmi seismic lines is the presence of seismically highly reflective units, typically with gentle apparent dips, and consisting of a series of very strong, subparallel reflections characterized by a reversal in reflection polarity at the base compared with the top. These highly reflective units have a seismic velocity of about 6500 ms⁻¹, higher than the surrounds (Ivanic et al., 2013b, this volume). They are very similar in geometry and seismic character to dolerite sills in Sweden imaged in seismic sections and intersected in a deep bore hole (Juhlin, 1990), and to sills imaged in Canada (Welford and Clowes, 2004). They are best observed at the western end of line 11GA-YU1, where they have been interpreted to extend for distances of up to 90 km (Fig. 1), but are less common in seismic line 10GA-YU2 (Fig. 2). One gabbro sill which crops out near Sandstone (probably the sill interpreted at about CDP 10300 on line 10GA-YU2, Fig. 2) has a crystallization age of c. 1070 Ma (U–Pb SHRIMP date on baddeleyite and zircon, Wingate et al., 2008). The inferred sills are commonly intruded along shear zones, and commonly link into higher level splay faults (e.g. about CDP 15800 on line 10GA-YU2, Fig. 2). A subhorizontal shear zone, intruded by a sill, at about 5.5 s TWT depth between about CDPs 3900 to 5600 on line 10GA-YU1 (Fig. 1), has a sinistral (top to the northwest) sense of tectonic transport. A major sill has been emplaced at the contact between the Youanmi Terrane and the Yarraquin Seismic Province, and this sill (or sills) extends for a distance of over 180 km on line 10GA-YU1 (Fig. 1). The Youanmi Terrane has been intruded by an

extensive suite of mafic dykes (see Frontispiece 2), but they are typically subvertical, and hence have not been imaged in the seismic sections.

Neodymium model ages for granites from the Youanmi Terrane have average crustal ages of c. 3200–3100 Ma (Champion and Cassidy, 2007, 2008). Within the Murchison Domain, however, there is a north-northeast trending belt, centred on Mount Magnet, which has slightly younger Nd model ages of c. 3100–2950 Ma. This implies the addition of juvenile material into the crust, possibly related to a rifting event at about 2900 Ma and formation of VHMS deposits (Champion and Cassidy, 2007; Ivanic et al., 2010). Evidence for rift structures is not obvious in the seismic sections (Figs 1, 3), although it is possible that some of the structures imaged in the seismic sections, which have been interpreted as thrusts, could have been early extensional faults later inverted during contractional events. Also, within the Southern Cross Domain, in the vicinity of the seismic survey, there are slightly older Nd model ages of 3500–3200 Ma (Champion and Cassidy, 2007, 2008).

Hafnium data from the Murchison Domain also suggest a significant juvenile crust-forming event at c. 3000 Ma (Ivanic et al., 2012; Wyche et al., 2012). Both this material and older material with Narryer-equivalent model ages were then sampled by granites from c. 2820 to 2600 Ma, with continued juvenile input especially at c. 2810 Ma and c. 2720 Ma (Van Kranendonk et al., 2012). Therefore an autochthonous development is possible for the Narryer and Youanmi terranes (Ivanic et al. 2012; Van Kranendonk et al., 2012). This is inconsistent with Nd model-age data, however, which show a significant contrast across the boundary between the Narryer Terrane and the Murchison Domain.

Yarraquin Seismic Province

Below the Youanmi Terrane (*sensu stricto*), a highly reflective middle and lower crust extends from the Yalgarr Fault in the northwest (Figs 1, 4) to the Ida Fault in the east (Fig. 2). As mentioned above, we use the term Yarraquin Seismic Province to refer to the middle and lower crust in this region (Fig. 5). The seismic province varies in thickness from about 4.7 s TWT (approximately 14 km) at CDP 8800 on line 10GA-YU2 (Fig. 2) to about 8.7 s TWT (approximately 26 km) at about CDP 15100 on line 10GA-YU1 (Fig. 1). As we have not been able to track these rocks to the surface, we have no direct constraints on their lithology or age. We are not able to demonstrate that this rock package forms part of the Youanmi Terrane, but with a different structural fabric. Hence, at this stage, we treat this seismic province as a discrete package of rocks that forms the current basement to the granite–greenstone rocks of the Youanmi Terrane.

The Nd model ages for granites from the Youanmi Terrane, discussed above, suggest an average crustal age of c. 3200–3100 Ma (Champion and Cassidy, 2007, 2008). These model ages are supported by the rarity of inherited zircons older than c. 3100 Ma in felsic magmatic rocks from the Youanmi Terrane (Wyche, 2007). The Hf data suggest that granites of the Murchison Domain have

sampled c. 3800–3100 Ma model-aged material at depth (Ivanic et al., 2012).

The origin of the terrane-wide, listric to subhorizontal fabric of the Yarraquin Seismic Province is an enigma, but possibly could be due to large-scale, crustal extension. Analogue centrifuge modelling by Harris et al. (2002) and Bédard et al. (2013) have produced scenarios which resemble the current seismic architecture of the Yarraquin Seismic Province. One problem is that to produce the current thickness of the seismic province only by extension, the crust would have to have been originally of Himalayan thickness. A possible solution is that large-scale extension of a crust of normal thickness was followed by later contraction, which thickened the crust to about its current thickness.

Eastern Goldfields Superterrane

The western part of the Kalgoorlie Terrane, part of the Eastern Goldfields Superterrane, was imaged seismically on the eastern end of line 10GA-YU2, east of the Ida Fault and the Waroonga Fault (Fig. 2). At the eastern end of this line, the Kalgoorlie Terrane is about 11.7 s TWT (approximately 35 km) thick, with a reflective mid-lower crust and a less reflective upper crust consisting of disjointed reflections dipping both to the east and the west. The Bardoc Fault is interpreted to be west-dipping, soling onto the Table Hill Shear Zone (see Zibra et al., 2013b, this volume), and the Perseverance Shear Zone is interpreted as an east-dipping zone near the eastern end of line 10GA-YU2 (Fig. 2).

Yarlarweelor Gneiss Complex and Errabiddy Shear Zone

The Paleoproterozoic Yarlarweelor Gneiss Complex, the Errabiddy Shear Zone, and a small sliver of the Glenburgh Terrane have been interpreted to occur beneath the Southern Carnarvon Basin between the Meeberrie Fault and the Darling North Fault on line 11GA-SC1 (Korsch et al., 2013, this volume) (Fig. 4). The Errabiddy Shear Zone is only weakly reflective, compared to the adjacent Narryer Terrane and Pinjarra Orogen. In contrast, the Glenburgh Terrane is more reflective, consisting of predominantly west-dipping reflections (Fig. 4).

Pinjarra Orogen

The Mesoproterozoic–Neoproterozoic Pinjarra Orogen is a remnant of a former larger orogen, which now occurs as a relatively narrow sliver between the Yilgarn Craton and oceanic crust to the west of the Western Australian continental margin (Fig. 5). In the Southern Carnarvon seismic section, the Pinjarra Orogen is interpreted to occur below the Southern Carnarvon Basin, from the Darling North Fault westwards to beyond the western end of seismic line 11GA-SC1. The orogen is only moderately to weakly reflective, has not been subdivided, and is interpreted to extend to the Moho (Fig. 4).

Badgeradda Basin

Approximately 70 km south of seismic line 11GA-SC1, between the Darling and Meeberrie Faults (Plate 2), unfossiliferous sedimentary rocks of the Badgeradda Group unconformably overlie Archean rocks of the Narryer Terrane. Age constraints on these sedimentary rocks are limited, but U–Pb SHRIMP dating of detrital zircons from the Woodrarrung Sandstone yielded a late Mesoproterozoic preliminary maximum depositional age of c. 1080 Ma (GSWA, unpublished data). The Badgeradda Group is inferred to continue to the north, in the subsurface, beneath the Byro Sub-basin of the Southern Carnarvon Basin, with an outcrop cut by seismic line 11GA-SC1 at about CDP 6200 (Fig. 4).

Southern Carnarvon Basin

The western half of seismic line 11GA-SC1 crossed the southern Carnarvon Basin, a Paleozoic sedimentary basin consisting of the western Gascoyne Platform and the eastern Byro Sub-basin (Carr et al., 2012; Korsch et al., 2013, this volume). The Byro Sub-basin consists of two half-graben, with the Ballythanna Fault and the Meeberrie Fault as their west-dipping, basin-bounding structures (Fig. 4).

The Southern Carnarvon Basin rests unconformably on a quite variable basement (Korsch et al., 2013, this volume), consisting of the Pinjarra Orogen to the west of the Darling North Fault, a thin sliver of the Glenburgh Terrane immediately east of the Darling North Fault, the Yarlalweelor Gneiss Complex and Errabiddy Shear Zone between the Glenburgh Terrane and the Badgeradda Fault, and the Badgeradda Group between the Badgeradda Fault and the Meeberrie Fault (Fig. 4).

Crustal Sutures

Relationship between Narryer Terrane and Youanmi Terrane

There are significant differences in crustal reflectivity across the Yalgar Fault between the Narryer Terrane and the Murchison Domain of the Youanmi Terrane (compare Figs 1, 4). The geometry of the contact between the Narryer and Youanmi terranes observed in the seismic sections is not totally clear, however, since the boundary has been extensively modified due to later intensive reworking in the Neoproterozoic and Proterozoic (e.g. Myers, 1995; Spaggiari et al., 2008).

One possible explanation is that these units are discrete blocks of continental crust. Thus, one interpretation is that the Yalgar Fault marks the site of a suture zone (Fig. 5b), as inferred initially by Myers (1988) and Nutman et al. (1993). Champion et al. (2002) and Champion and Cassidy (2010) reported c. 2780–2740 Ma magmatism, which included sanukitoid-like rocks, in the northern Murchison Domain, and Wyman and Kerrich (2012) have described boninite-like rocks, also from the northern Murchison Domain. A subduction zone, interpreted to account for these rocks was inferred by these authors to be located between the Narryer Terrane and the Murchison Domain, and ceased with ocean closure and collision between the two terranes (Wyman and Kerrich, 2012). Champion and Cassidy (2002) suggested that collision occurred at, or just before, c. 2750 Ma, and Spaggiari et al. (2007) suggested that the two terranes were then stitched by plutons aged between 2750 and 2620 Ma. The polarity of the inferred subduction zone would have dipped to the (present) southeast (Fig. 6).

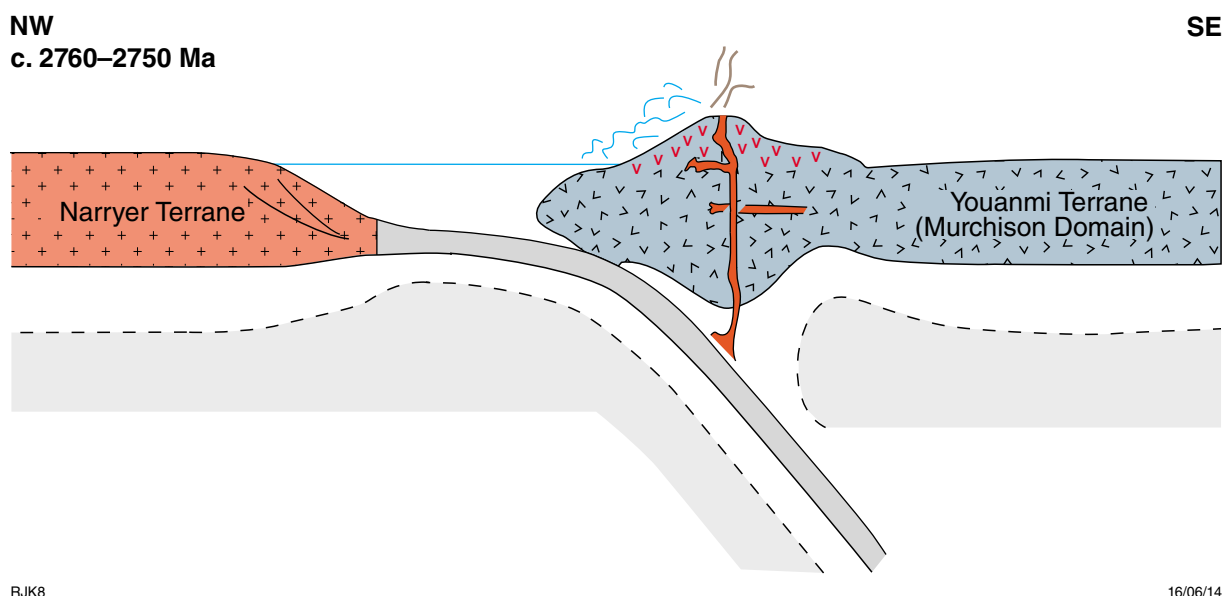


Figure 6. Schematic cross section, showing the magmatic arc in the Murchison Domain, prior to collision between the Narryer Terrane and the Murchison Domain of the Youanmi Terrane.

An alternative hypothesis, however, has been suggested for the tectonic evolution of the northern Murchison Domain. Owing to the presence of autochthonous contacts between greenstones deposited from c. 2850–2710 Ma, a continuously evolving geochemical cycle of both greenstones and granitic rocks, lack of thrusts, and the presence of komatiite and komatiitic volcanism, a plume-driven, autochthonous development of the Murchison Domain has been inferred (Fig. 7: Van Kranendonk et al., 2012; Ivanic et al., 2012).

If the Narryer–Youanmi boundary is a suture, then the Narryer Terrane may have been thrust over the northwestern part of Youanmi Terrane and Yarraquin Seismic Province. Alternatively, the marginally similar reflectance properties of the Narryer Terrane with the middle part of the crust beneath the Youanmi Terrane (*sensu stricto*), suggests that Narryer-type crust may continue beneath the Youanmi Terrane, and may have been exhumed along the northwestern margin of the craton during Proterozoic tectonism. This scenario is supported by the presence of c. 4000 Ma xenocrystic zircons in younger Murchison granites (Nelson et al., 2000), by Hf isotopic data of c. 4000 Ma crust in the source region of

younger Murchison granites (Ivanic et al., 2012), and by the presence of >3100 Ma detrital zircons and Hf isotopic evidence of >4000 Ma crust formation in the Southern Cross Domain (Wyche et al., 2004, 2012).

Relationship between Murchison Domain and Southern Cross Domain

In the vicinity of the seismic lines, the boundary between the Murchison and Southern Cross domains is the Youanmi Shear Zone, crossed at about CDP 9080 on seismic line 10GA-YU2 (Fig. 2). Here it is interpreted as a major, east-dipping, crustal-scale structure, soling onto the top of the lower crust. Nevertheless, there is no apparent difference in the nature of the upper crustal seismic reflectivity in the Youanmi Terrane (*sensu stricto*) across the Youanmi Shear Zone, suggesting that there is similar geology across this domain boundary. Also, we see no change in the seismic character of the Yarraquin Seismic Province across the Youanmi Shear Zone (Fig. 2).

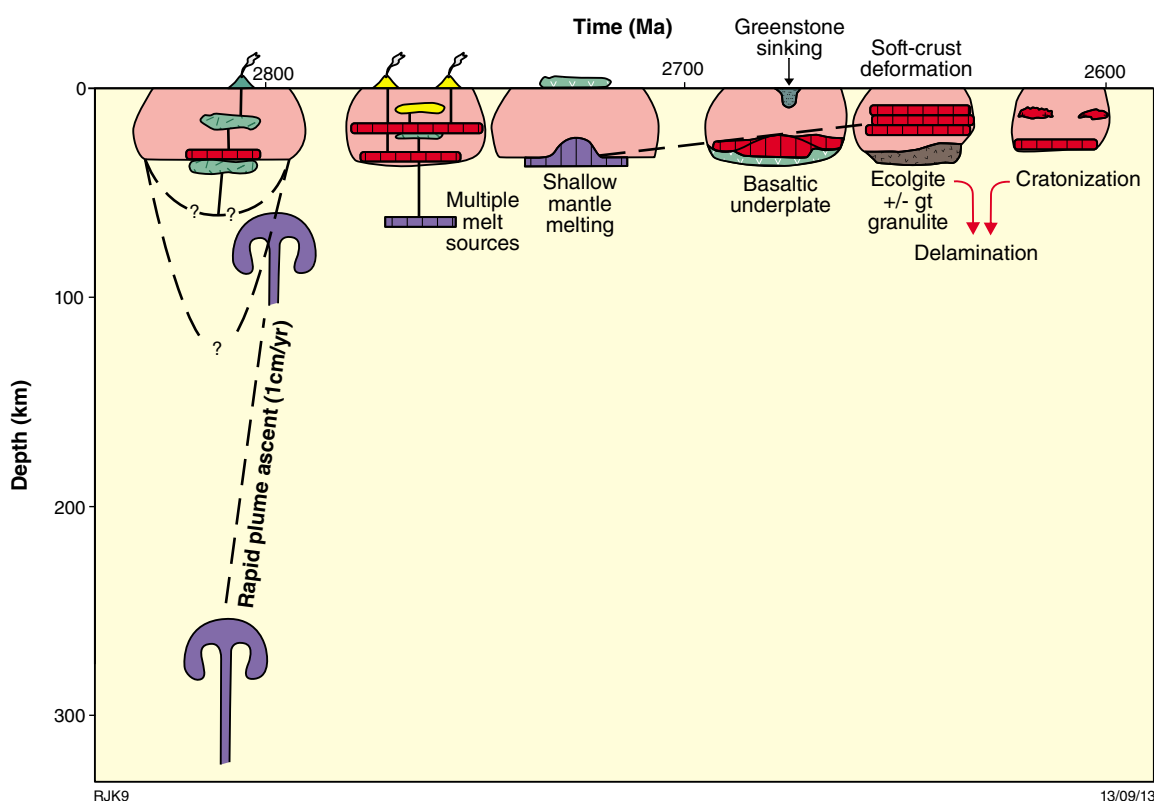


Figure 7. Schematic time–depth model of Murchison Domain evolution, commencing with the rise of deep-mantle derived melts at base of Murrouli Basalt (c. 2820 Ma), and followed quickly thereafter by the eruption of shallower-derived melts (2800 Ma) as the plume rose upwards. Conductive heating from the plume caused the onset of widespread partial melting of older crust at 2785–2760 Ma, and mingling of crust and mantle-derived magmas at 2760–2740 Ma. Subsequent eruption of crustally contaminated mantle melts of the c. 2730 Ma Glen Group derived from shallow mantle sources, indicating lithospheric extension and perhaps onset of a second plume. This was followed by further partial melting of the crust and development of an eclogitic residue at the base of the crust, which delaminated at c. 2640 Ma, giving rise to the emplacement of widespread post-tectonic granites.

Neodymium isotopic data on granites and the zircon inheritance data from granites (see above) suggest that the middle to lower crust below the Southern Cross Domain may contain older crust than that below the Murchison Domain. Hafnium isotopic data indicate, however, that granitic rocks from both of these terranes sample 3100–3800 Ma model-aged material beneath (Ivanic et al., 2012; Wyche et al. 2012), suggesting that these two domains share similar basement histories. Therefore, for the purpose of this discussion, we treat the Murchison and Southern Cross domains of the Youanmi Terrane as a single entity.

Relationship between Youanmi Terrane and Eastern Goldfields Superterrane

For most of its length, the Ida Fault forms the boundary between the Southern Cross Domain of the Youanmi Terrane and the Kalgoorlie Terrane of the Eastern Goldfields Superterrane (Frontispiece 1). In the vicinity of seismic line 11GA-YU2, however, the Waroonga Fault has excised the Ida Fault from the uppermost part of the crust, and becomes the boundary between the terranes at the surface (e.g. Cassidy, 2006) (Fig. 2).

Widely different geodynamic models have been proposed to explain the relationship between the Youanmi Terrane and the Kalgoorlie Terrane. Myers (1995) proposed that the two terranes were amalgamated at about 2650 Ma, with the Ida Fault as the suture between them. Krapež (2006) proposed that an east-dipping subduction zone was located to the west of the Kalgoorlie Terrane, and

that the Ida Fault was the suture with older continental crust to the west. Alternative models, by Czarnota et al. (2010) and Van Kranendonk et al. (2012), propose that the Youanmi and Kalgoorlie Terranes were part of the same continent, but that the Kalgoorlie Terrane was a stretched and thinned part of that continent. Van Kranendonk et al. (2012, fig. 32) suggested that the Ida Fault acted as a major extensional fault, allowing the crust to the east of it to be drastically thinned.

Neodymium isotopic data from granites (Champion and Cassidy, 2007, 2008) show that there is a marked contrast in the Nd isotopic character across the Ida Fault, probably the biggest contrast anywhere in the Yilgarn Craton, with the crust being much more juvenile to the east. Also, Champion et al. (2002) showed that the syenitic group of granites are a significant granitic component east of the Ida Fault, but that these granites are extremely rare to the west. Together, the Nd isotopes and distribution of syenites suggest that there is a major change in crustal composition at the Ida Fault, and this has been widely used to imply that it was a terrane boundary during Neoproterozoic subduction–accretion. Given this scenario, we consider that the Youanmi and Kalgoorlie terranes were, at some stage, probably separated by oceanic crust, and were amalgamated during ocean closure and collision. Recently, Angerer et al. (2013) described boninitic rocks from the Koolyanobbing greenstone belt in the Southern Cross Domain, which they considered erupted at an intra-oceanic island arc at about 3000 Ma. Currently, there are no direct isotopic age constraints on the Koolyanobbing greenstone belt, and hence it could be younger, at c. 2800 Ma or even younger in age. The arc-related boninites occur on the upper plate, suggesting that the subduction zone was west dipping (Fig. 8).

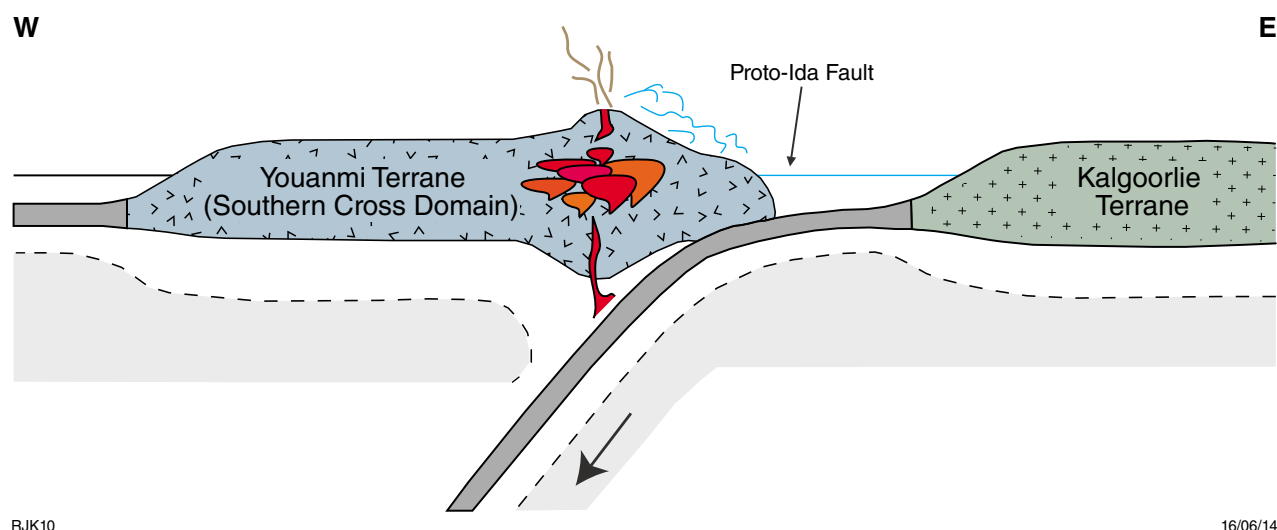


Figure 8. Schematic cross-section, showing a west-dipping subduction zone beneath the Southern Cross Domain, prior to collision between the Southern Cross Domain and the Kalgoorlie Terrane. Note that timing is poorly constrained, and collision could be c. 2800 Ma or younger.

Relationship between Narryer Terrane and Gascoyne Province

The Gascoyne Province is considered exotic to both the Pilbara and Yilgarn cratons (Occhipinti et al., 2004; Johnson et al., 2011a,b) and, as such, the Narryer Terrane and Gascoyne Province represent discrete continental blocks sutured by a collision/suture zone. At the surface, the boundary corresponds to the north-dipping Errabiddy Shear Zone, which was crossed in seismic line 10GA-CP3 (Johnson et al., 2011a, 2013). The Errabiddy Shear Zone is interpreted also to occur in the subsurface beneath the Southern Carnarvon Basin in seismic line 11GA-SC1 (Korsch et al., 2013, this volume). Another key structure interpreted in seismic line 10GA-CP3 is a south-dipping, middle- to lower-crustal fault, termed the Cardilya Fault (Johnson et al., 2011a).

Sheppard et al. (2004) demonstrated that the Dalgaringa Supersuite in the Glenburgh Terrane of the southern Gascoyne Province was an Andean-type, continental-margin magmatic arc that was active from c. 2005 to 1985 Ma, although Johnson et al. (2011b) instead considered that the initiation of arc magmatism occurred at about 2080 Ma. The magmatic arc developed along the southern margin of the Gascoyne Province (Sheppard et al., 2004; Johnson et al., 2011b), constraining the polarity of subduction: that is, dipping northwards under the Gascoyne Province (Fig. 9).

Ocean closure and collision between the Glenburgh Terrane of the Gascoyne Province and the Narryer Terrane took place during the c. 1965–1950 Ma event termed the

Glenburgh Orogeny (Johnson et al., 2011b). The collision resulted in the imbrication of the northern margin of the Yilgarn Craton with slices of the Glenburgh Terrane along the Errabiddy Shear Zone. The collisional event was accompanied by the intrusion of granitic rocks of the c. 1965–1945 Ma Bertibubba Supersuite. These granitic rocks are the first common magmatic element of the northern margin of the Yilgarn Craton, the Yarlalweelor Gneiss Complex, the Errabiddy Shear Zone, and the Glenburgh Terrane (Johnson et al., 2011b).

Interpretation of seismic line 10GA-CP3 (Johnson et al., 2011a) shows that the main crustal structure, the Cardilya Fault, is moderately south-dipping, opposite to the inferred subduction geometry (Fig. 9). The intricate relationship of this fault with the Errabiddy Shear Zone, and the imbrication of the Moho, imply a complex setting for the collision. The imbrication of lithologies from both the and Narryer Terrane along the Errabiddy Shear Zone suggests that this structure is possibly the suture zone. Following the initial collision and interleaving of lithologies along the Errabiddy Shear Zone, the zone was reworked by the Cardilya Fault, which underthrust the southern margin of the Glenburgh Terrane beneath the Narryer Terrane (see Johnson et al., 2011a). Alternatively, during oceanic closure and collision, the Narryer Terrane was obducted onto the Gascoyne Province at the present site of the Cardilya Fault. During the post-collisional phase of the Glenburgh Orogeny, backthrusting at the Errabiddy Shear Zone resulted in a slice of the Glenburgh Terrane being thrust back to the south, over the upper part of the Narryer Terrane, thus producing the present crustal architecture imaged in seismic line 10GA-CP3 (Johnson et al., 2011a).

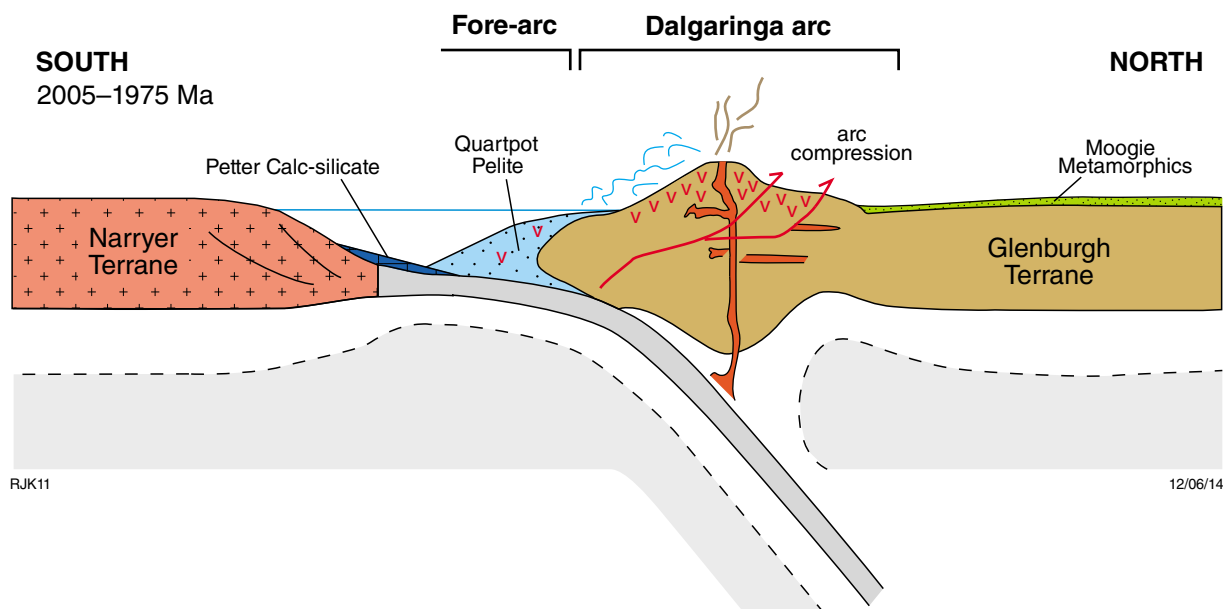


Figure 9. Schematic cross-section, showing the evolution of the Dalgaringa Arc, prior to the collision between the Yilgarn Craton and the Gascoyne Province (after Korsch et al., 2011a).

Relationship between Narryer Terrane and Pinjarra Orogen

To the south of seismic line 11GA-SC1, the boundary between the Yilgarn Craton and the Pinjarra Orogen, is the north-south striking Darling Fault, which extends for over 1000 km. In the area of seismic line 11GA-SC1, however, the Darling Fault splays into the Ballythanna Fault and the Darling North Fault, and the contact between the two terranes is interpreted to be the Darling North Fault (Korsch et al., 2013, this volume). To the south of our area of interest, Myers (1990) suggested that thrust movements on the Darling Fault may be related to continental collision between about 750 and 600 Ma and, presumably, the suturing of the Pinjarra Orogen to the Yilgarn Craton, whereas Wilde (1999) put the age of collision at about 1080 Ma, based on granulite facies metamorphism of this age in the orogen. Fitzsimons (2003), in contrast, suggested that the Pinjarra Orogen developed to the south of its present position, where it was deformed at about 1080 Ma and, between about 750 and 550 Ma, was translated northwards to its present position by dextral strike-slip movement along the Darling Fault.

Boger (2011) suggested that rifting between about 1140 and 1080 Ma removed that part of the Yilgarn Craton to the west of the current Darling Fault, which was present prior to inception of the Darling Fault, so that this margin faced an open ocean, whereas Ksienzyk et al. (2012) put the rifting at about 1345 to 1140 Ma. In agreement with Wilde (1999), Boger (2011) and Ksienzyk et al. (2012) considered that collision occurred at about 1090–1080 Ma, which resulted in the Pinjarra Orogen being sutured to the Yilgarn Craton.

There is no evidence for Mesoproterozoic arc magmatism in the western Yilgarn Craton, implying that the subduction zone must have dipped to west beneath the Pinjarra Orogen (Fig. 10). Evidence for this magmatism is likely to be on the part of the orogen that has been removed, probably during the breakup of the Gondwana supercontinent.

Geodynamic Implications

The new deep seismic imaging, extending from the Pinjarra Orogen to the eastern Yilgarn Craton, provides, for the first time, a holistic view of the crustal architecture across much of the Yilgarn Craton, and the architectural relationships with adjacent orogens to the northwest and west. Based on the nature of seismic reflectivity, the upper part of the Narryer Terrane is distinctly different from the Youanmi Terrane, which is here confined to the upper crust. The crust which underlies the exposed surface of the Youanmi Terrane is seismically distinct, and cannot be tracked anywhere to the surface. Therefore, a new seismic province, the Yarraquin Seismic Province, is proposed. The seismic images, combined with geological and geophysical data can be used to help constrain geodynamic models for the region.

There is considerable and ongoing debate about the Neoproterozoic evolution of the Yilgarn Craton, centred

essentially on two opposed models: 1) a convergent plate tectonic model, based on analogies with modern-day plate tectonic processes, involving subduction zone magmatism and the accretion of allochthonous continental slivers as discrete terranes (e.g. Barley et al., 1989; Myers, 1995; Krapež and Barley, 2008; Czarnota et al., 2010; Korsch et al., 2011b), and 2) an autochthonous model, involving mantle plumes and partial convective overturn of the upper and middle crust (e.g. Campbell and Hill, 1988; Barnes et al., 2012; Van Kranendonk et al., 2012; Ivanic et al., 2012). Our interpretations, discussed above, suggest support and disagreement with aspects of each model.

Assembly of the Yilgarn Craton and the West Australian Craton

Assuming the first model of subduction-related, progressive accretion of continental slivers onto the margins of the Youanmi Terrane (and its basement, the Yarraquin Seismic Province), several conclusions may be drawn. Using a convergent plate tectonic model, based on analogies with modern-day plate tectonic processes, several groups of workers (e.g. Barley et al., 1989; Myers, 1995; Krapež and Barley, 2008; Czarnota et al., 2010; Korsch et al., 2011b) have proposed geodynamic models for the Eastern Goldfields Superterrane which involve the accretion of allochthonous continental slivers as discrete terranes. The geochemistry of volcanic rocks in the Kurnalpi Terrane (including intra-arc extension in the Gindalbie Domain) are consistent with an island arc signature, leading Barley et al. (2008), Kositsin et al. (2008) and Korsch et al. (2011b) to suggest that the Eastern Goldfields Superterrane was a collage of narrow slivers, which were amalgamated late in the Neoproterozoic, between about 2672 and 2660 Ma (Fig. 11). A modern analogue is possibly the eastern margin of Australia today, where narrow, thin, continental slivers, such as the Lord Howe Rise, are located outboard, and may be accreted to the Australian continent in the future. For example, it is inferred that the Burtville Terrane, a narrow sliver of older continental crust, collided with the Kurnalpi island arc at about 2672 Ma, and that the marginal sea between the Kalgoorlie Terrane and the Kurnalpi Terrane closed, resulting in another collision at about 2660 Ma (see Korsch et al., 2011b for full details).

Recently, Pawley et al. (2012) subdivided the Burtville Terrane of Cassidy et al. (2006) into two, with the Burtville Terrane (*sensu stricto*) being confined to the area west of the Yamarna Shear Zone, and they proposed a new terrane, the Yamarna Terrane, for the region to the east of the Yamarna Shear Zone. Pawley et al. (2012) considered that the c. 2715–2630 Ma successions in the Yamarna Terrane were deposited on thinned continental crust, similar to that exposed in the Burtville Terrane. Because most of the Yamarna Terrane is hidden under younger sedimentary cover, there is, at yet, insufficient information available to assess the relative merits of convergent margin versus intracontinental autochthonous processes for the formation of this terrane.

The pre-3000 Ma history of the Yilgarn Craton is patchy, but recent work by Thern and Nelson (2012) suggests

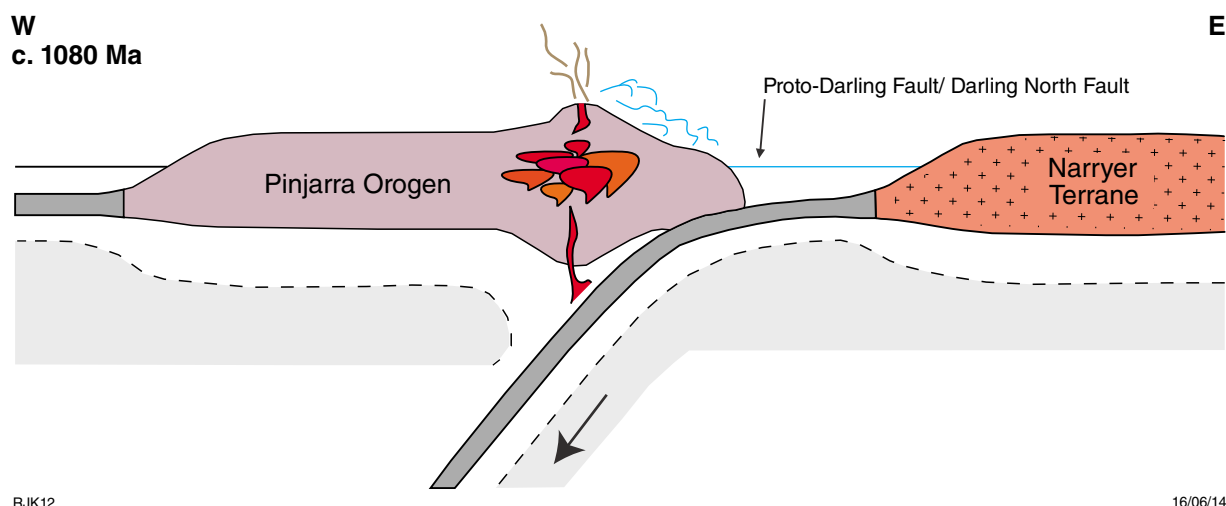


Figure 10. Schematic cross-section, showing the subduction system between the Pinjarra Orogen and Yilgarn Craton, just prior to 1080 Ma, when collision between the orogen and craton is inferred to have occurred.

that the early history of the Yilgarn Craton involved the collision of at least two Hadean terranes at c. 3750 Ma, resulting in their amalgamation and subsequent intrusion by several granite-forming events. Thus, it is possible that the Yilgarn Craton has undergone a series of terrane amalgamations over a period of at least one billion years (c. 3750–2660 Ma), of which the older events have yet to be deciphered in detail.

In summary, the arc-accretion model contends that the Yilgarn Craton was built through the amalgamation of several discrete terranes, possibly over a long period of time. This was followed, at about 1965 Ma, by the amalgamation of the Yilgarn Craton with the Gascoyne Province to the north (which previously had been sutured to Pilbara Craton at about 2215 Ma) to form the West Australian Craton. Finally, suturing of the Pinjarra Orogen to the Western Yilgarn Craton occurred at about 1080 Ma (Fig. 12).

According to the second model, that of plume-driven autochthonous development, the Yilgarn Craton, or at least the Youanmi Terrane, was a large Eoarchean to Paleoarchean continent affected by several plume-related magmatic events (e.g. Barnes et al., 2012; Van Kranendonk et al., 2012). These events were particularly voluminous, with juvenile crust formation at c. 2810 Ma and c. 2720 Ma, with associated komatiitic volcanism and large mafic-ultramafic intrusions. Conductive heating at the base of the lithosphere combined with greenstone blanketing allowed prolonged granitic magmatism to continue from c. 2700 to 2600 Ma. Crustal melting may have been aided at a late stage by delamination of

eclogitic underplated material. Sanukitoid-like rocks and andesites at c. 2750 Ma, at least in the northern Murchison Domain, are attributed to mafic–felsic magma-mixing events, producing features such as mafic clots in tonalitic suites (e.g. Ivanic et al., 2012). With this model, discrete extensional events, and hence structures, also precede and are reactivated by east–west contractional tectonics which started at least at about 2660 Ma. This contractional event formed the majority of structures evident at the surface and in the seismic lines, which are interpreted to be transpressional shear zones accommodating roughly east–west shortening.

This approximately east–west contractional event is possibly the same event as that across the whole of the Eastern Goldfields Superterrane. The source of such far-field compressive stress is uncertain, but given the clear truncations of aeromagnetic and gravity anomalies at the current margins of the Yilgarn Craton, it is likely that the craton once formed part of a much larger supercraton (e.g. Bleeker, 2003). The presence of large c. 2420 Ma dykes in both the Yilgarn Craton and also in the Nain Craton (northwest Scotland), led Bleeker (2003) to suggest that these two cratons preserve different parts of an originally much larger supercraton. Using paleomagnetic data, Smirnov et al. (2013) suggested that the Yilgarn Craton and the Zimbabwe Craton in Africa formed part of a supercraton, which was in existence at least at about 2420 Ma, given the presence of dykes of this age in both cratons. Smirnov et al. (2013) also suggested that breakup of this supercontinent probably took place sometime between 2200 and 2000 Ma.

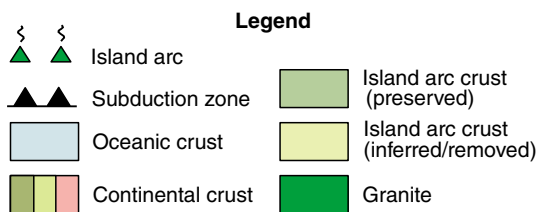
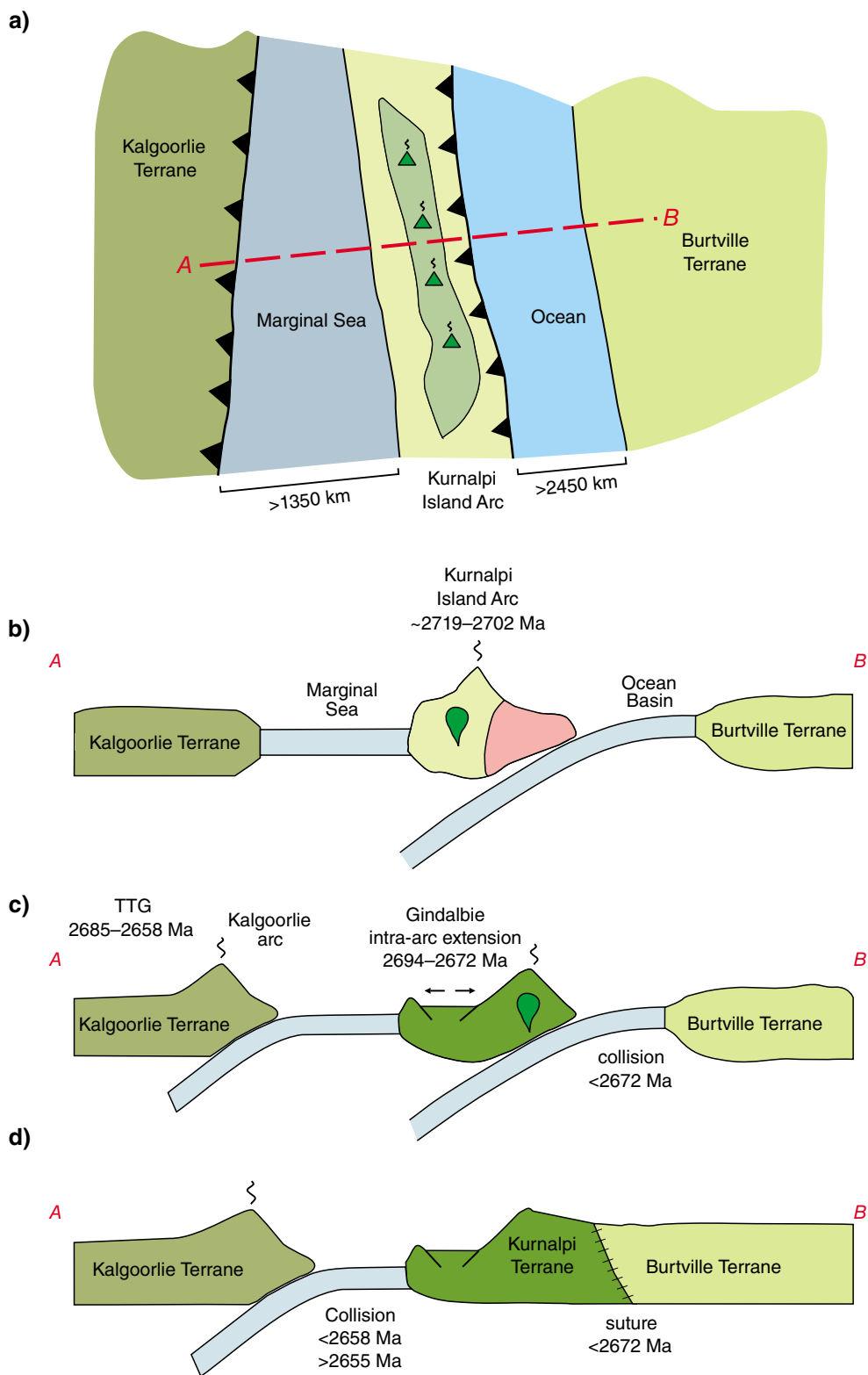


Figure 11. (facing) Proposed tectonic scenario during formation of the Kurnalpi island arc: a) sketch map; b) cartoon cross-section showing tectonic scenario at c. 2719–2702 Ma, during formation of the Kurnalpi island arc; c) cartoon cross-section showing tectonic scenario at c. 2694–2672 Ma, during formation of the Kalgoorlie continental margin arc and Gindalbie intra-arc rift; d) cartoon cross-section showing tectonic scenario at c. 2670–2660 Ma after collision and amalgamation of the Kurnalpi island arc with the Burtville Domain.

Transect across the Yilgarn Craton

It is now possible to combine the seismic sections from the current Youanmi and Southern Carnarvon surveys with the seismic sections from earlier surveys to produce a 1300 km traverse across almost the entire Yilgarn Craton (Kennett et al., 2013), which is shown in cartoon form in Figure 12. Although there have been several previous deep seismic surveys in the Yilgarn Craton, the key surveys of interest here are the Eastern Goldfields survey, acquired in 1991 (line BMR91-EGF01, commonly known as EGF1, Drummond et al., 1993, 2000; Swager et al., 1997), and the Northeast Yilgarn survey, acquired in 2001 (lines 01AGS-NY1 and 01AGS-NY3, Goleby et al., 2004, 2006). These surveys showed that the terranes which make up the Eastern Goldfields Superterrane are separated from each other by major, crustal-scale, east-dipping faults or shear zones.

The overall architecture of the Yilgarn Craton is dominated by a central nucleus, consisting of the Youanmi Terrane and underlying Yarraquin Seismic Province (Fig. 12). Based on Nd isotopic data, it has been proposed that the Youanmi Terrane has behaved as a coherent crustal block since at least about 3000–2900 Ma (Champion and Cassidy, 2010; Ivanic et al., 2012; Van Kranendonk et al., 2012). Others have suggested that it then acted as

a nucleus, or protocraton, onto which the Narryer Terrane and Eastern Goldfields Superterrane accreted (Cassidy et al., 2006). Terranes on either side of the Youanmi Terrane are seen to be bounded by crustal-scale faults that dip away from the nucleus, towards the west and northwest on the northwestern side, and towards the east on the eastern side.

The terrane accretion model of the Yilgarn Craton is likely to have produced an irregular Moho topography. The Moho, however, is remarkably flat for several hundred kilometres across almost the entire the Yilgarn Craton. This suggests that the Moho imaged in the seismic section either did not form during Archean terrane amalgamation but is a younger feature, superimposed on the older architecture, or that the terrane accretion model is incorrect. The formation of the imaged Moho is possibly related to the post-tectonic, low-Ca granites (possibly due to re-equilibration of the lower crust), which intruded across the entire craton at approximately the same time. Their emplacement ceased at c. 2630 Ma, which is about the time of final cratonization of the Yilgarn Craton (Champion et al., 2002). Alternatively, it could be related to possible delamination or convective thinning at about this time, related to felsic alkaline intrusions, as suggested by Smithies and Champion (1999). Another possibility is that the Moho could be related to underplating of mafic magma at the time(s) of intrusion of the Proterozoic dykes, or possibly a combination of the above processes.

Acknowledgements

This paper forms part of a collaborative project between the Geological Survey of Western Australia and Geoscience Australia. Terrex Seismic Pty Ltd carried out the seismic data acquisition. Dynamic Satellite Surveys Pty Ltd undertook the transect line survey pegging at 40 m intervals along a predefined route prior to the data acquisition phase, and also collected the gravity readings on the Youanmi seismic lines at 400 m intervals.

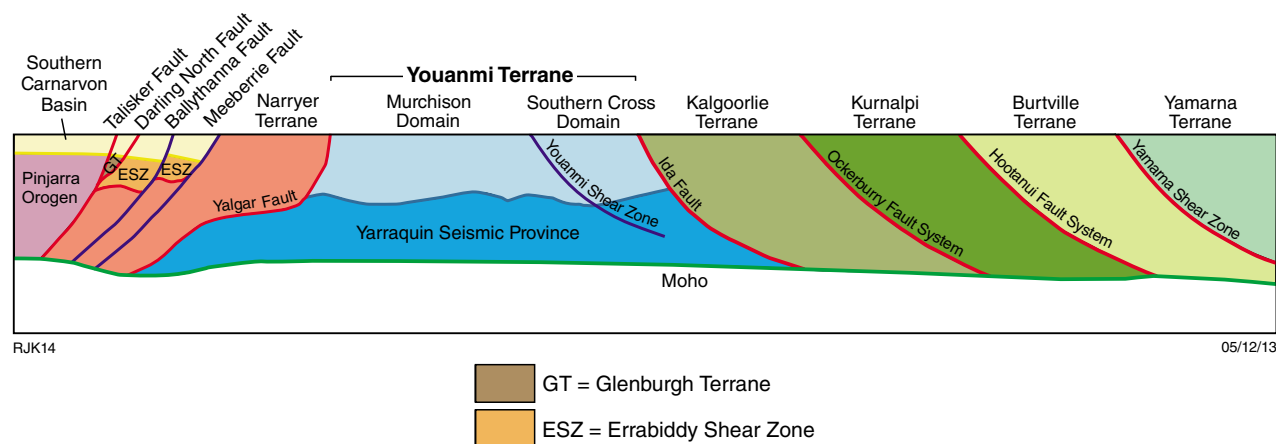


Figure 12. Cartoon of present day architecture of the crust from the Pinjarra Orogen, across most of the Yilgarn Craton from the Narryer Terrane in the west, to the Yamarna Terrane in the east, showing the key terranes, domains and significant faults. Note that this is approximate only and is not to scale.

We thank the following for their contributions to the project: Jenny Maher and Tristan Kemp for project management during the planning, acquisition and processing phase of the seismic data; Narelle Neumann for project management during the interpretation phase of the project; Lindsay Highet and Weiping Zhang for producing the maps and the digital versions of the interpretations of the seismic sections, respectively; and David Champion for many fruitful discussions and for reviewing the manuscript. Authors from Geoscience Australia publish with permission of the Chief Executive Officer, Geoscience Australia.

References

- Angerer, T, Kerrich, R and Hagemann, SG 2013, Geochemistry of a komatiitic, boninitic, and tholeiitic basalt association in the Mesoarchean Koolyanobbing greenstone belt, Southern Cross Domain, Yilgarn craton: Implications for mantle sources and geodynamic setting of banded iron formation: *Precambrian Research*, v. 224, p. 110–128.
- Barley, ME, Brown, SJ, Krapež, B and Kositsin, N 2008, Physical volcanology and geochemistry of a late Archaean volcanic arc: Kurnalpi and Gindalbie terranes, eastern Goldfields Superterrane, Western Australia: *Precambrian Research*, v. 161, p. 53–76.
- Barley, ME, Eisenlohr, BN, Groves, DI, Perring, CS and Verancombe, JR 1989, Late Archean convergent margin tectonics and gold mineralization: a new look at the Norseman–Wiluna Belt, Western Australia: *Geology*, v. 17, p. 826–829.
- Barnes, S, Van Kranendonk, MJ and Sontag, I 2012, Geochemistry and tectonic setting of basalts from the Eastern Goldfields Superterrane: *Australasian Journal of Earth Sciences*, v. 59, p. 707–735.
- Bédard, JH, Harris, LB and Thurston, PC 2013, The hunting of the snArc: *Precambrian Research*, v. 229, p. 20–48.
- Bleeker, W 2003, The late Archean record: a puzzle in ca. 35 pieces: *Lithos*, v. 71, p. 99–134.
- Boger, SD 2011, Antarctica – before and after Gondwana: *Gondwana Research*, v. 19, p. 335–371.
- Campbell, IH and Hill, RI 1988, A two-stage model for the formation of the granite–greenstone terrains of the Kalgoorlie–Norseman area, Western Australia: *Earth and Planetary Science Letters*, v. 90, p. 11–25.
- Carr, LK, Korsch, RJ, Mory, AJ, Hocking, RM, Marshall, SK, Costelloe, RD, Holzschuh, J and Maher, JL 2012, Structural and stratigraphic architecture of Australia's frontier onshore sedimentary basins: the Western Officer and Southern Carnarvon basins, Western Australia: *APPEA Journal and Conference Proceedings*, v. 52, 4p. (CD-ROM).
- Cassidy, KF 2006, Geological Evolution of the eastern Yilgarn Craton (EYC), and terrane, domain and fault system nomenclature, in *Final Report, 3D Geological models of the eastern Yilgarn Craton, Project Y2, September 2001 – December 2004* edited by RS Blewett and AP Hitchman: Geoscience Australia, Record 2006/05, p. 1–38.
- Cassidy, KF, Champion, DC, Krapež, B, Barley, ME, Brown, SJA, Blewett, RS, Groenewald, PB and Tyler, IM 2006, A revised geological framework for the Yilgarn Craton, Western Australia: *Geological Survey of Western Australia, Record* 2006/8, 8p.
- Cavosie, AJ, Valley, JW and Wilde, SA 2007, The oldest terrestrial mineral record: a review of 4400 to 4000 Ma detrital zircons from Jack Hills, Western Australia, in *Earth's oldest rocks* edited by MJ Van Kranendonk, RH Smithies and VC Bennett: *Developments in Precambrian Geology*, v. 15, p. 91–111.
- Champion, DC and Cassidy, KF 2002, Granites in the Leonora–Laverton transect area, north eastern Yilgarn Craton, in *Geology, geochronology and geophysics of the north eastern Yilgarn Craton, with an emphasis on the Leonora–Laverton transect area* edited by KF Cassidy: Geoscience Australia, Record 2002/18, p. 13–35.
- Champion, DC and Cassidy, KF 2007, An overview of the Yilgarn Craton and its crustal evolution: *Geoscience Australia, Record* 2007/14, p. 8–13.
- Champion, DC and Cassidy, KF 2008, Geodynamics: using geochemistry and isotopic signatures of granites to aid mineral systems studies: an example from the Yilgarn Craton: *Geoscience Australia, Record*, 2008/09, p. 7–16.
- Champion, DC and Cassidy, KF 2010, Granitic magmatism in the Yilgarn Craton: implications for crustal growth and Metallogeny, in *Yilgarn–Superior Workshop — Abstracts, Fifth International Archean Symposium, 10 September 2010: Geological Survey of Western Australia, Record* 2010/20, p. 12–18.
- Champion, DC, Cassidy, KF and Budd, A 2002, Overview of the Yilgarn Craton magmatism: Implications for crustal development, in *The characterisation and metallogenic significance of Archaean granitoids of the Yilgarn Craton*, edited by KF Cassidy, DC Champion, NJ McNaughton, IR Fletcher, AJ Whitaker, IV Bastrakova and AR Budd: Australian Mineral Industry Research Association (AMIRA) Project P482/MERIWA Project M281, Final Report, p. 8.1 – 8.21.
- Clowes, RM and Oueity, J 2010, The nature of the Moho transition in NW Canada from combined near-vertical and wide-angle seismic reflection studies, in *14th International Symposium on Deep Seismic Profiling of the Continents and their Margins* compiled by DM Finlayson: Geoscience Australia, Record 2010/24, p. 40.
- Czarnota, K, Champion, DC, Goscombe, B, Blewett, RS, Cassidy, KF, Henson, PA and Groenewald, PB 2010, Geodynamics of the eastern Yilgarn Craton: *Precambrian Research*, v. 183, p. 175–202.
- Drummond, BJ, Goleby, BR and Swager, CP 2000, Crustal signature of Late Archaean tectonic episodes in the Yilgarn craton, Western Australia: evidence from deep seismic sounding: *Tectonophysics*, v. 329, p. 193–221.
- Drummond, BJ, Goleby, BR and Swager, CP and Williams, PR 1993, Constraints on Archaean crustal composition and structure provided by deep seismic sounding in the Yilgarn Block: *Ore Geology Reviews*, v. 8, p. 117–124.
- Fitzsimons, ICW, 2003, Proterozoic basement provinces of southern and southwestern Australia, and their correlation with Antarctica, in *Proterozoic East Gondwana: Supercontinent assembly and breakup* edited by M Yoshida, BF Windley and S Dasgupta: Geological Society, London, Special Publication 206, p. 93–130.
- Froude, CF, Ireland, TR, Kinny, PD, Williams, IS, Compston, W, Williams, IR and Myers, JS 1983, Ion-microprobe identification of 4100–4200 Myr old terrestrial zircons: *Nature*, v. 304, p. 616–618.
- Gessner, K, Jones, T, Goodwin, JA, Gallardo, LA, Milligan, PR, Brett, J and Murdie, R 2013, Interpretation of magnetic and gravity data across the South Carnarvon Basin, and the Narryer and Youanmi Terranes, in *Youanmi and Southern Carnarvon seismic and magnetotelluric (MT) workshop 2013* compiled by S Wyche, TJ Ivanic and I Zibra: Geological Survey of Western Australia, Record 2013/6, p. 65–77.
- Goleby, BR, Blewett, RS, Fomin, T, Fishwick, S, Reading, AM, Henson, PA, Kennett, BLN, Champion, DC, Jones, LEA, Drummond, BJ and Nicoll, M, 2006, An integrated multi-scale 3D seismic model of the Archaean Yilgarn Craton, Australia: *Tectonophysics*, v. 420, p. 75–90.
- Goleby, BR, Blewett, RS, Korsch, RJ, Champion, DC, Cassidy, KF, Jones, LEA, Groenewald, PB and Henson, PA 2004, Deep seismic reflection profiling in the Archaean northeastern Yilgarn Craton, Western Australia: implications for crustal architecture and mineral potential: *Tectonophysics*, v. 388, p. 119–133.

- Hammer, PTC and Clowes, RM 1997. Moho reflectivity patterns – a comparison of Canadian Lithoprobe transects. *Tectonophysics*, v. 269, p. 179–198.
- Harris, L, Koyi, H and Fossen, H 2002 Mechanisms for folding of high-grade rocks in extensional tectonic settings: *Earth-Science Reviews*, v. 59, p. 163–210.
- Ivanic, TJ, Korsch, RJ, Wyche, S, Jones, LEA, Zibra, I, Blewett, RS, Jones, T, Milligan, PR, Costelloe, RD, Van Kranendonk, MJ, Doublier, MP, Hall, CE, Romano, SS, Pawley, MJ, Gessner, K, Patison, N, Kennett, BLN and Chen, SF 2013a, Preliminary interpretation of the 2010 Youanmi deep seismic reflection lines and magnetotelluric data for the Windimurra Igneous Complex, *in* Youanmi and Southern Carnarvon seismic and magnetotelluric (MT) workshop 2013 *compiled by* S Wyche, TJ Ivanic and I Zibra: Geological Survey of Western Australia, Record 2013/6, p. 97–111.
- Ivanic, TJ, Van Kranendonk, MJ, Kirkland, CL, Wyche, S, Wingate, MTD and Belousova, EA 2012, Zircon Lu–Hf isotopes and granite geochemistry of the Murchison Domain of the Yilgarn Craton: Evidence for reworking of Eoarchean crust during Meso-Neoproterozoic plume-driven magmatism: *Lithos*, v. 148, p. 112–127.
- Ivanic, TJ, Wingate, MTD, Kirkland, CL, Van Kranendonk, MJ and Wyche, S 2010, Age and significance of voluminous mafic–ultramafic magmatic events in the Murchison Domain, Yilgarn Craton: *Australian Journal of Earth Sciences* v. 57, p. 597–614.
- Ivanic, TJ, Wingate, MTD, Korsch, RJ, Blewett, RS, Jones, LEA, Wyche, S, Zibra, I, Doublier, MP, Romano, SS, Pawley, MJ, Van Kranendonk, MJ, Gessner, K, Hall, CE, Chen, SF, Patison, NL and Costelloe, RD 2013b, Preliminary interpretation of the Youanmi deep seismic reflection lines for Proterozoic intrusive rocks, *in* Youanmi and Southern Carnarvon seismic and magnetotelluric (MT) workshop 2013 *compiled by* S Wyche, TJ Ivanic and I Zibra: Geological Survey of Western Australia, Record 2013/6, p. 81–85.
- Johnson, SP, Sheppard, S, Rasmussen, B, Wingate, MTD, Kirkland, CL, Muhling, JR, Fletcher, IR and Belousova, EA 2011b, Two collisions, two sutures: punctuated pre-1950 Ma assembly of the West Australian Craton during the Ophthalmanian and Glenburgh Orogenies: *Precambrian Research*, v. 189, p. 239–262.
- Johnson SP, Thorne, AM and Tyler IM (editors) 2011a, Capricorn Orogen seismic and magnetotelluric (MT) workshop 2011: extended abstracts: Geological Survey of Western Australia, Record 2011/25, 120p.
- Johnson SP, Thorne, AM, Tyler IM, Korsch, RJ, Kennett, BLN, Cutten, HN, Blay, O, Blewett, RS, Joly, A, Dentith, MC, Aitken, ARA, Goodwin, JA, Holzschuh, J, Salmon, M, Reading, A, Boren, G, Ross, J, Costelloe, RD and Fomin, T 2013, Crustal architecture of the Capricorn Orogen, Western Australia: results from the 2010 deep crustal reflection seismic survey: *Australian Journal of Earth Sciences* v. 60, no. 6–7, p. 681–705.
- Juhlin, C 1990, Interpretation of the reflections in the Siljan Ring area based on results from the Gravberg-1 borehole: *Tectonophysics*, v. 173, p. 345–360.
- Kennett, BLN, Saygin, E, Fomin, T and Blewett, R 2013, Deep Crustal Seismic Reflection Profiling: Australia 1978–2011: ANU E Press and Commonwealth of Australia (Geoscience Australia), Canberra, Australia, 180p.
- Kinny, PD, Williams, IS, Froude, DO, Ireland, TR and Compston W 1988, Early Archaean zircon ages from orthogneisses and anorthosites at Mount Narryer, Western Australia: *Precambrian Research*, v. 38, p. 325–341.
- Korsch, RJ, Doublier, MP, Romano, SS, Johnson, SP, Mory, AJ, Carr, LK, Zhan, Y and Blewett, RS 2013, Geological interpretation of deep seismic reflection line 11GA-SC1: Narryer Terrane, Yilgarn Craton and Southern Carnarvon Basin, *in* Youanmi and Southern Carnarvon seismic and magnetotelluric (MT) workshop 2013 *compiled by* S Wyche, TJ Ivanic and I Zibra: Geological Survey of Western Australia, Record 2013/6, p. 129–145.
- Korsch, RJ, Huston, DL, Henderson, RA, Blewett, RS, Withnall, IW, Fergusson, CL, Collins, WJ, Saygin, E, Kositsin, N, Meixner, AJ, Chopping, R, Henson, PA, Champion, DC, Hutton, LJ, Wormald, R, Holzschuh, J and Costelloe, RD 2012, Crustal architecture and of North Queensland, Australia: insights from deep seismic reflection profiling: *Tectonophysics*, v. 572–573, p. 76–99.
- Korsch, RJ, Johnson, SP, Tyler, IM, Thorne, AM, Blewett, RS, Cutten, HN, Joly, A, Dentith, MC, Aitken, ARA, Goodwin, JA and Kennett, BLN 2011a, Geodynamic implications of the Capricorn deep seismic survey: from the Pilbara Craton to the Yilgarn Craton, *in* Capricorn Orogen seismic and magnetotelluric (MT) workshop 2011: extended abstracts *edited by* SP Johnson, AM Thorne and IM Tyler: Geological Survey of Western Australia, Record 2011/25, p. 107–114.
- Korsch, RJ, Kositsin, N and Champion, DC 2011b, Australian island arcs through time: geodynamic implications for the Archean and Proterozoic: *Gondwana Research*, v. 19, p. 716–734.
- Korsch, RJ, Preiss, WV, Blewett, RS, Cowley, WM, Neumann, NL, Fabris, AJ, Fraser, GL, Dutch, R, Fomin, T, Holzschuh, J, Fricke, CE, Reid, AJ, Carr, LK and Bendall, BR 2010, Deep seismic reflection transect from the western Eyre Peninsula in South Australia to the Darling Basin in New South Wales: Geodynamic implications, *in* South Australian Seismic and MT Workshop, extended abstracts *edited by* RJ Korsch and N Kositsin: Geoscience Australia, Record 2010/10, p. 105–116.
- Kositsin, N, Brown, SJA, Barley, ME, Krapež, B, Cassidy, KF, Champion, DC, 2008, SHRIMP U–Pb zircon age constraints on the Late Archaean tectonostratigraphic architecture of the Eastern Goldfields Superterrane, Yilgarn Craton, Western Australia: *Precambrian Research*, v. 161, p. 5–33.
- Krapež, B 2006, Terrane Stratigraphy of the Eastern Goldfields Superterrane, and review of the geotectonic history, *in* Tectonostratigraphic and structural architecture of the eastern Yilgarn Craton: Australian Mineral Industry Research Association (AMIRA) Project P763/pmd* CRC Project Y1, Final Report, p. 1–107.
- Krapež, B and Barley, ME 2008, Late Archaean synorogenic basins of the Eastern Goldfields Superterrane, Yilgarn Craton, Western Australia. Part III. Signatures of tectonic escape in an arc-continent collision zone: *Precambrian Research*, v. 161, p. 183–199.
- Ksienzyk, AK, Jacobs, J, Boger, SD, Kosler, J, Sircombe, KN and Whitehouse, MJ 2012, U–Pb ages of metamorphic monazite and detrital zircon from the Northampton Complex: evidence of two orogenic cycles in Western Australia: *Precambrian Research*, v. 198–199, p. 37–50.
- Milligan, PR, Duan, J, Fomin, T, Nakamura, A and Jones, T 2013, The Youanmi magnetotelluric (MT) transects, *in* Youanmi and Southern Carnarvon seismic and magnetotelluric (MT) workshop 2013 *compiled by* S Wyche, TJ Ivanic and I Zibra: Geological Survey of Western Australia, Record 2013/6, p. 13–25.
- Myers, JS 1988, Early Archaean Narryer Gneiss Complex, Yilgarn Craton, Western Australia: *Precambrian Research*, v. 38, p. 297–307.
- Myers JS 1990, Pinjarra Orogen: Geological Survey of Western Australia, Memoir 3, p. 265–274.
- Myers, JS 1995, The generation and assembly of an Archaean supercontinent: evidence from the Yilgarn Craton, Western Australia, *in* Early Precambrian Processes *edited by* MP Coward and AC Ries: Geological Society, London, Special Publication 95, p. 143–154.
- Nelson, DR, Robinson, BW and Myers, JS 2000, Complex geological histories extending for ≥ 4.0 Ga deciphered from xenocryst zircon microstructures: *Earth and Planetary Science Letters*, v. 181, p. 89–102.
- Nutman, AP, Bennett, VC, Kinny, PD and Price, R 1993, Large-scale crustal structure of the northwestern Yilgarn Craton, Western Australia: Evidence from Nd isotopic data and zircon geochronology: *Tectonics*, v. 12, p. 971–981.

- Occhipinti, SA, Sheppard, S, Passchier, C, Tyler, IM and Nelson, DR 2004, Palaeoproterozoic crustal accretion and collision in the southern Capricorn Orogen: the Glenburgh Orogeny: *Precambrian Research*, v. 128, p. 237–255.
- Pawley, MJ, Wingate, MTD, Kirkland, CL, Wyche, S, Hall, CE, Romano, SS and Doublier, MP 2012, Adding pieces to the puzzle: episodic crustal growth and a new terrane in the northeast Yilgarn Craton, Western Australia: *Australian Journal of Earth Sciences*, v. 59, p. 603–623.
- Pidgeon, RT and Wilde, SA 1990, The distribution of 3.0 Ga and 2.7 Ga volcanic episodes in the Yilgarn Craton of Western Australia: *Precambrian Research*, v. 91, p. 309–325.
- Romano, SS, Ivanic, TJ, Korsch, RJ, Wyche, S, Van Kranendonk, MJ, Jones, LEA, Zibra, I, Blewett, RS, Jones, T, Milligan, PR, Costelloe, RD, Doublier, MP, Pawley, MJ, Gessner, K, Hall, CE, Patison, N, Kennett, BLN and Chen, SF 2013, Preliminary interpretation of the northern section of deep seismic line 10GA-YU1: Narryer Terrane to Murchison Domain of the Youanmi Terrane, in *Youanmi and Southern Carnarvon seismic and magnetotelluric (MT) workshop 2013 compiled by S Wyche, TJ Ivanic and I Zibra*: Geological Survey of Western Australia, Record 2013/6, p. 123–128.
- Sheppard, S, Occhipinti, SA and Tyler, IM 2004, A 2005–1970 Ma Andean-type batholith in the southern Gascoyne Complex, Western Australia: *Precambrian Research*, v. 128, p. 257–277.
- Smirnov, AV, Evans, ADA, Ernst, RE, Soderlund, U and Li, ZX 2013, Trading partners: Tectonic ancestry of southern Africa and Western Australia, in *Archean supercratons Vaalbara and Zimgarn*: *Precambrian Research*, v. 224, p. 11–22.
- Smithies, RH and Champion, DC 1999, Late Archean felsic alkaline igneous rocks in the Eastern Goldfields, Yilgarn Craton, Western Australia: a result of lower crustal delamination?: *Journal of the Geological Society, London*, v. 156, p. 561–576.
- Spaggiari, CV, 2007, Structural and lithological evolution of the Jack Hills greenstone belt, Narryer Terrane, Yilgarn craton, Western Australia: Geological Survey of Western Australia, Record 2007/3, 49p.
- Spaggiari, CV, Pidgeon, RT and Wilde, SA 2007, The Jack Hills greenstone belt, Western Australia, Part 2: Lithological relationships and implications for the deposition of ≥ 4.0 Ga detrital zircons: *Precambrian Research*, v. 155, p. 261–286.
- Spaggiari, CV, Wartho, J-A and Wilde, SA 2008, Proterozoic deformation in the northwest of the Archean Yilgarn Craton, Western Australia: *Precambrian Research*, v. 162, p. 354–384.
- Swager, CP, Goleby, BR, Drummond, BJ, Rattenbury, MS and Williams, PR 1997, Crustal structure of granite–greenstone terranes in the Eastern Goldfields, Yilgarn Craton, as revealed by seismic reflection profiling: *Precambrian Research*, v. 83, p. 43–56.
- Thern, ER and Nelson, DR 2012, Detrital zircon age structure within ca. 3 Ga metasedimentary rocks, Yilgarn Craton: Elucidation of Hadean source terranes by principal component analysis: *Precambrian Research*, v. 214–215, p. 28–43.
- Van Kranendonk, MJ, Ivanic, TJ, Wingate, MTD, Kirkland, CL and Wyche S 2012, Long-lived, autochthonous development of the Archean Murchison Domain, and implications for Yilgarn Craton tectonics: *Precambrian Research*, v. 229, p. 49–92.
- Welford, JK and Clowes, RM 2004, Deep 3-D seismic reflection imaging of Precambrian sills in southwestern Alberta, Canada: *Tectonophysics*, v. 388, p. 161–172.
- Wilde, SA 1999, Evolution of the Western Margin of Australia during the Rodinian and Gondwanan Supercontinent Cycles: *Gondwana Research*, v. 2, p. 481–499.
- Wilde, SA, Valley, JW, Peck, WH and Graham, CM 2001, Evidence from detrital zircons for the existence of continental crust and oceans on the Earth 4.4 Gyr ago: *Nature*, v. 409, p. 175–178.
- Wingate, MTD, Bodorkos, S and Kirkland, CL 2008, 178113: gabbro sill, Kurratong Bore: Geochronology dataset 732 in *Compilation of geochronology data*, Geological Survey of Western Australia.
- Wyche, S 2007, Evidence of pre-3100 Ma crust in the Youanmi and South West Terranes and Eastern Goldfields Superterrane, of the Yilgarn Craton, in *Earth's oldest rocks edited by MJ Van Kranendonk, RH Smithies and VC Bennett*: *Developments in Precambrian Geology*, v. 15, p. 113–123.
- Wyche, S, Kirkland, CL, Riganti, A, Pawley, MJ, Belousova, EA and Wingate, MTD 2012, Isotopic constraints on stratigraphy in the central and eastern Yilgarn Craton, Western Australia: *Australian Journal of Earth Sciences*, v. 59, p. 657–670.
- Wyche, S, Nelson, DR and Riganti, A 2004, 4350–3130 Ma detrital zircons in the Southern Cross Granite–Greenstone Terrane, Western Australia: implications for the early evolution of the Yilgarn Craton: *Australian Journal of Earth Sciences*, v. 51, p. 31–45.
- Wyche, S, Pawley, MJ, Chen, SF, Ivanic, TJ, Zibra, I, Van Kranendonk, MJ, Spaggiari, CV and Wingate MTD 2013, Geology of the northern Yilgarn Craton, in *Youanmi and Southern Carnarvon seismic and magnetotelluric (MT) workshop 2013 compiled by S Wyche, TJ Ivanic and I Zibra*: Geological Survey of Western Australia, Record 2013/6, p. 33–63.
- Wyman, DA and Kerrich, R 2012, Geochemical and isotopic characteristics of Youanmi terrane volcanism: the role of mantle plumes and subduction tectonics in the western Yilgarn Craton: *Australian Journal of Earth Sciences*, v. 51, p. 671–694.
- Zibra, I, Gessner, K, Korsch, RJ, Blewett, RS, Jones, T, Milligan, PR, Jones, LEA, Wyche, S, Doublier, MP, Hall, CE, Chen, SF, Romano, SS, Ivanic, TJ, Pawley, MJ, Patison, N, Kennett, BLN and Van Kranendonk, MJ 2013a, Preliminary interpretation of deep seismic lines 10GA-YU3 and the southeastern part of 10GA-YU1: Murchison Domain of the Youanmi Terrane, in *Youanmi and Southern Carnarvon seismic and magnetotelluric (MT) workshop 2013 compiled by S Wyche, TJ Ivanic and I Zibra*: Geological Survey of Western Australia, Record 2013/6, p. 113–122.
- Zibra, I, Gessner, K, Pawley, MJ, Wyche, S, Chen, SF, Korsch, RJ, Blewett, RS, Jones, T, Milligan, PR, Jones, LEA, Doublier, MP, Hall, CE, Romano, SS, Ivanic, TJ, Patison, N, Kennett, BLN and Van Kranendonk, MJ 2013b, Preliminary interpretation of deep seismic line 10GA-YU2: Youanmi Terrane and western Kalgoorlie Terrane, in *Youanmi and Southern Carnarvon seismic and magnetotelluric (MT) workshop 2013 compiled by S Wyche, TJ Ivanic and I Zibra*: Geological Survey of Western Australia, Record 2013/6, p. 87–95.

The 2010 Youanmi deep-crustal seismic lines: implications for mineral systems

by

S Wyche, TJ Ivanic, I Zibra, K Gessner, M Doublier, RJ Korsch¹, and RS Blewett¹

Introduction

The Youanmi and Southern Carnarvon seismic lines (Costelloe, 2013, this volume; Costelloe and Jones, 2013, this volume) traverse the western half of the northern Yilgarn Craton from the western side of the Kalgoorlie Terrane of the Eastern Goldfields Superterrane, across the Paleo- to Neoproterozoic rocks of the Youanmi and Narryer terranes. The western end of the Southern Carnarvon seismic line, 11GA-SC1, passes from the Yilgarn Craton to cross Archean to Proterozoic rocks of the Glenburgh Terrane, Meso- to Neoproterozoic rocks of the Pinjarra Orogen, and Phanerozoic sedimentary rocks of the Southern Carnarvon Basin (Fig. 1). Only aspects of mineralization in the Yilgarn Craton will be discussed in this contribution.

The distribution and endowment of various mineral commodities in the Yilgarn Craton is best understood in terms of the various factors which control development of a mineral system. These include: 1) geodynamic setting; 2) architecture; 3) fluid reservoirs; 4) fluid-flow pathways and drivers; and 5) metal transport and deposition (Barnicoat et al., 2007). Seismic reflection and MT traverses provide key insights into the understanding of the lithospheric architecture (Blewett et al., 2010a). They are particularly helpful in understanding the structure of the middle and lower crust, shape and depth of greenstone belts, and the orientations and depth penetration of major shear zones.

The northern Yilgarn Craton is a richly endowed region that contains economic deposits of gold, nickel, iron, base metals, vanadium and uranium, with potential for chromium and PGE mineralization. The three Youanmi seismic traverses cross several greenstone intervals, each of which has a particular character in terms of age, style and volume of metal endowment.

Seismic and MT data provide constraints on geodynamic models (see Korsch et al., 2013, this volume), which, in

turn, determine the exploration potential for commodities such as base metals and iron. They are especially valuable, however, for the interpretation of late structural history and shapes of basins. Thus, in the northern Yilgarn Craton, they are perhaps of most direct relevance in understanding the late structural history which hosted gold mineralization, and in determining the shape and orientation of the layered igneous complexes, which host, or have the potential to host, magmatic chromium, nickel, vanadium and PGE deposits.

The eastern end of line 10GA-YU2 crosses the Ida Fault, which is the boundary between the Kalgoorlie Terrane of the Eastern Goldfields Superterrane and the Youanmi Terrane. This boundary is considered to be a fundamental division within the Yilgarn Craton, separating two areas of crust with significantly different crustal histories (Cassidy et al., 2006; Wyche et al., 2013, this volume). The greenstones near and immediately to the east of the interpreted position of the Ida Fault (see Zibra et al., 2013, this volume) host world-class gold (Thébaud et al., 2012) and nickel deposits (Barnes et al., 2011). The fundamental nature of this structure is evident in a range of datasets from seismic (Swager et al., 1997; Drummond et al., 2000) to aeromagnetic and gravity data (Plate 1A), and Nd and Hf model-age isotopic data (Fig. 2; Champion and Cassidy, 2007). In the Nd and Hf model-age data, there is a marked change from relatively juvenile crust in the Eastern Goldfields Superterrane to older, reworked crust in the Youanmi Terrane (Wyche et al., 2012). Regions of very old, reworked crust may overlie thick remnants of subcontinental lithospheric mantle (SCLM; Begg et al., 2010). The Ida Fault also marks a change from the richly gold- and nickel-endowed Eastern Goldfields Superterrane to the apparently more sparsely-endowed Youanmi Terrane where economic nickel and gold mineralization is more locally focused. The only known economic VMS deposit in the Eastern Goldfields, is the Jaguar – Bentley – Teutonic Bore deposit, about 70 km south of the eastern end of line 10GA-YU2.

West of the Ida Fault, seismic line 10GA-YU2 crosses the Southern Cross Domain of the Youanmi Terrane, which is dominated by granite with several small greenstone intervals, most notably the Sandstone greenstone belt.

¹ Minerals and Natural Hazards Division, Geoscience Australia, GPO Box 378, Canberra ACT 2601

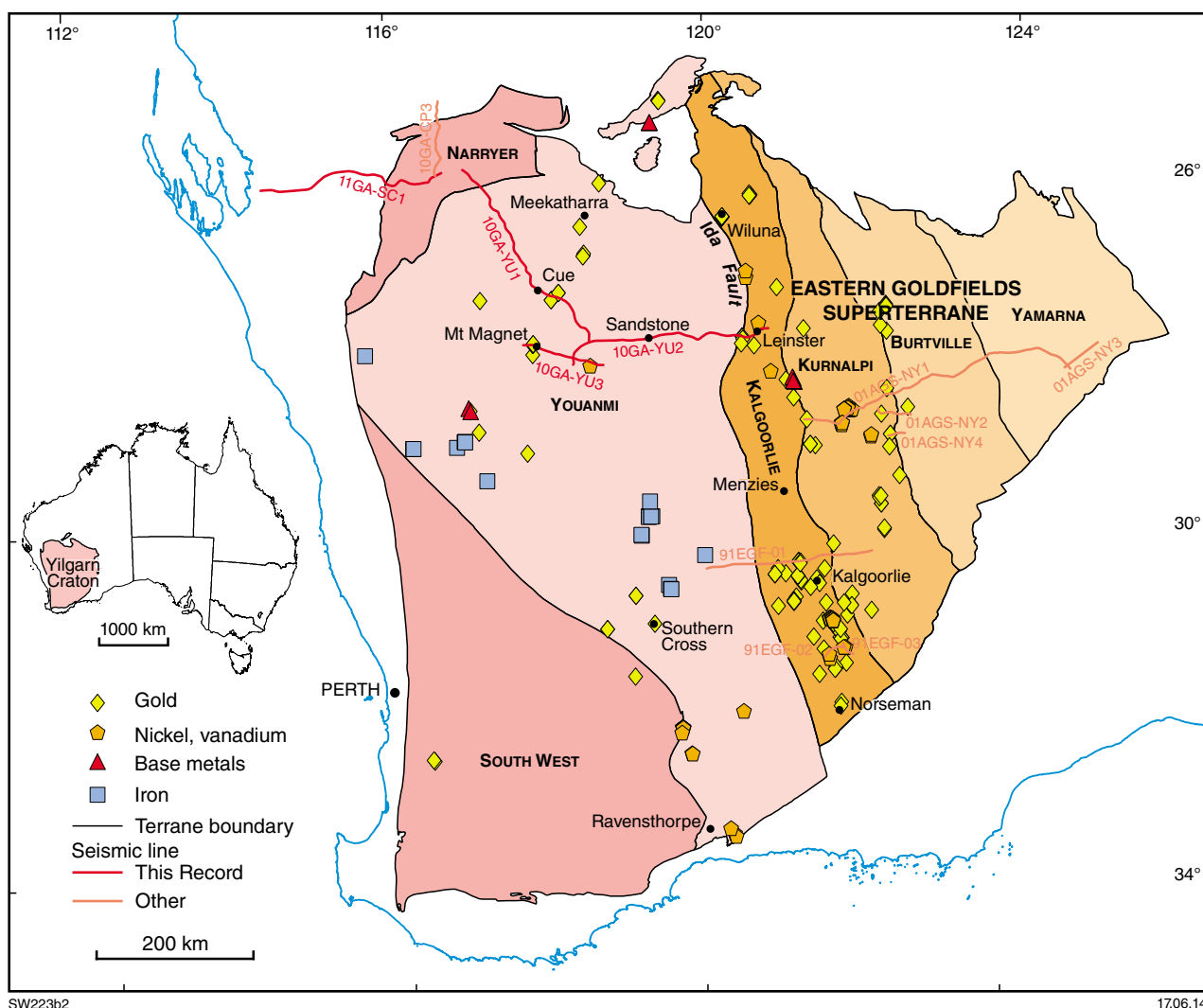


Figure 1. Tectonic units along the seismic traverses showing the distribution of operating mines

In this part of the traverse, east of the boundary with the Murchison Domain, the Nd and Hf model-age data indicate the presence of old, stable, reworked crust (Fig. 2; Wyche et al., 2012). There are no known large gold deposits in this interval. Although there are mapped komatiites (Chen et al., 2005) in the greenstone successions, no economic nickel mineralization has been found in this region. The nearest Southern Cross Domain deposits lie about 500 km to the south at Forrestania and Lake Johnston (Barnes and Fiorentini, 2012). Greenstones of the Southern Cross Domain host iron deposits in banded iron-formation, with economic deposits or active prospects in most greenstone belts. No economic base-metal deposits have been found in this region.

West of the Southern Cross Domain, line 10GA-YU2 links lines 10GA-YU1 and 10GA-YU3 at the Windimurra Igneous Complex in the Murchison Domain of the Youanmi Terrane. This layered mafic-ultramafic intrusion is part of the Meeline Suite of similar intrusions (Ivanic et al., 2010, 2013, this volume; see also below), which host economic vanadium deposits and have potential for

chromium, nickel and PGE mineralization. To the west and northwest of the Windimurra Igneous Complex, lines 10GA-YU3 and 10GA-YU1 cross a region with substantial gold endowment and a number of base-metal prospects which, along with the Meeline Suite of mafic-ultramafic layered intrusions, coincides with a zone of relatively juvenile crust (Fig. 2; Champion and Cassidy, 2007; Ivanic et al., 2012). The only operating base-metal mine in the Murchison Domain is hosted in c. 2950 Ma felsic volcanic and volcanoclastic rocks at Golden Grove, about 100 km southwest of western end of line 10GA-YU3. Iron deposits and prospects hosted in banded iron-formation are rare in the vicinity of the zone of juvenile crust, but abundant in the older greenstone successions to the north, notably in the Jack Hills greenstone belt near the northwestern end of 10GA-YU1, which lies near the interpreted boundary between the Youanmi Terrane and the Narryer Terrane (Spaggiari et al., 2007; Romano et al., 2013, this volume).

The northwestern end of line 10GA-YU1 and the eastern end of line 11GA-SC1 cross the Narryer Terrane. Here,

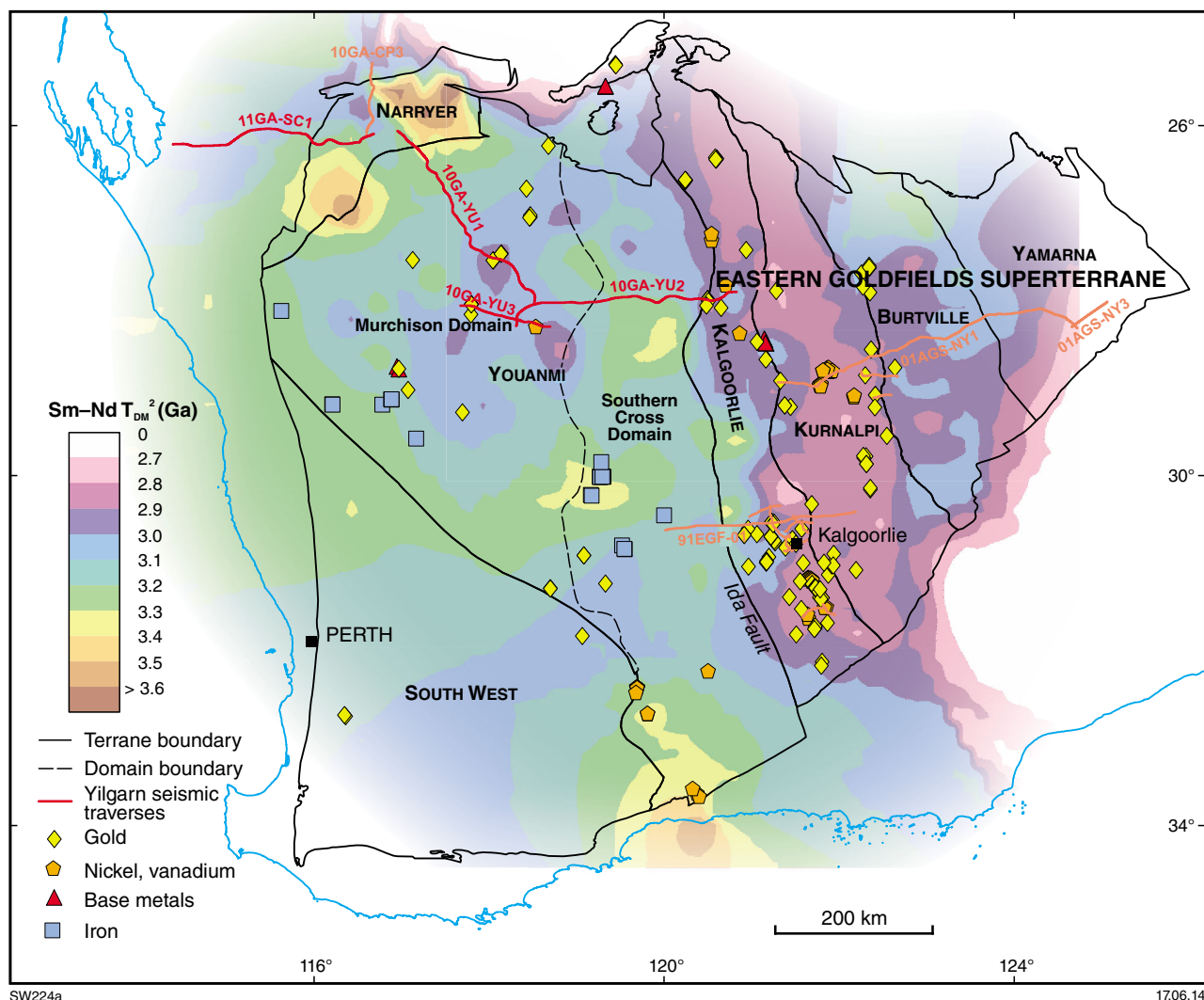


Figure 2. Nd depleted-mantle model age map for the Yilgarn Craton showing operating mines and tectonic subdivisions

the Nd model-age data (Fig. 2) indicate the presence of very old crust, which is in accordance with the known presence of very old rocks and detrital zircons in clastic sedimentary rocks. This region is dominated by extensive areas of granite and granitic gneiss, with minor mafic gneiss and supracrustal rocks, including mafic rocks, banded iron-formation and clastic sedimentary rocks (Wyche et al., 2013, this volume, and references therein). This region is not known to host any economic mineral deposits.

Gold

Eastern Goldfields Superterrane

Cassidy et al. (2003) and Blewett et al. (2010a,b) described the key elements in the architecture of the Eastern Goldfields Superterrane which play a role in the localization of gold deposits. In particular, they recognized

that crustal-penetrating shear zones are potentially important pathways for fluids, but that not all apparently prominent structures penetrate deeply into the crust. Blewett et al. (2010b) suggested that the best endowed areas are those which have a long history of structural preparation through repeated deformation, perhaps back to the earliest basin-forming events (e.g. Miller et al., 2010). In these places, there are likely to have been multiple episodes of mineralization. The most abundant and largest gold deposits have a spatial association with the relatively juvenile crust in the Kalgoorlie and Kurnalpi terranes in the western part of the Eastern Goldfields Superterrane (Fig. 2).

Although there is evidence for multiple episodes of gold mineralization in the Eastern Goldfields Superterrane, all are considered to be relatively late in the tectonic history (Blewett and Czarnota, 2007; Blewett et al., 2010b; Thébaud et al., 2012). Blewett et al. (2010b) proposed that the first prominent gold mineralization event coincided with their D₃ doming event, which was associated with widespread granite intrusion after c. 2665 Ma. The shear

zones produced by this deformation are characterized as extensional, as shown by S–C–C' fabrics (Blewett et al., 2010b) and anticlockwise P–T–t paths (Goscombe et al., 2009). The presence of clastic 'late-basin' successions (Krapež et al., 2000), which are commonly found near large gold deposits (Hall, 2007), in the hangingwall of the D₃ extensional shear zones, is a common feature of these structures.

According to Blewett et al. (2010b), the major gold mineralization event in the Eastern Goldfields coincided with west-northwesterly – east-northeasterly oriented shortening (D4b and D5 of Blewett et al., 2010b), which commenced during the waning stages of high-Ca granite magmatism, and produced brittle–ductile shear zones and thrusts with local development of dilational and contractional jogs. These proved to be favourable loci for the deposition of gold mineralization.

Eastern end of seismic line 10GA-YU2

The eastern end of line 10GA-YU2 is about 40 km east of the Youanmi Terrane – Eastern Goldfields Superterrane boundary, marked in most places by the Ida Fault. At the surface, the position of the fault is apparently masked by overprinting structures in this area (Liu and Chen, 1998; Zibra et al., this volume). However, it is clearly imaged as a prominent, east-dipping feature in the 10GA-YU2 MT survey (Milligan et al., 2013, this volume). The largest gold deposits in this region have been found near this boundary.

Beardsmore (2002) provides detailed descriptions of historical gold mines in the Lawlers region near the eastern end of line 10GA-YU2. Thébaud et al. (2012) described the structural setting of four gold deposits along the western side of the Lawlers Anticline. They interpreted two main periods of gold mineralization: an early event at c. 2662 Ma, broadly contemporaneous with the intrusion of the Lawlers Tonalite (Songvang and Crusader; Fig. 3); and later, possibly multistage, mineralization within late-basin sedimentary rocks (Waroonga, New Holland and Genesis; Fig. 3). Blewett et al. (2010b) interpreted the Sunrise Birthday deposit, which lies within the greenstone succession near the hinge of the Lawlers Anticline (Fig. 3), as having formed in an extensional setting associated with the emplacement of the Lawlers Tonalite.

The seismic data (Fig. 4; Zibra et al., 2013, this volume) show overprinting relationships between large-scale features, such as the Lawlers Anticline, and very early structures, such as the Ida Fault, which is interpreted to have been truncated during the intrusion of the Lawlers Tonalite. In this instance, the tonalite may have intruded and enhanced a pre-existing fold. The structural sequence immediately postdating the intrusion of the Lawlers Tonalite is not readily decipherable from the seismic data, but relationships are consistent with some westward-directed thrust movement. The seismic line ends just to the east of the surface trace of the Perseverance Fault, which is not a prominent feature in the seismic images (Fig. 4). However, none of the interpreted east- or west-dipping structures in this part of the line penetrates deeper

than about 4 s two-way travel time (TWT), so the only structures at the eastern end of line 10GA-YU2 which appear likely to pass through the crust are the Ida Fault, interpreted below the Lawlers Tonalite, and the Table Hill Shear Zone, which bounds the eastern side of the Lawlers Anticline (Fig. 4). Apart from the Proterozoic sills, which may occupy very late, shallow-dipping structures, the latest structures evident in the seismic data are the Waroonga and Emu shear zones, which bound the late-basin succession to the west of New Holland, and show duplex structures indicating eastward-directed movement. Both of these structures are highly mineralized.

Beneath the eastern limb of the Lawlers Anticline, a broad zone of diffuse reflectance extends to the base of the crust and beyond (Fig. 4). This feature coincides with the deepening of the Moho and a change in texture of the reflections, from shallow east-dipping to flat lying in the middle and lower crust in the Youanmi Terrane, to a more pronounced dip to the east in the Eastern Goldfields Superterrane. The zone of diffuse reflectance embraces the interpreted position of the Ida Fault. It may be an artefact due to a loss of data, but it could also represent an alteration or damage zone generated as result of complexly overprinting structures in a craton-scale terrane boundary.

In summary, in terms of gold mineralization, the most endowed part of the southern end of the Agnew–Wiluna greenstone belt lies along the western side of the belt. The seismic data show this part of the belt to have the most complex overprinting structural relationships, with both the earliest and latest recognized structures in this part of the line. The long history of structural overprinting and reworking, accompanied by intrusion of the Lawlers Tonalite to provide fluids and a heat source, has created numerous opportunities for gold deposition. The latest structures, the Waroonga and Emu shear zones, generated new sites for gold deposition in what was already a very fertile region.

Youanmi Terrane

Although the structural setting and other factors affecting gold mineralization in the Eastern Goldfields Superterrane have been the subject of many studies, much less attention has been given to the gold deposits in the Youanmi Terrane. This terrane has numerous gold deposits and prospects spread across most greenstone belts, with significant production from the Southern Cross greenstone belt, in the south of the Southern Cross Domain, and from the greenstones between Meekatharra and Mount Magnet, a region crossed by lines 10GA-YU1 and 10GA-YU3 in this survey. The other major gold producer in the western Yilgarn Craton is the Boddington gold mine in the South West Terrane (Allibone et al., 1998).

The Youanmi Terrane includes several distinct crustal elements, which are clearly delineated on the Yilgarn Nd model-age map (Fig. 2). Immediately west of the Ida Fault and across most of the Southern Cross Domain traversed by line 10GA-YU2, the Nd model-age map shows old, reworked crust. The nature of the crust changes in the eastern part of the Murchison Domain, where the three

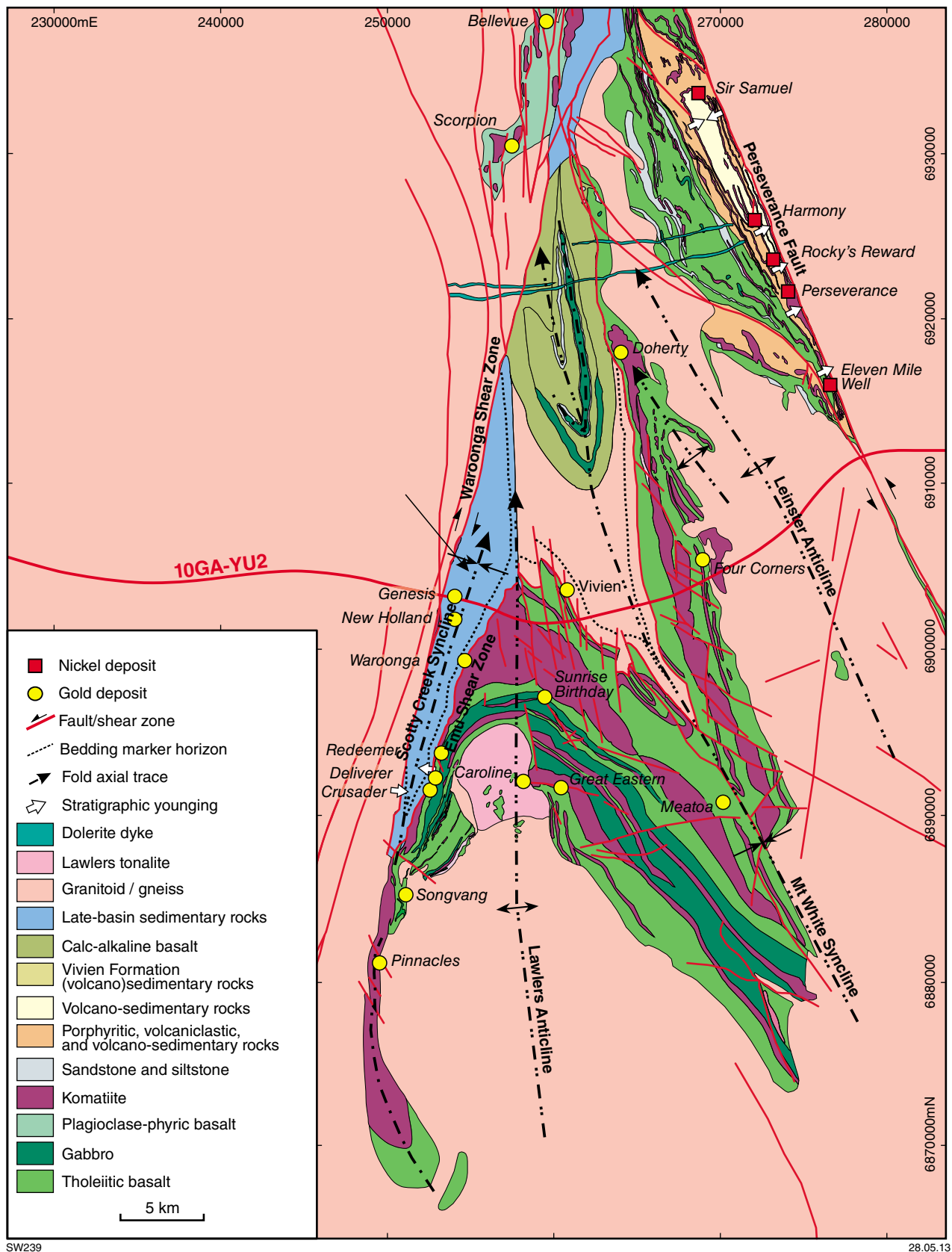


Figure 3. Lawlers Anticline area of the Agnew–Wiluna greenstone belt showing major gold deposits (modified from Duuring et al., 2012)

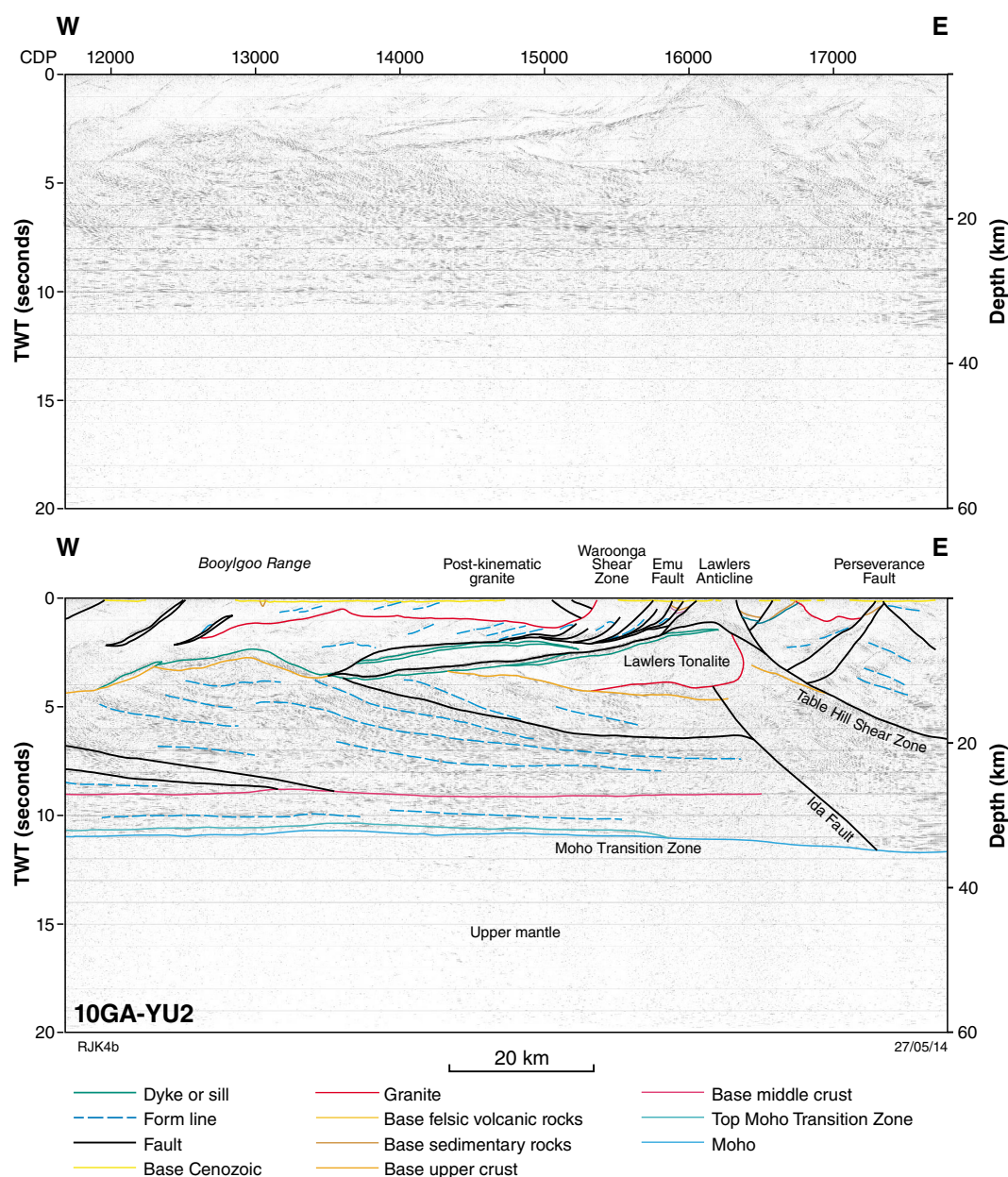


Figure 4. Migrated seismic section for eastern end of the seismic line 10GA-YU2 with interpretation

Youanmi seismic lines intersect, becoming dominated by more juvenile crust along a structural corridor which is occupied by greenstones of the Murchison Supergroup and associated granites (Van Kranendonk et al., 2012; Wyche et al., 2013, this volume). This corridor contains the most abundant and well-endowed gold deposits (Robert et al., 2005; Geological Survey of Western Australia, 2013). West of the corridor, lines 10GA-YU1 and 11GA-SC1 cross old, reworked crust, which is similar in character to that between the Ida Fault and the eastern side of the Murchison Domain.

Greenstone successions in the Youanmi Terrane are typically older, cover a broader age range, and differ

in character from those in the gold-rich Kalgoorlie and Kurnalpi terranes of Eastern Goldfields Superterrane. Thus they have a longer and possibly more complex structural history, although there is a strong commonality across the Yilgarn Craton in the later history of granite intrusion and age of large-scale deformation (Wyche et al., 2013, this volume). Although there is ongoing discussion concerning the number and age of mineralizing events in individual deposits, all evidence indicates that gold mineralization postdates formation of most of the supracrustal rocks, and took place mostly after c. 2700 Ma across the entire Yilgarn Craton (Duuring et al., 2007).

In the vicinity of the seismic traverses across northern

Youanmi Terrane, there are gold prospects, historical gold mines and/or operating gold mines in all greenstone belts except the Booylgoo Range greenstone belt (Geological Survey of Western Australia, 2013). The greenstone belts in the northern Southern Cross Domain, however, have relatively small historical production. The Sandstone greenstone belt produced about 30 t of gold, with 7 t having come from the Bulchina openpit, which closed in 2004. Here, gold appeared to be hosted in late structures (Wyche, 2007).

Although there has been substantial documentation of individual gold deposits in the northern Murchison Domain (e.g. Watkins and Hickman, 1990; Mueller et al., 1996; Timms et al., 2011), there has been no attempt to synthesize the regional controls on mineralization. Deposits are typically hosted in late structures but there are very few constraints on the age of the mineralizing events. Wang et al. (1993) dated the mineralization at Reedy at c. 2639 Ma using a Pb–Pb isochron on titanate and pyrite; Mueller et al. (1996) obtained a U–Pb almandine age of c. 2662 Ma on an alteration assemblage from the structurally hosted Big Bell deposit; and Yeats et al. (1996) dated hydrothermal zircons associated with gold mineralization at Mount Gibson in the south of the region at c. 2627 Ma.

Southern Cross Domain: seismic line 10GA-YU2

Although several large-scale shear zones are apparent in outcrop and on aeromagnetic images (Plate 1A), the only structure interpreted as penetrating the lower crust is the east-dipping Youanmi Shear Zone (Zibra et al., 2013, this volume). However, even this structure is not well defined in the seismic data (Fig. 5). Shallow-dipping Proterozoic sills are common in this part of line 10GA-YU2. Extensive areas of high-level, sill-like intrusions of post-tectonic granites further obscure potential fluid pathways in the upper crust.

West-dipping structures between the Ida Fault and the Sandstone greenstone belt, including the Waroonga Shear Zone immediately west of the terrane boundary (Fig. 4), postdate and, in some cases, truncate east-dipping structures. These structures rarely penetrate to more than about 2 s TWT (~6 km). However, it is likely that movement on the Waroonga Shear Zone played a role in preparing depositional sites for gold mineralization along the western side of the Kalgoorlie Terrane, so these late structures may be significant in areas where other factors suggest gold fertility. One of the west-dipping shear zones,

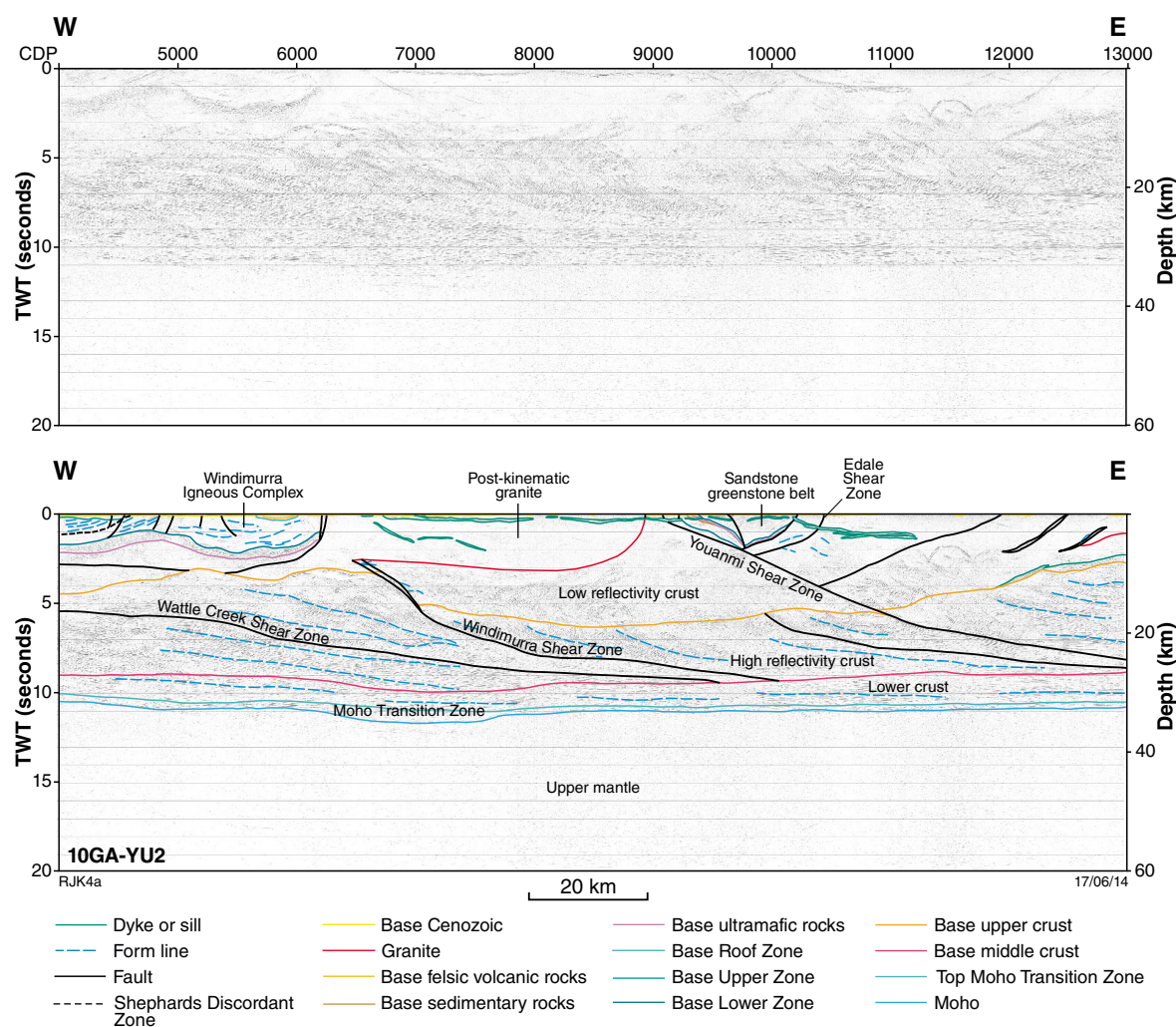


Figure 5. Migrated seismic section for western end of the seismic line 10GA-YU2 with interpretation

at about CDP 12500 (Zibra et al., 2013, this volume), corresponds to an area of relatively low resistivity on the 10GA-YU2 MT image (Plate 3; Milligan et al., 2013, this volume), suggesting that this may be a more deeply penetrating feature. This broad structure may extend for more than 50 kilometres to the north where it disrupts and dismembers greenstones at the northern end of the Booylgoo Range greenstone belt (Wyche and Doyle, 2006).

In summary, the lack of substantial gold deposits in the northern part of the Southern Cross Domain may be attributed to a lack of clearly-defined, crustal-penetrating structures, the dominance of old, stable, reworked crust, and widespread emplacement of sheetlike post-tectonic granites.

Murchison Domain: southeastern end of line 10GA-YU1; western end of line 10GA-YU2; line 10GA-YU3

In contrast with the Southern Cross Domain, the eastern part of the Murchison Domain is a region of relatively juvenile crust (Fig. 2), with a long history of greenstone deposition and granite emplacement, and considerable structural complexity (Wyche et al., 2013, this volume).

Seismic lines 10GA-YU1 and 10GA-YU3 (Fig. 6) show a number of large-scale shear zones, some of which penetrate at least into the lower crust. There are clearly overprinting relationships between early, deeply penetrating, east-dipping structures and later, shallower, west-dipping structures, some of which are duplexes.

The most notable of the early, deeply penetrating structures is the Wattle Creek Shear Zone, which can be traced to at least the top of the lower crust. Zibra (2012) has interpreted this structure as a large-scale, synmagmatic shear zone, which developed during the emplacement of the adjacent tonalitic to monzogranitic Lakeside Granite. It comes to the surface in the Mount Magnet greenstone belt on line 10GA-YU3 on the eastern side of the Lakeside Granite, and is truncated by overprinting, west-dipping structures in the vicinity of Cue and Big Bell on line 10GA-YU1. It also coincides with a clear resistivity discontinuity in the MT images, particularly on line 10GA-YU3. Its surface projection, however, can also be seen as an area of low resistivity on line 10GA-YU1 (Milligan et al., 2013, this volume). These areas are among the most significant gold producers in the Murchison Domain, with historical production of >170 t from Mount Magnet (Ramelius Resources, 2013), >80 t from Big Bell (Mueller et al., 1996) and >40 t from the nearby Day Dawn deposit at Cue (Watkins and Hickman, 1990).

Although the dataset which forms the basis of the Nd model-age map is patchy, the historically largest gold deposits appear to be focused along the western side of the corridor of relatively juvenile crust, in areas directly above the most deeply penetrating structures. The deposit with the largest historical gold production in the Murchison Domain, the Mount Magnet deposit, is very close to the surface expression of the Wattle Creek Shear

Zone. The large deposits at Big Bell and Day Dawn lie above late structures that have deformed and overprinted the Wattle Creek Shear Zone. The endowment at Mount Magnet is substantially larger than appears to be the case at Big Bell and Day Dawn combined. This suggests that there may have been some reworking or remobilization of gold mineralization related to the Wattle Creek Shear Zone at the latter deposits, possibly as a result of the late structural overprint. The other large gold deposit in the northern Murchison Domain, at Meekatharra, about 100 km northeast of line 10GA-YU1, lies just to the east of a prominent shear zone, the Chunderloo Shear Zone (Spaggiari, 2006), which is interpreted to link with the structures at Big Bell (Van Kranendonk et al., 2012).

In summary, the largest gold deposits in the Murchison Domain appear to be related to structures that were able to directly access or tap into deeply penetrating structures in relatively juvenile crust. The most deeply penetrating structures are broadly contemporaneous with TTG-style granites.

Northwestern Murchison Domain and Narryer Terrane: northwestern end of line 10GA-YU1 and eastern end of line 11GA-SC1

Northwest of Big Bell (Plate 1A), seismic line 10GA-YU1 traverses old, reworked crust of the Murchison Domain before passing into the even older crust of the Narryer Terrane to the west. The eastern part of line 11GA-SC1 crosses ancient crust of the Narryer Terrane before encountering Proterozoic and Phanerozoic rocks to the west (Plate 2).

There are few Archean gold prospects, and no known deposits, in the Narryer Terrane. The seismic data reveal no major crustal-penetrating structures of Archean age. The major shear zones near its eastern margin, evident in the seismic data, are considered to be Proterozoic in age, or at least reworked during the Proterozoic (Korsch et al., 2013, this volume). Thus, the lack of suitable structures, combined with old, reworked nature of the crust in this region, suggest that it is not prospective for gold mineralization.

Comparison with Yilgarn seismic lines 91EGF-01 and 01AGS-NY1

Cassidy et al. (2003) compared the seismic profiles from lines 01AGS-NY1 and 91EGF-01 to highlight similarities and differences between the northern and southern parts of the Eastern Goldfields Superterrane, and between the Eastern Goldfields Superterrane and the eastern part of the Youanmi Terrane. The three Youanmi seismic lines have many similarities with the earlier seismic lines, but there are also some distinct differences.

- All lines show a three-layered crust. The reflections in the middle crust in the Youanmi lines and the western

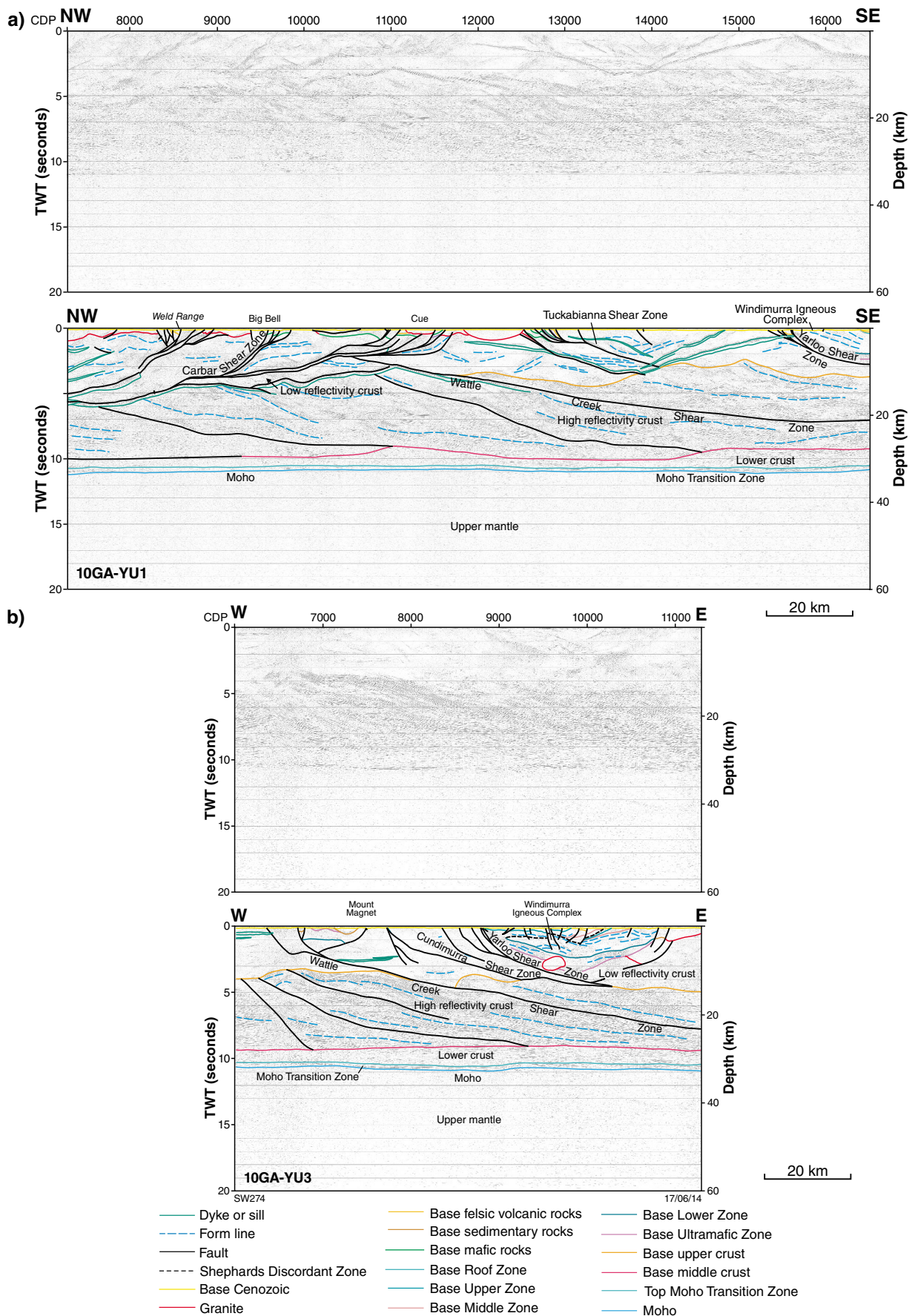


Figure 6. Migrated seismic sections for Cue – Mount Magnet region: a) southeastern end of 10GA-YU1 in the Cue area with interpretation; b) line 10GA-YU3 with interpretation

part of line 91EGF-01, however, are more prominent than in the Eastern Goldfields Superterrane. There is a distinct difference between the character of the middle and lower crust in the Youanmi Terrane (the Yarraquin Seismic Province of Korsch et al., 2013, this volume) compared with the equivalent crustal levels under the Eastern Goldfields Superterrane.

- As in the Youanmi seismic lines, the Moho is clearly defined in line 01AGS-NY1 (Goleby et al., 2004) and line 91EGF-01 (Drummond et al., 2000). Under the Youanmi Terrane, it is typically a flat structure between 10.5 and 11 s TWT (about 31 to 33 km), and becomes deeper to the east under the Eastern Goldfields Superterrane.
- Greenstones are typically between about 4 and 7 km thick and sheet-like granite bodies are clearly imaged in the upper crust.
- All lines show deeply penetrating structures that dip to the east. The Youanmi lines and line 91EGF-01, however, have abundant west-dipping structures in the upper crust, which are not so apparent in line 01AGS-NY1.
- A detachment surface interpreted at base of the greenstones and some granites in line 91EGF-01 (Drummond et al., 2000) has not been recognized in line 01AGS-NY1 or in the Youanmi seismic lines.

Mineralization associated with layered igneous complexes

Cu–Ni–Cr–PGE

The layered mafic–ultramafic intrusions of the Meeline Suite are prospective for Cu, Ni, Cr and PGEs. The Wondinong Cr–PGE prospect, in the lower part of the lower zone of the Windimurra Igneous Complex, is exposed at the surface in its northeasternmost outcrop. Here, mineralization is contained within a <1 cm thick chromitite, the only chromitite yet identified in the main body of the complex. PGE sulfides have been noted at the base of this layer. It is possible that there are many more of these chromitites at depth, especially given that a critical zone (cf. Bushveld Igneous Complex), lying between the lower zone and a postulated ultramafic zone, may be present. Historic drilling projects have never succeeded in breaching beyond the depths of the lower zone of the complex and it is not known which parts of the complex are the likely shallowest targets for a critical or ultramafic zone intersection.

The three Youanmi seismic lines, each of which intersects parts of the Windimurra Igneous Complex, show that there is a thick region of strong reflections beneath at least the northern half of the complex (Ivanic et al., 2013, this volume). These reflections indicate the presence of a strongly compositionally layered, basal zone in the

complex that has no expression in the surface geology. In the current interpretation of the seismic data, we have suggested that this is likely the ultramafic zone of the complex, but it is possible that it also contains a ‘critical zone’ where accumulations of significant chromitite may be found (e.g. Bushveld Complex, Cawthorn and Waldraven, 1998; see Fig. 7).

In the central part of the Windimurra Igneous Complex, the lower zone extends down from 1 s TWT to about 2.3 s TWT, a thickness of about 1.3 s TWT (~4 km), as seen on line 10GA-YU3. The overall funnel shape of the intrusion in 3D is such that the base of the lower zone is shallowest at the margins. The seismic lines indicate the shallowest part to the base of the lower zone, or top of the ultramafic zone, is at about 0.2 s TWT (~600 m depth) in the northernmost part of the complex on line 10GA-YU1, and the westernmost part of the complex on line 10GA-YU3. The 3D seismic model for the complex suggests that the northeastern marginal part of the complex is most favorable for a shallow-base to the lower zone. In this area, it is not terminated by major shear zones, and it is not very deep, as line 10GA-YU2 indicates is the case for the eastern part of the complex.

The presence of a significant ultramafic zone at the base of the Windimurra Igneous Complex would enhance the prospectivity of other igneous complexes in the Meeline Suite. These complexes typically have unknown relationships with their affiliated ultramafic components (Fig. 7), which are typically interpreted to be partially dismembered, and commonly assumed to no longer be present directly beneath them.

Not only is the discovery of a thick ultramafic zone important for Cr–PGE mineralization associated with chromitites, but it also opens up the potential for reefs containing Cu–Ni sulfides. The formation of the upper zone of the western lobe of the complex has been attributed to a single pulse of a 1.5 km-thick sheet (Nebel et al., 2010). Seismic data and 3D modeling show that this sheet is relatively flat lying and consistent with truncation of underlying stratigraphy. If a new pulse of magma was responsible for this zone, it is possible that a second phase of PGE enrichment may be present in the upper zone of the western lobe of the Windimurra Igneous Complex, in a style similar to the Stella intrusion in South Africa (Maier, 2005).

The Inky prospect in the southwestern part of the Youanmi Igneous Complex has recently yielded indications of Ni–Cu sulfide mineralization (Sirius Resources, 2013). The seismic data across the Windimurra Igneous Complex, which show a possible, large, unexposed ultramafic zone, may signify the presence of similar components in the Youanmi Igneous Complex. These two closely juxtaposed Meeline Suite complexes are relatively flat lying and have similar lithological associations.

V–Ti–Fe

Unpublished 3D modelling of the Windimurra Igneous Complex has provided a model compatible with available

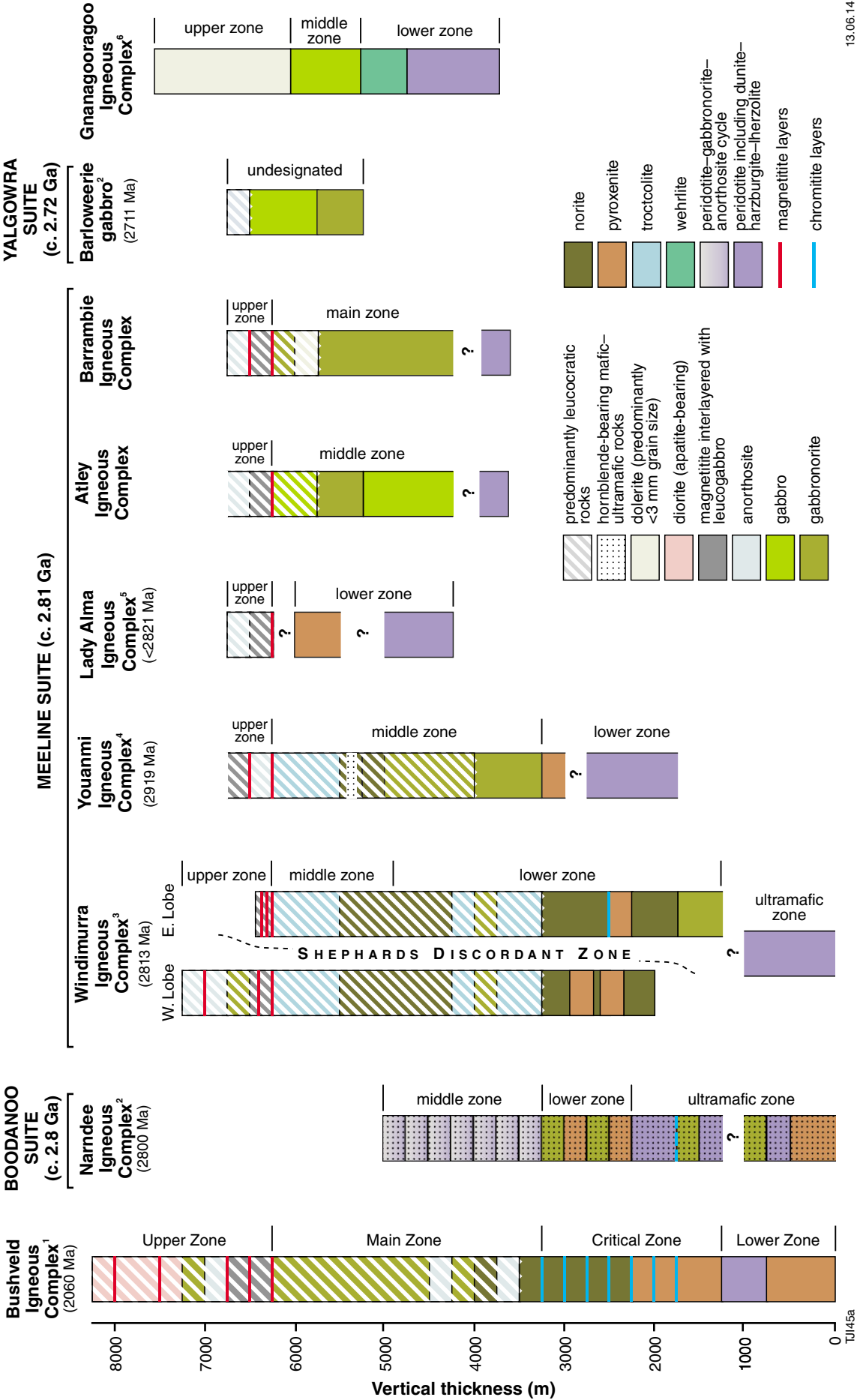


Figure 7. Comparative igneous stratigraphic columns (simplified) for layered igneous complexes of the Murchison Domain, compared with the Bushveld Igneous Complex. Stratigraphy is aligned with occurrence of the lowermost upper zone, typically associated with thick magnetite horizons in the Meeline Suite. Note identified chromitite horizons, in comparison to the critical zone of the Bushveld Igneous Complex. Notes: 1) adapted from Cawthorn and Walraven (1998); 2) zone nomenclature adapted from Scowen (1991), age from Ivanic et al. (2010); 3) age from Wingate et al. (2012); 4) Gill (unpublished); 5) Wang (2009), zones adapted from Parks (1998).

geological and geophysical data at approximately 1:250 000 scale. The geometry of all the various zones of the complex (Fig. 7) has been defined, and the location of the upper zone volumes has the potential to be used to estimate the overall reserves of V–Ti–Fe ore.

In the 3D model, there is a significant break in the igneous stratigraphy along the Shephards Discordant Zone. This zone divides the complex into an early eastern lobe and a late western lobe, the latter of which has a nested, funnel-shaped intrusive form. The formation of this apparent dual-lobe stratigraphy is interpreted to be the result of tectonic instability during crystallization of the magma. The 3D geometry of the truncation of the eastern lobe by the western lobe shows that the main V–Ti mineralization at the Windimurra vanadium mine is truncated at the surface to the north by the western lobe, approximately at the point where the complex is overlain by the roof zone and Kantie Murdana Volcanics Member.

In terms of structure, line 10GA-YU3 shows the Shephards Discordant Zone dipping approximately 30° west, down to at least 1 s TWT (~3 km depth). In the western lobe, many faults can be seen to offset the magnetite layers and other strongly reflective horizons. These features provide good 3D constraints for feasibility studies on the displacements along late northerly striking brittle faults in the Canegrass prospect (Wyche et al., 2013, this volume, fig. 16).

References

- Allibone, AH, Windh, J, Etheridge, MA, Burton, D, Anderson, G, Edwards, PW, Miller, A, Graves, C, Fanning, CM and Wysoczanski, R 1998, Timing relationships and structural controls on the location of Au–Cu mineralisation at the Boddington gold mine: *Economic Geology*, v. 93, p. 245–270.
- Barnes, S-J and Fiorentini, ML, 2012, Komatiite magmas and sulfide nickel deposits: A comparison of variably endowed Archean terranes: *Economic Geology*, v. 107, p. 755–780.
- Barnes, S-J, Fiorentini, ML, Duuring, P, Grguric, BA and Perring, CS 2011, The Perseverance and Mount Keith Ni deposits of the Agnew–Wiluna Belt, Yilgarn Craton, Western Australia: *Reviews in Economic Geology*, v. 17, p. 51–88.
- Barnicoat and the pmd*CRC Y4 Team 2007, Putting it all together: anatomy of a giant mineral system, *in* Proceedings of Geoconferences (WA) Inc. Kalgoorlie '07 Conference, 25–27 September 2007 *edited by* FP Bierlein and CM Knox-Robinson: Geoscience Australia, Record 2007/14, p. 47–51.
- Beardmore, TJ 2002, The geology, tectonic evolution and gold mineralization of the Lawlers region: a synopsis of present knowledge: Barrick Gold of Australia Ltd, Confidential Technical Report 1026, 279p.
- Begg, GC, Hronsky, JMA, Arndt, NT, Griffin, WL, O'Reilly, S and Hayward, N 2010, Lithospheric, cratonic, and geodynamic setting of Ni–Cu–PGE sulfide deposits: *Economic Geology*, v. 105, p. 1057–1070.
- Blewett, RS and Czarnota, K 2007, Diversity of structurally controlled gold through time and space of the central Eastern Goldfields Superterrane — a field guide: Geological Survey of Western Australia, Record 2007/19, 65p.
- Blewett, RS, Czarnota, K and Henson, PA 2010b, Structural-event framework for the eastern Yilgarn Craton, Western Australia, and its implications for orogenic gold: *Precambrian Research*, v. 183, p. 203–209.
- Blewett, RS, Henson, PA, Roy, IG, Champion, DC and Cassidy, KF 2010a, Scale-integrated architecture of a world-class gold mineral system: The Archaean eastern Yilgarn Craton, Western Australia: *Precambrian Research*, v. 183, p. 230–250.
- Cassidy, KF, Blewett, RS, Champion, DC and Goleby, BR 2003, Northeastern Yilgarn seismic reflection survey: implications for orogenic gold systems, *in* The 2001 Northeastern Yilgarn Deep Seismic Reflection Survey *edited by* BR Goleby, RS Blewett, PB Groenewald, KF Cassidy, DC Champion, LEA Jones, RJ Korsch, S Schevchenko and SN Apak: Geoscience Australia, Record 2003/28, p. 127–143.
- Cassidy, KF, Champion, DC, Krapež, B, Barley, ME, Brown, SJA, Blewett, RS, Groenewald, PB and Tyler, IM 2006, A revised geological framework for the Yilgarn Craton, Western Australia: Geological Survey of Western Australia, Record 2006/8, 8p.
- Cawthorn, RG and Walraven, F 1998, Emplacement and crystallization time for the Bushveld complex: *Journal of Petrology*, v. 39, p. 1669–1687.
- Champion, DC and Cassidy, KF 2007, An overview of the Yilgarn craton and its crustal evolution, *in* Proceedings of Geoconferences (WA) Inc. Kalgoorlie '07 Conference, 25–27 September 2007 *edited by* FP Bierlein and CM Knox-Robinson: Geoscience Australia, Record 2007/14, p. 8–13.
- Chen, SF, Morris, PA and Pirajno, FP 2005, Occurrence of komatiites in the Sandstone greenstone belt, north-central Yilgarn Craton: *Australian Journal of Earth Sciences*, v. 52, p. 959–963.
- Costelloe, RD 2013, 2011 Southern Carnarvon seismic survey: acquisition and processing, *in* Youanmi and Southern Carnarvon seismic and magnetotelluric (MT) workshop 2013 *compiled by* S Wyche, TJ Ivanic and I Zibra: Geological Survey of Western Australia, Record 2013/6, p. 7–12.
- Costelloe, RD and Jones, LEA 2013, 2010 Youanmi seismic survey:–acquisition and processing, *in* Youanmi and Southern Carnarvon seismic and magnetotelluric (MT) workshop 2013 *compiled by* S Wyche, TJ Ivanic and I Zibra: Geological Survey of Western Australia, Record 2013/6, p. 1–6.
- Drummond, BJ, Goleby, BR and Swager, CP 2000, Crustal signature of Late Archean tectonic episodes in the Yilgarn craton, Western Australia: evidence from deep seismic sounding: *Tectonophysics*, v. 329, p. 193–221.
- Duuring, P, Cassidy, KF and Hagemann, SG 2007, Granitoid-associated orogenic, intrusion-related, and porphyry style metal deposits in the Archaean Yilgarn Craton, Western Australia: *Ore Geology Reviews*, v. 32, p. 157–186.
- Geological Survey of Western Australia, 2013, Mines and Mineral deposits (MINEDEX): Department of Mines and Petroleum, <www.dmp.wa.gov.au/minedex>, viewed January 2013.
- Gill, M 2011, The petrogenesis and FeTiO accumulation of the Youanmi Igneous Complex (Yilgarn Craton), Western Australia: University of Tasmania, Hobart, Honours thesis (unpublished).
- Goleby, BR, Blewett, RS, Korsch, RJ, Champion, DC, Cassidy, KF, Jones, LEA, Groenewald, PB and Henson, P 2004, Deep seismic reflection profiling in the Archaean northeastern Yilgarn Craton, Western Australia: implications for crustal architecture and mineral potential: *Tectonophysics*, v. 388, p. 119–133.
- Goscombe, B, Blewett, RS, Czarnota, K, Groenewald, PB and Maas, R 2009, Metamorphic evolution and integrated terrane analysis of the Eastern Yilgarn Craton: rationale, methods, outcomes and interpretation: Geoscience Australia, Record 2009/23, 270p.

- Hall, G 2007, Exploration success in the Yilgarn Craton: insights from the Placer Dome experience – the need for integrated research, in *Proceedings of Geoconferences (WA) Inc. Kalgoorlie '07 Conference, 25–27 September 2007 edited by FP Bierlein and CM Knox-Robinson: Geoscience Australia, Record 2007/14, p. 199–202.*
- Ivanic, TJ 2009, The Windimurra and Narndee mafic–ultramafic intrusions: mineralization and geological context, in *GSWA 2009 extended abstracts: promoting the prospectivity of Western Australia: Geological Survey of Western Australia, Record 2009/2, p. 4–6.*
- Ivanic, TJ, Korsch, RJ, Wyche, S, Jones, LEA, Zibra, I, Blewett, RS, Jones, T, Milligan, PR, Costelloe, RD, Van Kranendonk, MJ, Doublier, MP, Hall, CE, Romano, SS, Pawley, MJ, Gessner, K, Patison, N, Kennett, BLN and Chen, SF 2013, Preliminary interpretation of the 2010 Youanmi deep seismic reflection lines and magnetotelluric data for the Windimurra Igneous Complex, in *Youanmi and Southern Carnarvon seismic and magnetotelluric (MT) workshop 2013 compiled by S Wyche, TJ Ivanic and I Zibra: Geological Survey of Western Australia, Record 2013/6, p. 97–111.*
- Ivanic, TJ, Van Kranendonk, MJ, Kirkland, CL, Wyche, S, Wingate, MTD and Belousova, EA 2012, Zircon Lu–Hf isotopes and granite geochemistry of the Murchison Domain of the Yilgarn Craton: Evidence for reworking of Eoarchean crust during Meso-Neoproterozoic plume-driven magmatism: *Lithos*, v. 148, p. 112–127.
- Ivanic, TJ, Wingate, MTD, Kirkland, CL, Van Kranendonk, MJ and Wyche, S 2010, Age and significance of voluminous mafic–ultramafic magmatic events in the Murchison Domain, Yilgarn Craton: *Australian Journal of Earth Sciences*, v. 57, p. 597–614.
- Korsch, RJ, Blewett, RS, Wyche, S, Zibra, I, Ivanic, TJ, Doublier, MP, Romano, SS, Pawley, MJ, Johnson, SP, Van Kranendonk, MJ, Jones, LEA, Kositsin, N, Gessner, K, Hall, CE, Chen, SF, Patison, N, Kennett, BLN, Jones, T, Goodwin, JA, Milligan, PR and Costelloe, RD 2013, Geodynamic implications of the Youanmi and Southern Carnarvon deep seismic reflection surveys: a ~1300 km traverse from the Pinjarra Orogen to the eastern Yilgarn Craton, in *Youanmi and Southern Carnarvon seismic and magnetotelluric (MT) workshop 2013 compiled by S Wyche, TJ Ivanic and I Zibra: Geological Survey of Western Australia, Record 2013/6, p. 147–166.*
- Krapež, B, Brown, SJA, Hand, J, Barley, ME and Cas, RAF 2000, Age constraints of recycled crustal and supracrustal sources of Archaean metasedimentary sequences, Eastern Goldfields Province, Western Australia: evidence from SHRIMP zircon dating: *Tectonophysics*, v. 332, no. 1–2, p. 89–133.
- Liu, SF and Chen, SF 1998, Structural framework of the northeastern Yilgarn Craton and implications for hydrothermal gold mineralisation: *AGSO Research Newsletter*, no. 29.
- Maier, WD 2005, Platinum-group element (PGE) deposits and occurrences: mineralization styles, genetic concepts, and exploration criteria: *Journal of African Earth Sciences*, v. 41, no. 3, p. 165–191.
- Miller, J, Blewett, R, Tunjic, J and Connors, K 2010, The role of early formed structures on the development of the world class St Ives Oldfield, Yilgarn, WA: *Precambrian Research*, v. 183, p. 292–315.
- Milligan, PR, Duan, J, Fomin, T, Nakamura, A and Jones, T 2013, The Youanmi magnetotelluric (MT) transects, in *Youanmi and Southern Carnarvon seismic and magnetotelluric (MT) workshop 2013 compiled by S Wyche, TJ Ivanic and I Zibra: Geological Survey of Western Australia, Record 2013/6, p. 13–25.*
- Mueller, AG, Campbell, IH, Schiøtte, L, Sevigny, JH and Layer, PW 1996, Constraints on the age of granitoid emplacement, metamorphism, gold mineralization, and subsequent cooling of the Archaean greenstone terrane at Big Bell, Western Australia: *Economic Geology*, v. 91, p. 896–915.
- Nebel, O, Mavrogenes, J, Arculus, R, Ivanic, T and Langford, R 2010, Geochemical depth-profiling of late-stage melts from the ~2.8 Ga Windimurra Igneous Complex, Western Australia, in *Fifth International Archean Symposium Abstracts edited by IM Tyler and CM Knox-Robinson: Geological Survey of Western Australia, Record 2010/8, p. 320–322.*
- Parks, J 1998, Weld Range platinum group element deposit, in *Geology of Australian and Papua New Guinean mineral deposits edited by DA Berman and DH Mackenzie: The Australian Institute of Mining and Metallurgy, Monograph 22, p. 279–286.*
- Rameli Resources 2013, Rameli Resources, <www.rameliresources.com.au>, viewed 28 January 2013.
- Robert, R, Poulsen, KH, Cassidy KF and Hodgson, CJ 2005, Gold metallogeny of the Superior and Yilgarn Cratons: *Economic Geology*, 100th Anniversary Volume, p. 1001–1033.
- Romano, SS, Ivanic, TJ, Korsch, RJ, Wyche, S, Van Kranendonk, MJ, Jones, LEA, Zibra, I, Blewett, RS, Jones, T, Milligan, PR, Costelloe, RD, Doublier, MP, Pawley, MJ, Gessner, K, Hall, CE, Patison, N, Kennett, BLN and Chen, SF 2013, Preliminary interpretation of the northern section of deep seismic line 10GA-YU1: Narryer Terrane to Murchison Domain of the Youanmi Terrane, in *Youanmi and Southern Carnarvon seismic and magnetotelluric (MT) workshop 2013 compiled by S Wyche, TJ Ivanic and I Zibra: Geological Survey of Western Australia, Record 2013/6, p. 123–128.*
- Scowen, PAH 1991, The geology and geochemistry of the Narndee intrusion: Australian National University, Canberra, Australian Capital Territory, PhD thesis, 214p (unpublished).
- Sirius Resources 2013, Youanmi, Western Australia, <www.siriusresources.com.au/projects-youanmi.php>, viewed 4 February 2013.
- Spaggiari CV, 2006, Interpreted bedrock geology of the northern Murchison Domain, Youanmi Terrane, Yilgarn Craton: *Geological Survey of Western Australia, Record 2006/10, 19p.*
- Spaggiari, CV 2007, The Jack Hills greenstone belt, Western Australia — Part 1: Structural and tectonic evolution over >1.5 Ga: *Precambrian Research*, v. 155, p. 204–228.
- Swager, CP, Goleby, BR, Drummond, BJ, Rattenbury, MS and Williams, PR 1997, Crustal structure of granite–greenstone terranes in the Eastern Goldfields, Yilgarn Craton, as revealed by seismic profiling: *Precambrian Research*, v. 83, p. 43–56.
- Thébaud, N, Miller, J, McCuaig, C, Hilliard P, Pegg, I and Fisher, L 2012, Structural and Mineralisation Evolution of the Agnew Camp, in *Structural Geology and Resources 2012, Extended Abstracts, compiled by J Vearncombe: Australian Institute of Geoscientists, Bulletin 56, p. 159–163.*
- Timms, N, Hollingsworth, D, Culpan, N, Penkethman, A, Vearncombe, S and Gates, K 2011, Geological mapping report, Yaloginda Area, Murchison Region, Western Australia: *Geological Survey of Western Australia, Record 2011/21, 86p.*
- Van Kranendonk, MJ, Ivanic, TJ, Wingate, MTD, Kirkland, CL and Wyche, S 2012, Long-lived, autochthonous development of the Archaean Murchison Domain, and implications for Yilgarn Craton tectonics: *Precambrian Research*, v. 229, p. 49–92.
- Wang, LG, McNaughton, NJ and Groves, DI 1993, An overview of the relationship between granitoid intrusions and gold mineralisation in the Archaean Murchison Province, Western Australia: *Mineralium Deposita*, v. 28, p. 482–494.
- Wang, Q 1998, Geochronology of the granite–greenstone terranes in the Murchison and Southern Cross Provinces of the Yilgarn Craton, Western Australia: Australian National University, Canberra, PhD thesis, 186p (unpublished).

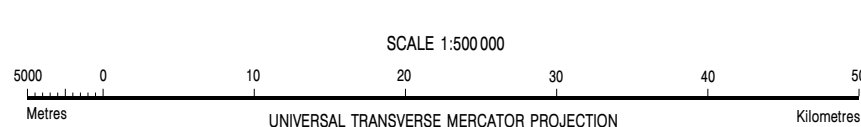
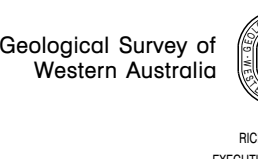
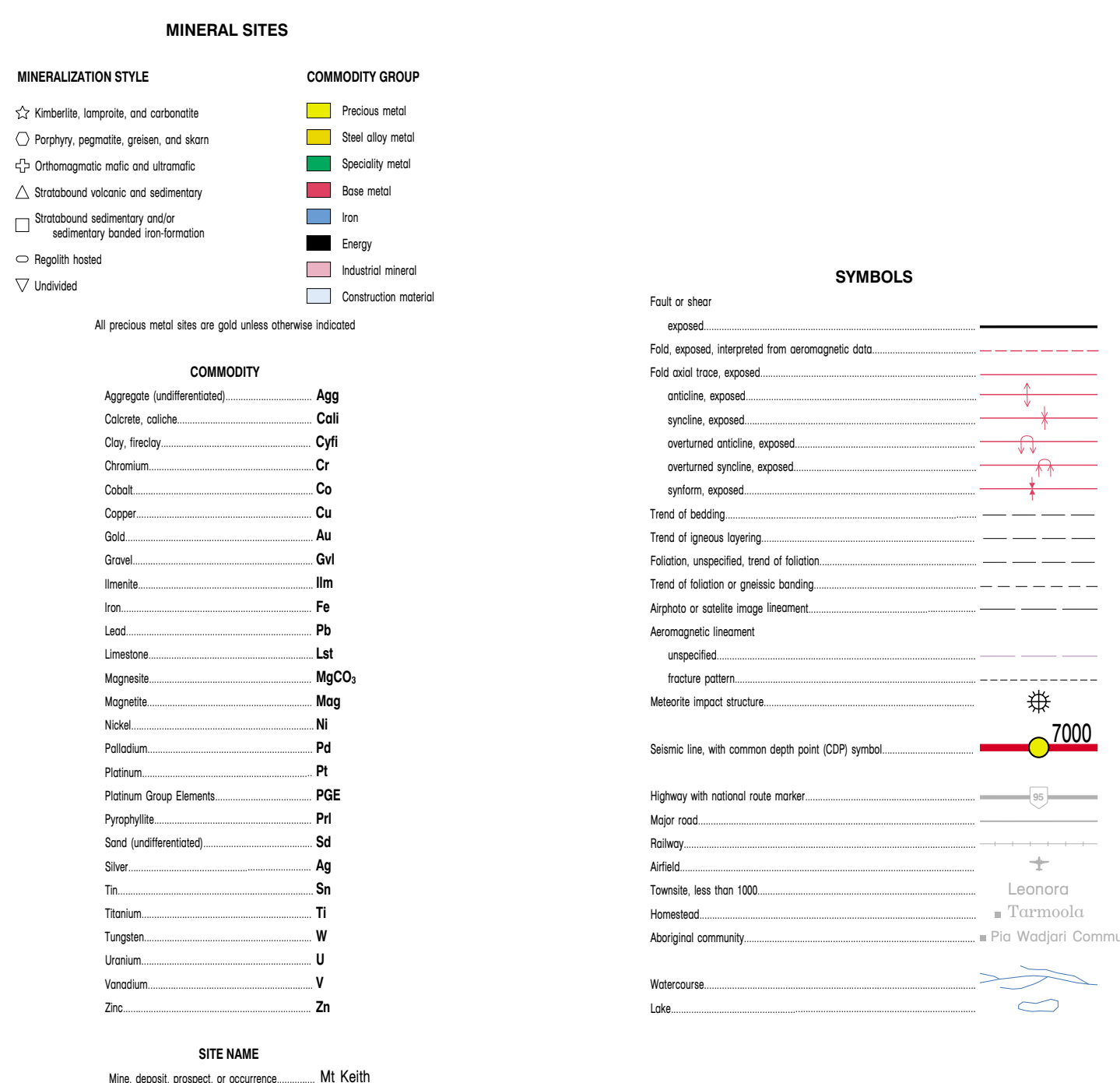
- Watkins, KP and Hickman, AH 1990, Geological evolution and mineralization of the Murchison Province, Western Australia: Geological Survey of Western Australia, Bulletin 137, 267p.
- Wingate, MTD, Kirkland, CL and Ivanic, TJ 2012, 194747: metagabbro, Malamiter Well; Geochronology Record 1013: Geological Survey of Western Australia, 4p.
- Wyche, S (compiler), 2007, A geological traverse across the northern Yilgarn Craton — a field guide: Geological Survey of Western Australia, Record 2007/20, 68p.
- Wyche, S, Kirkland, CL, Riganti, A, Pawley, MJ, Belousova, E and Wingate, MTD 2012, Isotopic constraints on stratigraphy in the central and eastern Yilgarn Craton, Western Australia: Australian Journal of Earth Sciences, v. 59, p. 657–670.
- Wyche, S and Doyle, MG 2007, Montagu, WA Sheet 2843: Geological Survey of Western Australia, 1:100 000 Geological Series.
- Wyche, S, Pawley, MJ, Chen, SF, Ivanic, TJ, Zibra, I, Van Kranendonk, MJ, Spaggiari, CV and Wingate MTD 2013, Geology of the northern Yilgarn Craton, *in* Youanmi and Southern Carnarvon seismic and magnetotelluric (MT) workshop 2013 *compiled by* S Wyche, TJ Ivanic and I Zibra: Geological Survey of Western Australia, Record 2013/6, p. 33–63.
- Yeats, CJ, McNaughton, NJ and Groves, DI 1996, SHRIMP U–Pb geochronological constraints on Archean volcanic-hosted massive sulfide and lode gold mineralization at Mount Gibson, Yilgarn Craton, Western Australia: Economic Geology, v. 91, p. 1354–1371
- Zibra, I 2012, Syndeformational granite crystallisation along the Mount Magnet greenstone belt, Yilgarn Craton: evidence of large-scale magma-driven strain localisation during Neoarchean time: Australian Journal of Earth Sciences, v. 59, p. 793–806.
- Zibra, I, Gessner, K, Pawley, MJ, Wyche, S, Chen, SF, Korsch, RJ, Blewett, RS, Jones, T, Milligan, PR, Jones, LEA, Doublier, MP, Hall, CE, Romano, SS, Ivanic, TJ, Patison, N, Kennett, BLN and Van Kranendonk, MJ 2013, Preliminary interpretation of deep seismic line 10GA-YU2: Youanmi Terrane and western Kalgoorlie Terrane, *in* Youanmi and Southern Carnarvon seismic and magnetotelluric (MT) workshop 2013 *compiled by* S Wyche, TJ Ivanic and I Zibra: Geological Survey of Western Australia, Record 2013/6, p. 87–95.

This Record is published in digital format (PDF) and is available as a free download from the DMP website at
<<http://www.dmp.wa.gov.au/GSWApublications>>.

Further details of geological products produced by the Geological Survey of Western Australia can be obtained by contacting:

Information Centre
Department of Mines and Petroleum
100 Plain Street
EAST PERTH WESTERN AUSTRALIA 6004
Phone: (08) 9222 3459 Fax: (08) 9222 3444
<http://www.dmp.wa.gov.au/GSWApublications>

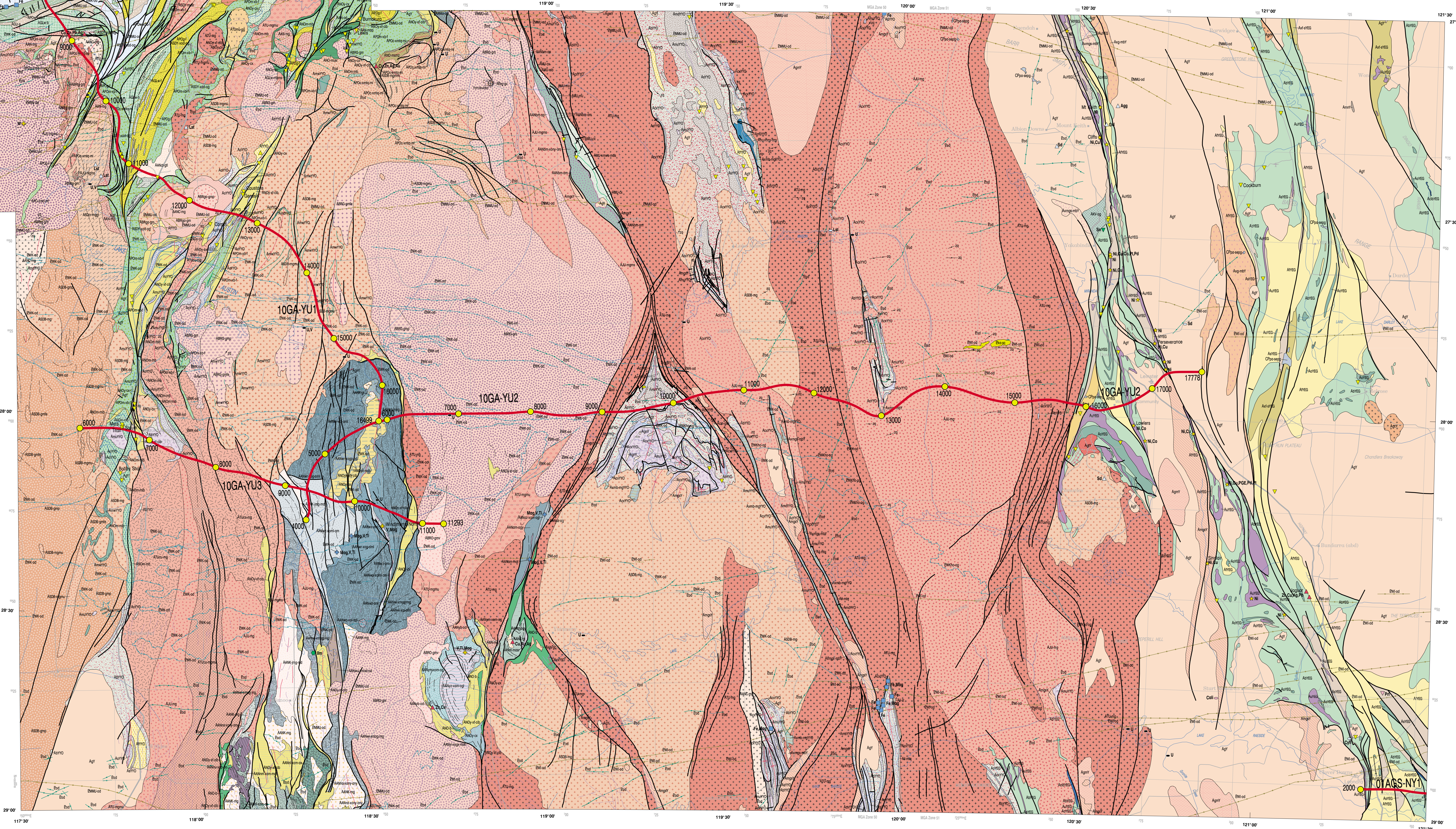
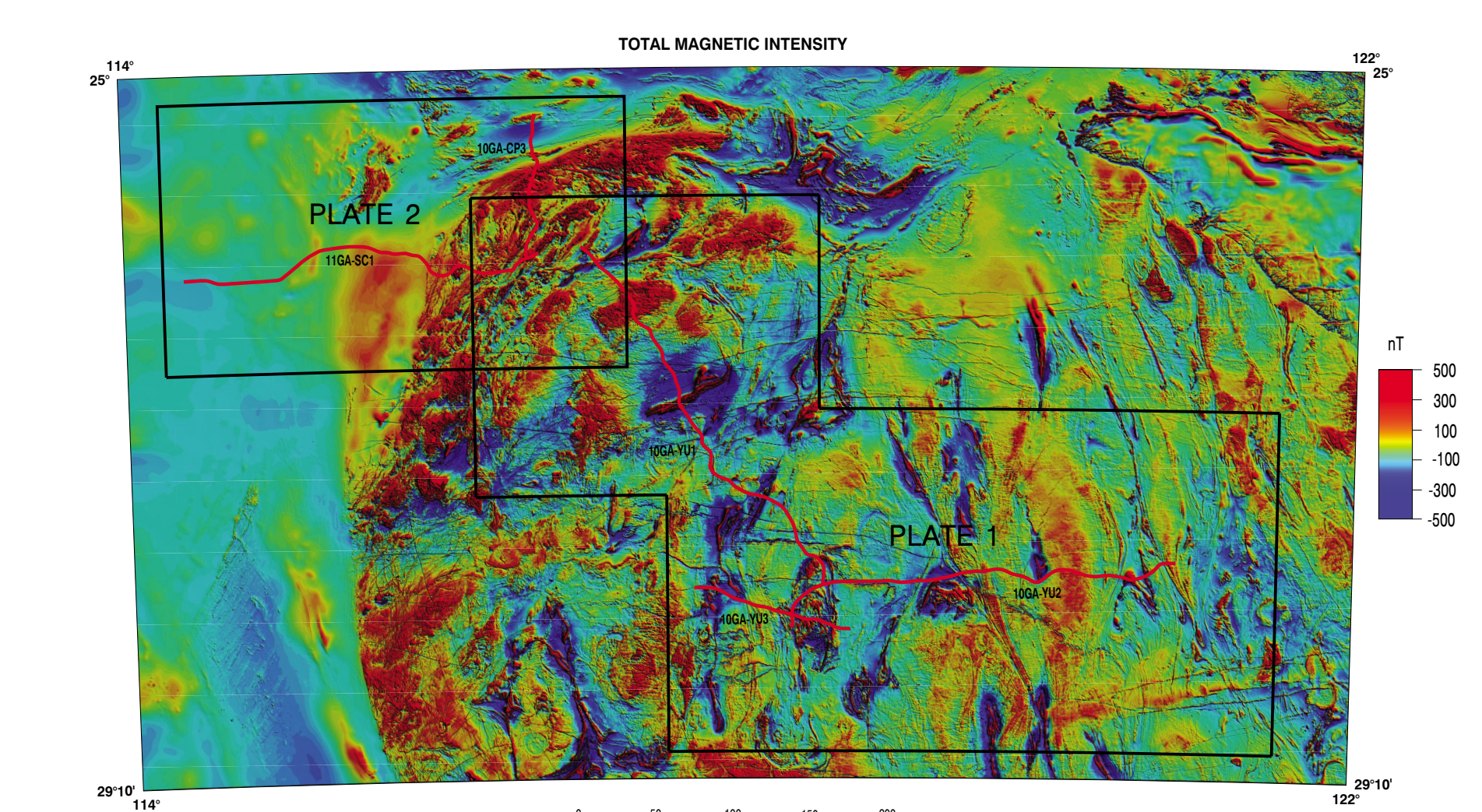


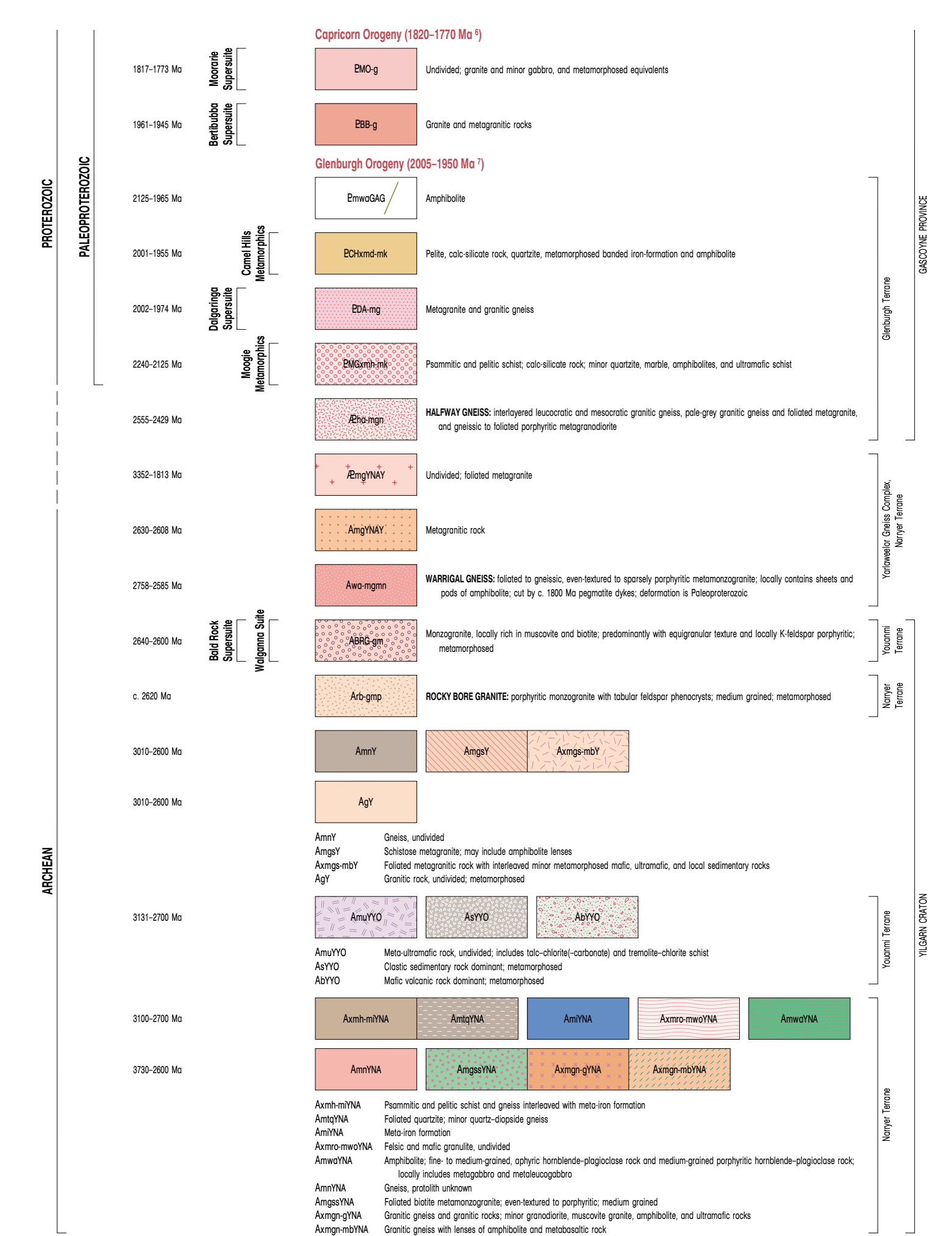
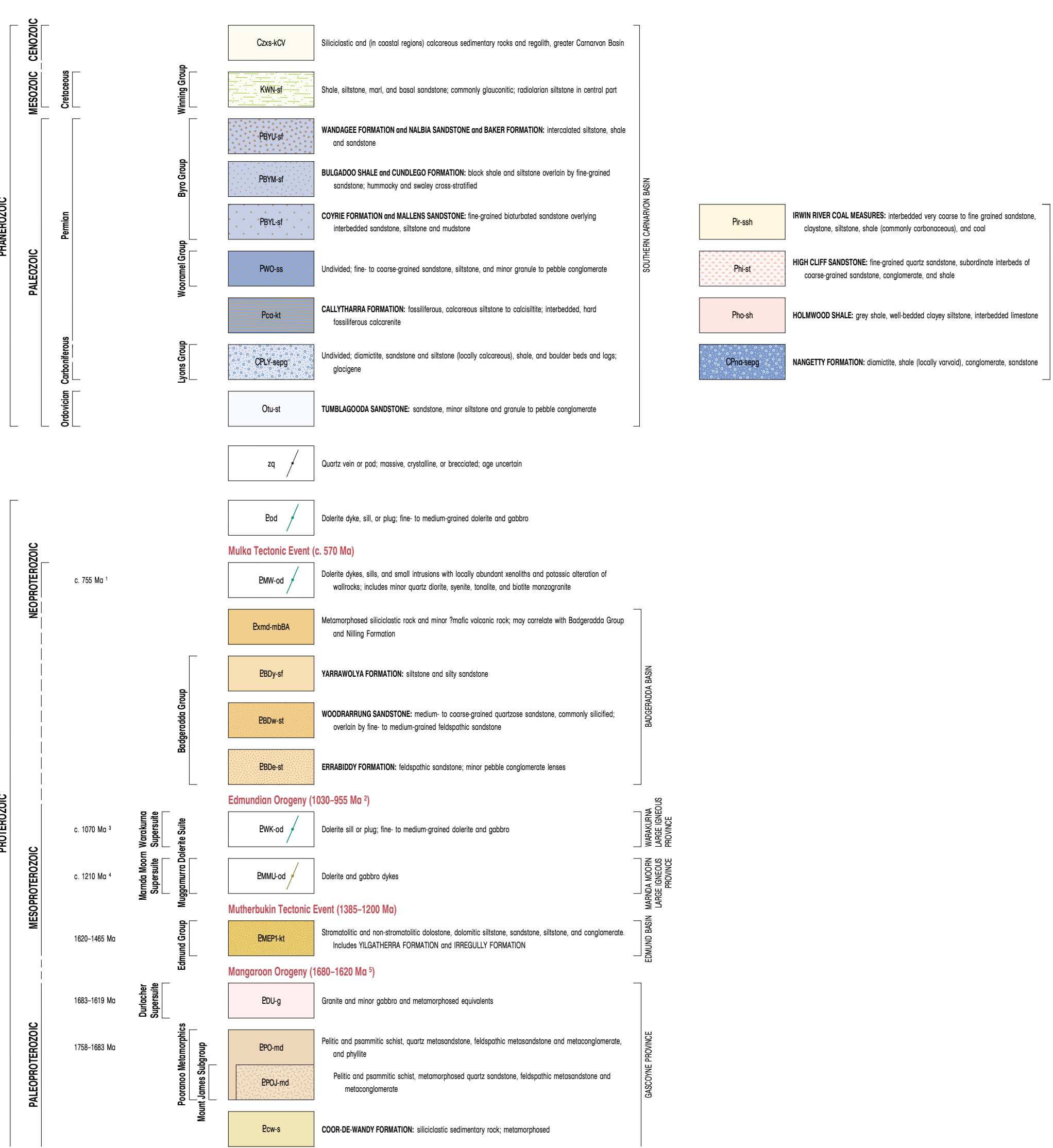
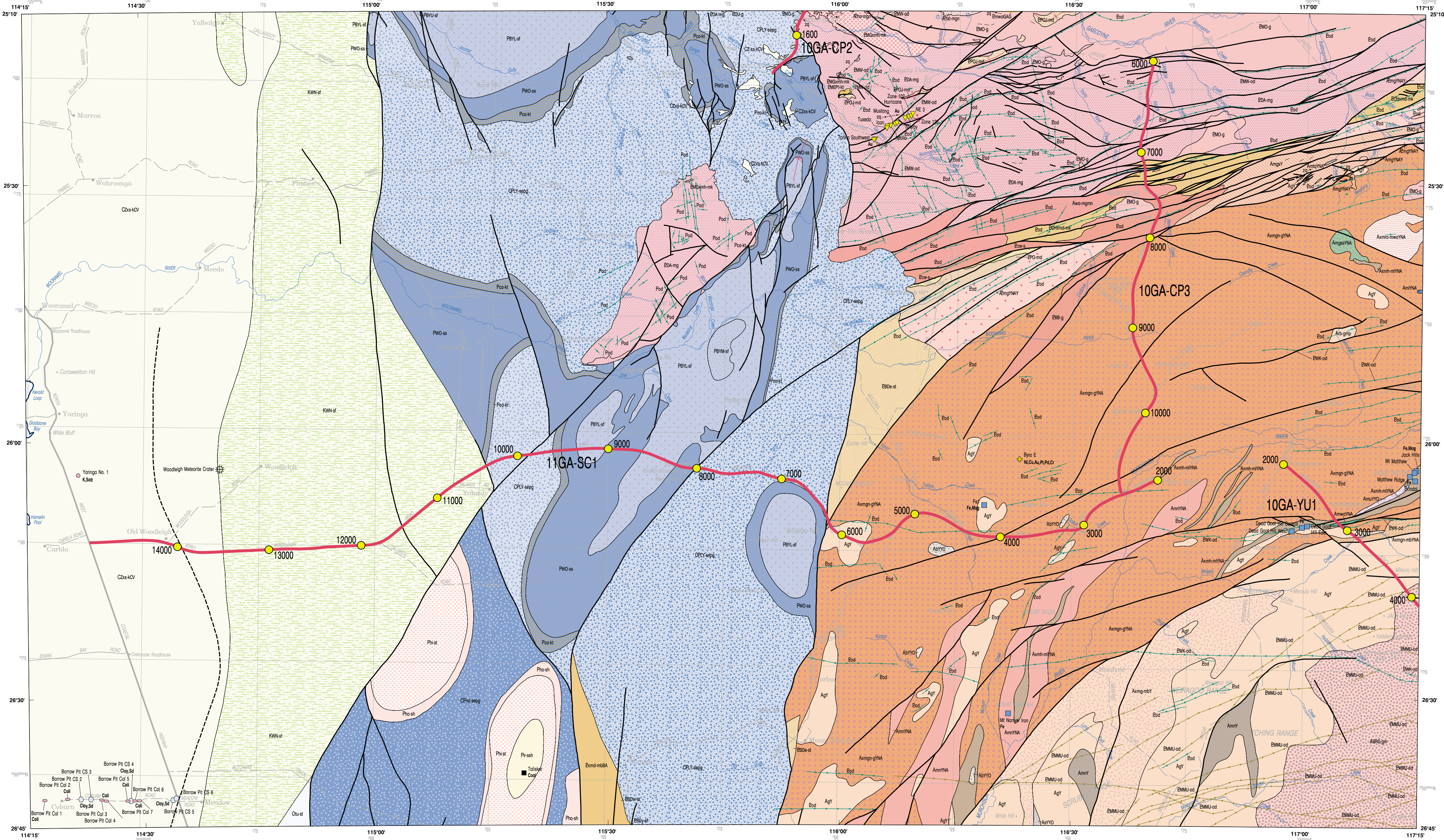


DATA DIRECTORY			
Theme	Date/Version		Organization
Geology*	2012	Geological Survey of Western Australia, Department of Mines and Petroleum	
Mineral sites*	JAN 2013	Geological Survey of Western Australia, Department of Mines and Petroleum	
Stratigraphic data	JAN 2013	Geological Survey of Western Australia, Department of Mines and Petroleum	
Horizontal control	JAN 2013		Land
Topographic nomenclature	2012		Land
Topography	2012		Land

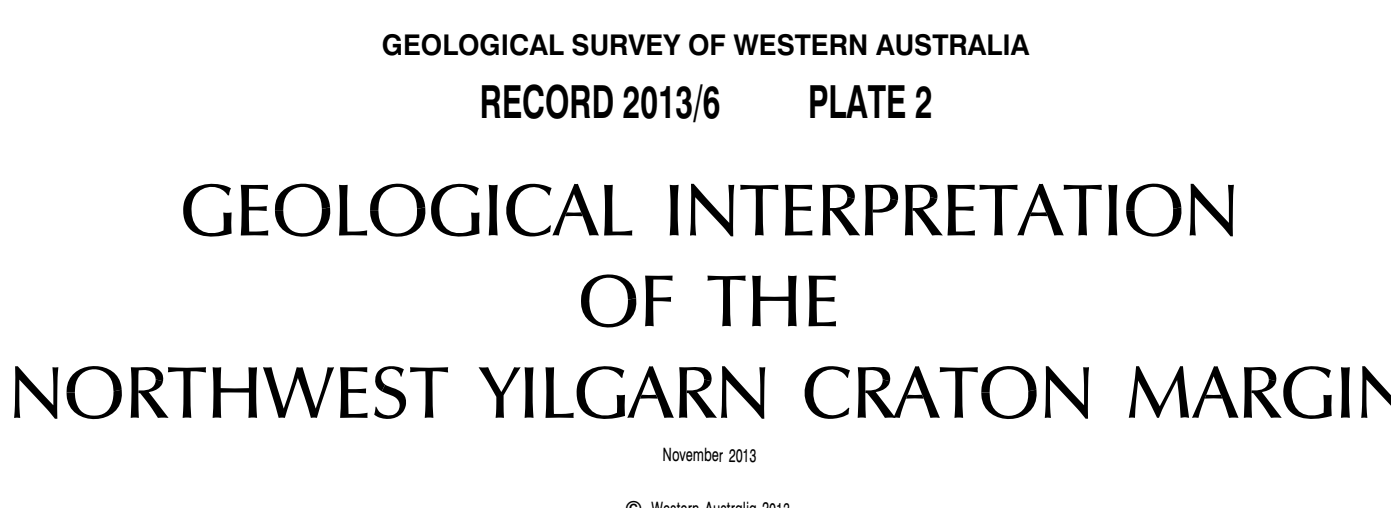
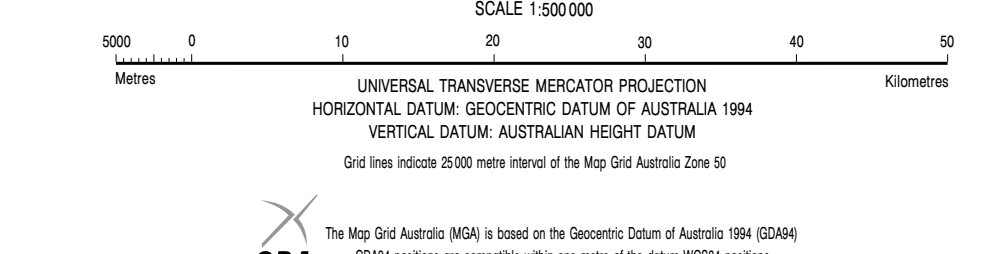
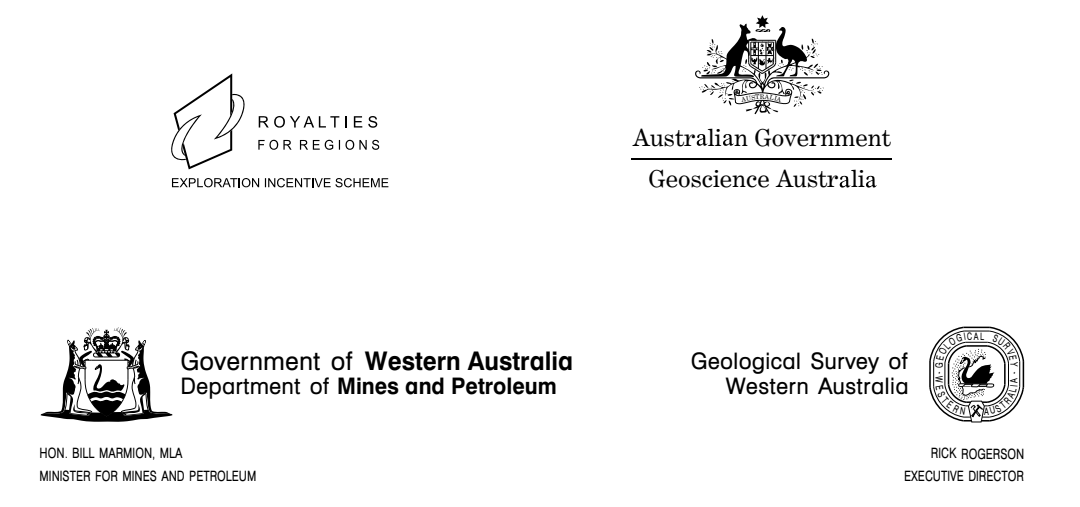
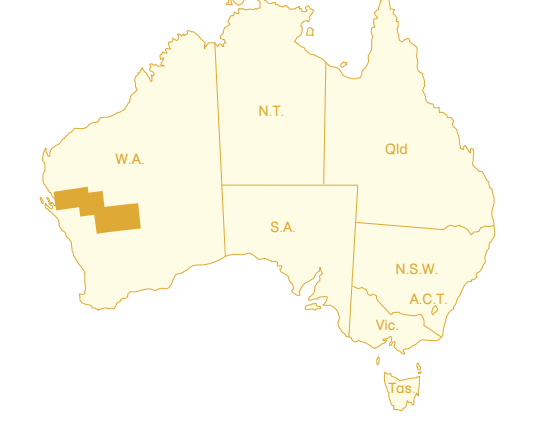
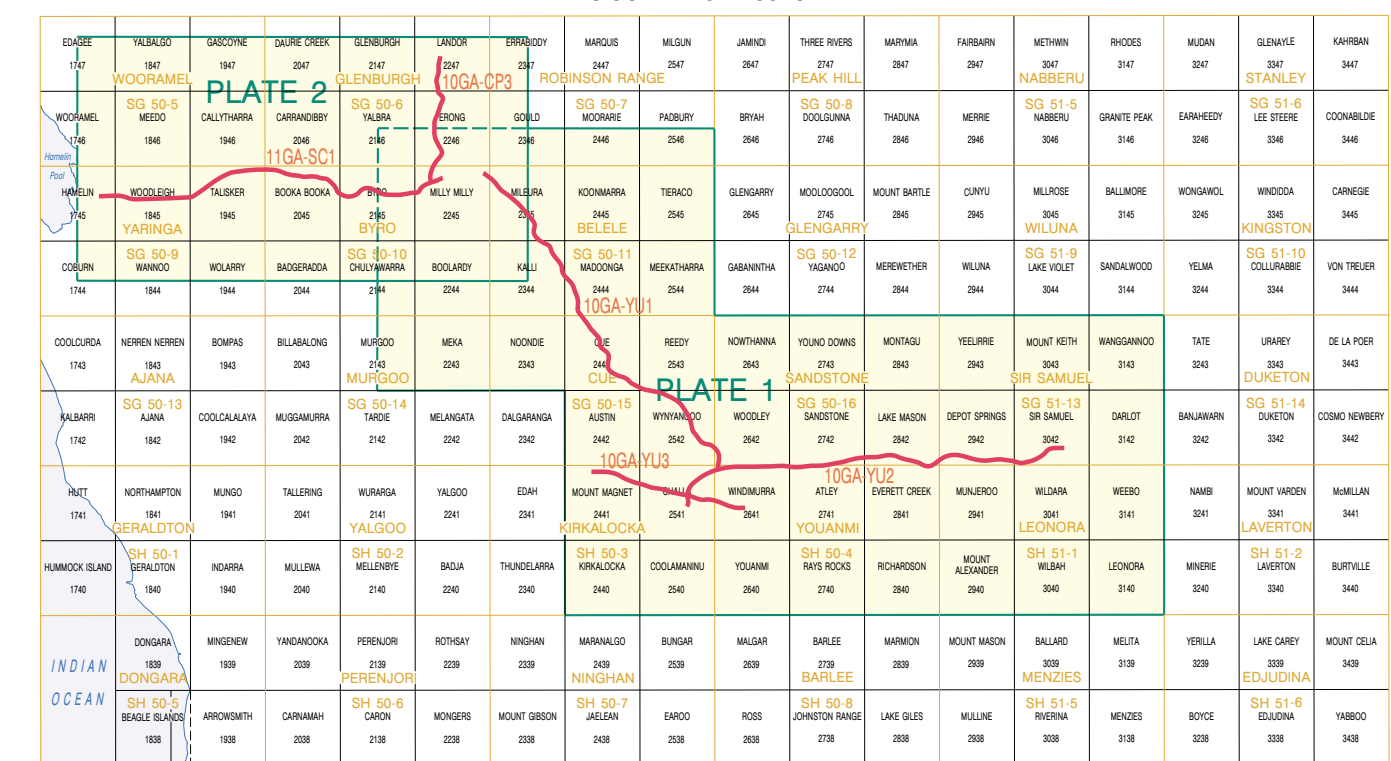
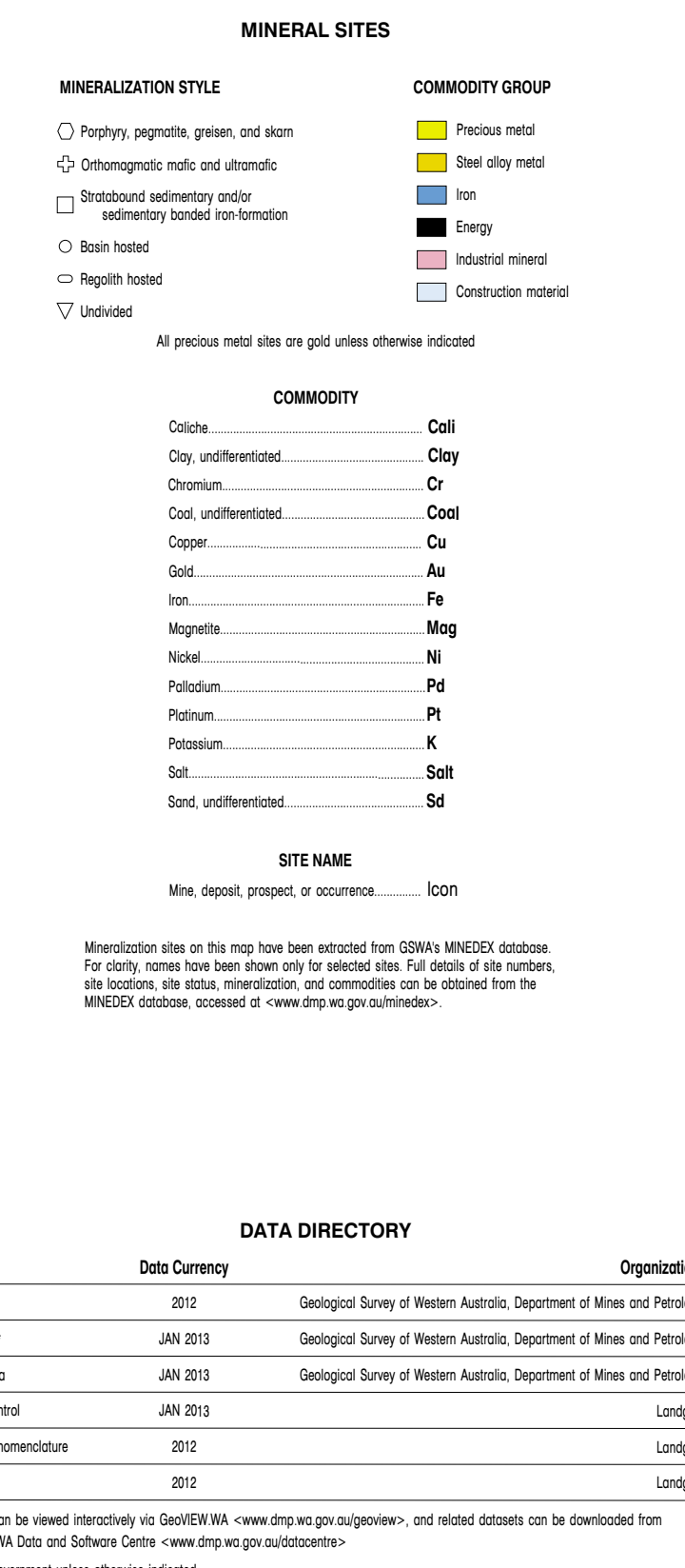
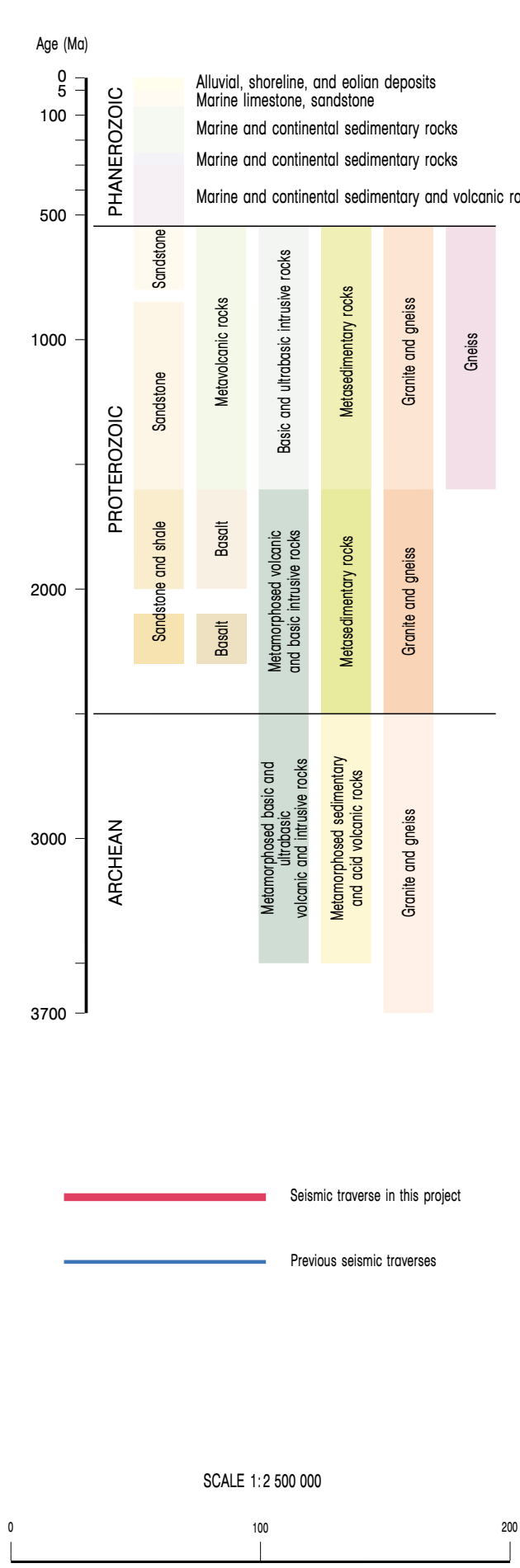
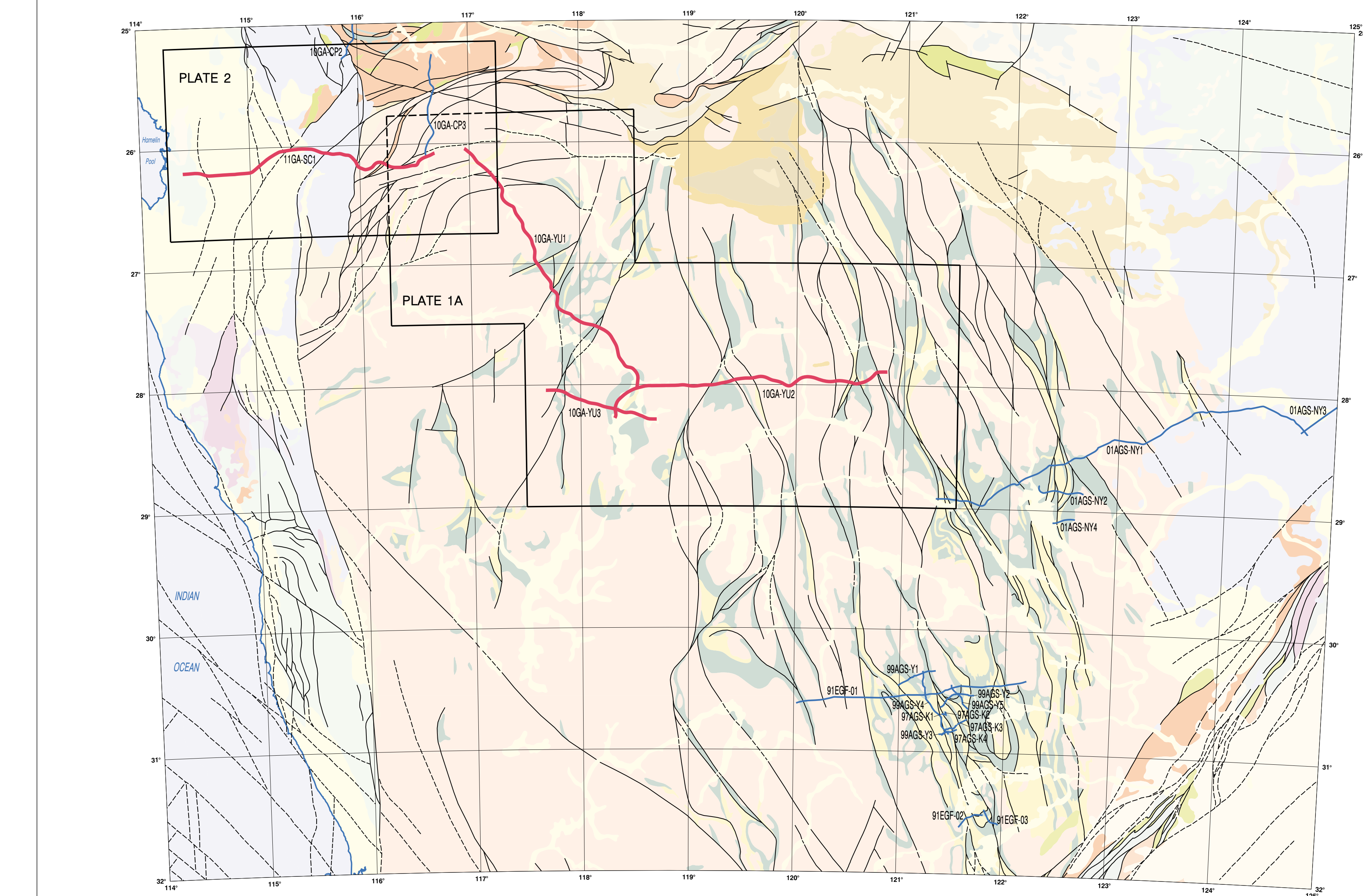
*DMP data can be viewed interactively via www.dmp.wa.gov.au/viewer/, and related datasets can be downloaded from the [DMP Data and Software Centre](http://www.dmp.wa.gov.au/dataset/) www.dmp.wa.gov.au/dataset/

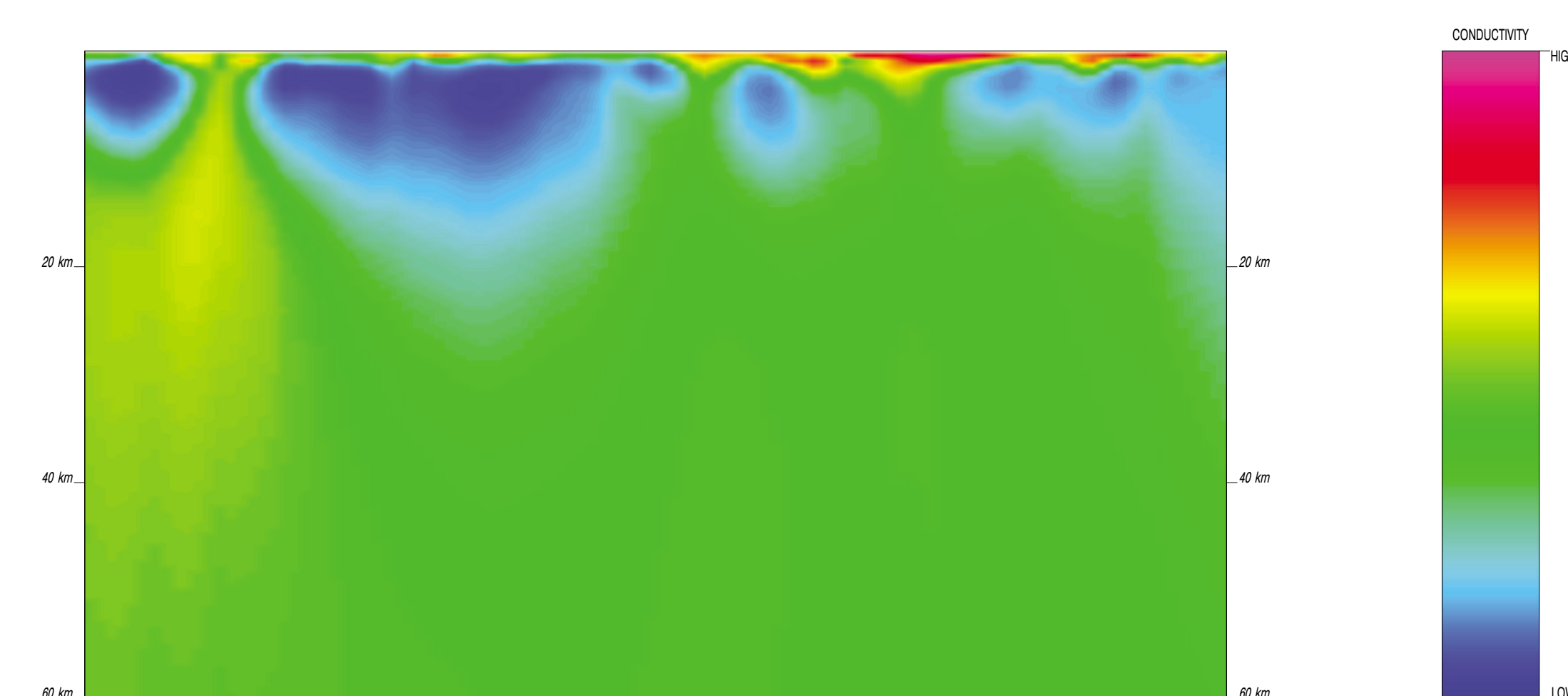
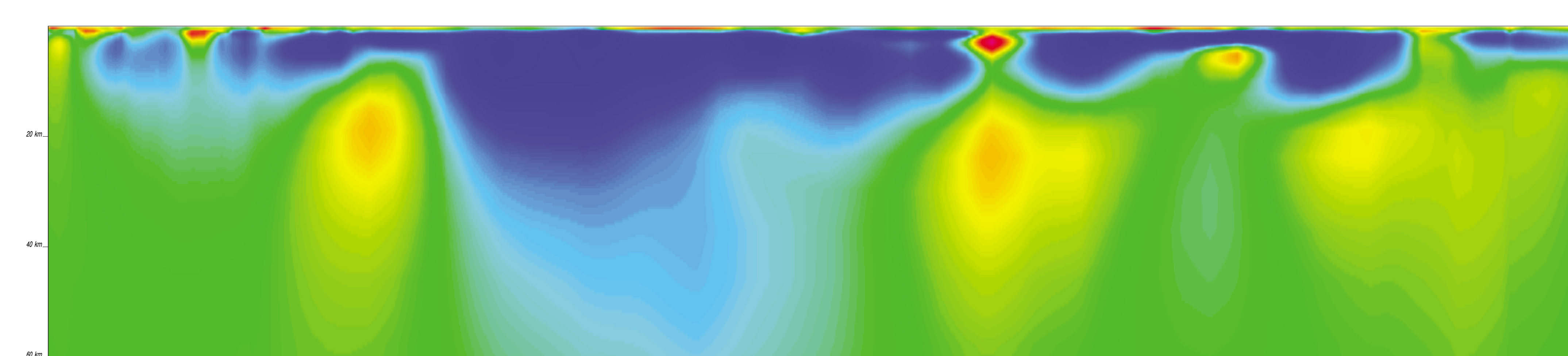
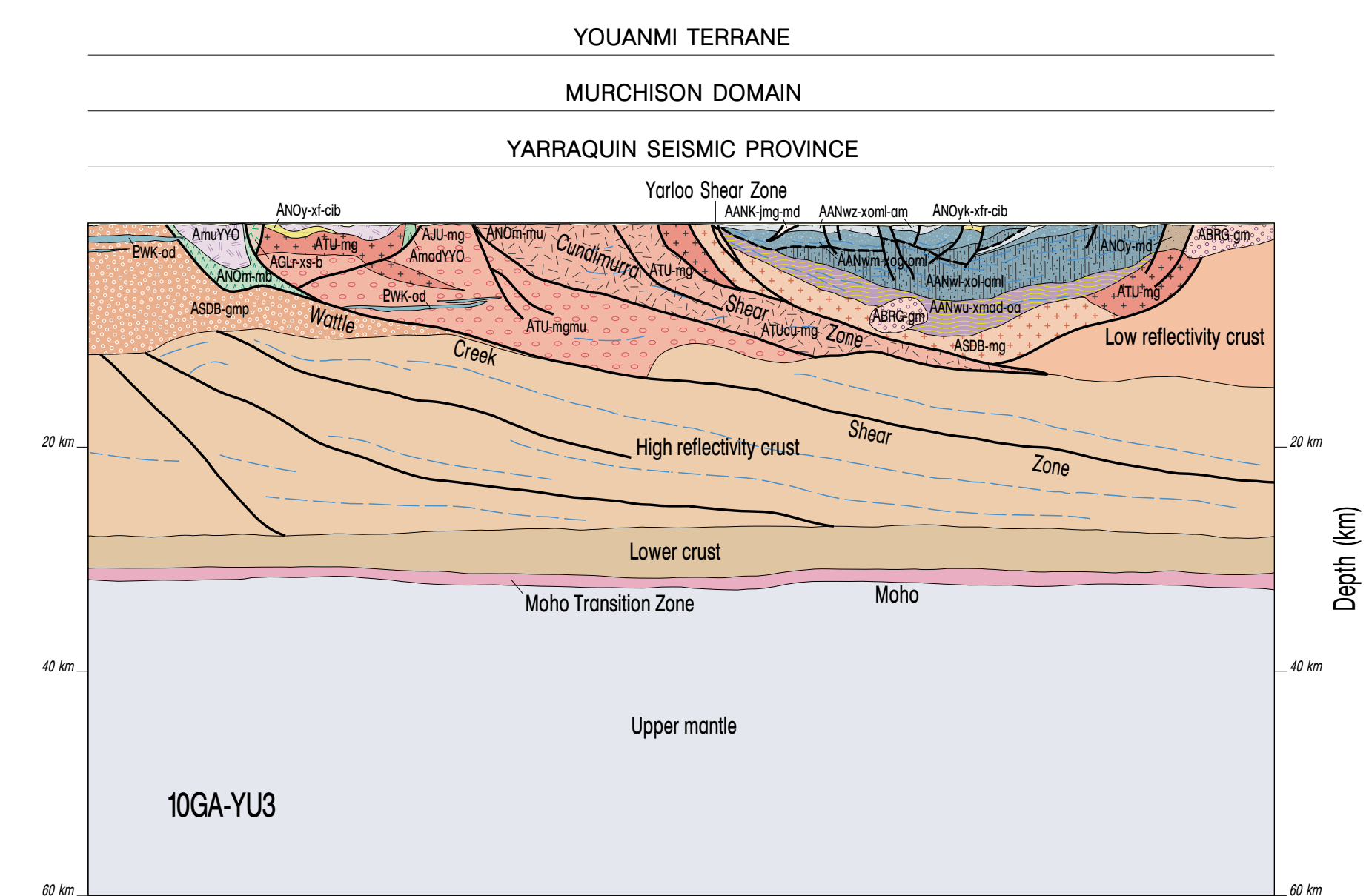
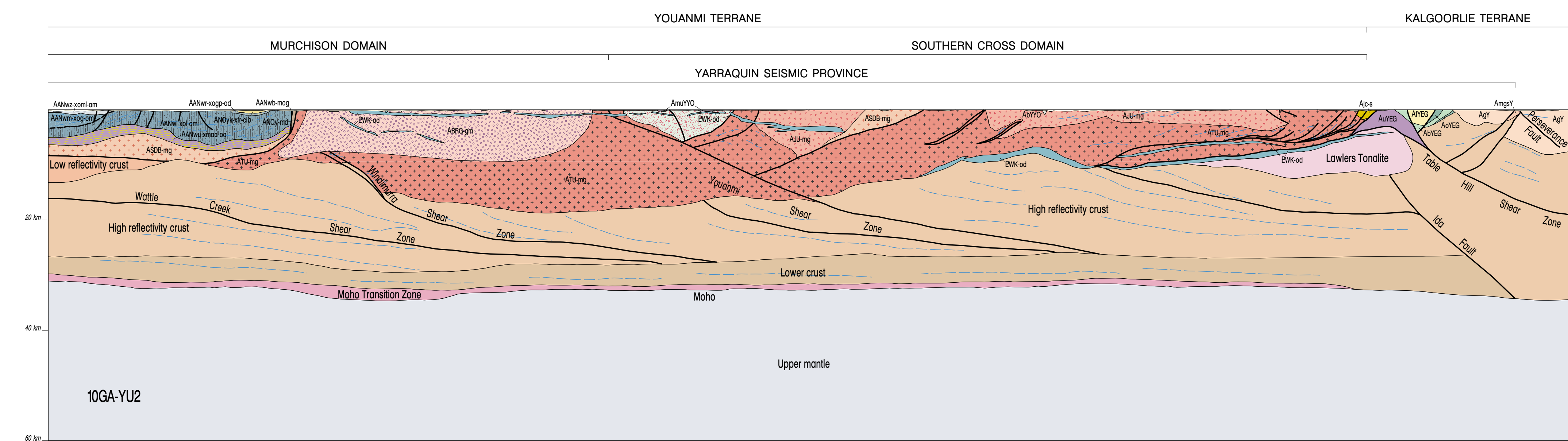
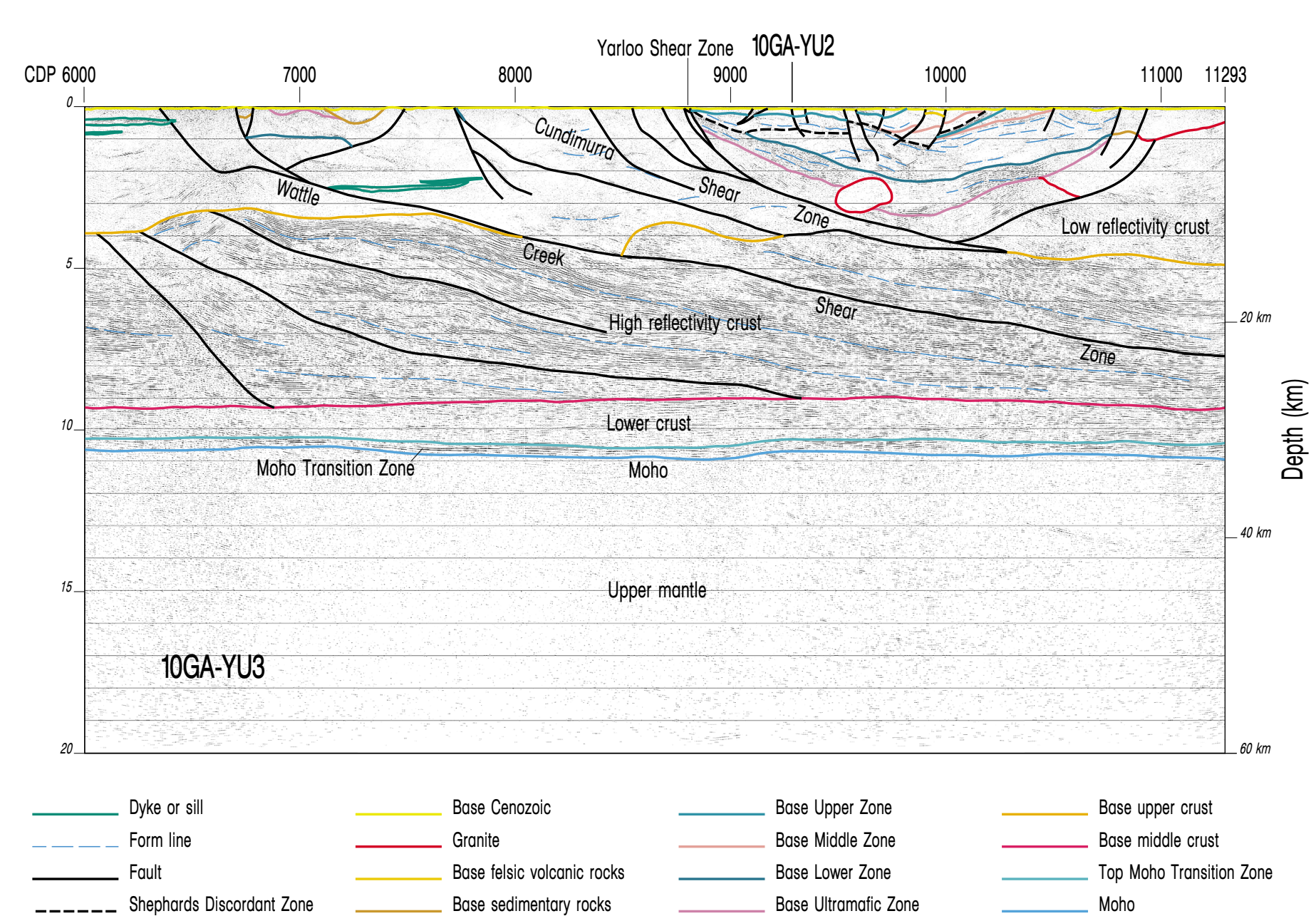
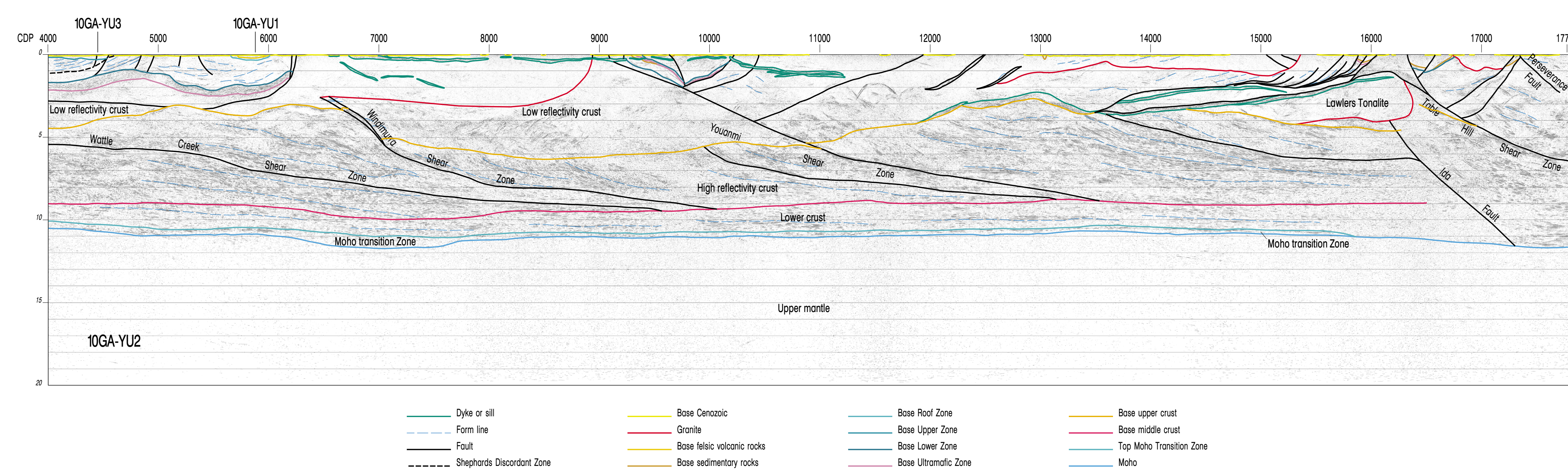
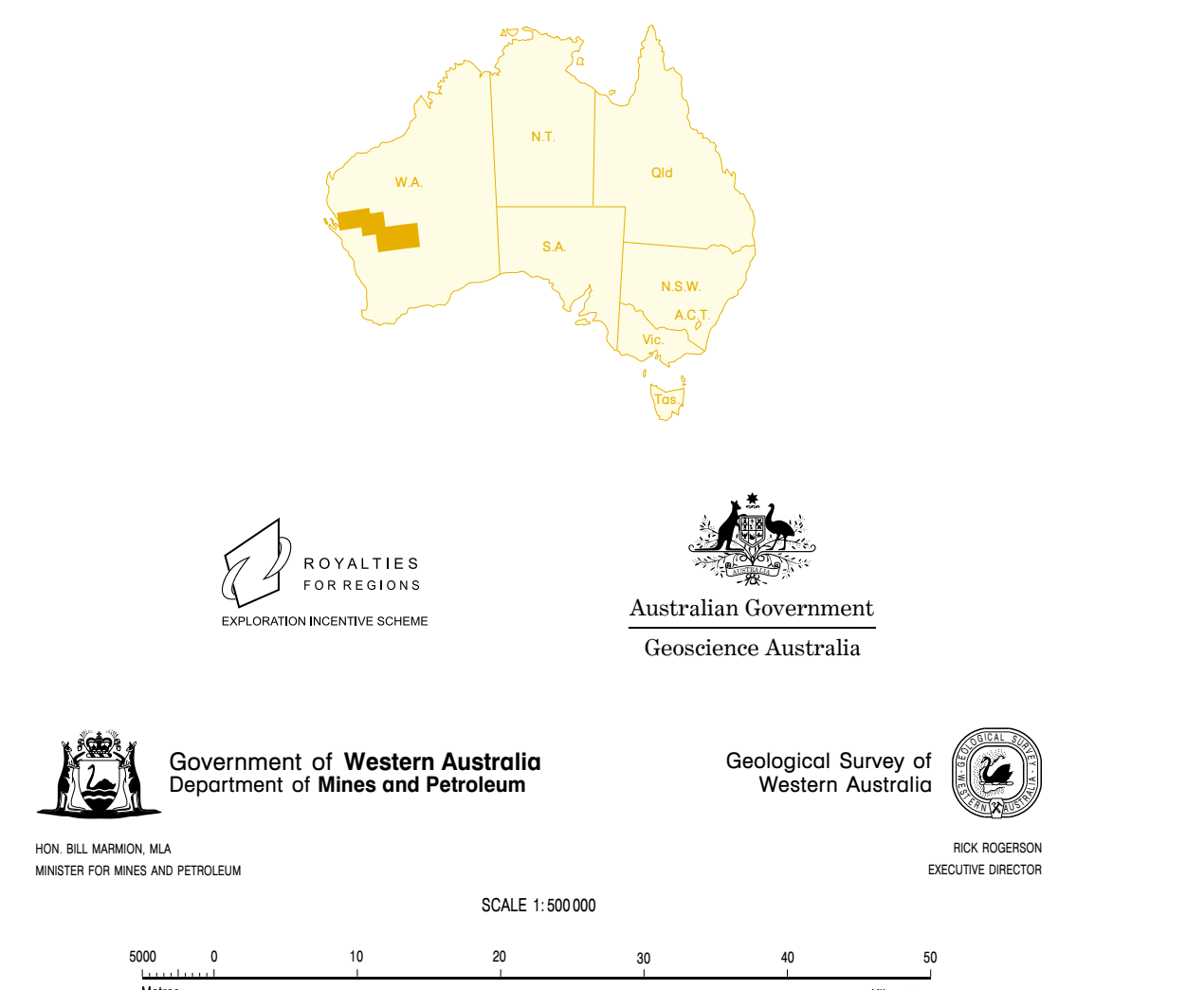
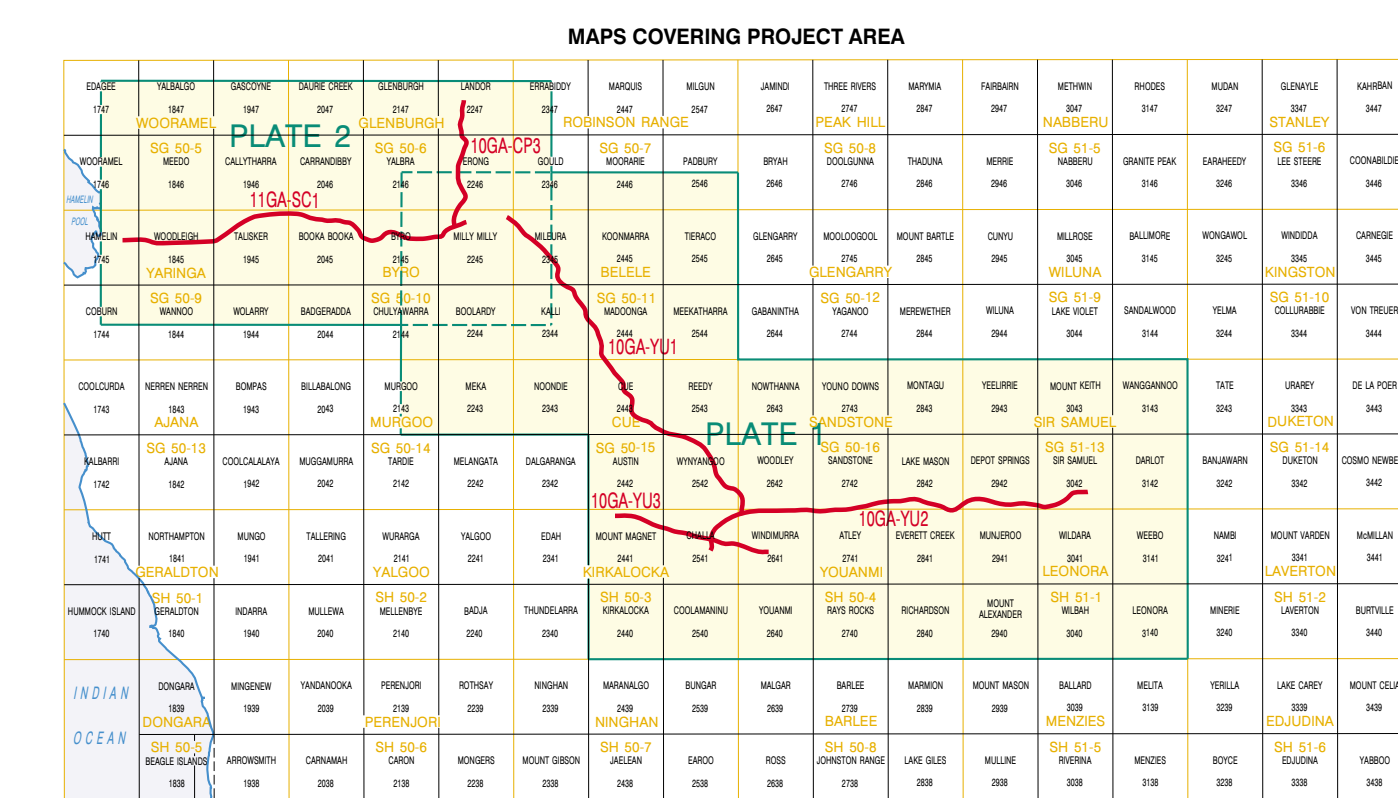
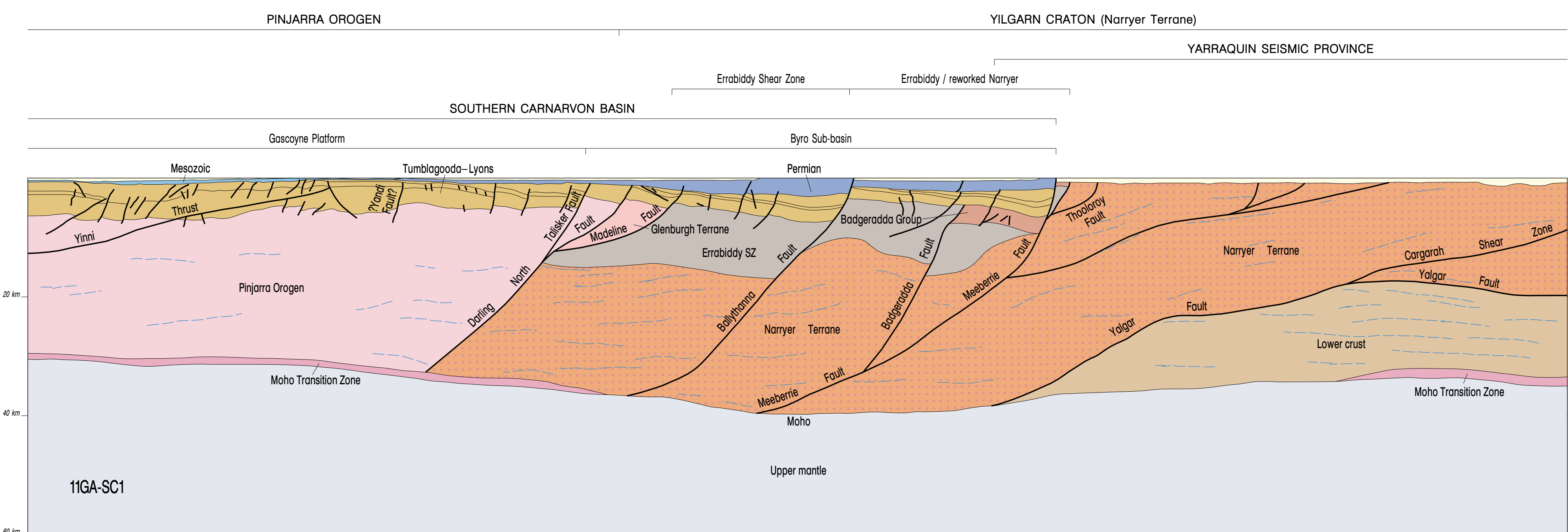
Compiled by Tu, Jizhen, Z. Liang, MP Doublaire, and S. Weythe 2013
Geology by a factor to individual 1:50000 and 1:250,000 map sheets
 Cartography by a factor to individual 1:50000
 Edited by S. Weythe
 Published by Geological Survey of Western Australia
 This work is published in digital format (PDF) and is available online at <www.dmp.wa.gov.au/GSA/MapAccess/>.
 Copies are available from:
 Information Centre
 Department of Mines and Petroleum
 120 Plain Street
 East Perth, Western Australia 6004
 Phone: +61 8 9222 3448
 Fac: +61 8 9222 3444
 Website: www.dmp.wa.gov.au/dmp/
 The nomenclature followed in this work is:
 Tu, J. Zhen, Z. Liang, M. P. Doublaire, M. Weythe, J. (compilers) 2013. Geological interpretation of the northern Yilgarn Craton, in *Proterozoic and Southern Cratonian orogenic belts and megacratons* (MGT workshop compiled by J. Zhen, J. Tu, Jizhen and Z. Liang). Geological Survey of Western Australia, Record 2013/06, Plate A1.





GEOLOGICAL SETTING OF THE YILGARN CRATON SEISMIC LINES



[illegible]

GEOLOGICAL INTERPRETATION
OF THE
YOUANMI AND SOUTHERN CARNARVON
SEISMIC LINES
10GA-YU1, 10GA-YU2,
10GA-YU3, and 11GA-SC1